Synthesis of Advanced Aliphatic Amines via Catalytic C(sp3)–N Bond–Formation or C(sp3)–H Functionalization

JINHONG CHEN

UNIVERSITAT ROVIRA i VIRGILI

ICIQ Institute of Chemical Research of Catalonia

Synthesis of Advanced Aliphatic Amines via Catalytic C(sp^3)–N Bond–Formation or C(sp^3)–H Functionalization

Jinhong Chen

DOCTORAL THESIS
2024

UNIVERSITAT ROVIRA I VIRGILI
Synthesis of Advanced Aliphatic Amines via Catalytic C(sp3)–N Bond-Formation or C(sp3)–H Functionalization
JINHONG CHEN

UNIVERSITAT ROVIRA I VIRGILI
Synthesis of Advanced Aliphatic Amines via Catalytic C(sp3)–N Bond-Formation or C(sp3)–H Functionalization
JINHONG CHEN

UNIVERSITAT ROVIRA I VIRGILI
Synthesis of Advanced Aliphatic Amines via Catalytic C(sp3)–N Bond-Formation or C(sp3)–H Functionalization
JINHONG CHEN

Synthesis of Advanced Aliphatic Amines via Catalytic C(sp^3)–N Bond-Formation or C(sp^3)–H Functionalization

Jinhong Chen

Doctoral Thesis

Supervised by Prof. Rubén Martín Romo

Institut Català d'Investigació Química (ICIQ)

Universitat Rovira i Virgili (URV)

Department of Analytical Chemistry & Organic Chemistry

Tarragona 2024

UNIVERSITAT ROVIRA I VIRGILI
Synthesis of Advanced Aliphatic Amines via Catalytic C(sp3)–N Bond-Formation or C(sp3)–H Functionalization
JINHONG CHEN

Prof. Dr. Rubén Martín Romo, Group Leader at the Institute of Chemical Research of Catalonia (ICIQ) and Research Professor at the Catalan Institution for Research and Advanced Studies (ICREA).

STATES that the present study, entitled "Synthesis of Advanced Aliphatic Amines via Catalytic C(sp^3)-N Bond-Formation or C(sp^3)-H Functionalization", presented by Jinhong Chen for the award of the degree of Doctor, has been carried out under my supervision at the Institute of Chemical Research of Catalonia (ICIQ).

Tarragona, October 2024

Doctoral Thesis Supervisor

Ruben Martin Romo - DNI 38129823D (TCAT)

Firmado digitalmente por Ruben Martin Romo - DNI 38129823D (TCAT)
Fecha: 2024.10.08 22:09:15 +02'00'

Prof. Rubén Martín Romo

UNIVERSITAT ROVIRA I VIRGILI
Synthesis of Advanced Aliphatic Amines via Catalytic C(sp3)–N Bond-Formation or C(sp3)–H Functionalization
JINHONG CHEN

List of Publications

At the time of printing, the results reported herein have been published as:

1. **Jinhong Chen**, Hao, Wang, Craig S. Day, and Ruben Marti, Nickel-Catalyzed Site-Selective Intermolecular C(sp^3)−H Amidation. *Angew. Chem. Int. Ed.* **2022**, *61*, e202212983. (*Very Important Paper*)

2. **Jinhong Chen**, Clarence Tan, Jesus Rodrigalvarez, Shuai Zhang, and Ruben Martin. Site-Selective Distal C(sp^3)−H Bromination of Aliphatic Amines as a Gateway for Forging Nitrogen-Containing sp^3 Architectures. *Angew. Chem. Int. Ed.* **2024**, *63*, e202406485. (*Among most accessed articles in ACIE in July 2024*)

The author has also contributed to the following:

3. Fei Cong, Riccardo S. Mega, **Jinhong Chen**, Craig S. Day, and Ruben Martin, Trifluoromethylation of Carbonyl and Unactivated Olefin Derivatives by C(sp^3)−C Bond Cleavage. *Angew. Chem. Int. Ed.* **2023**, *62*, e202214633.

UNIVERSITAT ROVIRA I VIRGILI
Synthesis of Advanced Aliphatic Amines via Catalytic C(sp3)–N Bond-Formation or C(sp3)–H Functionalization
JINHONG CHEN

Table of Contents

UNIVERSITAT ROVIRA I VIRGILI
Synthesis of Advanced Aliphatic Amines via Catalytic C(sp3)–N Bond-Formation or C(sp3)–H Functionalization
JINHONG CHEN

Acknowledgement

Time flies, and my journey of studying in Spain is nearing its end. Looking back on 3 and a half years, I have not only gained knowledge and honed my skills but also experienced significant personal growth in this unique cultural environment. The fusion of diverse thoughts and cultures has deepened my understanding of the pursuit of truth and goodness. I am deeply grateful for the opportunity to have had such an extraordinary experience in my life.

First and foremost, I would like to express my deepest gratitude to my supervisor, **Rubén Martín**, for giving me this incredible opportunity to pursue my PhD study in this group and for guiding me over these years. Your patient guidance in academics and your care in daily life have been like a refreshing breeze, nurturing my growth. Whether it was showing me how to present research, advising on personal interactions, or sharing your life experiences, every bit of your guidance has been a treasure. Without the platform you provided, none of the work in the following chapters would have been possible. Your support has shaped my academic path and deeply influenced my approach to life.

Second, I would like to sincerely thank the members of the committee, **Prof. Miquel Costas**, **Prof Mariola Tortosa**, and **Prof. Francisco Juliá** for kindly accepting our invitation to assess my work.

A special note of appreciation goes to **Ingrid Mateu**, **Eva Casco**, and **Dr. David Sádaba** for their indispensable administrative and technical support. I also thank the **ICIQ Research Support Units** for their experimental assistance. A heartfelt thank to the **China Scholarship Council** for their financial support, which made this journey possible.

I would like to acknowledge the invaluable collaboration and support of **Dr. Fei Cong**, **Dr. Riccardo Salvatore Mega**, **Hao Wang**, **Dr. Craig Day**, **Clarence Tan**, **Dr. Jesús Rodrigalvarez**, and **Shuai Zhang**. Special thanks to **Dr. Jacob Davies** for guiding me during the early stages of my PhD, and **Dr. Franz-Lucas Haut** for his valuable discussions and dedicated support. Your involvement has been instrumental in elevating the quality and impact of my research.

I owe my sincerest thanks to the past and present members of the Martín group, who have made this journey memorable through their support, discussions, and shared moments of joy. **Jacob**, your unwavering help, especially when I first joined, remains in my heart. I fondly remember the time you patiently showed me how to set up photoreactions, our project discussions, and, of course, your amazing homemade cakes. **Fei**, thank you for helping me settle into life and work in Spain and for your invaluable advice. I wish you the very best in your future endeavors. **Craig**, your efficiency and breadth of knowledge have been an inspiration. I'm confident you'll excel wherever you go. **Franz**, thank you for helping revise my manuscripts and for our insightful discussions, particularly around Quantum yield determination, good luck in your research career! **Jesús**, your timely support when I struggled in research made a significant difference—best of luck with your project. **Ciro**, your brilliance and sense of humor have always been a pleasure, making the lab an enjoyable place. **Hongfei**, a very warm guy, thank you for showing me the ropes when I first arrived. **Álvaro**, **Tomás**, I'll never forget our Spanish lessons and the fun we shared in Lab 2.7, una cerveza, por favor! **Liangliang**, thank you for your guidance with SFC and for sharing your postdoc application experience. **Christopher**, **Roman**, **Riccardo**, **Robert**, your assistance during my tenure has been invaluable. **Zhong**, **Ana**, **Hui-qing** and **Daniel**, it's been a pleasure to have you around.

Carlota, you have been such a kind and generous lab mate—I feel incredibly lucky to have worked with you for three years. The memories we created will always stay with me. I wish you every success as you pursue your goals in the US. **Wenjun**, thank you for the guidance throughout my PhD application process and hosting so many unforgettable parties. **Xinyang**, as a fellow undergraduate alum, I truly enjoyed our lunch discussions at URV. Best of luck to both of you in your journeys in the US. **Bradley**, **Laura**, **Julien**, your support during my time here has been invaluable. **Victoria** and **Dmitry**, I'm especially grateful for the warm welcome you both extended when I first arrived in Spain. **Adrian** and **Júlia**, I wish you both the best of luck in completing your PhDs! **Hao** and **Huihui**, you guys are wonderful friends to me, I truly enjoyed the dinner parties and hiking, best wishes to you both, and keep up the great work! **Yubiao** and **Xuemen**, your

work ethic has been a profound source of inspiration. Keep striving forward—I have no doubt that you'll achieve great things in your research careers. **Filip**, thank you for our valuable discussions and the insights you've shared with me. I hope your PhD journey is as fulfilling as you've hoped.

Clarence, your timely assistance with the bromination reaction was a turning point when I needed it most. I also cherish the stories you've shared about your travels and Singapore's culture. I sincerely wish you great success in your PhD at Berna, and I look forward to seeing your accomplishments! **Shuai**, thank you for tackling numerous challenging topics with me—your research skills are extraordinary. Keep up the fantastic work! **Ricardo**, as my desk mate, your energy and passion have always been contagious. Thank you for all the exciting moments we've shared. **Jonathan**, though we only worked together briefly, I truly appreciated your contributions. I look forward to hearing more about your progress in Germany! **Wei**, **Zuoyu**, and **Huilin**, it has been a pleasure sharing wonderful times with you during our stay in Spain. **Joan** and **Eva**, your presence has made my time in the Martín group much more enjoyable.

Finally, I would like to thank my wife, **Ningyi Zhu**, my parents, my brother, and my many family members and friends. Despite the thousands of miles between us, your support, encouragement, and companionship helped me regain confidence time and again during moments of doubt and frustration, enabling me to overcome countless challenges throughout my academic journey. Now, as my doctoral dissertation draws to a close, the chapter of life filled with love only grows more vibrant. (最后，我想感谢我的妻子朱宁艺，我的父母、弟弟以及众多家人朋友们。正是因为你们在我彷徨惆怅的困难时，给予了支持，鼓励和陪伴，尽管相隔万里，使我一次次重拾信心，克服求学生涯中的重重挑战。至此，博士论文已近结束，但充满爱的人生篇章愈发绚丽。)

Abbreviations & Acronyms

ACN = Acetonitrile

Ad = Adamantane

aq. = Aqueous

AIBN = Azobisisobutyronitrile

bpy = 2,2′-Bipyridine

BDE = Bond dissociation energy

Bac = *tert*-Butylaminocarbonyl

Boc = *tert*-Butyloxycarbonyl

BTMG = 2-tert-Butyl-1,1,3,3-tetramethylguanidine

Cat. = Catalyst

Cbz = Benzyloxycarbonyl

CFL = Compact fluorescent lamp

COD = 1,5-Cyclooctadiene

diglyme = Diglycol methyl ether

dtbppy = 4,4′-Di-tert-butyl-2,2′-dipyridyl

dppe = 1,2-Bis(diphenylphosphino)ethane

DBDMH = 1,3-Dibromo-5,5-dimethylhydantoin

DCC = Dicyclohexylcarbodiimide

DCE = 1,2-Dichloroethane

DCM = Dichloromethane

DFT = Density functional theory

DG = Directing group

DIPEA = *N*,*N*-Diisopropylethylamine

DMA = Dimethylacetamide

DME = Ethylene glycol dimethyl ether

DMF = *N*,*N*-Dimethylformamide

DMMS = Dimethoxymethylsilane

DMSO = Dimethyl sulfoxide

DTBP = Di-*tert*-butyl peroxide

EPR = Electron paramagnetic resonance

equiv. = Equivalent

EtOAc = Ethyl acetate

h = Hour

HAA = Hydrogen atom abstraction

HAT = Hydrogen atom transfer

HBpin = Pinacolborane

HOMO = Highest occupied molecular orbital

LED = Light-emitting diode

LMCT = Ligand-to-metal charge transfer

LUMO = Lowest unoccupied molecular orbital

m = meta

Mes = Mesityl

MLCT = Metal-to-ligand charge transfer

MTBE = Methyl *tert*-butyl ether

NHC = *N*-heterocyclic carbene

NMP = *N*-Methyl-2-pyrrolidone

o = ortho

p = para

PC = Photocatalyst

PCET = Proton-coupled electron transfer

Phen = 1,10-Phenanthroline

rt (RT) = Room temperature

SCE = Saturated calomel electrode

SET = Single electron transfer

SOMO = Singly occupied molecular orbital

t = *tert*

TBAB = Tetrabutylammonium bromide

TBADT = Tetra-*n*-butylammonium decatungstate

TBAI = Tetrabutylammonium iodide

TBS = *tert*-butyldimethylsilyl

TDAE = Tetrakis(dimethylamino)ethylene

TEMPO = 2,2,6,6-Tetramethyl-1-piperidinyloxy

TFE = 2,2,2-Trifluoroethanol

THF = Tetrahydrofuran

TMG = 1,1,3,3-Tetramethylguanidine

TMHD = 2,2,6,6-Tetramethyl-3,5-heptanedione

TMS = Tetramethylsilane

Tp = Trispyrazolylborate

Tf = triflate

Ts = Tosyl

TTMSS = Tris(trimethylsilyl)silane

UV = Ultraviolet

XAT = Halogen atom transfer

Abstract

Amines are highly ubiquitous in bioactive natural products, pharmaceuticals, and materials. A close look at the literature data reveals that 82 % of the top 200 small molecule prescription medicines by global sales in 2022 contain at least an amine moiety or a nitrogen-containing heterocycle. Therefore, the development of new catalytic manifolds aimed at promoting *de novo* C–N bond-forming reactions operating with broad applicability and practicality would be particularly valuable in both pharmaceutical and industrial laboratories.

In line with our ongoing interest in Ni-catalyzed cross-coupling reactions, this doctoral thesis focuses on two main areas: 1) nickel-catalyzed C(sp^3)–N bond formation via functionalization of C(sp^3)–H linkages or olefins via nitrene transfer, and 2) site-selective, diverse functionalization of C(sp^3)–H bonds in aliphatic amines.

The initial study unravels the possibility of conducting a site-selective C(sp^3)–H amidation enabled by nickel-nitrenoid catalysis. The approach is characterized by a predictable reactivity by selective C–N bond formation at sp^3 sites adjacent to heteroatoms via open-shell species, thereby offering a complementary profile to traditional oxidative-type manner via two-electron transfer processes.

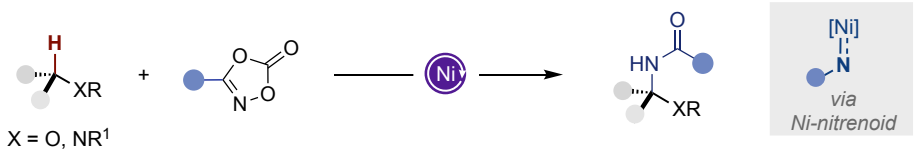

Scheme 1 Ni-catalyzed intermolecular site-selective C(sp^3)–H amidation.

The following chapter focuses on stereodivergent *N*-glycosylation via nickel catalyzed hydroamidation of glycals. The protocol provides access to either α- or β-*N*-glycosides through forging C(sp^3)–N glycosidic bonds on kinetic or thermodynamic grounds.

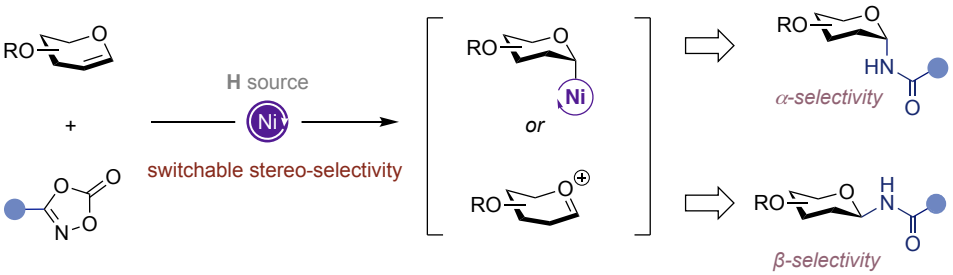

Scheme 2 Ni-catalyzed stereodivergent *N*-glycosylation.

On the other hand, we have developed a new platform for enabling remote functionalization of aliphatic amines via a site-selective bromination event at distal C(sp^3)–H sites enabled by the intermediacy of ammonium salts in acidic media. The resulting brominated scaffolds serve as a synthetic linchpin that can be easily transformed to a series of carbon–carbon and carbon–heteroatom bonds, thus offering access to advanced sp^3 architectures possessing valuable aliphatic amine moieties.

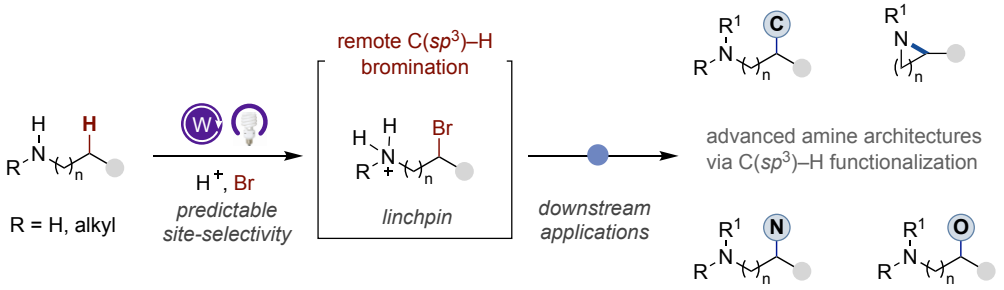

Scheme 3 Remote functionalization of C(sp^3)–H bonds in aliphatic amines.

Chapter 1. General Introduction

1.1 Properties of Nickel

Nickel, a first-row transition metal first isolated and classified as an element by Axel Fredrik Cronstedt in the 1750s,[1] is one of most abundant first-row transition metals presenting a ground-state configuration of $3d^8\ 4s^2$. Compared to heavier metals like palladium, nickel's smaller d-orbital splitting enables access to multiple oxidation states ranging from Ni(0) to Ni(IV) (Scheme 1.1). In addition, nickel's unpaired 3d electrons allow the implementation of both two- and single-electron transfer (SET) reactions with exceptional ease, an observation that is in sharp contrast with the canonical two-electron pathways typically encountered in the other d^{10} metal series. This redox promiscuity has recently been leveraged for enabling a wide number of bond-forming reactions.[2] Moreover, nickel complexes have a strong affinity to unsaturated π-systems such as alkenes, alkynes, and carbonyls, where electrons from nickel's filled d orbitals are donated into the π* anti-bonding orbitals of the ligand.[3] Not surprisingly, the unique properties of nickel have attracted considerable attention, offering new vistas when accessing new chemical space in synthetic endeavors.[4]

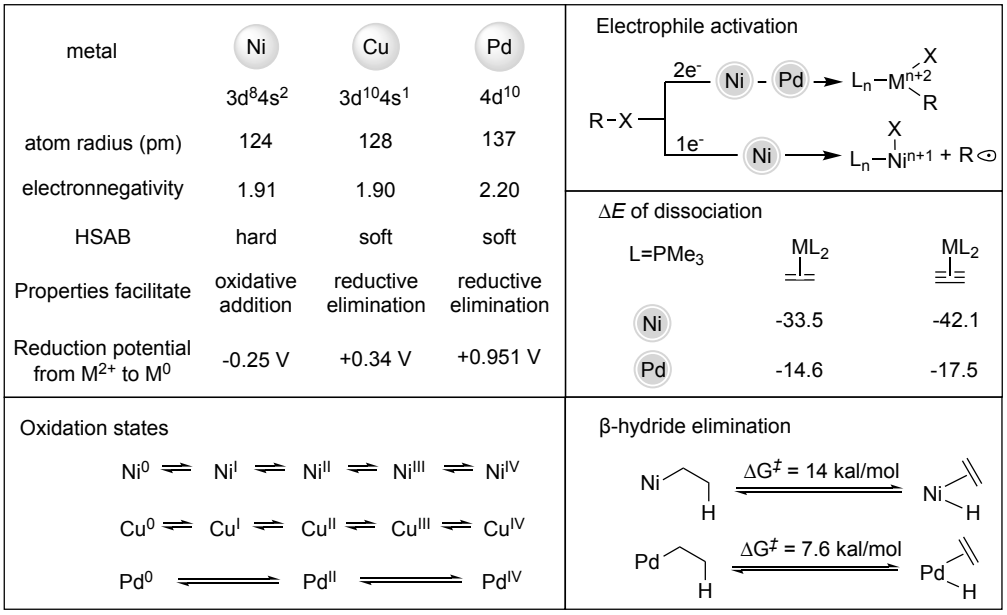

Scheme 1.1 General features of Ni for synthetic transformations.

1.2 Nickel-Catalyzed C–H Functionalization Reactions

The recent years have witnessed considerable advances in the area of transition metal-catalyzed cross-coupling reactions, offering conceptually new pathways for forging new carbon-carbon and carbon-heteroatom bond-linkages.[5] Indeed, these reactions have been widely adopted in both academic and industrial settings, as illustrated by the countless examples found in the literature when implementing exceedingly complex endeavors, for example in the venerable Pd-catalyzed Heck, Negishi, Suzuki-Miyayra or Buchwald-Hartwig cross-coupling reactions for forging carbon-carbon or carbon-nitrogen bonds.[6] Despite the advances realized, the requirement for prefunctionalized substrates spurred the development of C–H functionalization reactions where similar transformations can be effected in the presence of suitable reagents and counterparts by utilizing simple C–H bonds as nucleophilic handles (Scheme 1.2),[7] with the potential to be applied in the context of late-stage functionalization (LSF) of advanced ingredients.[8]

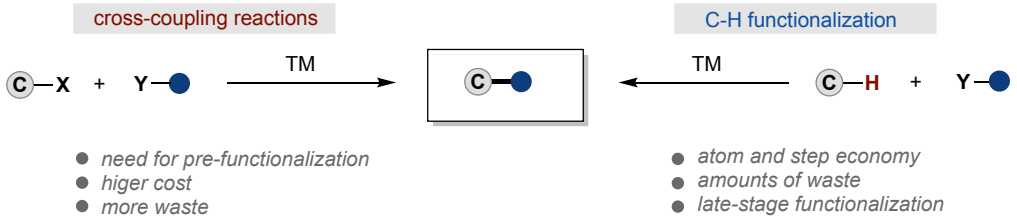

Scheme 1.2 Conventional cross-coupling vs C–H functionalization techniques.

Despite the attractiveness in designing C–H functionalization reactions, the inherent thermodynamic stability of C–H bonds makes them particularly difficult to activate under mild conditions (Scheme 1.3), particularly in the presence of multiple, yet similar, C–H bonds present in a regular small molecule.[9]

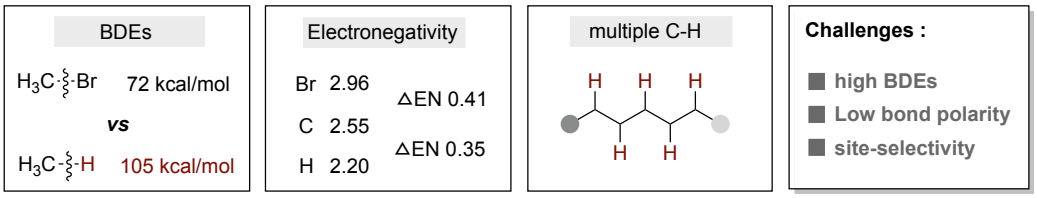

Scheme 1.3 Challenges for C–H functionalization.

Over the past two decades, nickel has gained significant momentum in C–H functionalization when compared to other d^{10} metals due to the flexibility for enabling a series of C–C or C–heteroatom bonds by one- or two-electron manifolds via inner/outer-sphere type mechanisms (Scheme 1.4).[10] The latter observation is particularly attractive, not only showing the dual nature that nickel catalysis offer in the context of organic synthesis, but also as versatile and powerful vehicle for bond-construction.

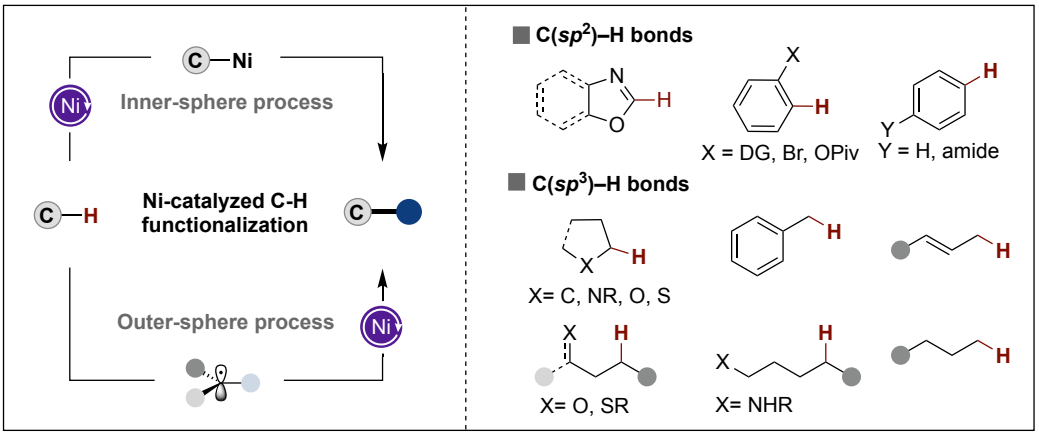

Scheme 1.4 Ni-catalyzed C–H functionalization.

1.2.1 Chelation-Assisted Ni-Catalyzed Functionalization of C–H Bonds

In 1963, Kleiman and Dubeck found that exposure of azobenzene to dicyclopentadienyl nickel leads to the formation of a nickelacycle, with azobenzene utilized as a formal directing group (Scheme 1.5).[11] This finding can hardly be underestimated, as it represents the very first time that an organometallic intermediate was isolated by means of C–H functionalization. Intriguingly, this result remained dormant, probably due to the meteoric development of Pd-, Rh- and Ir-catalyzed C–H functionalization events.[12] In 2011, Chatani revisited the seminal discovery from Kleiman and Dubeck and described a Ni-catalyzed regioselective cycloaddition of aromatic amides with alkynes.[13] In this reaction, the utilization the 2-pyridinylmethylamine as a chelating group enabled coordination to nickel center in an *N*,*N*-fashion, facilitating the C–H metalation via a σ-complex-assisted metathesis (σ-CAM) mechanism,[14] thus setting the basis for functionalizing the ortho C(sp^2)–H bond.

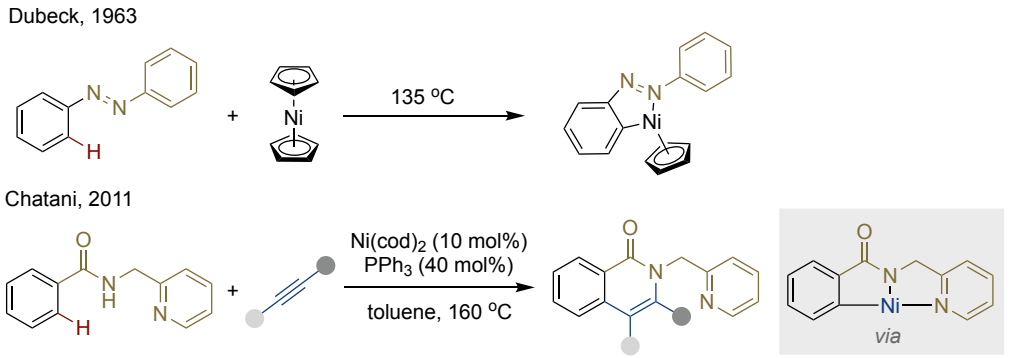

Scheme 1.5 Initial Ni-mediated C(sp^2)–H bond functionalization reactions.

Spurred by the potential implications of the work of Kleiman, Dübeck and Chatani, the subsequent years witnessed the development of a series of C–H functionalization reactions assisted by proximal nitrogen-based chelating groups.[15] As shown in Scheme 1.6, notable examples include 8-aminoquinoline (AQ),[16] (pyridine-2-yl)isopropyl (PIP) amine,[17] 2-pyridyl,[18] 2-pyrimidylamine,[19] purine[20] or amides,[21] among others. The incorporation of these chelating groups has allowed a series of C–C and C–heteroatom bond-forming reactions via concerted metalation deprotonation (CMD) or σ-bond

metathesis utilizing Ni catalysts. In most instances, however, these reactions require high temperatures and strong bases, thus reinforcing a change in strategy for expanding the potential applicability of these reactions in organic synthesis.

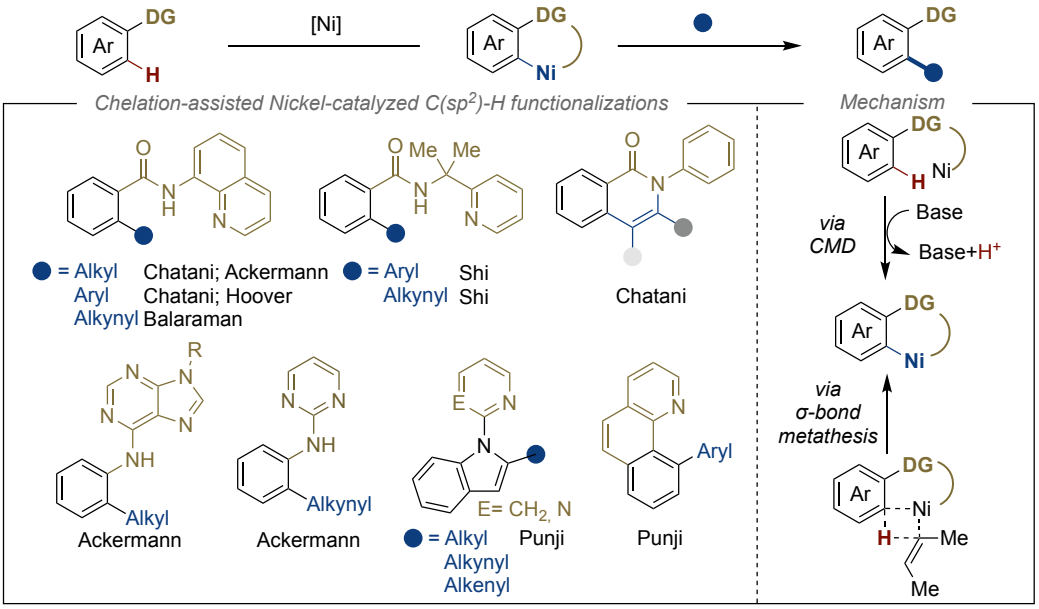

Scheme 1.6 Chelation-assisted Ni-catalyzed C(sp^2)–H functionalization.

From a both conceptual and chemical standpoint, the functionalization of C(sp^3)–H bonds is considerably more challenging than their C(sp^2)–H congeners. This is due to the fact that sp^3 C–H bonds are less acidic and lack proximal empty low-energy or filled high-energy orbitals that interact with the d electrons of the transition metal. Additionally, we should take into consideration site-selectivity principles due to the presence of multiple, yet similar, sp^3 C–H bonds, and observation that raises important questions when promoting site-selective C–H functionalization in simple aliphatic hydrocarbon side-chains. Spurred by the successful implementation of directing group methodologies in the sp^2 C–H series, in 2014 Chatani reported a nickel-catalyzed C(sp^3)–H arylation with 8-aminoquinoline as bidentate chelating group, even in presence of free C(sp^2)–H sites (Scheme 1.7).[22] A Ni(II)/Ni(IV) catalytic cycle mechanism was proposed, where a

reversible concerted metalation deprotonation (CMD) event was proposed to drive the targeted C(sp^3)–H functionalization.

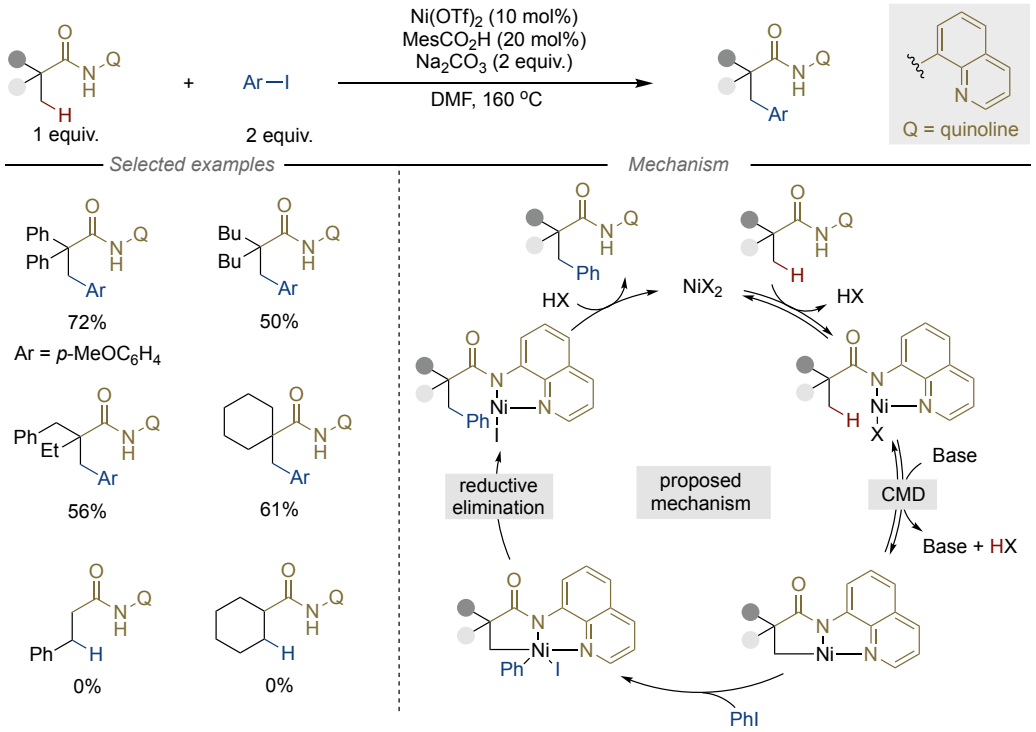

Scheme 1.7 8-Aminoquinoline directed Ni-catalyzed C(sp^3)–H arylation.

Driven by the potential of chelation assistance, the recent years have witnessed the development of a series of C(sp^3)–H alkylation,[23] alkenylation,[24] alkynylation,[25] carbonylation,[26] amination[27] or thiolation[28] events (Scheme 1.8). However, the majority of these endeavors still rely on the utilization of strongly chelating 8-aminoquinoline directing groups, harsh conditions. Unfortunately, these reactions showed a rather limited substrate scope. In addition, a non-negligible number of these protocols occur at terminal methyl C(sp^3)–H bonds possessing a neighboring quaternary carbon center that prevents parasitic β-hydride elimination from occurring.

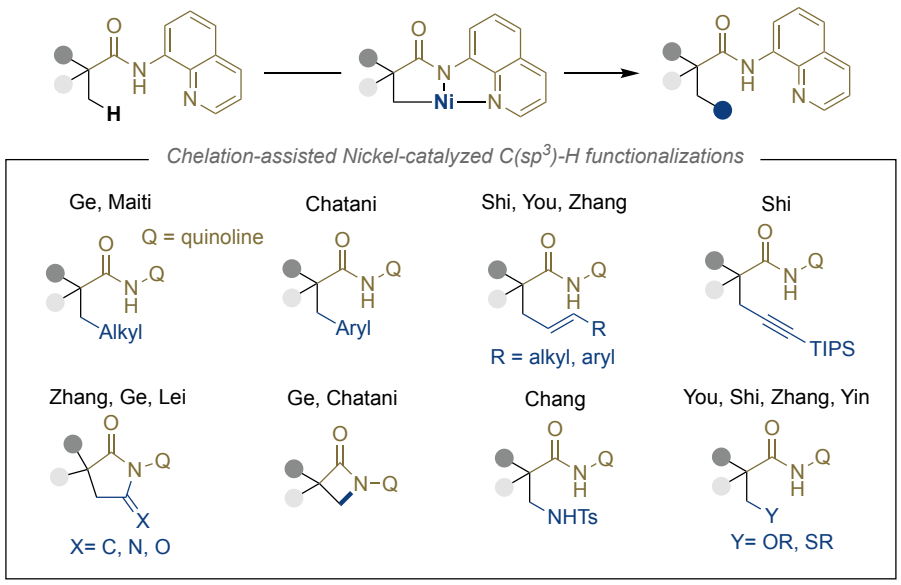

Scheme 1.8 Chelation-assisted Ni-catalyzed C(sp^3)–H functionalization.

1.2.2 Undirected Ni-catalyzed Functionalization of C(sp^2)–H Bonds

In 2004, Cavell described a Ni-catalyzed C–H alkylation of imidazolium salts with simple olefins in the absence of directing groups (Scheme 1.9).[29] This protocol is believed to proceed via oxidative addition of a particularly acidic C(sp^2)–H bond to a low-valent Ni complex in the presence of PPh_3 as ligand, resulting in a Ni(II)–H species that undergoes a migratory insertion into the alkene.

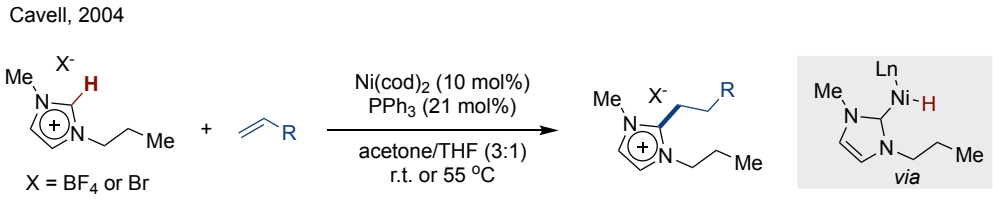

Scheme 1.9 Ni-catalyzed C(sp^2)–H alkylation of imidazolium salts.

In the subsequent years, Hiyama, Itami, Miura or Ackermann, among many others, showed the implementation of a series of C(sp^3)–H alkylations,[30] arylations,[31] alkenylations,[32] alkynylations[33] and borylations[34] of acidic C(sp^2)–H bonds (Scheme 1.10, left).[35] These transformations likely operate via C–H nickelation in the presence of a

strong base. On the other hand, nickel-catalyzed alkylation and alkenylation of neutral C(sp^2)–H bonds have been proposed to proceed via ligand-to-ligand hydrogen transfer (Scheme 1.10, right).[36] As for other Ni-catalyzed C–H functionalizations, however, the majority of these transformations require a specific backbone or proceeds at high temperatures or require harsh reaction conditions.

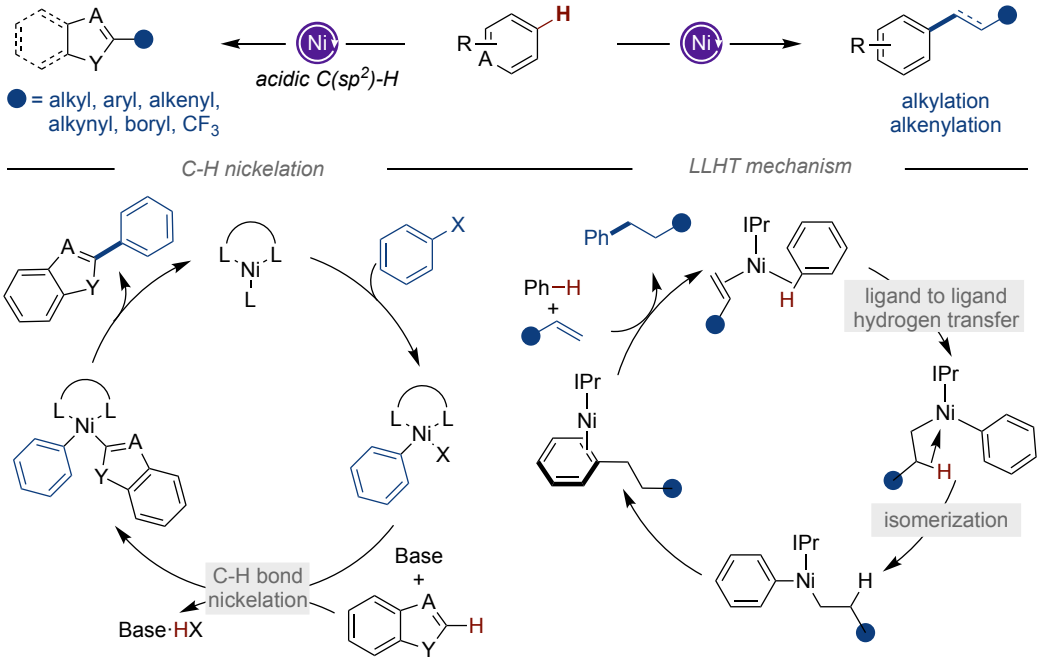

Scheme 1.10 Strategies for undirected Ni-catalyzed C(sp^2)–H functionalization.

1.2.3 Ni-Catalyzed C(sp^3)–H Functionalization via Hydrogen Atom Transfer

Driven by the redox promiscuity of nickel complexes to populate both two- and one-electron pathways, it comes as no surprise that nickel catalysis has successfully been interfaced with open-shell species generated by means of hydrogen-atom transfer (HAT). As shown in Scheme 1.11, Lei and MacMillan independently described a site-selective arylation of C(sp^3)–H bonds via hydrogen-atom transfer enabled by either di-*tert*-butyl peroxide or in the context of a photochemical endeavor.[37] These reactions exhibited a strong preference for promoting the functionalization of C(sp^3)–H bonds adjacent to amino groups.

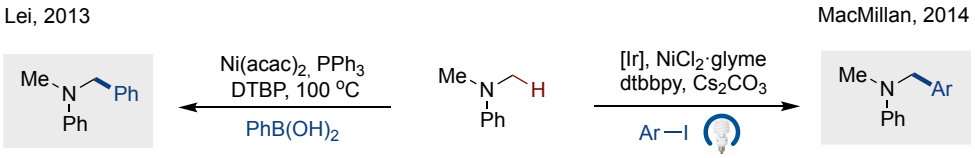

Scheme 1.11 Ni-catalyzed functionalization of α-amino C(sp^3)–H.

Driven by the mild conditions required for enabling photoredox reactions and the flexibility exerted by nickel complexes for bond-formation, dual Ni/photoredox manifolds have offered innovative new grounds for building up complex molecular architectures.[38] Additionally, selective functionalization at δ-C(sp^3)–H sites can be promoted by 1,5-hydrogen atom transfer (HAT) processes.[39] In these endeavors, the utilization of HAT-mediators such as alkoxy radicals,[40] amine radical cations,[41] amidyl radicals,[42] halogens,[43] metal oxo species[44] or triplet carbonyls[45] can facilitate the generation of open-shell species (Scheme 1.12). The resulting nucleophilic carbon-centered radicals can be interfaced by nickel complexes, thus setting the foundation for enabling a formal C(sp^3)–H functionalization in the presence of an appropriate electron acceptor.

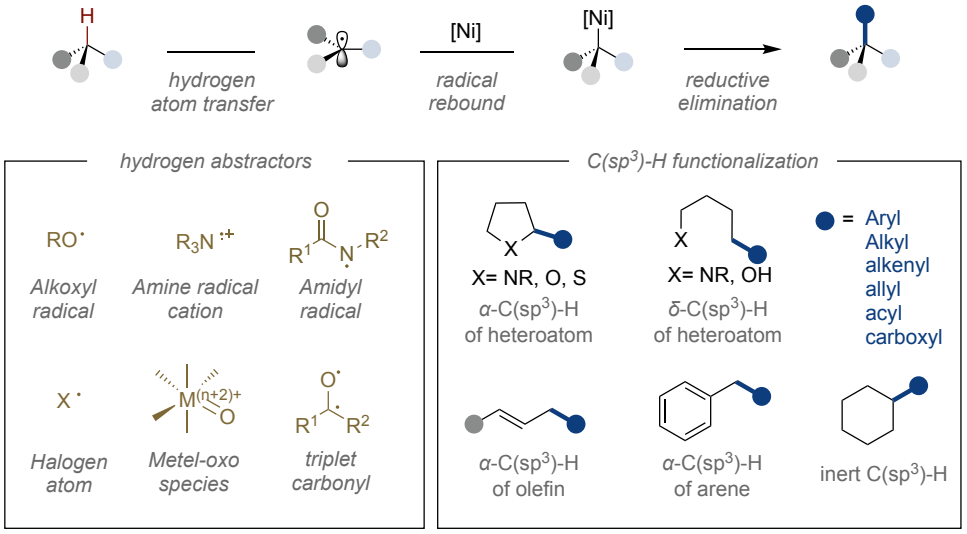

Scheme 1.12 Ni-catalyzed functionalization of C(sp^3)–H via HAT

1.2.4 Ni-Catalyzed C(sp^3)–H Functionalization via Nitrene Transfer

Metal-catalyzed C(sp^3)–H amination can be enabled via nitrene transfer,[46] highly reactive species due to the exceptional electron deficiency at the nitrogen atom. Specifically, singlet nitrenes possess two nonbonding electrons that occupy one p orbital with antiparallel spins, with a remaining empty p orbital that makes singlet nitrenes particularly electrophilic and not particularly stable (Scheme 1.13). On the contrary, triplet nitrenes exhibit two nonbonding electrons that occupy separate p orbitals with parallel spins, giving them a diradical character. This configuration leads to distinct reactivity patterns compared to singlet nitrenes. For example, singlet nitrenes undergo cycloaddition reactions, rearrangements and electrophilic substitutions whereas triplet nitrenes normally are involved in transition-metal catalyzed C–H insertion reactions.[47]

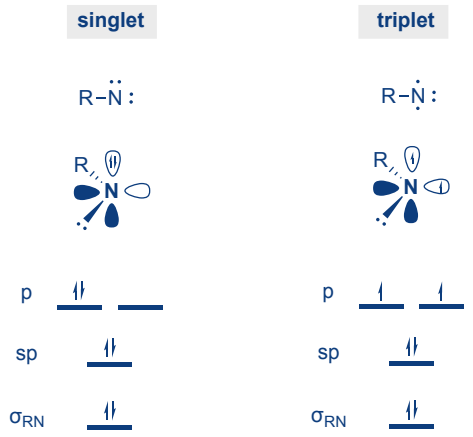

Scheme 1.13 General features of Nitrenes.

In 2001, pioneering work from Hillhouse and co-workers led to isolation of the first imido nickel complex, featuring a nickel-nitrogen double bond and a three-coordination with a bulky bidentate phosphine ligand (Scheme 1.14).[48] The oxidation of arylamido nickel(I), followed by deprotonation, results in the formation of an imido nickel complex that facilitates a cycloaddition event with ethylene.[49] Later on, Hillhouse reported two high valent Ni(III)-imide complexes capable of abstracting hydrogen atoms from ether an ethereal solvent or the hydrogen donor *n*-BuSnH. On the other hand, Warren and co-

workers described a high valent nickel(III)-imide complex–[Me$_3$NN]Ni=NAd, generated from the reaction of Ni(I) and an azide in 2005.[50] Additional studies in 2011 showed the viability for enabling stochiometric C(sp^3)–H amination of [Me$_3$NN]Ni=NAd species with benzylic C–H precursors via hydrogen atom abstraction (HAA) and radical bound processes.[51]

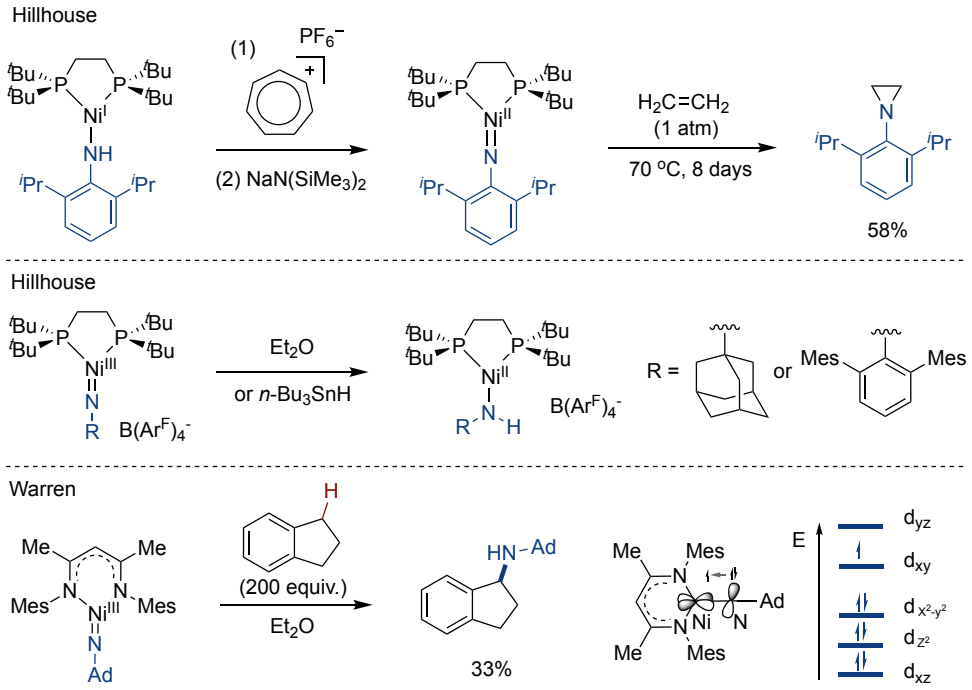

Scheme 1.14 Imido nickel complexes and their reactivities.

Driven by the potential of nickel-catalyzed nitrene transfer for forging C(sp^3)–N linkages, in 2020 Betley described the utilization of a dipyrrin-supported monovalent nickel catalyst. This combination enabled an intramolecular C–H amination of aliphatic azides en route to a variety of pyrrolidines through the cleavage of primary, secondary, or tertiary C(sp^3)–H bonds (Scheme 1.15).[52] Mechanistic studies suggested the involvement of a nickel-nitrenoid, which facilitates intramolecular δ-hydrogen atom abstraction via a six-membered transition state.[53] A subsequent radical recombination ultimately delivered the desired pyrrolidine. However, the requirement for tertiary alkyl azides to prevent facile

β-hydride elimination, along with the use of expensive benzene-d_6 underscores the necessity for designing more practical and accessible C(sp^3)–H amination protocols.

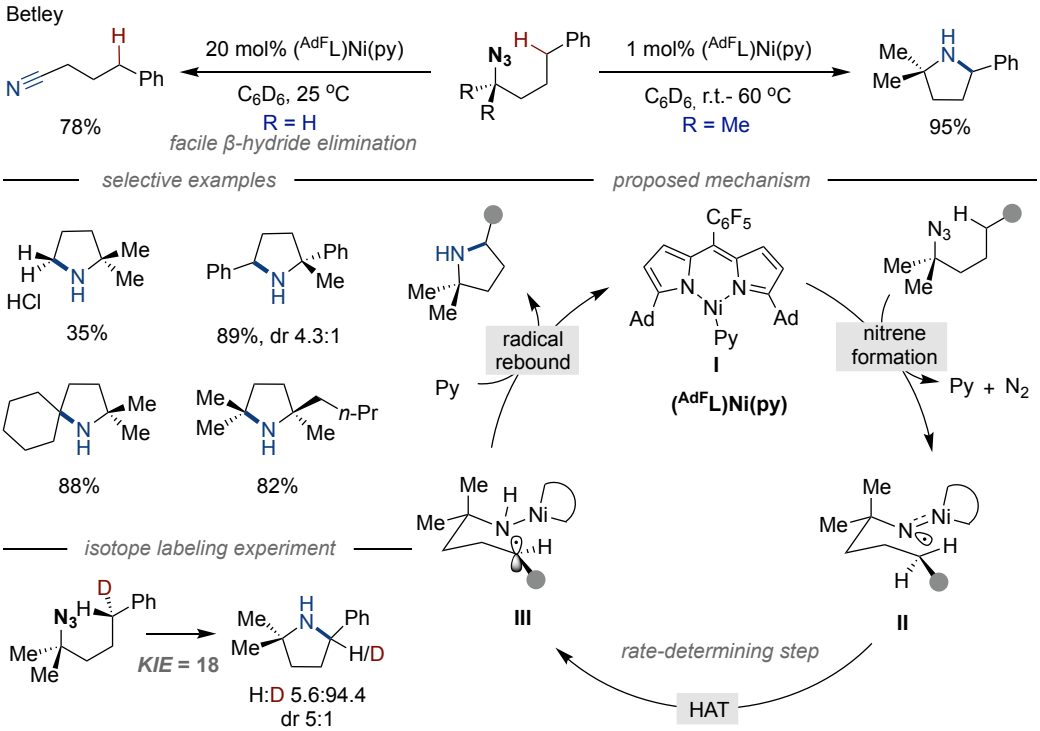

Scheme 1.15 Ni-catalyzed intramolecular C(sp^3)–H amination of aliphatic azides.

1.2.5 Catalytic Functionalization of C–H bonds via Ni Migration

Although significant advances have been realized in Ni-catalyzed C(sp^2)–H functionalization through chelation assistance or by targeting substrates possessing acidic C(sp^2)–H linkages, the recent years have witnessed the functionalization of unreactive C(sp^2)–H bonds distal from the initial reactive functional group via nickel migration. In 2020, our group disclosed a remote, regioselective C(sp^2)–H carboxylation protocol through 1,4-nickel shift from vinyl to aryl moieties, enabling incorporation of CO_2 at C(sp^2)–H sites (Scheme 1.16).[54] In a later collaboration with Zhu, this 1,4-nickel shift strategy could be extended beyond CO_2, allowing to promote an ipso/ortho-difunctionalization of aryl bromides with alkyl halides and alkyne congeners.[55] In 2023,

this approach was further adapted to a nickel-catalyzed 1,4-shift with N_2O as coupling partner, thus facilitating the formation of either carbonyl or phenol derivatives.[56]

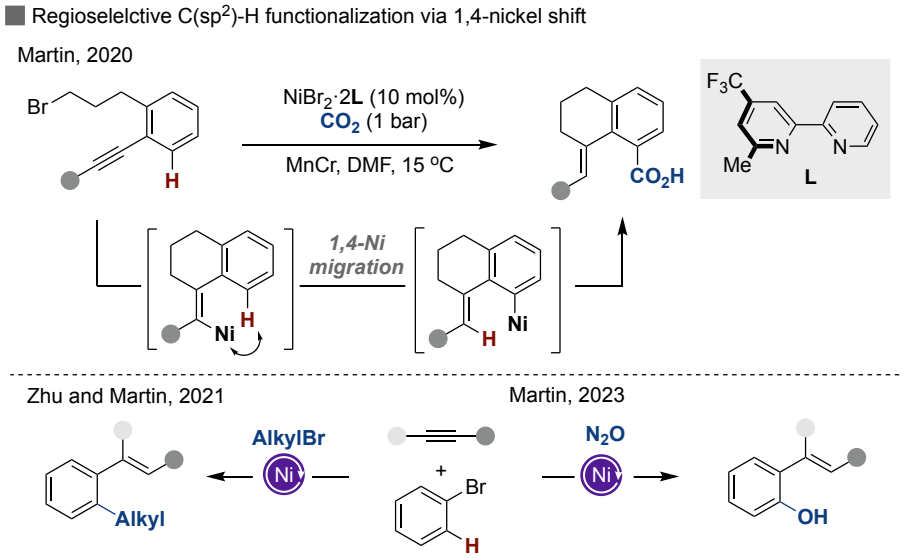

Scheme 1.16 Remote C(sp^2)–H functionalization via nickel-1,4 migration.

More recently, our group explored the utilization of Ni–Ni species as a new manifold to enable distal C(sp^2)–H arylation of aryl pivalates through nickel translocations at arene backbones via a 1,2-hydride shift process (Scheme 1.17).[57]

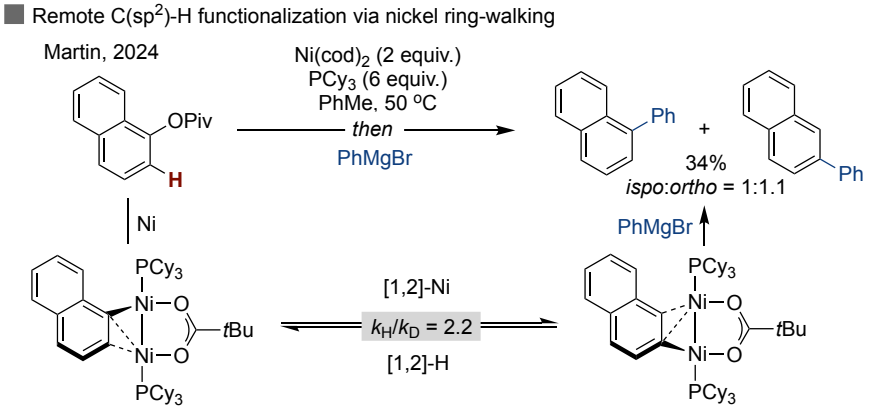

Scheme 1.17 Remote C(sp^2)–H functionalization via Ni ring-walking.

The dynamic displacement of a metal throughout an alkyl chain, coined as "chain-walking", has undoubtedly unlocked new powerful platforms for functionalizing distal C(sp^3)–H bonds[58] through iterative 1,2- or 1,3-hydride shifts along saturated backbones (Scheme 1.18).[59]

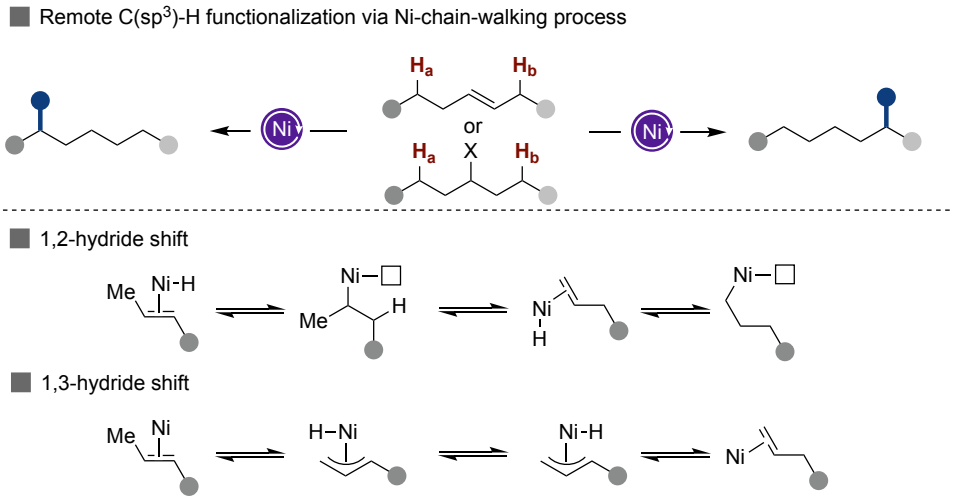

Scheme 1.18 Ni-catalyzed remote C(sp^3)–H functionalization.

In recent years, a variety of reactions have been accomplished by controlling the motion at which the nickel catalyst is translocated along the hydrocarbon side chain.[60] For example, as illustrated in Scheme 1.19, site-selective functionalization of C–H bonds adjacent to arenes,[61] boron atoms, or heteroatoms[62] have been implemented, with site-selectivity dictated by the stability of neighboring groups. On the other hand, the kinetic preference for terminal primary C(sp^3)–H sites could be demonstrated by independent disclosures from our group and Zhu.[63] More recently, significant advances have shown that chain-walking events can be interrupted to override thermodynamic and steric considerations by using thioethers, ketimines, or amides as directing groups through five- or six-membered nickelacycles, thus enabling the functionalization of otherwise inaccessible, yet unactivated methylene C(sp^3)–H bonds.[64]

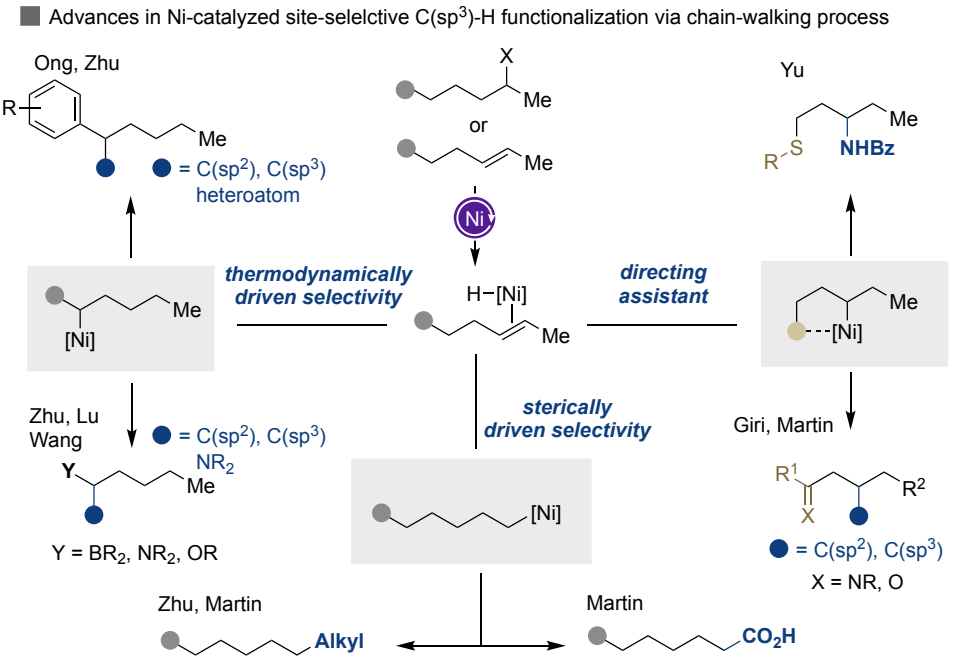

Scheme 1.19 Selected examples for C(sp^3)–H functionalization via Ni chain-walking.

1.3 Nickel-Catalyzed Functionalization of Olefins

Olefins are present in a variety of commodity chemicals and bioactive molecules.[65] Not surprisingly, their site-selective functionalization has prompted chemists to come up with new protocols to be applied at late-stages.[66] Among these, particularly attractive are recent catalytic methods that form polyethylene,[67] Wacker oxidation that convert olefins into ketones,[68] hydroboration-oxidation reactions give rise to alcohols in an anti-Markovnikov pattern[69] or Heck-type reaction that offer the possibility to forge new C–C bonds under mild conditions.[70] On the other hand, olefin metathesis facilitates the formation of new C=C bonds, a reaction that has been rapidly adopted in material science and drug discovery.[71]

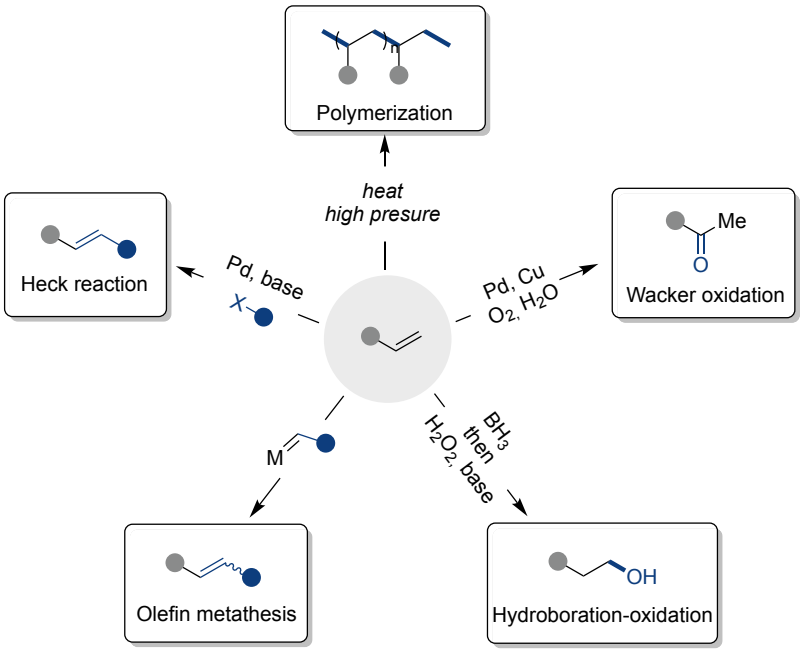

Scheme 1.20 Advances in catalytic functionalization of olefin feedstocks.

1.3.1 Ni-Catalyzed Hydrofunctionalization of Olefins

Driven by nickel's strong affinity to unsaturated systems, its low proclivity to promote β-hydride elimination, and the ability to engage in both one-electron or two-electron events, [72] recent years have witnessed a series of nickel-catalyzed hydrofunctionalization of olefins as a new manifold to forge carbon-carbon or carbon-heteroatom sp^3 linkages from simple olefin building blocks. [73] A priori, multiple catalytic cycles might be conceivable, including Ni(I)/Ni(III) or Ni(0)/Ni(II) cycles. As shown in Scheme 1.21, a Ni(I)/Ni(III) regime involves the formation of a nickel-hydride species through σ-bond metathesis or ligand substitution with an appropriate hydride source (left).[74] Sequential nickel-hydride migratory insertion resulted in an alkyl nickel(I) species, facilitating oxidative addition with an appropriate electrophile to form high valent Ni(III) intermediate. A final reductive elimination results in the targeted hydrofunctionalized product and recovers back the propagating Ni(I) catalyst. On the other hand, a mechanism involving a Ni(0)/Ni(II) could be initiated by direct oxidative addition of an acidic R-H bond with low-valent Ni(0) to yield Ni(II) intermediate,[75] followed by migratory insertion into the olefin, and reductive elimination. In some cases, ligand exchange or transmetalation at Ni(II) intermediate are required to form the targeted products.[76]

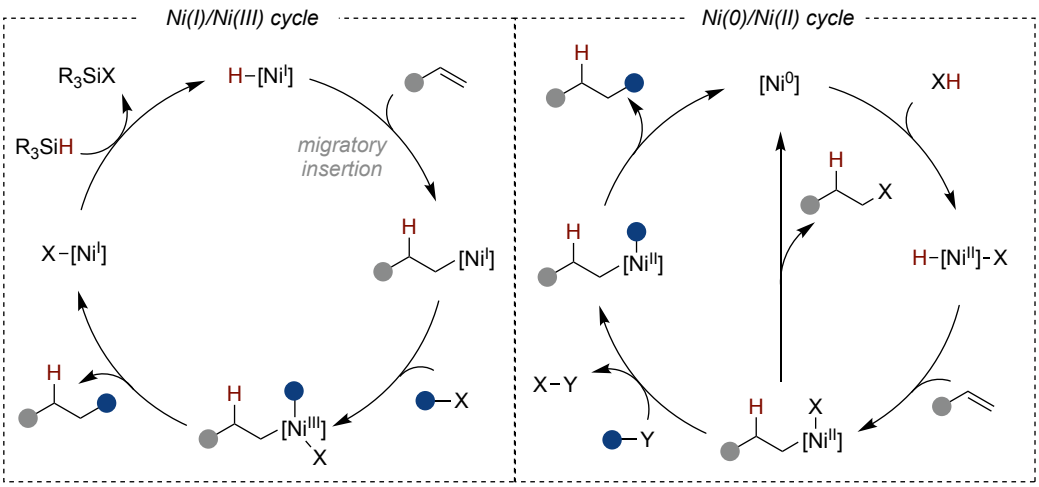

Scheme 1.21 Strategies for Ni-catalyzed hydrofunctionalization of olefins.

In 2016, Fu and co-workers disclosed a nickel-catalyzed hydrofunctionalization of unactivated olefins with alkyl and aryl (pseudo) halides and a silane as hydride source (Scheme 1.22).[77] Notably, the utilization of a 2,2'-bipyridine ligand was critical for forging C(sp^3)–C(sp^3) and C(sp^3)–C(sp^2) bonds at terminal positions with exclusive anti-Markovnikov selectivities. The transformation could even be conducted in the presence of bis(pinacolato)diborons, aromatic rings, esters, and ethers, which might a priori interfere with a competing nickel chain-walking.

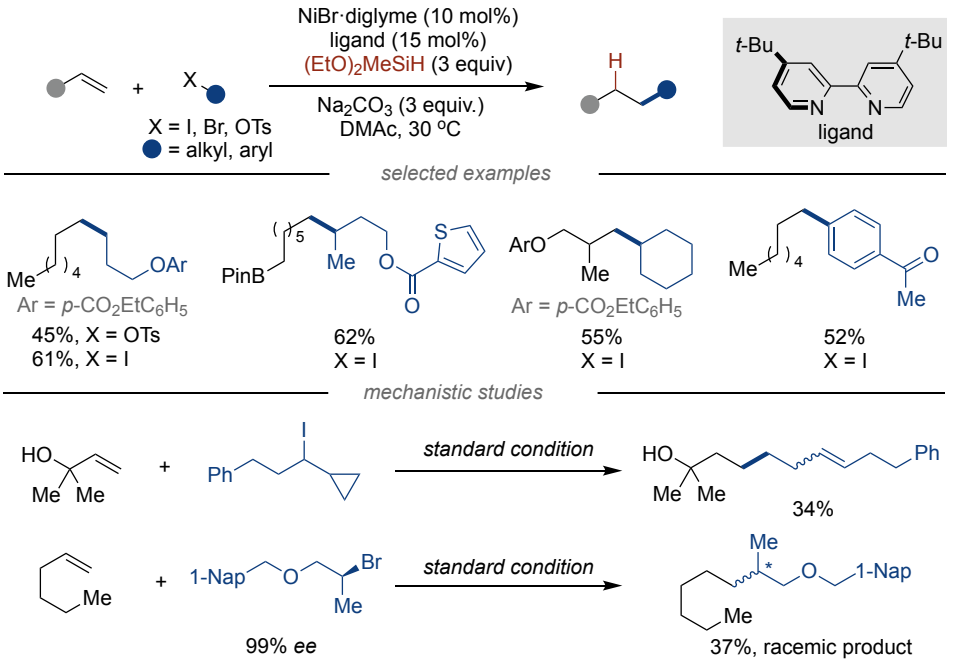

Scheme 1.22 Ni-catalyzed hydroalkylation of unactivated olefins.

In 2017, Martin and co-workers disclosed a nickel catalyzed carboxylation of olefins with CO_2 using water as the hydride source, leading to a variety of carboxylic acids including Ibuprofen (Scheme 1.23).[78] The reaction is distinguished by a site-selectivity pattern that results in anti-Markovnikov selectivity for unactivated olefins or Markovnikov selectivity for styrenes, respectively. Notably, internal olefins also could be subjected to this protocol, yielding linear aliphatic acids via nickel chain-walking processes with equal ease (left).

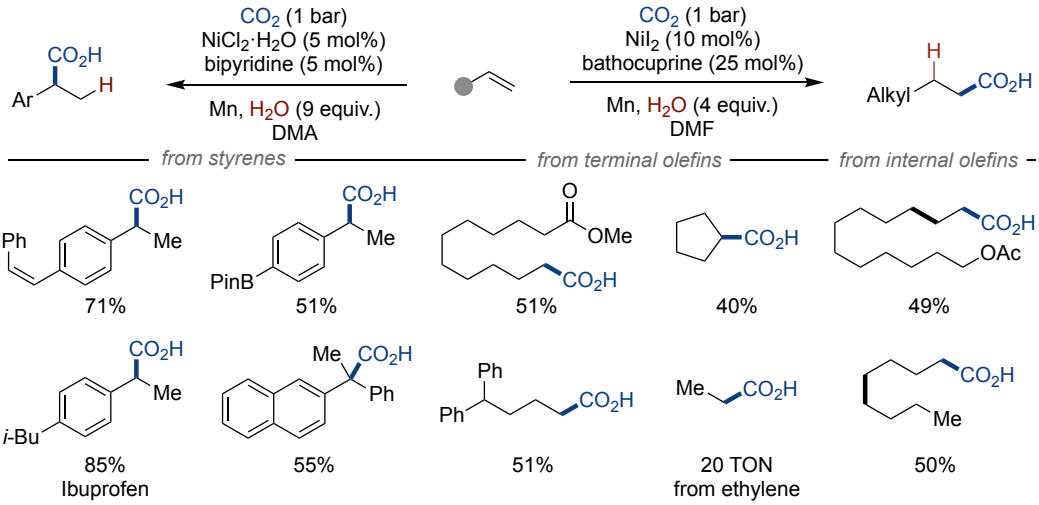

Scheme 1.23 Ni-catalyzed hydrocarboxylation of olefins.

In recent years, metal-hydride hydrogen atom transfer (MHAT) reactions have expanded the range of transformations from simple olefins, providing access to products with Markovnikov selectivity.[79] For example, in 2016 Shenvi and co-workers described that the combination of cobalt and nickel catalysis enables a Markovnikov-selective hydroaylation of terminal olefins with aryl iodides (Scheme 1.24).[80] Mechanistic studies indicated that the reaction was initiated by a Co-hydride migratory insertion into the terminal olefin followed by a transmetalation between the Co-alkyl species and a high-valent nickel intermediate. The resulted Ni-alkyl intermediate undergoes reductive elimination, ultimately affording the α-branched product.[81]

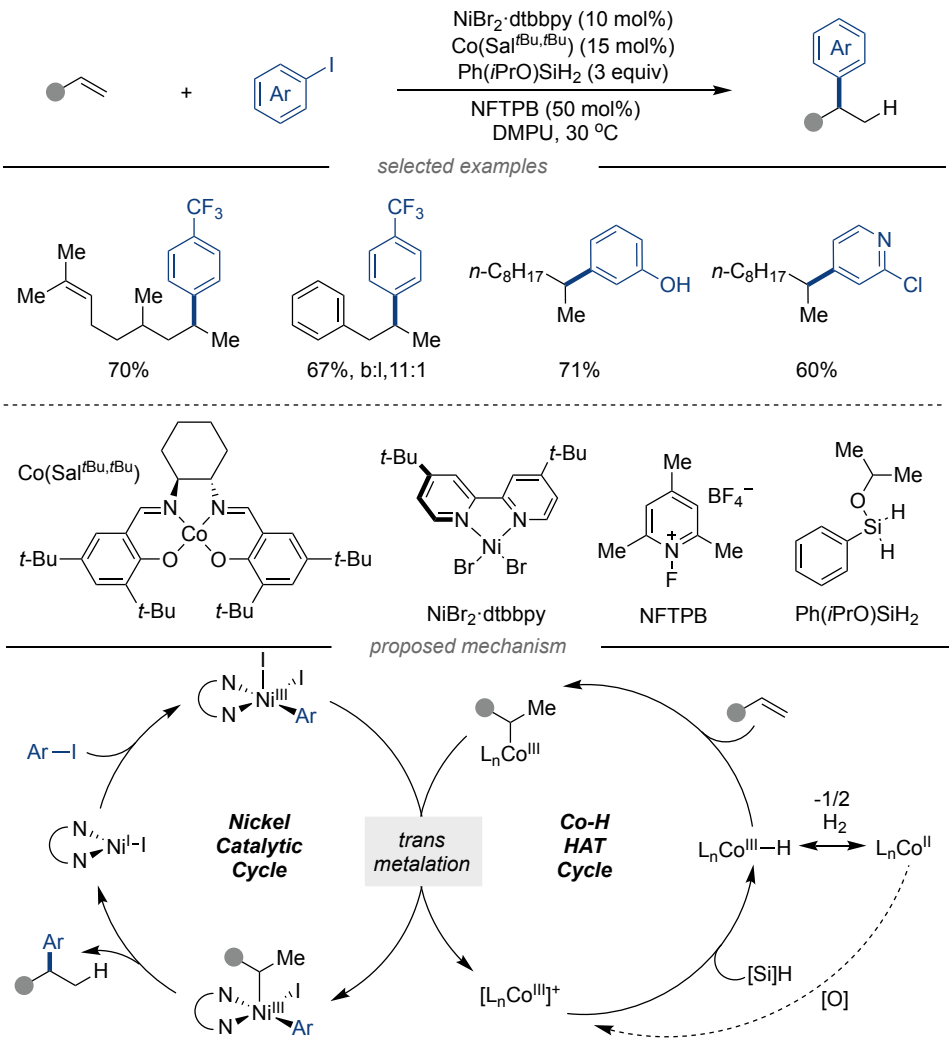

Scheme 1.24 Ni-catalyzed Markovnikov hydrocarboxylation of olefins.

1.3.2 Ni-Catalyzed Difunctionalization of Olefins

Difunctionalization of olefins via cross-coupling with more than two fragments can promote multiple carbon-carbon or carbon-heteroatom bond-formations from simple precursors.[82] Over the last decade, nickel has gained considerable momentum in the catalytic difunctionalization of alkenes via classic two-electron pathways (Scheme 1.25, top). In these endeavors, initial oxidative addition of an electrophile or transmetalation of a nucleophile to the nickel catalyst results in organometallic nickel species that undergoes

migratory insertion with an olefin to afford a metal–alkyl intermediate. On the other hand, nickel catalysts can mediate the formation of radicals from electrophiles and engage in radical processes, leading to different regioselectivity in difunctionalization of olefins compared to that obtained from migratory insertion.[83]

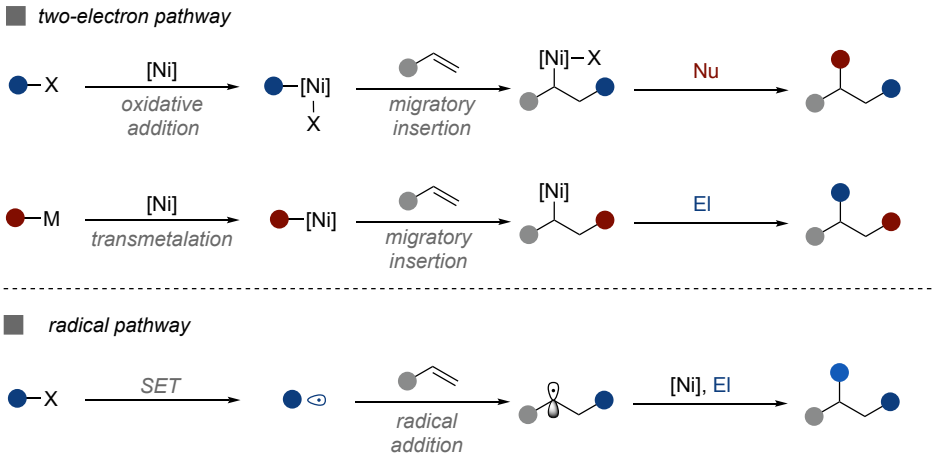

Scheme 1.25 Strategies for Ni-catalyzed difunctionalization of olefins.

In 2018, Brown and co-workers disclosed a 1,2-diarylation of styrenes enabled by nickel catalysis, which featured high chemoselectivity by employing aryl boron reagents and aryl bromides as counterparts (Scheme 1.26).[84] The proposed mechanism involves an oxidative addition of the aryl bromide to Ni(0), and the resulting Ni(II) intermediate undergoes a subsequent migratory insertion into the styrene to form a benzyl-Ni complex. Sequential transmetalation with the aryl boron reagent ultimately facilitates a reductive elimination event, thus resulting in a formal 1,2–diarylation of styrene.

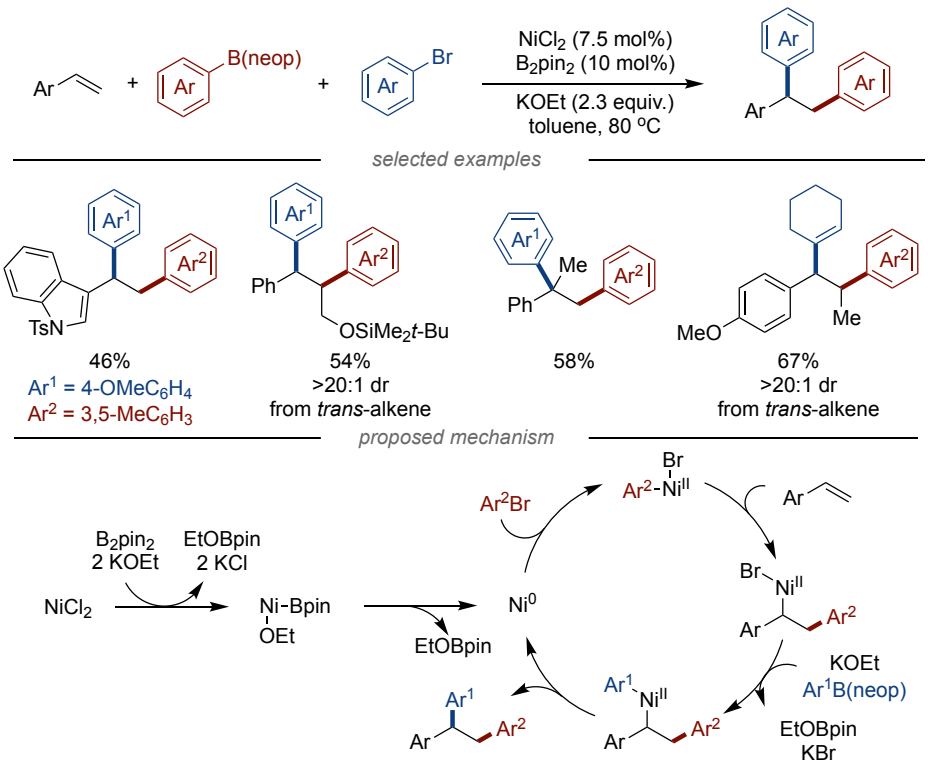

Scheme 1.26 Ni-catalyzed 1,2-diarylation of styrenes.

In 2019, Yin and co-workers discovered that the utilization of an unusual pyridyl carboxamide ligand enables regioselective 1,1-alkylboration of olefins using B_2pin_2 and benzyl halides as coupling partners in the presence of a nickel catalyst (Scheme 1.27).[85] The reaction was characterized by a broad substrate scope, even when utilizing internal olefins. Mechanistic studies suggested an initial transmetalation en route to Ni-Bpin species followed by a migratory insertion with olefin that results in an alkyl nickel intermediate. Notably, facile β-hydride elimination and a migratory insertion sequence leads to a 1,1-boryl nickel species. The site-selectivity is probably dictated by π-back bonding between the nickel and an empty p-orbital of the adjacent boron atom. This was further evidenced by the exclusive 1,1-difunctionlization of olefins bearing an amide group, and a 6:1 regioisomeric ratio in alkylboration of allyl benzene.

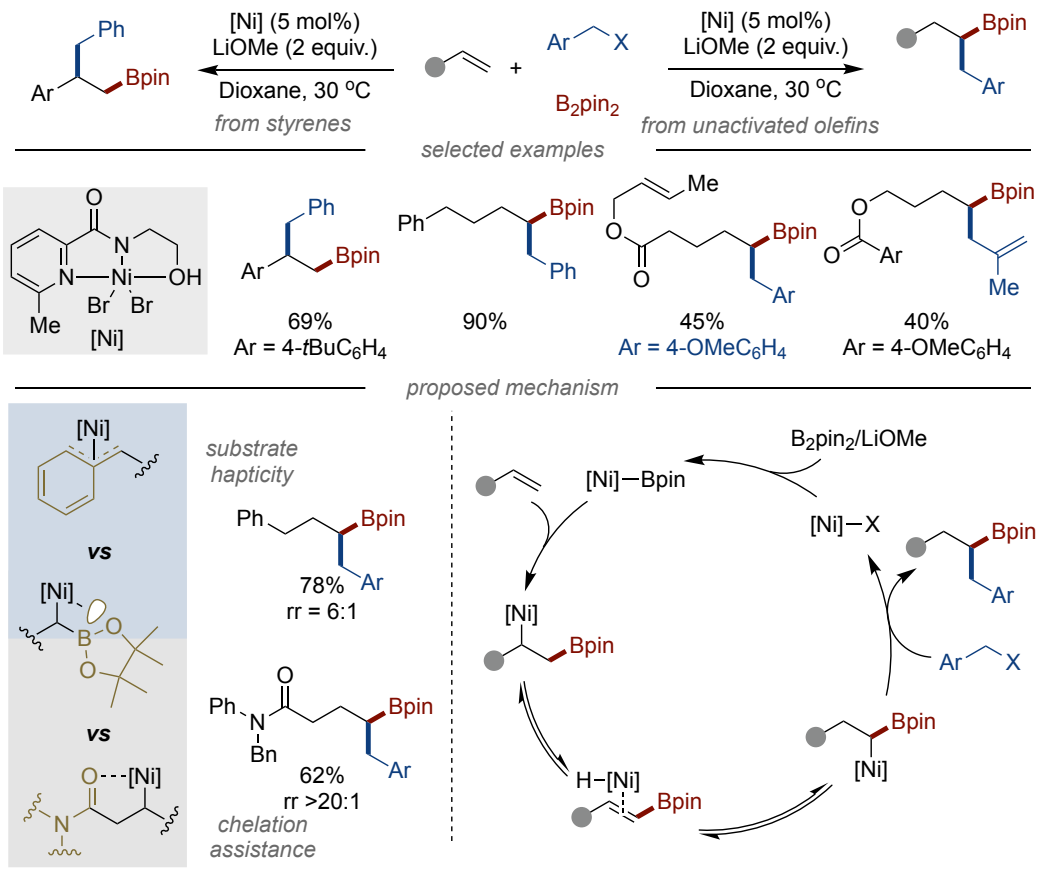

Scheme 1.27 Ni-catalyzed alkylboration of olefins.

In 2018, Nevado described a nickel-catalyzed reductive coupling of olefins, aryl iodides, and alkyl iodides, resulting in a neat 1,2-difunctionalization that forges C(sp^3)-C(sp^3) and C(sp^3)-C(sp^2) bonds in a formal cross-electrophile endeavor (Scheme 1.28).[86] Success is driven by to utilization of tetrakis(dimethylamino)ethylene (TDAE) as organic reductant, which can promote the reduction from Ni(II) to Ni(0). The latter species undergo oxidative addition with the aryl bromide, resulting in the aryl-Ni intermediate. In parallel, a single-electron reduction of alkyl iodide by Ni(I) results in an alkyl radical that adds across the double bond to generate a new open-shell intermediate. The latter can be interfaced with an aryl-Ni intermediate, leading to a high-valent Ni complex that

facilitates reductive elimination, ultimately affording the dicarbofunctionalized product while regenerating the propagating Ni(I) species.

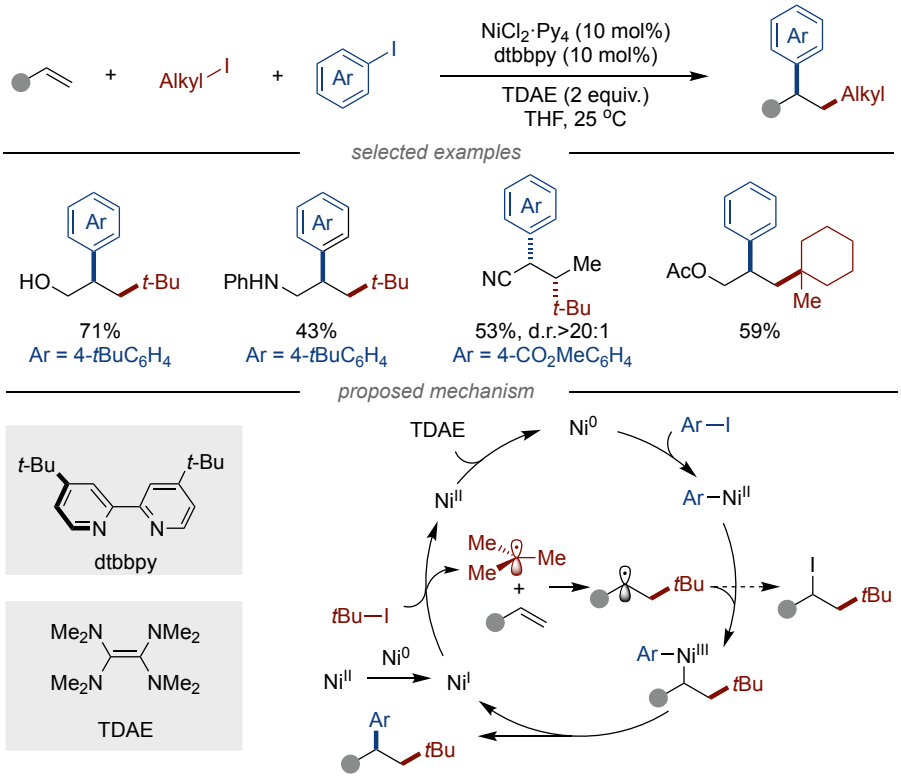

Scheme 1.28 Ni-catalyzed 1,2-dicarbonylation of unactivated olefins.

.

1.4 General Aim of the Thesis

Over the last two decades, nickel catalysis has emerged as a powerful platform for forging sp^3-hybridized architectures via functionalization of C(sp^3)–H bonds or by harnessing the potential of olefins as latent sp^3 nucleophiles. Although remarkable advances have been realized, efficient and reliable construction of sp^3-hybridized carbon-heteroatom linkages still constitutes a challenge in synthetic endeavors. As part of our group's interests in nickel-catalyzed cross-couplings, this thesis has the following objectives:

1. To develop a site-selective intermolecular amidation of C(sp^3)–H bonds via nickel-catalyzed nitrene transfer, offering a new platform for forging C(sp^3)–N bond from ubiquitous C–H linkages under mild conditions.
2. To develop a nickel catalyzed hydroamidation of glycals, enabling access to either α- or β-*N*-glycosides through stereodivergent C(sp^3)-N bond-formations.
3. To promote a predictable site-selective remote C(sp^3)–H functionalization of aliphatic amines, providing a new gateway for forging advanced nitrogen-containing sp^3 architectures.

1.5 References

[1] D. G. E. Kerfoot, Nickel. In Ullmann's Encyclopedia of Industrial Chemistry, (Ed.). **2000**.

[2] Selected reviews: a) J. Diccianni, T. Diao, *Trends Chem.* **2019**, 1, 830; b) J. Diccianni, Q. Lin, T. Diao, *Acc. Chem. Res.* **2020**, 53, 906.

[3] C. Massera, G. Frenking, *Organometallics*, **2003**, 22, 2758–2765.

[4] Selected reviews: a) S. Z. Tasker, E. A. Standley, T. F. Jamison, *Nature* **2014**, *509*, 299; b) K. E. Poremba, S. E. Dibrell, S. E. Reisman, *ACS Catal.* **2020**, *10*, 8237.

[5] Selected reviews: a) Ranjan JanaTejas P. PathakMatthew S. Sigman, *Chem. Rev.* **2011**, *111*, 1417; b) J. Choi, G. C. Fu, *Science* **2017**, *356*, 152.

[6] C. C. C. Johansson Seechurn, M. O. Kitching, T. J. Colacot, V. Snieckus, *Angew. Chem. Int. Ed.* **2012**, *51*, 5062.

[7] Selected reviews: a) T. Rogge, N. Kaplaneris, N. Chatani, J. Kim, S. Chang, B. Punji, L. L. Schafer, D. G. Musaev, J. Wencel-Delord, C. A. Roberts, R. Sarpong, Z. E. Wilson, M. A. Brimble, M. J. Johansson, L. Ackermann, *Nat. Rev. Methods Primers* **2021**, *1*, 43; b) D. L. Golden, S.-E. Suh, S. S. Stahl, *Nat. Rev. Chem.* **2022**, *6*, 405; c) C. Zhang, Z.-L. Li, Q.-S. Gu, X.-Y. Liu, *Nat. Commun.* **2021**, *12*, 475; d) T. G. Saint-Denis, R. Y. Zhu, G. Chen, Q. F. Wu, J. Q. Yu, *Science.* **2018**, *359*, eaao4798; e) H. M. L. Davies, J. R. Manning, *Nature* **2008**, *451*, 417.

[8] L. Guillemard, N. Kaplaneris, L. Ackermann, M. J. Johansson, *Nat. Rev. Chem.* **2021**, *5*, 522.

[9] S. J. Blanksby, G. B. Ellison, *Acc. Chem. Res.* **2003**, *36*, 255.

[10] Selected reviews: a) S. M. Khake, N. Chatani, *Chem*. **2020**, *6*, 1056; b) C. E. Johnson, S. Li, R. Arora, B Mirabi, M. Lautens, *Synlett.* **2024**; *35*, 851.

[11] J. P. Kleiman, M. Dubeck, *J. Am. Chem. Soc.* **1963**, *85*, 1544.

[12] Selected reviews: a) Parthasarathy Gandeepan, Thomas Müller, Daniel Zell, Gianpiero Cera, Svenja Warratz, Lutz Ackermann, *Chem. Rev.* **2019**, *119*, 2192; b) J. H. Docherty,

T. M. Lister, G. Mcarthur, M. T. Findlay, P. Domingo-Legarda, J. Kenyon, S. Choudhary, I. Larrosa, *Chem. Rev.* **2023**, *123*, 7692.

[13] H. Shiota, Y. Ano, Y. Aihara, Y. Fukumoto, N. Chatani, *J. Am. Chem. Soc.* **2011**, 133, 14952.

[14] H. M. Omer, P. Liu, *ACS Omega* **2019**, *4*, 5209.

[15] Selected review: a) S. M. Khake, N. Chatani, *Trends Chem.* **2019**, *1*, 524; b) Y.-H. Liu, Y.-N. Xia, B.-F. Shi, *Chin. J. Chem.* **2020**, *38*, 635.

[16] Y. Aihara, N. Chatani, *J. Am. Chem. Soc.* **2013**, 135, 5308. W. Song, S. Lackner, L. Ackermann, *Angew. Chem. Int. Ed.* **2014**, *53*, 2477. V. Soni, R. A. Jagtap, R. G. Gonnade, B. Punji, *ACS Catal.* **2016**, *6*, 5666. A. Yokota, Y. Aihara, N. Chatani, *J. Org. Chem*. **2014**, *79*, 11922. V. G. Landge, C. H. Shewale, G. Jaiswal, M. K. Sahoo, S. P. Midya, E. Balaraman, *Catal. Sci. Technol.* **2016**, *6*, 1946.

[17] Y.-J. Liu, Y.-H. Liu, S.-Y. Yan, B.-F. Shi, *Chem. Commun.* **2015**, *51*, 6388; S. Zhao, B. Liu, B.-B. Zhan, W.-D. Zhang, B.-F. Shi, *Org. Lett*. **2016**, *18*, 4586. B. Liu, Z.-Z. Zhang, X. Li, B.-F. Shi, *Org. Chem. Front.* **2016**, *3*, 897.

[18] V. Soni, R. A. Jagtap, R. G. Gonnade, B. Punji, *ACS Catal.***2016**, *6*, 5666.

[19] Z. Ruan, S. Lackner, L. Ackermann, *ACS Catal.* **2016**, *6*, 4690.

[20] Z. Ruan, D. Ghorai, G. Zanoni, L. Ackermann, *Chem. Commun*. **2017**, *53*, 9113.

[21] A. Obata, Y. Ano, N. Chatani, *Chem. Sci.* **2017**, *8*, 6650.

[22] Y. Aihara, N. Chatani, *J. Am. Chem. Soc.* **2014**, *136*, 898.

[23] X. Wu, Y. Zhao, H. Ge, *J. Am. Chem. Soc.* **2014**, *136*, 1789.

[24] Y.-J. Liu, Z.-Z. Zhang, S.-Y. Yan, Y.-H. Liu, B.-F. Shi, *Chem. Commun.* **2015**, *51*, 7899.

[25] F.-X. Luo, Z.-C. Cao, H.-W. Zhao, D. Wang, Y.-F. Zhang, Xu, X.; Shi, Z.-J. *Organometallics* **2017**, *36*, 18.

[26] X. Wu, Y. Zhao, H. Ge, *J. Am. Chem. Soc*. **2015**, *137*, 4924–4927.

[27] X. Wu, Y. Zhao, H. Ge, *Chem. Eur. J.* **2014**, *20*, 9530; Y. B. Kim, J. Won, J. Lee, J. Kim, B. Zhou, J.-W. Park, M.-H. Baik, S. Chang, *ACS Catal.* **2021**, *11*, 3067.

[28] X. Ye, J. L. Petersen, X. Shi, *Chem. Commun.* **2015**, *51*, 7863.

[29] N. D. Clement, K. J. Cavell, *Angew. Chem. Int. Ed.* **2004**, *43*, 3845.

[30] Y. Nakao, N. Kashihara, K. S. Kanyiva, T. Hiyama, *J. Am. Chem. Soc.* **2008**, *130*, 16170.

[31] J. Canivet, J. Yamaguchi, I. Ban, K. Itami, *Org. Lett.* **2009**, *11*, 1733.

[32] Y. Nakao, K. S. Kanyiva, S. Oda, T. Hiyama, *J. Am. Chem. Soc.* **2006**, *128*, 8146.

[33] N. Matsuyama, K. Hirano, T. Satoh, M. Miura, *Org. Lett.* **2009**, *11*, 4156.

[34] H. Zhang, S. Hagihara, K. Itami, *Chem. Lett.* **2015**, *44*, 779.

[35] Selected review: S. M. Khake, N. Chatani, *Chem.* **2020**, *6*, 1056.

[36] S. Tang, O. Eisenstein, Y. Nakao, S. Sakaki, *Organometallics* **2017**, *36*, 2716.

[37] a) D. Liu, C. Liu, H. Li, A. W. Lei, *Angew. Chem. Int. Ed.* **2013**, *52*, 4453; b) Z. Zuo, D. T. Ahneman, L. Chu, J. A. Terrett, A. G. Doyle, D. W. C. MacMillan, *Science* **2014**, *345*, 437.

[38] L. Mantry, R. Maayuri, V. Kumar, P. Gandeepan, *Beilstein J. Org. Chem.* **2021**, *17*, 2209.

[39] W.-J. Yue, C. S. Day, R. Martin, *J. Am. Chem. Soc.* **2021**, *143*, 6395.

[40] A. Vasilopoulos, S. W. Krska, S. S. Stahl, *Science* **2021**, *372*, 398.

[41] M. H. Shaw, V. W. Shurtleff, J. A. Terrett, J. D. Cuthbertson, D. W. C. MacMillan, *Science* **2016**, *352*, 1304.

[42] S. M. Thullen, S. M. Treacy, T. Rovis, *J. Am. Chem. Soc.* **2019**, *141*, 14062.

[43] B. J. Shields, A. G. Doyle, *J. Am. Chem. Soc.* **2016**, *138*, 12719.

[44] I. B. Perry, T. F. Brewer, P. J. Sarver, D. M. Schultz, D. A. DiRocco, D. W. C. MacMillan, *Nature* **2018**, *560*, 70.

[45] W.-J. Yue, C. S. Day, R. Martin, *J. Am. Chem. Soc.* **2021**, *143*, 6395.

[46] a) H. M. L. Davies, J. R. Manning, *Nature* **2008**, *451*, 417; b) Y. Park, Y. Kim, S. Chang, *Chem. Rev.* **2017**, *117*, 9247; c) J. L. Roizen, M. E. Harvey, J. Du Bois, *Acc. Chem. Res.* **2012**, *45*, 911; d) M. Ju, J. M. Schomaker, *Nat. Rev. Chem.* **2021**, *5*, 580.

[47] a) G. Dequirez, V. Pons, P. Dauban, *Angew. Chem. Int. Ed.* **2012**, *51*, 7384; b) P. F. Kuijpers, J. Ivar van der Vlugt, S. Schneider, B. de Bruin, *Chem. Eur. J.* **2017**, 23, 13819.

[48] D. J. Mindiola, G. L. Hillhouse, *J. Am. Chem. Soc.* **2001**, *123*, 4623.

[49] R. Waterman, G. L. Hillhouse, *J. Am. Chem. Soc.* **2003**, *125*, 13350.

[50] E. Kogut, H. L. Wiencko, L. Zhang, D. E. Cordeau, T. H. Warren, *J. Am. Chem. Soc.* **2005**, *127*, 11248.

[51] S. Wiese, J. L. McAfee, D. R. Pahls, C. L. McMullin, T. R. Cundari, T. H. Warren, *J. Am. Chem. Soc.* **2012**, *134*, 10114.

[52] a) Y. Dong, J. T. Lukens, R. M. Clarke, S.-L. Zheng, K. M. Lancaster, T. A. Betley, *Chem. Sci.* **2020**, *11*, 1260; b) Y. Dong, R. M. Clarke, G. J. Porter, T. A. Betley, *J. Am. Chem. Soc.* **2020**, *142*, 10996.

[53] Y. Dong, C. J. Lund, G. J. Porter, R. M. Clarke, S.-L. Zheng, T. R. Cundari, T. A. Betley, *J. Am. Chem. Soc.* **2021**, *143*, 817.

[54] M. Börjesson,; D. Janssen-Müller, B. Sahoo, Y. Duan, X. Wang, R. Martin, *J. Am. Chem. Soc.* **2020**, *142*, 20594.

[55] Y. He, M. Börjesson, H. Song, Y. Xue, D. Zeng, R. Martin, S. Zhu, *J. Am. Chem. Soc.* **2021**, *143*, 20064.

[56] H. Zhang, J. Rodrigalvarez, R. Martin, *J. Am. Chem. Soc.* **2023**, *145*, 17564.

[57] C. Odena,; E. Gómez-Bengoa,; R. Martin, *J. Am. Chem. Soc.* **2024**, *146*, 112.

[58] A. Vasseur, J. Bruffaerts, I. Marek, *Nat. Chem.* **2016**, *8*, 209.

[59] a) H. Sommer, F. Juliá-Hernández, R. Martin, I. Marek, *ACS Cent. Sci.* **2018**, *4*, 153; b) S. Ghosh, S. Patela, I. Chatterjee, *Chem. Commun.* **2021**, *57*, 11110.

[60] a) C. Romano, R. Martin, *Nat. Rev. Chem*. **2024**, https://doi.org/10.1038/s41570-024-00649-4; b) J. Rodrigalvarez, F. L. Haut, R. Martin, *JACS Au* **2023**, *3*, 3270; c) Y. Wang, Y. He, S. Zhu, *Acc. Chem. Res.* **2022**, *55*, 3519.

[61] a) W.-C. Lee, C.-H. Wang, Y.-H. Lin, W.-C. Shih, T.-G. Ong, *Org. Lett.* **2013**, *15*, 5358; b) Y. He, Y. Cai, S. Zhu, *J. Am. Chem. Soc.* **2017**, *139*, 1061; c) J. Xiao, Y. He, F. Ye, S. Zhu, *Chem*. **2018**, *4*, 1645; d) Y. Zhang, B. Han, S. Zhu, *Angew. Chem. Int. Ed.* **2019**, *58*, 13860.

[62] a) Y. Zhang, J. Ma, J. Chen, L. Meng, Y. Liang, S. Zhu, *Chem.* **2021**, *7*, 3171; b) J.-W. Wang, D.-G. Liu, Z. Chang, Z. Li, Y. Fu, X. Lu, *Angew. Chem. Int. Ed.* **2022**, *61*, e202205537; c) J-W Wang, Z Li, D Liu, J.-Y. Zhang, X. Lu, Y. Fu, *J. Am. Chem. Soc.* **2023**, *145*, 10411.

[63] a) F. Juliá-Hernández, T. Moragas, J. Cornella, R. Martin, *Nature* **2017**, *545*, 84; b) S. Z. Sun, C. Romano, R. Martin, *J. Am. Chem. Soc.* **2019**, *141*, 16197; c) F. Zhou, J. Zhu, Y. Zhang, S. Zhu, Angew. Chem. Int. Ed. 2018, 57, 4058.

[64] a) P. Basnet, R. K. Dhungana, S. Thapa, B. Shrestha, Shekhar KC, J. M. Sears, R. Giri, *J. Am. Chem. Soc.* **2018**, *140*, 7782; b) B. Du, Y. Ouyang, Q. Chen, W.-Y. Yu, *J. Am. Chem. Soc.* **2021**, *143*, 14962; c) J. Rodrigalvarez, H. Wang, R. Martin, *J. Am. Chem. Soc.* **2023**, *145*, 3869.

[65] a) H. M. Torres Galvis, K. P. de Jong, *ACS Catal.* **2013**, *3*, 2130; b) S. M. Sadrameli, *Fuel* **2015**, *140*, 102.

[66] a) H. Jiang, A. Studer, *Chem. Soc. Rev.* **2020**, 49, 1790; b) S. W. M. Crossley, C. Obradors, R. M. Martinez, R. A. Shenvi, *Chem. Rev.* **2016**, 116, 8912; c) H.-Q. Ni, P. Cooper, K. Engle, *Chem. Commun.* **2021**, *57*, 7610.

[67] P. S. Chum, K. W. Swogger, *Prog. Polym. Sci.* **2008**, *22*, 797.

[68] J. M. Takacs, X. Jiang, *Curr. Org. Chem.* **2003**, *7*, 369.

[69] a) H. C. Brown, Hydroboration, W. A. Benjamin, New York, NY, 1962; b) S. J. Geier, C. M. Vogels, J. A. Melanson, S. A. Westcott, *Chem. Soc. Rev.* **2022**, *51*, 8877.

[70] I. P. Beletskaya, A. V. Cheprakov, *Chem. Rev.* **2000**, *100*, 3009.

[71] a) O. M. Ogba, N. C. Warner, D. J. O'Leary, R. H. Grubbs, *Chem. Soc. Rev.* **2018**, *47*, 4510; b) A. H. Hoveyda, A. R. Zhugralin, *Nature* **2007**, *450*, 243.

[72] a) A. Velasco-Rubio, R. Martin, *Adv. Synth. Catal.* **2023**, *365*, 1; b) J. Derosa, O. Apolinar, T. Kang, V. T. Tran, K. M. Engle, *Chem. Sci.*, **2020**, *11*, 4287; c) X.-Y. Sun, B.-Y. Yao, B. Xuan, L.-J. Xiao, Q.-L. Zhou, *Chem Catal.* **2022**, *2*, 3140.

[73] J. Diccianni, Q. Lin, T. Diao, *Acc. Chem. Res.* **2020**, *53*, 906.

[74] a) N. A. Eberhardt, H. Guan, *Chem. Rev.* **2016**, *116*, 8373; b) Y. Wang, Y. He, S. Zhu, *Acc. Chem. Res.* **2022**, *55*, 3519; c) Z. Zhang, S. Bera, C. Fan, X. Hu, *J. Am. Chem. Soc.* **2022**, 144, 7015; d) Y. K. Mirza, P. S. Bera, S. B. Mohite, *Org. Chem. Front.* **2024**, *11*, 4290.

[75] Y. Nakao, N. Kashihara, K. S. Kanyiva, T. Hiyama, *Angew. Chem. Int. Ed.* **2010**, *49*, 4451.

[76] L. Cheng, M.-M. Li, M.-L. Li, L.-J. Xiao, J.-H. Xie, Q.-L. Zhou, *CCS Chem.* **2021**, *3*, 3260.

[77] X. Lu, B. Xiao, Z. Zhang, T. Gong, W. Su, J. Yi, Y. Fu, L. Liu, *Nat. Commun.* **2016**, *7*, 11129.

[78] M. Gaydou, T. Moragas, F. Juliá-Hernández, R. Martin, *J. Am. Chem. Soc.* **2017**, *139*, 12161.

[79] S. A. Green, S. W. M. Crossley, J. L. M. Matos, S. Vásquez Céspedes, S. L. Shevick, R. A. Shenvi, *Acc. Chem. Res.* **2018**, *51*, 2628.

[80] S. A. Green, J. L. M. Matos, A. Yagi, R. A. Shenvi, *J. Am. Chem. Soc.* **2016**, *138*, 12779.

[81] S. L. Shevick, C. Obradors, R. A. Shenvi, *J. Am. Chem. Soc.* **2018**, *140*, 12056.

[82] a) R. K. Dhungana, S. KC, P. Basnet, R. Giri, *Chem. Rec.* **2018**, *18*, 1314; b) J.-S. Zhang, L. Liu, T. Chen, L. B. Han, *Chem.-Asian J.* **2018**, *13*, 2277; c) J. Lin, R.-J. Song, M. Hu, J.-H. Li, *Chem. Rec.* **2019**, *19*, 440.

[83] a) X. Qi, T. Diao, *ACS Catal.* **2020**, *10*, 8542; b) Y. Li, D. Wu, H. Cheng, G. Yin, *Angew. Chem., Int. Ed.* **2020**, *59*, 7990.

[84] P. Gao, L.-A. Chen, M. K. Brown, *J. Am. Chem. Soc.* **2018**, *140*, 10653.

[85] Y. Li, H. Pang, D. Wu, Z. Li, W. Wang, H. Wei, Y. Fu, G. Yin, *Angew. Chem. Int. Ed*. **2019**, *58*, 8872

[86] A. García-Domínguez, Z. Li, C. Nevado, *J. Am. Chem. Soc.* **2017**, *139*, 6835.

Chapter 2. Nickel-Catalyzed Site-Selective Intermolecular C(sp^3)–H Amidation.

————In collaboration with Hao Wang and Dr. Craig S. Day

2.1 General Introduction

Amines are ubiquitous structures in natural products, pharmaceuticals and materials, among others. A close inspection into the literature data reveals that 82% of the top 200 small molecule prescription medicines by 2022 global sales contain at least an amine moiety or nitrogen-containing heterocycle.[1] These observations challenged chemists to design new catalytic protocols for C–N bond-forming reactions.[2] Thus, a myriad of elegant protocols has been design towards this goal, including the Jordan-Ullmann-Goldberg synthesis, Chan-Lam coupling, and Buchwald-Hartwig amination, among others.[3] On the other hand, conventional strategies consisting of nucleophilic N-alkylation, hydroamination, reductive amination are now essential tools in the synthetic chemist's repertoire for forging more common C(sp^3)–N linkages (Scheme 2.1).[4] However, these transformations often require prefunctionalized coupling partners such as alkyl (pseudo)halides, alkenes, or carbonyls. To this end, the recent years have witnessed direct functionalization of ubiquitous C(sp^3)–H bonds as a new route to rapidly build up C(sp^3)–N architectures,[5] minimizing the number of synthetic manipulations while offering new chemical space to be applied in the context of late-stage modification of advanced ingredients.[6]

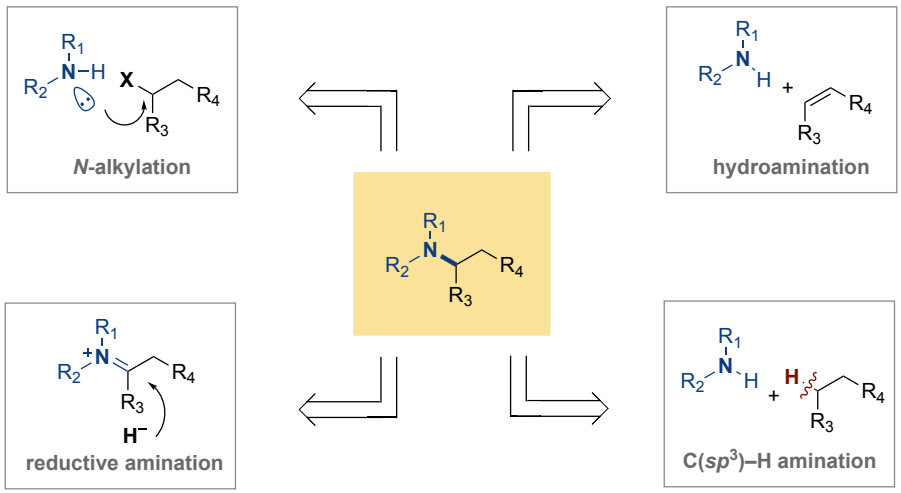

Scheme 2.1 The state-of-art for preparing C(sp^3)–N bonds.

2.1.1 C(sp^3)–H Amination through Oxidative Dehydrogenation

Cross-dehydrogenative coupling reactions have gained considerable momentum for forging carbon-carbon and carbon-heteroatom bonds from C–H linkages.[7] For example, in 2010, Warren and co-workers described a Cu-catalyzed oxidative dehydrogenative amination of alkanes with amines in the presence of stoichiometric peroxide (Scheme 2.2).[8] Notably, the protocol was found to be applicable to both benzylic C(sp^3)–H and unactivated secondary C(sp^3)–H bonds, resulting in secondary and tertiary amines with equal ease. Note, however, that a large excess of hydrocarbon was required for the reaction to occur.

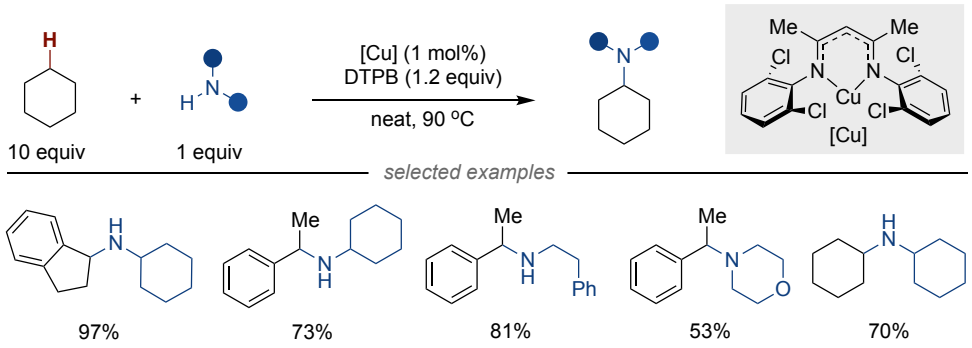

Scheme 2.2 Cu(I)-catalyzed oxidative C(sp^3)–H amination.

In 2017, Soulé and co-workers disclosed that the use of phenanthroline as ligands enabled an efficient amination across a series of primary, secondary, and tertiary C(sp^3)–H bonds via Cu-catalyzed oxidative C(sp^3)–H/N-H coupling approach (Scheme 2.3). Although 1 equivalent of alkane was used as C(sp^3)–H donor, the reaction required harsh reaction conditions.[9] The proposed mechanism involved a hydrogen atom abstraction (HAA) process from alkane by *tert*-butoxy radical. The in situ formed carbon-centered radical was then interfaced with a nitrogen-bound copper intermediate followed by reductive elimination, thus ultimately resulting in the desired amination product.

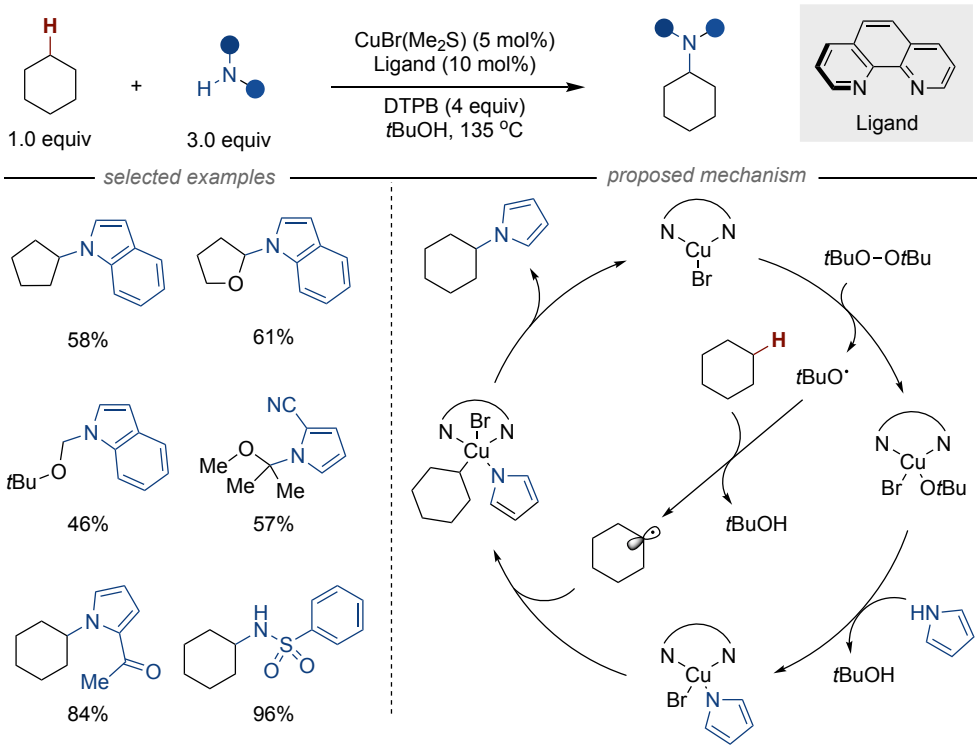

Scheme 2.3 Cu-catalyzed C(sp^3)–H amination via oxidative dehydrogenation.

The acid-induced Ritter-type reaction, which involves conversion of carbocations into the corresponding amides offers a valuable strategy for C–N bond construction.[10] Although most carbocations are typically generated in situ from alcohols, halides, and other electrophilic alkylating reagents, in 2012 Baran and co-workers disclosed a copper-catalyzed intermolecular C(sp^3)–H amination of unactivated hydrocarbons via carbocation intermediates (**Scheme 2.4**).[11] Notably, either secondary or tertiary C(sp^3)–H precursors could be used as limiting reagents and oxidized to the corresponding carbocations in the presence of F-TEDA-PF_6. Reaction with acetonitrile results in nitrilium ion intermediates that generates the aminated products under basic conditions.

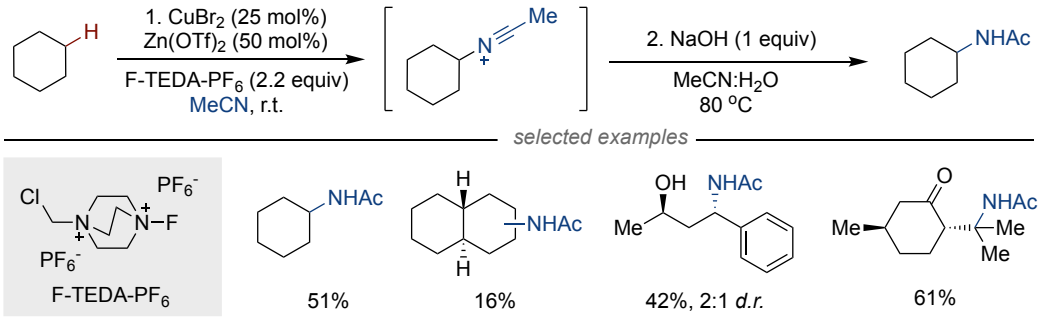

Scheme 2.4 Cu-catalyzed C(sp^3)–H amination via ritter reaction.

2.1.2 C(sp^3)–H Amination via Metal-catalyzed Nitrene Transfer

Prompted by the pioneering work of Smolinsky,[12] Mattingly,[13] and Edwards[14] on the utilization of nitrenes capable of reacting with simple C–H bonds and olefins, modern metal-catalyzed nitrene transfers have emerged as cutting-edge methods to forge C(sp^3)–N linkages.[15] In 2018, White and co-workers explored a manganese-catalyzed intermolecular C(sp^3)–H amination via nitrene insertion, exhibiting exclusive site-selectivity toward benzylic sites (Scheme 2.5).[16] The protocol can be applied to late-stage functionalization of bioactive molecules and natural products with equal ease, with site-selectivity dictated by steric and electronic differentiation among multiple C–H bonds. The proposed mechanism involves the formation of an electrophilic metallonitrene intermediate, which facilitates intermolecular hydrogen-atom transfer with C–H linkages. The resulting benzylic radicals then interact with a nitrogen-bound manganese complex, ultimately resulting in the desired products.

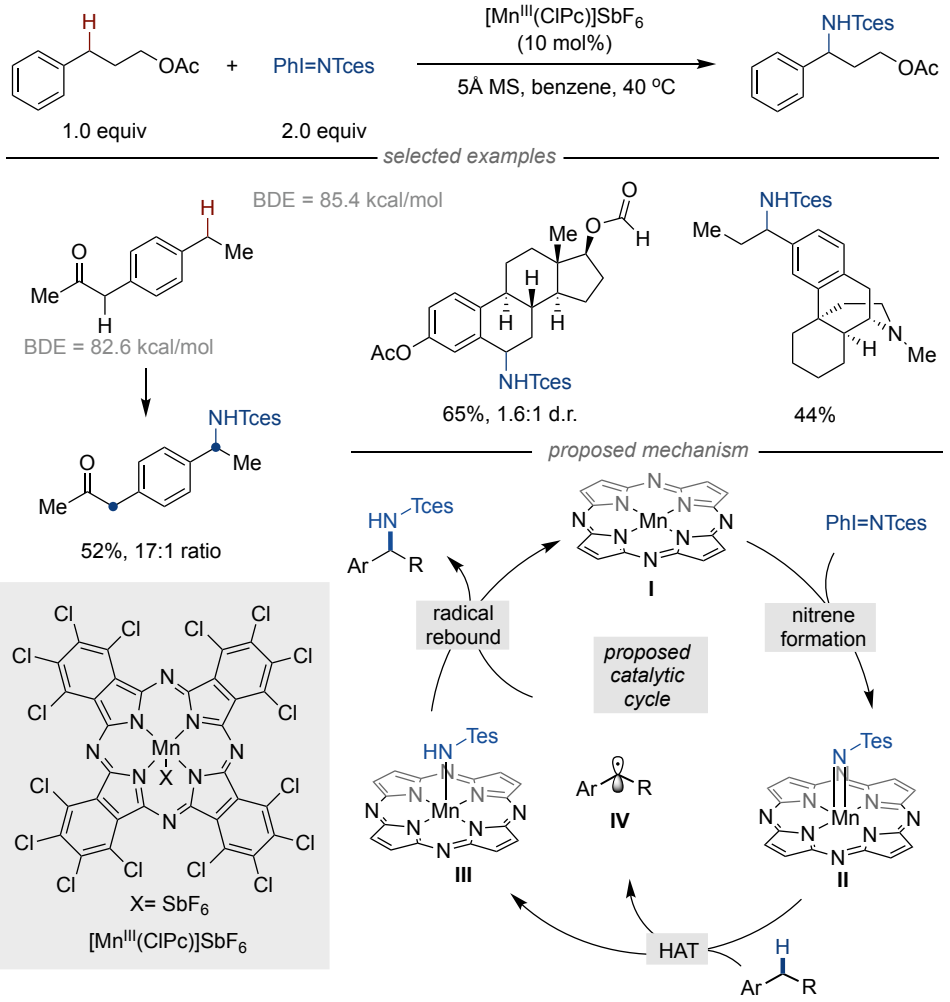

Scheme 2.5 Mn-catalyzed benzylic C(sp^3)–H amination via nitrene insertion.

Driven by their high catalytic efficiency and mild reaction conditions, it is not particularly surprising that enzymatic reactions have offered a complementary approach to enable C−H functionalization.[17] In 2020, Arnold and co-workers[18] reported the use of a P411BPA variant featuring a Ser axial ligand at iron, facilitating C(sp^3)–N bond formation at benzylic and allylic sites with excellent enantioselectivity using readily available hydroxylamines as amine sources (Scheme 2.6). This biocatalytic protocol was also demonstrated to operate with high efficiency and >100 turnover number.

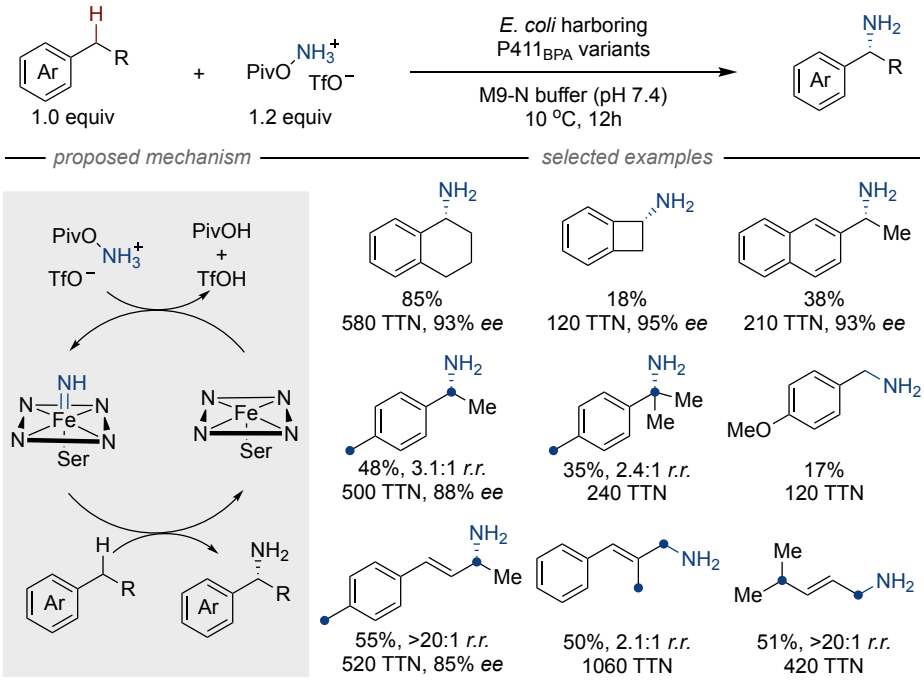

Scheme 2.6. C(sp^3)–H amination enabled by enzymatic nitrene insertion.

Despite the significant advances realized in benzylic and allylic C–N bond formation via nitrene insertion, the means to promote C(sp^3)–H amination beyond activated sites remains particularly challenging due to higher BDEs associated to less-activated C–H bonds, the presence of multiple, yet similar C–H bonds within an alkyl side chain and steric considerations that might hinder the targeted C–N bond-formation (Scheme 2.7).[19]

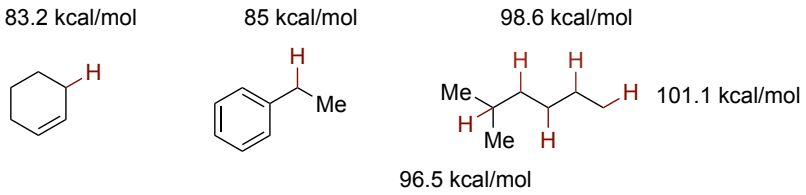

Scheme 2.7 BDEs of C(sp^3)–H bonds.

In 2021, Chang and co-workers demonstrated that electronic modulation of the ligand in cobalt catalyst facilitated the amidation toward sterically less hindered secondary

C(sp^3)–H sites in alkanes (Scheme 2.8).[20] Mechanistic studies revealed that the reaction may proceed via a radical pathway involving a triplet cobalt nitrenoid intermediate.

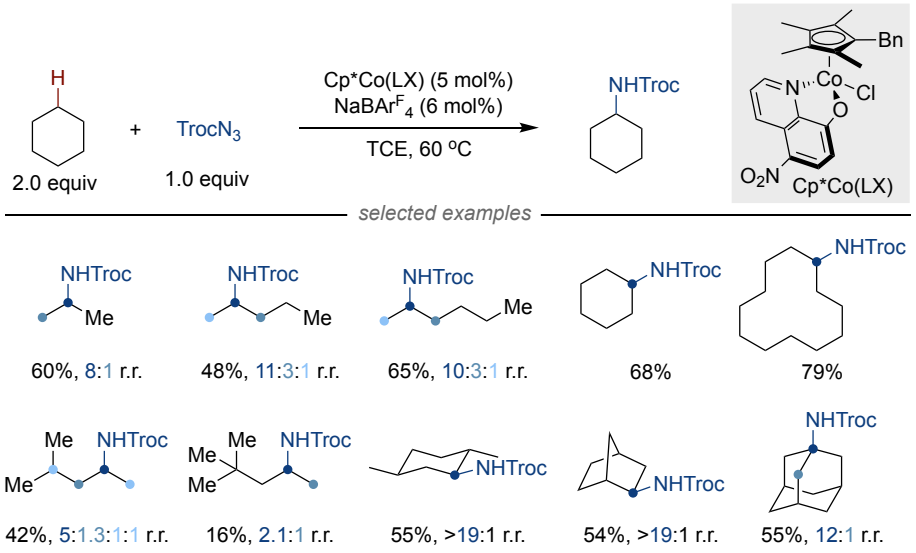

Scheme 2.8 Co-catalyzed amination of unactivated C(sp^3)–H bonds.

Dauban and co-workers in 2021 disclosed the utilization of a Rh_2(*S*-tfpttl)$_4$ catalyst possessing a well-defined catalytic pocket in combination with $TBPhsNH_2$ as amine source as a means to enable amination at tertiary C(sp^3)–H sites. The reaction occurred with excellent site-selectivitites, even in the presence of more reactive benzylic and propargylic sites (Scheme 2.9). [21]

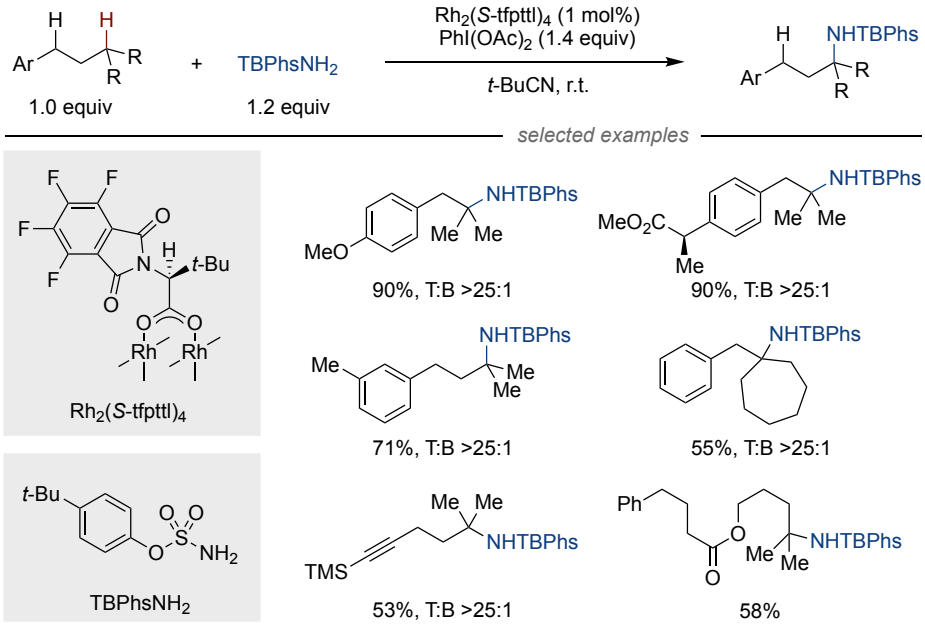

Scheme 2.9. Rh-catalyzed amination of tertiary C(sp^3)–H.

In 2023, Meggers and co-workers disclosed a highly stereocontrolled, iron-catalyzed α-amination of abundant carboxylic acids (**Scheme 2.10**).[22] Notably, the reaction can be extended to bioactive molecules and drugs, even containing activated C(sp^3)–H sites. Mechanistic studies revealed that the process is initiated by nitrene formation in the presence of a base, followed by the coordination with carboxylic acid. This facilitates intramolecular 1,5-HAT of the carboxylic acid-bound iron–nitrenoid species, leading to the formation of an α-carbon radical. The subsequent radical rebound, which serves as the enantio-determining step, ultimately yields the chiral amino acid product.

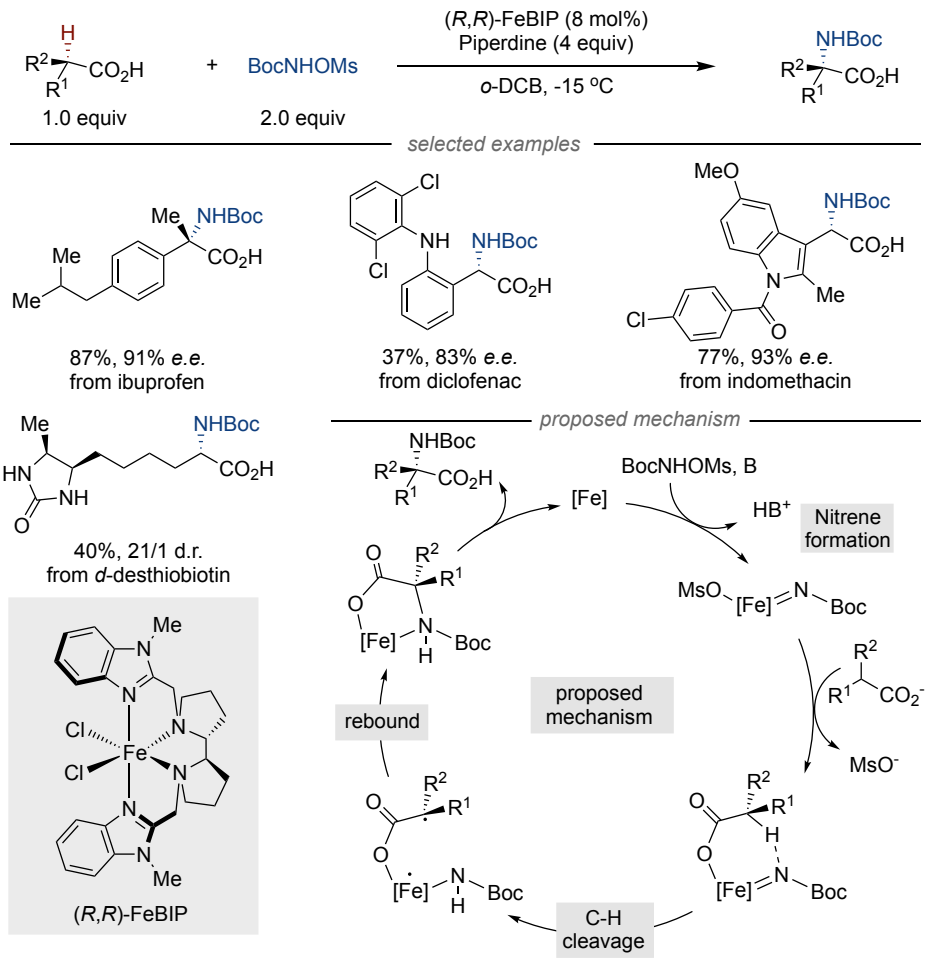

Scheme 2.10 Fe-catalyzed enantioselective C(sp^3)–H amination of carboxylic acids.

2.1.3 Photocatalyzed Intermolecular C(sp^3)–N Bond Formation

Over the past decade, photoredox catalysis has emerged as an innovative tool to rapidly and reliably build up molecular complexity under mild conditions. In particular, photoredox catalysis has been particularly suited for generating high-energy heteroatom-centered radicals that can abstract a hydrogen atom from hydrocarbons en route to sp^3 carbon-centered radicals (Scheme 2.11). These carbon-centered radicals can then add to *N*-based radical acceptors, laying the foundation for a C(sp^3)–N bond formation.[23]

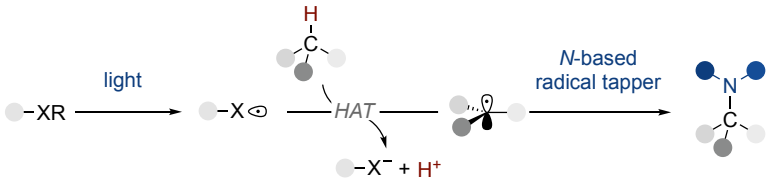

Scheme 2.11 General strategy for photocatalyzed C(sp^3)–H amination.

In 2018, Zuo and co-workers demonstrated that photoinduced ligand-to-metal charge transfer (LMCT) catalysis enables remote δ-C(sp^3)–H amination of alcohols by using azodicarboxylates as *N*-based radical acceptors (Scheme 2.12).[24] Specifically, an electrophilic alkoxy radical is formed by coordination-LMCT-homolysis with a cerium salt and alcohol under blue light irradiation. The alkoxy radical undergoes a 1,5-HAT process, resulting in a δ-carbon-center radical, which is subsequently trapped into electrophilic azodicarboxylate. Single-electron reduction and protonation sequence ultimately afford amidated product, along with the regeneration of Ce(IV) catalyst.

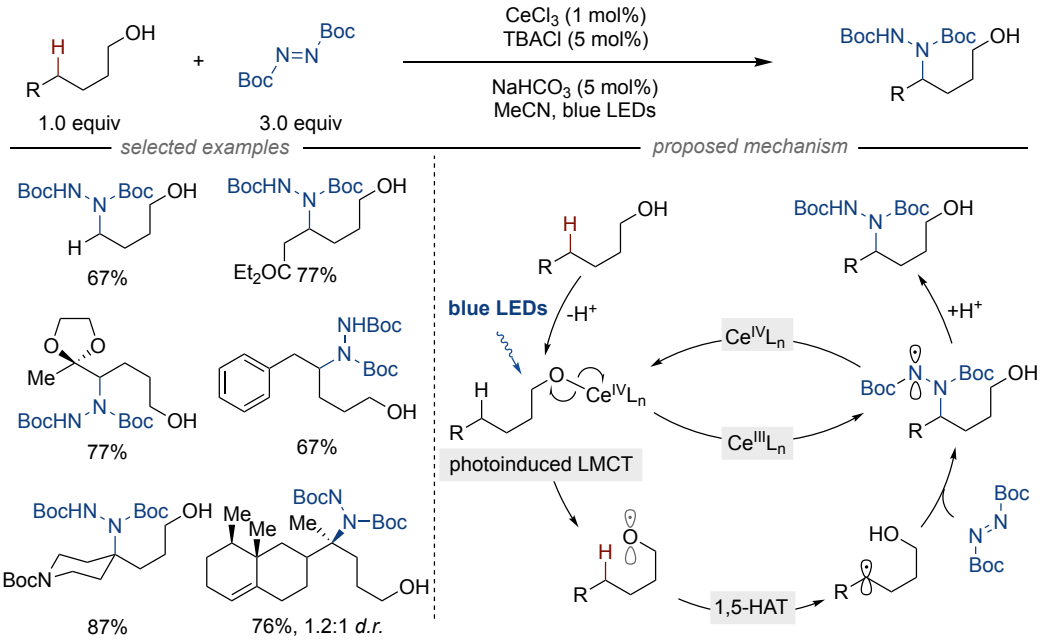

Scheme 2.12 δ-C(sp^3)–H amination of alcohols enabled by Ce- and photocatalysis.

In 2022, Noël and coworkers developed a photocatalyzed regioselective C(sp^3)–H amination of aliphatic C(sp^3)–H bonds within a flow reactor setup (Scheme 2.13).[25] The utilization of decatungstate (TBADT) as the photocatalyst enabled amination at either allylic and aldehyde C–H sites, or at unactivated secondary and tertiary C(sp^3)–H linkages dictated by BDEs of C–H bonds and polar effects.[26] In addition, this platform allowed for both rapid production (314 mmol/h) and scalability, enabling the synthesis of up to 23.6 grams of the aminated product.

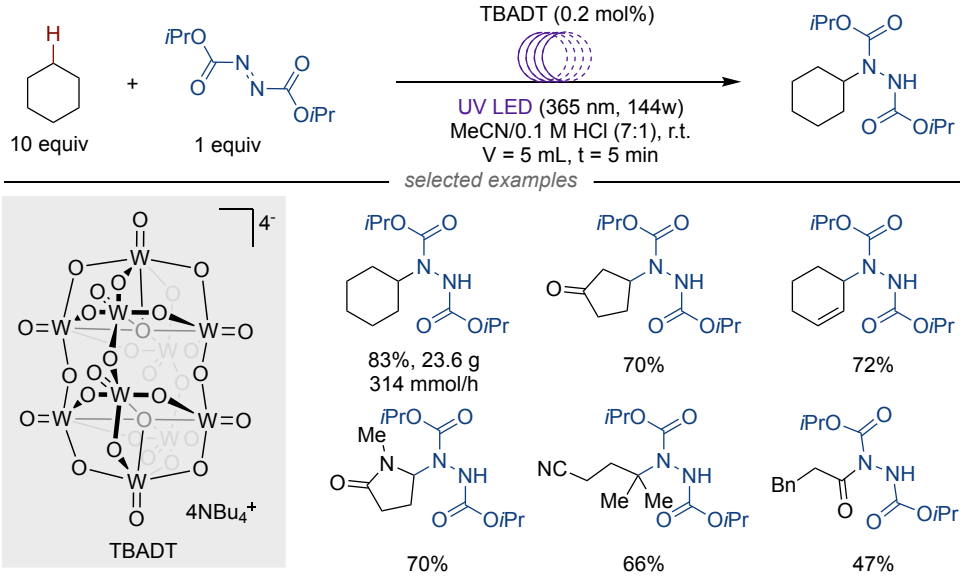

Scheme 2.13. Decatungstate-catalyzed C(sp^3)–H amination.

2.2 General Aim of the Project

Metal-catalyzed nitrene transfer has emerged as an effective strategy for forging C(sp^3)–N bond at benzylic, allylic, or sterically less-encumbered C(sp^3)-H linkages. However, the development of a new catalytic scenario for site-selective amidation of C(sp^3)–H sites adjacent to heteroatoms remains largely unexplored. This chapter aims at exploring the integration of nickel catalysts into nitrene transfer to achieve site-selective sp^3 C−H amidation, with regioselectivity arising from the intrinsic properties of both the C–H bonds and the nickel nitrenoids generated in situ.

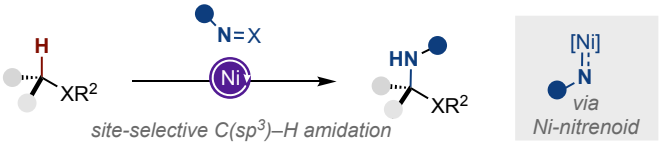

Scheme 2.13 Nickel-catalyzed site-selective C(sp^3)–H amidation.

2.3 Optimization of the Reaction Conditions

Our investigation began by evaluating the C(sp^3)–H amidation of tetrahydrofuran (THF, **1a**) utilizing phenyl dioxazolone (**2a**) as the nitrene precursor. The choice of the latter was not arbitrary given the ease at which these precursors are made from ubiquitous carboxylic acids. As shown in Table 2.1, the reaction was conducted with 10 mol% $Ni(ClO_4)_2·6H_2O$ as the precatalyst, 15 mol% bathocuproine as the ligand, and HBpin as the reductant at room temperature. After 12 hours, the desired *N*,*O*-acetal product (**3a**) was obtained in 75% yield (entry 1). Control experiments confirmed that the presence of nickel, the ligand, and the reductant were essential for the success of this transformation (entries 2-4).

Table 2.1 Control experiments for Ni-catalyzed C(sp^3)–H amidation.[a]

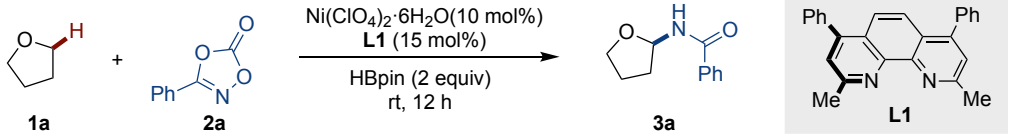

Entry	Deviation from standard conditions	**3a** (%)[b]
1	none	75
2	No $Ni(ClO_4)_2·6H_2O$	0
3	No **L1**	0
4	No HBpin	0

Conditions: [a] **2a** (0.1 mmol), $Ni(ClO_4)_2·6H_2O$ (10 mol%), **L1** (15 mol%), HBpin (2.0 equiv.), in THF (1 mL) at r.t. for 24 h. [b] GC yield with dodecane as internal standard.

Next, we investigated the impact of various nickel precatalysts on the reaction outcome (Table 2.2). Notably, only $Ni(ClO_4)_2 \cdot 6H_2O$ and $Ni(OTf)_2$ facilitated the formation of **3a**, whereas other Ni(II) and Ni(0) sources showed no reactivity. We hypothesize that nickel sources with non-coordinating counteranions such as ClO_4^- and OTf^- may facilitate reduction of nickel by HBpin due to the formation of strong B–O bonds.

Table 2.2 Screening of Ni catalysts.[a]

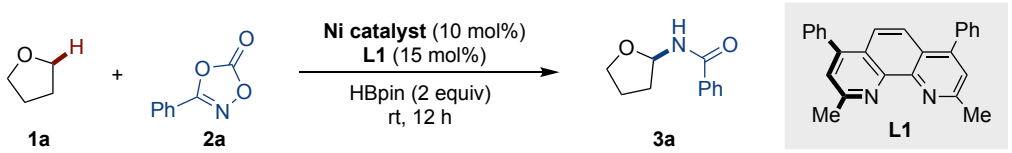

Entry	Ni catalyst	**3a** (%)[b]
1	$Ni(ClO_4)_2 \cdot 6H_2O$	75
2	$Ni(OTf)_2$	20
3	$Ni(acac)_2$	0
4	NiI_2	0
5	$NiCl_2$	0
6	$Ni(OAc)_2 \cdot 4H_2O$	0
7	$NiBr_2 \cdot DME$	0
8	$Ni(cod)_2$	0
9	$Ni(cod)_2$ + $NaClO_4$	0

Conditions: [a] **2a** (0.1 mmol), nickel catalyst (10 mol%), **L1** (15 mol%), HBpin (2.0 equiv.), in THF (1 mL) at r.t. for 24 h. [b] GC yield with dodecane as internal standard.

As expected, the nature of the ligand was critical for the reaction's success (Table 2.3). The use of phenanthroline ligand **L1**, which features a methyl group at C2 and a phenyl group at C4, provided the best results (entry 1). Notably, trace amounts of **3a** were observed in the absence of the methyl groups adjacent to nitrogen atom in phenanthroline backbone (entry 2). On the other hand, removal of the phenyl substituents at C4 led to a diminished yield of **3a** (entry 3). The use of more flexible bipyridine **L7** and pyridine-oxazoline ligand **L8** had a deleterious effect on reactivity (entries 7-8). In addition, **3a** was not detected when employing **L10** as ligand.

Table 2.3. Screening of ligands.[a]

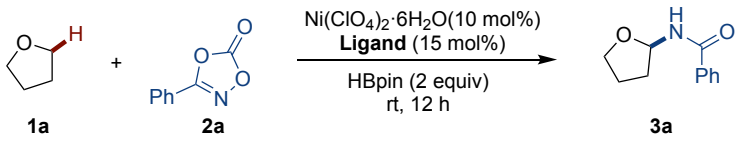

Entry	ligand	**3a** (%)[b]
1	**L1**	77
2	**L2**	trace
3	**L3**	33
4	**L4**	71
5	**L5**	0
6	**L6**	0
7	**L7**	32
8	**L8**	57
9	**L9**	63
10	**L10**	0

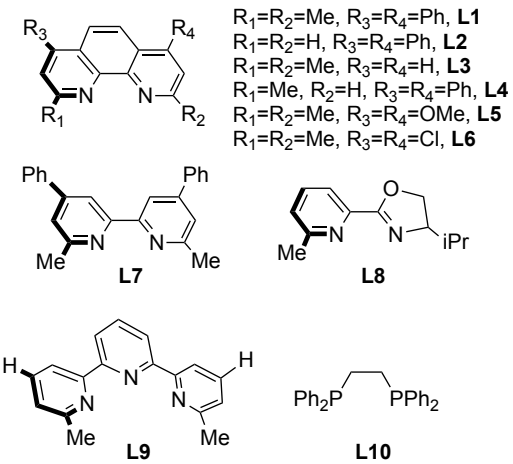

Conditions: [a] **2a** (0.1 mmol), $Ni(ClO_4)_2·6H_2O$ (10 mol%), ligand (15 mol%), HBpin (2.0 equiv.), in THF (1 mL) at r.t. for 24 h. [b] GC yield with dodecane as internal standard.

Table 2.4 highlights the impact of different reductants on the reaction outcome. The replacement of HBpin with organosiloxanes, such as $(EtO)_3SiH$ and TMDSO, led to no formation of the desired product (entries 2-3), whereas the use of phenylsilane resulted in **3a** with an excellent 93% yield (entry 5). In contrast, other metal-based reductants, such as manganese and zinc, were ineffective in promoting the transformation (entries 6-7).

Table 2.4. Screening of reductants.[a]

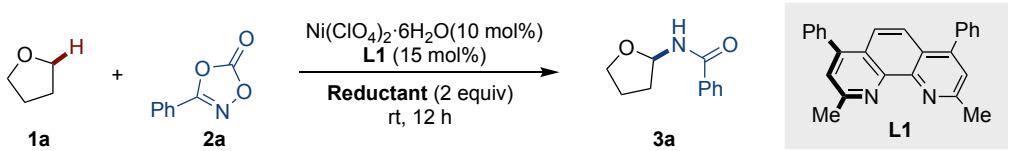

Entry	Reductants	**3a** (%)
1	HBpin	75
2	$(EtO)_3SiH$	0
3	TMDSO	0
4	Ph_2SiH_2	0
5	$PhSiH_3$	93
6	Mn	0
7	Zn	0
8	B_2Pin_2	0

Conditions: [a] **2a** (0.1 mmol), $Ni(ClO_4)_2·6H_2O$ (10 mol%), **L1** (15 mol%), reductant (2.0 equiv.), in THF (1 mL) at r.t. for 24 h. [b] GC yield with dodecane as internal standard.

Aiming at extending the impact that this technique might have, we next focused our attention on utilizing solvents lacking hydrogen atoms amenable for parasitic HAT (Table 2.5). Notably, the utilization of hindered pivalonitrile (*t*BuCN), which lacks activated C–H bonds, gave a promising yield of 34% when 5 equivalents of THF were used as the C–H precursor (entry 5). Additionally, benzamide arising from reduction of dioxazolone was observed as byproduct.

Table 2.5 Screening of solvents.[a]

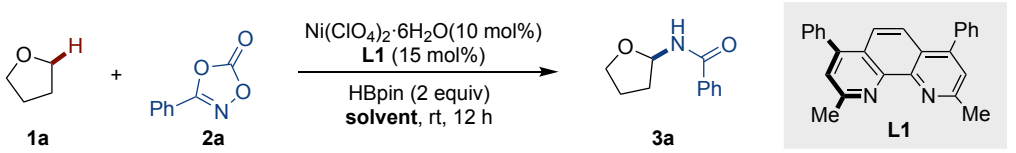

Entry	Solvents	**3a** (%)[b]
1	$PhCF_3$	12
2	benzene	13
3	DCE	0
4	MeCN	trace
5	PhCN	3
6	*t*BuCN	34

Conditions: [a] **2a** (0.1 mmol), 5 equiv. of THF, $Ni(ClO_4)_2 \cdot 2$**L1** (10 mol%), HBpin (2.0 equiv.), in solvent (1 mL) at r.t. for 24 h. [b] GC yield with dodecane as internal standard.

As shown in Table 2.6, the utilization of 15 mol% $PhSiH_3$ in pivalonitrile as solvent significantly increased the reaction outcome, resulting in a 82% isolated yield of **3a**.

Table 2.6 Screening of amounts of $PhSiH_3$.[a]

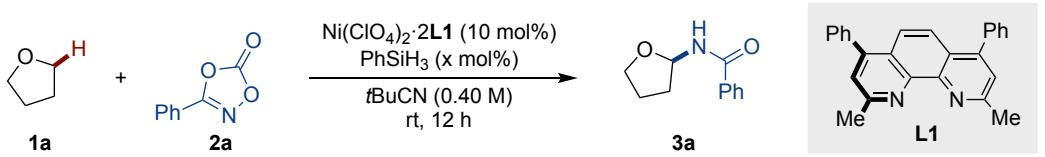

Entry	Conditions	**3a** (%)[b]
1	$PhSiH_3$ (50 mol%)	60
2	$PhSiH_3$ (25 mol%)	73
3	$PhSiH_3$ (15 mol%)	82[c]
4	$PhSiH_3$ (15 mol%) & THF (5 equiv)	73

Conditions: [a] **2a** (0.4 mmol), 10 equiv. of THF, $Ni(ClO_4)_2$·2**L1** (10 mol%), $PhSiH_3$ (x mol%) in *t*BuCN (1 mL) at r.t. for 24 h. [b] GC yield with dodecane as internal standard.. [c] isolated yield.

2.4 Substrate Scope

2.4.1 Scope of C(sp^3)–H Precursors

With optimized conditions in hand (Table 2.6, entry 3), we turned our attention to exploring the generality of the C(sp^3)–H amidation across a range of structurally diverse C(sp^3)–H precursors. As shown in Scheme 2.14, a variety of cyclic ethers can be subjected to the conditions with similar ease, resulting in the targeted products **3a**-**3g** in good yields. Interestingly, the use of 2-Me THF resulted in **3b** as the predominant regioisomer (3.4:1 ratio), suggesting that steric effects largely dictate our C(sp^3)–H amidation process. Nevertheless, it is worth noting that C–N bond formation can be implemented at tertiary C(sp^3)–H centers, as observed in **3f**, albeit in lower yields. Of particular interest, (–)–Ambroxide could be employed in this C-H amidation, thus offering a rapid and efficient means to access novel scaffolds that could be valuable for the fragrance industry (**3g**).[27]

No reactivity was observed for cyclohexane, probably due to the lack of feasible interaction with nickel catalyst and/or the high BDEs of the targeted C(sp^3)–H bonds.

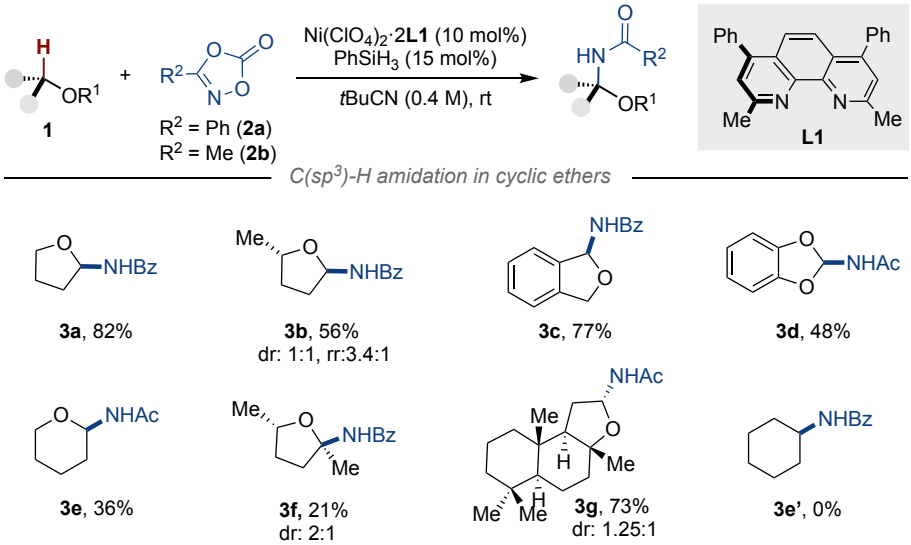

Scheme 2.14 Scope of C(sp^3)–H precursors in cyclic ethers and cyclohexane. Conditions: **1** (4 mmol), **2** (0.40 mmol), Ni(ClO_4)$_2$·2**L1** (10 mol%), $PhSiH_3$ (15 mol%), *t*BuCN (1 mL), see experimental section for details.

Encouraged by these results, we next investigated the potential of our amidation protocol across C−H precursors other than simple ethers. Gratifyingly, as indicated in Scheme 2.15, a diverse array of *N*-protected amines was successfully subjected to this protocol with higher efficiency, enabling access to a series of aminal architectures **3h**-**3x**. A variety of pyrrolidine derivatives possessing Boc, Bac, Bz, Cbz, and phenyl groups could all be accommodated with similar ease, resulting **3h**-**3l** in good yields. Notably, amidation of cyclopropyl-fused pyrrolidine afforded **3q** as the major diastereomer (11:1 d.r.); under the limits of detection, no relative radical ring-opening products were found in the crude reaction mixtures. The utilization of *N*-methylpyrrolidine (NMP) led to exclusive C(sp^3)–H amidation at the endocyclic secondary position (**3r**). Interestingly, the formation of **3u** clearly demonstrated that amidation was preferentially occurring at the C–H sites adjacent to the nitrogen atom in morpholine backbones, as confirmed by X-ray

crystallography. It is worth noting that acyclic amines could also be subjected to this reaction to produce **3v-x**. While a 1.4:1 regioselectivity was observed for **3v**, exclusive amidation at the primary C–H site was observed in **3w**. In the case of **3y**, free NH groups did not impede productive C–N bond formation at the proximal C(sp^3)–H position.

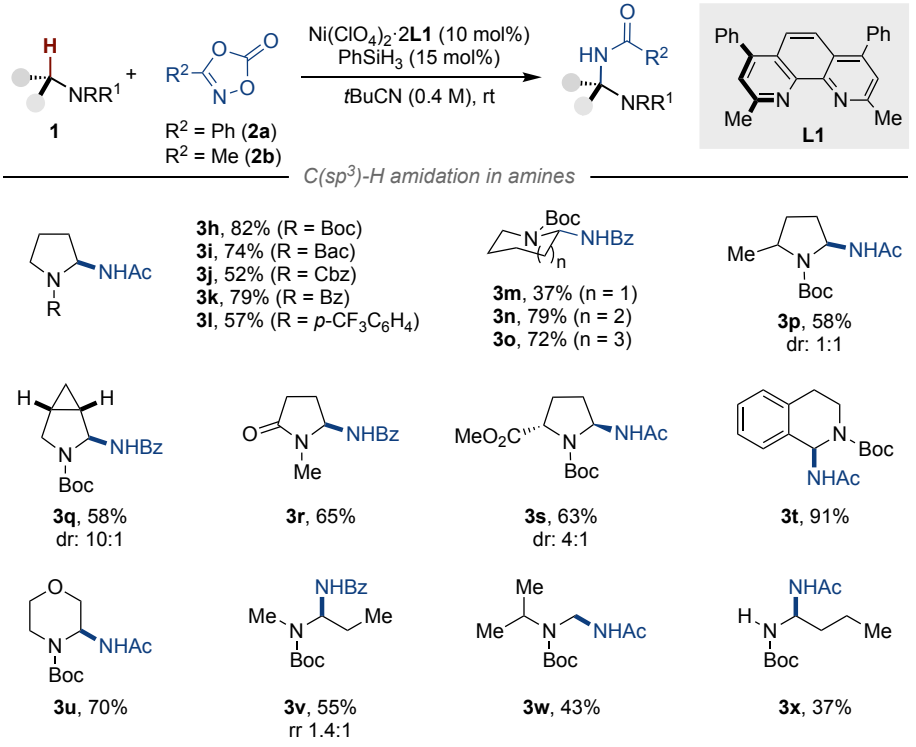

Scheme 2.15 Scope of C(sp^3)–H precursors in protected amines. Conditions: **1** (0.8 mmol), **2** (0.40 mmol), $Ni(ClO_4)_2 \cdot 2$**L1** (10 mol%), $PhSiH_3$ (15 mol%), *t*BuCN (1 mL), see experimental section for details.

2.4.2 Scope of Dioxazolones

Next, we assessed the suitability of various dioxazolones to perform the C–H amidation. As shown in Scheme 2.16, a range of alkyl-substituted dioxazolones were successfully subjected to the optimized conditions, resulting in the corresponding C(sp^3)–H amidation products **4a-k** in moderate to high yields. Notably, no intramolecular C(sp^3)–

H amidation was detected in dioxazolones bearing pendant C(sp^3)–H linkages on the alkyl chain, leading to exclusive formation of **4a**, **4c**, and **4k**. Although the presence of benzylic C(sp^3)–H sites might interfere with efficient C(sp^3)–H amidation through competitive hydrogen atom transfer, this was not the case and **4b**, **4i**, and **4j** were obtained as the sole products. In addition, the successful collection of **4i**, **4j** and **4k** highlights the potential impact of this C(sp^3)–H amidation strategy, particularly in the preparation of advanced synthetic intermediates and for late-stage molecular diversification.[28]

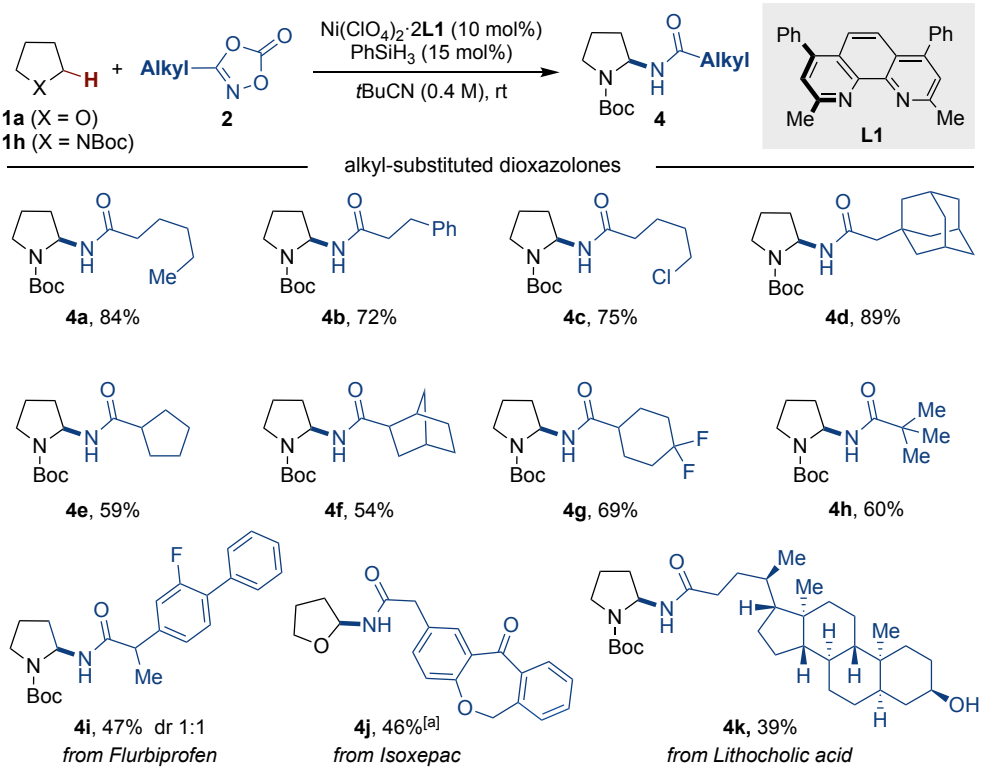

Scheme 2.16 Scope of alkyl dioxazolones. Conditions: **1h** (0.8 mmol), **2** (0.40 mmol), Ni(ClO_4)$_2$·2**L1** (10 mol%), $PhSiH_3$ (15 mol%), *t*BuCN (1 mL). [a] THF were used instead of *t*BuCN. See experimental section for details.

As shown in Scheme 2.17, similar results were found with aryl dioxazolones possessing either electron-donating or electron-withdrawing substituents, affording the

targeted products (**4l-4t**) in good yields and exquisite selectivities. In addition, heterocycles (**4u**), methoxy (**4q**) and functional groups, such as halides (**4n**, **4p**), nitriles (**4o**), could all be well-accommodated under the optimized conditions.

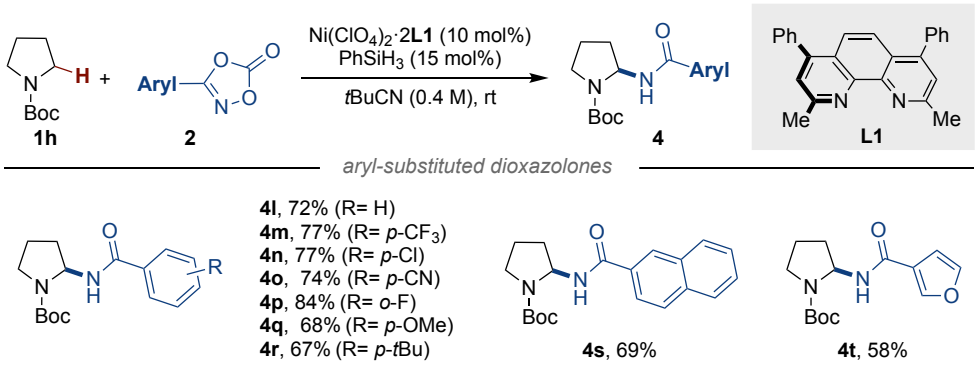

Scheme 2.17 Scope of aryl dioxazolones. Conditions: **1h** (2.0 mmol), **2** (0.40 mmol), $Ni(ClO_4)_2 \cdot 2$**L1** (10 mol%), $PhSiH_3$ (15 mol%), *t*BuCN (1 mL). See experimental section for details.

2.4.2 Scope of Difunctionalization of Ethers

Given the inherent synthetic potential of *N*,*O*-acetals for subsequent functionalization via the intermediacy of iminium ions,[29] we wondered whether we could utilize readily available acyclic ether feedstocks as unorthodox bifunctional linchpins via sequential C(sp^3)–H amidation / C(sp^3)–O(alkyl) functionalization *en route* to valuable alkyl amine scaffolds. As shown in Scheme 2.18, **3aa-3ac** were easily within reach from diethyl ether by telescoping the formation of *N*,*O*-acetal **I** and subsequent reaction with amine source (**3aa**), Et_3SiH (**3ab**) or an appropriate vinyl ether (**3ac**). Similarly, the utilization of DME with **2a** resulted in an exhaustive amination event *en route* to **3ad**. Although in modest yields, these results should be interpreted against the challenge that is addressed, not only offering new knowledge in retrosynthetic analysis but also new chemical space when accessing valuable nitrogen-containing compounds from simple alkyl ether feedstocks.

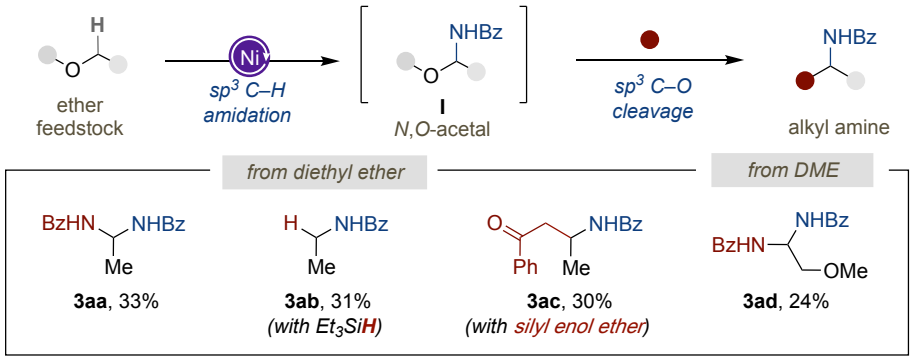

Scheme 2.18 Scope of difunctionalization of ethers.

2.5 Mechanistic Studies

2.5.1 Intercepting Radical Intermediates with Methyl Acrylate

To gain insight into the possible reaction pathway of this amidation process, a set of preliminary mechanistic experiments were conducted. As shown in Scheme 2.19, a crossover experiment of **1a** in the presence of both **2a** and methyl acrylate led to the formation of **3a** in a diminished 31% yield, along with the corresponding alkyl radical adduct **5a** in 16% yield. This observation indicates the involvement of open-shell alkyl radical species during this transformation.

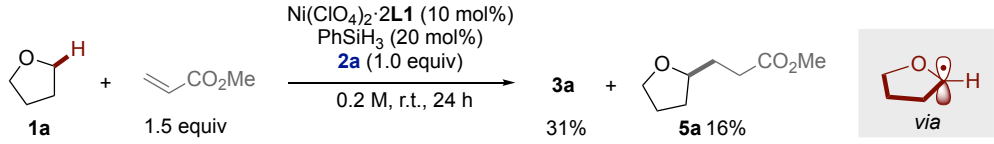

Scheme 2.19 Radical intercept experiment.

2.5.2 Intermolecular Kinetic Isotope Effect

To further investigate the C–H cleavage step, intermolecular kinetic isotope effect experiments were conducted using THF and THF-d_8 respectively, yielding a k_H/k_D value of 3.8. This kinetic isotope effect suggests that sp^3 C–H cleavage may be involved in the rate-determining step of the reaction.[30]

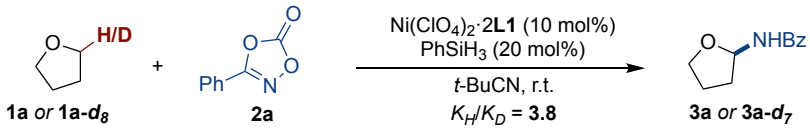

1a *or* **1a-d_8** + **2a** → **3a** *or* **3a-d_7**

Graph S1. Initial rates of THF and THF-d_8.

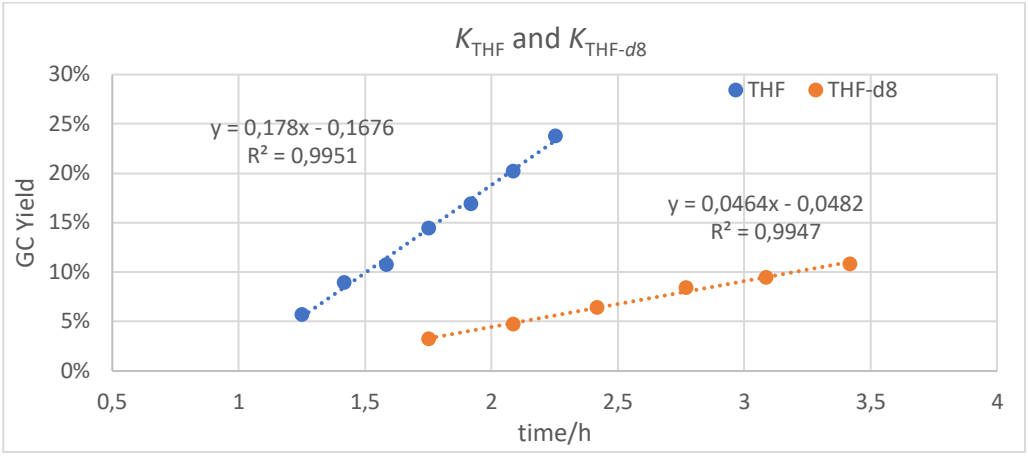

2.5.3 Stochiometric Organometallic Reactions

Next, we turned our attention to monitor the reaction of $Ni(ClO_4)_2 \cdot 2$**L1** and $PhSiH_3$ via EPR spectroscopy, providing compelling evidence for the involvement of Ni(I) intermediates (Scheme 2.20, top). This was supported by the observation of an otherwise identical EPR signal for $NiClO_4 \cdot 2$**L1**, which can be synthesized by oxidizing $Ni(cod)_2$ with $AgClO_4$.[31] Upon addition of **2a**, the lack of an EPR signal (**Scheme 2.20**, top left) is consistent with consumption of $NiClO_4 \cdot 2$**L1** species rapidly. Although the reactive and transient nature of the intermediates precluded their isolation in a pure, analyzable form, a stoichiometric reaction of $NiClO_4 \cdot 2$L1 with **2a** and **1a** afforded the expected product **3a** in 37% yield (**Scheme 2.20**, bottom), suggesting that Ni(I) might play a critical role as a key intermediate in the reaction.

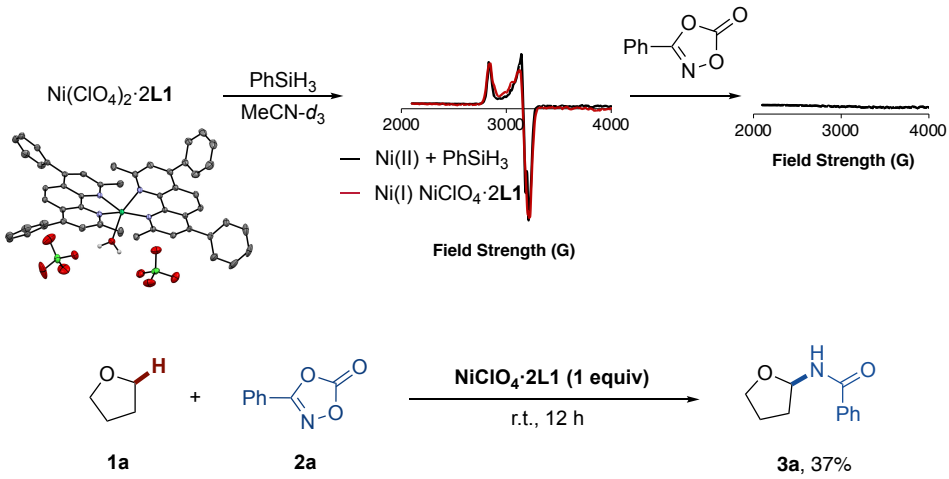

Scheme 2.20 Stochiometric organometallic reactions.

2.5.4 Proposed Mechanism

With all this information in hand, our transformation might follow the mechanistic rationale depicted in Figure 2.1. Initial single electron reduction of pre-catalyst $Ni(ClO_4)_2 \cdot 2$**L1** by $PhSiH_3$ results in Ni(I) species **I**, followed by reaction with dioxazolone that ultimately generates an electrophilic Ni–nitrenoid species (**II**). This Ni–nitrenoid selectively abstracts a hydrogen atom from the C–H nucleophile, affording an open-shell carbon-centered radical **IV** and Ni(II) species **III**. The carbon-centered radical can be intercepted by Ni(II) species **III**, resulting in Ni(III) intermediate **V**. Subsequent reductive elimination of **V** ultimately delivers the amidated product and regenerates Ni(I), thus closing the catalytic cycle.

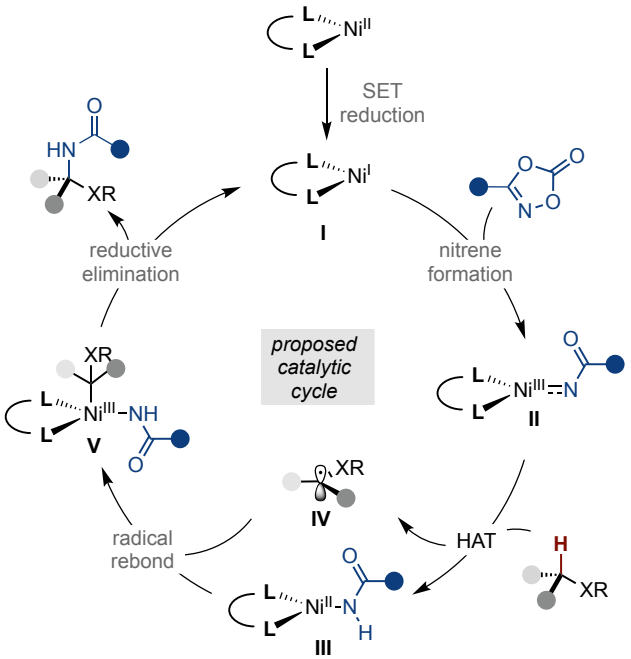

Figure 2.1 Proposed mechanism.

2.6 Conclusion

In this chapter, we have disclosed a nickel-catalyzed, intermolecular C(sp^3)–H amidation protocol to access a series of *N*, *O*-acetals and *N*, *N*-aminals. This catalytic scenario is based on the intermediacy of nickel–nitrenoid species that are capable of functionalizing C(sp^3)–H bonds adjacent to heteroatoms. The reaction is characterized by its mild conditions, and broad scope, accommodating a wide range of C–H precursors, including ethers and *N*-protected amines, and by utilizing alkyl/aryl dioxazolones as nitrene precursors. Moreover, the difunctionalization of acyclic ethers also offers an opportunity to improve upon existing nonactivated C(sp^3)-O functionalization scenarios.

2.7 Experimental Section

2.7.1 General Considerations

Reagents. Commercially available materials were used as received without further purification. $Ni(ClO_4)_2 \cdot 6H_2O$ (99% purity) was purchased from Strem. Bathocuproine (99% purity) was purchased from Acros. Anhydrous tetrahydrofuran (THF, 99.5% purity) was purchased from Acros. Anhydrous pivalonitrile (*t*-BuCN, 98% purity) was purchased from Aldrich, which was dealt with freeze-pump-thaw degassing before using. Pinacolborane (HBpin, 97% purity) was purchased from Acros and Phenylsilane ($PhSiH_3$, 97% purity) was purchased from TCI.

Analytical methods. ^{1}H and ^{13}C NMR and ^{19}F spectra were recorded on Bruker 300 MHz, Bruker 400 MHz and Bruker 500 MHz at 20 °C. All ^{1}H NMR spectra are reported in parts per million (ppm) downfield of TMS and were calibrated using the residual solvent peak of $CHCl_3$ (7.26 ppm), unless otherwise indicated. All ^{13}C NMR spectra are reported in ppm relative to TMS, were calibrated using the signal of residual $CHCl_3$ (77.16 ppm). Coupling constants, *J* are reported in Hertz. Gas chromatographic analyses were performed on Hewlett-Packard 6890 gas chromatography instrument with FID detector. Melting points were measured using open glass capillaries in a Büchi B540 apparatus. Infrared spectra (FT-IR) measurements were carried out on a Bruker Optics FT-IR Alpha spectrometer equipped with a DTGS detector, KBr beamsplitter at 4 cm^{-1} resolution using a one bounce ATR accessory with diamond windows. High-resolution mass spectra were recorded on a Waters LCT Premier spectrometer or in a MicroTOF Focus, Bruker Daltonics spectrometer. UV/Vis absorption spectra were recorded using a Agilent Technologies Cary 300 UV/Vis spectrophotometer and UV-1800PC spectrophotometer in quartz cuvettes with a path length of 1.0 cm. Bulk electrolysis was conducted on a PARSTAT 2273 potentiometer using a 3-electrode cell configuration at room temperature, The same electrodes were used as for CV experiments, namely a glassy carbon working electrode, platinum flag counter electrode and Ag/AgCl (KCl sat.) reference electrode. Flash chromatography was performed with EM Science silica gel 60 (230-400 mesh).

Thin layer chromatography was used to monitor reaction progress and analysed fractions from column chromatography. To this purpose TLC Silica gel 60 F_{254} aluminium sheets from Merck were used and visualization was achieved using UV irradiation and/or staining with Potassium Permanganate or Phosphomolybdic acid solution. The yields reported refer to isolated yields and represent an average of at least two independent runs. The procedures described in this section are representative. Thus, the yields may differ slightly from those given in the tables of the manuscript.

2.7.2 Synthesis of Catalysts and Substrates

Synthesis of $Ni(ClO_4)_2$·2L1. In a round- bottom flask, $Ni(ClO_4)_2·6H_2O$ (5.0 mmol, 1.0 equiv.) was dissolved in 20 mL anhydrous MeOH. Bathocuproine (10.0 mmol, 2.0 equiv.) was added in one batch. Then the reaction mixture was stirred at 55 °C for 3 h. After cooling to r.t., the resulting mixture was filtered, obtained green solid was washed once by cold methanol and dried under vacuum at 50 °C overnight. Yield: 65%.

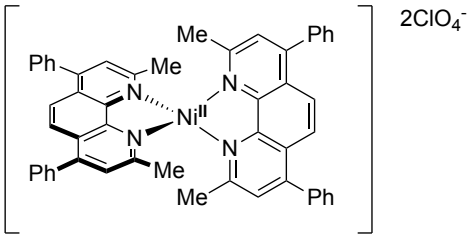

^{1}H NMR (500 MHz, $CDCl_3$, paramagnetic) δ 60.52 (s, 1H), 26.09 (s, 1H), 8.34 (s, 2H), 8.08 (t, *J* = 7.3 Hz, 1H), 7.21 (s, 2H), -8.44 (br. s, 3H) ppm.

Synthesis of Nitrene Precursors Dioxazolones. 3-methyl-1,4,2-dioxazol-5-one, 3-pentyl-1,4,2-dioxazol-5-one, 3-phenethyl-1,4,2-dioxazol-5-one, 3-(4-chlorobutyl)-1,4,2-dioxazol-5-one, 3-(but-3-en-1-yl)-1,4,2-dioxazol-5-one, 3-cyclopentyl-1,4,2-dioxazol-5-one, 3-(4,4-difluorocyclohexyl)-1,4,2-dioxazol-5-one, 3-(bicyclo[2.2.1]heptan-2-yl)-1,4,2-dioxazol-5-one, 3-(*tert*-butyl)-1,4,2-dioxazol-5-one, 3-((11-oxo-6,11-dihydrodibenzo[b,e]oxepin-2-yl)methyl)-1,4,2-dioxazol-5-one, 3-phenyl-1,4,2-dioxazol-

5-one, 3-(4-(trifluoromethyl)phenyl)-1,4,2-dioxazol-5-one, 3-(4-chlorophenyl)-1,4,2-dioxazol-5-one, 3-(4-cyanophenyl)-1,4,2-dioxazol-5-one, 3-(2-fluorophenyl)-1,4,2-dioxazol-5-one, 3-(4-methoxyphenyl)-1,4,2-dioxazol-5-one, 3-(4-(*tert*-butyl)phenyl)-1,4,2-dioxazol-5-one, 3-(naphthalen-2-yl)-1,4,2-dioxazol-5-one, 3-(furan-3-yl)-1,4,2-dioxazol-5-one were prepared following the literature procedure.[32]

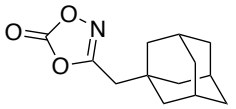

3-((adamantan-1-yl)methyl)-1,4,2-dioxazol-5-one (2c). To an oven-dried 100 mL round-bottom flask was charged with 1,1′-carbonyldiimidazole (CDI, 1.9 g, 1.2 equiv) and THF (40 mL) under argon atmosphere. To this suspension was added 1-adamantaneacetic acid (1.9 g, 10 mmol), and the resulting mixture was stirred for 2 h at room temperature. Then hydroxylamine hydrochloride (NH_2OH•HCl, 1.4 g, 2.0 equiv) was quickly added, and allowed to stir for another 14 h. After completion, the mixture was diluted with 5% $KHSO_4$ (aq.) and extracted with EtOAc (2 times). The combined organic layers were dried over anhydrous Na_2SO_4, filtered, and concentrated under reduced pressure. To a stirred solution of hydroxamic acid (950 mg, 1.0 equiv) in dichloromethane (0.1 M) was added 1,1′-carbonyldiimidazole (900 mg, 1.2 equiv) in one portion at room temperature. After stirring for 1 h, the reaction mixture was quenched with 1 N HCl(aq), extracted with dichloromethane (3 times), and dried over anhydrous Na_2SO_4. The mixture was concentrated under reduced pressure and filtered through a pad of silica with an eluent (EtOAc/n-hexane, 5:1). The filtrate was concentrated under reduced pressure to afford the title compound (942 mg, 40%, two steps) as a white solid. **^{1}H NMR** (400 MHz, $CDCl_3$) δ 2.37 (s, 2H), 2.02 (br. m, 3H), 1.75 (br. m, 1H), 1.72 (br. m, 2H), 1.65 (br. m, 2H), 1.60 (br. m, 7H). **^{13}C NMR** (101 MHz, $CDCl_3$) δ 165.13, 154.43, 42.24, 38.93, 36.44, 33.30, 28.49. **IR (neat):** 2905, 2887, 2850, 1883, 1871, 1860, 1814, 1645, 1630, 1446, 1408, 1380, 1360, 1344, 1274, 1224, 1153, 985, 762, 708 cm^{-1}. **HRMS (APCI)** *calcd.* for ($C_{13}H_{18}NO_3$) $[M+H]^+$: 236.1281, *found* 236.1279.

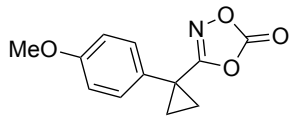

3-(1-(4-methoxyphenyl)cyclopropyl)-1,4,2-dioxazol-5-one (2d). To an oven-dried 100 mL round-bottom flask was charged with 1,1′-carbonyldiimidazole (CDI, 1.9 g, 1.2 equiv) and THF (20 mL) under argon atmosphere. To this suspension was added 1-(4-methoxyphenyl)cyclopropanecarboxylic acid (1.9 g, 10 mmol), and the resulting mixture was stirred for 2 h at room temperature. Then hydroxylamine hydrochloride (NH_2OH•HCl, 1.4 g, 2.0 equiv) was quickly added, and allowed to stir for another 14 h. After completion, the mixture was diluted with 5% $KHSO_4$(aq) and extracted with EtOAc (2 times). The combined organic layers were dried over anhydrous Na_2SO_4, filtered, and concentrated under reduced pressure. To a stirred solution of hydroxamic acid (870 mg, 1.0 equiv) in dichloromethane (0.1 M) was added 1,1′-carbonyldiimidazole (816 mg, 1.2 equiv) in one portion at room temperature. After stirring for 1 h, the reaction mixture was quenched with 1 N HCl(aq), extracted with dichloromethane (3 times), and dried over anhydrous Na_2SO_4. The mixture was concentrated under reduced pressure and filtered through a pad of silica with an eluent (EtOAc/n-hexane, 5:1). The filtrate was concentrated under reduced pressure to afford the title compound (652 mg, 28%, two steps) as a white solid. **^{1}H NMR** (400 MHz, $CDCl_3$) δ 7.40 – 7.32 (m, 2H), 6.95 – 6.87 (m, 2H), 3.81 (s, 3H), 1.66 – 1.59 (m, 2H), 1.50 – 1.40 (m, 2H). **^{13}C NMR** (101 MHz, $CDCl_3$) δ 169.54, 159.86, 154.25, 131.55, 127.22, 114.36, 55.43, 21.18, 15.09. **IR (neat):** 2928, 2862, 1858, 1825 1635, 1447, 1365, 1337, 1149, 1035, 982, 763 cm^{-1}. **HRMS (APCI)** *calcd*. for ($C_{12}H_{12}NO_4$) $[M+H]^+$: 234.0761, *found* 234.0759.

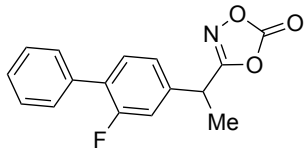

3-(1-(2-fluoro-[1,1'-biphenyl]-4-yl)ethyl)-1,4,2-dioxazol-5-one (2e). To an oven-dried 100 mL round-bottom flask was charged with 1,1′-carbonyldiimidazole (CDI, 1.9 g, 1.2

equiv) and THF (20 mL) under argon atmosphere. To this suspension was added Flurbiprofen (2.4 g, 10 mmol), and the resulting mixture was stirred for 2 h at room temperature. Then hydroxylamine hydrochloride (NH_2OH•HCl, 1.4 g, 2.0 equiv) was quickly added, and allowed to stir for another 14 h. After completion, the mixture was diluted with 5% $KHSO_4$ (aq.) and extracted with EtOAc (2 times). The combined organic layers were dried over anhydrous Na_2SO_4, filtered, and concentrated under reduced pressure. To a stirred solution of hydroxamic acid (1.3 g, 1.0 equiv) in dichloromethane (0.1 M) was added 1,1′-carbonyldiimidazole (1.0 g, 1.2 equiv) in one portion at room temperature. After stirring for 1 h, the reaction mixture was quenched with 1 N HCl(aq), extracted with dichloromethane (3 times), and dried over anhydrous Na_2SO_4. The mixture was concentrated under reduced pressure and filtered through a pad of silica with an eluent (EtOAc/n-hexane, 5:1). The filtrate was concentrated under reduced pressure to afford the title compound (714 mg, 25%, two steps) as a white solid. **^{1}H NMR** (500 MHz, $CDCl_3$) δ 7.57 (m, 2H), 7.53 – 7.47 (m, 3H), 7.45 – 7.40 (m, 1H), 7.22 – 7.13 (m, 2H), 4.14 (q, *J* = 7.2 Hz, 1H), 1.75 (d, *J* = 7.3 Hz, 3H). **^{13}C NMR** (126 MHz, $CDCl_3$) δ 168.01, 160.98, 159.00, 154.00, 138.02, 137.96, 135.02, 131.71, 131.67, 129.54, 129.43, 129.08, 129.05, 128.69, 128.17, 123.55, 123.52, 115.50, 115.31, 36.68, 36.66, 17.20. **^{19}F NMR** (376 MHz, $CDCl_3$) δ -116.18, -116.21, -116.23. **IR (neat):** 1872, 1831, 1620, 1485, 1422, 1378, 1257, 1235, 1212, 1147, 1133, 1067, 984, 934, 915, 887, 830, 761, 723, 700, 658, 572 cm^{-1}. **HRMS** *calcd*. for ($C_{16}H_{12}FNNaO_3$) $[M+Na]^+$: 308.0693, *found* 308.0688.

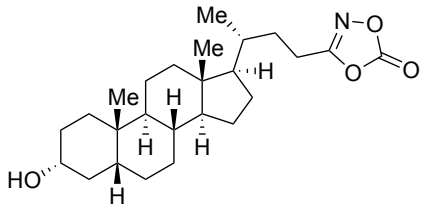

3-((*R*)-3-((3*R*,5*R*,8*R*,9*S*,10*S*,13*R*,14*S*,17*R*)-3-hydroxy-10,13-dimethylhexadecahydro-1*H*-cyclopenta[a]phenanthren-17-yl)butyl)-1,4,2-dioxazol-5-one (2f). To an oven-dried 100 mL round-bottom flask was charged with 1,1′-carbonyldiimidazole (CDI, 1.9 g, 1.2 equiv) and THF(20 mL) under argon atmosphere.

To this suspension was added Lithocholic acid (3.8 g, 10 mmol), and the resulting mixture was stirred for 5 h at 0 °C. Then hydroxylamine hydrochloride (NH_2OH•HCl, 1.4 g, 2.0 equiv) was quickly added, and allowed to stir for another 14 h. After completion, the mixture was diluted with 5% $KHSO_4$ (aq.) and extracted with EtOAc (2 times). The combined organic layers were dried over anhydrous Na_2SO_4, filtered, and concentrated under reduced pressure. The residue was purified by flash column chromatography to give the hydroxamic acid. To a stirred solution of hydroxamic acid (1.2 g, 1.0 equiv) in dichloromethane (0.1 M) was added 1,1′-carbonyldiimidazole (576 mg, 1.2 equiv) in one portion at 0 °C. After stirring for 3 h, the reaction mixture was quenched with 1 N HCl(aq), extracted with dichloromethane (3 times), and dried over anhydrous Na_2SO_4. The mixture was concentrated in vacuo. The residue was purified by flash column chromatography to give the title compound as a white solid (350 mg, 8.4%, two steps) as a white solid. **^{1}H NMR** (500 MHz, $CDCl_3$) δ 3.63 (m, 1H), 2.66 (m, 1H), 2.53 (m, 1H), 1.95 (m, 1H), 1.89 – 1.70 (m, 5H), 1.68 – 1.04 (m, 22H), 0.97 (d, J = 6.3 Hz, 3H), 0.92 (s, 3H), 0.65 (s, 3H). **^{13}C NMR** (126 MHz, $CDCl_3$) δ 167.32, 154.38, 71.97, 56.60, 55.78, 42.96, 42.19, 40.54, 40.28, 36.57, 35.96, 35.46, 35.34, 34.70, 30.75, 30.67, 28.35, 27.29, 26.52, 24.29, 23.49, 21.95, 20.94, 18.25, 12.20. **IR (neat):** 2928, 2862, 1858, 1825, 1635, 1447, 1365, 1337, 1149, 1035, 982, 763 cm^{-1}. **HRMS** *calcd*. for ($C_{25}H_{39}NNaO_4$) $[M+Na]^+$: 440.2771, *found* 440.2771.

2.7.3 Synthesis of Product

General procedure for the optimization of the *sp*^{3} C–H amidation of THF with 2a. An oven-dried 20 mL reaction tube containing a stir bar was charged with $Ni(ClO_4)_2·6H_2O$ (3.7 mg, 10 mol%), bathocuproine (**L1**) (5.4 mg, 15 mol%), **2a** (0.1 mmol, 1.0 equiv). The reaction tube was connected to a vacuum line where it was evacuated and backfilled with Ar at least three times. Then anhydrous THF (1.0 mL) was added, and the mixture was stirred at r.t. for 5 minutes under Ar flow before adding HBpin (29.0μL, 2.0 equiv). The tube was sealed under Ar atmosphere and stirred at rt. for 12 h. The reaction mixture was then quenched with air and diluted with EtOAc. Dodecane

(internal standard, 22.5 μL, 0.1 mmol) was added to the mixture for analyzing yields by GC.

Ni-catalyzed intermolecular site-selective C(*sp*^{3})–H amidation

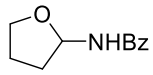

***N*-(tetrahydrofuran-2-yl)benzamide (3a)** An oven-dried 20 mL reaction tube containing a stir bar was charged with $Ni(ClO_4)_2$·2Bathocuproine (39 mg, 10 mol%), **2a** (0.4 mmol, 1.0 equiv). The reaction tube was connected to a vacuum line where it was evacuated and backfilled with Ar at least three times. Then anhydrous pivalonitrile (1.0 mL) was added and the mixture was stirred at r.t. for 5 minutes under Ar flow before adding tetrahydrofuran (325 μL, 4.0 mmol) and $PhSiH_3$ (7.4 μL, 15 mol%) sequentially. The tube was sealed under Ar atmosphere and stirred at r.t. for 24 h. The reaction mixture was quenched with air and diluted with EtOAc, then concentrated in vacuo. The residue was purified by flash column chromatography to give the title compound as a white solid (63 mg, 82% yield). **M.P.** 136 °C. **^{1}H NMR** (400 MHz, $CDCl_3$) δ 7.81 – 7.71 (m, 2H), 7.52 – 7.43 (m, 1H), 7.44 – 7.34 (m, 2H), 6.60 (br. m, 1H), 5.89 (m, 1H), 3.98 (m, 1H), 3.83 (m, 1H), 2.26 (ddt, *J* = 12.9, 8.5, 6.6 Hz, 1H), 2.05 – 1.94 (m, 2H), 1.92 – 1.83 (m, 1H). **^{13}C NMR** (126 MHz, $CDCl_3$) δ 167.35, 134.30, 131.81, 128.64, 127.18, 81.98, 67.81, 32.41, 24.81. **IR (neat):** 3309, 3058, 2971, 2883, 1641, 1578, 1528, 1488, 1448, 1313, 1293, 1262, 1192, 1059, 1040, 1025, 984, 911, 878, 715, 693, 645, 550 cm^{-1}. **HRMS** *calcd*. for ($C_{11}H_{13}NNaO_2$) $[M+Na]^+$: 214.0838, *found* 214.0831.

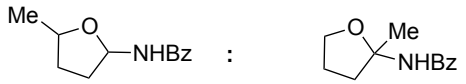

3a **3ab**

r.r. 3.4:1

***N*-(5-methyltetrahydrofuran-2-yl)benzamide (3b)** An oven-dried 20 mL reaction tube containing a stir bar was charged with $Ni(ClO_4)_2$·2Bathocuproine (39 mg, 10 mol%), **2a**

(0.4 mmol, 1.0 equiv). The reaction tube was connected to a vacuum line where it was evacuated and backfilled with Ar at least three times. Then anhydrous pivalonitrile (1.0 mL) was added and the mixture was stirred at r.t. for 5 minutes under Ar flow before adding 2-methyltetrahydrofuran (400 μL, 4.0 mmol) and $PhSiH_3$ (9.9 μL, 20 mol%) sequentially. The tube was sealed under Ar atmosphere and stirred at r.t. for 24 h. The reaction mixture was quenched with air and diluted with EtOAc, then concentrated in vacuo. The residue was purified by flash column chromatography to give the title compound (35 mg, 43% yield, d.r. 1:1., white solid) and **3ba** (10 mg, 13% yield, colorless oil), r.r. (**3b**:**3ba**) 3.4:1. ***N*-(5-methyltetrahydrofuran-2-yl)benzamide (3b)**. **M.P.** 70 °C. **^{1}H NMR** (400 MHz, $CDCl_3$) δ 7.75 (dt, *J* = 8.3, 1.1 Hz, 4H), 7.52 – 7.43 (m, 2H), 7.43 – 7.31 (m, 4H), 6.73 (d, *J* = 7.4 Hz, 1H), 6.65 – 6.50 (m, 1H), 5.95 (dt, *J* = 7.9, 5.8 Hz, 1H), 5.83 (m, 1H), 4.29 – 4.16 (m, 1H), 4.14 – 3.99 (m, 1H), 2.37 (m, 1H), 2.24 (m, 1H), 2.13 – 1.99 (m, 2H), 1.96 – 1.80 (m, 2H), 1.63 – 1.48 (m, 2H), 1.29 (d, *J* = 6.1 Hz, 3H), 1.23 (d, *J* = 6.1 Hz, 3H). **^{13}C NMR** (126 MHz, $CDCl_3$) δ 167.37, 167.06, 134.39, 134.29, 131.77, 131.72, 128.62, 128.59, 127.18, 127.16, 81.95, 81.72, 75.73, 75.12, 32.95, 32.85, 32.63, 31.92, 21.75, 21.15. **IR (neat):** 3317, 2966, 2872, 1738, 1645, 1537, 1488, 1368, 1285, 1076, 1000, 876, 802, 714, 688, 655 cm^{-1}. **HRMS** *calcd*. for ($C_{12}H_{15}NNaO_2$) $[M+Na]^+$: 228.0995, *found* 228.1004.

***N*-(2-methyltetrahydrofuran-2-yl)benzamide (3ba).** **^{1}H NMR** (400 MHz, $CDCl_3$) δ 7.78 – 7.71 (m, 2H), 7.56 – 7.45 (m, 1H), 7.46 – 7.36 (m, 2H), 6.30 (s, 1H), 4.10 – 4.00 (m, 1H), 4.01 – 3.89 (m, 1H), 2.86 – 2.72 (m, 1H), 2.18 – 1.90 (m, 3H), 1.72 (s, 3H). **^{13}C NMR** (101 MHz, $CDCl_3$) δ 166.24, 135.06, 131.57, 128.67, 126.94, 93.85, 68.72, 36.81, 25.95, 25.54. **IR (neat):** 3315, 3062, 2987, 2934, 2873, 1644, 1604, 1536, 1489, 1368, 1313, 1285, 1274, 1214, 1133, 1076, 999, 987, 876, 862, 802, 688, 655 cm^{-1}. **HRMS** *calcd*. for ($C_{12}H_{15}NNaO_2$) $[M+Na]^+$: 228.0995, *found* 228.0996

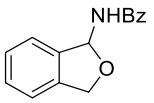

***N*-(1,3-dihydroisobenzofuran-1-yl)benzamide (3c)** An oven-dried 20 mL reaction tube containing a stir bar was charged with $Ni(ClO_4)_2 \cdot 2$Bathocuproine (39 mg, 10 mol%), **2a** (0.4 mmol, 1.0 equiv). The reaction tube was connected to a vacuum line where it was evacuated and backfilled with Ar at least three times. Then anhydrous pivalonitrile (1.0 mL) was added and the mixture was stirred at r.t. for 5 minutes under Ar flow before adding Phthalan (324 μL, 4.0 mmol) and $PhSiH_3$ (9.9 μL, 20 mol%) sequentially. The tube was sealed under Ar atmosphere and stirred at r.t. for 24 h. The reaction mixture was quenched with air and diluted with EtOAc, then concentrated in vacuo. The residue was purified by flash column chromatography to give the title compound as a white solid (73 mg, 77% yield). **M.P.** 147 °C.**^{1}H NMR** (500 MHz, $CDCl_3$) δ 7.83 – 7.75 (m, 2H), 7.55 – 7.46 (m, 1H), 7.45 – 7.32 (m, 5H), 7.30 – 7.25 (m, 1H), 7.19 – 7.11 (m, 1H), 6.84 (d, J = 9.4 Hz, 1H), 5.19 (dd, J = 12.5, 2.6 Hz, 1H), 5.07 (d, J = 12.5 Hz, 1H). **^{13}C NMR** (126 MHz, $CDCl_3$) δ 167.48, 140.00, 137.84, 133.91, 132.03, 129.29, 128.66, 128.12, 127.34, 122.73, 121.39, 85.02, 72.16. **IR (neat):** 3319, 2866, 1642, 1512, 1484, 1361, 1273, 1250, 1012, 912, 753, 696, 661 cm^{-1}. **HRMS** *calcd*. for ($C_{15}H_{13}NNaO_2$) $[M+Na]^+$: 262.0851, *found* 262.0838

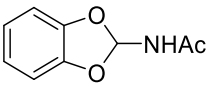

***N*-(benzo[d][1,3]dioxol-2-yl)acetamide (3d)** An oven-dried 20 mL reaction tube containing a stir bar was charged with $Ni(ClO_4)_2 \cdot 2$Bathocuproine (39 mg, 10 mol%). The reaction tube was connected to a vacuum line where it was evacuated and backfilled with Ar at least three times. Then anhydrous pivalonitrile (1.0 mL) was added and the mixture was stirred at r.t. for 5 minutes under Ar flow before adding 1,3-benzodioxole (488 mg, 4.0 mmol), **2b** (0.4 mmol, 1.0 equiv) and $PhSiH_3$ (9.9 μL, 20 mol%) sequentially. The tube was sealed under Ar atmosphere and stirred at r.t. for 24 h. The reaction mixture was quenched with air and diluted with EtOAc, then concentrated in vacuo. The residue was purified by flash column chromatography to give the title compound as a colorless oil (34 mg, 48% yield). **^{1}H NMR** (500 MHz, $CDCl_3$) δ 7.50 (d, J = 8.6 Hz, 1H), 6.85 (m, 4H),

6.67 (s, 1H), 2.05 (s, 3H). **^{13}C NMR** (126 MHz, $CDCl_3$) δ 169.91, 145.70, 122.17, 108.94, 105.55, 23.60. **IR (neat):** 3275, 1739, 1680, 1601, 1511, 1469, 1370, 1187, 1096, 745 cm^{-1}. **HRMS** *calcd*. for ($C_9H_9NNaO_3$) $[M+Na]^+$: 202.0475, *found* 202.0473

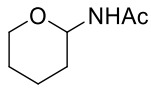

***N*-(tetrahydro-2H-pyran-2-yl)acetamide (3e)** An oven-dried 20 mL reaction tube containing a stir bar was charged with $Ni(ClO_4)_2$·2Bathocuproine (39 mg, 10 mol%) The reaction tube was connected to a vacuum line where it was evacuated and backfilled with Ar at least three times. Then anhydrous pivalonitrile (1.0 mL) was added and the mixture was stirred at r.t. for 5 minutes under Ar flow before adding tetrahydropyran (391 μL, 4.0 mmol), **2b** (0.4 mmol, 1.0 equiv). and $PhSiH_3$ (9.9 μL, 20 mol%) sequentially. The tube was sealed under Ar atmosphere and stirred at r.t. for 26 h. The reaction mixture was quenched with air and diluted with EtOAc, then concentrated in vacuo. The residue was purified by flash column chromatography to give the title compound as a colorless oil (21 mg, 36% yield). **^{1}H NMR** (500 MHz, $CDCl_3$) δ 6.13 – 5.96 (m, 1H), 5.09 (m, 1H), 3.98 – 3.92 (m, 1H), 3.67 – 3.53 (m, 1H), 1.99 (s, 3H), 1.88 (m, 1H), 1.77 (dq, *J* = 12.8, 3.3 Hz, 1H), 1.64 – 1.47 (m, 3H), 1.36 (m, 1H). **^{13}C NMR** (101 MHz, $CDCl_3$) δ 169.77, 77.82, 67.50, 31.62, 25.15, 23.54, 22.96. **IR (neat):** 3293, 2940, 2853, 1663, 1540, 1440, 1367, 1207, 1078, 1034 cm^{-1}. **HRMS** *calcd*. for ($C_7H_{13}NNaO_2$) $[M+Na]^+$: 166.0838, *found* 166.0843.

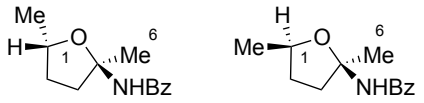

3f **3fa**

d.r. 2:1

***N*-((2R,5S)-2,5-dimethyltetrahydrofuran-2-yl)benzamide (3f)** An oven-dried 20 mL reaction tube containing a stir bar was charged with $Ni(ClO_4)_2$·2Bathocuproine (39 mg, 10 mol%), **2a** (0.4 mmol, 1.0 equiv). The reaction tube was connected to a vacuum line

where it was evacuated and backfilled with Ar at least three times. Then anhydrous pivalonitrile (1.0 mL) was added and the mixture was stirred at r.t. for 5 minutes under Ar flow before adding 2,5-dimethyltetrahydrofuran (480 μL, 5.0 mmol) and $PhSiH_3$ (7.4 μL, 15 mol%) sequentially. The tube was sealed under Ar atmosphere and stirred at r.t. for 24 h. The reaction mixture was quenched with air and diluted with EtOAc, then concentrated in vacuo. The residue was purified by flash column chromatography to give the title compound as a white solid (18 mg, 21% yield, d.r. 2:1, **3f**:**3fa**). **M.P.** 95 °C. **^{1}H NMR** (400 MHz, $CDCl_3$) δ 7.73 (m, 2H), 7.52 – 7.45 (m, 1H), 7.45 – 7.37 (m, 2H), 6.37 (s, 0.58H), 6.28 (s, 0.33H), 4.42 – 4.29 (m, 0.61H), 4.21 (m, 0.37H), 2.87 (m, 0.35H), 2.78 – 2.65 (m, 0.63H), 2.20 – 1.88 (m, 2H), 1.70 (d, 3H), 1.65 – 1.54 (m, 1H), 1.34 (d, *J* = 6.1 Hz, 1.1H), 1.26 (d, *J* = 6.1 Hz, 2.1H). **^{13}C NMR** (101 MHz, CDCl3) δ 166.34, 165.69, 135.06, 135.04, 131.53, 128.66, 128.63, 126.92, 126.90, 93.98, 93.83, 76.84, 76.29, 37.47, 37.13, 33.24, 32.97, 26.93, 26.20, 22.30, 21.43. **IR (neat):** 3364, 2969, 1656, 1617, 1577, 1376, 1299, 1211, 728, 626 cm^{-1}. **HRMS** *calcd*. for ($C_{13}H_{17}NNaO_2$) $[M+Na]^+$: 242.1151, *found* 242.1159. The relative stereochemistry of **3f** and **3fa** were corroborated by *NOESY* experiments (as indicated on the compound structure). *NOE* was observed between C_1-H and C_6-H for **3fa**, *NOE* was not observed between C_1-H and C_6-H for **3f**.

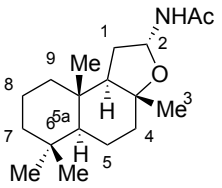

***N*-((3aR,5aS,9aS,9bR)-3a,6,6,9a-tetramethyldodecahydronaphtho[2,1-b]furan-2-yl)acetamide (3g)** An oven-dried 20 mL reaction tube containing a stir bar was charged with $Ni(ClO_4)_2$·2Bathocuproine (39 mg, 10 mol%) and (-)-Ambroxide (946 mg, 4.0 mmol). The reaction tube was connected to a vacuum line where it was evacuated and backfilled with Ar at least three times. Then anhydrous pivalonitrile (2.0 mL) was added and the mixture was stirred at r.t. for 5 minutes under Ar flow before adding **2b** (0.4 mmol, 1.0 equiv) and $PhSiH_3$ (9.9 μL, 20 mol%) sequentially. The tube was sealed under Ar

atmosphere and stirred at r.t. for 24 h. The reaction mixture was quenched with air and diluted with EtOAc, then concentrated in vacuo. The residue was purified by flash column chromatography to give the title compound as a white solid (85 mg, 73% yield, d.r. 5:4). **M.P.** 162 °C. **^{1}H NMR** (400 MHz, $CDCl_3$) δ 6.21 (d, *J* = 8.5 Hz, 0.58H), 6.14 (d, *J* = 8.7 Hz, 0.40H), 5.76 (td, *J* = 8.0, 1.4 Hz, 0.57H), 5.73 – 5.64 (m, 0.42H), 2.17 – 2.04 (m, 1H), 1.95 (m, 4H), 1.73 (m, 1H), 1.69 – 1.57 (m, 1H), 1.57 – 1.36 (m, 6H), 1.35 – 1.08 (m, 4H), 0.97 (m, 3H), 0.90 – 0.75 (m, 9H). **^{13}C NMR** (101 MHz, $CDCl_3$) δ 170.14, 169.41, 82.09, 81.21, 80.05, 79.22, 60.39, 58.83, 57.50, 56.96, 42.49, 42.40, 40.11, 40.02, 39.90, 39.89, 36.19, 36.17, 33.62, 33.52, 33.17, 33.14, 30.82, 30.44, 24.24, 23.56, 23.52, 22.03, 21.15, 21.13, 20.66, 20.59, 18.39, 15.49, 15.04. **IR (neat):** 3282, 2939, 1654, 1546, 1444, 1376, 1280, 1154, 1033, 998, 975, 941 cm^{-1}. **HRMS** *calcd*. for ($C_{18}H_{31}NNaO_2$) $[M+Na]^+$: 316.2247, *found* 316.2253. The relative stereochemistry of **3g** (major one, as indicated on the compound structure) were corroborated by *NOESY* experiments. *NOE* was observed between C_2-H and C_3-H for major product, *NOE* was observed between N-H and C_3-H for minor product.

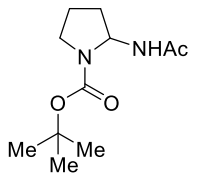

***tert*-butyl 2-acetamidopyrrolidine-1-carboxylate (3h)** An oven-dried 20 mL reaction tube containing a stir bar was charged with $Ni(ClO_4)_2 \cdot 2$Bathocuproine (39 mg, 10 mol%). The reaction tube was connected to a vacuum line where it was evacuated and backfilled with Ar at least three times. Then anhydrous pivalonitrile (1.0 mL) was added and the mixture was stirred at r.t. for 5 minutes under Ar flow before adding *tert*-butyl pyrrolidine-1-carboxylate (140 μL, 0.8 mmol), **2b** (0.4 mmol, 1.0 equiv) and $PhSiH_3$ (9.9 μL, 20 mol%) sequentially. The tube was sealed under Ar atmosphere and stirred at r.t. for 10 h. The reaction mixture was quenched with air and diluted with EtOAc, then concentrated in vacuo. The residue was purified by flash column chromatography to give the title

compound as a white solid (75 mg, 82% yield). **M.P.** 113 °C. **^{1}H NMR** (400 MHz, $CDCl_3$) δ 5.91 (d, *J* = 6.7 Hz, 1H), 5.62 (s, 1H), 3.43 (dt, *J* = 10.6, 5.4 Hz, 1H), 3.25 (q, *J* = 8.7 Hz, 1H), 1.93 (m, 7H), 1.42 (s, 9H). **^{13}C NMR** (101 MHz, $CDCl_3$) δ 168.98, 154.21, 80.18, 64.06, 46.00, 33.88, 28.49, 23.39, 22.49. **IR (neat):** 3253, 2976, 1649, 1541, 1387, 1162, 1109 cm^{-1}. **HRMS** *calcd*. for ($C_{11}H_{20}N_2NaO_3$) $[M+Na]^+$: 251.1366, *found* 251.1368.

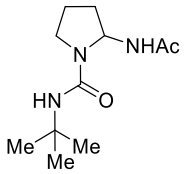

2-acetamido–N-(*tert*-butyl)pyrrolidine-1-carboxamide (3i) An oven-dried 20 mL reaction tube containing a stir bar was charged with $Ni(ClO_4)_2$·2Bathocuproine (39 mg, 10 mol%), *N*-(*tert*-butyl)pyrrolidine-1-carboxamide (153 mg, 0.8 mmol). The reaction tube was connected to a vacuum line where it was evacuated and backfilled with Ar at least three times. Then anhydrous pivalonitrile (1.0 mL) was added and the mixture was stirred at r.t. for 5 minutes under Ar flow before adding **2b** (0.4 mmol, 1.0 equiv) and $PhSiH_3$ (9.9 μL, 20 mol%) sequentially. The tube was sealed under Ar atmosphere and stirred at r.t. for 10 h. The reaction mixture was quenched with air and diluted with EtOAc, then concentrated in vacuo. The residue was purified by flash column chromatography to give the title compound as a white solid (67 mg, 74% yield). **M.P.** 159 °C. **^{1}H NMR** (500 MHz, $CDCl_3$) δ 6.99 (d, *J* = 9.4 Hz, 1H), 6.31 (s, 1H), 5.56 (m, 1H), 3.50 – 3.38 (m, 1H), 3.34 (m, 1H), 2.15 (m, 1H), 1.98 (s, 3H), 1.91 – 1.76 (m, 3H), 1.30 (s, 9H). **^{13}C NMR** (126 MHz, $CDCl_3$) δ 171.26, 156.28, 62.15, 50.74, 45.87, 33.82, 29.44, 23.19, 22.60. **IR (neat):** 3277, 3065, 2970, 1738, 1671, 1627, 1576, 1365, 1218 cm^{-1}. **HRMS** *calcd*. for ($C_{11}H_{21}N_3NaO_2$) $[M+Na]^+$: 250.1526, *found* 250.1536.

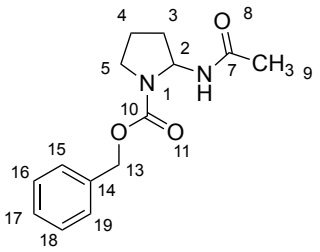

benzyl 2-acetamidopyrrolidine-1-carboxylate (3j) An oven-dried 20 mL reaction tube containing a stir bar was charged with $Ni(ClO_4)_2 \cdot 2$Bathocuproine (39 mg, 10 mol%). The reaction tube was connected to a vacuum line where it was evacuated and backfilled with Ar at least three times. Then anhydrous pivalonitrile (1.0 mL) was added and the mixture was stirred at r.t. for 5 minutes under Ar flow before adding benzyl pyrrolidine-1-carboxylate (164 mg, 0.8 mmol), **2b** (0.4 mmol, 1.0 equiv) and $PhSiH_3$ (9.9 μL, 20 mol%) sequentially. The tube was sealed under Ar atmosphere and stirred at r.t. for 24 h. The reaction mixture was quenched with air and diluted with EtOAc, then concentrated in vacuo. The residue was purified by flash column chromatography to give the title compound as a white solid (54 mg, 52% yield, 1.5:1 mixture of rotamers, A:B). **M.P.** 82 °C. **^{1}H NMR** (500 MHz, $CDCl_3$) δ 7.23 (m, 5H), 6.23 (br. s, 0.56H, N-H, A), 6.14 (br. s, 0.35H, N-H, B), 5.73 (s, 0.54H, C_2-H, A), 5.56 (br. s, 0.37H, C_2-H, B), 5.31 – 4.96 (m, 2H), 3.49 (s, 1H), 3.32 (t, J = 8.9 Hz, 1H), 2.12 – 1.75 (m, 7H). **^{13}C NMR** (126 MHz, $CDCl_3$) δ 169.67 (C_7, B), 169.15 (C_7, A), 154.59 (C_{10}), 136.53, 128.52, 128.09, 127.93, 66.95 (C_{13}), 65.53 (C_2, B), 64.03 (C_2, A), 46.51(C_5), 33.87 (C_3, A), 32.60 (C_3, B), 23.22 ((C9), (C_4, B)), 22.27 (C_4, A). **IR (neat):** 3244, 3062, 2971, 2990, 1695, 1637, 1551, 1407, 1359, 1338, 1284, 1189,1117, 995, 772, 733, 696 cm^{-1}. **HRMS** *calcd*. for ($C_{14}H_{18}N_2NaO_3$) $[M+Na]^+$: 285.1210, *found* 285.1221.

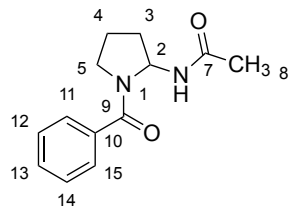

***N*-(1-benzoylpyrrolidin-2-yl)acetamide (3k)** An oven-dried 20 mL reaction tube containing a stir bar was charged with $Ni(ClO_4)_2 \cdot 2$Bathocuproine (39 mg, 10 mol%). The reaction tube was connected to a vacuum line where it was evacuated and backfilled with Ar at least three times. Then anhydrous pivalonitrile (1.0 mL) was added and the mixture was stirred at r.t. for 5 minutes under Ar flow before adding phenyl(pyrrolidin-1-yl)methanone (140 mg, 0.8 mmol), **2b** (0.4 mmol, 1.0 equiv) and $PhSiH_3$ (9.9 μL, 20 mol%) sequentially. The tube was sealed under Ar atmosphere and stirred at r.t. for 24 h. The reaction mixture was quenched with air and diluted with EtOAc, then concentrated in vacuo. The residue was purified by flash column chromatography to give the title compound as a white solid (73 mg, 79% yield, 1:1 mixture of rotamers, A:B). **M.P.** 156 °C. **^{1}H NMR** (400 MHz, $CDCl_3$) δ 7.65 – 7.28 (m, 5H), 7.11 (s, 0.46H, N-H, A) 6.81 (s, 0.44H, N-H, B), 5.56 (s, 1H), 3.89 – 3.25 (m, 2H), 2.21 (m, 1H), 2.05 – 1.82 (m, 4H), 1.69 (m, 2H). **^{13}C NMR** (126 MHz, $CDCl_3$) δ 170.46 (C_7, A), 168.62 (C_7, B), 136.42 (C_9), 130.36, 128.42, 127.41, 126.53, 66.05 (C_2, B), 65.57 (C_2, A), 50.33 (C_5, A), 46.26 (C_5, B), 34.17 (C_3, B), 30.74 (C_3, A), 24.85 (C_8, A), 23.58 (C_8, B), 22.72 (C_4, B), 21.38 (C_4, A). **IR (neat):** 3294, 2971, 2886, 1738, 1673, 1611, 1524, 1425, 1372, 1275, 1191, 785, 740, 701, 635, 600, 577 cm^{-1}. **HRMS** *calcd*. for ($C_{13}H_{15}N_2O_2$) $[M-H]^-$: 231.1139, *found* 231.1137.

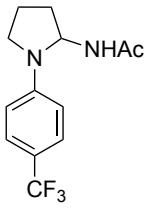

***N*-(1-(4-(trifluoromethyl)phenyl)pyrrolidin-2-yl)acetamide (3l)** An oven-dried 20 mL reaction tube containing a stir bar was charged with $Ni(ClO_4)_2 \cdot 2$Bathocuproine (39 mg, 10 mol%), 1-(4-(trifluoromethyl)phenyl)pyrrolidine (430 mg, 2.0 mmol). The reaction tube was connected to a vacuum line where it was evacuated and backfilled with Ar at least three times. Then anhydrous pivalonitrile (1.0 mL) was added and the mixture was stirred at r.t. for 5 minutes under Ar flow before adding **2b** (0.4 mmol, 1.0 equiv) and

$PhSiH_3$ (9.9 μL, 20 mol%) sequentially. The tube was sealed under Ar atmosphere and stirred at r.t. for 24 h. The reaction mixture was quenched with air and diluted with EtOAc, then concentrated in vacuo. The residue was purified by flash column chromatography to give the title compound as a white solid (62 mg, 57% yield). **M.P.** 175 °C. **^{1}H NMR** (500 MHz, $CDCl_3$) δ 7.45 (d, *J* = 8.4 Hz, 1H), 6.68 (d, *J* = 8.3 Hz, 1H), 5.71 (m, 2H), 3.52 (m, 1H), 3.21 (m, 1H), 2.23 – 1.99 (m, 4H), 1.97 (s, 3H). **^{13}C NMR** (126 MHz, $CDCl_3$) δ 169.62, 147.95, 126.74 (q, *J* = 3.7 Hz), 125.08 (q, *J* = 270.3 Hz), 119.22 (q, *J* = 32.5 Hz), 112.16, 65.58, 47.84, 34.19, 23.50, 22.83. **^{19}F NMR** (282 MHz, $CDCl_3$) δ -61.06. **IR (neat):** 3237, 3049, 2980, 2866, 1631, 1614, 1550, 1525, 1371, 1320, 1286, 1203, 1156, 1101, 1068, 982, 837, 810, 759, 600 cm^{-1}. **HRMS** *calcd*. for ($C_{13}H_{14}F_3N_2O$) $[M-H]^-$: 271.1064, *found* 271.1058.

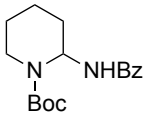

***tert*-butyl 2-benzamidopiperidine-1-carboxylate (3m)** An oven-dried 20 mL reaction tube containing a stir bar was charged with $Ni(ClO_4)_2 \cdot 2$Bathocuproine (39 mg, 10 mol%), **2a** (0.4 mmol, 1.0 equiv). The reaction tube was connected to a vacuum line where it was evacuated and backfilled with Ar at least three times. Then anhydrous pivalonitrile (1.0 mL) was added and the mixture was stirred at r.t. for 5 minutes under Ar flow before adding *tert*-butyl piperidine-1-carboxylate (370 mg, 2.0 mmol) and $PhSiH_3$ (9.9 μL, 20 mol%) sequentially. The tube was sealed under Ar atmosphere and stirred at r.t. for 24 h. The reaction mixture was quenched with air and diluted with EtOAc, then concentrated in vacuo. The residue was purified by flash column chromatography to give the title compound as a white solid (45 mg, 37% yield). **M.P.** 122 °C. **^{1}H NMR** (500 MHz, $CDCl_3$) δ 7.77 – 7.70 (m, 2H), 7.53 – 7.46 (m, 1H), 7.45 – 7.37 (m, 2H), 6.68 (s, 1H), 6.30 – 6.17 (m, 1H), 3.96 (d, *J* = 13.8 Hz, 1H), 2.96 (t, *J* = 12.5 Hz, 1H), 1.99 – 1.90 (m, 1H), 1.81 – 1.65 (m, 3H), 1.63 – 1.48 (m, 2H), 1.46 (s, 9H). **^{13}C NMR** (126 MHz, $CDCl_3$) δ 166.43, 154.87, 134.79, 131.66, 128.72, 127.00, 80.57, 58.94, 40.45, 29.78, 28.43, 24.90, 19.35.

IR (neat): 3309, 2932, 1636, 1522, 1487, 1365, 1313, 1262, 1159, 1029, 998, 867, 722, 692 cm^{-1}. **HRMS** *calcd*. for ($C_{17}H_{24}N_2NaO_3$) $[M+Na]^+$: 327.1679, *found* 327.1685.

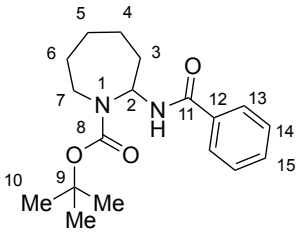

***tert*-butyl 2-benzamidoazepane-1-carboxylate (3n)** An oven-dried 20 mL reaction tube containing a stir bar was charged with $Ni(ClO_4)_2$·2Bathocuproine (39 mg, 10 mol%), **2a** (0.4 mmol, 1.0 equiv). The reaction tube was connected to a vacuum line where it was evacuated and backfilled with Ar at least three times. Then anhydrous pivalonitrile (1.0 mL) was added and the mixture was stirred at r.t. for 5 minutes under Ar flow before adding *tert*-butyl azepane-1-carboxylate (398 mg, 2.0 mmol) and $PhSiH_3$ (9.9 μL, 20 mol%) sequentially. The tube was sealed under Ar atmosphere and stirred at r.t. for 12 h. The reaction mixture was quenched with air and diluted with EtOAc, then concentrated in vacuo. The residue was purified by flash column chromatography to give the title compound as a white solid (100 mg, 79% yield, 5:4 mixture of rotamers, A:B). **M.P.** 124 °C. **^{1}H NMR** (500 MHz, $CDCl_3$) δ 7.83 – 7.67 (m, 2H), 7.61 (d, *J* = 8.4 Hz, 0.63H, N-H, A), 7.46 (t, *J* = 7.4 Hz, 1H), 7.39 (t, *J* = 7.5 Hz, 2H), 6.58 (br. s, 0.41H, N-H, B), 5.84 (br. s, 0.41H, C_2-H, B), 5.47 (br. s, 0.55H, C_2-H, A), 3.69 (m, 1H), 3.20 (m, 1H), 2.36 – 2.09 (m, 1H), 1.45 (m, 16H). **^{13}C NMR** (126 MHz, $CDCl_3$) δ 166.46 (C_{11}, A), 166.26 (C_{11}, B), 155.84 (C_8, A), 155.22 (C_8, B), 134.71 (C_{12}, B), 134.53 (C_{12}, A), 131.55 (C_{15}), 128.65 (C_{14}, B), 128.55 (C_{14}, A), 127.23 (C_{14}, A), 126.95 (C_{13}, B), 80.49 (C_9, B), 79.97 (C_9, A), 65.33 (C_2, A), 63.82 (C_2, B), 47.45 (C_7, A), 43.77 (C_7, B), 34.25 (C_3, B), 32.38 (C_3, A), 29.74 (C_6, A), 29.51 (C_6, B), 28.53 (C10), 28.38 (C_4, B), 26.27 (C_4, A), 25.17 (C_5, A), 24.61 (C_5, B). **IR (neat):** 3310, 2978, 2930, 2862, 1688, 1643, 1536, 1490, 1402, 1365, 1343, 1315, 1286, 1162, 1072, 984, 883, 695, 666 cm^{-1}. **HRMS** *calcd*. for ($C_{18}H_{26}N_2NaO_3$) $[M+Na]^+$: 341.1836, *found* 341.1840.

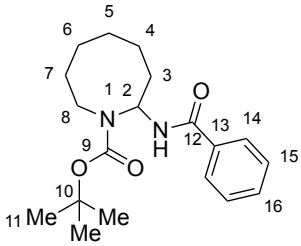

***tert*-butyl 2-benzamidoazocane-1-carboxylate (3o)** An oven-dried 20 mL reaction tube containing a stir bar was charged with $Ni(ClO_4)_2 \cdot 2$Bathocuproine (39 mg, 10 mol%), **2a** (0.4 mmol, 1.0 equiv). The reaction tube was connected to a vacuum line where it was evacuated and backfilled with Ar at least three times. Then anhydrous pivalonitrile (1.0 mL) was added and the mixture was stirred at r.t. for 5 minutes under Ar flow before adding *tert*-butyl azocane-1-carboxylate (426 mg, 2.0 mmol) and $PhSiH_3$ (9.9 μL, 20 mol%) sequentially. The tube was sealed under Ar atmosphere and stirred at r.t. for 20 h at r.t., the reaction mixture was quenched with air and diluted with EtOAc, then concentrated in vacuo. The residue was purified by flash column chromatography to give the title compound as a white solid (95 mg, 72% yield, 2:1 mixture of rotamers, A:B). **M.P.** 118 °C. **^{1}H NMR** (400 MHz, $CDCl_3$) δ 7.81 – 7.70 (m, 2H), 7.67 (d, J = 7.6 Hz, 0.61H, N-H, A), 7.52 – 7.42 (m, 1H), 7.39 (td, J = 8.1, 1.6 Hz, 2H), 6.93 (d, J = 7.9 Hz, 0.3H, N-H, B), 5.66 (br. s, 0.32H, C_2-H, B), 5.49 (m, 0.67H, C_2-H, A), 3.81 (m, 1H), 3.17 (m, 0.31H, C_8-Hb, B), 3.07 (m, 0.69H, C_8-Hb, A), 2.42 – 2.29 (m, 0.66H, C_3-Ha, B), 2.06 (m, 0.49H, C_3-Ha, B), 1.85 – 1.38 (m, 18H). **^{13}C NMR** (101 MHz, $CDCl_3$) δ 166.43 (C_{12}, A), 166.12 (C_{12}, B), 155.26 (C_9, A), 154.74 (C_9, B), 134.39 (C_{13}, A+B), 131.72 (C_{16}, B), 131.57 (C_{16}, A), 128.72 (C_{14}, B), 128.55 (C_{14}, A), 127.21 (C_{15}, A), 126.86 (C_{15}, B), 80.42 (C_{10}, B), 79.88 (C_{10}, A), 64.41 (C_2, A), 62.55 (C_2, B), 49.52 (C_8, A+B), 33.14 (C_3, B), 32.17 (C_3, A), 28.79 (C_{11}, B), 28.55 (C_{11}, A), 26.96 (C_7, B), 26.87 (C_7, A), 26.67 (C_4, A), 26.56 (C_4, B), 26.12 (C_6, A+B), 24.32 (C_5, A), 24.01 (C_5, B). **IR (neat):** 3329, 2971, 2933, 2856, 1678, 1638, 1540, 1466, 1407, 1366, 1345, 1318, 1287, 1216, 1154, 1133, 1033, 1017, 953, 723, 692, 656, 586 cm^{-1}. **HRMS** *calcd*. for ($C_{19}H_{28}N_2NaO_3$) $[M+Na]^+$: 355.1992, *found* 355.1993.

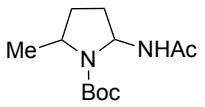

***tert*-butyl 2-acetamido-5-methylpyrrolidine-1-carboxylate (3p)** An oven-dried 20 mL reaction tube containing a stir bar was charged with $Ni(ClO_4)_2 \cdot 2$Bathocuproine (39 mg, 10 mol%). The reaction tube was connected to a vacuum line where it was evacuated and backfilled with Ar at least three times. Then anhydrous pivalonitrile (1.0 mL) was added and the mixture was stirred at r.t. for 5 minutes under Ar flow before adding *tert*-butyl 2-methylpyrrolidine -1-carboxylate (148 mg, 0.8 mmol), **2b** (0.4 mmol, 1.0 equiv) and $PhSiH_3$ (9.9 μL, 20 mol%) sequentially. The tube was sealed under Ar atmosphere and stirred at r.t. for 5 h. The reaction mixture was quenched with air and diluted with EtOAc, then concentrated in vacuo. The residue was purified by flash column chromatography to give the title compound as a colorless oil (56 mg, 58% yield, 1:1 d.r. (A:B, 1:1), 1:1 mixture of rotamers (A1:A2 and B1:B2)). **^{1}H NMR** (500 MHz, $CDCl_3$) δ 6.14 – 5.83 (m, 1H), 5.70 – 5.45 (m, 1H), 4.01 – 3.84 (m, 0.47H), 3.80 – 3.69 (m, 0.51H), 2.24 (s, 0.54H), 2.00 (m, 2H), 1.92 (s, 1.5H), 1.90 (s, 1.5H),1.78 (d, J = 11.6 Hz, 0.47H), 1.59 – 1.48 (m, 1H), 1.41 (s, 9H), 1.26 (d, J = 6.2 Hz, 1.5H), 1.10 (d, J = 6.3 Hz, 1.5H). **^{13}C NMR** (101 MHz, $CDCl_3$) δ 169.28, 168.72, 154.47, 153.36, 80.09, 79.94, 66.20, 64.94, 63.80, 54.23, 54.03, 53.41, 52.90, 31.89, 31.33, 30.16, 29.97, 29.15, 28.49, 28.45, 23.39, 23.23, 21.82, 19.99, 19.16. **IR (neat):** 3295, 2973, 1655, 1541, 1366, 1167, 1134, 910, 729 cm^{-1}. **HRMS** *calcd*. for ($C_{12}H_{22}N_2NaO_3$) $[M+Na]^+$: 265.1523, *found* 265.1531.

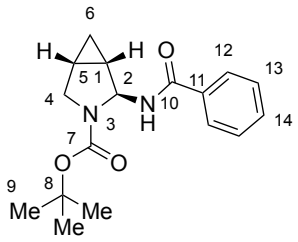

***tert*-butyl (1*S*,2*S*,5*R*)-2-benzamido-3-azabicyclo[3.1.0]hexane-3-carboxylate (3q)** An oven-dried 20 mL reaction tube containing a stir bar was charged with

$Ni(ClO_4)_2 \cdot 2$Bathocuproine (39 mg, 10 mol%), **2a** (0.4 mmol, 1.0 equiv). The reaction tube was connected to a vacuum line where it was evacuated and backfilled with Ar at least three times. Then anhydrous pivalonitrile (1.0 mL) was added and the mixture was stirred at r.t. for 5 minutes under Ar flow before adding *tert*-butyl (1*R*,5*S*)-3-azabicyclo[3.1.0]hexane-3-carboxylate (366 mg, 2.0 mmol) and $PhSiH_3$ (9.9 μL, 20 mol%) sequentially. The tube was sealed under Ar atmosphere and stirred at r.t. for 24 h. The reaction mixture was quenched with air and diluted with EtOAc, then concentrated in vacuo. The residue was purified by flash column chromatography to give the title compound as a white solid (70 mg, 58% yield, 10:1 d.r. (A:B, 10:1), 3:1 mixture of rotamers (A1:A2 3:1), 5:3 mixture of rotamers for B (B1:B2, 5:3)).[7] **M.P.** 153 °C. **^{1}H NMR** (300 MHz, $CDCl_3$) δ 7.85 – 7.79 (m, 0.25H, B), 7.79 – 7.69 (m, 1.70H, A), 7.57 – 7.34 (m, 3H), 6.65 (br, s, 0.19H, N-H, A2), 6.44 (d, J = 8.2 Hz, 0.6H, N-H, A1), 5.92 (d, J = 8.2 Hz, 0.6H, C_2-H, A1), 5.63 (s, 0.2H, C_2-H, A2), 5.42 (s, 0.05H, C_2-H, B1), 5.32 (s, 0.03H, C_2-H, B2), 3.68 – 3.48 (m, 1.83H, C_4-H, A), 3.39 (m, 0.11H, C_4-H, B) 1.75 – 1.51 (m, 2H), 1.39 (m, 9H), 0.76 (td, J = 7.9, 5.4 Hz, 0.85H, C_6-Hb, A), 0.66 (m, 0.14H, C_6-Hb, B), 0.33 – 0.15 (m, 0.79H, C_6-Ha, A), 0.12 (m, 0.11H, C_6-Ha, B). **^{13}C NMR** (126 MHz, $CDCl_3$) δ 167.18 (C_{10}, A2), 166.53 (C_{10}, A1), 154.38 (C_7, A1+A2), 134.63 (C_{11}, A1+A2), 131.64 (C_{14}, A1+A2), 128.68 (C_{13}, A1), 128.51 (C_{13}, A2), 127.18 (C_{12}, A2), 127.01 (C_{12}, A1), 80.56 (C_8, A1), 80.26 (C_8, A2), 67.19 (C_2, A2), 65.82 (C_2, A1), 48.73 (C_4, A2), 47.40 (C_2, A1), 28.47 (C_9, A2), 28.45 (C_9, A1), 22.26 (C_1, A1), 21.37 (C_1, A2), 15.99 (C_5, A2), 14.57 (C_5, A1), 8.76 (C_2, A1+A2). **IR (neat):** 3388, 3289, 2987, 2887, 1653, 1528, 1397, 1366, 1319, 1276, 1167, 1126, 905, 818, 779, 693 cm^{-1}. **HRMS** *calcd.* for ($C_{17}H_{22}N_2NaO3$) $[M+Na]^+$: 325.1523, *found* 325.1524. The relative stereochemistry of the major diastereomer A of the title compound was corroborated by *NOESY* experiments (as indicated on the compound structure). *NOE* was observed between C_6-Ha and C_2-H.

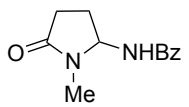

***N*-(1-methyl-5-oxopyrrolidin-2-yl)benzamide (3r)** An oven-dried 20 mL reaction tube containing a stir bar was charged with $Ni(ClO_4)_2$·2Bathocuproine (39 mg, 10 mol%), **2a** (0.4 mmol, 1.0 equiv). The reaction tube was connected to a vacuum line where it was evacuated and backfilled with Ar at least three times. Then anhydrous pivalonitrile (1.0 mL) was added and the mixture was stirred at r.t. for 5 minutes under Ar flow before adding 1-methylpyrrolidin-2-one (193 μL, 2.0 mmol) and $PhSiH_3$ (9.9 μL, 20 mol%) sequentially. The tube was sealed under Ar atmosphere and stirred at r.t. for 5 h. The reaction mixture was quenched with air and diluted with EtOAc, then concentrated in vacuo. The residue was purified by flash column chromatography to give the title compound as a white solid (57 mg, 65% yield). **M.P.** 133 °C. **^{1}H NMR** (500 MHz, $CDCl_3$) δ 7.98 – 7.88 (m, 2H), 7.79 (d, *J* = 9.1 Hz, 1H), 7.52 – 7.46 (m, 1H), 7.41 (dd, *J* = 8.4, 7.0 Hz, 2H), 5.86 (dt, *J* = 8.7, 4.2 Hz, 1H), 2.78 (s, 3H), 2.47 (dq, *J* = 13.8, 7.0 Hz, 2H), 2.32 (dq, *J* = 15.7, 7.9 Hz, 1H), 1.95 (td, *J* = 12.3, 8.0 Hz, 1H). **^{13}C NMR** (126 MHz, $CDCl_3$) δ 167.57, 133.42, 132.06, 128.62, 127.44, 66.20, 29.39, 27.44, 25.84. **IR (neat):** 3289, 1682, 1653, 1530, 1491, 1401, 1364, 1283, 1179, 1113, 1080, 993, 701, 664 cm^{-1}. **HRMS** *calcd*. for ($C_{12}H_{14}N_2NaO_2$) $[M+Na]^+$: 241.0947, *found* 241.0950.

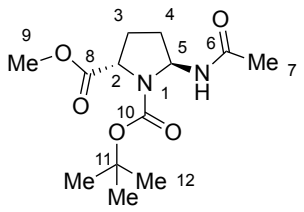

1-(*tert*-butyl) 2-methyl (2*S*,5*S*)-5-acetamidopyrrolidine-1,2-dicarboxylate (3s) An oven-dried 20 mL reaction tube containing a stir bar was charged with $Ni(ClO_4)_2$·2Bathocuproine (39 mg, 10 mol%). The reaction tube was connected to a vacuum line where it was evacuated and backfilled with Ar at least three times. Then anhydrous pivalonitrile (1.0 mL) was added and the mixture was stirred at r.t. for 5 minutes under Ar flow before adding 1-(*tert*-butyl) 2-methyl (*S*)-pyrrolidine-1,2-dicarboxylate (183 mg, 0.8 mmol), **2b** (0.4 mmol, 1.0 equiv) and $PhSiH_3$ (12.4 μL, 25 mol%) sequentially. The tube was sealed under Ar atmosphere and stirred at r.t. for 24 h.

The reaction mixture was quenched with air and diluted with EtOAc, then concentrated in vacuo. The residue was purified by flash column chromatography to give amidated product (72 mg, 63% yield, 4:1 d.r. (**3s**:**3sa**, 4:1)).[8] **3s:** 5:4 mixture of rotamers, A1:A2. Colorless oil.**^{1}H NMR** (500 MHz, $CDCl_3$) δ 5.99 (br. s, 0.46H, N-H, A2), 5.84 (br. s, 0.47H, N-H, A1), 5.81 (t, J = 6.4 Hz, 0.53H, C_5-H, A2), 5.62 (t, *J* = 6.2 Hz, 0.53H, C_5-H, A1), 4.37 (d, *J* = 8.0 Hz, 0.44H, C_2-H, A2), 4.32 (d, *J* = 8.9 Hz, 0.57H, C_2-H, A1), 3.71 (s, 3H), 2.46 – 2.11 (m, 2H), 2.09 – 1.93 (m, 4H), 1.87 (m, 1H), 1.43 (s, 4H, C_{12}-H, A2), 1.39 (s, 5H, C_{12}-H, A1). **^{13}C NMR** (126 MHz, $CDCl_3$) δ 173.18 (C_8, A1), 172.62 (C_8, A2), 169.93 (C_6, A2), 168.91 (C_6, A1), 153.84 (C_{12}, A1), 153.52 (C_{12}, A2), 81.23 (C_{11}, A2), 81.16 (C_{11}, A1), 66.05 (C_5, A2), 64.63 (C_5, A2), 60.06 (C_2, A1), 59.16 (C_2, A2), 52.38 (C_9, A2), 52.22 (C_9, A1), 32.06 (C_4, A2), 30.65 (C_4, A1), 28.42 (C_{12}, A2), 28.28 (C_{12}, A1), 28.11 (C_7, A1), 27.12 (C_7, A2), 23.57 (C_3, A1), 23.37 (C_3, A2). **IR (neat):** 3284, 2978, 1745, 1702, 1650, 1541, 1365, 1201, 1160, 1094 cm^{-1}. **HRMS** *calcd*. for ($C_{13}H_{22}N_2O_5$) $[M+Na]^+$: 309.1421, *found* 309.1425.

The relative stereochemistry of the major diastereomer **3s** was corroborated by *NOESY* experiments (as indicated on the compound structure). *NOE* was observed between C_2-Ha and N-H.

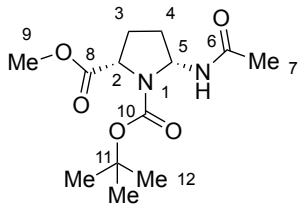

1-(*tert*-butyl) 2-methyl (2*S*,5*R*)-5-acetamidopyrrolidine-1,2-dicarboxylate. (3sa) 5:3 mixture of rotamers, B1:B2. **^{1}H NMR** (500 MHz, $CDCl_3$) δ 6.45 (s, 0.48H, N-H, B1), 6.24 (s, 0.28H, N-H, B2), 5.82 (t, *J* = 6.9 Hz, 0.56H, C_5-H, B1), 5.76 (br. s, 0.34H, C_5-H, B2), 4.38 (t, *J* = 7.0 Hz, 0.54H, C_2-H, B1), 4.26 (t, *J* = 8.2 Hz, 0.34H, C_5-H, B2), 3.78 (s, 3H), 2.38 – 2.02 (m, 2H), 2.01 – 1.75 (m, 5H), 1.43 (s, 5.53H, C_{12}-H, B1), 1.42 – 1.39 (s, 3.13H, C_{12}-H, B2). **^{13}C NMR** (126 MHz, $CDCl_3$) δ 175.49, 169.07, 153.31, 81.27, 65.59

(C_5, B2), 64.69 (C_5, B1), 59.52 (C_2, B2), 58.92 (C_2, B1), 52.76 (C_9, B1), 52.55 (C_9, B2), 33.11 (C_4, B1), 32.42 (C_4, B2), 28.43, 28.30, 27.67, 23.44. **IR (neat):** 3356, 2977, 1700, 1520, 1438, 1365, 1306, 1203, 1162, 1124 cm^{-1}. **HRMS** *calcd*. for ($C_{13}H_{22}N_2NaO_5$) $[M+Na]^+$: 309.1421, *found* 309.1423.

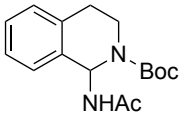

***tert*-butyl 1-acetamido-3,4-dihydroisoquinoline-2(1*H*)-carboxylate (3t)** An oven-dried 20 mL reaction tube containing a stir bar was charged with $Ni(ClO_4)_2$·2Bathocuproine (39 mg, 10 mol%). The reaction tube was connected to a vacuum line where it was evacuated and backfilled with Ar at least three times. Then anhydrous pivalonitrile (1.0 mL) was added and the mixture was stirred at r.t. for 5 minutes under Ar flow before adding *tert*-butyl 3,4-dihydroisoquinoline-2(1*H*)-carboxylate (187 mg, 0.8 mmol), **2b** (0.4 mmol, 1.0 equiv) and $PhSiH_3$ (9.9 μL, 20 mol%) sequentially. The tube was sealed under Ar atmosphere and stirred at r.t. for 2 h. The reaction mixture was quenched with air and diluted with EtOAc, then concentrated in vacuo. The residue was purified by flash column chromatography to give the title compound as a white solid (105 mg, 91% yield). **M.P.** 161 °C. **^{1}H NMR** (500 MHz, $CDCl_3$) δ 7.32 – 7.26 (m, 1H), 7.21 – 7.14 (m, 2H), 7.11 – 7.04 (m, 1H), 6.92 (d, J = 8.6 Hz, 1H), 6.70 (d, J = 8.6 Hz, 1H), 4.17 (s, 1H), 3.13 (s, 1H), 2.86 (m, 1H), 2.66 (dt, J = 16.2, 3.2 Hz, 1H), 1.90 (s, 3H), 1.44 (s, 9H). **^{13}C NMR** (101 MHz, $CDCl_3$) δ 168.74, 154.29, 134.89, 134.74, 128.67, 128.07, 127.83, 126.76, 80.77, 58.45, 37.58, 28.63, 28.37, 23.32. **IR (neat):** 3243, 2975, 2925, 1709, 1691, 1650, 1542, 1414, 1366, 1334, 1234, 1154, 1119, 1063, 1043, 931, 891, 772, 742 cm^{-1}. **HRMS** *calcd*. for ($C_{16}H_{22}N_2NaO_3$) $[M+Na]^+$: 313.1523, *found* 313.1534.

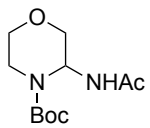

***tert*-butyl 3-acetamidomorpholine-4-carboxylate (3u)** An oven-dried 20 mL reaction tube containing a stir bar was charged with $Ni(ClO_4)_2 \cdot 2$Bathocuproine (39 mg, 10 mol%), *tert*-butyl morpholine-4-carboxylate (150 mg, 0.8 mmol). The reaction tube was connected to a vacuum line where it was evacuated and backfilled with Ar at least three times. Then anhydrous pivalonitrile (1.0 mL) was added and the mixture was stirred at r.t. for 5 minutes under Ar flow before adding **2b** (0.4 mmol, 1.0 equiv) and $PhSiH_3$ (9.9 μL, 20 mol%) sequentially sequentially. The tube was sealed under Ar atmosphere and stirred at r.t. for 24 h. The reaction mixture was quenched with air and diluted with EtOAc, then concentrated in vacuo. The residue was purified by flash column chromatography to give the title compound as a white solid (68 mg, 70% yield). **M.P.** 113 °C. **^{1}H NMR** (500 MHz, $CDCl_3$) δ 6.46 (d, *J* = 8.5 Hz, 1H), 5.94 (dt, *J* = 8.5, 1.8 Hz, 1H), 3.89 (dd, *J* = 11.5, 3.8 Hz, 1H), 3.83 – 3.70 (m, 2H), 3.61 (dd, *J* = 11.7, 2.4 Hz, 1H), 3.52 (m, 1H), 3.12 (m, 1H), 1.98 (s, 3H), 1.46 (s, 9H). **^{13}C NMR** (126 MHz, $CDCl_3$) δ 169.16, 154.01, 80.66, 70.21, 66.64, 56.61, 39.07, 28.02, 22.83. **IR (neat):** 3261, 2973, 2862, 1704, 1653, 1543, 1397, 1365, 1299, 1267, 1227, 1160, 1117, 1101, 1078, 1012, 862, 746, 648 cm^{-1}. **HRMS** *calcd.* for ($C_{11}H_{20}N_2NaO_4$) $[M+Na]^+$: 267.1315, *found* 267.1318.

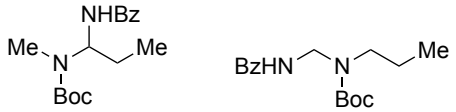

3v **3va**

r.r. 1.4:1

***tert*-butyl (1-benzamidopropyl)(methyl)carbamate (3v)**. An oven-dried 20 mL reaction tube containing a stir bar was charged with $Ni(ClO_4)_2 \cdot 2$Bathocuproine (39 mg, 10 mol%), **2a** (0.4 mmol, 1.0 equiv). The reaction tube was connected to a vacuum line where it was evacuated and backfilled with Ar at least three times. Then anhydrous pivalonitrile (1.0 mL) was added and the mixture was stirred at r.t. for 5 minutes under Ar flow before adding *tert*-butyl methyl(propyl)carbamate (346 mg, 2.0 mmol) and $PhSiH_3$ (9.9 μL, 20 mol%) sequentially. The tube was sealed under Ar atmosphere and stirred at r.t. for 36 h. The reaction mixture was quenched with air and diluted with EtOAc, then concentrated

in vacuo. The residue was purified by flash column chromatography to give **3v** (37 mg, 32% yield) and **3va** (27 mg, 23% yield), r.r. 1.4:1. **3v**, white solid. **M.P.** 109 °C. **^{1}H NMR** (500 MHz, $CDCl_3$) δ 7.77 (dt, *J* = 7.2, 1.3 Hz, 2H), 7.60 – 7.46 (m, 1H), 7.46 – 7.34 (m, 2H), 5.31 (s, 1H), 2.95 (s, 3H), 2.19 – 1.78 (m, 2H), 1.47 (s, 9H), 0.95 (t, *J* = 7.4 Hz, 3H). **^{13}C NMR** (126 MHz, $CDCl_3$) δ 166.72, 155.49, 134.38, 131.76, 128.70, 127.14, 80.28, 67.63, 29.81, 28.60, 26.43, 10.43. **IR (neat):** 3346, 2972, 2937, 1688, 1639, 1520, 1489, 1461, 1445, 1397, 1362, 1335, 1314, 1285, 1166, 1138, 1109, 1081, 931, 887, 764, 730, 698, 629 cm^{-1}. **HRMS** *calcd*. for ($C_{16}H_{24}N_2NaO_3$) $[M+Na]^+$: 315.1679, *found* 315.1688.

***tert*-butyl (benzamidomethyl)(propyl)carbamate (3va).** White solid. **M.P.** 93 °C. **^{1}H NMR** (500 MHz, $CDCl_3$) δ 7.77 (d, *J* = 7.6 Hz, 2H), 7.51 (t, *J* = 7.3 Hz, 1H), 7.43 (t, *J* = 7.6 Hz, 2H), 7.15 (s, 1H), 4.87 (d, *J* = 6.4 Hz, 2H), 3.32 (t, *J* = 7.3 Hz, 2H), 1.59 (q, J = 7.3 Hz, 2H), 1.47 (s, 9H), 0.88 (t, *J* = 7.4 Hz, 3H). **^{13}C NMR** (126 MHz, $CDCl_3$) δ 167.56, 156.77, 134.24, 131.88, 128.75, 127.20, 80.32, 52.74, 49.95, 28.54, 22.50, 11.37. **IR (neat):** 3663, 2970, 2927, 1694, 1650, 1542, 1416, 1366, 1286, 1244, 1142, 1090, 1058, 1028, 876, 771, 706 cm^{-1}. **HRMS** *calcd*. for ($C_{16}H_{24}N_2NaO_3$) $[M+Na]^+$: 315.1679, *found* 315.1684.

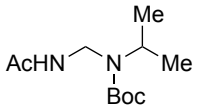

***tert*-butyl (acetamidomethyl)(isopropyl)carbamate (3w)** An oven-dried 20 mL reaction tube containing a stir bar was charged with $Ni(ClO_4)_2$·2Bathocuproine (39 mg, 10 mol%). The reaction tube was connected to a vacuum line where it was evacuated and backfilled with Ar at least three times. Then anhydrous pivalonitrile (1.0 mL) was added and the mixture was stirred at r.t. for 5 minutes under Ar flow before adding *tert*-butyl isopropyl(methyl)carbamate (346 mg, 2.0 mmol), **2b** (0.4 mmol, 1.0 equiv) and $PhSiH_3$ (14.9 μL, 30 mol%) sequentially. The tube was sealed under Ar atmosphere and stirred at r.t. for 36 h. The reaction mixture was quenched with air and diluted with EtOAc, then concentrated in vacuo. The residue was purified by flash column chromatography to give

the title compound as a colorless oil (40 mg, 43% yield). **^{1}H NMR** (400 MHz, $CDCl_3$) δ 6.52 (s, 1H), 4.62 (d, *J* = 6.2 Hz, 2H), 4.07 (s, 1H), 1.94 (s, 3H), 1.47 (s, 9H), 1.14 (d, *J* = 6.8 Hz, 6H). **^{13}C NMR** (101 MHz, $CDCl_3$) δ 169.33, 156.67, 80.43, 48.08, 28.61, 23.55, 20.98. **IR (neat):** 3309, 2973, 1655, 1541, 1452, 1407, 1366, 1348, 1253, 1167, 1135, 1083 cm^{-1}. **HRMS** *calcd*. for ($C_{11}H_{22}N_2NaO_3$) $[M+Na]^+$: 253.1523, *found* 253.1532.

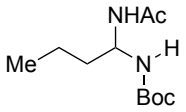

***tert*-butyl (1-acetamidobutyl)carbamate (3x)** An oven-dried 20 mL reaction tube containing a stir bar was charged with $Ni(ClO_4)_2$·2Bathocuproine (39 mg, 10 mol%). The reaction tube was connected to a vacuum line where it was evacuated and backfilled with Ar at least three times. Then anhydrous pivalonitrile (1.0 mL) was added and the mixture was stirred at r.t. for 5 minutes under Ar flow before adding *tert*-butyl butylcarbamate (693 mg, 4.0 mmol), **2b** (0.4 mmol, 1.0 equiv) and $PhSiH_3$ (15.9 μL, 30 mol%) sequentially. The tube was sealed under Ar atmosphere and stirred at r.t. for 3 h. The reaction mixture was quenched with air and diluted with EtOAc, then concentrated in vacuo. The residue was purified by flash column chromatography to give the title compound as a colorless oil (34 mg, 37% yield). **^{1}H NMR** (400 MHz, CD_2Cl_2) δ 6.45 (s, 1H), 5.48 (s, 1H), 5.09 (m, 1H), 1.91 (s, 3H), 1.82 – 1.64 (m, 2H), 1.41 (s, 9H), 1.34 (dt, *J* = 8.3, 7.1 Hz, 2H), 0.92 (t, *J* = 7.4 Hz, 3H). **^{13}C NMR** (101 MHz, CD_2Cl_2) δ 170.07, 155.52, 80.03, 58.87, 37.03, 28.63, 23.66, 19.46, 13.93. **IR (neat):** 3296, 2968, 2933, 1660, 1510, 1366, 1250, 1171, 1049, 1019 cm^{-1}. **HRMS** *calcd*. for ($C_{11}H_{22}N_2NaO_3$) $[M+Na]^+$: 253.1523, *found* 253.1531.

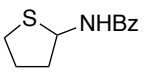

***N*-(tetrahydrothiophen-2-yl)benzamide (3y)** An oven-dried 20 mL reaction tube containing a stir bar was charged with $Ni(ClO_4)_2$·2Bathocuproine (39 mg, 10 mol%). The reaction tube was connected to a vacuum line where it was evacuated and backfilled with

Ar at least three times. Then anhydrous pivalonitrile (1.0 mL) was added and the mixture was stirred at r.t. for 5 minutes under Ar flow before adding Tetrahydrothiophene (4.0 mmol), **2a** (0.4 mmol, 1.0 equiv) and $PhSiH_3$ (15.9 μL, 30 mol%) sequentially. The tube was sealed under Ar atmosphere and stirred at r.t. for 24 h. The reaction mixture was quenched with air and diluted with EtOAc, then concentrated in vacuo. The residue was purified by flash column chromatography to give the title compound as a colorless oil (23 mg, 27% yield). **^{1}H NMR** (400 MHz, $CDCl_3$) δ 7.77 – 7.74 (m, 2H), 7.50 (ddt, *J* = 8.3, 6.5, 1.4 Hz, 1H), 7.43 (ddt, *J* = 8.3, 6.6, 1.3 Hz, 2H), 6.33 (s, 1H), 5.77 (dt, *J* = 7.9, 4.6 Hz, 1H), 3.14 – 3.04 (m, 1H), 2.91 – 2.80 (m, 1H), 2.24 – 2.10 (m, 3H), 2.04 – 1.95 (m, 1H). **^{13}C NMR** (101 MHz, $CDCl_3$) δ 166.60, 134.19, 131.83, 128.73, 127.09, 58.71, 38.74, 32.84, 29.08. **HRMS** *calcd*. for ($C_{11}H_{13}NNaOS$) $[M+Na]^+$: 230.0610, *found* 230.0607.

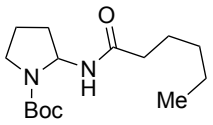

***tert*-butyl 2-hexanamidopyrrolidine-1-carboxylate (4a)** An oven-dried 20 mL reaction tube containing a stir bar was charged with $Ni(ClO_4)_2 \cdot 2$Bathocuproine (39 mg, 10 mol%). The reaction tube was connected to a vacuum line where it was evacuated and backfilled with Ar at least three times. Then anhydrous pivalonitrile (1.0 mL) was added and the mixture was stirred at r.t. for 5 minutes under Ar flow before adding *tert*-butyl pyrrolidine-1-carboxylate (140 μL, 0.8 mmol, 2.0 equiv), 3-pentyl-1,4,2-dioxazol-5-one (63 mg, 0.4 mmol, 1.0 equiv) and $PhSiH_3$ (9.9 μL, 20 mol%) sequentially. The tube was sealed under Ar atmosphere and stirred at r.t. for 12 h. The reaction mixture was quenched with air and diluted with EtOAc, then concentrated in vacuo. The residue was purified by flash column chromatography to give the title compound as a white solid (95 mg, 84% yield). **M.P.** 116 °C. **^{1}H NMR** (500 MHz, $CDCl_3$) δ 5.96 (s, 1H), 5.60 (s, 1H), 3.39 (m, 1H), 3.28 – 3.15 (m, 1H), 2.07 (t, *J* = 7.6 Hz, 2H), 2.04 – 1.93 (m, 1H), 1.89 – 1.77 (m, 3H), 1.55 (p, *J* = 7.5 Hz, 2H), 1.38 (s, 9H), 1.31 – 1.18 (m, 4H), 0.82 (t, *J* = 6.8 Hz, 3H). **^{13}C NMR** (126 MHz, $CDCl_3$) δ 171.91, 154.11, 80.03, 63.93, 45.96, 36.75, 33.92, 31.44, 28.43,

25.45, 22.41, 22.32, 13.92. **IR (neat):** 3261, 2961, 2930, 2880, 1695, 1645, 1544, 1386, 1159, 1130, 1110 cm^{-1}. **HRMS** *calcd*. for ($C_{15}H_{28}N_2NaO_3$) $[M+Na]^+$: 307.1992, *found* 307.2005.

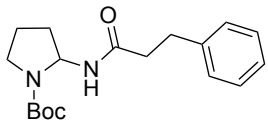

***tert*-butyl 2-(3-phenylpropanamido)pyrrolidine-1-carboxylate (4b)** An oven-dried 20 mL reaction tube containing a stir bar was charged with $Ni(ClO_4)_2 \cdot 2$Bathocuproine (39 mg, 10 mol%). The reaction tube was connected to a vacuum line where it was evacuated and backfilled with Ar at least three times. Then anhydrous pivalonitrile (1.0 mL) was added and the mixture was stirred at r.t. for 5 minutes under Ar flow before adding *tert*-butyl pyrrolidine-1-carboxylate (140 μL, 0.8 mmol, 2.0 equiv), 3-phenethyl-1,4,2-dioxazol-5-one (76 mg, 0.4 mmol, 1.0 equiv) and $PhSiH_3$ (9.9 μL, 20 mol%) sequentially. The tube was sealed under Ar atmosphere and stirred at r.t. for 12 h. The reaction mixture was quenched with air and diluted with EtOAc, then concentrated in vacuo. The residue was purified by flash column chromatography to give the title compound as a white solid (92 mg,72% yield). **M.P.** 129 °C. **^{1}H NMR** (400 MHz, $CDCl_3$) δ 7.30 – 7.21 (m, 2H), 7.22 – 7.06 (m, 3H), 5.78 (d, J = 6.9 Hz, 1H), 5.69 – 5.43 (m, 1H), 3.37 (m, 1H), 3.28 – 3.14 (m, 1H), 3.00 – 2.86 (m, 2H), 2.53 – 2.31 (m, 2H), 2.04 – 1.63 (m, 4H), 1.41 (s, 9H). **^{13}C NMR** (101 MHz, $CDCl_3$) δ 170.82, 154.12, 140.89, 128.56, 128.40, 126.27, 80.14, 64.02, 45.96, 38.41, 33.80, 31.73, 28.48, 22.35. **IR (neat):** 3287, 2969, 1693, 1642, 1535, 1394, 1365, 1229, 1159, 1110, 695 cm^{-1}. **HRMS** *calcd*. for ($C_{18}H_{26}N_2NaO_3$) $[M+Na]^+$: 341.1836, *found* 341.1831.

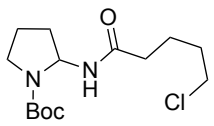

***tert*-butyl 2-(5-chloropentanamido)pyrrolidine-1-carboxylate (4c)** An oven-dried 20 mL reaction tube containing a stir bar was charged with $Ni(ClO_4)_2 \cdot 2$Bathocuproine (39 mg, 10 mol%). The reaction tube was connected to a vacuum line where it was evacuated and backfilled with Ar at least three times. Then anhydrous pivalonitrile (1.0 mL) was added and the mixture was stirred at r.t. for 5 minutes under Ar flow before adding *tert*-butyl pyrrolidine-1-carboxylate (140 μL, 0.8 mmol, 2.0 equiv), 3-(4-chlorobutyl)-1,4,2-dioxazol-5-one (71 mg, 0.4 mmol, 1.0 equiv) and $PhSiH_3$ (9.9 μL, 20 mol%) sequentially. The tube was sealed under Ar atmosphere and stirred at r.t. for 12 h. The reaction mixture was quenched with air and diluted with EtOAc, then concentrated in vacuo. The residue was purified by flash column chromatography to give the title compound as a white solid (91 mg, 75% yield). **M.P.** 115 °C. **^{1}H NMR** (500 MHz, $CDCl_3$) δ 5.88 (d, J = 6.7 Hz, 1H), 5.70 – 5.39 (m, 1H), 3.51 (t, *J* = 6.1 Hz, 2H), 3.42 (dt, *J* = 10.7, 5.4 Hz, 1H), 3.24 (q, *J* = 8.9 Hz, 1H), 2.15 (t, *J* = 6.9 Hz, 2H), 2.09 – 1.97 (m, 1H), 1.94 – 1.70 (m, 7H), 1.41 (s, 9H). **^{13}C NMR** (126 MHz, $CDCl_3$) δ 171.08, 154.15, 80.20, 64.09, 46.06, 44.66, 35.73, 33.96, 31.98, 28.50, 22.98, 22.42. **IR (neat):** 3258, 2979, 2883, 1649, 1645, 1543, 1457, 1385, 1235, 1158, 1127 cm^{-1}. **HRMS** *calcd*. for ($C_{14}H_{25}ClN_2NaO_3$) $[M+Na]^+$: 327.1446, *found* 327.1457.

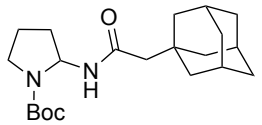

***tert*-butyl 2-(2-((adamantan-1-yl)acetamido)pyrrolidine-1-carboxylate (4d)** An oven-dried 20 mL reaction tube containing a stir bar was charged with $Ni(ClO_4)_2 \cdot 2$Bathocuproine (39 mg, 10 mol%), 3-((adamantan-1-yl)methyl)-1,4,2-dioxazol-5-one (94 mg, 0.4 mmol, 1.0 equiv). The reaction tube was connected to a vacuum line where it was evacuated and backfilled with Ar at least three times. Then anhydrous pivalonitrile (1.0 mL) was added and the mixture was stirred at r.t. for 5 minutes under Ar flow before adding *tert*-butyl pyrrolidine-1-carboxylate (140 μL, 0.8 mmol, 2.0 equiv) and $PhSiH_3$ (9.9 μL, 20 mol%) sequentially. The tube was sealed under

Ar atmosphere and stirred at r.t. for 2 h. The reaction mixture was quenched with air and diluted with EtOAc, then concentrated in vacuo. The residue was purified by flash column chromatography to give the title compound as a white solid (129 mg, 89% yield). **M.P.** 168 °C. **^{1}H NMR** (400 MHz, $CDCl_3$) δ 5.78 – 5.65 (m, 1H), 5.57 (s, 1H), 3.41 (dt, *J* = 10.5, 5.3 Hz, 1H), 3.31 – 3.15 (m, 1H), 2.05 – 1.76 (m, 9H), 1.73 – 1.51 (m, 12H), 1.40 (s, 9H). **^{13}C NMR** (101 MHz, $CDCl_3$) δ 169.77, 154.07, 80.15, 64.31, 51.78, 46.09, 42.60, 36.78, 33.93, 32.82, 28.65, 28.46, 22.28. **IR (neat):** 3293, 2974, 2906, 2847, 1697, 1633, 1531, 1450, 1395, 1364, 1244, 1164, 1147 cm^{-1}. **HRMS** *calcd.* for ($C_{21}H_{34}N_2NaO_3$) $[M+Na]^+$: 385.2462, *found* 385.2450.

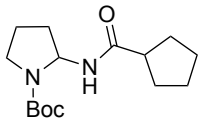

***tert*-butyl 2-(cyclopentanecarboxamido)pyrrolidine-1-carboxylate (4e)** An oven-dried 20 mL reaction tube containing a stir bar was charged with $Ni(ClO_4)_2 \cdot 2$Bathocuproine (39 mg, 10 mol%). The reaction tube was connected to a vacuum line where it was evacuated and backfilled with Ar at least three times. Then anhydrous pivalonitrile (1.0 mL) was added and the mixture was stirred at r.t. for 5 minutes under Ar flow before adding *tert*-butyl pyrrolidine-1-carboxylate (140 μL, 0.8 mmol, 2.0 equiv), 3-cyclopentyl-1,4,2-dioxazol-5-one (62 mg, 0.4 mmol, 1.0 equiv) and $PhSiH_3$ (9.9 μL, 20 mol%) sequentially. The tube was sealed under Ar atmosphere and stirred at r.t. for 24 h. The reaction mixture was quenched with air and diluted with EtOAc, then concentrated in vacuo. The residue was purified by flash column chromatography to give the title compound as a white solid (67 mg, 59% yield). **M.P.** 171 °C. **^{1}H NMR** (500 MHz, $CDCl_3$) δ 5.81 (d, *J* = 6.7 Hz, 1H), 5.59 (s, 1H), 3.41 (dt, *J* = 10.6, 5.4 Hz, 1H), 3.22 (dt, *J* = 10.4, 8.1 Hz, 1H), 2.43 (p, *J* = 8.0 Hz, 1H), 2.11 – 1.61 (m, 10H), 1.59 – 1.46 (m, 2H), 1.38 (s, 9H). **^{13}C NMR** (126 MHz, $CDCl_3$) δ 174.85, 154.13, 80.05, 63.98, 46.01, 45.78, 33.98, 30.65, 30.12, 28.46, 25.97, 25.94, 22.42. **IR (neat):** 3268, 2961, 2873, 1696, 1642, 1546, 1386, 1364, 1234, 1198,

1158, 1127, 1106 cm^{-1}. **HRMS** *calcd*. for ($C_{15}H_{26}N_2NaO_3$) $[M+Na]^+$: 305.1836, *found* 305.1838.

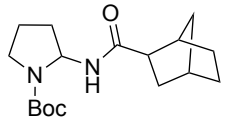

***tert*-butyl 2-(bicyclo[2.2.1]heptane-2-carboxamido)pyrrolidine-1-carboxylate (4f)** An oven-dried 20 mL reaction tube containing a stir bar was charged with $Ni(ClO_4)_2 \cdot 2$Bathocuproine (39 mg, 10 mol%). The reaction tube was connected to a vacuum line where it was evacuated and backfilled with Ar at least three times. Then anhydrous pivalonitrile (1.0 mL) was added and the mixture was stirred at r.t. for 5 minutes under Ar flow before adding *tert*-butyl pyrrolidine-1-carboxylate (140 μL, 0.8 mmol, 2.0 equiv), 3-(bicyclo[2.2.1]heptan-2-yl)-1,4,2-dioxazol-5-one (72 mg, 0.4 mmol, 1.0 equiv) and $PhSiH_3$ (15.9 μL, 30 mol%) sequentially. The tube was sealed under Ar atmosphere and stirred at r.t. for 24 h. The reaction mixture was quenched with air and diluted with EtOAc, then concentrated in vacuo. The residue was purified by flash column chromatography to give the title compound as a white solid (67 mg, 54% yield). **M.P.** 153 °C. **^{1}H NMR** (500 MHz, $CDCl_3$) δ 5.68 (s, 1H), 5.56 (s, 1H), 3.43 (td, J = 9.0, 5.1 Hz, 1H), 3.23 (dt, J = 10.5, 8.4 Hz, 1H), 2.58 – 2.48 (m, 1H), 2.35 (m, 1H), 2.20 (s, 1H), 2.06 – 1.91 (m, 2H), 1.84 (s, 2H), 1.66 – 1.52 (m, 2H), 1.51 – 1.20 (m, 15H). **^{13}C NMR** (126 MHz, $CDCl_3$) δ 172.88, 154.18, 154.14, 80.22, 64.69, 47.19, 47.09, 46.16, 40.99, 40.60, 40.50, 37.06, 33.95, 31.24, 29.22, 28.47, 24.59, 24.31, 22.25. **IR (neat):** 3305, 2958, 2873, 1692, 1639, 1522, 1386, 1364, 1200, 1158, 1124, 1104 cm^{-1}. **HRMS** *calcd*. for ($C_{17}H_{28}N_2NaO_3$) $[M+Na]^+$: 331.1992, *found* 331.1986.

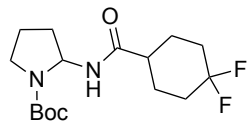

***tert*-butyl 2-(4,4-difluorocyclohexane-1-carboxamido)pyrrolidine-1-carboxylate (4g)** An oven-dried 20 mL reaction tube containing a stir bar was charged with $Ni(ClO_4)_2 \cdot 2$Bathocuproine (39 mg, 10 mol%). The reaction tube was connected to a vacuum line where it was evacuated and backfilled with Ar at least three times. Then anhydrous pivalonitrile (1.0 mL) was added and the mixture was stirred at r.t. for 5 minutes under Ar flow before adding *tert*-butyl pyrrolidine-1-carboxylate (140 μL, 0.8 mmol, 2.0 equiv), 3-(4,4-difluorocyclohexyl)-1,4,2-dioxazol-5-one (82 mg, 0.4 mmol, 1.0 equiv) and $PhSiH_3$ (9.9 μL, 20 mol%) sequentially. The tube was sealed under Ar atmosphere and stirred at r.t. for 24 h. The reaction mixture was quenched with air and diluted with EtOAc, then concentrated in vacuo. The residue was purified by flash column chromatography to give the title compound as a white solid (92 mg, 69% yield). **M.P.** 163 °C. **^{1}H NMR** (400 MHz, CD_2Cl_2) δ 5.80 (d, J = 6.8 Hz, 1H), 5.57 (s, 1H), 3.48 – 3.37 (m, 1H), 3.23 (dt, J = 10.5, 8.0 Hz, 1H), 2.21 – 2.07 (m, 3H), 2.03 (m, 1H), 1.93 – 1.84 (m, 4H), 1.82 – 1.64 (m, 5H), 1.41 (s, 9H). **^{13}C NMR** (101 MHz, CD_2Cl_2) δ 173.02, 154.44, 123.54 (t, J = 240.8 Hz), 80.29, 64.56, 46.65, 43.10, 34.39, 33.55, 33.50, 33.30, 33.26, 33.24, 33.06, 33.01, 28.71, 26.38, 26.29, 22.94. **^{19}F NMR** (282 MHz, $CDCl_3$) δ -92.70, -93.54, -100.30, -101.14. **IR (neat):** 3263, 2973, 2871, 1697, 1640, 1547, 1387, 1370, 1224, 1159, 1107 cm^{-1}. **HRMS** *calcd*. for ($C_{16}H_{27}F_2N_2O_3$) $[M+H]^+$: 333.1984, *found* 333.1982.

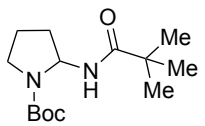

***tert*-butyl 2-pivalamidopyrrolidine-1-carboxylate (4h)** An oven-dried 20 mL reaction tube containing a stir bar was charged with $Ni(ClO_4)_2 \cdot 2$Bathocuproine (39 mg, 10 mol%). The reaction tube was connected to a vacuum line where it was evacuated and backfilled with Ar at least three times. Then anhydrous pivalonitrile (1.0 mL) was added and the mixture was stirred at r.t. for 5 minutes under Ar flow before adding *tert*-butyl pyrrolidine-1-carboxylate (140 μL, 0.8 mmol, 2.0 equiv), 3-(*tert*-butyl)-1,4,2-dioxazol-5-one (57 mg,

0.4 mmol, 1.0 equiv) and $PhSiH_3$ (9.9 μL, 20 mol%) sequentially. The tube was sealed under Ar atmosphere and stirred at r.t. for 24 h. The reaction mixture was quenched with air and diluted with EtOAc, then concentrated in vacuo. The residue was purified by flash column chromatography to give the title compound as a white solid (65 mg, 60% yield). **M.P.** 168 °C. **^{1}H NMR** (500 MHz, $CDCl_3$) δ 5.70 (s, 1H), 5.50 (s, 1H), 3.43 (dt, *J* = 10.8, 5.3 Hz, 1H), 3.22 (dt, *J* = 10.4, 8.1 Hz, 1H), 2.11 – 1.96 (m, 1H), 1.82 (s, 3H), 1.38 (s, 9H), 1.12 (s, 9H). **^{13}C NMR** (126 MHz, $CDCl_3$) δ 177.20, 154.12, 80.09, 64.60, 46.20, 38.59, 33.91, 28.44, 27.55, 22.42. **IR (neat):** 3313, 2971, 2874, 1698, 1631, 1525, 1385, 1364, 1196, 1159, 1125, 1105 cm^{-1}. **HRMS** *calcd*. for ($C_{14}H_{26}N_2NaO_3$) $[M+Na]^+$: 293.1836, *found* 293.1826.

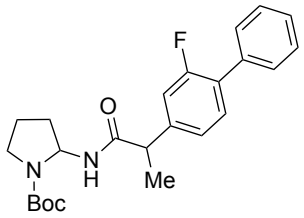

***tert*-butyl 2-(2-(2-fluoro-[1,1'-biphenyl]-4-yl)propanamido)pyrrolidine-1-carboxylate (4i).** An oven-dried 20 mL reaction tube containing a stir bar was charged with $Ni(ClO_4)_2$·2Bathocuproine (39 mg, 10 mol%), 3-(1-(2-fluoro-[1,1'-biphenyl]-4-yl)ethyl)-1,4,2-dioxazol-5-one (114 mg, 0.4 mmol, 1.0 equiv). The reaction tube was connected to a vacuum line where it was evacuated and backfilled with Ar at least three times. Then anhydrous pivalonitrile (1.0 mL) was added and the mixture was stirred at r.t. for 5 minutes under Ar flow before adding *tert*-butyl pyrrolidine-1-carboxylate (140 μL, 0.8 mmol, 2.0 equiv) and $PhSiH_3$ (9.9 μL, 20 mol%) sequentially. The tube was sealed under Ar atmosphere and stirred at r.t. for 24 h. The reaction mixture was quenched with air and diluted with EtOAc, then concentrated in vacuo. The residue was purified by flash column chromatography to give amidated product with 1:1 d.r. **4g:** 37 mg, 23% yield. colorless oil. **^{1}H NMR** (500 MHz, $CDCl_3$) δ 7.53 (dt, *J* = 8.1, 1.4 Hz, 2H), 7.46 – 7.40 (m, 2H), 7.40 – 7.33 (m, 2H), 7.19 – 7.05 (m, 2H), 5.69 (s, 1H), 5.60 (s, 1H), 3.55 (q, *J* = 7.1

Hz, 1H), 3.42 (m, 1H), 3.25 (m, 1H), 2.03 (m, 1H), 1.89 – 1.72 (m, 3H), 1.53 (d, *J* = 7.2 Hz, 3H), 1.43 (s, 9H). **^{13}C NMR** (126 MHz, $CDCl_3$) δ 172.34, 160.87, 158.89, 154.18, 142.60 135.49, 131.13, 129.03, 129.01, 128.58, 127.83, 123.64, 123.61, 115.44, 115.25, 80.33, 64.57, 46.75, 46.18, 33.81, 28.50, 22.52, 18.71. **^{19}F NMR** (376 MHz, $CDCl_3$) δ -117.18, -117.47. **IR (neat):** 3236, 2977, 2932, 2891, 1701, 1638, 1550, 1482, 1388, 1375, 1384, 1220, 1166, 1109, 1068, 971, 911, 864, 764, 726, 696 cm^{-1}. **HRMS** *calcd*. for ($C_{24}H_{29}FN_2NaO_3$) $[M+Na]^+$: 435.2054, *found* 435.2061. **4ga:** 40 mg, 24% yield. colorless oil. **^{1}H NMR** (500 MHz, $CDCl_3$) δ 7.54 – 7.47 (m, 2H), 7.46 – 7.40 (m, 2H), 7.40 – 7.32 (m, 2H), 7.20 – 7.08 (m, 2H), 5.75 (s, 1H), 5.57 (s, 1H), 3.49 (d, *J* = 6.4 Hz, 1H), 3.45 – 3.37 (m, 1H), 3.23 (dt, *J* = 10.4, 8.2 Hz, 1H), 2.11 – 2.01 (m, 1H), 2.00 – 1.77 (m, 3H), 1.52 (d, *J* = 7.1 Hz, 3H), 1.27 (s, 9H). **^{13}C NMR** (126 MHz, $CDCl_3$) δ 172.10, 160.86, 158.88, 154.07, 142.92, 142.86, 135.50, 131.14, 131.11, 128.99, 128.97, 128.58, 127.83, 123.75, 115.46, 115.27, 80.30, 64.65, 46.72, 46.15, 33.97, 28.26, 22.38, 18.57. **^{19}F NMR** (376 MHz, $CDCl_3$) δ -117.29. **IR (neat):** 3256, 2979, 2932, 2868, 1697, 1638, 1546, 1483, 1386, 1365, 1229, 1159, 1126, 1106, 968, 950, 914, 855, 764, 694 cm^{-1}. **HRMS** *calcd*. for ($C_{24}H_{29}FN_2NaO_3$) $[M+Na]^+$: 435.2054, *found* 435.2056.

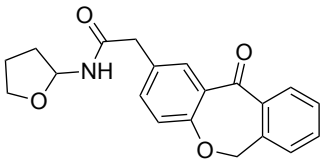

2-(11-oxo-6,11-dihydrodibenzo[*b*,*e*]oxepin-2-yl)–N-(tetrahydrofuran-2-yl)acetamide (4j) An oven-dried 20 mL reaction tube containing a stir bar was charged with $Ni(ClO_4)_2$·2Bathocuproine (20 mg, 10 mol%), 3-((11-oxo-6,11-dihydrodibenzo[b,e]oxepin-2-yl)methyl)-1,4,2-dioxazol-5-one (62 mg, 0.2 mmol, 1.0 equiv). The reaction tube was connected to a vacuum line where it was evacuated and backfilled with Ar at least three times. Anhydrous THF (1.0 mL) was added, and the mixture was stirred at r.t. for 5 minutes under Ar flow before adding $PhSiH_3$ (5.0 μL, 20 mol%). The tube was sealed under Ar atmosphere and stirred at r.t. for 24 h. The reaction mixture was quenched with air and diluted with EtOAc, then concentrated in vacuo. The

residue was purified by flash column chromatography to give the title compound as a white solid (31 mg, 46% yield). **M.P.** 143 °C. **^{1}H NMR** (400 MHz, $CDCl_3$) δ 8.06 (d, *J* = 2.4 Hz, 1H), 7.87 (dd, *J* = 7.7, 1.4 Hz, 1H), 7.56 (td, *J* = 7.4, 1.4 Hz, 1H), 7.50 – 7.41 (m, 2H), 7.36 (dd, *J* = 7.5, 1.3 Hz, 1H), 7.03 (d, *J* = 8.4 Hz, 1H), 5.99 (d, *J* = 8.0 Hz, 1H), 5.68 (m, 1H), 5.18 (s, 2H), 3.86 (dt, *J* = 8.5, 6.7 Hz, 1H), 3.75 (dt, *J* = 8.4, 6.9 Hz, 1H), 3.54 (s, 2H), 2.14 (m, 1H), 1.95 – 1.84 (m, 2H), 1.66 (m, 1H). **^{13}C NMR** (101 MHz, $CDCl_3$) δ 190.97, 170.57, 160.70, 140.47, 136.53, 135.64, 132.99, 132.51, 129.59, 129.42, 128.51, 127.98, 125.35, 121.62, 81.46, 73.75, 67.64, 42.81, 32.13, 24.69. **IR (neat):** 3280, 2921, 2872, 1650, 1610, 1537, 1484, 1408, 1298 1238, 1205, 1120, 1045, 1014, 899, 828, 760, 721, 643 cm^{-1}. **HRMS** *calcd*. for ($C_{20}H_{20}NO_4$) $[M+H]^+$: 338.1387, *found* 338.1385.

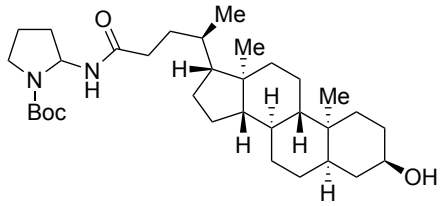

***tert*-butyl 2-((*R*)-4-((3*R*,5*R*,8*R*,9*S*,*10S*,13*R*,14*S*,17*R*)-3-hydroxy-10,13-dimethylhexadecahydro-1*H*-cyclopenta[*a*]phenanthren-17-yl)pentanamido)pyrrolidine-1-carboxylate (4k)** An oven-dried 20 mL reaction tube containing a stir bar was charged with $Ni(ClO_4)_2$·2Bathocuproine (20 mg, 10 mol%), 3-((*R*)-3-((3*R*,5*R*,8*R*,9*S*,10*S*,13*R*,14*S*,17*R*)-3-hydroxy-10,13-dimethylhexadecahydro-1*H*-cyclopenta[a]phenanthren-17-yl)butyl)-1,4,2-dioxazol-5-one (83 mg, 0.2 mmol, 1.0 equiv). The reaction tube was connected to a vacuum line where it was evacuated and backfilled with Ar at least three times. Anhydrous pivalonitrile (1.0 mL) was added and the mixture was stirred at r.t. for 5 minutes under Ar flow before adding *tert*-butyl pyrrolidine-1-carboxylate (70 μL, 0.4 mmol, 2.0 equiv) and $PhSiH_3$ (5.0 μL, 20 mol%) sequentially. The tube was sealed under Ar atmosphere and stirred at r.t. for 24 h. The reaction mixture was quenched with air and diluted with EtOAc, then concentrated in vacuo. The residue was purified by flash column chromatography to give the title compound as a colorless oil (42 mg, 39% yield, d.r. 1:1). **^{1}H NMR** (400 MHz, $CDCl_3$) δ

5.60 (s, 2H), 3.61 (tt, *J* = 11.0, 4.7 Hz, 1H), 3.46 (dt, *J* = 10.4, 5.3 Hz, 1H), 3.34 – 3.20 (m, 1H), 2.26 – 2.13 (m, 1H), 2.09 – 1.61 (m, 13H), 1.60 – 1.19 (m, 23H), 1.19 – 0.98 (m, 5H), 0.97 – 0.87 (m, 4H), 0.82 (d, *J* = 6.3 Hz, 2H), 0.64 (d, *J* = 6.3 Hz, 3H). **^{13}C NMR** (101 MHz, $CDCl_3$) δ 176.04, 154.27, 80.26, 71.96, 64.32, 56.69, 56.64, 56.17, 56.13, 55.84, 55.76, 46.07, 42.90, 42.24, 40.64, 40.59, 40.34, 40.24, 36.59, 35.99, 35.59, 35.49, 34.91, 34.88, 34.71, 33.77, 31.17, 31.12, 30.68, 28.59, 28.56, 28.38, 28.20, 27.34, 26.56, 24.34, 24.23, 23.49, 22.80, 20.97, 20.94, 18.64, 18.60, 18.53, 18.50, 12.37, 12.19. **IR (neat):** 3305, 2935, 1635, 1580, 1522, 1487, 1365, 1314, 1264, 1158, 1029, 998, 692 cm^{-1}. **HRMS** *calcd*. for ($C_{33}H_{56}N_2NaO_4$) $[M+Na]^+$: 567.4132, *found* 567.4134.

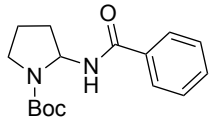

***tert*-butyl 2-benzamidopyrrolidine-1-carboxylate (4l)** An oven-dried 20 mL reaction tube containing a stir bar was charged with $Ni(ClO_4)_2 \cdot 2$Bathocuproine (39 mg, 10 mol%), 3-phenyl-1,4,2-dioxazol-5-one (65 mg, 0.4 mmol, 1.0 equiv). The reaction tube was connected to a vacuum line where it was evacuated and backfilled with Ar at least three times. Anhydrous pivalonitrile (1.0 mL) was added and the mixture was stirred at r.t. for 5 minutes under Ar flow before adding *tert*-butyl pyrrolidine-1-carboxylate (350 μL, 2.0 mmol, 5.0 equiv) and $PhSiH_3$ (9.9 μL, 20 mol%) sequentially. The tube was sealed under Ar atmosphere and stirred at r.t. for 24 h. The reaction mixture was quenched with air and diluted with EtOAc, then concentrated in vacuo. The residue was purified by flash column chromatography to give the title compound as a white solid (84 mg, 72% yield). **M.P.** 163 °C. **^{1}H NMR** (300 MHz, $CDCl_3$) δ 7.73 (dt, *J* = 8.2, 1.2 Hz, 2H), 7.44 (m, 3H), 6.31 (br. s, 1H), 5.82 (br. s, 1H), 3.53 (dt, *J* = 10.7, 5.4 Hz, 1H), 3.33 (dt, *J* = 10.5, 8.1 Hz, 1H), 2.38 – 1.75 (m, 4H), 1.40 (s, 9H). **^{13}C NMR** (101 MHz, $CDCl_3$) δ 166.58, 154.31, 134.62, 131.65, 128.70, 127.01, 80.41, 64.86, 46.27, 34.07, 28.52, 22.68. **IR (neat):** 3309, 2980, 2886, 1691, 1635, 1529, 1490, 1396, 1364, 1243, 1161, 972, 915, 690, 658 cm^{-1}. **HRMS** *calcd*. for ($C_{16}H_{22}N_2NaO_3$) $[M+Na]^+$: 313.1523, *found* 313.1524.

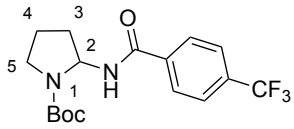

***tert*-butyl 2-(4-(trifluoromethyl)benzamido)pyrrolidine-1-carboxylate (4m)** An oven-dried 20 mL reaction tube containing a stir bar was charged with $Ni(ClO_4)_2 \cdot 2$Bathocuproine (39 mg, 10 mol%), 3-(4-(trifluoromethyl)phenyl)-1,4,2-dioxazol-5-one (92 mg, 0.4 mmol, 1.0 equiv). The reaction tube was connected to a vacuum line where it was evacuated and backfilled with Ar at least three times. Anhydrous pivalonitrile (1.0 mL) was added and the mixture was stirred at r.t. for 5 minutes under Ar flow before adding *tert*-butyl pyrrolidine-1-carboxylate (350 µL, 2.0 mmol, 5.0 equiv) and $PhSiH_3$ (9.9 µL, 20 mol%) sequentially. The tube was sealed under Ar atmosphere and stirred at r.t. for 24 h. The reaction mixture was quenched with air and diluted with EtOAc, then concentrated in vacuo. The residue was purified by flash column chromatography to give the title compound as a white solid (110 mg, 77% yield). **M.P.** 186 °C. **^{1}H NMR** (400 MHz, $CDCl_3$) δ 7.82 (d, J = 7.9 Hz, 2H), 7.63 (d, J = 7.9 Hz, 2H), 6.63 (d, J = 6.6 Hz, 1H), 5.93 – 5.57 (m, 1H), 3.50 (dt, J = 10.8, 5.4 Hz, 1H), 3.31 (dt, J = 10.5, 8.0 Hz, 1H), 2.25 – 1.85 (m, 4H), 1.39 (s, 9H). **^{13}C NMR** (126 MHz, $CDCl_3$) δ 165.27, 154.20, 137.83, 133.50, 133.24 (q, J =32.9 Hz), 132.98, 132.72, 127.57, 126.93, 125.50, 124.77 (q, J =272.5), 122.60, 120.43, 80.32, 65.86 (C2, Rotamer B), 65.72 (C2, Rotamer A), 46.79 (C5, Rotamer B), 46.14 (C5, Rotamer A), 33.92 (C3, Rotamer B), 32.71 (C3, Rotamer A), 28.41, 23.15 (C4, Rotamer B), 22.50 (C4, Rotamer A). **^{19}F NMR** (282 MHz, $CDCl_3$) δ -62.96. **IR (neat):** 3297, 2980, 1694, 1637, 1541, 1385, 1362, 1324, 1166, 1128, 1108, 1066, 1016, 966, 911, 862, 774, 699 cm^{-1}. **HRMS** *calcd*. for ($C_{17}H_{21}F_3N_2NaO_3$) $[M+Na]^+$: 381.1396, *found* 381.1399.

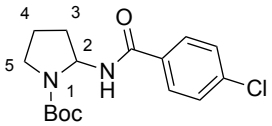

***tert*-butyl 2-(4-chlorobenzamido)pyrrolidine-1-carboxylate (4n)** An oven-dried 20 mL reaction tube containing a stir bar was charged with $Ni(ClO_4)_2 \cdot 2$Bathocuproine (39 mg, 10 mol%), 3-(4-chlorophenyl)-1,4,2-dioxazol-5-one (79 mg, 0.4 mmol, 1.0 equiv). The reaction tube was connected to a vacuum line where it was evacuated and backfilled with Ar at least three times. Anhydrous pivalonitrile (1.0 mL) was added and the mixture was stirred at r.t. for 5 minutes under Ar flow before adding *tert*-butyl pyrrolidine-1-carboxylate (350 μL, 2.0 mmol, 5.0 equiv) and $PhSiH_3$ (9.9 μL, 20 mol%) sequentially. The tube was sealed under Ar atmosphere and stirred at r.t. for 12 h. The reaction mixture was quenched with air and diluted with EtOAc, then concentrated in vacuo. The residue was purified by flash column chromatography to give the title compound as a white solid (100 mg, 77% yield, 2.3:1 mixture of rotamers, A:B). **M.P.** 149 °C. **^{1}H NMR** (400 MHz, $CDCl_3$) δ 7.64 (d, J = 8.1 Hz, 2H), 7.31 (d, J = 8.9 Hz, 2H), 6.66 (d, J = 7.3 Hz, 1H), 5.80 (br. m, 0.68 H, C_2-H, A), 5.66 (br. m, 0.29 H, C_2-H, B), 3.46 (m, 1H), 3.27 (dt, J = 10.4, 7.6 Hz, 1H), 2.18 – 1.79 (m, 4H), 1.36 (s, 9H). **^{13}C NMR** (101 MHz, $CDCl_3$) δ 165.45, 154.19, 137.68, 132.89, 128.75, 128.50, 80.27, 64.69, 46.14, 33.94, 28.44, 22.55. **IR (neat):** 3260, 2979, 2900, 1688, 1633, 1594, 1543, 1486, 1383, 1360, 1284, 1164, 1107,1088, 1014, 966, 911, 844, 777, 673 cm^{-1}. **HRMS** *calcd*. for ($C_{16}H_{21}ClN_2NaO_3$) $[M+Na]^+$: 347.1133, *found* 347.1135.

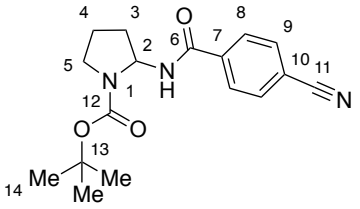

***tert*-butyl 2-(4-cyanobenzamido)pyrrolidine-1-carboxylate (4o)** An oven-dried 20 mL reaction tube containing a stir bar was charged with $Ni(ClO_4)_2 \cdot 2$Bathocuproine (39 mg, 10 mol%), 3-(4-cyanophenyl)-1,4,2-dioxazol-5-one (75 mg, 0.4 mmol, 1.0 equiv). The reaction tube was connected to a vacuum line where it was evacuated and backfilled with Ar at least three times. Anhydrous pivalonitrile (1.0 mL) was added and the mixture was stirred at r.t. for 5 minutes under Ar flow before adding *tert*-butyl pyrrolidine-1-

carboxylate (350 μL, 2.0 mmol, 5.0 equiv) and $PhSiH_3$ (9.9 μL, 20 mol%) sequentially. The tube was sealed under Ar atmosphere and stirred at r.t. for 24 h. The reaction mixture was quenched with air and diluted with EtOAc, then concentrated in vacuo. The residue was purified by flash column chromatography to give the title compound as a white solid (93 mg, 74% yield, 2:1 mixture of rotamers, A:B). **M.P.** 170 °C. **^{1}H NMR** (500 MHz, $CDCl_3$) δ 7.83 (d, *J* = 8.7 Hz, 2H), 7.74 – 7.56 (m, 2H), 6.85 (br. m, 1H, N-H, A+B), 5.83 (br. m, 0.62 H, C_2-H, A), 5.65 (br. m, 0.33 H, C_2-H, B), 3.47 (m, 1H), 3.29 (dt, *J* = 10.4, 7.9 Hz, 1H), 2.21 – 1.82 (m, 4H), 1.35 (s, 9H). **^{13}C NMR** (126 MHz, $CDCl_3$) δ 167.51 (C6, B), 164.61 (C6, A), 154.12, 138.43 (C7, A), 137.42 (C7, B), 132.41, 128.22 (C8, B), 127.83 (C8, A), 118.05, 115.32 (C10, B), 114.91 (C10, A), 80.37, 65.98 (C2, B), 64.81 (C2, A), 46.16 (C5, A), 33.90 (C3, A), 32.69 (C3, B), 28.43, 23.17 (C4, B), 22.51(C4, A). **IR (neat):** 3363, 2975, 2887, 2228, 1700, 1636, 1531, 1494, 1385, 1364, 1242, 1163, 1104, 917, 876, 766 cm^{-1}. **HRMS** *calcd*. for ($C_{17}H_{21}N_3NaO_3$) $[M+Na]^+$: 338.1475, *found* 338.1478.

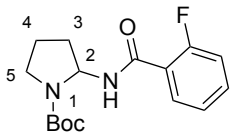

***tert*-butyl 2-(2-fluorobenzamido)pyrrolidine-1-carboxylate (4p)** An oven-dried 20 mL reaction tube containing a stir bar was charged with $Ni(ClO_4)_2 \cdot 2$Bathocuproine (39 mg, 10 mol%), 3-(2-fluorophenyl)-1,4,2-dioxazol-5-one (72 mg, 0.4 mmol, 1.0 equiv). The reaction tube was connected to a vacuum line where it was evacuated and backfilled with Ar at least three times. Anhydrous pivalonitrile (1.0 mL) was added and the mixture was stirred at r.t. for 5 minutes under Ar flow before adding *tert*-butyl pyrrolidine-1-carboxylate (350 μL, 2.0 mmol, 5.0 equiv) and $PhSiH_3$ (9.9 μL, 20 mol%) sequentially. The tube was sealed under Ar atmosphere and stirred at r.t. for 12 h. The reaction mixture was quenched with air and diluted with EtOAc, then concentrated in vacuo. The residue was purified by flash column chromatography to give the title compound as a white solid (103 mg, 84% yield). **M.P.** 95 °C. **^{1}H NMR** (400 MHz, $CDCl_3$) δ 7.99 (td, *J* = 7.9, 1.9

Hz, 1H), 7.41 (q, *J* = 4.7 Hz, 1H), 7.20 (t, *J* = 7.6 Hz, 1H), 7.13 – 6.98 (m, 1H), 6.79 (br. m., 1H), 5.79 (br. m., 1H), 3.50 (dt, *J* = 10.7, 5.4 Hz, 1H), 3.37 – 3.21 (m, 1H), 2.24 – 1.97 (m, 2H), 1.89 (dq, *J* = 8.2, 3.7 Hz, 2H), 1.37 (s, 9H). **^{13}C NMR** (101 MHz, $CDCl_3$) δ 162.15, 160.51 (d, *J* = 247.2 Hz), 154.07, 133.29 (d, *J* = 9.2 Hz), 131.90, 124.82, 121.19 (d, *J* = 11.6 Hz), 116.00 (d, *J* = 24.6 Hz), 80.25, 64.76, 46.14, 33.88, 28.37, 22.50. **^{19}F NMR** (282 MHz, $CDCl_3$) δ -112.74, -112.76, -112.77, -112.79, -112.80, -113.62, -114.10. **IR (neat):** 3390, 3295, 3191, 2979, 2875, 1684, 1634, 1614, 1530, 1485, 1454, 1391, 1364, 1244, 1217, 1156, 1118, 968, 920, 837, 761, 619, 538 cm^{-1}. **HRMS** *calcd*. for ($C_{16}H_{21}FN_2NaO_3$) $[M+Na]^+$: 331.1428, *found* 331.1432.

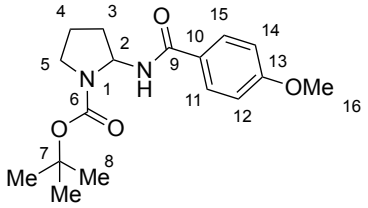

***tert*-butyl 2-(4-methoxybenzamido)pyrrolidine-1-carboxylate (4q)** An oven-dried 20 mL reaction tube containing a stir bar was charged with $Ni(ClO_4)_2$·2Bathocuproine (39 mg, 10 mol%), 3-(4-methoxyphenyl)-1,4,2-dioxazol-5-one (77 mg, 0.4 mmol, 1.0 equiv). The reaction tube was connected to a vacuum line where it was evacuated and backfilled with Ar at least three times. Anhydrous pivalonitrile (1.0 mL) was added and the mixture was stirred at r.t. for 5 minutes under Ar flow before adding *tert*-butyl pyrrolidine-1-carboxylate (350 μL, 2.0 mmol, 5.0 equiv) and $PhSiH_3$ (9.9 μL, 20 mol%) sequentially. The tube was sealed under Ar atmosphere and stirred at r.t. for 24 h. The reaction mixture was quenched with air and diluted with EtOAc, then concentrated in vacuo. The residue was purified by flash column chromatography to give the title compound as a white solid (87 mg, 68% yield, 10:1 mixture of rotamers, A:B). **M.P.** 128 °C. **^{1}H NMR** (400 MHz, $CDCl_3$) δ 7.81 – 7.73 (m, 0.12H, $C_{11,15}$-H, B), 7.74 – 7.64 (m, 1.9H, $C_{11,15}$-H, A), 6.99 – 6.74 (m, 2H), 6.42 (d, *J* = 6.3 Hz, 1H), 5.80 (br. m, 0.79H, A), 5.67 (br. m, 0.11H, B), 3.80 (s, 3H), 3.49 (m, 1H), 3.29 (dt, *J* = 10.5, 8.0 Hz, 1H), 2.27 – 1.85 (m, 4H), 1.48 – 1.28 (s, 9H). **^{13}C NMR** (101 MHz, $CDCl_3$) δ 168.99 (C_6, B), 166.09 (C_6, A), 162.53 (C_{13},

B), 162.21 (C_{13}, A+B), 154.28 (C_9, A+B), 129.45 ($C_{11,15}$, B), 128.82 ($C_{11,15}$, A), 126.82 (C_{10}, A), 125.74 (C_{10}, B), 113.74 ($C_{12,14}$, B), 113.73 ($C_{12,14}$, A), 81.77 (C_7, B), 80.19 (C_7, A), 65.92 (C_2, B), 64.71 (C_2, A), 55.45 (C_{16}, B), 55.42 (C_{16}, A), 46.17 (C_5, A), 45.97 (C_5, B), 34.03 (C_3, A), 32.78 (C_3, B), 28.51 (C_8, B), 28.44 (C_8, A), 22.76 (C_4, B), 22.57 (C_4, A). **IR (neat):** 3323, 2982, 2873, 1738, 1687, 1630, 1607, 1577, 1538, 1504, 1405, 1359, 1286, 1258, 1242, 1161, 1112, 1204, 915, 845, 769, 659, 634, 608 cm^{-1}. **HRMS** *calcd*. for ($C_{17}H_{24}N_2NaO_4$) $[M+Na]^+$: 343.1628, *found* 343.1630.

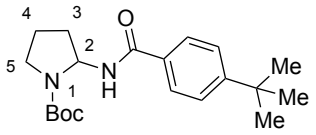

***tert*-butyl 2-(4-(*tert*-butyl)benzamido)pyrrolidine-1-carboxylate (4r)** An oven-dried 20 mL reaction tube containing a stir bar was charged with $Ni(ClO_4)_2 \cdot 2$Bathocuproine (39 mg, 10 mol%), 3-(4-(*tert*-butyl)phenyl)-1,4,2-dioxazol-5-one (88 mg, 0.4 mmol, 1.0 equiv). The reaction tube was connected to a vacuum line where it was evacuated and backfilled with Ar at least three times. Anhydrous pivalonitrile (1.0 mL) was added and the mixture was stirred at r.t. for 5 minutes under Ar flow before adding *tert*-butyl pyrrolidine-1-carboxylate (350 μL, 2.0 mmol, 5.0 equiv) and $PhSiH_3$ (9.9 μL, 20 mol%) sequentially. The tube was sealed under Ar atmosphere and stirred at r.t. for 12 h. The reaction mixture was quenched with air and diluted with EtOAc, then concentrated in vacuo. The residue was purified by flash column chromatography to give the title compound as a white solid (93 mg, 67% yield). **M.P.** 110 °C. **^{1}H NMR** (400 MHz, $CDCl_3$) δ 7.72 – 7.61 (m, 2H), 7.43 (d, J = 8.1 Hz, 2H), 6.25 (br. m, 1H), 5.83 (br. m, 1H), 3.54 (dt, J = 10.7, 5.4 Hz, 1H), 3.33 (dt, J = 10.5, 8.1 Hz, 1H), 2.24 – 1.81 (m, 4H), 1.41 (s, 9H), 1.32 (s, 9H). **^{13}C NMR** (101 MHz, $CDCl_3$) δ 166.52, 154.19, 134.58, 131.46, 128.53, 126.98, 80.18, 64.65, 46.11, 33.95, 32.94, 28.42, 28.05, 22.55. **IR (neat):** 3329, 2962, 2876, 1692, 1626, 1531, 1499, 1397, 1364, 1279, 1243, 1155, 1145, 1104, 969, 917, 853, 774, 756, 645, 630 cm^{-1}. **HRMS** *calcd*. for ($C_{20}H_{30}N_2NaO_3$) $[M+Na]^+$: 369.2149, *found* 369.2154.

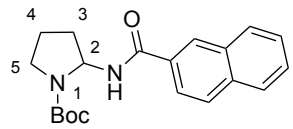

***tert*-butyl 2-(2–Naphthamido)pyrrolidine-1-carboxylate (4s)** An oven-dried 20 mL reaction tube containing a stir bar was charged with $Ni(ClO_4)_2 \cdot 2$Bathocuproine (39 mg, 10 mol%), 3-(naphthalen-2-yl)-1,4,2-dioxazol-5-one (85 mg, 0.4 mmol, 1.0 equiv). The reaction tube was connected to a vacuum line where it was evacuated and backfilled with Ar at least three times. Anhydrous pivalonitrile (1.0 mL) was added and the mixture was stirred at r.t. for 5 minutes under Ar flow before adding *tert*-butyl pyrrolidine-1-carboxylate (350 μL, 2.0 mmol, 5.0 equiv) and $PhSiH_3$ (9.9 μL, 20 mol%) sequentially. The tube was sealed under Ar atmosphere and stirred at r.t. for 12 h. The reaction mixture was quenched with air and diluted with EtOAc, then concentrated in vacuo. The residue was purified by flash column chromatography to give the title compound as a white solid (94 mg, 69% yield). **M.P.** 142 °C. **^{1}H NMR** (400 MHz, $CDCl_3$) δ 8.23 (s, 1H), 7.94 – 7.71 (m, 4H), 7.50 (qt, *J* = 6.9, 3.6 Hz, 2H), 6.74 (d, *J* = 6.7 Hz, 1H), 5.90 (br. m, 1H), 3.55 (m, 1H), 3.31 (m, 1H), 2.24 – 1.83 (m, 4H), 1.40 (s, 9H). **^{13}C NMR** (101 MHz, $CDCl_3$) δ 169.51 (rotamer), 166.61, 154.29, 134.76, 132.61, 131.79, 128.90, 128.45, 127.75, 127.65, 127.44, 126.74, 123.71, 80.27, 64.78, 46.19, 34.02, 28.47, 22.61. **IR (neat):** 3304, 2980, 2883, 1689, 1625, 1532, 1503, 1396, 1356, 1296, 1240, 1159, 1112, 916, 860, 822, 775, 669 cm^{-1}. **HRMS** *calcd*. for ($C_{20}H_{24}N_2NaO_3$) $[M+Na]^+$: 363.1679, *found* 363.1681.

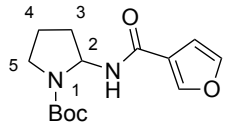

***tert*-butyl 2-(furan-3-carboxamido)pyrrolidine-1-carboxylate (4t)** An oven-dried 20 mL reaction tube containing a stir bar was charged with $Ni(ClO_4)_2 \cdot 2$Bathocuproine (39 mg, 10 mol%), 3-(furan-3-yl)-1,4,2-dioxazol-5-one (61 mg, 0.4 mmol, 1.0 equiv). The reaction tube was connected to a vacuum line where it was evacuated and backfilled with

Ar at least three times. Anhydrous pivalonitrile (1.0 mL) was added and the mixture was stirred at r.t. for 5 minutes under Ar flow before adding *tert*-butyl pyrrolidine-1-carboxylate (350 μL, 2.0 mmol, 5.0 equiv) and $PhSiH_3$ (9.9 μL, 20 mol%) sequentially. The tube was sealed under Ar atmosphere and stirred at r.t. for 12 h. The reaction mixture was quenched with air and diluted with EtOAc, then concentrated in vacuo. The residue was purified by flash column chromatography to give the title compound as a white solid (64 mg, 58% yield, 3.5:1 mixture of rotamers, A:B). **M.P.** 179 °C. **^{1}H NMR** (500 MHz, $CDCl_3$) δ 7.92 (s, 1H), 7.39 (s, 1H), 6.62 (s, 1H), 6.30 (d, J = 6.8 Hz, 1H), 5.80 (br. m, 0.70 H, C_2-H, A), 5.64 (br. m, 0.22 H, C_2-H, B), 3.52 – 3.43 (m, 1H), 3.29 (dt, J = 10.5, 8.0 Hz, 1H), 2.13 (br. m, 2H), 2.01 – 1.83 (m, 2H), 1.39 (s, 9H). **^{13}C NMR** (126 MHz, $CDCl_3$) δ 161.59, 154.33, 144.91, 143.81, 122.64, 108.46, 80.41, 64.21, 46.15, 34.01, 28.48, 22.57. **IR (neat):** 3311, 3129, 2983, 2880, 1680, 1632, 1567, 1533, 1403, 1387, 1364, 1245, 1187, 1152, 1121, 1011, 907, 876, 830, 758, 662 cm^{-1}. **HRMS** *calcd*. for ($C_{14}H_{20}N_2NaO_4$) $[M+Na]^+$: 303.1315, *found* 303.1323.

Difunctionalization of Acyclic Ethers via C-O Bond Cleavage

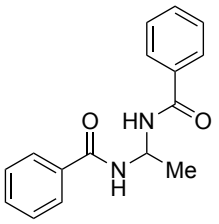

***N,N'*-(ethane-1,1-diyl)dibenzamide (3aa) from <u>diethyl ether</u>**. An oven-dried 20 mL reaction tube containing a stir bar was charged with $Ni(ClO_4)_2 \cdot$2Bathocuproine (20 mg, 10 mol%), 3-phenyl-1,4,2-dioxazol-5-one **2a** (32 mg, 0.2 mmol, 1.0 equiv). The reaction tube was connected to a vacuum line where it was evacuated and backfilled with Ar at least three times. Then anhydrous pivalonitrile (1.0 mL) was added and the mixture was stirred at r.t. for 5 minutes under Ar flow before adding degassed diethyl ether (415 μL, 4.0 mmol, 20.0 equiv) and $PhSiH_3$ (25 μL, 1.0 equiv) sequentially. The tube was sealed under Ar atmosphere and stirred at r.t. for 12 h. The reaction mixture was quenched with

air and diluted with EtOAc, then concentrated in vacuo. The residue was purified by flash column chromatography to give the title compound as a white solid (18 mg, 33% yield). **M.P.** 212 °C. **^{1}H NMR** (400 MHz, $CDCl_3$) δ 7.81 – 7.76 (m, 4H), 7.67 (d, *J* = 7.5 Hz, 2H), 7.57 – 7.46 (m, 2H), 7.45 – 7.37 (m, 4H), 5.74 (td, *J* = 7.3, 6.5 Hz, 1H), 1.81 (d, *J* = 6.8 Hz, 3H). **^{13}C NMR** (101 MHz, $CDCl_3$) δ 167.74, 134.09, 131.98, 128.73, 127.26, 55.82, 20.59. **IR (neat):** 3225, 2984, 1645, 1602, 1557, 1515, 1481, 1366, 1346, 1287, 1124, 1081, 712 696, 603 cm^{-1}. **HRMS** *calcd*. for ($C_{16}H_{17}N_2O_2$) $[M+H]^+$: 269.1285, *found* 269.1286.

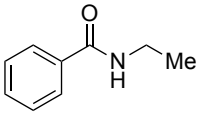

***N*-ethylbenzamide (3ab) <u>from diethyl ether</u>.** An oven-dried 20 mL reaction tube containing a stir bar was charged with $Ni(ClO_4)_2$·2Bathocuproine (20 mg, 10 mol%), 3-phenyl-1,4,2-dioxazol-5-one **2a** (32 mg, 0.2 mmol, 1.0 equiv). The reaction tube was connected to a vacuum line where it was evacuated and backfilled with Ar at least three times. Then anhydrous pivalonitrile (1.0 mL) was added and the mixture was stirred at r.t. for 5 minutes under Ar flow before adding degassed diethyl ether (415 µL, 4.0 mmol, 20.0 equiv) and $PhSiH_3$ (25 µL, 1.0 equiv) sequentially. The tube was sealed under Ar atmosphere and stirred at r.t. for 24 h. Then Et_3SiH (64 µL, 0.4 mmol, 2.0 equiv) and methanesulfonic acid (20 µL, 0.3 mmol, 1.5 equiv) was added and reaction was stirred at r.t. for another 12 h. Then, the reaction mixture was diluted with aq. $NaHCO_3$ and EtOAc, and the aqueous layer was extracted with three portions of EtOAc. The combined organic layers were dried over Na2SO4, filtered, and concentrated. The residue was purified by flash column chromatography to give the title compound as a white solid (9 mg, 31% yield). **M.P.** 70 °C. **^{1}H NMR** (300 MHz, $CDCl_3$) δ 7.86 – 7.70 (m, 2H), 7.49 – 7.38 (m, 1H), 7.34 (m, 2H), 6.81 (s, 1H), 3.42 (qd, *J* = 7.2, 5.6 Hz, 2H), 1.18 (t, *J* = 7.3 Hz, 3H). **^{13}C NMR** (75 MHz, $CDCl_3$) δ 167.63, 134.79, 131.20, 128.40, 126.95, 34.91, 14.83. **IR (neat):** 3316, 2979, 2936, 1633, 1602, 1578, 1544, 1487, 1432, 1359, 1309, 1286, 1145,

1088, 866, 692, 674, 657, 615 cm^{-1}. **HRMS** *calcd*. for ($C_9H_{12}NO$) $[M+H]^+$: 150.0913, *found* 150.0914.

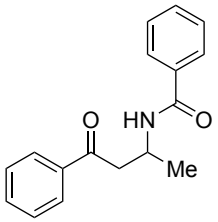

***N*-(4-oxo-4-phenylbutan-2-yl)benzamide (3ac) <u>from diethyl ether</u>.** An oven-dried 20 mL reaction tube containing a stir bar was charged with $Ni(ClO_4)_2 \cdot 2$Bathocuproine (20 mg, 10 mol%), 3-phenyl-1,4,2-dioxazol-5-one **2a** (32 mg, 0.2 mmol, 1.0 equiv). The reaction tube was connected to a vacuum line where it was evacuated and backfilled with Ar at least three times. Then anhydrous pivalonitrile (1.0 mL) was added and the mixture was stirred at r.t. for 5 minutes under Ar flow before adding degassed diethyl ether (415 µL, 4.0 mmol, 20.0 equiv) and $PhSiH_3$ (4.9 µL, 20 mol%) sequentially. The tube was sealed under Ar atmosphere and stirred at r.t. for 2 h and then 1-Phenyl-1-trimethylsiloxyethylene (80 µL, 0.4 mmol, 2.0 equiv) was added. After stirring for another 22 h, the reaction mixture was quenched with air and diluted with EtOAc, then concentrated in vacuo. The residue was purified by flash column chromatography to give the title compound as a white solid (16 mg, 30% yield). **M.P.** 165 °C. **^{1}H NMR** (300 MHz, $CDCl_3$) δ 8.04 – 7.94 (m, 2H), 7.83 – 7.74 (m, 2H), 7.63 – 7.55 (m, 1H), 7.53 – 7.38 (m, 5H), 7.05 (d, J = 8.4 Hz, 1H), 4.77 – 4.62 (m, 1H), 3.48 (dd, J = 16.8, 4.2 Hz, 1H), 3.20 (dd, J = 16.8, 5.9 Hz, 1H), 1.41 (d, J = 6.9 Hz, 3H). **^{13}C NMR** (101 MHz, $CDCl_3$) δ 199.84, 166.82, 137.06, 134.74, 133.68, 131.56, 128.89, 128.68, 128.29, 127.06, 43.36, 43.10, 20.23. **IR (neat):** 3311, 2977, 1685, 1635, 1602, 1578, 1545, 1492, 1448, 1405, 1367, 1347, 1293, 1220, 1164, 1100, 1068, 1000, 759, 689, 653 cm^{-1}. **HRMS** *calcd*. for ($C_{17}H_{17}NNaO_2$) $[M+Na]^+$: 290.1151, *found* 290.1153.

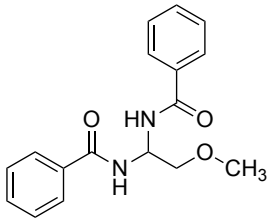

***N,N'*-(2-methoxyethane-1,1-diyl)dibenzamide (3ad) <u>from ethylene glycol dimethyl ether</u>**. An oven-dried 20 mL reaction tube containing a stir bar was charged with $Ni(ClO_4)_2 \cdot 2$Bathocuproine (20 mg, 10 mol%), 3-phenyl-1,4,2-dioxazol-5-one **2a** (32 mg, 0.2 mmol, 1.0 equiv). The reaction tube was connected to a vacuum line where it was evacuated and backfilled with Ar at least three times. Then anhydrous pivalonitrile (1.0 mL) was added and the mixture was stirred at r.t. for 5 minutes under Ar flow before adding anhydrous ethylene glycol dimethyl ether (416 μL, 4.0 mmol, 20.0 equiv) and $PhSiH_3$ (25 μL, 1.0 equiv) sequentially. The tube was sealed under Ar atmosphere and stirred at r.t. for 24 h. The reaction mixture was quenched with air and diluted with EtOAc, then concentrated in vacuo. The residue was purified by flash column chromatography to give the title compound as a white solid (14 mg, 24% yield). **M.P.** 185 °C. **^{1}H NMR** (400 MHz, $CDCl_3$) δ 7.83 – 7.77 (m, 4H), 7.54 – 7.48 (m, 2H), 7.43 (m, 4H), 7.34 (d, J = 7.6 Hz, 2H), 5.99 (tt, J = 7.7, 5.2 Hz, 1H), 3.87 (d, J = 5.2 Hz, 2H), 3.43 (s, 3H). **^{13}C NMR** (101 MHz, $CDCl_3$) δ 167.51, 133.81, 132.10, 128.76, 127.33, 72.82, 59.40, 57.76. **IR (neat):** 3247,2927, 1648, 1303, 1558, 1515, 1486, 1366, 1334, 1292, 1142, 1129, 1091, 1078, 713, 692, 666 cm^{-1}. **HRMS** *calcd*. for ($C_{17}H_{18}N_2NaO_3$) $[M+Na]^+$: 321.1210, *found* 321.1211.

2.7.4 Preliminary mechanistic studies

Intercepting radical intermediates with methyl acrylate

An oven-dried 20 mL reaction tube containing a stir bar was charged with $Ni(ClO_4)_2 \cdot 2$Bathocuproine (19 mg, 10 mol%), **2a** (0.2 mmol, 1.0 equiv). The reaction tube was connected to a vacuum line where it was evacuated and backfilled with Ar at

least three times. Then anhydrous THF (1.0 mL) was added, and the mixture was stirred at r.t. for 5 minutes under Ar flow before adding $PhSiH_3$ (4.9 μL, 20 mol%) and methyl acrylate 17 μL, 0.3 mmol) sequentially. The tube was sealed under Ar atmosphere and stirred at r.t. for 24 h. The reaction mixture was quenched with air and diluted with EtOAc, then concentrated in vacuo. The residue was purified by flash column chromatography to give **3a** (12 mg, 31% yield) and **5a** (5 mg, 16% yield).

Methyl 3-(tetrahydrofuran-2-yl)propanoate 5a. White solid. **^{1}H NMR** (400 MHz, $CDCl_3$) δ 3.88 – 3.78 (m, 2H), 3.76 – 3.69 (m, 1H), 3.67 (s, 3H), 2.52 – 2.32 (m, 2H), 1.99 (m, 1H), 1.93 – 1.78 (m, 4H), 1.47 (m, 1H). **^{13}C NMR** (101 MHz, $CDCl_3$) δ 174.23, 78.30, 67.86, 51.71, 31.33, 31.08, 30.86, 25.84. Data consistent with those previously reported.

Intermolecular kinetic isotope effect.

An oven-dried 20 mL reaction tube containing a stir bar was charged with $Ni(ClO_4)_2$·2Bathocuproine (39 mg, 10 mol%), **2a** (0.4 mmol, 1.0 equiv). The reaction tube was taken into a nitrogen-filled glove box. Then anhydrous pivalonitrile (1.0 mL) was added and the mixture was stirred at r.t. for 5 minutes before adding THF (325 μL, 4.0 mmol) or THF-*d8* (325 μL, 4.0 mmol), dodecane (internal standard, 45 μL, 0.2 mmol) and $PhSiH_3$ (9.9 μL, 20 mol%). The tube was sealed and stirred at r.t. Aliquots were taken from the reaction mixture at the indicated time points, and were then quenched with air, diluted with EtOAc, and analyzed by GC. KIE: k_H/k_D= 0.1780/0.0646 = 3.8

Stochiometric organometallic reactions

Reaction between $[(L1)_2Ni^{II}][ClO_4]_2$ and $PhSiH_3$

In the glovebox, $[(\mathbf{L1})_2Ni^{II}][ClO_4]_2$ (14.6 mg, 0.015 mmol) was added to a 4 mL vial and dissolved in 1 mL MeCN-d_3 with a stir bar. To the stirred solution, $PhSiH_3$ (3.2 mg, 0.03 mmol, 2 equiv.) was added. This solution was then stirred for 30 minutes and an aliquot was taken for EPR analysis which identified the formation of paramagnetic species

(Figure 2.2, below) with line shape and g values (g(x) = 2.07876, g(y) = 2.12142, g(z) = 2.36243) matching Ni(I) perchlorate complex $[(L1)_2Ni^{I}][ClO_4]$. The remaining solution was transferred to a J-young NMR tube and analyzed by paramagnetic ^1H NMR (Figure 2.4, below t_1) which revealed paramagnetic ^1H NMR signals consistent with the formation of $[(\mathbf{L1})2Ni^{I}][ClO_4]$ and remaining Ni(II). To determine if reduction to Ni(0) species or free ligand was liberated had occurred, the solution was brought back into the glovebox, the solvent was removed, redissolved in C_6D_6 and analyzed by ^1H NMR. Analysis of the ^1H NMR spectra (Figure 2.4, top, t_{final}) shows no formation of Ni(0) complexes such as $(\mathbf{L1})_2Ni$ or the liberation of L1 and is consistent with the reaction between $[(\mathbf{L1})_2Ni^{II}][ClO_4]_2$ and $PhSiH_3$ forming $[(\mathbf{L1})_2Ni^{I}][ClO_4]$. **Conclusion**: $[(\mathbf{L1})_2Ni^{II}][ClO_4]_2$ is reduced to $[(L1)_2Ni^{I}][ClO_4]$ by $PhSiH_3$.

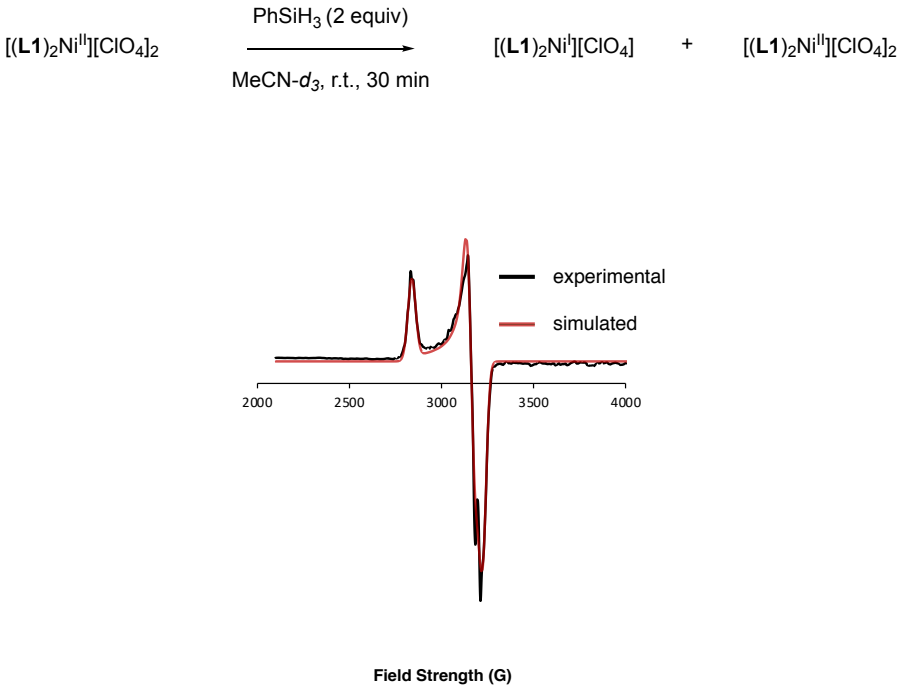

Figure 2.2 X-band EPR spectra (MeCN, 77 K) of the reaction between $[(\mathbf{L1})_2Ni^{II}][ClO_4]_2$ and $PhSiH_3$. g(z) = 2.36243, g(y) = 2.12142, g(x) = 2.07876.

EPR Spectra of Synthesized Complexes

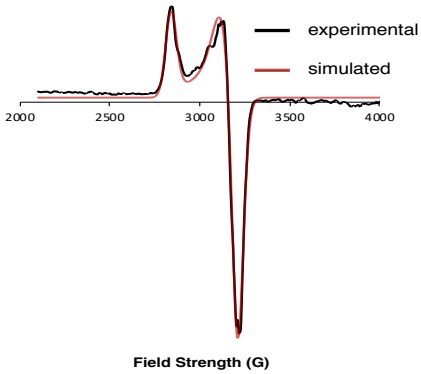

Figure 2.3 X-band EPR spectra (THF, 77 K) of $[(\mathbf{L1})_2Ni^{I}][ClO_4]$. g(z) = 2.36059, g(y) = 2.1198, g(x) = 2.09323.

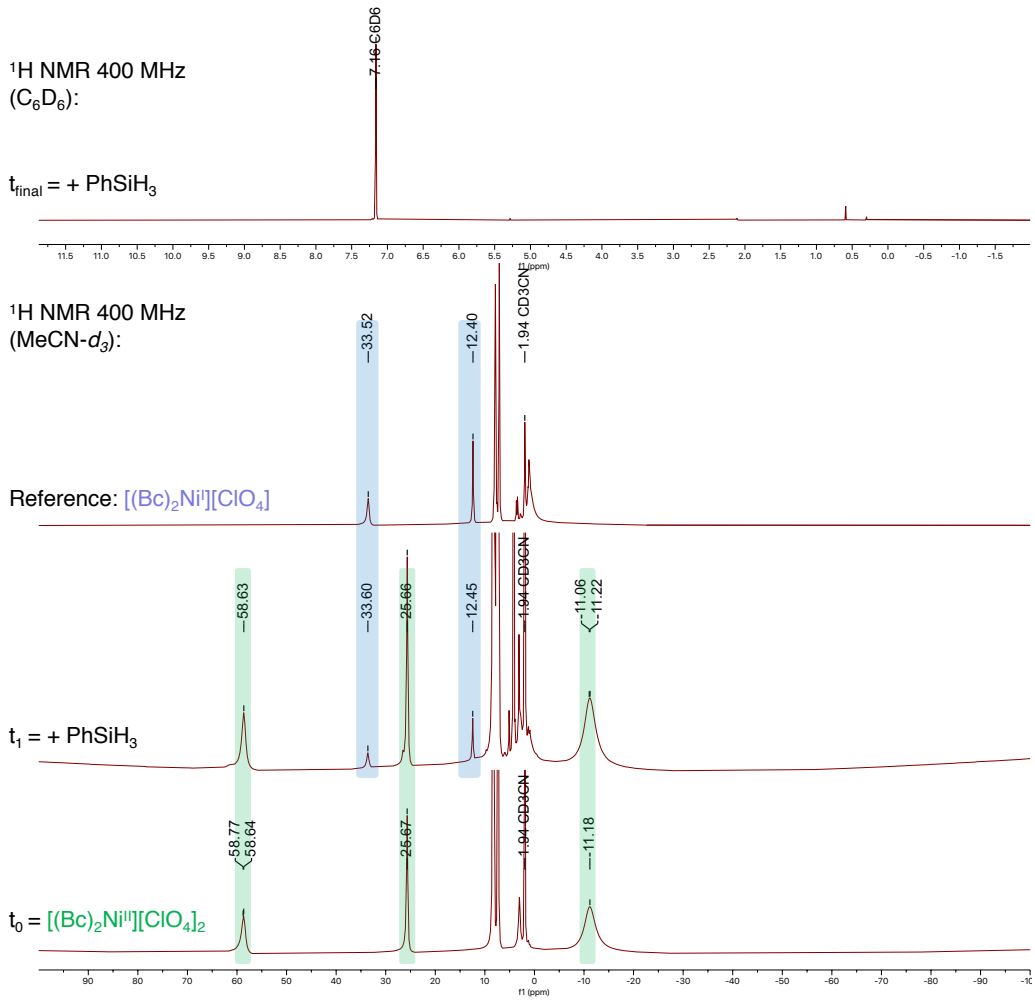

Figure 2.4 ^{1}H spectra (MeCN-d_3/C_6D_6, 400 MHz) of the reaction between $[(\mathbf{L1})_2Ni^{II}][ClO_4]_2$ and $PhSiH_3$. $[(\mathbf{L1})_2Ni^{II}][ClO_4]_2$ (green), $[(\mathbf{L1})_2Ni^{I}][ClO_4]$ (blue).

Analyzing resting state species by paramagnetic ^{1}H NMR, EPR and UV-VIS

The standard reaction of **1a** with **2a** was setup and reacted for 3 hours at which point it was brought into the glovebox and an aliquot was added to an EPR tube, diluted in MeCN and analyzed by EPR. The lack of an EPR signal (Figure 2.5) is consistent with no Ni(I) species as resting state intermediates in catalysis. The remaining solvent of the reaction mixture was then removed. The reaction mixture was redissolved in MeCN-d_3 and transferred to a J-young NMR tube and analyzed by paramagnetic ^{1}H NMR (Figure 2.6, middle, catalytic reaction mixture). By paramagnetic ^{1}H NMR, Ni(II) complex $[(\mathbf{L1})_2Ni^{II}][ClO_4]_2$ is the resting state nickel species in catalysis. In a separate experiment, the UV-VIS of the standard reaction was measured and displayed an absorption peak (l_{max} = 585 nm, Figure 2.7, blue trace) that overlaid nearly identically to $[(\mathbf{L1})_2Ni^{II}][ClO_4]_2$ (l_{max} = 585 nm, Figure 2.7, red trace). **Conclusion**: $[(\mathbf{L1})_2Ni^{II}][ClO_4]_2$ is the primary resting state species in catalysis.

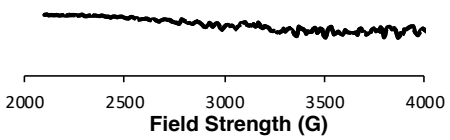

Figure 2.5 X-band EPR spectra (MeCN, 77 K) of the catalytic reaction.

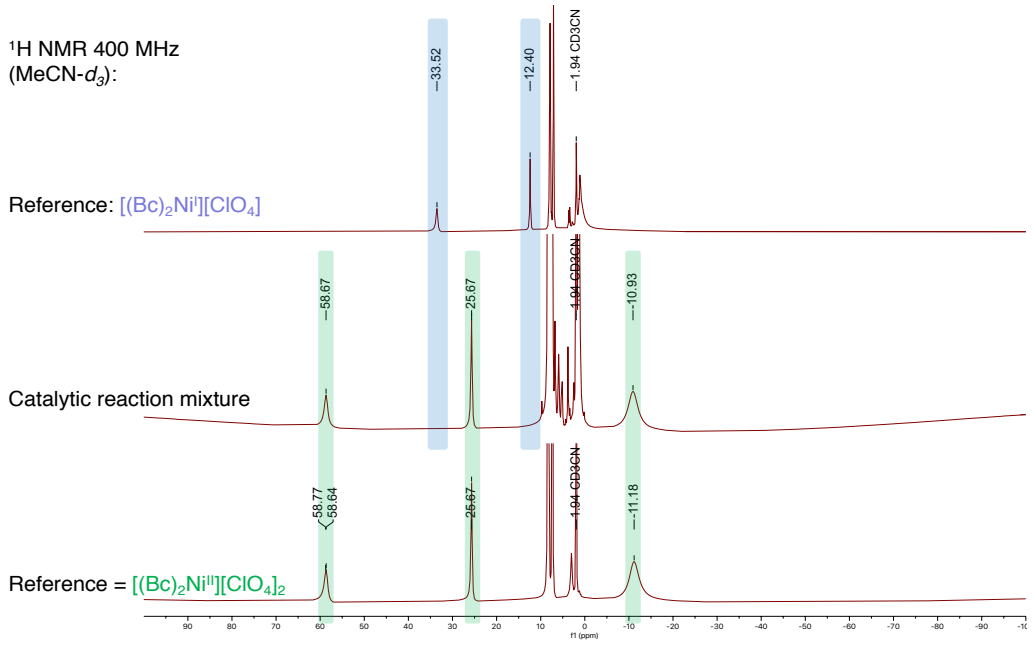

Figure 2.6 ^{1}H spectra (MeCN-d$_3$, 400 MHz) of the catalytic reaction. [(**L1**)$_2$Ni^{II}][ClO$_4$]$_2$ (green), [(**L1**)$_2$Ni^{I}][ClO$_4$] (blue).

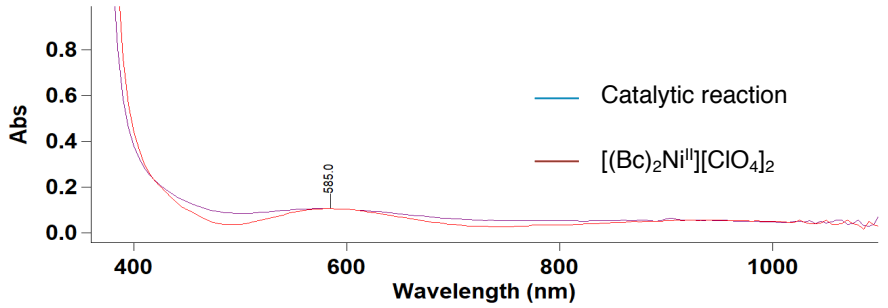

Figure 2.7 UV-VIS spectra (MeCN) of the catalytic reaction. [(**L1**)$_2$Ni^{II}][ClO$_4$]$_2$ (red trace), catalytic reaction mixture (blue trace).

Stochiometric $[(L1)_2Ni^I][ClO_4]$ and nitrene precursor 2a.

In the glovebox, $[(\mathbf{L1})_2Ni^I][ClO_4]$ (8.8 mg, 0.01 mmol) was added to a 4 mL vial and dissolved in 0.5 mL THF with a stir bar. To the sirred solution, 3-phenyl-1,4,2-dioxazol-5-one **2a** (1.6 mg, 0.01 mmol, 1.0 equiv) was added. The reaction was stirred at r.t. for 12 h. Then the reaction mixture was quenched with air, diluted with EtOAc and analyzed by GC, which gave the **3a** with 37% yield.

In the glovebox, $[(\mathbf{L1})_2Ni^I][ClO_4]$ (8.8 mg, 0.01 mmol) was added to a 4 mL vial and dissolved in 1 mL MeCN-d_3 with a stir bar. To the sirred solution, 3-phenyl-1,4,2-dioxazol-5-one **2a** (2.0 mg, 0.01 mmol, 1.1 equiv) was added in which a rapid colour change to orange was observed. This solution was then stirred for 30 minutes and an aliquot was taken for EPR analysis which identified full conversion of Ni(I), and no EPR active species (Figure 2.8, below), consistent with the formation of Ni(II) or Ni(III) complexes. The remaining solution was transferred to a J-young NMR tube and analyzed by paramagnetic ^{1}H NMR (Figure 2.9, below t_1) which displayed a complex mixture of paramagnetic products. Multiple attempts to isolate and characterized the resulting complexes were unsuccessful. **Conclusion**: $[(\mathbf{L1})_2Ni^I][ClO_4]$ reacts readily with 3-phenyl-1,4,2-dioxazol-5-one **2a** to form a mixture of Ni(II) and/or Ni(III) complexes. We hypothesize that an intermediate Ni(III) nitrene complex is generated which rapidly reacts at the high concentrations of synthesis to a complex mixture of Ni(II) and/or Ni(III) products.

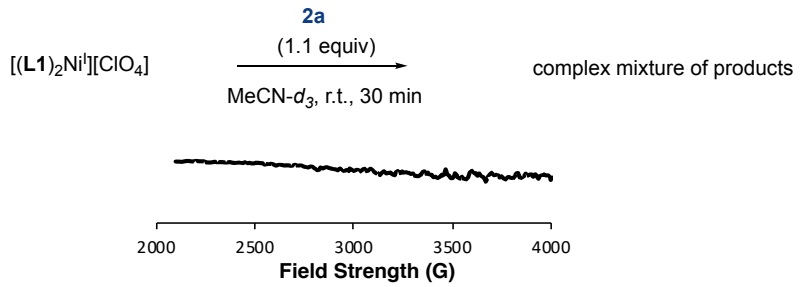

Figure 2.8 X-band EPR spectra (MeCN, 77 K) of the catalytic reaction.

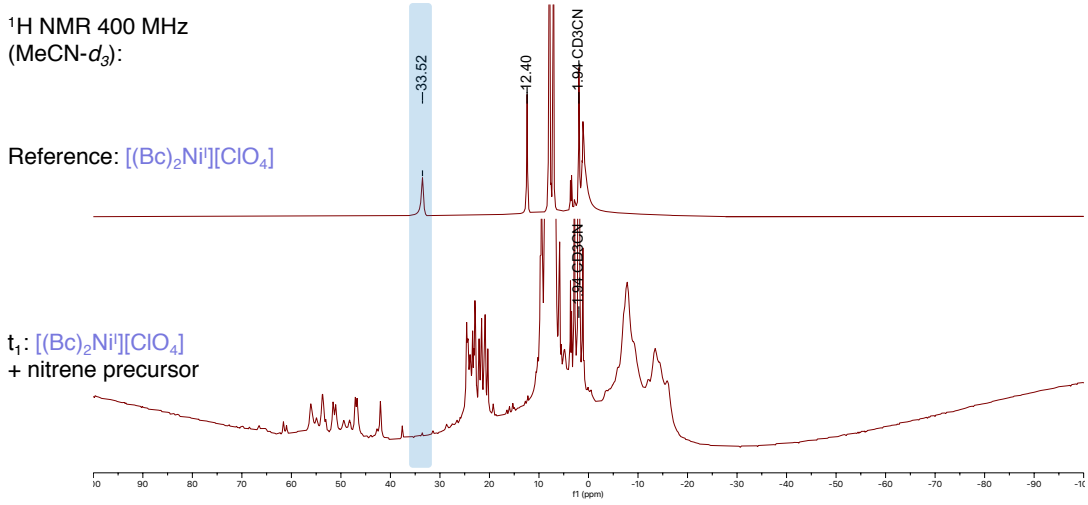

Figure 2.9 ^{1}H spectra (MeCN-d_3, 400 MHz) of the reaction between [(**L1**)$_2$Ni^I][ClO$_4$] and 3-phenyl-1,4,2-dioxazol-5-one. [(**L1**)$_2$Ni^I][ClO$_4$] (blue).

Cyclic voltammetry experiments

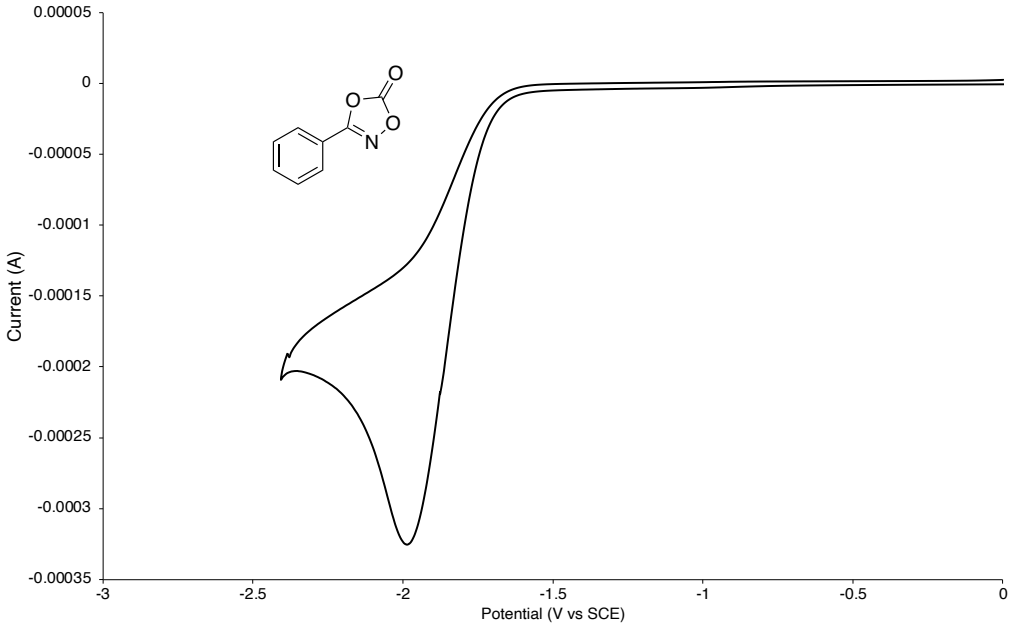

Figure 2.10 Cyclic voltammogram of 3-phenyl-1,4,2-dioxazol-5-one **2a**. Voltammograms were taken using a glassy carbon working electrode in a 0.1 M [$^{n}Bu_4N$][PF_6] supporting electrolyte MeCN solution with a 100 mV/s scan rate and 0.01 M of sample referenced to Fc (+0.38 V vs SCE). Scans were started at the open-circuit potential and scanned in the anode direction first. E_p value for 3-phenyl-1,4,2-dioxazol-5-one radical anion reduction = -1.98 V vs SCE.

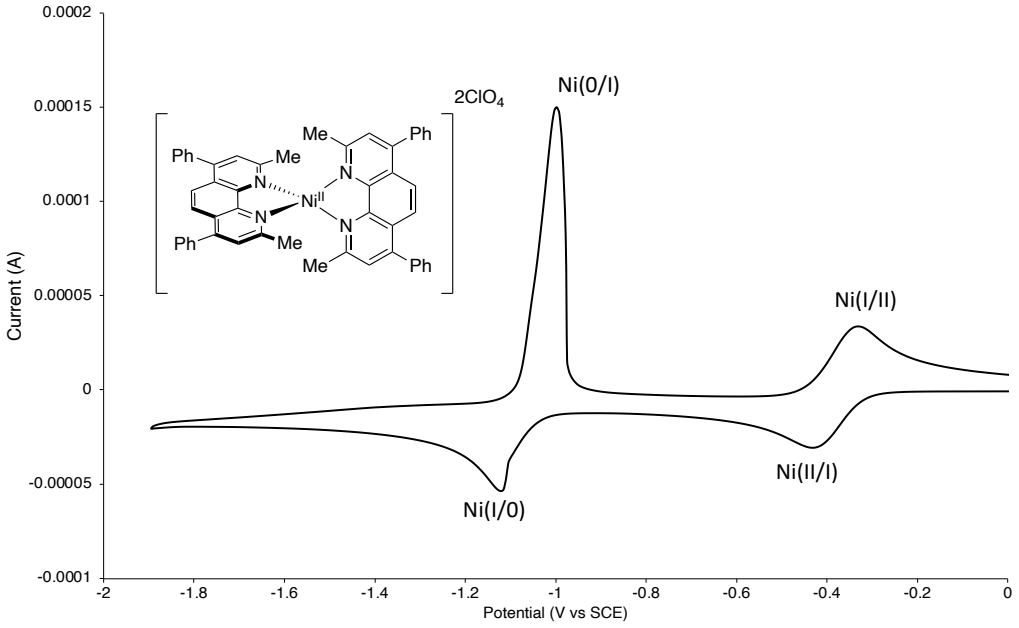

Figure 2.11 Cyclic voltammogram of $[(\mathbf{L1})_2Ni^{II}][ClO_4]_2$. Voltammograms were taken using a glassy carbon working electrode in a 0.1 M $[^nBu_4N][PF_6]$ supporting electrolyte MeCN solution with a 100 mV/s scan rate and 0.01 M of sample referenced to Fc (+0.38 V vs SCE). Scans were started at the open-circuit potential and scanned in the anode direction first. Redox potential value for $[(\mathbf{L1})_2Ni^{II}][ClO_4]_2$ are $E^o(Ni(II/I))$ = -0.38 V vs SCE and $E^o(Ni(I/0))$ = -1.06 V vs SCE.

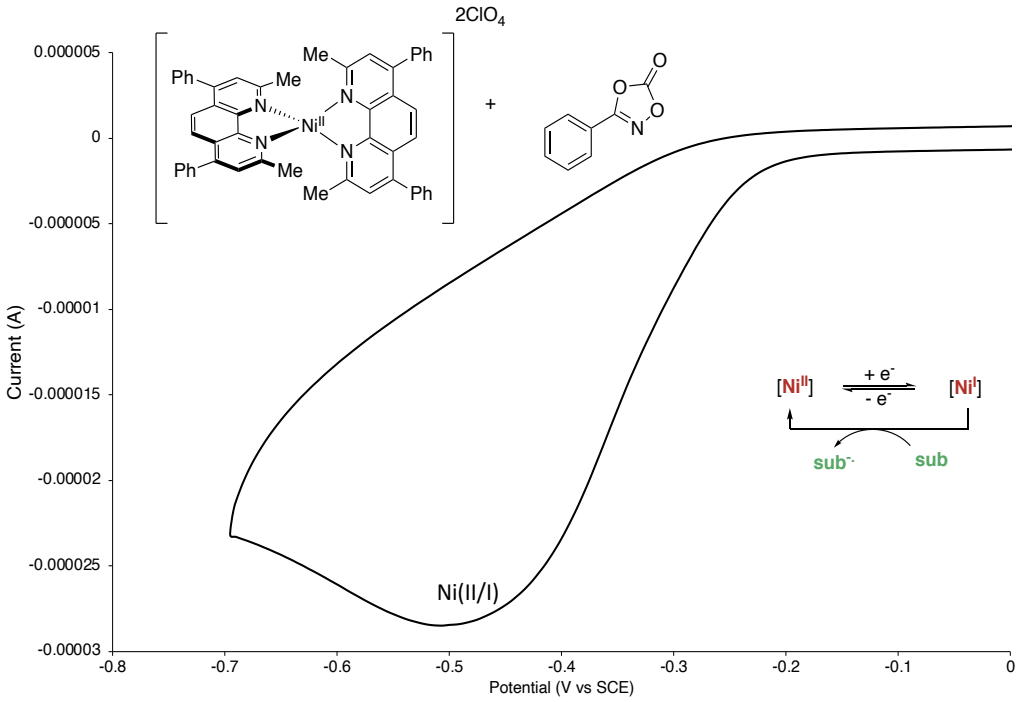

Figure 2.12 Cyclic voltammogram of $[(\mathbf{L1})_2Ni^{II}][ClO_4]_2$ with 3-phenyl-1,4,2-dioxazol-5-one **2a** added (1:1 mol ratio). Voltammograms were taken using a glassy carbon working electrode in a 0.1 M $[^nBu_4N][PF_6]$ supporting electrolyte MeCN solution with a 100 mV/s scan rate and 0.01 M of sample referenced to Fc (+0.38 V vs SCE). Scans were started at the open-circuit potential and scanned in the anode direction first. The previously reversible reduction of Ni(II/I) for $[(\mathbf{L1})_2Ni^{II}][ClO_4]_2$ is now irreversible, which is consistent with the electrochemically generated Ni(I) species $[(\mathbf{L1})_2Ni^{I}][ClO_4]$ reacting rapidly with 3-phenyl-1,4,2-dioxazol-5-one **2a** to form Ni(II) or Ni(III) compounds.

2.7.5 X-ray Diffraction

X-ray diffraction of $Ni(ClO_4)_2 \cdot 2L1$ (Ni-1)

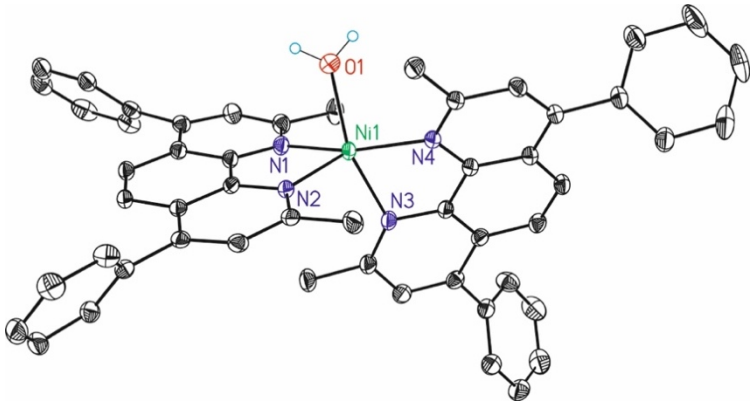

Figure 2.13 ORTEP diagram of **Ni-1**, CCDC: 2194347

Table 2.7 Crystal data and structure refinement for **Ni-1**.

Empirical formula	C56H50.40Cl2N4NiO11.20
Formula weight	1088.21
Temperature/K	100(2)
Wavelength	0.71073 Å
Crystal system	triclinic
Space group	P -1
a/Å	11.0288(2)
b/Å	14.3085(3)
c/Å	16.7284(3)
α/°	75.870(2)
β/°	85.509(2)
γ/°	85.669
Volume/$Å^3$	2547.76(9)

Table 2.7 Crystal data and structure refinement for **Ni-1**.

Z	2
ρ_{calc}Mg/cm^3	1.419
μ/mm^{-1}	0.553
F(000)	1132
Crystal size/mm^3	0.40 × 0.25 × 0.10
Theta range for data collection/°	3.326 to 29.856
Index ranges	-15<=h<=15,-19<=k<=19,-23<=l<=23
Reflections collected	61974
Independent reflections	13316[R(int) = 0.0501]
Completeness to theta =29.856°	90.8%
Absorption correction	Multi-scan
Max. and min. transmission	1.00 and 0.80
Refinement method	Full-matrix least-squares on F^2
Data/restraints/parameters	13316/ 102/ 774
Goodness-of-fit on F^2	0.954
Final R indexes [I>=2σ (I)]	R1 = 0.0396, wR2 = 0.1077
Final R indexes [all data]	R1 = 0.0514, wR2 = 0.1149
Largest diff. peak/hole / e Å^{-3}	0.753 and -0.570

Table 2.8 Bond Lengths for **Ni-1**.

Atom	**Atom**	**Length/Å**	**Atom**	**Atom**	**Length/Å**
Ni1	N2	2.0477(13)	C51	C46	1.403(2)
Ni1	N4	2.0666(13)	C51	H51	0.9500
Ni1	N3	2.0721(13)	C1	N4	1.335(2)
Ni1	O1	2.0743(12)	C1	C13	1.497(2)
C2	C3	1.374(2)	N2	C27	1.337(2)

Atom	Atom	Length/Å	Atom	Atom	Length/Å
C2	C1	1.404(2)	N2	C31	1.3722(19)
C2	H2	0.9500	N3	C12	1.338(2)
C3	C4	1.425(2)	N3	C9	1.3701(19)
C3	C14	1.484(2)	N4	C5	1.3705(18)
C4	C5	1.404(2)	C5	C9	1.439(2)
C4	C6	1.430(2)	C8	C9	1.404(2)
C6	C7	1.356(2)	C8	C10	1.427(2)
C6	H6	0.9500	C10	C20	1.487(2)
O1	H1W	0.8494	C12	C26	1.497(2)
O1	H2W	0.9079	C13	H13A	0.9800
N1	C38	1.333(2)	C13	H13B	0.9800
N1	C35	1.3609(19)	C13	H13C	0.9800
C7	C8	1.428(2)	C26	H26A	0.9800
C7	H7	0.9500	C26	H26B	0.9800
C11	C10	1.369(2)	C26	H26C	0.9800
C11	C12	1.409(2)	C27	C39	1.496(2)
C11	H11	0.9500	C29	C30	1.424(2)
C15	C16	1.390(3)	C29	C40	1.480(2)
C15	C14	1.397(2)	C30	C31	1.404(2)
C15	H15	0.9500	C31	C35	1.437(2)
C16	C17	1.380(4)	C34	C35	1.406(2)
C16	H16	0.9500	C34	C36	1.428(2)
C17	C18	1.382(3)	C36	C46	1.485(2)
C17	H17	0.9500	C38	C52	1.497(2)
C18	C19	1.392(3)	C39	H39A	0.9800
C18	H18	0.9500	C39	H39B	0.9800
C19	C14	1.392(2)	C39	H39C	0.9800
C19	H19	0.9500	C52	H52A	0.9800
C21	C22	1.387(3)	C52	H52B	0.9800
C21	C20	1.389(3)	C52	H52C	0.9800
C21	H21	0.9500	O1A	Cl1A	1.4078(14)
C22	C23	1.390(3)	O1A	Cl1B	1.520(3)
C22	H22	0.9500	Cl1A	O3A	1.4253(18)
C23	C24	1.375(3)	Cl1A	O2A	1.437(2)

Atom	Atom	Length/Å	Atom	Atom	Length/Å
C23	H23	0.9500	Cl1A	O4A	1.4610(18)
C24	C25	1.391(2)	Cl1B	O2B	1.361(12)
C24	H24	0.9500	Cl1B	O3B	1.374(8)
C25	C20	1.395(2)	Cl1B	O4B	1.527(15)
C25	H25	0.9500	O2W	H3W	1.0235
C28	C29	1.383(2)	O2W	H4W	0.9424
C28	C27	1.404(2)	Cl2A	O6A	1.4113(15)
C28	H28	0.9500	Cl2A	O7A	1.4136(16)
C32	C33	1.355(2)	Cl2A	O8A	1.4314(18)
C32	C30	1.432(2)	Cl2A	O5A	1.4524(14)
C32	H32	0.9500	C1S	C2S	1.480(8)
C33	C34	1.426(2)	C1S	H1SA	0.9800
C33	H33	0.9500	C1S	H1SB	0.9800
C37	C36	1.380(2)	C1S	H1SC	0.9800
C37	C38	1.407(2)	C2S	O2S	1.210(5)
C37	H37	0.9500	C2S	O1S	1.352(6)
C41	C42	1.386(3)	C3S	O1S	1.454(6)
C41	C40	1.397(2)	C3S	C4S	1.499(7)
C41	H41	0.9500	C3S	H3SA	0.9900
C42	C43	1.387(3)	C3S	H3SB	0.9900
C42	H42	0.9500	C4S	H4SA	0.9800
C43	C44	1.385(3)	C4S	H4SB	0.9800
C43	H43	0.9500	C4S	H4SC	0.9800
C44	C45	1.391(2)	C1S'	C2S'	1.481(7)
C44	H44	0.9500	C1S'	H1SD	0.9800
C45	C40	1.397(2)	C1S'	H1SE	0.9800
C45	H45	0.9500	C1S'	H1SF	0.9800
C47	C48	1.390(2)	C2S'	O2S'	1.210(4)
C47	C46	1.397(2)	C2S'	O1S'	1.352(6)
C47	H47	0.9500	C3S'	O1S'	1.456(6)
C48	C49	1.388(3)	C3S'	C4S'	1.497(8)
C48	H48	0.9500	C3S'	H3SC	0.9900
C49	C50	1.379(3)	C3S'	H3SD	0.9900
C49	H49	0.9500	C4S'	H4SD	0.9800

Atom	Atom	Length/Å	Atom	Atom	Length/Å
C50	C51	1.391(3)	C4S'	H4SE	0.9800
C50	H50	0.9500	C4S'	H4SF	0.9800

Table 2.9 Bond Angles for **Ni-1**.

Atom	Atom	Atom	Angle/°	Atom	Atom	Atom	Angle/°
N1	Ni1	N2	81.43(5)	C11	C10	C20	120.20(14)
N1	Ni1	N4	160.58(5)	C8	C10	C20	121.91(14)
N2	Ni1	N4	117.76(5)	N3	C12	C11	121.03(14)
N1	Ni1	N3	98.87(5)	N3	C12	C26	119.76(14)
N2	Ni1	N3	103.28(5)	C11	C12	C26	119.20(14)
N4	Ni1	N3	80.38(5)	C1	C13	H13A	109.5
N1	Ni1	O1	82.79(5)	C1	C13	H13B	109.5
N2	Ni1	O1	99.27(5)	H13A	C13	H13B	109.5
N4	Ni1	O1	90.63(5)	C1	C13	H13C	109.5
N3	Ni1	O1	157.39(5)	H13A	C13	H13C	109.5
C3	C2	C1	121.72(14)	H13B	C13	H13C	109.5
C3	C2	H2	119.1	C19	C14	C15	119.33(16)
C1	C2	H2	119.1	C19	C14	C3	121.74(15)
C2	C3	C4	117.61(14)	C15	C14	C3	118.91(15)
C2	C3	C14	119.70(14)	C21	C20	C25	119.55(15)
C4	C3	C14	122.69(13)	C21	C20	C10	121.16(15)
C5	C4	C3	117.66(13)	C25	C20	C10	119.27(16)
C5	C4	C6	118.73(14)	C12	C26	H26A	109.5
C3	C4	C6	123.61(14)	C12	C26	H26B	109.5
C7	C6	C4	121.33(14)	H26A	C26	H26B	109.5
C7	C6	H6	119.3	C12	C26	H26C	109.5
C4	C6	H6	119.3	H26A	C26	H26C	109.5
Ni1	O1	H1W	123.9	H26B	C26	H26C	109.5
Ni1	O1	H2W	121.5	N2	C27	C28	121.25(14)
H1W	O1	H2W	100.6	N2	C27	C39	118.95(14)
C38	N1	C35	119.08(13)	C28	C27	C39	119.80(15)
C38	N1	Ni1	127.77(11)	C28	C29	C30	117.26(14)

Atom	Atom	Atom	Angle/°	Atom	Atom	Atom	Angle/°
C35	N1	Ni1	112.36(10)	C28	C29	C40	120.07(14)
C6	C7	C8	121.08(14)	C30	C29	C40	122.66(13)
C6	C7	H7	119.5	C31	C30	C29	117.92(13)
C8	C7	H7	119.5	C31	C30	C32	118.51(14)
C10	C11	C12	121.65(14)	C29	C30	C32	123.56(14)
C10	C11	H11	119.2	N2	C31	C30	123.37(14)
C12	C11	H11	119.2	N2	C31	C35	116.95(13)
C16	C15	C14	119.92(19)	C30	C31	C35	119.65(13)
C16	C15	H15	120.0	C35	C34	C33	118.06(14)
C14	C15	H15	120.0	C35	C34	C36	117.63(14)
C17	C16	C15	120.3(2)	C33	C34	C36	124.29(14)
C17	C16	H16	119.9	N1	C35	C34	123.03(14)
C15	C16	H16	119.9	N1	C35	C31	116.46(13)
C16	C17	C18	120.28(18)	C34	C35	C31	120.51(13)
C16	C17	H17	119.9	C37	C36	C34	117.59(14)
C18	C17	H17	119.9	C37	C36	C46	120.70(14)
C17	C18	C19	119.89(19)	C34	C36	C46	121.71(14)
C17	C18	H18	120.1	N1	C38	C37	121.11(14)
C19	C18	H18	120.1	N1	C38	C52	117.70(15)
C18	C19	C14	120.29(18)	C37	C38	C52	121.18(15)
C18	C19	H19	119.9	C27	C39	H39A	109.5
C14	C19	H19	119.9	C27	C39	H39B	109.5
C22	C21	C20	120.48(18)	H39A	C39	H39B	109.5
C22	C21	H21	119.8	C27	C39	H39C	109.5
C20	C21	H21	119.8	H39A	C39	H39C	109.5
C21	C22	C23	119.56(19)	H39B	C39	H39C	109.5
C21	C22	H22	120.2	C45	C40	C41	119.21(15)
C23	C22	H22	120.2	C45	C40	C29	121.50(14)
C24	C23	C22	120.32(17)	C41	C40	C29	119.20(14)
C24	C23	H23	119.8	C47	C46	C51	118.87(16)
C22	C23	H23	119.8	C47	C46	C36	120.39(15)
C23	C24	C25	120.39(18)	C51	C46	C36	120.73(15)
C23	C24	H24	119.8	C38	C52	H52A	109.5
C25	C24	H24	119.8	C38	C52	H52B	109.5

Atom	Atom	Atom	Angle/°	Atom	Atom	Atom	Angle/°
C24	C25	C20	119.68(18)	H52A	C52	H52B	109.5
C24	C25	H25	120.2	C38	C52	H52C	109.5
C20	C25	H25	120.2	H52A	C52	H52C	109.5
C29	C28	C27	121.88(15)	H52B	C52	H52C	109.5
C29	C28	H28	119.1	O1A	Cl1A	O3A	109.57(11)
C27	C28	H28	119.1	O1A	Cl1A	O2A	109.97(13)
C33	C32	C30	121.35(14)	O3A	Cl1A	O2A	110.92(14)
C33	C32	H32	119.3	O1A	Cl1A	O4A	108.28(10)
C30	C32	H32	119.3	O3A	Cl1A	O4A	109.41(13)
C32	C33	C34	121.64(14)	O2A	Cl1A	O4A	108.64(13)
C32	C33	H33	119.2	O2B	Cl1B	O3B	115.8(8)
C34	C33	H33	119.2	O2B	Cl1B	O1A	119.3(6)
C36	C37	C38	121.36(15)	O3B	Cl1B	O1A	114.5(4)
C36	C37	H37	119.3	O2B	Cl1B	O4B	101.3(10)
C38	C37	H37	119.3	O3B	Cl1B	O4B	100.6(8)
C42	C41	C40	120.12(16)	O1A	Cl1B	O4B	100.5(6)
C42	C41	H41	119.9	H3W	O2W	H4W	110.7
C40	C41	H41	119.9	O6A	Cl2A	O7A	110.91(13)
C41	C42	C43	120.37(17)	O6A	Cl2A	O8A	109.12(11)
C41	C42	H42	119.8	O7A	Cl2A	O8A	111.02(14)
C43	C42	H42	119.8	O6A	Cl2A	O5A	109.64(10)
C44	C43	C42	119.95(16)	O7A	Cl2A	O5A	107.94(10)
C44	C43	H43	120.0	O8A	Cl2A	O5A	108.15(10)
C42	C43	H43	120.0	C2S	C1S	H1SA	109.5
C43	C44	C45	120.05(16)	C2S	C1S	H1SB	109.5
C43	C44	H44	120.0	H1SA	C1S	H1SB	109.5
C45	C44	H44	120.0	C2S	C1S	H1SC	109.5
C44	C45	C40	120.25(16)	H1SA	C1S	H1SC	109.5
C44	C45	H45	119.9	H1SB	C1S	H1SC	109.5
C40	C45	H45	119.9	O2S	C2S	O1S	124.1(5)
C48	C47	C46	120.49(17)	O2S	C2S	C1S	126.5(6)
C48	C47	H47	119.8	O1S	C2S	C1S	108.9(5)
C46	C47	H47	119.8	O1S	C3S	C4S	112.0(4)
C49	C48	C47	120.13(18)	O1S	C3S	H3SA	109.2

Atom	Atom	Atom	Angle/°	Atom	Atom	Atom	Angle/°
C49	C48	H48	119.9	C4S	C3S	H3SA	109.2
C47	C48	H48	119.9	O1S	C3S	H3SB	109.2
C50	C49	C48	119.84(17)	C4S	C3S	H3SB	109.2
C50	C49	H49	120.1	H3SA	C3S	H3SB	107.9
C48	C49	H49	120.1	C3S	C4S	H4SA	109.5
C49	C50	C51	120.70(18)	C3S	C4S	H4SB	109.5
C49	C50	H50	119.7	H4SA	C4S	H4SB	109.5
C51	C50	H50	119.7	C3S	C4S	H4SC	109.5
C50	C51	C46	119.97(18)	H4SA	C4S	H4SC	109.5
C50	C51	H51	120.0	H4SB	C4S	H4SC	109.5
C46	C51	H51	120.0	C2S	O1S	C3S	116.3(4)
N4	C1	C2	121.41(14)	C2S'	C1S'	H1SD	109.5
N4	C1	C13	120.26(13)	C2S'	C1S'	H1SE	109.5
C2	C1	C13	118.32(14)	H1SD	C1S'	H1SE	109.5
C27	N2	C31	118.29(13)	C2S'	C1S'	H1SF	109.5
C27	N2	Ni1	129.96(10)	H1SD	C1S'	H1SF	109.5
C31	N2	Ni1	111.75(10)	H1SE	C1S'	H1SF	109.5
C12	N3	C9	118.19(13)	O2S'	C2S'	O1S'	123.2(4)
C12	N3	Ni1	131.77(11)	O2S'	C2S'	C1S'	124.6(4)
C9	N3	Ni1	108.77(10)	O1S'	C2S'	C1S'	112.2(4)
C1	N4	C5	118.12(13)	O1S'	C3S'	C4S'	109.7(6)
C1	N4	Ni1	130.72(10)	O1S'	C3S'	H3SC	109.7
C5	N4	Ni1	109.23(10)	C4S'	C3S'	H3SC	109.7
N4	C5	C4	123.40(14)	O1S'	C3S'	H3SD	109.7
N4	C5	C9	116.76(13)	C4S'	C3S'	H3SD	109.7
C4	C5	C9	119.82(13)	H3SC	C3S'	H3SD	108.2
C9	C8	C10	117.42(14)	C3S'	C4S'	H4SD	109.5
C9	C8	C7	118.92(14)	C3S'	C4S'	H4SE	109.5
C10	C8	C7	123.54(14)	H4SD	C4S'	H4SE	109.5
N3	C9	C8	123.33(14)	C3S'	C4S'	H4SF	109.5
N3	C9	C5	116.67(13)	H4SD	C4S'	H4SF	109.5
C8	C9	C5	119.93(13)	H4SE	C4S'	H4SF	109.5
C11	C10	C8	117.83(14)	C2S'	O1S'	C3S'	115.5(4)

Table 2.10 Torsion Angles for **Ni-1**.

A	B	C	D	Angle/°	A	B	C	D	Angle/°
C1	C2	C3	C4	-1.5(2)	C24	C25	C20	C21	1.4(3)
C1	C2	C3	C14	178.08(15)	C24	C25	C20	C10	-179.80(15)
C2	C3	C4	C5	0.3(2)	C11	C10	C20	C21	122.57(19)
C14	C3	C4	C5	-	C8	C10	C20	C21	-60.2(2)
C2	C3	C4	C6	179.91(15)	C11	C10	C20	C25	-56.2(2)
C14	C3	C4	C6	0.3(2)	C8	C10	C20	C25	121.01(18)
C5	C4	C6	C7	-4.1(2)	C31	N2	C27	C28	0.5(2)
C3	C4	C6	C7	176.33(15)	Ni1	N2	C27	C28	-179.94(11)
C4	C6	C7	C8	0.6(2)	C31	N2	C27	C39	-179.90(14)
C14	C15	C16	C17	0.3(4)	Ni1	N2	C27	C39	-0.3(2)
C15	C16	C17	C18	-1.2(4)	C29	C28	C27	N2	0.0(2)
C16	C17	C18	C19	0.9(3)	C29	C28	C27	C39	-179.64(15)
C17	C18	C19	C14	0.3(3)	C27	C28	C29	C30	-1.2(2)
C20	C21	C22	C23	-0.8(3)	C27	C28	C29	C40	178.61(14)
C21	C22	C23	C24	1.1(3)	C28	C29	C30	C31	1.9(2)
C22	C23	C24	C25	-0.1(3)	C40	C29	C30	C31	-177.92(13)
C23	C24	C25	C20	-1.1(3)	C28	C29	C30	C32	-177.26(14)
C30	C32	C33	C34	1.6(2)	C40	C29	C30	C32	3.0(2)
C40	C41	C42	C43	2.1(3)	C33	C32	C30	C31	0.6(2)
C41	C42	C43	C44	-0.7(3)	C33	C32	C30	C29	179.67(14)
C42	C43	C44	C45	-1.3(3)	C27	N2	C31	C30	0.3(2)
C43	C44	C45	C40	1.9(2)	Ni1	N2	C31	C30	-179.34(11)
C46	C47	C48	C49	0.0(3)	C27	N2	C31	C35	-177.55(13)
C47	C48	C49	C50	-1.0(3)	Ni1	N2	C31	C35	2.80(16)
C48	C49	C50	C51	0.9(3)	C29	C30	C31	N2	-1.5(2)
C49	C50	C51	C46	0.1(3)	C32	C30	C31	N2	177.66(13)
C3	C2	C1	N4	0.5(2)	C29	C30	C31	C35	176.30(13)
C3	C2	C1	C13	180.00(15)	C32	C30	C31	C35	-4.5(2)
C2	C1	N4	C5	1.8(2)	C32	C33	C34	C35	0.4(2)
C13	C1	N4	C5	-	C32	C33	C34	C36	178.43(14)
C2	C1	N4	Ni1	-	C38	N1	C35	C34	-0.4(2)
C13	C1	N4	Ni1	19.9(2)	Ni1	N1	C35	C34	170.21(11)
C1	N4	C5	C4	-3.1(2)	C38	N1	C35	C31	178.85(13)

Table 2.10 Torsion Angles for **Ni-1**.

A	B	C	D	Angle/°	A	B	C	D	Angle/°
Ni1	N4	C5	C4	162.83(12)	Ni1	N1	C35	C31	-10.57(16)
C1	N4	C5	C9	175.21(14)	C33	C34	C35	N1	174.75(14)
Ni1	N4	C5	C9	-18.88(16)	C36	C34	C35	N1	-3.4(2)
C3	C4	C5	N4	2.0(2)	C33	C34	C35	C31	-4.4(2)
C6	C4	C5	N4	-	C36	C34	C35	C31	177.40(13)
C3	C4	C5	C9	-	N2	C31	C35	N1	5.28(19)
C6	C4	C5	C9	4.2(2)	C30	C31	C35	N1	-172.67(13)
C6	C7	C8	C9	2.6(2)	N2	C31	C35	C34	-175.48(13)
C6	C7	C8	C10	-	C30	C31	C35	C34	6.6(2)
C12	N3	C9	C8	7.6(2)	C38	C37	C36	C34	-3.7(2)
Ni1	N3	C9	C8	-	C38	C37	C36	C46	176.79(15)
C12	N3	C9	C5	-	C35	C34	C36	C37	5.2(2)
Ni1	N3	C9	C5	21.81(17)	C33	C34	C36	C37	-172.79(15)
C10	C8	C9	N3	-3.3(2)	C35	C34	C36	C46	-175.21(14)
C7	C8	C9	N3	-	C33	C34	C36	C46	6.8(2)
C10	C8	C9	C5	173.75(14)	C35	N1	C38	C37	2.2(2)
C7	C8	C9	C5	-2.4(2)	Ni1	N1	C38	C37	-166.75(12)
N4	C5	C9	N3	-2.1(2)	C35	N1	C38	C52	-179.15(14)
C4	C5	C9	N3	176.25(14)	Ni1	N1	C38	C52	11.9(2)
N4	C5	C9	C8	-	C36	C37	C38	N1	-0.1(2)
C4	C5	C9	C8	-1.0(2)	C36	C37	C38	C52	-178.72(16)
C12	C11	C10	C8	6.0(2)	C44	C45	C40	C41	-0.5(2)
C12	C11	C10	C20	-	C44	C45	C40	C29	176.08(14)
C9	C8	C10	C11	-3.5(2)	C42	C41	C40	C45	-1.5(2)
C7	C8	C10	C11	172.45(16)	C42	C41	C40	C29	-178.15(15)
C9	C8	C10	C20	179.21(15)	C28	C29	C40	C45	-123.95(16)
C7	C8	C10	C20	-4.8(2)	C30	C29	C40	C45	55.8(2)
C9	N3	C12	C11	-5.0(2)	C28	C29	C40	C41	52.6(2)
Ni1	N3	C12	C11	160.54(13)	C30	C29	C40	C41	-127.60(16)
C9	N3	C12	C26	175.32(16)	C48	C47	C46	C51	1.1(2)
Ni1	N3	C12	C26	-19.1(3)	C48	C47	C46	C36	179.40(15)
C10	C11	C12	N3	-1.8(3)	C50	C51	C46	C47	-1.1(2)
C10	C11	C12	C26	177.89(17)	C50	C51	C46	C36	-179.44(15)

Table 2.10 Torsion Angles for **Ni-1**.

A	B	C	D	Angle/°	A	B	C	D	Angle/°
C18	C19	C14	C15	-1.2(3)	C37	C36	C46	C47	-131.73(16)
C18	C19	C14	C3	-	C34	C36	C46	C47	48.7(2)
C16	C15	C14	C19	0.9(3)	C37	C36	C46	C51	46.6(2)
C16	C15	C14	C3	179.23(19)	C34	C36	C46	C51	-132.97(16)
C2	C3	C14	C19	122.96(18)	O2S	C2S	O1S	C3S	-1.7(11)
C4	C3	C14	C19	-57.5(2)	C1S	C2S	O1S	C3S	-174.2(8)
C2	C3	C14	C15	-55.4(2)	C4S	C3S	O1S	C2S	-82.5(7)
C4	C3	C14	C15	124.20(18)	O2S'	C2S'	O1S'	C3S'	-3.2(8)
C22	C21	C20	C25	-0.5(3)	C1S'	C2S'	O1S'	C3S'	178.9(6)
C22	C21	C20	C10	-	C4S'	C3S'	O1S'	C2S'	145.1(8)

X-ray diffraction of 3u

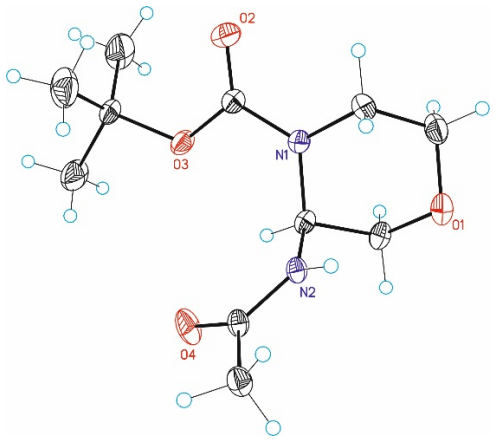

Figure 2.14 ORTEP diagram of **3u**, CCDC: 2194348

Table 2.11 Crystal data and structure refinement for **3u**.

Empirical formula	C11H20N2O4
Formula weight	244.29
Temperature/K	100(2)

Table 2.11 Crystal data and structure refinement for **3u**.

Wavelength	0.71073 Å
Crystal system	orthorhombic
Space group	P b c a
a/Å	8.9426(2)
b/Å	9.4420(3)
c/Å	30.9968(11)
α/°	90
β/°	90
γ/°	90
Volume/$Å^3$	2617.26(14)
Z	8
$\rho_{calc}Mg/cm^3$	1.240 Mg/m3
Absorption coefficient μ/mm^{-1}	0.094 mm-1
F(000)	1056
Crystal size/mm^3	0.300 x 0.300 x 0.300 mm3
Theta range for data collection/°	2.628 to 32.931°.
Index ranges	-12<=h<=13,-14<=k<=13,-46<=l<=46
Reflections collected	33893
Independent reflections	4761[R(int) = 0.0223]
Completeness to theta =29.856°	97.0%
Absorption correction	Multi-scan
Max. and min. transmission	1.00 and 0.86
Refinement method	Full-matrix least-squares on F2
Data/restraints/parameters	4761/ 245/ 263
Goodness-of-fit on F^2	1.025

Table 2.11 Crystal data and structure refinement for **3u**.

Final R indexes [I>=2σ (I)]	R1 = 0.0419, wR2 = 0.1148
Final R indexes [all data]	R1 = 0.0491, wR2 = 0.1195
Largest diff. peak/hole / e $Å^{-3}$	0.379 and -0.240 e.Å-3

Table 2.12 Bond Lengths for **3u**.

Atom	Atom	Length/Å	Atom	Atom	Length/Å
O1	C4	1.4170(12)	N1'	C3'	1.3479
O1	C1	1.4274(14)	N1'	C5'	1.4196
O2	C5	1.2107(11)	N1'	C2'	1.4649
O3	C5	1.3461(11)	C1'	C2'	1.3935
O3	C6	1.4777(10)	C1'	O1'	1.6776
O4	C10	1.2318(11)	C1'	H1'A	0.9700
N1	C5	1.3734(11)	C1'	H1'B	0.9700
N1	C3	1.4572(12)	C2'	H2'C	0.9700
N1	C2	1.4626(12)	C2'	H2'D	0.9700
N2	C10	1.3481(11)	C3'	C4'	1.3857
N2	C3	1.4560(11)	C3'	N2'	1.4910
N2	H2	0.8600	C3'	H3'	0.9800
C1	C2	1.5111(14)	O2'	C5'	1.0660
C1	H1A	0.9700	O3'	C5'	1.4469
C1	H1B	0.9700	O3'	C6'	1.4711
C8	C6	1.5143(15)	C6'	C9'	1.4703
C8	H8A	0.9600	C6'	C7'	1.5675
C8	H8B	0.9600	C6'	C8'	1.6340
C8	H8C	0.9600	C7'	H7'A	0.9600
C9	C6	1.5190(14)	C7'	H7'B	0.9600
C9	H9A	0.9600	C7'	H7'C	0.9600
C9	H9B	0.9600	C8'	H8'A	0.9600
C9	H9C	0.9600	C8'	H8'B	0.9600

Atom	Atom	Length/Å	Atom	Atom	Length/Å
C10	C11	1.5099(13)	C8'	H8'C	0.9600
C11	H11A	0.9600	O1'	C4'	1.6855
C11	H11B	0.9600	C4'	H4'A	0.9700
C11	H11C	0.9600	C4'	H4'B	0.9700
C2	H2A	0.9700	C9'	H9'A	0.9600
C2	H2B	0.9700	C9'	H9'B	0.9600
C3	C4	1.5329(12)	C9'	H9'C	0.9600
C3	H3	0.9800	O4'	C10'	1.4533
C4	H4A	0.9700	C10'	C11'	1.1508
C4	H4B	0.9700	C10'	N2'	1.4424
C6	C7	1.5090(15)	C11'	H11D	0.9600
C7	H7A	0.9600	C11'	H11E	0.9600
C7	H7B	0.9600	C11'	H11F	0.9600
C7	H7C	0.9600	N2'	H2'	0.8600

Table 2.13 Bond Angles for **3u**.

Atom	Atom	Atom	Angle/°	Atom	Atom	Atom	Angle/°
C4	O1	C1	110.39(8)	C3'	N1'	C5'	121.3
C5	O3	C6	120.44(7)	C3'	N1'	C2'	108.6
C5	N1	C3	124.43(7)	C5'	N1'	C2'	129.0
C5	N1	C2	118.26(7)	C2'	C1'	O1'	120.9
C3	N1	C2	114.77(7)	C2'	C1'	H1'A	107.1
C10	N2	C3	122.69(7)	O1'	C1'	H1'A	107.1
C10	N2	H2	118.7	C2'	C1'	H1'B	107.1
C3	N2	H2	118.7	O1'	C1'	H1'B	107.1
O1	C1	C2	110.72(8)	H1'A	C1'	H1'B	106.8
O1	C1	H1A	109.5	C1'	C2'	N1'	115.2

Atom	Atom	Atom	Angle/°	Atom	Atom	Atom	Angle/°
C2	C1	H1A	109.5	C1'	C2'	H2'C	108.5
O1	C1	H1B	109.5	N1'	C2'	H2'C	108.5
C2	C1	H1B	109.5	C1'	C2'	H2'D	108.5
H1A	C1	H1B	108.1	N1'	C2'	H2'D	108.5
C6	C8	H8A	109.5	H2'C	C2'	H2'D	107.5
C6	C8	H8B	109.5	N1'	C3'	C4'	128.1
H8A	C8	H8B	109.5	N1'	C3'	N2'	113.0
C6	C8	H8C	109.5	C4'	C3'	N2'	104.4
H8A	C8	H8C	109.5	N1'	C3'	H3'	102.7
H8B	C8	H8C	109.5	C4'	C3'	H3'	102.7
C6	C9	H9A	109.5	N2'	C3'	H3'	102.7
C6	C9	H9B	109.5	C5'	O3'	C6'	117.3
H9A	C9	H9B	109.5	O2'	C5'	N1'	127.5
C6	C9	H9C	109.5	O2'	C5'	O3'	127.0
H9A	C9	H9C	109.5	N1'	C5'	O3'	105.5
H9B	C9	H9C	109.5	C9'	C6'	O3'	107.7
O4	C10	N2	122.50(9)	C9'	C6'	C7'	114.5
O4	C10	C11	121.87(8)	O3'	C6'	C7'	100.6
N2	C10	C11	115.63(8)	C9'	C6'	C8'	114.6
C10	C11	H11A	109.5	O3'	C6'	C8'	108.5
C10	C11	H11B	109.5	C7'	C6'	C8'	109.9
H11A	C11	H11B	109.5	C6'	C7'	H7'A	109.5
C10	C11	H11C	109.5	C6'	C7'	H7'B	109.5
H11A	C11	H11C	109.5	H7'A	C7'	H7'B	109.5
H11B	C11	H11C	109.5	C6'	C7'	H7'C	109.5

Atom	Atom	Atom	Angle/°	Atom	Atom	Atom	Angle/°
N1	C2	C1	108.69(8)	H7'A	C7'	H7'C	109.5
N1	C2	H2A	110.0	H7'B	C7'	H7'C	109.5
C1	C2	H2A	110.0	C6'	C8'	H8'A	109.5
N1	C2	H2B	110.0	C6'	C8'	H8'B	109.5
C1	C2	H2B	110.0	H8'A	C8'	H8'B	109.5
H2A	C2	H2B	108.3	C6'	C8'	H8'C	109.5
N2	C3	N1	112.14(7)	H8'A	C8'	H8'C	109.5
N2	C3	C4	110.07(7)	H8'B	C8'	H8'C	109.5
N1	C3	C4	108.05(7)	C1'	O1'	C4'	103.4
N2	C3	H3	108.8	C3'	C4'	O1'	108.2
N1	C3	H3	108.8	C3'	C4'	H4'A	110.1
C4	C3	H3	108.8	O1'	C4'	H4'A	110.1
O1	C4	C3	111.25(7)	C3'	C4'	H4'B	110.1
O1	C4	H4A	109.4	O1'	C4'	H4'B	110.1
C3	C4	H4A	109.4	H4'A	C4'	H4'B	108.4
O1	C4	H4B	109.4	C6'	C9'	H9'A	109.5
C3	C4	H4B	109.4	C6'	C9'	H9'B	109.5
H4A	C4	H4B	108.0	H9'A	C9'	H9'B	109.5
O2	C5	O3	125.99(8)	C6'	C9'	H9'C	109.5
O2	C5	N1	123.27(9)	H9'A	C9'	H9'C	109.5
O3	C5	N1	110.71(7)	H9'B	C9'	H9'C	109.5
O3	C6	C7	110.23(8)	C11'	C10'	N2'	124.9
O3	C6	C8	110.67(8)	C11'	C10'	O4'	127.1
C7	C6	C8	111.87(10)	N2'	C10'	O4'	99.8
O3	C6	C9	102.41(7)	C10'	C11'	H11D	109.5

Atom	Atom	Atom	Angle/°	Atom	Atom	Atom	Angle/°
C7	C6	C9	111.62(10)	C10'	C11'	H11E	109.5
C8	C6	C9	109.66(9)	H11D	C11'	H11E	109.5
C6	C7	H7A	109.5	C10'	C11'	H11F	109.5
C6	C7	H7B	109.5	H11D	C11'	H11F	109.5
H7A	C7	H7B	109.5	H11E	C11'	H11F	109.5
C6	C7	H7C	109.5	C10'	N2'	C3'	129.9
H7A	C7	H7C	109.5	C10'	N2'	H2'	115.0
H7B	C7	H7C	109.5	C3'	N2'	H2'	115.0

Table 2.14 Torsion Angles for **3u**.

A	B	C	D	Angle/°	A	B	C	D	Angle/°
C4	O1	C1	C2	61.83(11)	O1'	C1'	C2'	N1'	-43.8
C3	N2	C10	O4	-5.34(15)	C3'	N1'	C2'	C1'	46.2
C3	N2	C10	C11	174.28(8)	C5'	N1'	C2'	C1'	-146.2
C5	N1	C2	C1	-143.46(8)	C5'	N1'	C3'	C4'	131.3
C3	N1	C2	C1	53.77(10)	C2'	N1'	C3'	C4'	-60.1
O1	C1	C2	N1	-56.24(11)	C5'	N1'	C3'	N2'	-96.3
C10	N2	C3	N1	118.28(9)	C2'	N1'	C3'	N2'	72.4
C10	N2	C3	C4	-121.41(9)	C3'	N1'	C5'	O2'	-10.1
C5	N1	C3	N2	-92.81(10)	C2'	N1'	C5'	O2'	-176.3
C2	N1	C3	N2	68.75(9)	C3'	N1'	C5'	O3'	170.8
C5	N1	C3	C4	145.71(8)	C2'	N1'	C5'	O3'	4.7
C2	N1	C3	C4	-52.73(10)	C6'	O3'	C5'	O2'	-6.7
C1	O1	C4	C3	-61.38(11)	C6'	O3'	C5'	N1'	172.4

Table 2.14 Torsion Angles for **3u**.

A	B	C	D	Angle/°	A	B	C	D	Angle/°
N2	C3	C4	O1	-67.45(10)	C5'	O3'	C6'	C9'	-60.9
N1	C3	C4	O1	55.30(10)	C5'	O3'	C6'	C7'	178.9
C6	O3	C5	O2	-1.83(14)	C5'	O3'	C6'	C8'	63.6
C6	O3	C5	N1	179.95(7)	C2'	C1'	O1'	C4'	37.0
C3	N1	C5	O2	168.60(9)	N1'	C3'	C4'	O1'	56.8
C2	N1	C5	O2	7.63(13)	N2'	C3'	C4'	O1'	-78.7
C3	N1	C5	O3	-13.12(12)	C1'	O1'	C4'	C3'	-35.5
C2	N1	C5	O3	-174.09(8)	C11'	C10'	N2'	C3'	162.7
C5	O3	C6	C7	64.98(12)	O4'	C10'	N2'	C3'	12.5
C5	O3	C6	C8	-59.30(11)	N1'	C3'	N2'	C10'	86.1
C5	O3	C6	C9	-176.12(9)	C4'	C3'	N2'	C10'	-130.8

X-ray diffraction of 3v

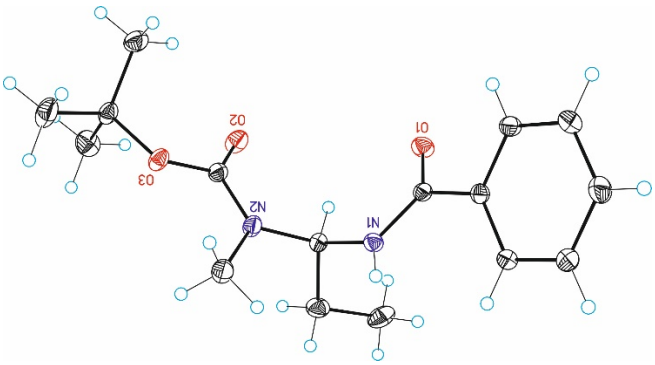

Figure 2.15 ORTEP diagram of **3v**, CCDC: 2193358

Table 2.15 Crystal data and structure refinement for **3v**.

Empirical formula	C16H24N2O3
Formula weight	292.37
Temperature/K	100(2)
Wavelength	0.71073 Å
Crystal system	monoclinic
Space group	P 21/c
a/Å	14.0708(2)
b/Å	9.46970(10)
c/Å	12.4275(2)
α/°	90
β/°	104.819(2)
γ/°	90
Volume/Å^3	1600.84(4)
Z	4
ρ_{calc}Mg/cm^3	1.213Mg/m3

Table 2.15 Crystal data and structure refinement for **3v**.

Absorption coefficient μ/mm^{-1}	0.084 mm-1
F(000)	632
Crystal size/mm^3	0.300 x 0.300 x 0.300 mm^3
Theta range for data collection/°	3.391 to 30.712°
Index ranges	-18<=h<=20,-13<=k<=13,-17<=l<=16
Reflections collected	34087
Independent reflections	4722[R(int) = 0.0225]
Completeness to theta =30.712°	94.9%
Absorption correction	Multi-scan
Max. and min. transmission	1.00 and 0.92
Refinement method	Full-matrix least-squares on F^2
Data/restraints/parameters	4722/ 0/ 195
Goodness-of-fit on F^2	1.045
Final R indexes [I>=2σ (I)]	R1 = 0.0364, wR2 = 0.1026
Final R indexes [all data]	R1 = 0.0412, wR2 = 0.1055
Largest diff. peak/hole / e Å^{-3}	0.451 and -0.259

Table 2.16 Bond Lengths for **3V**.

Atom	**Atom**	**Length/Å**	**Atom**	**Atom**	**Length/Å**
O1	C1	1.2364(10)	C2	C7	1.3987(11)
O2	C12	1.2177(10)	C3	C4	1.3923(12)
O3	C12	1.3524(10)	C4	C5	1.3911(12)
O3	C13	1.4705(10)	C5	C6	1.3930(12)
N1	C1	1.3524(10)	C6	C7	1.3894(12)
N1	C8	1.4574(10)	C8	C9	1.5247(11)
N2	C12	1.3577(10)	C9	C10	1.5219(14)

Atom	Atom	Length/Å	Atom	Atom	Length/Å
N2	C11	1.4611(11)	C13	C14	1.5195(13)
N2	C8	1.4654(10)	C13	C15	1.5205(12)
C1	C2	1.4964(11)	C13	C16	1.5219(12)
C2	C3	1.3960(11)			

Table 2.17 Bond Angles for **3v**.

Atom	Atom	Atom	Angle/°	Atom	Atom	Atom	Angle/°
C12	O3	C13	120.08(6)	C6	C7	C2	120.02(8)
C1	N1	C8	121.67(7)	N1	C8	N2	110.21(7)
C12	N2	C11	122.12(7)	N1	C8	C9	110.72(6)
C12	N2	C8	118.42(7)	N2	C8	C9	113.13(7)
C11	N2	C8	119.44(7)	C10	C9	C8	111.14(7)
O1	C1	N1	122.81(7)	O2	C12	O3	125.06(7)
O1	C1	C2	120.60(7)	O2	C12	N2	124.76(8)
N1	C1	C2	116.58(7)	O3	C12	N2	110.18(7)
C3	C2	C7	119.88(7)	O3	C13	C14	108.85(7)
C3	C2	C1	122.70(7)	O3	C13	C15	102.23(7)
C7	C2	C1	117.41(7)	C14	C13	C15	111.19(8)
C4	C3	C2	119.95(7)	O3	C13	C16	111.73(7)
C5	C4	C3	119.91(8)	C14	C13	C16	112.74(7)
C4	C5	C6	120.35(8)	C15	C13	C16	109.63(8)
C7	C6	C5	119.88(8)				

Table 2.18 Torsion Angles for **3v**.

A	B	C	D	Angle/°	A	B	C	D	Angle/°
C8	N1	C1	O1	-2.37(12)	C12	N2	C8	N1	122.75(8)
C8	N1	C1	C2	176.63(7)	C11	N2	C8	N1	-59.15(10)
O1	C1	C2	C3	-148.05(8)	C12	N2	C8	C9	-112.70(8)
N1	C1	C2	C3	32.93(11)	C11	N2	C8	C9	65.40(10)

Table 2.18 Torsion Angles for **3v**.

A	B	C	D	Angle/°	A	B	C	D	Angle/°
O1	C1	C2	C7	30.87(11)	N1	C8	C9	C10	-61.27(9)
N1	C1	C2	C7	-148.15(7)	N2	C8	C9	C10	174.46(7)
C7	C2	C3	C4	0.22(12)	C13	O3	C12	O2	11.43(12)
C1	C2	C3	C4	179.12(7)	C13	O3	C12	N2	-168.70(7)
C2	C3	C4	C5	0.60(13)	C11	N2	C12	O2	-172.85(9)
C3	C4	C5	C6	-0.91(14)	C8	N2	C12	O2	5.20(12)
C4	C5	C6	C7	0.39(14)	C11	N2	C12	O3	7.28(11)
C5	C6	C7	C2	0.44(13)	C8	N2	C12	O3	-174.67(7)
C3	C2	C7	C6	-0.74(12)	C12	O3	C13	C14	62.00(9)
C1	C2	C7	C6	-179.70(7)	C12	O3	C13	C15	179.69(7)
C1	N1	C8	N2	-109.66(8)	C12	O3	C13	C16	-63.16(10)
C1	N1	C8	C9	124.41(8)					

2.7.6 Representative set of NMR Spectra

For all the spectra, see the SI of *Angew. Chem. Int. Ed.* **2022**, 61, e202212983.

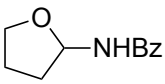
O
NHBz

3a

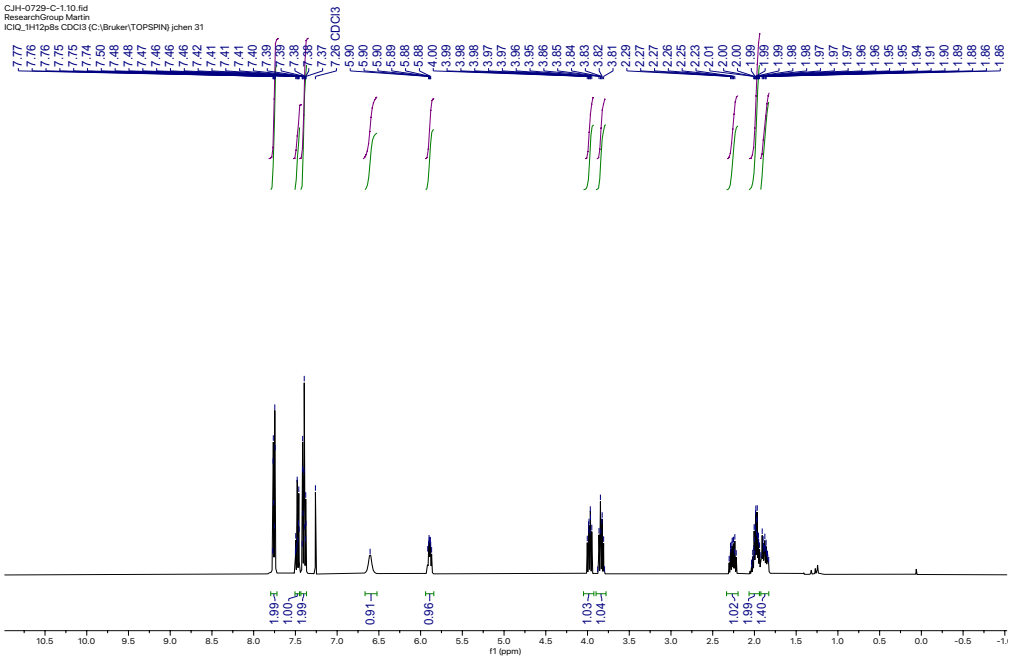
CJH-0729-C-1.10.fid
ResearchGroup Martin
ICIQ_1H12p8s CDCl3 (C:\Bruker\TOPSPIN) jchen 31
7.77 7.76 7.76 7.75 7.75 7.74 7.50 7.48 7.48 7.47 7.46 7.46 7.42 7.41 7.41 7.41 7.40 7.39 7.39 7.38 7.38 7.37 7.26 CDCl3 5.90 5.90 5.90 5.89 5.88 5.88 4.00 3.99 3.98 3.98 3.97 3.97 3.96 3.95 3.86 3.85 3.84 3.83 3.82 3.81 2.29 2.27 2.27 2.26 2.25 2.23 2.01 2.00 2.00 1.99 1.99 1.98 1.98 1.97 1.97 1.97 1.96 1.96 1.95 1.95 1.94 1.91 1.90 1.89 1.88 1.88 1.86 1.86
1.99 1.00 1.99 0.91 0.96 1.03 1.04 1.02 1.99 1.40
f1 (ppm)

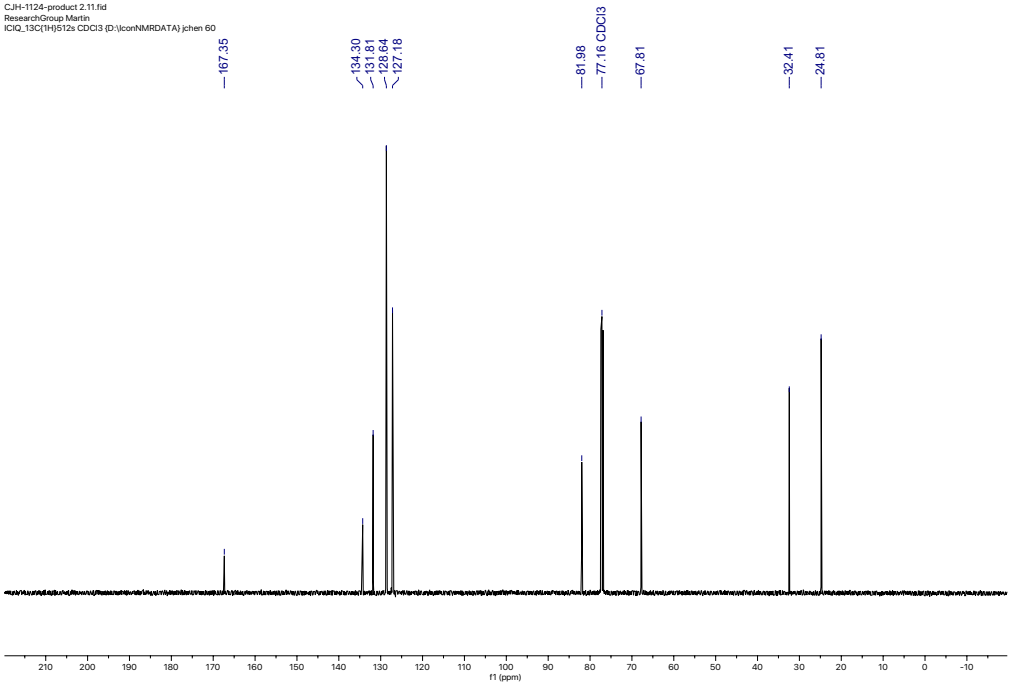
CJH-1124-product 2.11.fid
ResearchGroup Martin
ICIQ_13C{1H}512s CDCl3 (D:\IconNMRDATA) jchen 60
167.35
134.30 131.81 128.64 127.18
81.98 77.16 CDCl3 67.81
32.41 24.81
f1 (ppm)

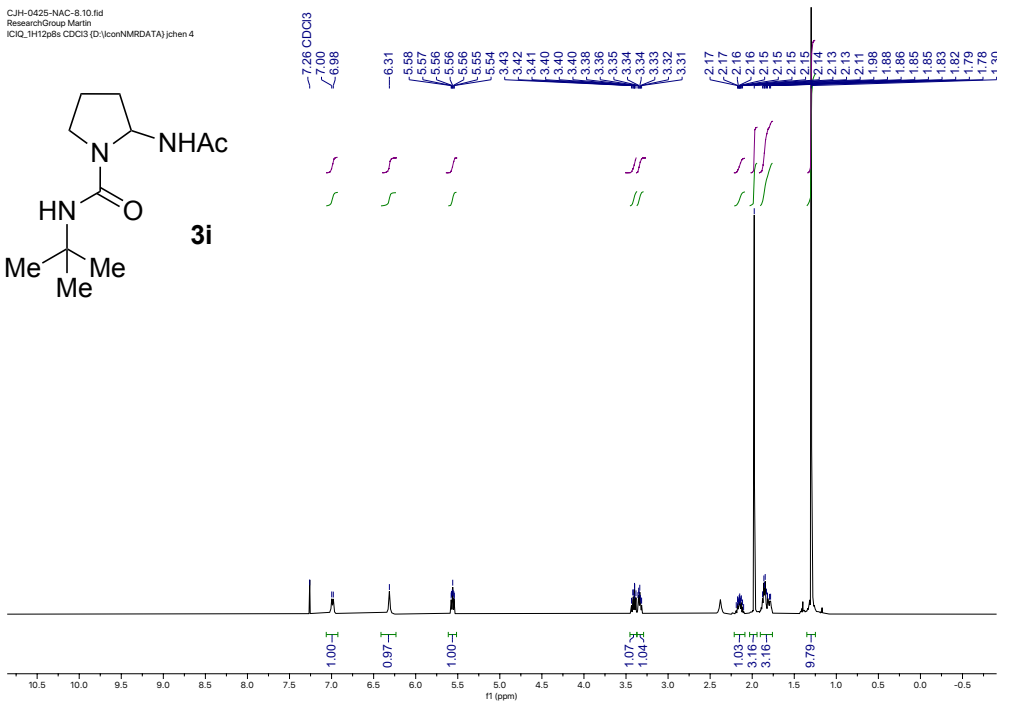
CJH-0425-NAC-8.10.fid
ResearchGroup Martin
ICIQ_1H12p8s CDCl3 (D:\IconNMRDATA) jchen 4
NHAc
HN
O
Me
Me
Me
3i
7.26 CDCl3
7.00
6.98
6.31
f1 (ppm)

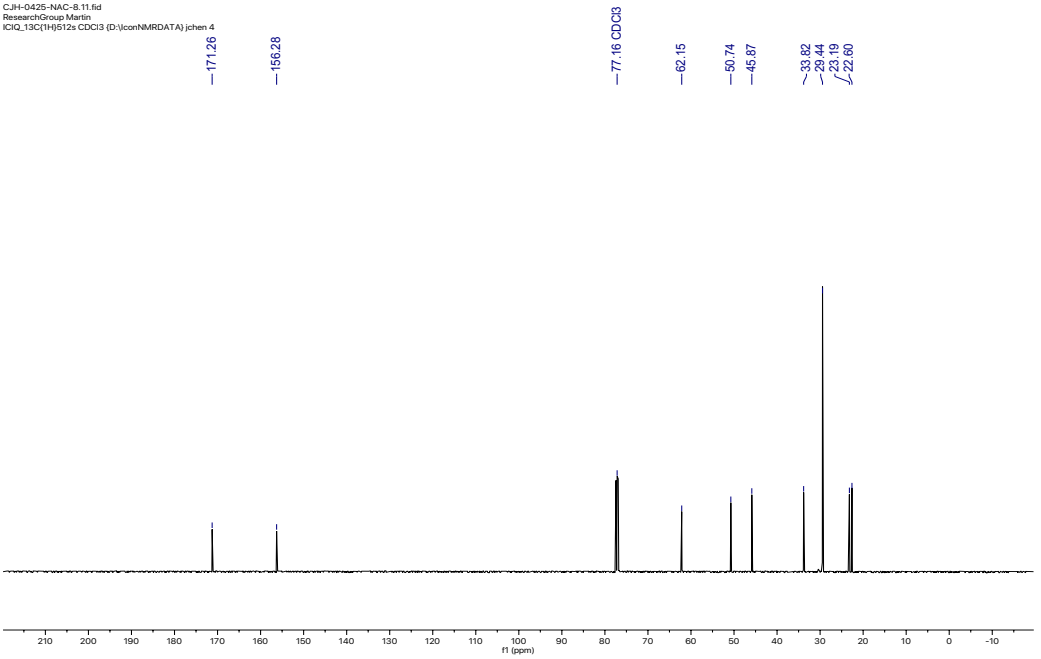
CJH-0425-NAC-8.11.fid
ResearchGroup Martin
ICIQ_13C(1H)512s CDCl3 (D:\IconNMRDATA) jchen 4
171.26
156.28
77.16 CDCl3
62.15
50.74
45.87
33.82
29.44
23.19
22.60
f1 (ppm)

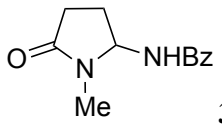
O
N
Me
NHBz

3r

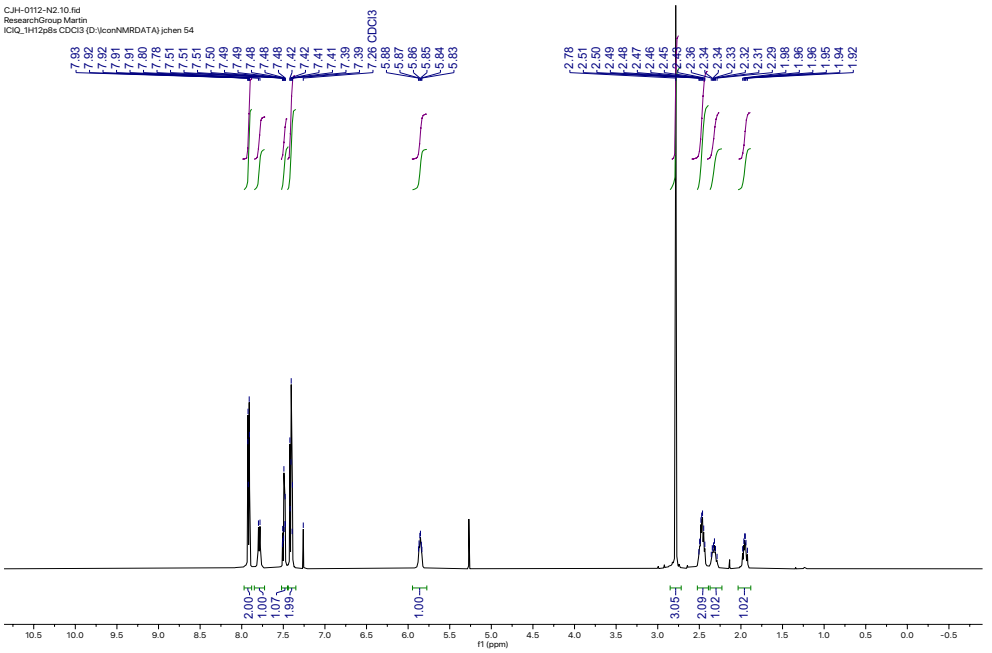
CJH-0112-N2.10.fid
ResearchGroup Martin
ICIQ_1H12p8s CDCl3 {D:\IconNMRDATA} jchen 54
CDCl3
f1 (ppm)

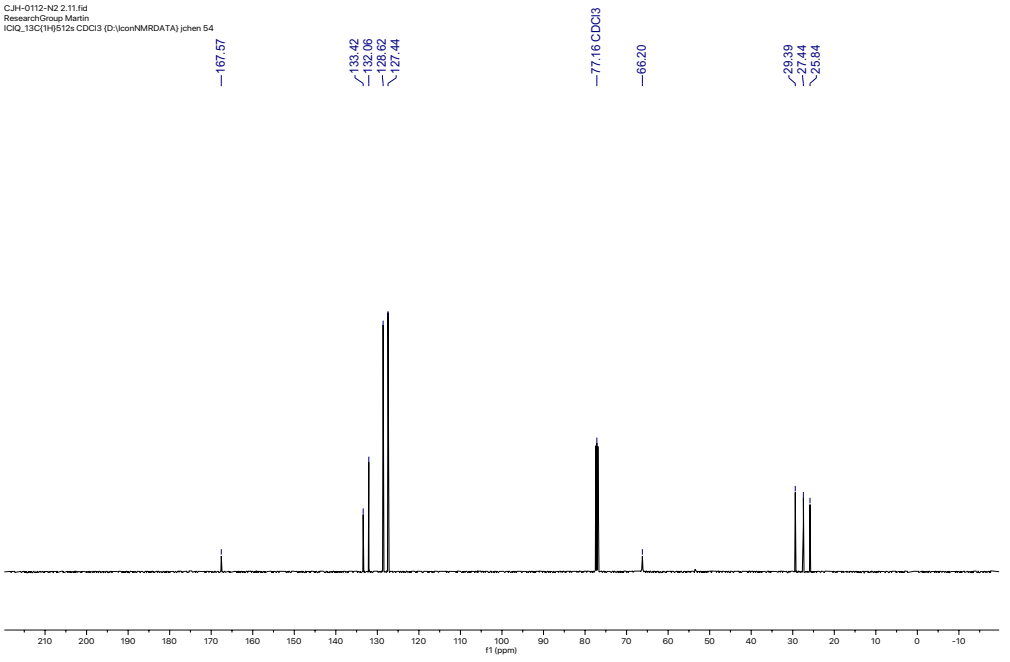
CJH-0112-N2 2.11.fid
ResearchGroup Martin
ICIQ_13C{1H}512s CDCl3 {D:\IconNMRDATA} jchen 54
167.57
133.42
132.06
128.62
127.44
77.16 CDCl3
66.20
29.39
27.44
25.84
f1 (ppm)

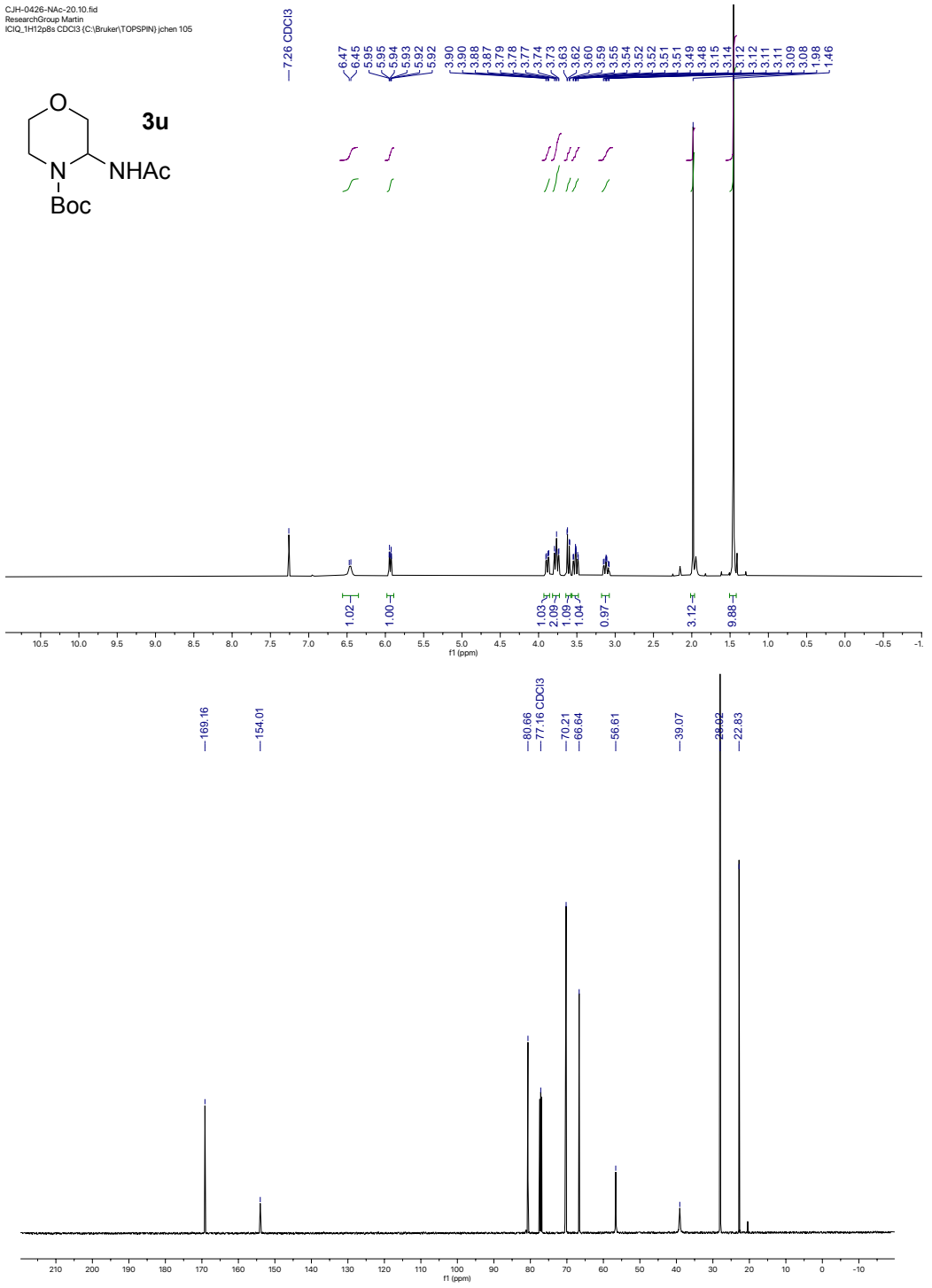
CJH-0426-NAc-20.10.fid
ResearchGroup Martin
ICIQ_1H12p8s CDCl3 (C:\Bruker\TOPSPIN) jchen 105
3u
NHAc
Boc
7.26 CDCl3
f1 (ppm)
169.16
154.01
80.66
77.16 CDCl3
70.21
66.64
56.61
39.07
28.02
22.83
f1 (ppm)

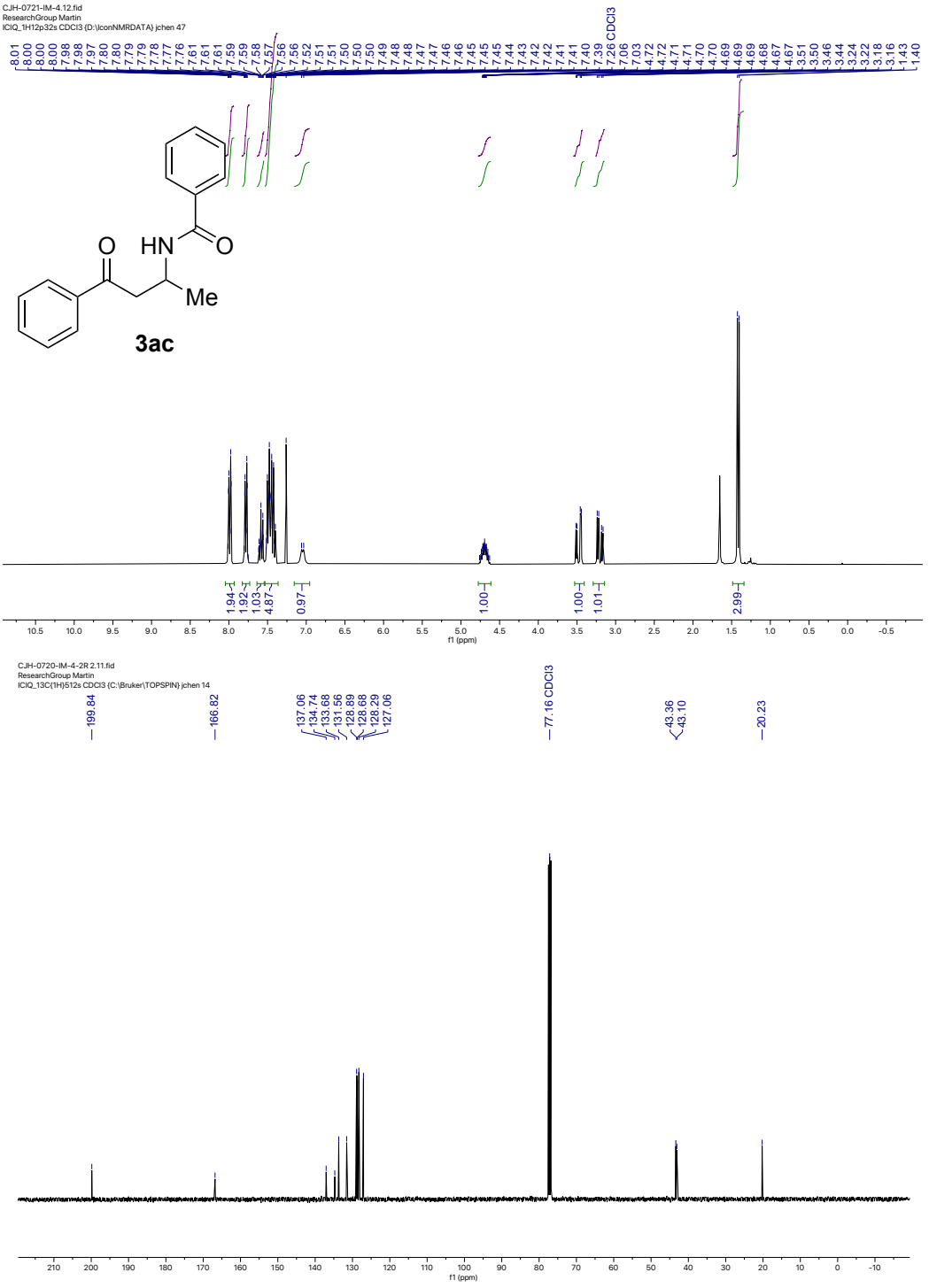
CJH-0721-IM-4.12.fid
ResearchGroup Martin
ICIQ_1H12p32s CDCl3 (D:\IconNMRDATA) jchen 47
O
HN
O
Me
3ac
f1 (ppm)
CJH-0720-IM-4-2R 2.11.fid
ResearchGroup Martin
ICIQ_13C{1H}512s CDCl3 (C:\Bruker\TOPSPIN) jchen 14
199.84
166.82
137.06
134.74
133.68
131.56
128.89
128.68
128.29
127.06
77.16 CDCl3
43.36
43.10
20.23
f1 (ppm)

2.8 References

[1] N. A. McGrath, M. Brichacek, J. T. Njardarson, *J. Chem. Educ.* **2010**, *87*, 1348. Top 200 Brand Name Drugs by Retail Sales in **2022** Poster; b) E. Vitaku, D. T. Smith, J. T. Njardarson, *J. Med. Chem.* **2014**, *57*, 10257; c) C. M. Marshall, J. G. Federice, C. N. Bell, P. B. Cox, J. T. Njardarson, *J. Med. Chem.* **2024**, *67*, 11622.

[2] a) A. M. Kaufmann, J. P. Krise, *J. Pharm. Sci.* **2007**, *96*, 729; b) N. Schneider, D. M. Lowe, R. A. Sayle, M. A. Tarselli, G. A. Landrum, *J. Med. Chem.* **2016**, *59*, 4385; c) D. C. Blakemore, L. Castro, I. Churcher, D. C. Rees, A. W. Thomas, D. M. Wilson, A. Wood, *Nat. Chem.* **2018**, *10*, 383; d) S. D. Roughley, A. M. Jordan, *J. Med. Chem.* **2011**, *54*, 3451.

[3] I. P. Beletskaya, A. D. Averin, *Russ. Chem. Rev.*, **2021**, *90*, 1359.

[4] J. Escorihuela, A. Lledós, G. Ujaque, *Chem. Rev.* **2023**, *123*, 9139.

[5] a) T. Rogge, N. Kaplaneris, N. Chatani, J. Kim, S. Chang, B. Punji, L. L. Schafer, D. G. Musaev, J. Wencel-Delord, C. A. Roberts, R. Sarpong, Z. E. Wilson, M. A. Brimble, M. J. Johansson, L. Ackermann, *Nat. Rev. Methods Prim.* **2021**, *1*, 43; b) D. L. Golden, S.-E. Suh, S. S. Stahl, *Nat. Rev. Chem.* **2022**, *6*, 405.

[6] a) T. Cernak, K. D. Dykstra, S. Tyagarajan, P. Vachal, S. W. Krska, *Chem. Soc. Rev.* **2016**, *45*, 546; b) L. Guillemard, N. Kaplaneris, L. Ackermann, M. J. Johansson, *Nat. Rev. Chem.* **2021**, *5*, 522; c) P. Bellotti, H.-M. Huang, T. Faber, F. Glorius, *Chem. Rev.* **2023**, *123*, 4237.

[7] a) C.-J. Li, *Acc. Chem. Res.* **2009**, *42*, 335; b) M. K. Lakshman, P. K. Vuram, *Chem. Sci.* **2017**,*8*, 5845.

[8] S. Wiese, Y. M. Badiei, R. T. Gephart, S. Mossin, M. S. Varonka, M. M. Melzer, K. Meyer, T. R. Cundari, T. H. Warren. *Angew. Chem. Int. Ed.* **2010**, *49*, 8850.

[9] C.-S. Wang, X.-F. Wu, P. H. Dixneuf, J.-F. Soulé, *Chem. Sus. Chem.* **2017**, *10*, 3075.

[10] M.-E, Chen, X.-W. Chen, Y.H. Hu, R. Ye, J.-W. Lv, B. Li, F.-M. Zhang, *Org. Chem. Front.* **2021**, *8*, 4623.

[11] Q. Michaudel, D. Thevenet, P. S. Baran, *J. Am. Chem. Soc.* **2012**, *134*, 2547.

[12] a) G. Smolinsky, *J. Am. Chem. Soc.* **1960**, *82*, 4717; b) G. Smolinsky, *J. Org. Chem.* **1961**, *26*, 4108.

[13] a) W. Lwowski, T. W. Mattingly, *Tetrahedron Lett.* **1962**, *3*, 277; b) W. Lwowski, T. W. Mattingly, *J. Am. Chem. Soc.* **1965**, *87*,1947.

[14] J. W. ApSimon, O. E. Edwards, *Can. J. Chem.* **1962**, *40*, 896.

[15] a) Y. Park, Y. Kim, S. Chang, *Chem. Rev.* **2017**, *117*, 9247; b) J. L. Roizen, M. E. Harvey, J. Du Bois, *Acc. Chem. Res.* **2012**, *45*, 911; c) G. Dequirez, V. Pons, P. Dauban, *Angew. Chem. Int. Ed.* **2012**, *51*, 7384; F. Collet, R. H. Dodda, P. Dauban, *Chem. Commun.* **2009**, 5061.

[16] J. R. Clark1, K. Feng, A. Sookezian, M. C. White, *Nat. Chem.* **2018**, *10*, 583.

[17] a) J. C. Lewis, P. S. Coelho, F. H. Arnold, *Chem. Soc. Rev.* **2011**, *40*, 2003; b) W.–N. Xu, Y.-D. Gao, P. Su, L. Huang, Z.-L. He, L.-C. Yang, *ACS Catal.* **2024**, *14*, 14139.

[18] Z.-J. Jia, S. Gao, F. H. Arnold, *J. Am. Chem. Soc.* **2020**, *142*, 10279.

[19] X. Tang, X. Jia, Z. Huang, *Chem. Sci.* **2018**, *9*, 288.

[20] J. Lee, S. Jin, D. Kim, S. H. Hong, S. Chang, *J. Am. Chem. Soc.* **2021**, *143*, 5191.

[21] E. Brunard, V. Boquet, E. V. Elslande, T. Saget, P. Dauban, *J. Am. Chem. Soc.* **2021**, *143*, 6407.

[22] C.-X. Ye, D. R. Dansby, S. Chen, E. Meggers, *Nat. Synth.* **2023**, *2*, 645.

[23] M. Rivas, V. Palchykov, X. Jia, V. Gevorgyan, *Nat. Rev. Chem.* **2022**, *6*, 544.

[24] A. Hu, J.-J. Guo, H. Pan, H. Tang, Z. Gao, Z. Zuo, *J. Am. Chem. Soc.* **2018**, *140*, 1612.

[25] T. Wan, Z. Wen, G. Laudadio, L. Capaldo, R. Lammers, J. A. Rincón, P. García-Losada, C. Mateos, M. O. Frederick, R. Broersma, T. Noël, *ACS Cent. Sci.* **2022**, *8*, 51.

[26] D. Ravelli, M. Fagnoni, T. Fukuyama, T. Nishikawa, I. Ryu, *ACS Catal.* **2018**, *8*, 1, 701.

[27] a) C. Chauffat, A. Morris, *Perfum. flavorist* **2004**, *29*, 34; b) S. I. Martínez-Guido, J. B. González-Campos, R. E. Del Río, J. M. Ponce-Ortega, F. Nápoles-Rivera, M. Serna-González, M. M. El-Halwagi, *ACS Sustain. Chem. Eng.* **2014**, *2*, 2380.

[28] a) L. Guillemard, N. Kaplaneris, L. Ackermann, M. J. Johansson, *Nat. Rev. Chem.* **2021**, *5*, 522; b) K. E. Kim, A. N. Kim, C. J. McCormick, B. M. Stoltz, *J. Am. Chem. Soc.* **2021**, *143*, 16890.

[29] a) W. N. Speckamp, M. J. Moolenaar, *Tetrahedron* **2000**, *56*, 3817; b) B. E. Maryanoff, H.-C. Zhang, J. H. Cohen, I. J. Turchi, C. A. Maryanoff, *Chem. Rev.* **2004**, *104*, 1431; c) M. Hamon, N. Dickinson, A. Devineau, D. Bolien, M. J. Tranchant, C. Taillier, I. Jabin, D. C. Harrowven, R. J. Whitby, A. Ganesan, V. Dalla, *J. Org. Chem.* **2014**, *79*, 1900.

[30] E. M. Simmons, J. F. Hartwig, *Angew. Chem. Int. Ed.* **2012**, *51*, 3066.

[31] D. C. Powers, B. L. Anderson, D. G. Nocera, *J. Am. Chem. Soc.* **2013**, *135*, 18876.

[32] a) K. M. van Vliet, B. de Bruin, *ACS Catal*. **2020**, *10*, 4751; b) X. Lyu, J. Zhang, D. Kim, S. Seo, S. Chang, *J. Am. Chem. Soc*. **2021**, *143*, 5867; c) B. Du, Y. Ouyang, Q. Chen, W.-Y. Yu, *J. Am. Chem. Soc.* **2021**, *143*, 14962.

Chapter 3. Ni-Catalyzed Stereodivergent *N*-Glycosylation of Glycals.

3.1 General Introduction

N-glycosides, compounds that contain a sugar-type backbone and a *N*-containing aglycon, are privileged structures in a wide variety of biologically-relevant compounds such as DNA or RNA, among others (Scheme 3.1).[1] For example, *N*-linked glycoproteins can be found on cell's surface and are known to improve the protein stability and solubility, contributing significatively to cell signaling.[2] On the other hand, a number of FDA approved antibodies such as Etanercept, Infliximab and Rituximab contain *N*-glycosylated therapeutic proteins in their structures. Moreover, a number of advanced ingredients have exhibited high inhibition against protein kinases or aldose reductases such as staurosporine or AKR1B1, among others.[3] The importance of the *N*-glycosisides is illustrated by the observation that mutations in eighteen genes involved in *N*-glycosylation result in a variety of diseases, most of which involve the nervous system.[4]

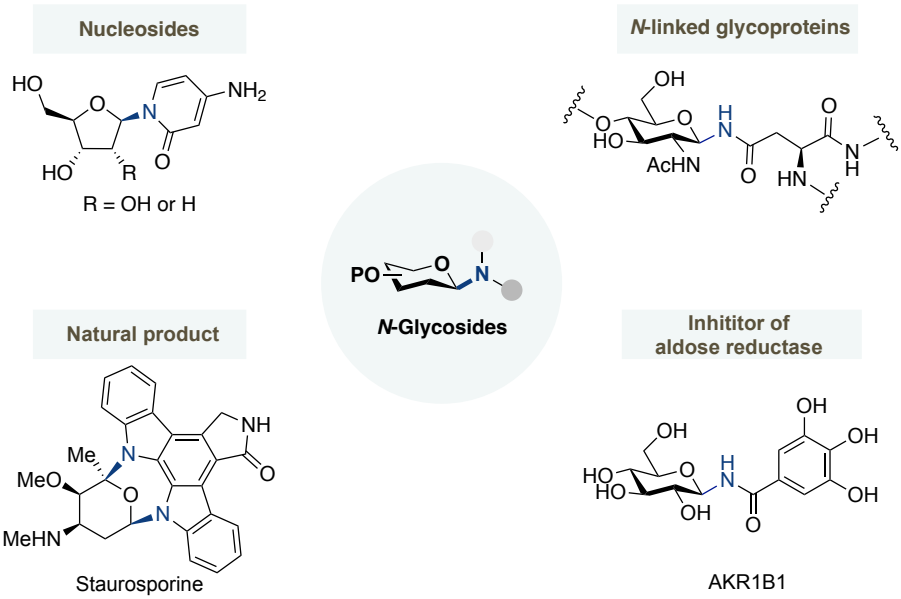

Scheme 3.1 Biologically active molecules containing *N*-glycosides.

3.1.1 Lewis Acid-Catalyzed *N*-Glycosylation

In 2005, Takahashi reported the stereoselective *N*-glycosylation of glycosyl donors with primary amides catalyzed by TMSOTf[5] by utilizing *N*-phenyltrifluoroimidates as leaving groups (Scheme 3.2). Interestingly, the presence of 2-*O*-benzoyl group resulted in exclusive 1,2-*trans*-stereoselectivity. However, a significant erosion in α:β ratio was observed with benzyl protecting groups in the D-galactose backbone, thus suggesting that neighboring assistance might play a decisive role in stereoselectivity.

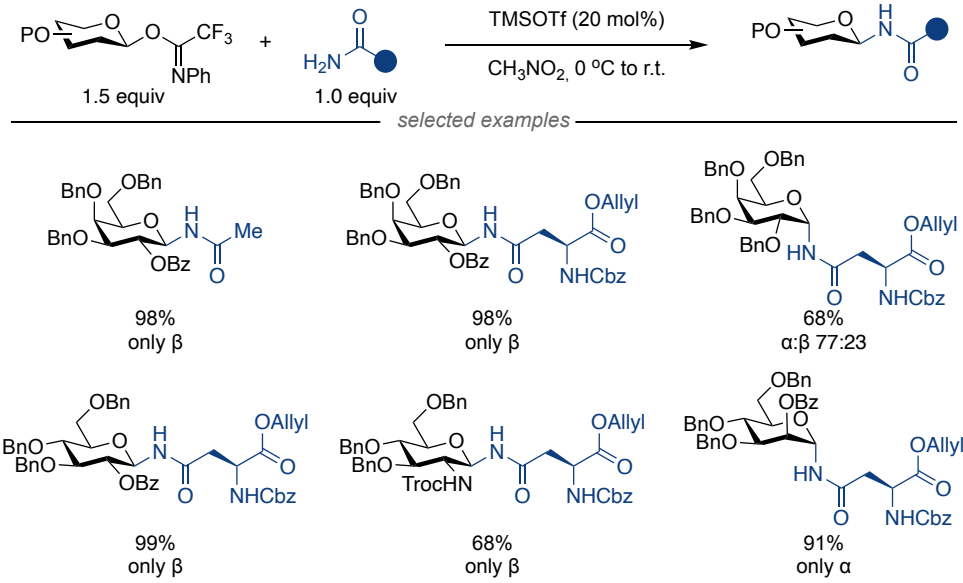

Scheme 3.2 TMSOTf-catalyzed *N*-glycosylation

In 2018, Takemoto and co-workers demonstrated the utilization of 2-iodoazolium salt **LA-1** as a soft and mild Lewis acid to facilitate the *N*-glycosylation with exclusive β-selectivity.[6] Not only pyranose, but also furanose derivatives could be employed as substates with equal ease. The proposed mechanism involves a Lewis acid catalyzed functionalization of the anomeric C-O bond, forming an oxocarbenium ion that can be stabilized by an adjacent carbonyl group. Subsequently, nucleophilic addition of the amide from less sterically hindered face results in the 1,2-*trans* *N*-glycosidic bond.

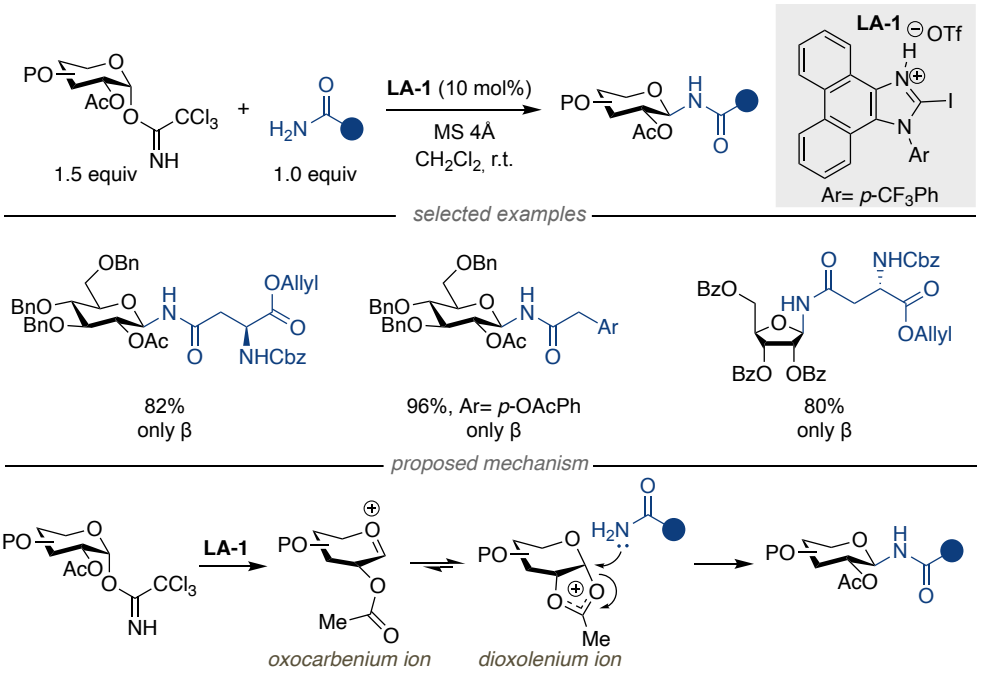

Scheme 3.3 2-Iodoazolium salt-catalyzed β-*N*-glycosylation.

1,2-unsaturated pyranoses or furanoses, coined as glycals, have been employed as readily available building blocks for the synthesis of natural products and the generation of novel structural features in diversity-oriented synthesis (DOS).[7] For instance, in 2019 Takemoto described the direct addition of glycals to amides en route to 2-deoxyglycosides under mild conditions and exclusive β-stereoselectivity for the D-galactal series (Scheme 3.4). [8] However, lower β-selectivities were observed in *N*-glycosylation of glucal derivatives with alkyl amides.

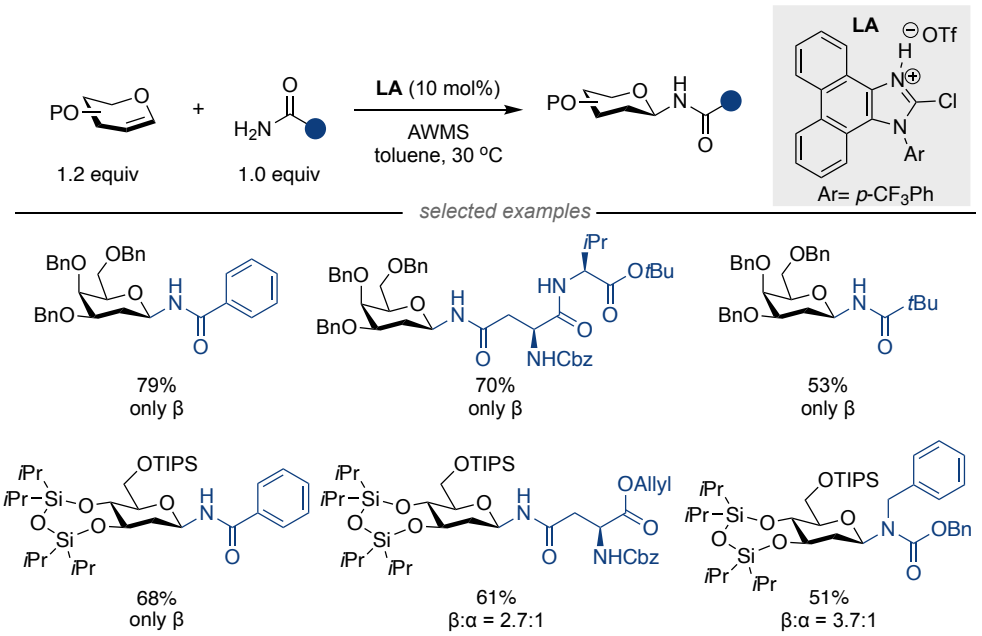

Scheme 3.4 Lewis acid-catalyzed *N*-glycosylation of glycals.

In 2013, Herzon and co-workers disclosed the utilization of azides as amine sources for forging β-*N*-glycosidic bonds by utilizing dimethylphenylphosphine as mediator (Scheme 3.5).[9] This approach allowed for the coupling of azides with a variety of protected and unprotected sugars without the need for preactivation at the anomeric position. The proposed mechanism involves a sequence consisting of Staudinger reduction and an aza-Wittig reaction, resulting in the formation of phosphine oxide byproducts.

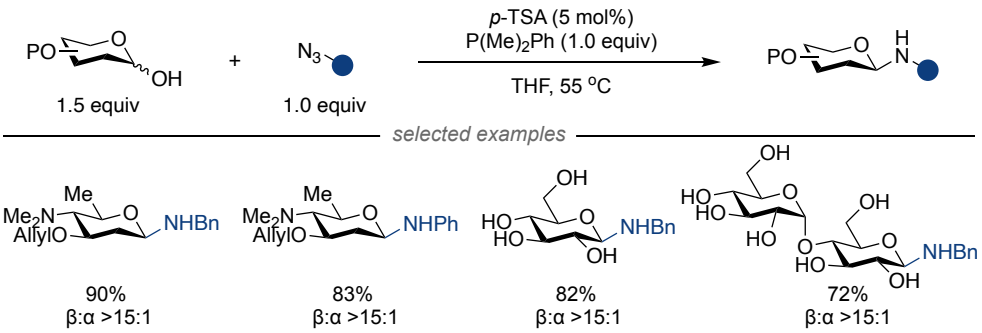

Scheme 3.5 *N*-glycosylation with azides as nitrogen sources.

3.1.2 Metal-Catalyzed *N*-Glycosylation

In 2023, Hotha's group reported a gold-catalyzed *N*-glycosylation of ethynylcyclohexyl glycosyl carbonate (Scheme 3.6).[10] This method allowed for the coupling of this glycosyl donor with various of *N*-based nucleophiles, including asparagine, as well as *N*-heterocycles such as purine, pyrimidine, and quinoline-2-one, affording the corresponding glycosides and nucleosides. Notably, the presence of a neighboring 2-*O*-carbonyl group was found to be essential for achieving high stereoselectivities.

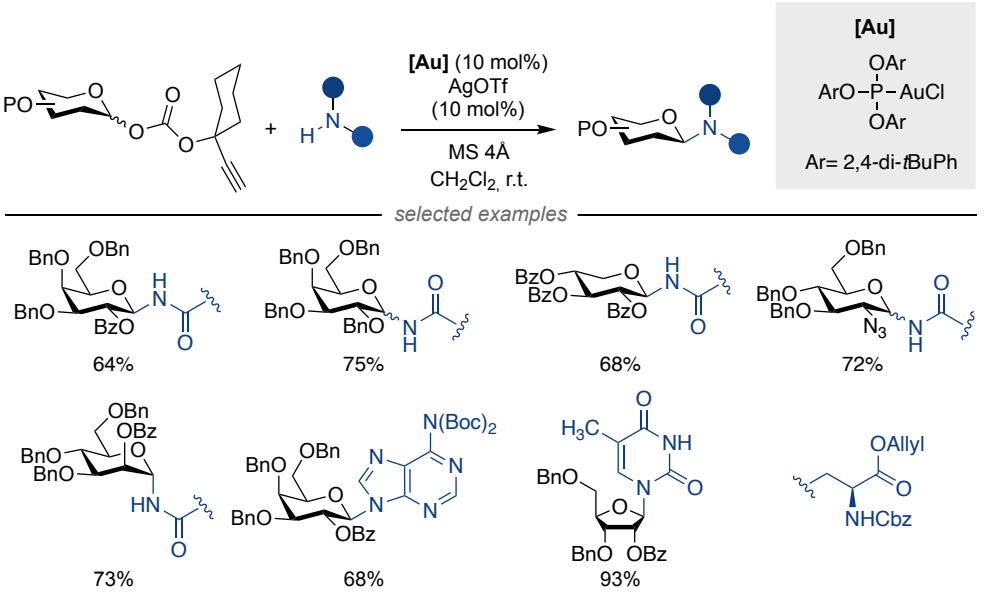

Scheme 3.6 Gold-catalyzed *N*-glycosylation.

In 2024, Chen and Koh reported the first *N*-glycosylation enabled by combination of copper and photo dual catalysis (Scheme 3.7). The authors developed novel glycosyl sulfones as glycosyl donors, which could be readily reduced to glycosyl radicals by the photocatalyst Ir(II) via single electron transfer event.[11] The formed glycosyl radical is then captured by Cu(II), followed by reductive elimination of the Cu(III) intermediate, resulting in the formation of *N*-glycosides and Cu(I). The propagating *N*-bound Cu(II) could be regenerated upon coordination of Cu(I) with an appropriate *N*-nucleophilic entity

and single-electron oxidation by photoexcited Ir(III)*. This approach could be applied not only to the *N*-glycosylation of furanoses but also to pyranoses, whereas significant erosions in α:β ratio were observed in the latter. Importantly, nucleophiles like amides do not work due to their lower nucleophilicity.

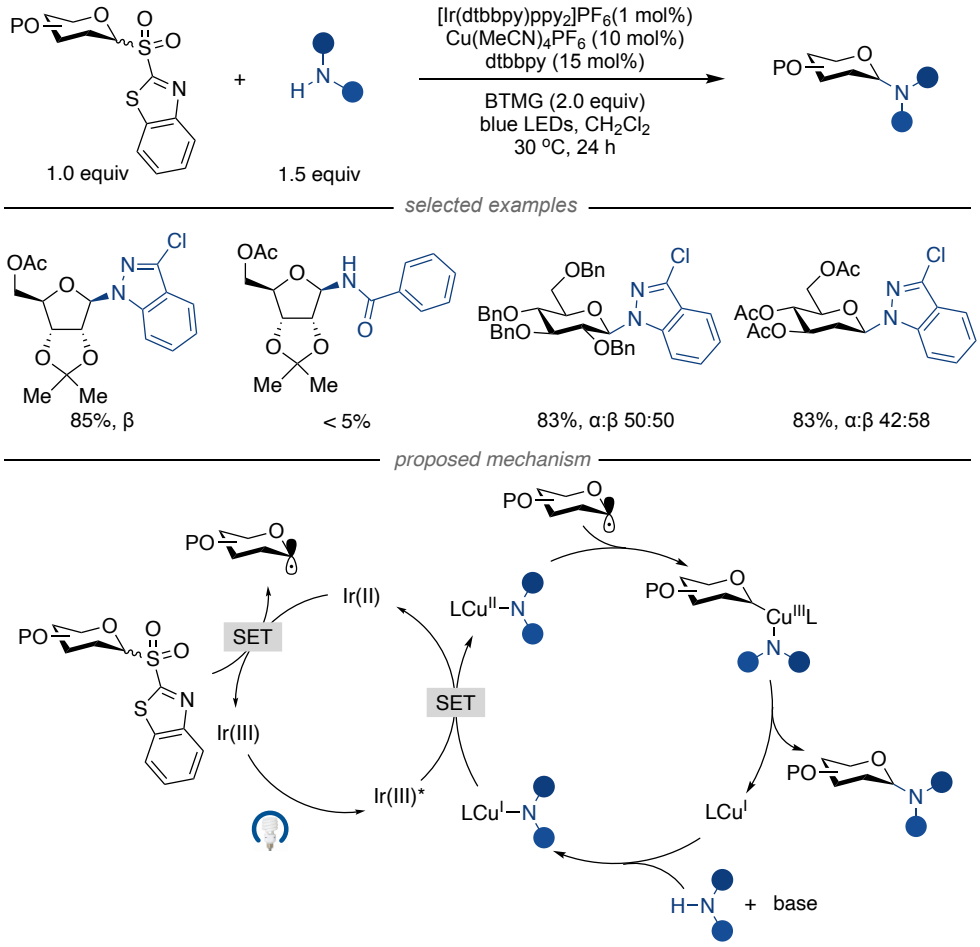

Scheme 3.7 Dual Cu/photoredox catalyzed *N*-glycosylation of glycosyl sulfones.

The Hu group demonstrated a dehydroxylative radical *N*-glycosylation protocol enabled by copper- and photocatalysis, yielding furanoses with 1,2-trans selectivity and α-selectivity for pyranoses (Scheme 3.8). In this approach, glycosyl radical precursors are formed via β-scission of hydroxyl groups bound to *N*-heterocyclic carbene (NHC).[12] The

reaction also exhibits a broad substrate scope, but it is worth noting that stoichiometric *t*-BuOOH is needed to oxidize $PC^{\bullet-}$ and Cu(I).

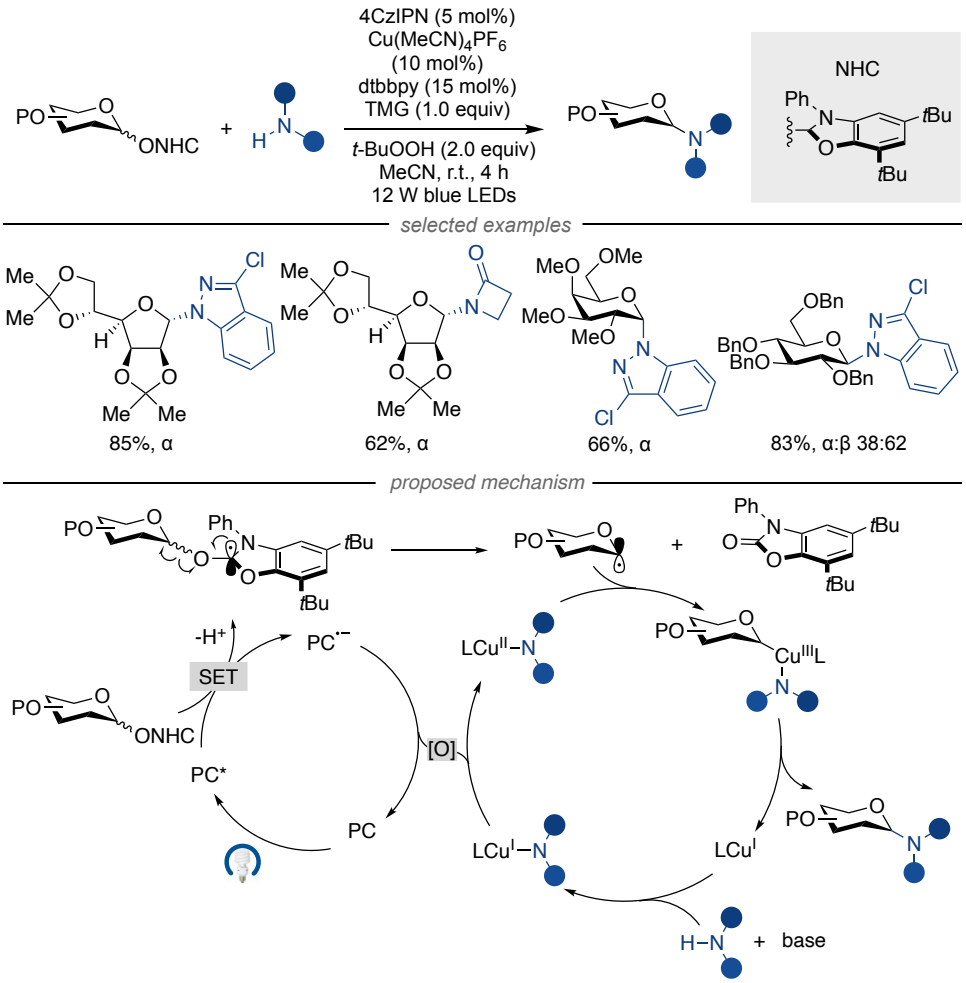

Scheme 3.8 Dehydroxylative *N*-glycosylation enabled by photo- and Cu-catalysis.

During the preparation of the manuscript emanating from the results of this chapter, Yin and Li reported a stereoselective *N*-glycosylation of glycals enabled by nickel catalysis using dioxazolones as nitrogen precursors (Scheme 3.9).[13] This approach yielded a series of 2-deoxy-*N*-glycosides with exclusive α-selectivities. However, the authors did not explore the preparation of β-*N*-glycosides in a high selectivity manner.

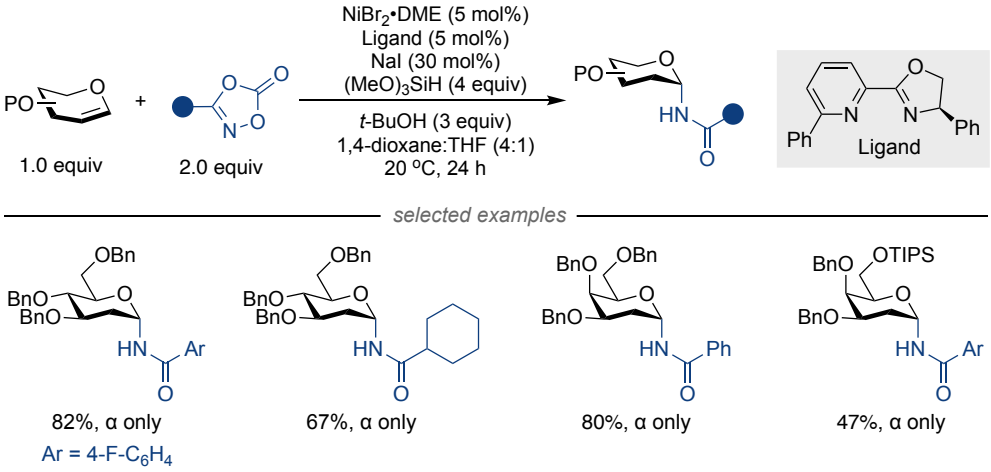

Scheme 3.9 Ni-catalyzed α-*N*-glycosylation of glycals.

3.2 General Aim of the Project

A series of disclosures have shown that the presence of neighboring groups can be an elegant vehicle for preparing 1,2-trans-*N*-glycosides from pre-functionalized glycals via the intermediacy of dioxolenium ions. Alternatively, Cu-catalyzed *N*-glycosylation can be achieved by the coupling of *N*-nucleophiles with in situ generated open-shell species, giving access to *N*-glycosides with variable selectivities. At the outset of our investigations, the design of a *de novo* catalytic *N*-glycosylation with improved flexibility and generality, capable of dictating α- or β-selectivity in *N*–glycosides avoiding neighboring groups or strong *N*-nucleophiles still constituted a considerable challenge.

Driven by the momentum of Ni catalysis to build up molecular complexity from simple precursors[14] and the prevalence of *N*-glycosides in a myriad of biologically relevant molecules, we aimed at establishing a Ni-catalyzed stereodivergent *N*-glycosylation protocol by leveraging the potential of in situ generated nitrenoids[15] en route to *N*–glycosides with improved modularity and flexibility (Scheme 3.10).

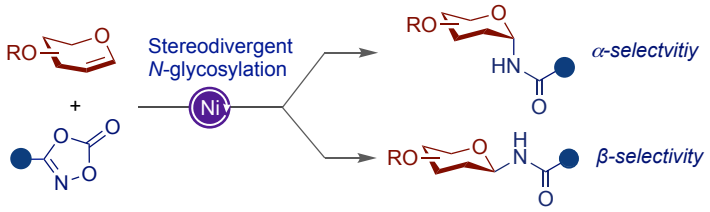

Scheme 3.10 Ni-catalyzed stereodivergent *N*-glycosylation.

3.3 Optimization of the Reaction Conditions for α-*N*-Glycosylation

We began our investigations by evaluating the *N*-glycosylation of 3,4,6-tri-*O*-benzyl-D-glucal (**1a**). Our initial efforts focused on identifying a nitrogen precursor that could afford the *N*-glycoside in both high yield and high stereoselectivity (Table 3.1). The best results were obtained by using 2 equivalents of phenyl-1,4,2-dioxazol-5-one (2a) as nitrogen precursor, leading to **3a** in 76% yield and 91% α-selectivity. In contrast, the utilization of benzoyl azide resulted in low yields, but high stereoselectivity. Additionally, no product was observed when using either sulfonyl azide or amide.

Table 3.1 Screening of nitrogen precursors.[a]

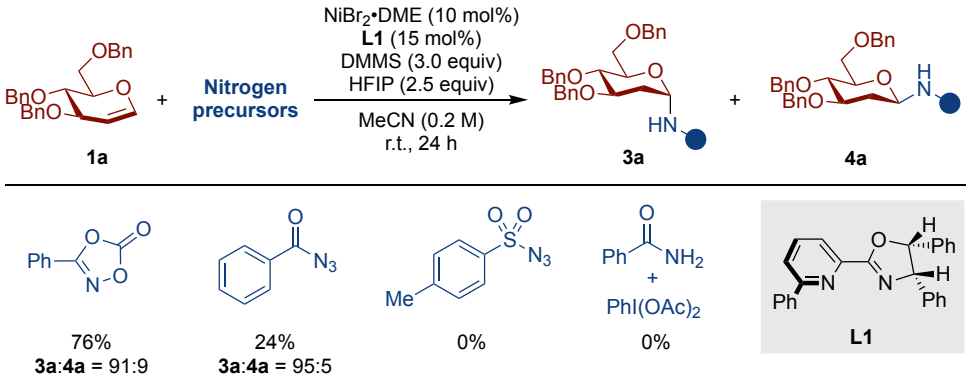

[a] Optimization of the reaction conditions: **1a** (0.20 mmol), nitrogen precursor (0.40 mmol), $NiBr_2$·DME (10 mol%), L1 (15 mol%), DMMS (0.60 mmol), HFIP (0.5 mmol) in MeCN (1 mL) at r.t. for 24 h. ^{1}H-NMR yield using CH_2Br_2 as internal standard. [b] Stereoselectivity en route to **3a** and **4a**.

Next, we investigated the effect of the nickel precatalyst on both reactivity and selectivity (Table 3.2). As anticipated, no product was formed in the absence of nickel. The use of nickel halide salts other than $NiBr_2$·DME resulted in diminished yields, albeit NiI_2 rendered an excellent stereoselectivity (entries 2-4). Additionally, the use of a Ni(0) source did not afford the desired product (entry 6), suggesting either that cod is detrimental for the reaction to occur or that a mechanism based on the intermediacy of Ni(0) is unlikely.

Table 3.2 Screening of nickel catalyst.[a]

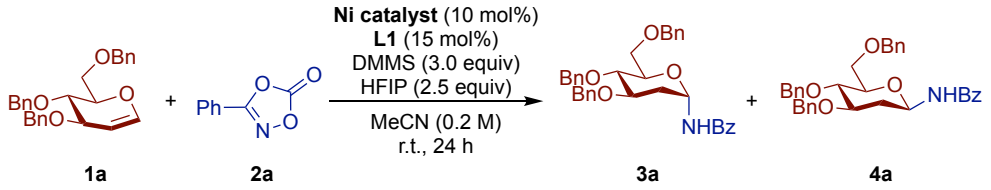

Entry	Ni catalyst	**3a** (%)	**3a**/**4a** (%)
1	No $NiBr_2$·DME	0	-
2	$NiBr_2$·DME	77	91:9
3	$NiCl_2$·DME	35	86:14
4	NiI_2	46	97:3
5	$Ni(ClO_4)_2·6H_2O$	0	-
6	$Ni(cod)_2$	0	-

[a] Optimization of the reaction conditions: **1a** (0.20 mmol), **2a** (0.40 mmol), nickel catalyst (10 mol%), **L1** (15 mol%), DMMS (0.60 mmol), HFIP (0.5 mmol) in MeCN (1 mL) at r.t. for 24 h. ^{1}H-NMR yield using CH_2Br_2 as internal standard.

As anticipated, the nature of the ligand was critical for success in both reactivity and stereoselectivity (Table 3.3), the use of pyridine-oxazoline-type (pyrox) ligand (**L4**) gave better results than 2,2′-bipyridine congeners (**L3**). Notably, the absence of phenyl substituents adjacent to the heteroatoms in either pyridine or oxazoline backbone resulted in diminished yields and low stereoselectivities. Interestingly, a stereoselectivity switch was not observed when employing (4*R*, 5*S*)-pyrox (**L2**) instead of **L1**, the suggesting that selectivity is not dictated by the chirality of the ligand backbone.

Table 3.3 Screening of ligands.[a]

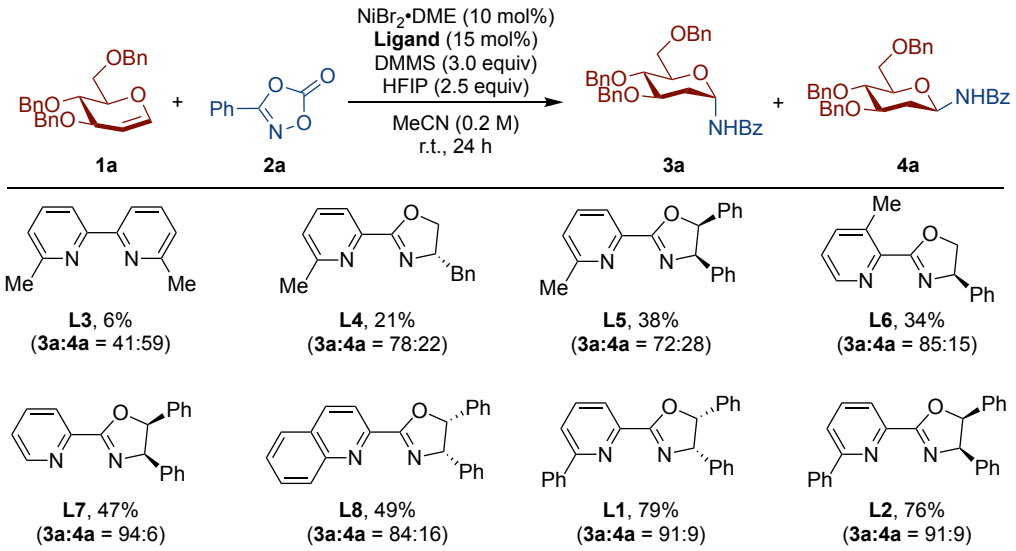

[a] Optimization of the reaction conditions: **1a** (0.20 mmol), **2a** (0.40 mmol), $NiBr_2$·DME (10 mol%), ligand (15 mol%), DMMS (0.60 mmol), HFIP (0.5 mmol) in MeCN (1 mL) at r.t. for 24 h. ^{1}H-NMR yield using CH_2Br_2 as internal standard.

With these results in hand, we next turned our attention to the nature of the hydride source (Table 3.4). As expected, the reaction required a hydride source to proceed (entry 1). The utilization of silanes other than DMMS resulted in lower yields (entries 3-5). Pinacolborane gave better selectivity but lower yield of **3a** (entry 6), whereas no reaction took place with sodium formate (entry 8).

Table 3.4 Screening of hydride sources.[a]

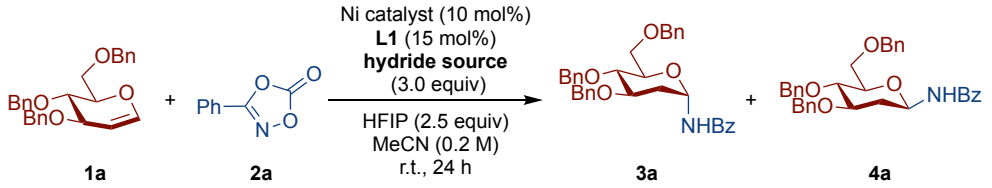

Entry	Hydride Sources	**3a** (%)	**3a**/**4a** (%)
1	No DMMS	0	-
2	DMMS	78	91:9
3	TMDSO	0	-
4	$PhMeSiH_2$	14	93:7
5	$PhSiH_3$	< 5%	-
6	HBpin	33	94:6
7	$Me_2S{\cdot}BH_3$	0	-
8	HCO_2Na	0	-

[a] Optimization of the reaction conditions: **1a** (0.20 mmol), **2a** (0.40 mmol), $NiBr_2{\cdot}DME$ (10 mol%), **L1** (15 mol%), hydride source (0.60 mmol), HFIP (0.5 mmol) in MeCN (1 mL) at r.t. for 24 h. ^{1}H-NMR yield using CH_2Br_2 as internal standard.

A thorough investigation on the proton source revealed that the use of TFE showed higher stereoselectivity than HFIP (Table 3.5). The utilization of other proton sources with lower pKa values such as acetic acid, or higher pKa values such as H_2O or EtOH all led to lower yields.

Table 3.5 Screening of proton sources.[a]

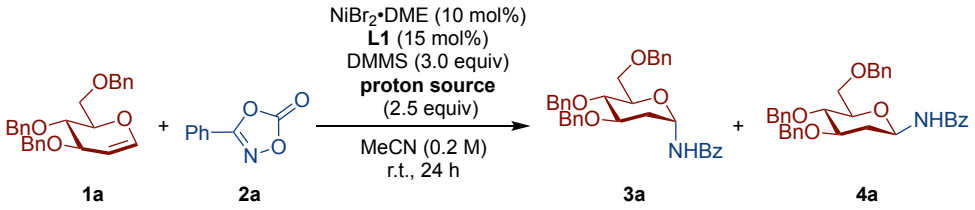

Entry	Proton Sources	**3a** (%)	**3a**/**4a** (%)
1	Acetic acid	0	-
2	HFIP	79	90:10
3	PhOH	31	98:2
4	TFE	77	92:8
5	H_2O	45	93:7
6	EtOH	27	96:4

[a] Optimization of the reaction conditions: **1a** (0.20 mmol), **2a** (0.40 mmol), $NiBr_2$·DME (10 mol%), **L1** (15 mol%), DMMS (0.60 mmol), proton source (0.5 mmol) in MeCN (1 mL) at r.t. for 24 h. ^{1}H-NMR yield using CH_2Br_2 as internal standard.

Next, we focused our attention on the influence of the additives on the reaction outcome. As shown in Table 3.6, the addition of stochiometric sodium carbonate or potassium phosphate tribasic led to lower yields of **3a** (entries 2-3). Although we hypothesized that a fluoride source might accelerate the formation of nickel-hydride species, this was unfortunately not the case (entry 4). The use of co-catalysts such as cobalt dibromide or lithium bromide also resulted in lower yields (entries 5-6). Finally, the addition of a catalytic amount of tetra-*n*-butylammonium iodide (TBAI) gave rise to **3a** in 83% yield with an exquisite 97:3 α:β selectivity (entry 7).

Table 3.6 Screening of additives.[a]

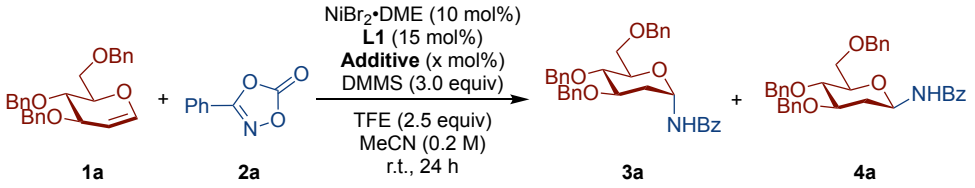

Entry	Additives	**3a** (%)	**3a/4a** (%)
1	No Additive	76	92:8
2	Na_2CO_3 (2.0 equiv.)	34	95:5
3	K_3PO_4 (2.0 equiv.)	< 5	-
4	KF (2.0 equiv.)	0	-
5	$CoBr_2$ (10 mol%)	< 5	-
6	LiBr (10 mol%)	0	-
7	TBAI (20 mol%)	83	97:3

[a] Optimization of the reaction conditions: **1a** (0.20 mmol), **2a** (0.40 mmol), $NiBr_2$·DME (10 mol%), **L1** (15 mol%), DMMS (0.60 mmol), TFE (0.5 mmol) in MeCN (1 mL) at r.t. for 24 h. ^{1}H-NMR yield using CH_2Br_2 as internal standard.

3.4 Substrate Scope of α-*N*-Glycosylation

3.4.1 Scope of Glycals

With optimized conditions in hand, we sought to examine the generality of the stereoselective *N*-glycosylation across a series of differently substituted glycals. As shown in Scheme 3.11, a variety of D-glucal derivatives with different protecting groups such as methyl, tert-butyldimethylsilyl (TBS), acetal and acyl groups could be employed as substrates with similar ease, resulting in the targeted *N*-glycosides (**3b**-**3e**) in good yields and α-selectivities. Notably, the installation of bulky TBS group as **3c** led to a α-selectivity greater than 99:1 compared to **3a** and **3b**, albeit in lower yield. It is worth noting that the formation of a relative rigid bicycle system from acetylation of 4,6-diols delivered *N*-glycoside **3d** and **3e** with exclusive α-selectivities. Although the presence of acyl group at C-3 sites might interfere with generation of 2,3-unsaturated *N*-glycosides via ferrier rearrangement,[16] this was not the case and **3e** could be obtained in 44% yield. As expected, L-rhamnal, 6-deoxy glucal, can be subjected to the optimized reaction conditions to produce **3f** with 95:5 α:β ratio, suggesting that the nature of the group at C5 might affect the stereoselectivity. In addition, **3g** was obtained in good yield and exclusive α-selectivity from the D-galactal series. Notably, D-arabinal containing a C3-axial C-O linkage yielded pure β-*N*-glycoside **3h** in 88% yield, thus suggesting that the configuration of substituents at C3 in pyran backbone plays a critical role in selectivity, probably due to unfavorable 1,3-diaxial interactions.[17] As shown by **3i**, our α-selective glycosylation can be extended to five-membered furanose rings with equal ease. It is worth noting that our protocol was equally effective when coupling disaccharide D-cellobial, resulting in **3i** in exclusive α-selectivity.

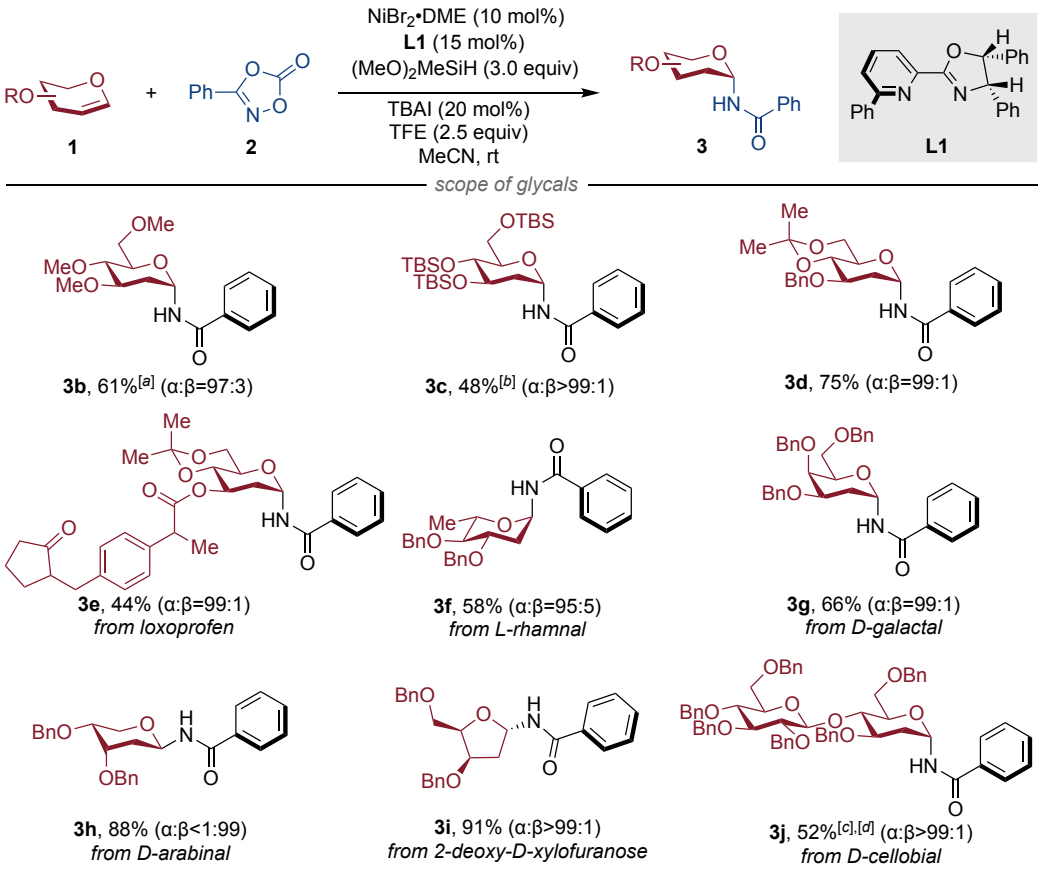

Scheme 3.11 Scope of glycals. **1** (0.20 mmol), **2** (0.40 mmol), $NiBr_2$·DME (10 mol%), **L1** (15 mol%), DMMS (0.60 mmol), TFE (0.5 mmol) in MeCN (1 mL) at r.t.. [a] additional DMMS (0.20 mmol) and TFE (0.1 mmol) were added after 48h. [b] HFIP (0.5 mmol) were used instead of TFE (0.5 mmol). [c] no TBAI added. [d] reactions were conducted on 0.1 mmol scale for **1**.

3.4.2 Scope of Dioxazolones

Encouraged by these results, we next turned our attention to explore the generality of the reaction by assessing the suitability of a family of different dioxazolones. As shown in Scheme 3.12, a wide variety of electron-rich or electron-poor aryl-substituted dioxazolones could be utilized as substrates, resulting in the corresponding *N*-glycosides (**3k-3q**) in good yields and excellent selectivities. In addition, primary, secondary, and even tertiary alkyl-substituted nitrogen precursors could be utilized equally well with different glycals to afford **3q-3v** in excellent stereoselectivities. Cyclic alkyl variants such

as cyclopropane (**3v**), cyclopentane (**3u**) or 4,4-difluorocyclohexane (**3t**) were all viable as amide precursors. Notably, dioxazolones containing nitriles (**3n**) or electrophilic sites such as chlorine (**3m, 3r**) and bromine (**3p**) susceptible for cross-coupling reactions could all be well-accommodated, thus providing an additional handle for further functionalization.[18] The absolute configuration of **3m** was confirmed by X-ray diffraction.

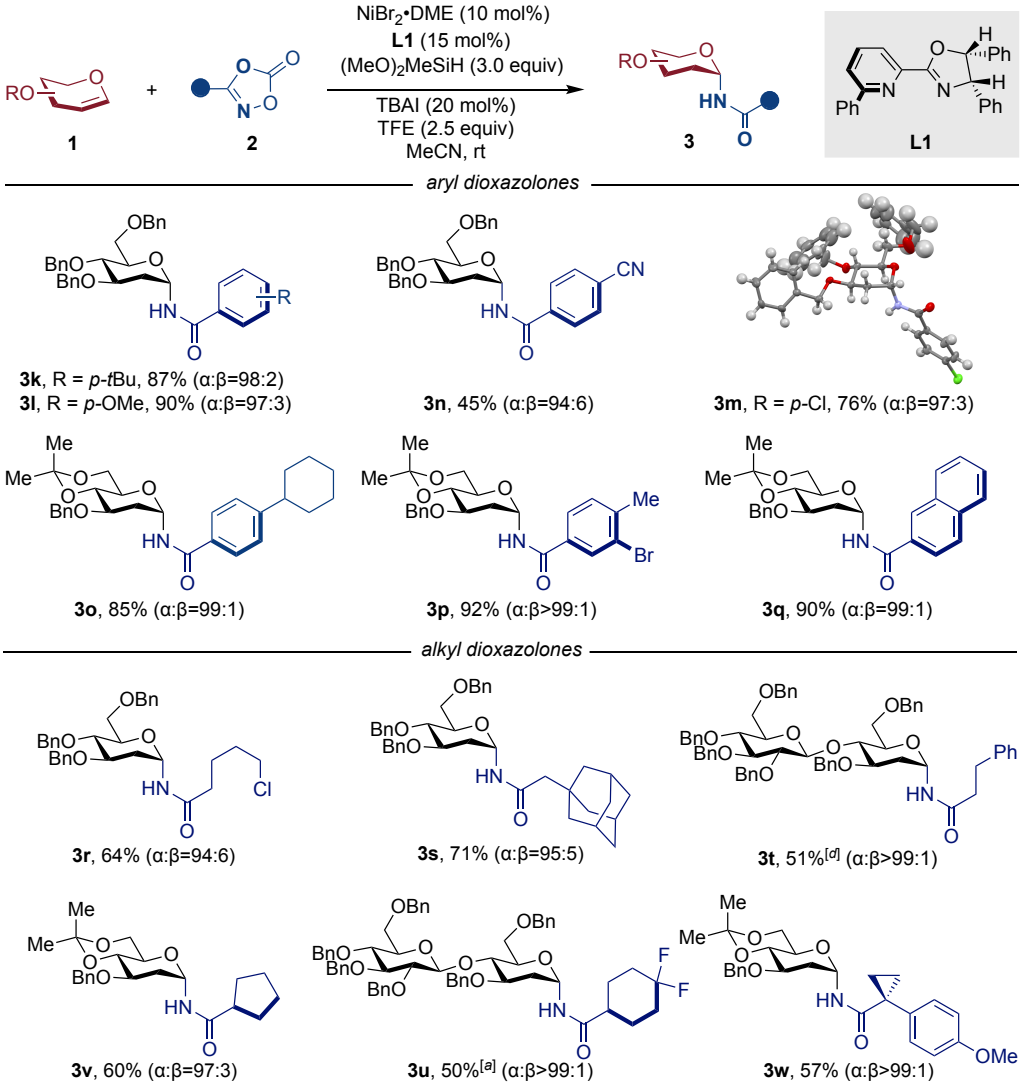

Scheme 3.12 Scope of aryl/alkyl dioxazolones. **1** (0.20 mmol), **2** (0.40 mmol), $NiBr_2$·DME (10 mol%), **L1** (15 mol%), DMMS (0.60 mmol), TFE (0.5 mmol) in MeCN (1 mL) at r.t.. [a] reactions were conducted on 0.1 mmol scale for **1**.

3.5 Optimization of the Reaction Conditions for β-*N*-Glycosylation

Taking into consideration the exquisite α-selectivity observed in Scheme 3.11, we wondered whether a nickel-catalyzed stereodivergent *N*-glycosylation could provide access to β-*N*-glycosides. However, all our attempts to optimize all reaction variables en route to the corresponding β-*N*-glycosides were met with failure. This is probably due to the observation that the reaction is kinetically-controlled, favoring the formation of the corresponding α-*N*-glycosides. We anticipated that a thermodynamically-controlled epimerization might provide a pathway to access the equatorial *N*-glycosidic bond.[19] As shown in Scheme Table 3.6, this approach turned out to be suited for our purposes. Indeed, simple exposure of α-*N*-glycosides to *p*-TSA (50 mol%) at 50 °C gave rise to desired β-*N*-glycosides **4b** with 93:7 selectivity (entry 1). In the absence of *p*-TSA, the reaction exclusively produced the α-*N*-glycoside, which was also observed when using 20 mol% *p*-TSA, likely due poisoning in the presence of basic nitrogen ligands (entries 2-3). It's worth noting that other Lewis acids, such as nickel chloride, zinc triflate, and zirconium(IV) chloride, were ineffective in promoting the epimerization (entries 4-6).

Table 3.6 Screening of additives.

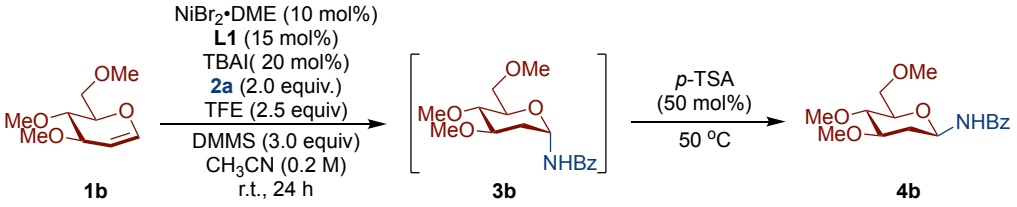

Entry	deviation	**4b** (yield%)	**4b**:**3b** (%)
1	no	64	93:7
2	no *p*-TSA	2	3:97
3	using *p*-TSA (20 mol%)	3	4:96
4	$NiCl_2$ instead of *p*-TSA	3	4:96
5	$Zn(OTf)_2$ instead of *p*-TSA	46	27:73
6	$ZrCl_4$ instead of *p*-TSA	61	87:13

3.6 Substrate Scope of β-*N*-Glycosylation

With optimized conditions in hand, we explored the generality of the epimerization across a wide range of glycals and dioxazolones. As shown in Scheme 3.13, D-glucals possessing benzyl- or methyl-protecting group were readily converted to **4k** and **4b** in good yields and high β-selectivities. Importantly, not only D-glucals, but also L-rhamnal, D-galactal and D-cellobial could be employed in this protocol, resulting in **4f**, **4x** and **4j** with similar efficiencies and selectivities. Notably, this acid-mediated epimerization protocol did not affect the *O*-glycosidic bond in **4j**. As anticipated, a 6:94 selectivity demonstrated the ability to extend this approach to alkyl amide-containing *N*-glycals (**4r**) with equal ease.

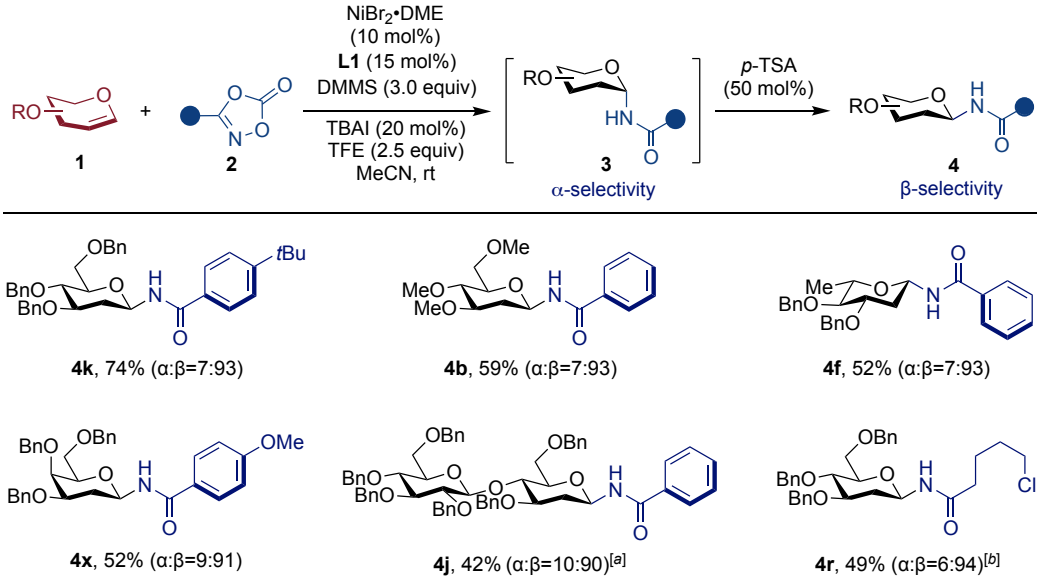

Scheme 3.13 Scope of β-*N*-glycosylation. **1** (0.20 mmol), **2** (0.40 mmol), $NiBr_2$·DME (10 mol%), **L1** (15 mol%), DMMS (0.60 mmol), TFE (0.5 mmol) in MeCN (1 mL) at r.t. for 24 h, then *p*-TSA (50 mol%) 50 °C. [a] reactions were conducted on 0.1 mmol scale for **1**, and without TBAI. [b] epimerization was conducted in toluene (1 mL).

3.7 Preliminary Mechanistic Studies

3.7.1 Crossover Experiments

To gain a deeper insight into the possible reaction pathway of our Ni-catalyzed N-glycosylation event, a set of preliminary mechanistic experiments were carried out. A crossover experiment of **1a** in the presence of both **2a** and *p*-methoxy benzamide led to exclusive formation of **3a** in 64% yield and 97:3 α:β selectivity and not even traces of **3l** were observed in the crude mixtures (Scheme 3.14). This observation argues against a pathway consisting of interception of an oxocarbenium ion with a free amide, thus supporting a scenario occurring via in situ generated nickel-nitrenoids prior to C-N bond-formation.[20]

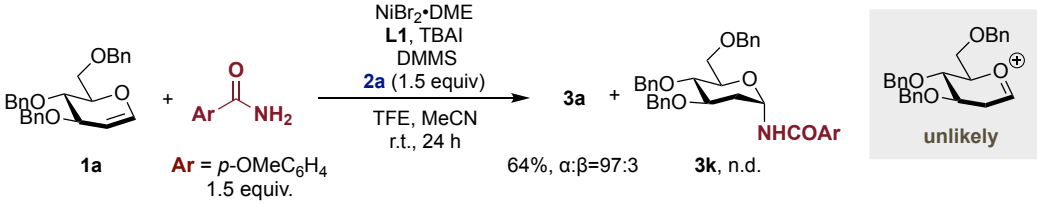

Scheme 3.14 Crossover experiment with amide.

3.7.2 Isotope-labelling Studies

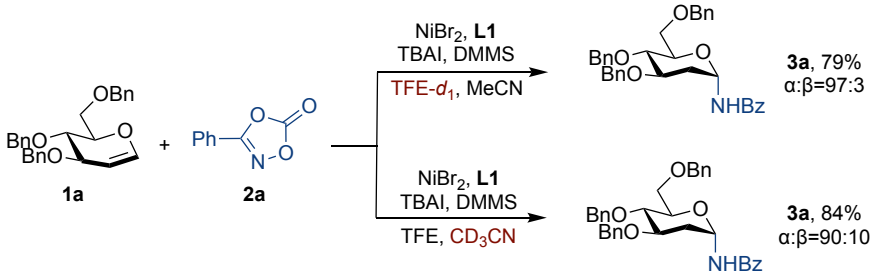

Scheme 3.15 Isotope-labelling with TFE-d_1 and CD_3CN.

No deuterium incorporation was detected in **3a** with either TFE-d_1 or CD_3CN, thus excluding the possibility of a pathway consisting of the generation of the nickel hydride from either TFE or MeCN (Scheme 3.15).

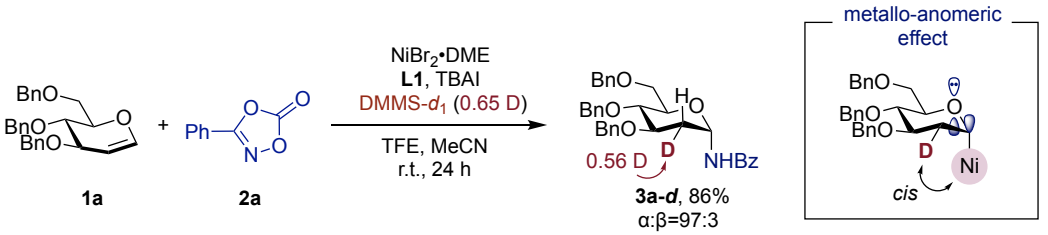

Scheme 3.16 Isotope-labelling with DMMS-d_1.

As anticipated, an equatorial 0.56 deuterium content at C2 was detected in **3a**-*d* when utilizing DMMS-d_1 (0.65D), strongly advocating the notion that the reaction involves a *syn*-migratory insertion of an in situ generated nickel hydride to glycals from the α-face (Scheme 3.16).[21] The high α-selectivity is consistent with the intervention of a kinetic metallo-anomeric effect, where the nickel center is located preferentially at the axial position prior to reaction with **2a** due to hyperconjugation between the endocyclic oxygen atom and the σ* orbitals of the C–Ni bond.[22]

3.7.3 Proposed Mechanism

On the basis of all our experiments, we believe that our results can be explained by a mechanism consisting of an initial reduction of a Ni(II) precatalyst by the DMMS, resulting in a nickel hydride complex **A** (Scheme 3.17). This complex can then undergo a migratory insertion to the glycal from α-face, resulting in **B** which features a stable anomeric carbon-nickel bond. Therefore, intermediate **B** subsequently reacts with dioxazolone to produce Ni-nitrenoid **C** with a neat loss of CO_2. Reductive elimination then forges the α-stereoselective *N*-glycosidic bond (**D**). A protonation in the presence of TFE and σ-bond metathesis with $(MeO)_2MeSiH$ ultimately releases the desired α-*N*-glycoside and regenerates Ni-hydride **A**.

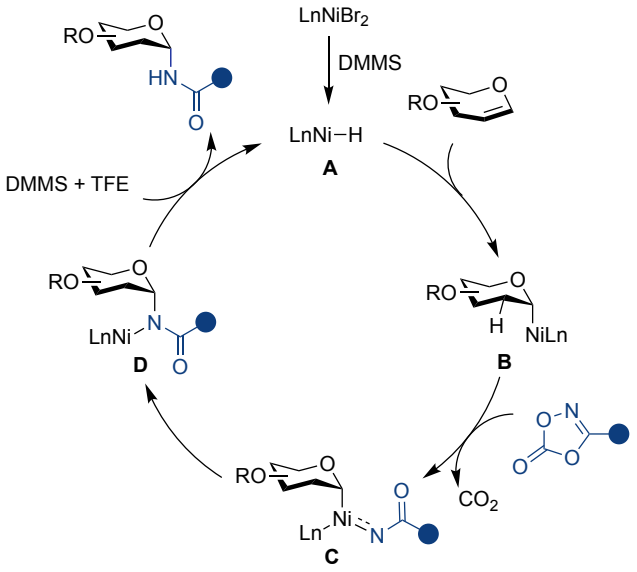

Scheme 3.17 Proposed Mechanism for the Ni-catalyzed α-*N*-glycosylation.

3.8 Conclusion

In this chapter, we disclose a nickel-catalyzed stereoselective α-*N*-glycosylation via a kinetically-controlled migratory insertion of a nickel-hydride into a glycal. The protocol is distinguished by its high stereoselectivity, mild conditions and broad scope. The corresponding β-*N*-glycosides can be obtained by an acid-mediated epimerization, thus offering a new modular and unified platform that expedites the access to stereodivergent *N*-glycosides with an exquisite control of the stereoselectivity.

3.9 Experimental Section

3.9.1 General Information

Analytical methods. ^{1}H and ^{13}C NMR were recorded on Bruker 300 MHz, Bruker 400 MHz and Bruker 500 MHz at 20 °C. All ^{1}H NMR spectra are reported in parts per million (ppm) downfield of TMS and were calibrated using the residual solvent peak of CD_2Cl_2 (5.32 ppm) or $CHCl_3$ (7.26 ppm), unless otherwise indicated. All ^{13}C NMR spectra are reported in ppm relative to TMS, were calibrated using the signal of residual CD_2Cl_2 (53.84 ppm) or $CHCl_3$ (77.16 ppm). Coupling constants, *J* are reported in Hertz. Gas chromatographic analyses were performed on Hewlett-Packard 6890 gas chromatography instrument with FID detector. Melting points were measured using open glass capillaries in a Büchi B540 apparatus. Infrared spectra (FT-IR) measurements were carried out on a Bruker Optics FT-IR Alpha spectrometer equipped with a DTGS detector, KBr beamsplitter at 4 cm^{-1} resolution using a one bounce ATR accessory with diamond windows. High-resolution mass spectra were recorded on a Waters LCT Premier spectrometer or in a MicroTOF Focus, Bruker Daltonics spectrometer. UV/Vis absorption spectra were recorded using a Agilent Technologies Cary 300 UV/Vis spectrophotometer and UV-1800PC spectrophotometer in quartz cuvettes with a path length of 1.0 cm. Flash chromatography was performed with EM Science silica gel 60 (230-400 mesh). Thin layer chromatography was used to monitor reaction progress and analyzed fractions from column chromatography. To this purpose TLC Silica gel 60 F_{254} aluminium sheets from Merck were used and visualization was achieved using UV irradiation and/or staining with Phosphomolybdic acid solution. The yields reported refer to isolated yields and represent an average of at least two independent runs. The procedures described in this section are representative. Thus, the yields may differ slightly from those given in the tables of the manuscript.

Reagents. Commercially available materials were used as received without further purification. Nickel bromide ethylene glycol dimethyl ether ($NiBr_2$·DME, 97% purity) was purchased from Sigma Aldrich. D-Glucal (98% purity) was purchased from BLD pharm. Dimethoxymethylsilane (DMMS, >97.0%(GC) purity) was purchased from TCI.

2,2,2-Trifluoroethanol (TFE, ⩾99% purity) was purchased from Sigma Aldrich. 1,1,1,3,3,3-Hexafluoro-2-propanol (HFIP, 99% purity) was purchased from Apollo Scientific. Extra dry MeCN (99.9+% purity, *note*: the utilization of MeCN containing molecular sieves afforded decreased yield and stereoselectivity) was purchased from Fisher Scientific.

General procedure for the optimization of the α-*N*-glycosylation of 1a with 2a. An oven-dried 20 mL reaction tube containing a stir bar was charged with $NiBr_2$·DME (6.2 mg, 10 mol%), **L1** (11.3 mg, 15 mol%), **1a** (0.2 mmol, 1.0 equiv., 83.4 mg), **2a** (0.4 mmol, 2.0 equiv., 65.2 mg). The reaction tube was connected to a vacuum line where it was evacuated and backfilled with Ar at least three times. Then anhydrous MeCN (1.0 mL) was added, and the mixture was stirred at r.t. for 5 minutes under Ar flow before adding DMMS (74.0 μL, 3.0 equiv.) and HFIP (52.6 μL, 2.5 equiv.). The tube was sealed under Ar atmosphere and stirred at rt. for 24 h. The reaction mixture was then quenched with air, concentrated under vacuum and purified by a short column to determine the yield and stereoselectivity via ^{1}H-NMR spectroscopy using CH_2Br_2 (0.2 mmol, 35mg, 13.5 μL) as internal standard.

3.9.2 Synthesis of Starting Materials

Synthesis of L1. 2-[(4*S*,5*R*)-4,5-Dihydro-4,5-diphenyl-2-oxazoyl]-6-phenylpyridine (**L1**) were prepared according to the literature procedure.[23]

Synthesis of glycals. 3,4,6-Tri-*O*-benzyl-D-glucal, 3,4,6-Tri-*O*-methyl-D-glucal, 3,4,6-Tri-*O*-tert-butyldimethylsilyl-D-glucal, 3,4-di-*O*-benzyl-L-rhamnal, 3,4,6-Tri-*O*-benzyl-D-galactal, 3,4-di-*O*-benzyl-D-arabinal, 2',3,3',4',6,6'-*O*-benzyl-D-cellobial were prepared according to the literature procedure,[24] 3-*O*-benzyl-4,6-di-*O*-isopropylidene-D-glucal were prepared according to the literature procedure,[25] 2-deoxy-3,5-di-*O*-benzyl-D-xylofuranose.[26]

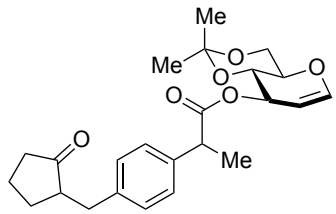

3-*O*-[α-methyl-4-[(2-oxocyclopentyl)methyl]benzeneacetate]-4,6-di-*O*-isopropylidene-D-glucal (1e). Loxoprofen (542 mg, 2.2 mmol) and DMAP (305 mg, 2.5 mmol) were dissolved in 10 mL of CH_2Cl_2 and cooled to 0 °C. After 10 min, *N*,*N*′-diisopropylcarbodiimide, (265 mg, 2.1 mmol) was added with vigorous stirring. After 5 min, a solution of 4,6-di-*O*-isopropylidene-D-glucal (372 mg, 2.0 mmol) in 10 mL of CH_2Cl_2 was added via cannula. The reaction mixture was stirred at room temperature for 12 h. The crude was filtered through a plug of silica gel, concentrated, and the residue was purified by flash silica gel chromatography, affording the title compound (618 mg, 70%, dr 1:1, colorless oil). **^{1}H NMR** (500 MHz, $CDCl_3$) δ 7.23 – 7.17 (m, 4H), 7.14 – 7.06 (m, 4H), 6.33 (dd, *J* = 6.1, 1.5 Hz, 1H), 6.26 (dd, *J* = 6.1, 1.5 Hz, 1H), 5.44 (dq, *J* = 7.7, 2.0 Hz, 1H), 5.38 (dt, *J* = 7.8, 1.8 Hz, 1H), 4.68 (dt, *J* = 6.1, 1.7 Hz, 1H), 4.57 (dd, *J* = 6.1, 1.5 Hz, 1H), 4.04 – 3.85 (m, 4H), 3.85 – 3.75 (m, 4H), 3.75 – 3.66 (m, 2H), 3.13 (d, *J* = 4.1 Hz, 1H), 3.10 (d, *J* = 4.1 Hz, 1H), 2.57 – 2.45 (m, 2H), 2.41 – 2.27 (m, 4H), 2.17 – 2.03 (m, 4H), 2.01 – 1.90 (m, 2H), 1.81 – 1.67 (m, 2H), 1.62 – 1.50 (m, 2H), 1.49 (s, 3H), 1.47 (d, *J* = 7.2 Hz, 6H), 1.40 (s, 3H), 1.34 – 1.28 (m, 6H) ppm. **^{13}C NMR** (126 MHz, $CDCl_3$) δ 174.42, 174.32, 145.58, 145.43, 138.92, 138.80, 138.53, 138.40, 129.19, 129.04, 127.76, 127.60, 100.90, 100.72, 99.89, 99.73, 70.16, 69.91, 69.88, 69.58, 69.07, 61.76, 61.73, 51.13, 51.08, 45.31, 45.21, 38.30, 38.28, 35.31, 35.29, 29.33, 29.02, 28.91, 20.65, 19.12, 18.83, 18.81, 18.50 ppm. **IR (neat):** 2991, 2970, 2939, 2878, 1732, 1639, 1513, 1375, 1269, 1232, 1200, 1168, 1110, 1091, 1067, 1053, 1003, 987, 943, 864, 755, 736 cm^{-1}. **HRMS (ESI)** *calcd*. for ($C_{24}H_{30}NaO_6$) $[M+Na]^+$: 437.1935, *found* 437.1947. **M.P.**: 72 °C.

Synthesis of Nitrene Precursors Dioxazolones. 3-pentyl-1,4,2-dioxazol-5-one, 3-phenethyl-1,4,2-dioxazol-5-one, 3-(4-chlorobutyl)-1,4,2-dioxazol-5-one, 3-cyclopentyl-

1,4,2-dioxazol-5-one, 3-(4,4-difluorocyclohexyl)-1,4,2-dioxazol-5-one, 3-(4-chlorophenyl)-1,4,2-dioxazol-5-one, 3-(4-cyanophenyl)-1,4,2-dioxazol-5-one, 3-(4-methoxyphenyl)-1,4,2-dioxazol-5-one, 3-(4-(*tert*-butyl)phenyl)-1,4,2-dioxazol-5-one, 3-(naphthalen-2-yl)-1,4,2-dioxazol-5-one, 3-((adamantan-1-yl)methyl)-1,4,2-dioxazol-5-one, 3-(1-(4-methoxyphenyl)cyclopropyl)-1,4,2-dioxazol-5-one were prepared following the literature procedure.[27]

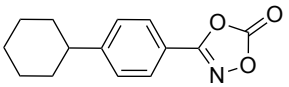

3-(4-(cyclohexyl)phenyl)-1,4,2-dioxazol-5-one (2o). 1,1′-carbonyldiimidazole (CDI, 1.9 g, 1.2 equiv.), 4-cyclohexylbenzoic acid (2.0 g, 10 mmol) and THF (40 mL) were added to an oven-dried 100 mL round-bottom flask under argon. The reaction mixture was stirred for 2 h at room temperature. Then, hydroxylamine hydrochloride (NH_2OH•HCl, 1.4 g, 2.0 equiv.) was quickly added to the crude mixture, and stirred for additional 14 h at room temperature. The mixture was diluted with 5% $KHSO_4$(aq.) and extracted with EtOAc (3 times). The combined organic layers were dried over anhydrous Na_2SO_4, filtered, and concentrated under reduced pressure and further crystallized in dichloromethane to afford hydroxamic acid (940 mg). Subsequently, 1,1′-carbonyldiimidazole (766 mg, 1.1 equiv.) was added in one portion at room temperature and stirred for 1 h before being quenched with cold HCl 1M (aqueous) at 0 ºC. The crude was extracted with CH_2Cl_2, dried over anhydrous Na_2SO_4, concentrated under reduced pressure and filtered through a pad of silica with an eluent (EtOAc/n-hexane, 5:1), affording the title compound (850 mg, 35%, two steps) as a white solid. **^{1}H NMR** (500 MHz, $CDCl_3$) δ 7.81 – 7.71 (m, 2H), 7.43 – 7.34 (m, 2H), 2.68 – 2.52 (m, 1H), 1.96 – 1.83 (m, 4H), 1.82 – 1.73 (m, 1H), 1.50 – 1.35 (m, 4H), 1.34 – 1.20 (m, 1H) ppm. **^{13}C NMR** (126 MHz, $CDCl_3$) δ 163.81, 154.81, 154.15, 128.06, 126.85, 117.60, 44.92, 34.16, 26.76, 26.08 ppm. **IR (neat):** 2927, 2900, 2852, 1859, 1830, 1613, 1563, 1509, 1449, 1420, 1365, 1353, 1165, 1065, 963, 836, 751, 671, 539 cm^{-1}. **HRMS (ESI)** *calcd*. for ($C_{15}H_{19}NNaO_4$) $[M+MeOH+Na]^+$: 300.1206, *found* 300.1210. **M.P.**: 108 °C.

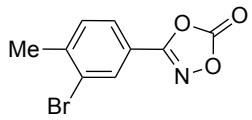

3-(3-(bromo)-4-(methyl)phenyl)-1,4,2-dioxazol-5-one (2p). Following a similar procedure to that shown for **2o**, the title compound could be obtained as a white solid (731 mg, 29%, two steps). **^{1}H NMR** (500 MHz, $CDCl_3$) δ 8.01 (d, *J* = 1.7 Hz, 1H), 7.69 (dd, *J* = 8.0, 1.8 Hz, 1H), 7.41 (d, *J* = 8.0 Hz, 1H), 2.49 (s, 3H) ppm. **^{13}C NMR** (126 MHz, $CDCl_3$) δ 162.57, 153.68, 144.83, 131.77, 130.39, 125.92, 125.42, 119.34, 23.55 ppm. **IR (neat):** 1867, 1828, 1777, 1615, 1548, 1492, 1397, 1346, 1273, 1171, 1039, 973, 932, 891, 819, 755, 703, 678, 621, 579 cm^{-1}. **HRMS (ESI)** *calcd*. for ($C_{10}H_{10}BrNNaO_4$) $[M+MeOH+Na]^+$: 309.9685, *found* 309.9692. **M.P.:** 65 °C.

3.9.3 Ni-catalyzed Stereoselective α-*N*-Glycosylation

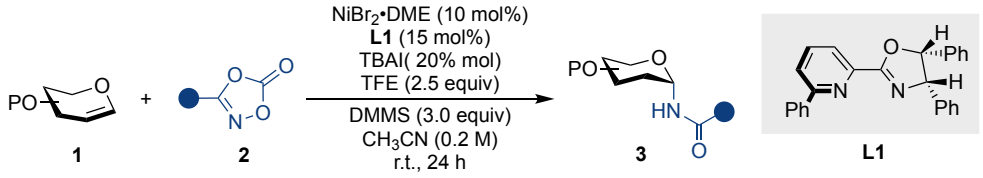

General Procedure A. An oven-dried 20 mL reaction tube containing a stir bar was charged with $NiBr_2$·DME (6.2 mg, 10 mol%), **L1** (11.3 mg, 15 mol%), **1** (0.2 mmol, 1.0 equiv.), **2** (0.4 mmol, 2.0 equiv.) and TBAI (14.7 mg, 20 mol%). The tube was connected to a vacuum line where it was evacuated and backfilled with Ar at least three times. Then, anhydrous MeCN (1.0 mL) was added, and the mixture was stirred at rt for 5 min under Ar flow before adding $(MeO)_2MeSiH$ (74.0 μL, 3.0 equiv.) and TFE (36.0 μL, 2.5 equiv.). The tube was sealed under Ar atmosphere and stirred at rt for 24 h. The reaction mixture was then opened to air and concentrated under vacuum. The residue was purified by flash column chromatography to give the targeted compounds.

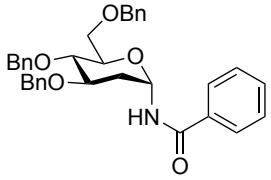

1-*N*-Benzoyl-(2-deoxyl-3,4,6-tri-*O*-benzyl-α-D-glucopyranosyl)-amine (3a). Following General Procedure A, 3,4,6-tri-*O*-benzyl-D-glucal (0.2 mmol, 83 mg) and **2a** (0.40 mmol, 65 mg) were used, affording **3a** as a white solid (first run, 86 mg, 80%; second run, 82 mg, 76%) and **4a** (first run, 2 mg, 2%; second run, 2 mg, 2%). **3a**: **^{1}H NMR** (400 MHz, CD_2Cl_2) δ 7.88 – 7.66 (m, 2H), 7.57 – 7.51 (m, 1H), 7.45 (t, *J* = 7.5 Hz, 2H), 7.39 – 7.22 (m, 15H), 6.74 (d, *J* = 7.8 Hz, 1H), 5.88 (dt, *J* = 8.2, 4.3 Hz, 1H), 4.83 (d, *J* = 11.0 Hz, 1H), 4.73 – 4.49 (m, 5H), 3.92 – 3.79 (m, 3H), 3.75 – 3.57 (m, 2H), 2.25 (dt, *J* = 13.6, 4.1 Hz, 1H), 2.03 (m, 1H). ppm. **^{13}C NMR** (101 MHz, CD_2Cl_2) δ 167.29, 139.06, 139.01, 138.97, 134.74, 132.41, 129.16, 128.94, 128.86, 128.53, 128.43, 128.27, 128.23, 128.10, 127.61, 77.35, 76.98, 74.86, 74.56, 73.95, 73.68, 72.03, 69.59, 34.02. ppm. **IR (neat):** 3309, 3062, 3030, 2866, 1645, 1524, 1488, 1453, 1364, 1269, 1204, 1090,

1027, 993, 734, 695, 618, 567 cm^{-1}. **HRMS (ESI)** *calcd*. for ($C_{34}H_{35}NNaO_5$) $[M+Na]^+$: 560.2407, *found* 560.2423. **M.P.**: 78 °C.

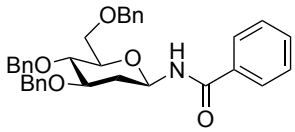

1-*N*-Benzoyl-(2-deoxyl-3,4,6-tri-*O*-benzyl-β-D-glucopyranosyl)-amine (4a). A white solid. **^{1}H NMR** (500 MHz, $CDCl_3$) δ 7.86 – 7.76 (m, 2H), 7.50 (t, *J* = 7.4 Hz, 1H), 7.42 (t, *J* = 7.6 Hz, 2H), 7.37 – 7.21 (m, 13H), 7.20 – 7.14 (m, 3H), 5.56 – 5.44 (m, 1H), 4.90 (d, *J* = 10.8 Hz, 1H), 4.66 (d, *J* = 11.6 Hz, 1H), 4.59 (d, *J* = 11.6 Hz, 1H), 4.52 (d, *J* = 10.9 Hz, 1H), 4.42 (d, *J* = 11.8 Hz, 1H), 4.32 (d, *J* = 11.8 Hz, 1H), 3.84 – 3.66 (m, 4H), 3.58 (d, *J* = 9.1 Hz, 1H), 2.29 – 2.19 (m, 1H), 1.85 – 1.73 (m, 1H) ppm. **^{13}C NMR** (126 MHz, $CDCl_3$) δ 166.84, 138.51, 138.44, 137.73, 133.81, 131.97, 128.61, 128.52, 128.47, 128.45, 128.40, 127.98, 127.93, 127.81, 127.76, 127.66, 127.39, 79.92, 77.49, 76.62, 75.14, 73.62, 71.49, 68.57, 36.67 ppm. **IR (neat):** 3347, 3060, 3030, 2955, 2893, 2860, 1656, 1523, 1491, 1453, 1364, 1307, 1267, 1155, 1086, 1047, 1027, 998, 971, 905, 736, 695, 649, 602, 567, 543 cm^{-1}. **HRMS (ESI)** *calcd*. for ($C_{34}H_{36}NO_5$) $[M+H]^+$: 538.2588, *found* 538.2588. **M.P.**: 143 °C.

NMR spectroscopy of the crude reaction mixture prior to purification revealed the formation of **3a**-**4a** with a 97:3 α:β selectivity.

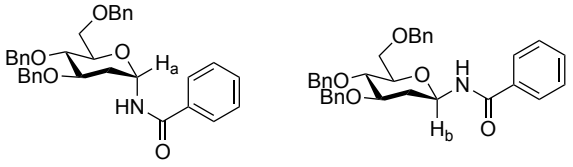

Ha:Hb = 97:3 (α:β)

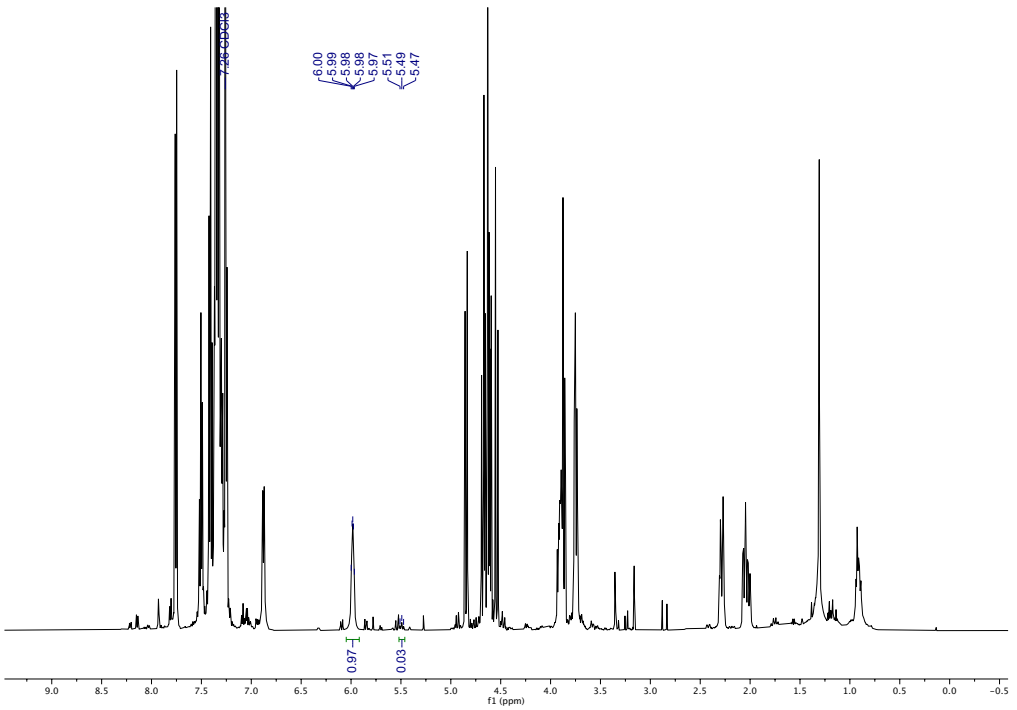

Crude ^{1}H-NMR (400 MHz, $CDCl_3$) en route to **3a**.

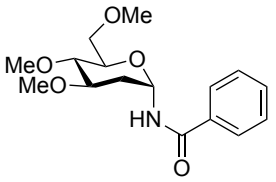

1-*N*-Benzoyl-(2-deoxyl-3,4,6-tri-*O*-methyl-α-D-glucopyranosyl)-amine (3b). Following General Procedure A, 3,4,6-tri-*O*-methyl-D-glucal (0.2 mmol, 38 mg) and **2a** (0.40 mmol, 65 mg) were used. The reactions were performed for 72 h, with additional DMMS (0.20 mmol, 25.0 μL) and TFE (0.1 mmol, 7.2 μL) added after 48 h, affording the title compound as a colorless oil (first run, 36 mg, 58%; second run, 39 mg, 63%). **^{1}H NMR** (500 MHz, CD_2Cl_2) δ 7.78 – 7.75 (m, 2H), 7.54 (t, J = 7.4 Hz, 1H), 7.46 (t, J = 7.6 Hz, 2H), 6.75 (d, J = 7.1 Hz, 1H), 5.81 (dt, J = 8.0, 4.4 Hz, 1H), 3.71 – 3.62 (m, 2H), 3.54 (m, 2H), 3.50 (s, 3H), 3.44 (s, 3H), 3.36 (s, 3H), 3.19 (t, J = 7.5 Hz, 1H), 2.15 (dt, J = 13.7, 4.2 Hz, 1H), 1.89 (m, 1H) ppm. **^{13}C NMR** (126 MHz, CD_2Cl_2) δ 167.28, 134.76,

132.40, 129.15, 127.61, 79.04, 78.51, 74.23, 73.40, 71.82, 60.14, 59.42, 57.56, 33.36 ppm. **IR (neat):** 3308, 2927, 2854, 2828, 1649, 1526, 1489, 1448, 1383, 1324, 1213, 1193, 1089, 1037, 998, 982, 714, 694, 575 cm^{-1}. **HRMS (ESI)** *calcd.* for ($C_{16}H_{23}NNaO_5$) $[M+Na]^+$: 332.1468, *found* 332.1474.

NMR spectroscopy of the crude reaction mixture prior to purification revealed the formation of **3b**-**4b** with a 97:3 α:β selectivity.

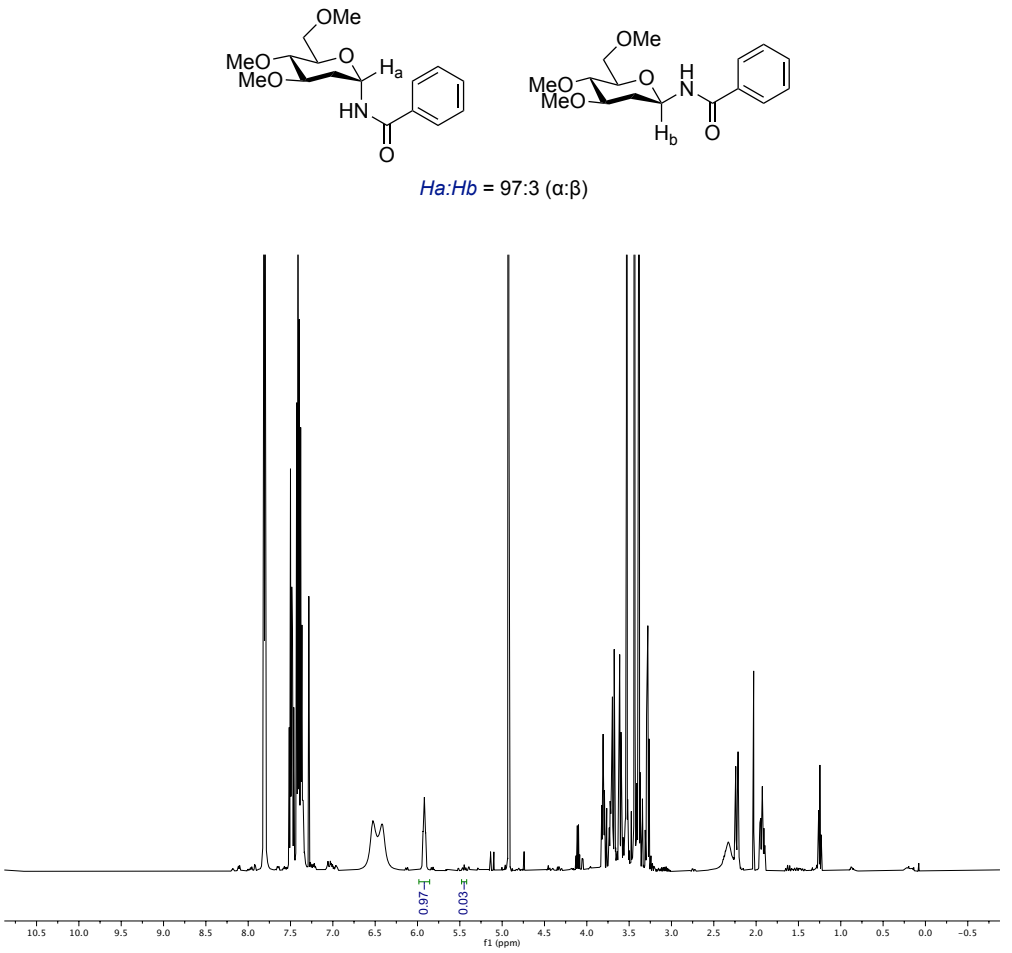

Crude ^{1}H-NMR (400 MHz, $CDCl_3$) en route to **3b**.

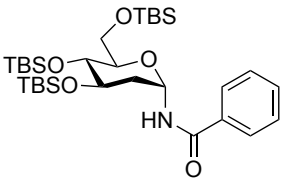

1-*N*-Benzoyl-(2-deoxyl-3,4,6-tri-*O*-tert-butyldimethylsilyl-α-D-glucopyranosyl)-amine (3c). Following General Procedure A, 3,4,6-tri-*O*-tert-butyldimethylsilyl-D-glucal (0.2 mmol, 98 mg), **2a** (0.40 mmol, 65 mg) and HFIP (0.5 mmol, 52.6 μL) were used, affording the title compound as a colorless oil (first run, 62 mg, 51%, second run, 54 mg, 44%). **^{1}H NMR** (400 MHz, CD_2Cl_2) δ 7.82 – 7.74 (m, 2H), 7.57 – 7.49 (m, 1H), 7.45 (t, *J* = 7.4 Hz, 2H), 6.62 (d, *J* = 8.9 Hz, 1H), 5.77 (td, *J* = 10.0, 2.4 Hz, 1H), 4.11 (m, 1H), 3.98 (m, 1H), 3.92 (m, 1H), 3.80 (t, *J* = 6.9 Hz, 1H), 3.72 (brs, 1H), 2.08 (m, 1H), 1.74 (dt, *J* = 13.2, 3.2 Hz, 1H), 1.02 – 0.82 (m, 27H), 0.10 (m, 18H) ppm. **^{13}C NMR** (101 MHz, CD_2Cl_2) δ 166.72, 134.95, 132.19, 129.08, 127.60, 81.56, 71.26, 70.85, 68.17, 62.35, 34.99, 26.30, 26.23, 18.72, 18.55, 18.52, -4.33, -4.36, -4.40, -4.63, -4.97 ppm. **IR (neat):** 3326, 2954, 2929, 2885, 2857, 1653, 1531, 1471, 1316, 1252, 1083, 1048, 1004, 891, 832, 773, 710, 692, 669 cm^{-1}. **HRMS (ESI)** *calcd*. for ($C_{31}H_{59}NNaO_5Si_3$) $[M+Na]^+$: 632.3593, *found* 632.3583.

NMR spectroscopy of the crude reaction mixture prior to purification revealed the formation of **3c** with an exquisite α selectivity.

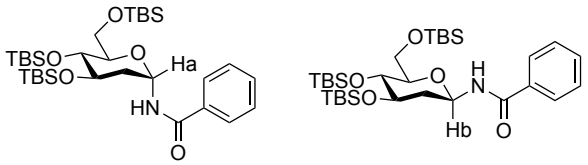

Ha:Hb > 99:1 (α:β)

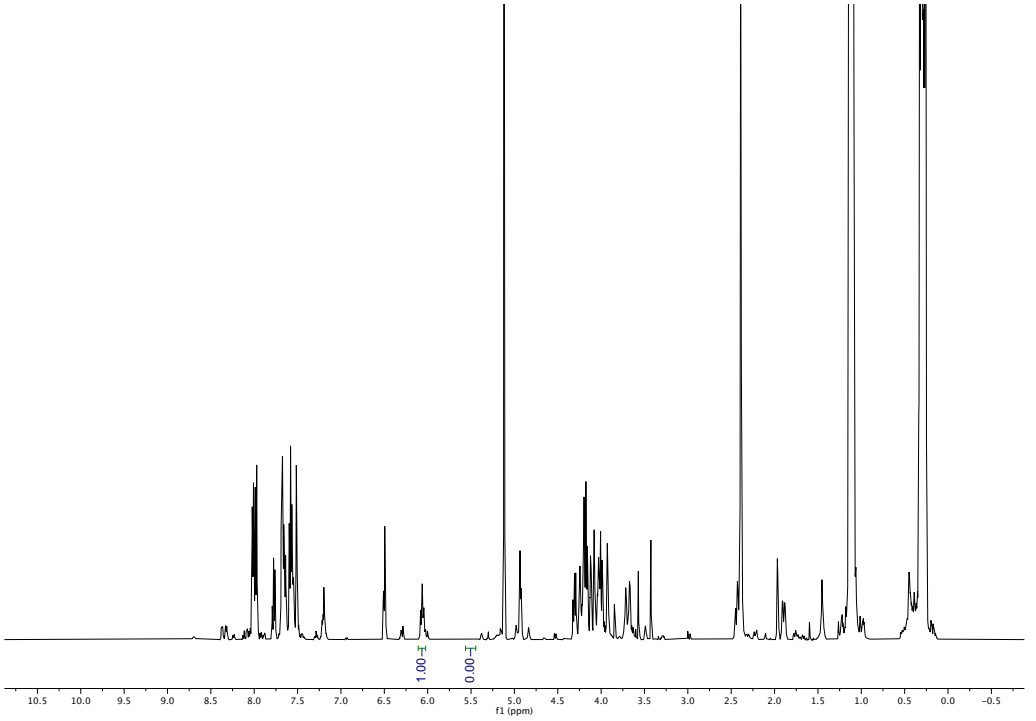

Crude ^{1}H-NMR (400 MHz, CD_3CN) en route to **3c**

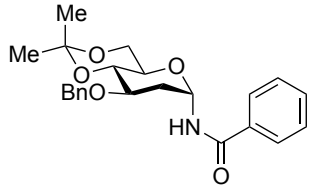

1-*N*-Benzoyl-(2-deoxyl-3-*O*-benzyl-4,6-di-*O*-isopropylidene-α-D-glucopyranosyl)-amine (3d). Following General Procedure A, 3-*O*-benzyl-4,6-di-*O*-isopropylidene-D-glucal (0.2 mmol, 55.2 mg) and **2a** (0.40 mmol, 65 mg) were used, affording the title compound as a colorless oil (first run, 57 mg, 72%; second run, 62 mg, 78%). **^{1}H NMR** (500 MHz, CD_2Cl_2) δ 7.82 – 7.72 (m, 2H), 7.60 – 7.52 (m, 1H), 7.51 – 7.42 (m, 2H), 7.38 – 7.33 (m, 4H), 7.33 – 7.23 (m, 1H), 6.88 (d, *J* = 7.6 Hz, 1H), 5.97 – 5.78 (m, 1H), 4.79 (d, *J* = 11.9 Hz, 1H), 4.67 (d, *J* = 11.9 Hz, 1H), 3.85 – 3.71 (m, 4H), 3.56 (td, *J* = 9.5, 5.8 Hz, 1H), 2.31-2.18 (m, 1H), 2.16 – 2.03 (m, 1H), 1.53 (s, 3H), 1.41 (s, 3H) ppm **^{13}C NMR**

(126 MHz, CD_2Cl_2) δ 167.43, 139.44, 134.60, 132.53, 129.19, 128.83, 128.14, 128.08, 127.65, 100.12, 76.94, 75.94, 73.66, 72.91, 65.81, 62.98, 35.53, 29.63, 19.58 ppm. **IR (neat):** 3306, 2992, 2926, 2892, 1644, 1580, 1525, 1488, 1454, 1372, 1336, 1263, 1206, 1172, 1156, 1115, 1089, 1029, 985, 949, 916, 854, 734, 713, 694, 616, 576, 520 cm^{-1}. **HRMS (ESI)** *calcd*. for ($C_{23}H_{27}NNaO_5$) $[M+Na]^+$: 420.1781, *found* 420.1786.

NMR spectroscopy of the crude reaction mixture prior to purification revealed the formation of **3d**-**4d** with a 99:1 α:β selectivity.

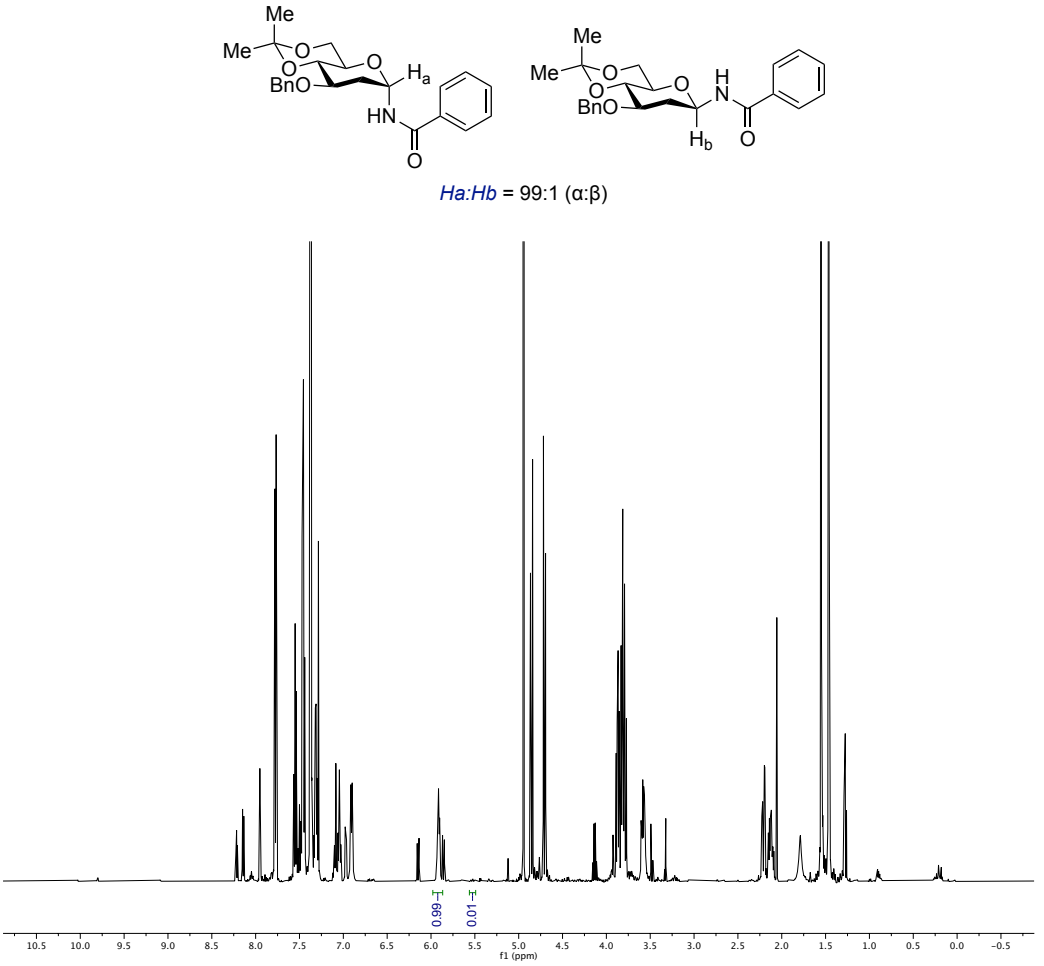

Crude ^{1}H-NMR (400 MHz, $CDCl_3$) en route to **3d**

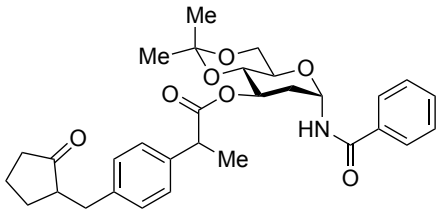

1-*N*-Benzoyl-(2-deoxyl-3-*O*-[α-methyl-4-[(2-oxocyclopentyl)methyl]-benzeneacetate]-4,6-di-*O*-isopropylidene-α-D-glucopyranosyl)-amine (3e). Following General Procedure A, 3-*O*-[α-methyl-4-[(2-oxocyclopentyl)methyl]-benzeneacetate]-4,6-di-*O*-isopropylidene-D-glucal (0.2 mmol, 83 mg) and **2a** (0.40 mmol, 65 mg) were used, affording the title compound as a white solid (first run, 44 mg, 41%; second run, 49 mg, 46%). **^{1}H NMR** (500 MHz, CD_2Cl_2) δ 7.85 – 7.74 (m, 2H), 7.63 – 7.50 (m, 1H), 7.49 – 7.40 (m, 2H), 7.38 – 7.22 (m, 1H), 7.22 – 7.15 (m, 2H), 7.15 – 7.08 (m, 2H), 5.95 – 5.76 (m, 1H), 5.30 – 5.18 (m, 1H), 3.87 – 3.59 (m, 5H), 3.12 – 3.03 (m, 1H), 2.53 – 2.42 (m, 1H), 2.38 – 2.24 (m, 2H), 2.22 – 2.01 (m, 3H), 2.00 – 1.88 (m, 2H), 1.78 – 1.66 (m, 1H), 1.59 – 1.51 (m, 1H), 1.51 – 1.34 (m, 6H), 1.32 – 1.23 (m, 3H) ppm. **^{13}C NMR** (126 MHz, CD_2Cl_2) δ 174.69, 174.53, 167.74, 139.76, 139.62, 138.85, 138.71, 134.46, 132.50, 129.59, 129.46, 129.11, 128.07, 127.96, 127.82, 100.32, 100.15, 75.67, 75.61, 74.02, 73.72, 68.80, 68.27, 65.77, 65.73, 62.86, 51.40, 51.35, 45.78, 45.54, 38.58, 38.56, 35.68, 34.55, 34.32, 29.84, 29.82, 29.81, 29.46, 29.35, 21.04, 19.47, 19.18, 19.15, 18.85, 18.63 ppm. **IR (neat):** 3366, 3335, 2969, 2938, 2875, 1734, 1655, 1603, 1580, 1516, 1487, 1450, 1373, 1336, 1264, 1205, 1176, 1158, 1091, 1051, 1032, 989, 950, 887, 854, 713, 693, 579 cm^{-1}. **HRMS (ESI)** *calcd*. for ($C_{31}H_{37}NNaO_7$) $[M+Na]^+$: 558.2462, *found* 558.2449. **M.P.**: 72 °C.

NMR spectroscopy of the crude reaction mixture prior to purification revealed the formation of **3e**-**4e** with a 99:1 α:β selectivity.

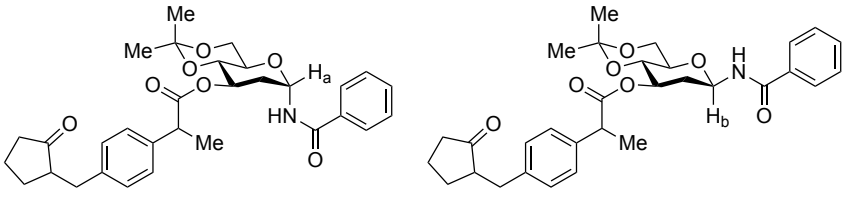

Ha:*Hb* = 99:1 (α:β)

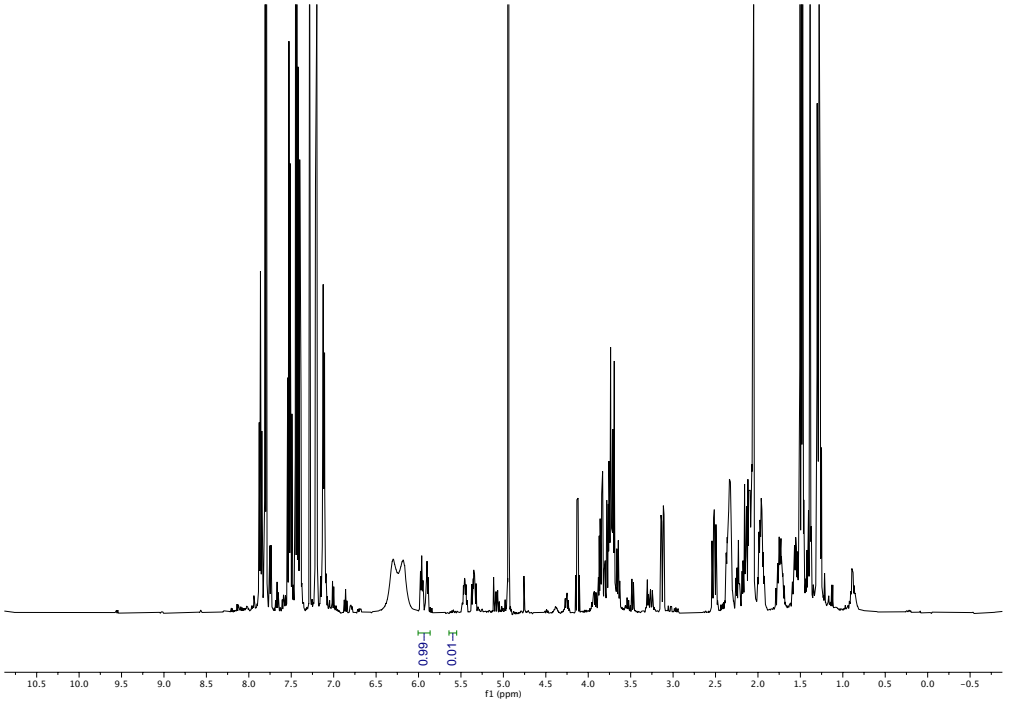

Crude ^{1}H-NMR (400 MHz, $CDCl_3$) en route to **3e**

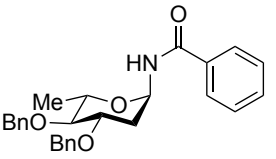

1-*N*-Benzoyl-(2,6-deoxyl-3,4-*O*-benzyl-α-L-glucopyranosyl)-amine (3f). Following General Procedure A, 3,4-di-*O*-benzyl-L-rhamnal (0.2 mmol, 62 mg) and **2a** (0.40 mmol, 65 mg) were used, affording the title compound as a white solid (first run, 52 mg, 60%;

second run, 48 mg, 56%). **^{1}H NMR** (400 MHz, CD_2Cl_2) δ 7.81 – 7.71 (m, 2H), 7.59 – 7.50 (m, 1H), 7.49 – 7.42 (m, 2H), 7.40 – 7.24 (m, 10H), 6.73 (d, *J* = 7.7 Hz, 1H), 5.91 – 5.77 (m, 1H), 4.88 (d, *J* = 11.0 Hz, 1H), 4.74 – 4.59 (m, 3H), 3.89 - 3.80 (m, 1H), 3.79 – 3.70 (m, 1H), 3.22 (t, *J* = 8.0 Hz, 1H), 2.27 (m, 1H), 2.01 (m, 1H), 1.33 (d, *J* = 6.3 Hz, 3H) ppm. **^{13}C NMR** (101 MHz, CD_2Cl_2) δ 167.27, 139.15, 139.02, 134.83, 132.39, 129.16, 128.94, 128.87, 128.55, 128.31, 128.24, 127.59, 83.27, 77.16, 75.24, 74.42, 72.00, 69.75, 34.40, 18.51 ppm. **IR (neat):** 4, 3063, 3031, 2930, 2873, 1638, 1603, 1580, 1528, 1489, 1453, 1363, 1341, 1273, 1212, 1093, 1069, 1028, 992, 733, 715, 694, 629, 572 cm^{-1}. **HRMS (ESI)** *calcd.* for ($C_{27}H_{29}BrNNaO_4$) $[M+Na]^+$: 454.1989, *found* 454.1991. **M.P.**: 101 °C.

NMR spectroscopy of the crude reaction mixture prior to purification revealed the formation of **3f-4f** with a 95:5 α:β selectivity.

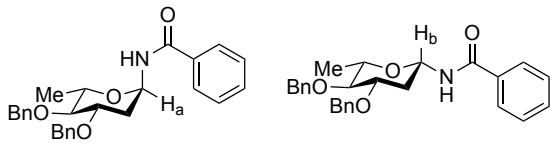

Ha:Hb = 95:5 (α:β)

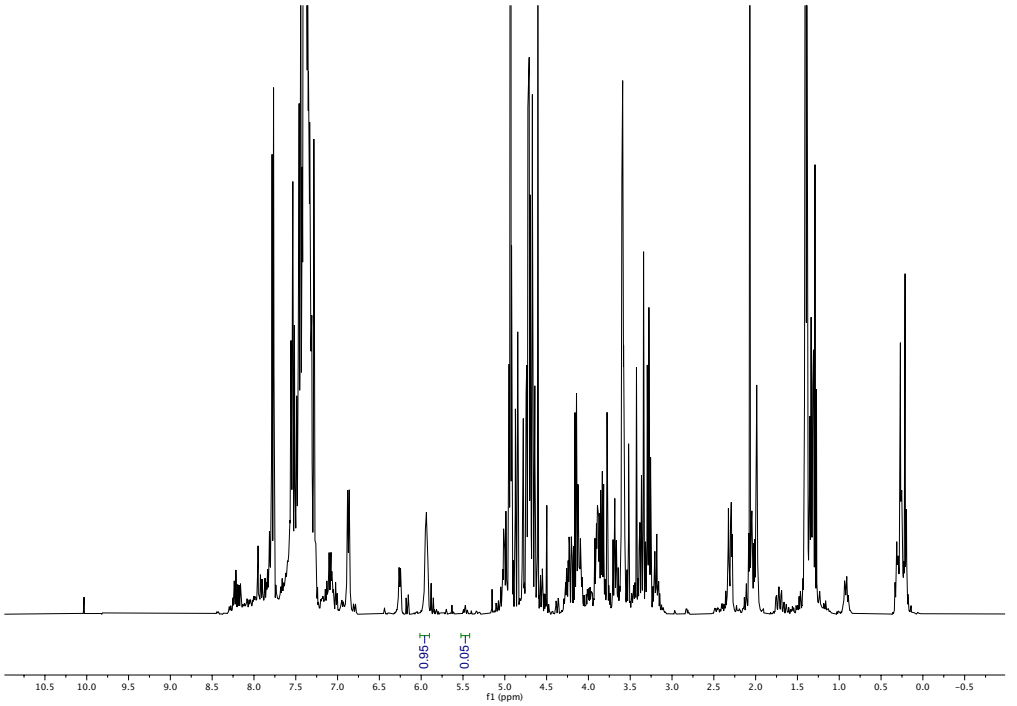

Crude ^{1}H-NMR (400 MHz, $CDCl_3$) en route to **3f**

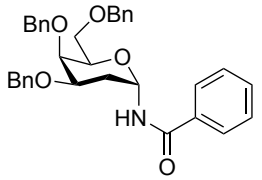

1-*N*-Benzoyl-(2-deoxyl-3,4,6-*O*-benzyl-α-D-galactopyranosyl)-amine (3g). Following General Procedure A, 3,4,6-tri-*O*-benzyl-D-galactal (0.2 mmol, 83 mg) and **2a** (0.40 mmol, 65 mg) were used, affording the title compound as a colorless oil (first run, 68 mg, 63%; second run, 74 mg, 69%). **^{1}H NMR** (500 MHz, CD_2Cl_2) δ 7.81 – 7.73 (m, 2H), 7.64 – 7.55 (m, 1H), 7.49 (t, *J* = 7.6 Hz, 2H), 7.45 – 7.27 (m, 15H), 6.72 (d, *J* = 7.4 Hz, 1H), 5.91 (brs, 1H), 4.91 (d, *J* = 11.2 Hz, 1H), 4.78 – 4.59 (m, 3H), 4.59 – 4.48 (m, 2H), 4.08 – 3.97 (m, 2H), 3.95 – 3.86 (m, 1H), 3.82 – 3.66 (m, 2H), 2.55 – 2.42 (m, 1H), 1.99 (dt, *J* = 13.3, 3.1 Hz, 1H) ppm. **^{13}C NMR** (126 MHz, CD_2Cl_2) δ 167.39, 139.44, 139.04, 138.98, 134.96, 132.39, 129.18, 129.02, 128.90, 128.86, 128.57, 128.51, 128.24, 128.19, 128.18,

128.10, 127.64, 75.33, 74.62, 74.59, 74.17, 74.03, 72.76, 71.32, 69.30, 31.54 ppm. **IR (neat):** 3307, 3062, 3029, 2921, 2862, 1643, 1603, 1580, 1523, 1488, 1453, 1368, 1331, 1301, 1268, 1208, 1164, 1088, 1058, 1027, 733, 694, 614, 561 cm^{-1}. **HRMS (ESI)** *calcd.* for ($C_{34}H_{36}NO_5$) $[M+H]^+$: 538.2588, *found* 538.2589.

NMR spectroscopy of the crude reaction mixture prior to purification revealed the formation of **3g**-**4g** with a 95:5 α:β selectivity.

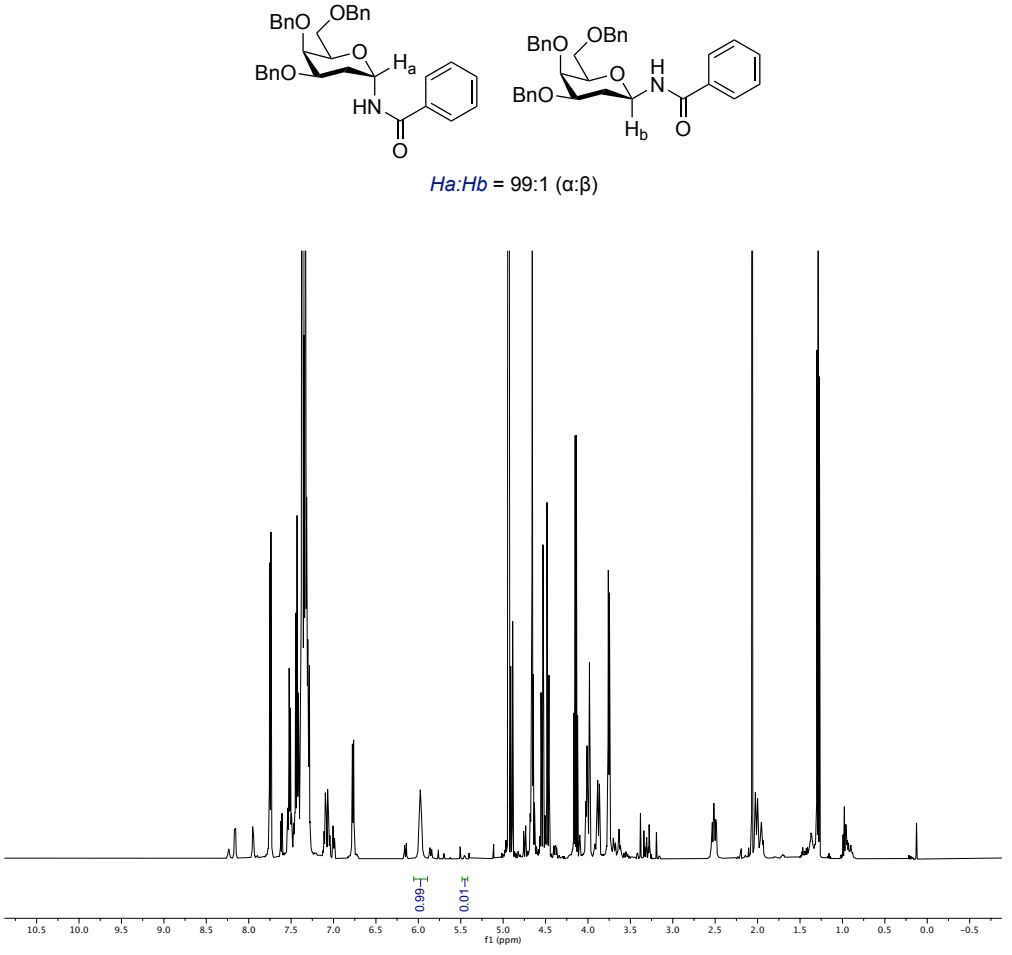

Crude ^{1}H-NMR (400 MHz, $CDCl_3$) en route to **3g**

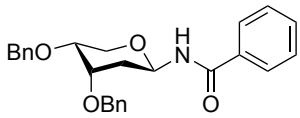

1-*N*-Benzoyl-(2-deoxyl-5-demethyl-3,4-*O*-benzyl-α-L-galactopyranosyl)-amine (3h). Following General Procedure A, 3,4-di-*O*-benzyl-D-arabinal (0.2 mmol, 60 mg) and **2a** (0.40 mmol, 65 mg) were used, affording the title compound as a white solid (first run, 77 mg, 92%; second run, 70 mg, 84%). **^{1}H NMR** (500 MHz, CD_2Cl_2) δ 7.82 – 7.71 (m, 2H), 7.58 – 7.49 (m, 1H), 7.49 – 7.38 (m, 4H), 7.39 – 7.28 (m, 8H), 6.58 (d, *J* = 8.9 Hz, 1H), 5.76 – 5.62 (m, 1H), 4.74 (s, 2H), 4.64 – 4.50 (m, 2H), 4.08 (s, 1H), 4.01 (t, *J* = 10.6 Hz, 1H), 3.85 (dd, *J* = 11.0, 3.9 Hz, 1H), 3.69 – 3.57 (m, 1H), 2.36 – 2.19 (m, 1H), 1.83 – 1.65 (m, 1H) ppm. **^{13}C NMR** (126 MHz, CD_2Cl_2) δ 167.19, 139.39, 139.03, 134.71, 132.33, 129.11, 128.91, 128.86, 128.21, 128.19, 128.08, 128.06, 127.59, 75.60, 74.96, 72.68, 72.43, 71.57, 64.30, 35.64 ppm. **IR (neat):** 3315, 3061, 3022, 2959, 2918, 2850, 1651, 1603, 1580, 1527, 1489, 1452, 1435, 1370, 1351, 1319, 1294, 1236, 1167, 1119, 1097, 1071, 1026, 983, 924, 896, 732, 711, 692, 666, 567 cm^{-1}. **HRMS (ESI)** *calcd*. for ($C_{26}H_{27}NNaO_4$) $[M+Na]^+$: 440.1832, *found* 440.1837. **M.P.**: 149 °C.

NMR spectroscopy of the crude reaction mixture prior to purification revealed the formation of **3h** with an exquisite β selectivity.

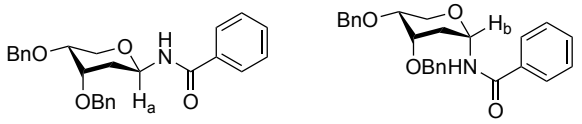

Ha:*Hb* > 99:1 (β:α)

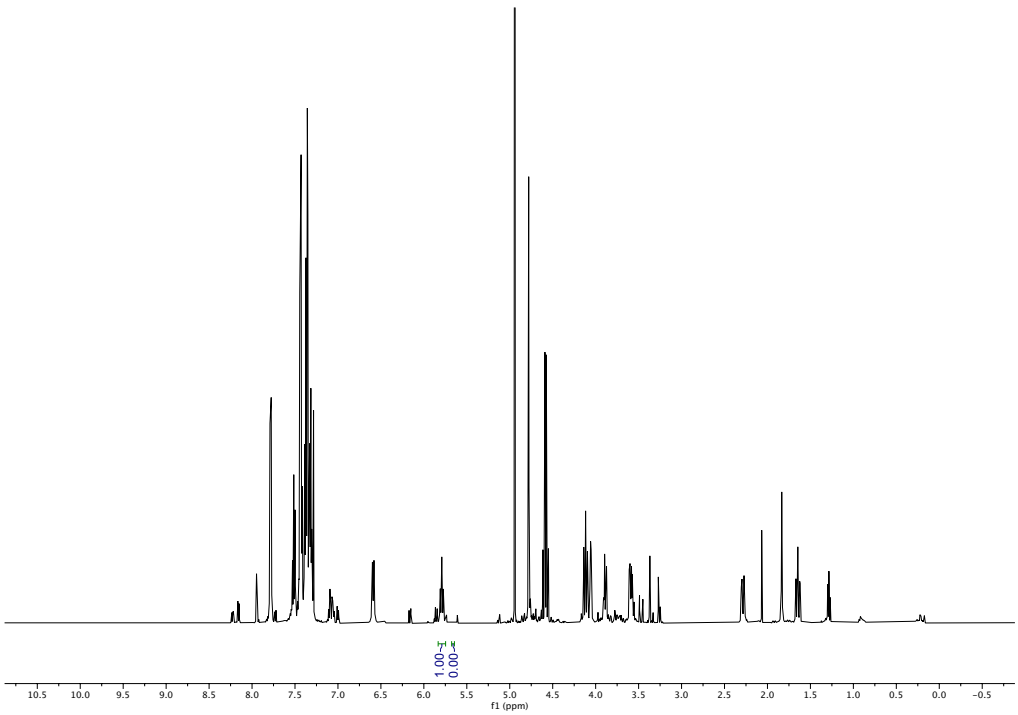

Crude ^{1}H-NMR (400 MHz, $CDCl_3$) en route to **3h**

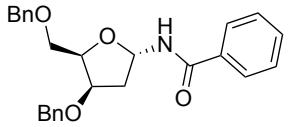

1-*N*-Benzoyl-(2-deoxyl-3,5-*O*-benzyl-α-D-xylofuranosyl)-amine (3i). Following General Procedure A, 2-deoxy-3,5-di-*O*-benzyl-D-arabinal (0.2 mmol, 60 mg) and **2a** (0.40 mmol, 65 mg) were used, affording the title compound as a white solid (first run, 79 mg, 95%; second run, 73 mg, 87%). **^{1}H NMR** (400 MHz, CD_2Cl_2) δ 7.82 – 7.74 (m, 2H), 7.55 – 7.48 (m, 1H), 7.48 – 7.40 (m, 2H), 7.40 – 7.24 (m, 10H), 6.74 (d, *J* = 8.2 Hz, 1H), 6.07 (q, *J* = 7.5 Hz, 1H), 4.62 (d, *J* = 11.9 Hz, 1H), 4.57 (d, *J* = 11.7 Hz, 1H), 4.51 (d, *J* = 11.7 Hz, 1H), 4.44 (d, *J* = 11.9 Hz, 1H), 4.36 – 4.28 (m, 1H), 4.27 – 4.18 (m, 1H), 3.79 (dd, *J* = 10.0, 4.9 Hz, 1H), 3.72 (dd, *J* = 10.0, 6.6 Hz, 1H), 2.65 – 2.51 (m, 1H), 2.04 – 1.91 (m, 1H) ppm. **^{13}C NMR** (101 MHz, CD_2Cl_2) δ 167.61, 139.03, 138.81, 134.81, 132.24, 129.07, 128.89, 128.83, 128.34, 128.16, 128.08, 127.60, 81.52, 81.25, 79.36,

74.00, 71.89, 69.75, 38.83 ppm. **IR (neat):** 3300, 3062, 3028, 2922, 2856, 1643, 1602, 1578, 1523, 1487, 1466, 1453, 1356, 1301, 1282, 1203, 1147, 1116, 1095, 1044, 973, 934, 921, 905, 846, 730, 693, 611, 445 cm^{-1}. **HRMS (ESI)** *calcd*. for ($C_{26}H_{27}NNaO_4$) $[M+Na]^+$: 440.1832, *found* 440.1827. **M.P.**: 125 °C.

NMR spectroscopy of the crude reaction mixture prior to purification revealed the formation of **3i** with an exquisite α selectivity.

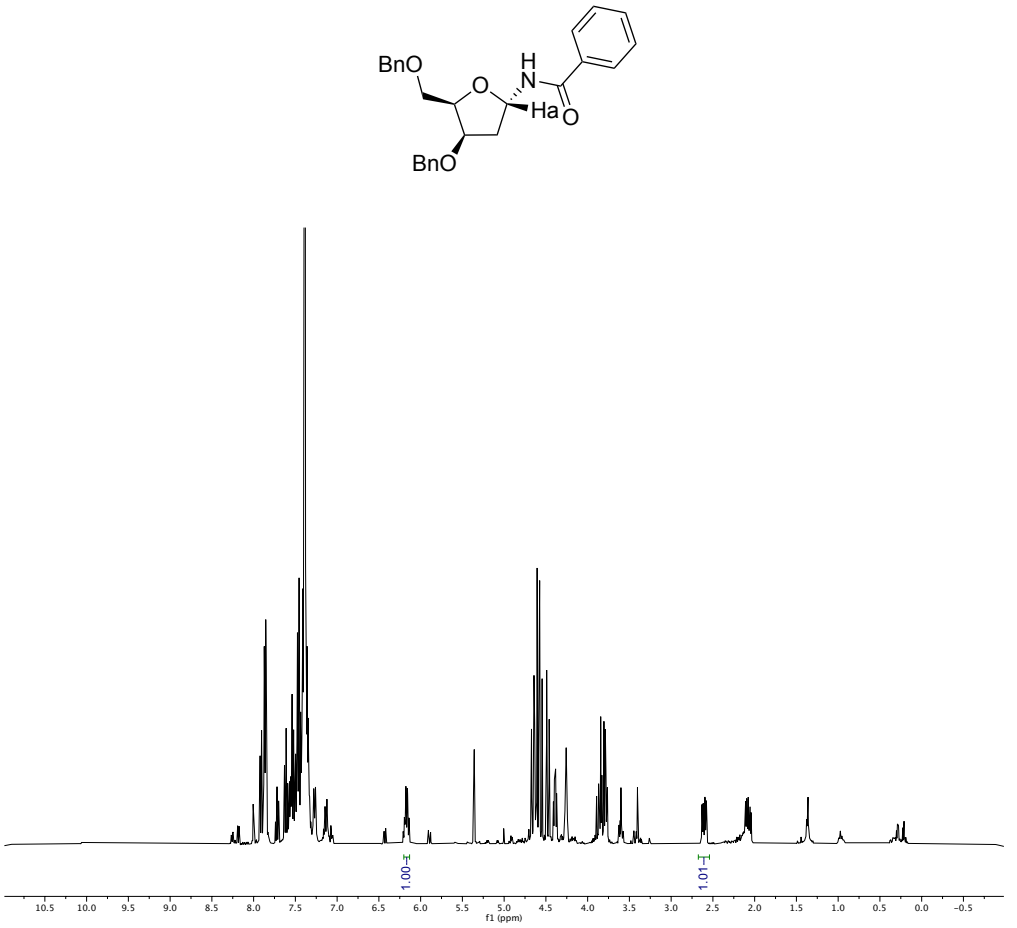

Crude ^{1}H-NMR (400 MHz, CD_2Cl_2) en route to **3i**

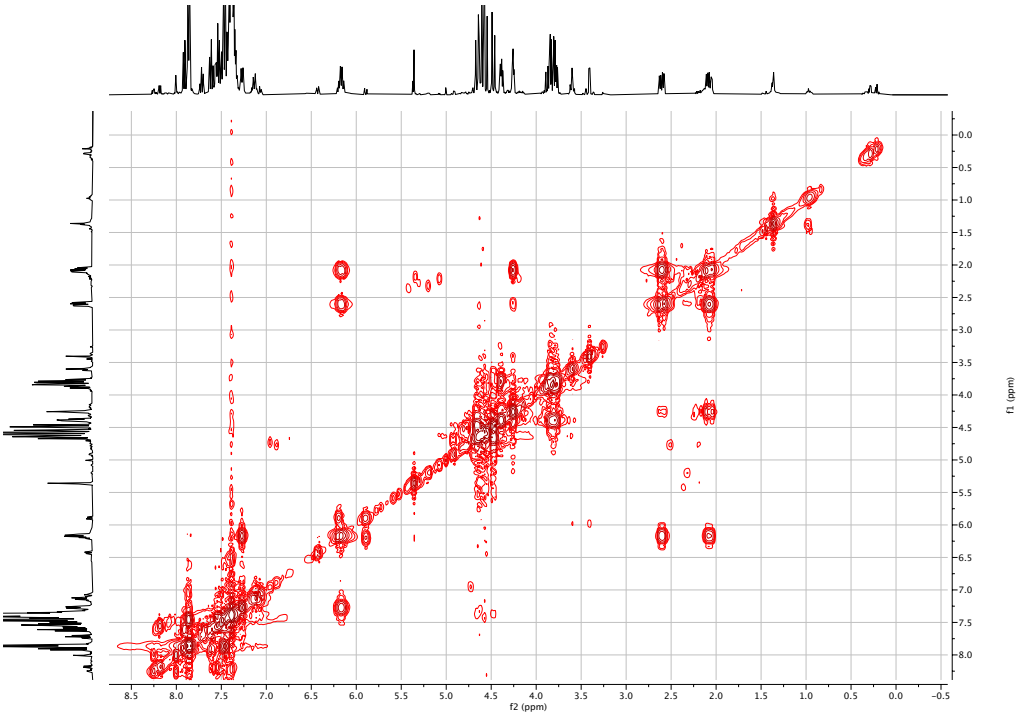

Crude ^{1}H-HCOSY (400 MHz, CD_2Cl_2) en route to **3i**

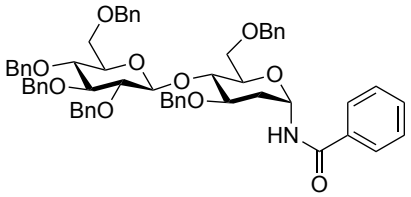

1-*N*-Benzoyl-(2-deoxyl-2',3,3',4',6,6'-*O*-benzyl-α-D-maltosyl)-amine (3j). Following General Procedure A, 2',3,3',4',6,6'-*O*-benzyl-D-cellobial (0.1 mmol, 1 equiv., 85 mg) and **2a** (0.20 mmol, 32 mg) were used. After 48 h, additional DMMS (0.1 mmol, 12.5 μL) and TFE (0.1 mmol, 7.2 μL) were added, affording the title compound as a white solid (first run, 51 mg, 53%; second run, 63 mg, 65%). **^{1}H NMR** (500 MHz, CD_2Cl_2) δ 7.83 – 7.71 (m, 2H), 7.55 (t, *J* = 7.4 Hz, 1H), 7.46 (t, *J* = 7.6 Hz, 2H), 7.40 – 7.15 (m, 30H), 6.61 (d, *J* = 8.5 Hz, 1H), 5.95 – 5.81 (m, 1H), 4.97 (d, *J* = 11.0 Hz, 1H), 4.91 (d, *J* = 11.0 Hz, 1H), 4.88 – 4.79 (m, 2H), 4.77 – 4.45 (m, 9H), 4.08 – 3.93 (m, 4H), 3.85 – 3.76 (m, 1H), 3.73 – 3.67 (m, 2H), 3.66 – 3.56 (m, 2H), 3.48 – 3.37 (m, 2H), 2.21 – 2.02 (m, 2H) ppm. **^{13}C**

NMR (126 MHz, CD_2Cl_2) δ 167.17, 139.43, 139.22, 139.06, 138.96, 134.80, 132.34, 129.12, 128.88, 128.87, 128.85, 128.82, 128.79, 128.65, 128.42, 128.38, 128.33, 128.26, 128.16, 128.11, 128.09, 128.07, 128.05, 128.03, 127.61, 103.65, 85.17, 82.95, 78.31, 76.01, 75.43, 75.39, 75.34, 74.97, 73.89, 73.82, 72.42, 72.21, 69.51, 68.89, 33.08 ppm. **IR (neat):** 3284, 3087, 3063, 3030, 2901, 2869, 1640, 1603, 1579, 1521, 1469, 1452, 1352, 1320, 1274, 1204, 1137, 1091, 1071, 741, 722, 693, 643, 540, 461 cm^{-1}. **HRMS (ESI)** *calcd*. for ($C_{61}H_{63}NNaO_{10}$) $[M+Na]^+$: 992.4344, *found* 992.4369. **M.P.**: 167 °C.

NMR spectroscopy of the crude reaction mixture prior to purification revealed the formation of **3j** with an exquisite α selectivity.

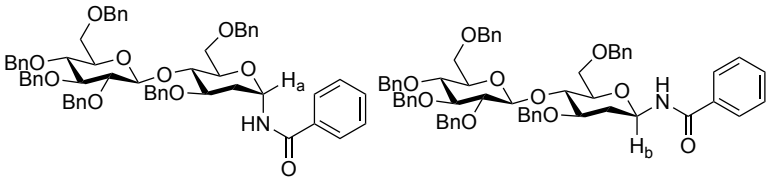

Ha:Hb > 99:1 (α:β)

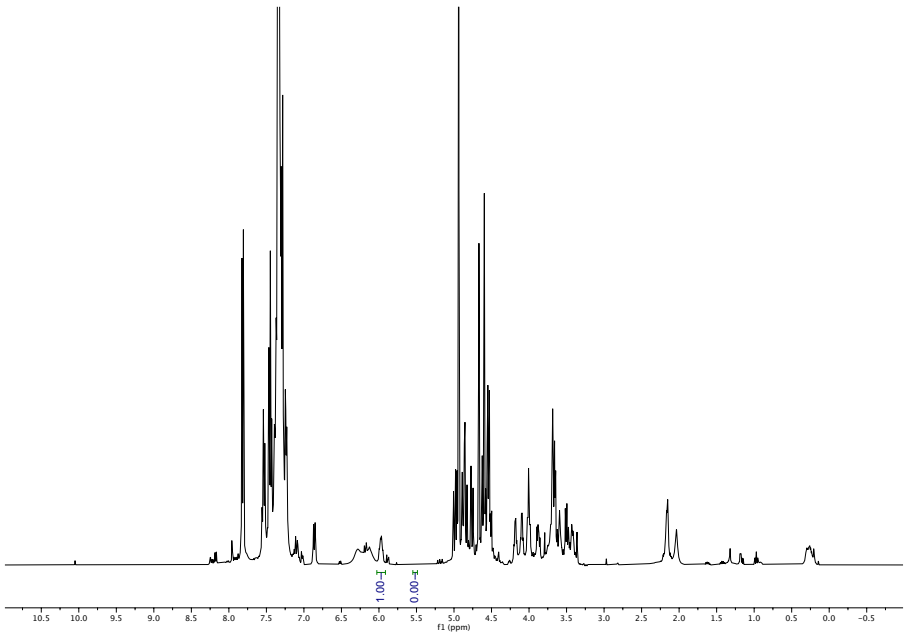

Crude ^{1}H-NMR (400 MHz, $CDCl_3$) en route to **3j**

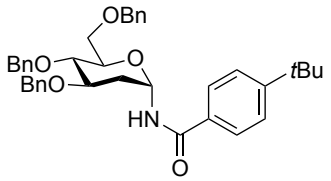

1-*N*-(4-*tert*-butylbenzoyl)-(2-deoxyl-3,4,6-tri-*O*-benzyl-α-D-glucopyranosyl)-amine (3k). Following General Procedure A, 3,4,6-tri-*O*-benzyl-D-glucal (0.2 mmol, 83 mg) and 3-(4-(*tert*-butyl)phenyl)-1,4,2-dioxazol-5-one (0.4 mmol, 88 mg) were used, affording the title compound as a white solid (first run, 108 mg, 91%; second run, 98 mg, 83%). **^{1}H NMR** (500 MHz, CD_2Cl_2) δ 7.75 – 7.66 (m, 2H), 7.55 – 7.43 (m, 2H), 7.43 – 7.23 (m, 15H), 6.72 (d, *J* = 7.9 Hz, 1H), 5.94 – 5.82 (m, 1H), 4.83 (d, *J* = 11.0 Hz, 1H), 4.68 (d, *J* = 11.6 Hz, 1H), 4.65 – 4.50 (m, 4H), 3.98 – 3.77 (m, 3H), 3.76 – 3.62 (m, 2H), 2.24 (dt, *J* = 13.6, 4.3 Hz, 1H), 2.14 – 1.97 (m, 1H), 1.34 (s, 9H) ppm. **^{13}C NMR** (101 MHz, CD_2Cl_2) δ 167.17, 156.12, 139.09, 139.03, 139.00, 131.80, 128.94, 128.86, 128.53, 128.43, 128.27, 128.22, 128.09, 127.43, 126.12, 77.43, 77.07, 74.88, 74.50, 73.95, 73.60, 72.03, 69.61, 35.42, 34.08, 31.43 ppm. **IR (neat):** 3305, 3031, 2960, 2925, 2866, 1640, 1610, 1529, 1497, 1454, 1363, 1339, 1270, 1204, 1143, 1090, 1046, 1027, 996, 854, 734, 696, 622 cm^{-1}. **HRMS (ESI)** *calcd*. for ($C_{38}H_{44}NO_5$) $[M+H]^+$: 594.3214, *found* 594.3206. **M.P.**: 95 °C.

NMR spectroscopy of the crude reaction mixture prior to purification revealed the formation of **3k**-**4k** with a 98:2 α:β selectivity.

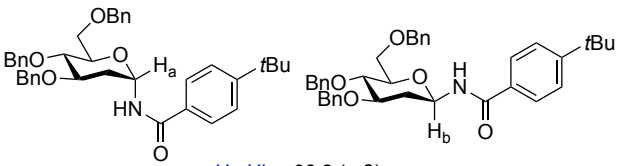

Ha:*Hb* = 98:2 (α:β)

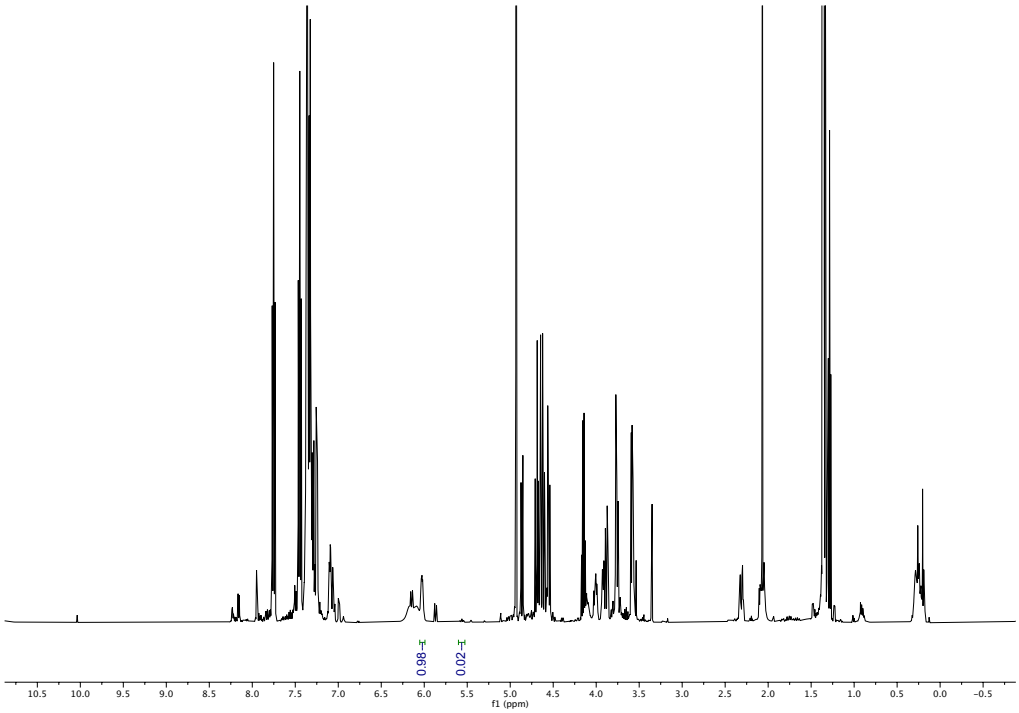

Crude ^{1}H-NMR (400 MHz, $CDCl_3$) en route to **3k**

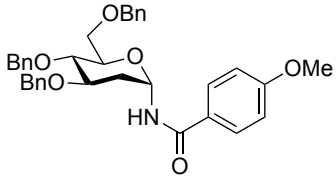

1-*N*-(4-methoxybenzoyl)-(2-deoxyl-3,4,6-tri-*O*-benzyl-α-D-glucopyranosyl)-amine (3l). Following General Procedure A, 3,4,6-tri-*O*-benzyl-D-glucal (0.2 mmol, 83 mg) and 3-(4-methoxyphenyl)-1,4,2-dioxazol-5-one (0.4 mmol, 77 mg) were used, affording the title compound as a white solid (first run, 97 mg, 86%; second run, 106 mg, 93%). **^{1}H NMR** (500 MHz, CD_2Cl_2) δ 7.77 – 7.70 (m, 2H), 7.42 – 7.23 (m, 15H), 7.02 – 6.89 (m, 2H), 6.70 (d, J = 8.0 Hz, 1H), 5.94 – 5.84 (m, 1H), 4.83 (d, J = 11.0 Hz, 1H), 4.69 (d, J = 11.7 Hz, 1H), 4.65 – 4.55 (m, 3H), 4.52 (d, J = 11.9 Hz, 1H), 3.92 – 3.86 (m, 1H), 3.86 – 3.79 (m, 5H), 3.75 – 3.63 (m, 2H), 2.25 (dt, J = 13.6, 4.3 Hz, 1H), 2.09 – 1.98 (m, 1H) ppm. **^{13}C NMR** (126 MHz, CD_2Cl_2) δ 166.73, 163.13, 139.08, 139.01, 138.99, 129.49,

128.92, 128.84, 128.52, 128.42, 128.25, 128.20, 128.08, 126.82, 114.28, 77.40, 77.03, 74.85, 74.48, 73.93, 73.53, 71.98, 69.60, 55.99, 34.06 ppm. **IR (neat):** 3509, 3418, 3230, 3064, 3030, 2927, 2871, 1626, 1607, 1578, 1541, 1508, 1453, 1371, 1345, 1328, 1283, 1252, 1207, 1178, 1078, 1029, 1008, 942, 852, 834, 732, 694, 638, 607, 577 cm^{-1}. **HRMS (ESI)** *calcd*. for ($C_{35}H_{38}NO_6$) $[M+H]^+$: 568.2694, *found* 568.2695. **M.P.**: 70 °C.

NMR spectroscopy of the crude reaction mixture prior to purification revealed the formation of **3l**-**4l** with a 97:3 α:β selectivity.

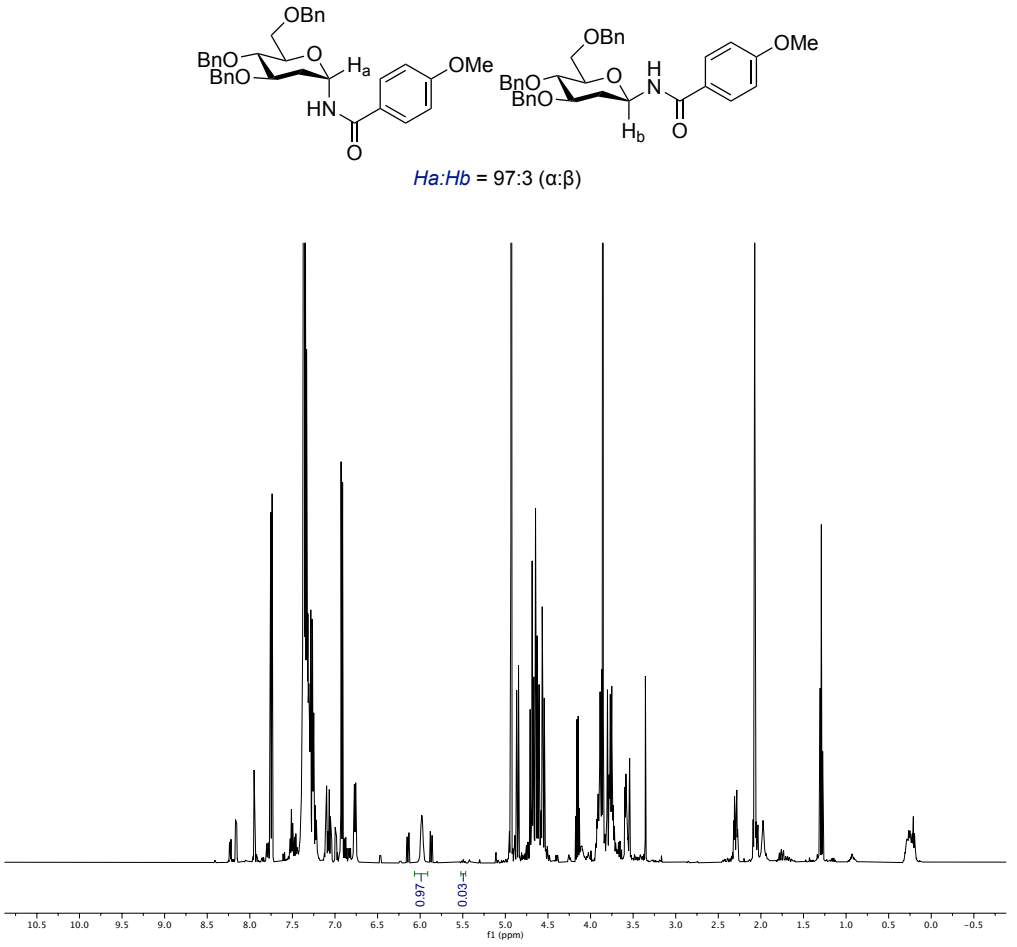

Crude ^{1}H-NMR (400 MHz, $CDCl_3$) en route to **3l**

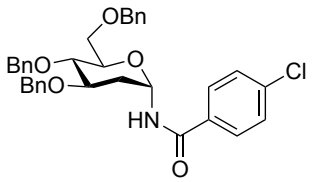

1-*N*-(4-chlorobenzoyl)-(2-deoxyl-3,4,6-tri-*O*-benzyl-α-D-glucopyranosyl)-amine (3m). Following General Procedure A, 3,4,6-tri-*O*-benzyl-D-glucal (0.2 mmol, 83 mg) and 3-(4-chlorophenyl)-1,4,2-dioxazol-5-one (0.4 mmol, 80 mg) were used, affording the title compound as a white solid (first run, 89 mg, 78%; second run, 83 mg, 73%). **^{1}H NMR** (500 MHz, CD_2Cl_2) δ 7.75 – 7.64 (m, 2H), 7.47 – 7.39 (m, 2H), 7.39 – 7.21 (m, 15H), 6.72 (d, *J* = 7.8 Hz, 1H), 5.89 – 5.83 (m, 1H), 4.81 (d, *J* = 11.0 Hz, 1H), 4.68 (d, *J* = 11.7 Hz, 1H), 4.65 – 4.57 (m, 2H), 4.60 – 4.49 (m, 2H), 3.90 – 3.79 (m, 3H), 3.73 – 3.66 (m, 1H), 3.65 (t, *J* = 7.5 Hz, 1H), 2.24 (dt, *J* = 13.6, 4.2 Hz, 1H), 2.08 – 1.97 (m, 1H) ppm. **^{13}C NMR** (126 MHz, CD_2Cl_2) δ 166.28, 138.98, 138.96, 138.92, 138.52, 133.15, 129.37, 129.17, 128.94, 128.87, 128.86, 128.53, 128.42, 128.25, 128.12, 77.11, 76.78, 74.78, 74.53, 73.94, 73.84, 72.00, 69.54, 33.86 ppm. **IR (neat):** 3387, 3064, 3035, 2923, 2856, 1667, 1592, 1514, 1480, 1453, 1366, 1328, 1238, 1204, 1086, 1062, 1026, 1010, 992, 970, 908, 843, 749, 734, 696, 622, 579, 528 cm^{-1}. **HRMS (ESI)** *calcd*. for ($C_{34}H_{34}ClNNaO_5$) $[M+Na]^+$: 594.2018, *found* 594.2024. **M.P.**: 110 °C.

NMR spectroscopy of the crude reaction mixture prior to purification revealed the formation of **3m**-**4m** with a 97:3 α:β selectivity.

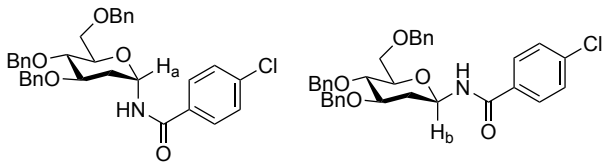

Ha:*Hb* = 97:3 (α:β)

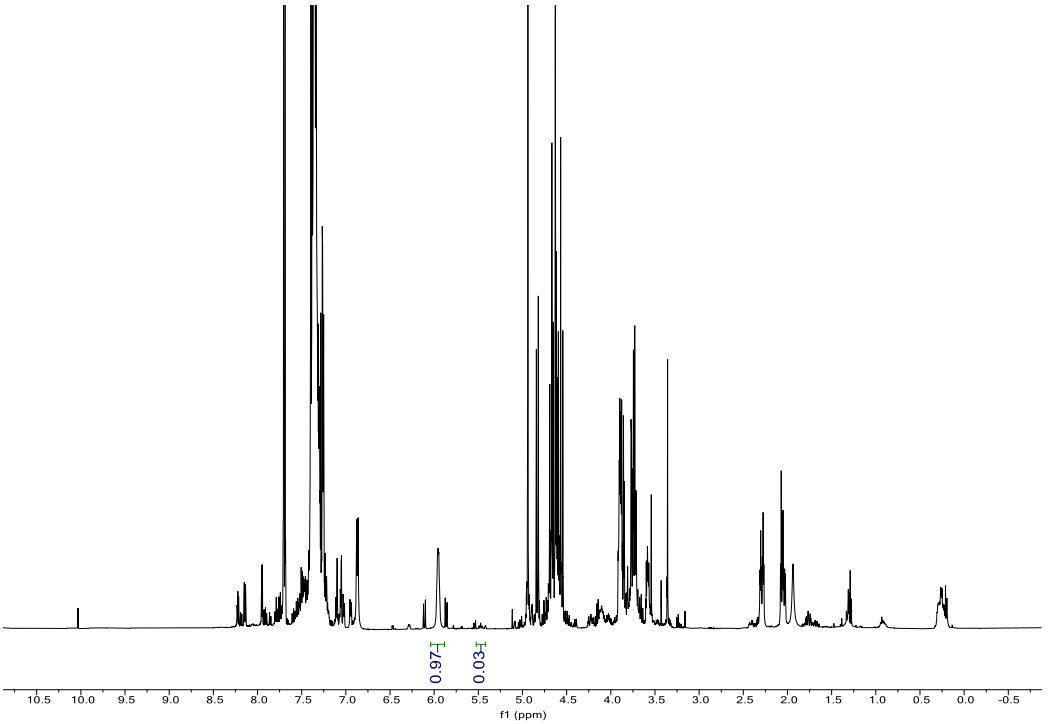

Crude ^{1}H-NMR (400 MHz, $CDCl_3$) en route to **3m**

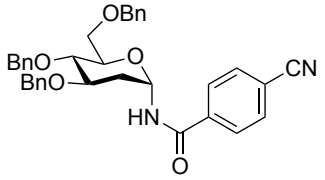

1-*N*-(4-cyanobenzoyl)-(2-deoxyl-3,4,6-tri-*O*-benzyl-α-D-glucopyranosyl)-amine (3n). Following General Procedure A, 3,4,6-tri-*O*-benzyl-D-glucal (0.2 mmol, 83 mg) and 3-(4-cyanophenyl)-1,4,2-dioxazol-5-one (0.4 mmol, 75 mg) were used, affording the title compound as a white solid (first run, 45 mg, 40%; second run, 55 mg, 49%). **^{1}H NMR** (300 MHz, CD_2Cl_2) δ 7.86 – 7.79 (m, 2H), 7.77 – 7.67 (m, 2H), 7.41 – 7.18 (m, 15H), 6.79 (d, J = 7.9 Hz, 1H), 5.99 – 5.78 (m, 1H), 4.80 (d, J = 11.0 Hz, 1H), 4.67 (d, J = 11.7 Hz, 1H), 4.64 – 4.51 (m, 4H), 3.91 – 3.78 (m, 3H), 3.76 – 3.59 (m, 2H), 2.26 (dt, J = 13.7, 4.3 Hz, 1H), 2.11 – 1.97 (m, 1H) ppm. **^{13}C NMR** (126 MHz, CD_2Cl_2) δ 165.78, 138.91, 138.90, 138.86, 138.52, 133.05, 128.95, 128.89, 128.87, 128.54, 128.41, 128.35, 128.30,

128.26, 128.22, 128.15, 118.50, 115.93, 76.83, 76.56, 74.68, 74.54, 74.12, 73.95, 72.00, 69.49, 33.66 ppm. **IR (neat):** 3445, 3064, 3025, 2924, 2886, 2855, 2229, 1685, 1675, 1522, 1488, 1454, 1363, ,1254, 1202, 1114, 1086, 1060, 1030, 1003, 967, 854, 751, 728, 693, 630, 550, 488 cm^{-1}. **HRMS (ESI)** *calcd*. for ($C_{35}H_{34}N_2NaO_5$) $[M+Na]^+$: 585.2360, *found* 585.2376. **M.P.**: 128 °C.

NMR spectroscopy of the crude reaction mixture prior to purification revealed the formation of **3n**-**4n** with a 94:6 α:β selectivity.

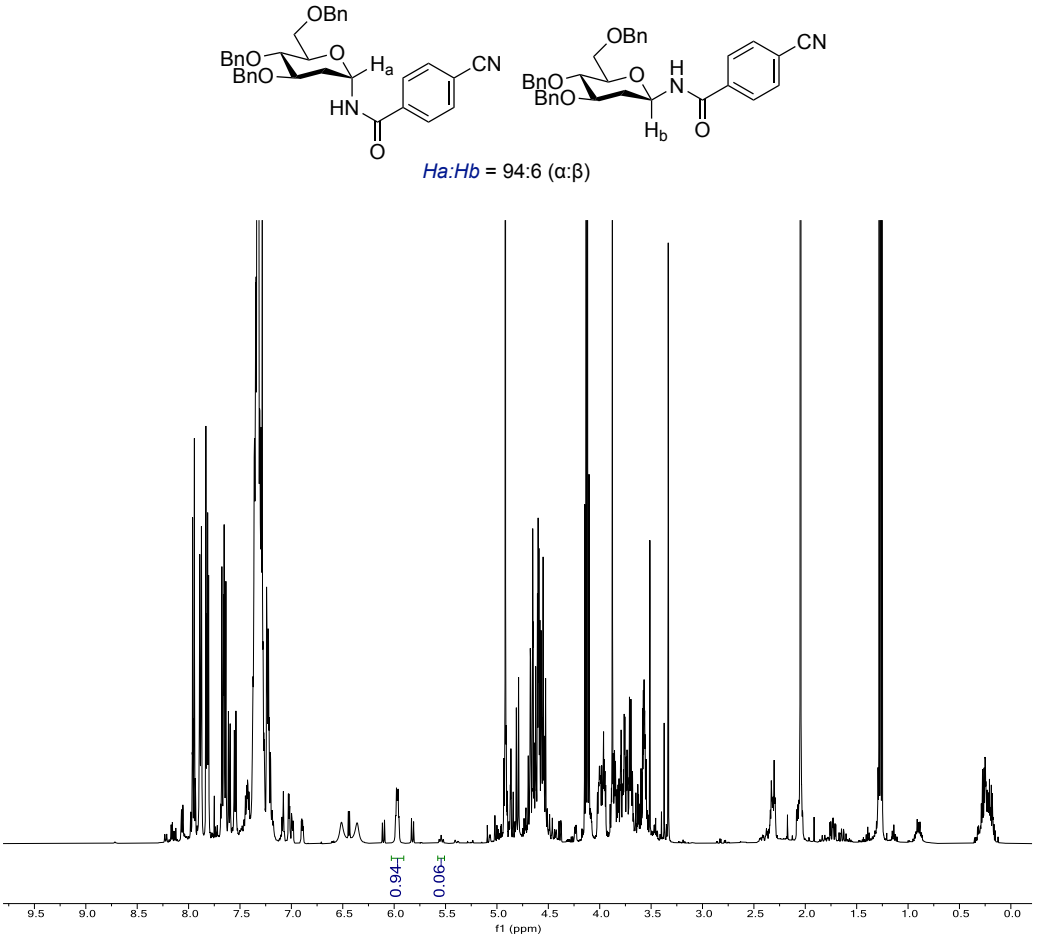

Crude ^{1}H-NMR (400 MHz, $CDCl_3$) en route to **3n**

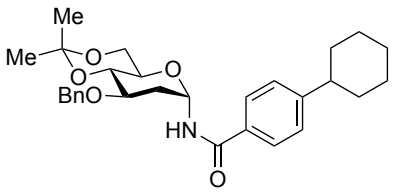

1-*N*-(4-cyclohexylbenzoyl)-(2-deoxyl-3-*O*-benzyl-4,6-di-*O*-isopropylidene-α-D-glucopyranosyl)-amine (3o). Following General Procedure A, 3-*O*-benzyl-4,6-di-*O*-isopropylidene-D-glucal (0.2 mmol, 55 mg) and 3-(4-(cyclohexyl)phenyl)-1,4,2-dioxazol-5-one (0.4 mmol, 98 mg) were used, affording the title compound as a white solid (first run, 83 mg, 87%; second run, 79 mg, 82%). **^{1}H NMR** (500 MHz, CD_2Cl_2) δ 7.78 – 7.64 (m, 2H), 7.43 – 7.23 (m, 7H), 6.81 (d, *J* = 7.8 Hz, 1H), 5.99 – 5.78 (m, 1H), 4.78 (d, *J* = 11.8 Hz, 1H), 4.67 (d, *J* = 11.9 Hz, 1H), 3.86 – 3.71 (m, 4H), 3.63 – 3.50 (m, 1H), 2.64 – 2.53 (m, 1H), 2.25 – 2.17 (m, 1H), 2.13 – 2.02 (m, 1H), 1.95 – 1.81 (m, 4H), 1.76 (d, *J* = 12.7 Hz, 1H), 1.52 (s, 3H), 1.49 – 1.36 (m, 7H), 1.35 – 1.23 (m, 1H) ppm. **^{13}C NMR** (126 MHz, CD_2Cl_2) δ 167.35, 153.27, 139.54, 132.15, 128.88, 128.19, 128.12, 127.74, 127.71, 100.17, 77.05, 75.97, 73.80, 72.98, 65.88, 63.08, 45.16, 35.68, 34.84, 34.83, 29.69, 27.39, 26.68, 19.66 ppm. **IR (neat):** 3307, 2992, 2923, 2851, 1642, 1610, 1530, 1498, 1448, 1369, 1262, 1205, 1090, 1030, 986, 916, 856, 733, 696, 578 cm^{-1}. **HRMS (ESI)** *calcd*. for ($C_{29}H_{38}NO_5$) $[M+H]^+$: 480.2744, *found* 480.2745. **M.P.**: 62 °C.

NMR spectroscopy of the crude reaction mixture prior to purification revealed the formation of **3o**-**4o** with a 99:1 α:β selectivity.

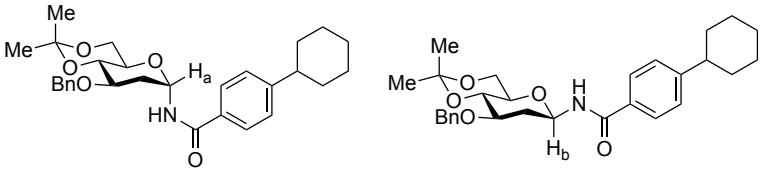

Ha:*Hb* = 99:1 (α:β)

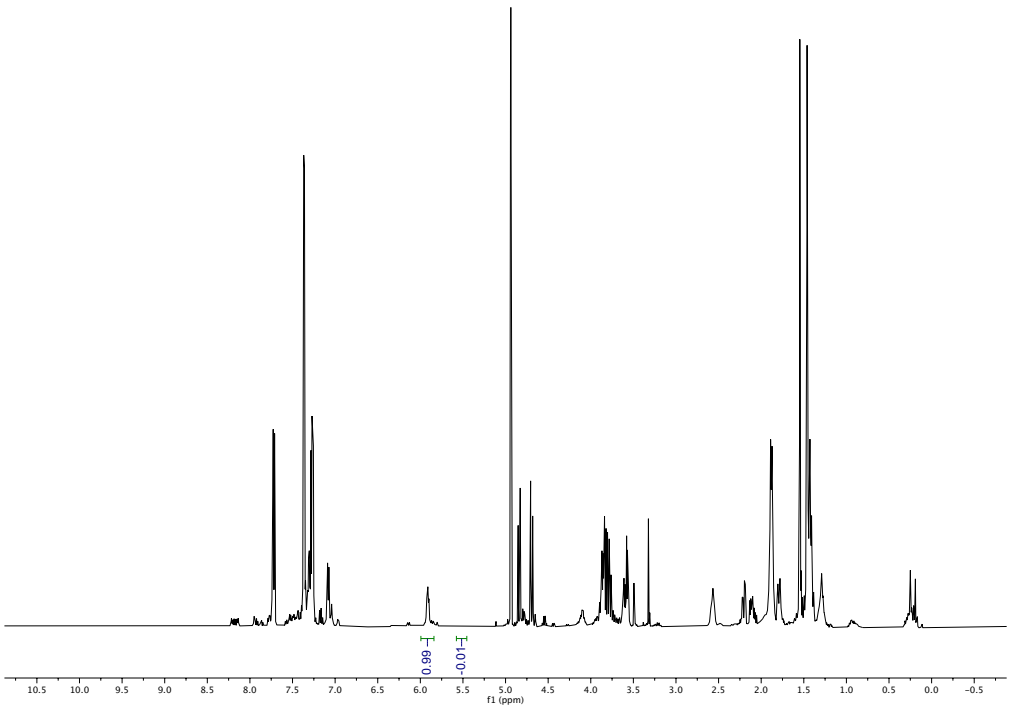

Crude ^{1}H-NMR (400 MHz, $CDCl_3$) en route to **3o**

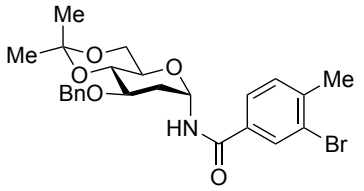

1-*N*-(3-(bromo)-4-(methyl) benzoyl)-(2-deoxyl-3-*O*-benzyl-4,6-di-*O*-isopropylidene-α-D-glucopyranosyl)-amine (3p). Following General Procedure A, 3-*O*-benzyl-4,6-di-*O*-isopropylidene-D-glucal (0.2 mmol, 55 mg) and 3-(3-(bromo)-4-(methyl) phenyl)-1,4,2-dioxazol-5-one (0.4 mmol, 102 mg) were used, affording the title compound as a white solid (first run, 87 mg, 89%; second run, 93 mg, 95%). **^{1}H NMR** (500 MHz, CD_2Cl_2) δ 7.96 (d, *J* = 1.8 Hz, 1H), 7.74 – 7.57 (m, 1H), 7.43 – 7.27 (m, 6H), 6.90 (d, *J* = 7.6 Hz, 1H), 5.93 – 5.79 (m, 1H), 4.83 (d, *J* = 11.8 Hz, 1H), 4.71 (d, *J* = 11.9 Hz, 1H), 3.94 – 3.71 (m, 4H), 3.65 – 3.53 (m, 1H), 2.48 (s, 3H), 2.33 – 2.21 (m, 1H), 2.19 – 2.03 (m, 1H), 1.56 (s, 3H), 1.45 (s, 3H) ppm. **^{13}C NMR** (101 MHz, CD_2Cl_2) δ 166.21, 142.87, 139.47, 133.80,

131.57, 131.40, 128.81, 128.09, 128.06, 126.70, 125.46, 100.10, 76.88, 76.06, 73.60, 72.86, 65.82, 62.94, 35.44, 29.64, 23.33, 19.57 ppm. **IR (neat):** 3293, 2991, 2938, 2875, 1642, 1527, 1484, 1454, 1373, 1335, 1306, 1262, 1205, 1090, 1029, 986, 948, 918, 858, 734, 696, 676, 576 cm^{-1}. **HRMS (ESI)** *calcd*. for ($C_{24}H_{29}BrNO_5$) $[M+H]^+$: 480.1224, *found* 490.1226. **M.P.**: 59 °C.

NMR spectroscopy of the crude reaction mixture prior to purification revealed the formation of **3p** with an exquisite α selectivity.

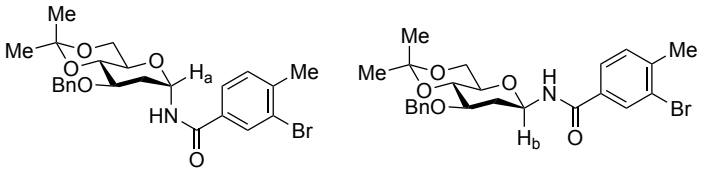

Ha:Hb > 99:1 (α:β)

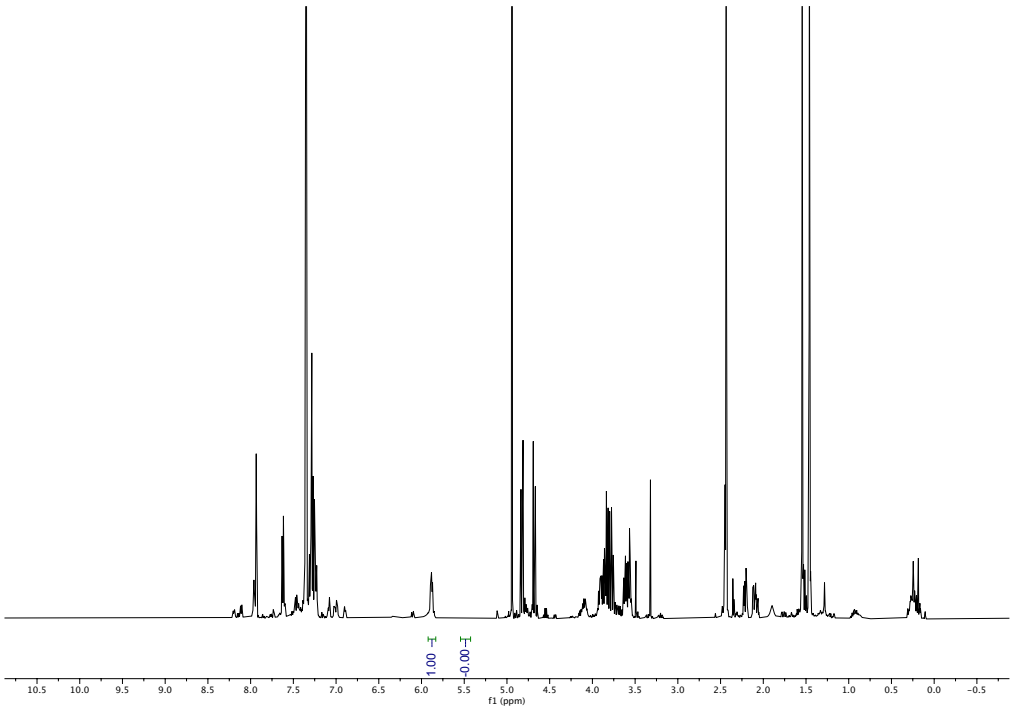

Crude ^{1}H-NMR (400 MHz, $CDCl_3$) en route to **3p**

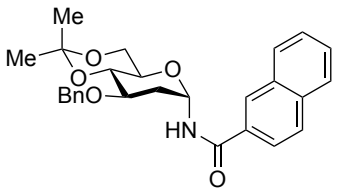

1-*N*-(2-naphthoyl)-(2-deoxyl-3-*O*-benzyl-4,6-di-*O*-isopropylidene-α-D-glucopyranosyl)-amine (3q). Following General Procedure A, 3-*O*-benzyl-4,6-di-*O*-isopropylidene-D-glucal (0.2 mmol, 55 mg) and 3-(naphthalen-2-yl)-1,4,2-dioxazol-5-one (0.4 mmol, 85 mg) were used, affording the title compound as a white solid (first run, 76 mg, 85%; second run, 84 mg, 94%). **^{1}H NMR** (400 MHz, CD_2Cl_2) δ 8.28 (s, 1H), 8.03 – 7.87 (m, 3H), 7.83 (m, 1H), 7.69 – 7.55 (m, 2H), 7.45 – 7.26 (m, 5H), 7.03 (d, *J* = 7.6 Hz, 1H), 6.12 – 5.80 (m, 1H), 4.81 (d, *J* = 11.9 Hz, 1H), 4.69 (d, *J* = 11.9 Hz, 1H), 3.93 – 3.75 (m, 4H), 3.73 - 3.58 (m, 1H), 2.33 – 2.23 (m, 1H), 2.19 – 2.06 (m, 1H), 1.54 (s, 3H), 1.42 (s, 3H) ppm. **^{13}C NMR** (101 MHz, CD_2Cl_2) δ 167.48, 139.46, 135.52, 133.10, 131.81, 129.42, 129.12, 128.85, 128.53, 128.33, 128.14, 128.10, 128.06, 127.54, 124.22, 100.17, 76.98, 76.06, 73.71, 72.93, 65.89, 63.02, 35.59, 29.65, 19.60 ppm. **IR (neat):** 3282, 3059, 29941, 2924, 2871, 1643, 1524, 1503, 1454, 1371, 1263, 1204, 1120, 1089, 1029, 985, 949, 861, 780, 735, 696, 569, 477 cm^{-1}. **HRMS (ESI)** *calcd.* for ($C_{27}H_{30}NO_5$) $[M+H]^+$: 448.2118, *found* 448.2124. **M.P.**: 65 °C.

NMR spectroscopy of the crude reaction mixture prior to purification revealed the formation of **3q**-**4q** with a 99:1 α:β selectivity.

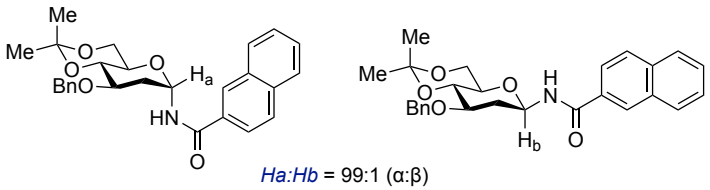

Ha:*Hb* = 99:1 (α:β)

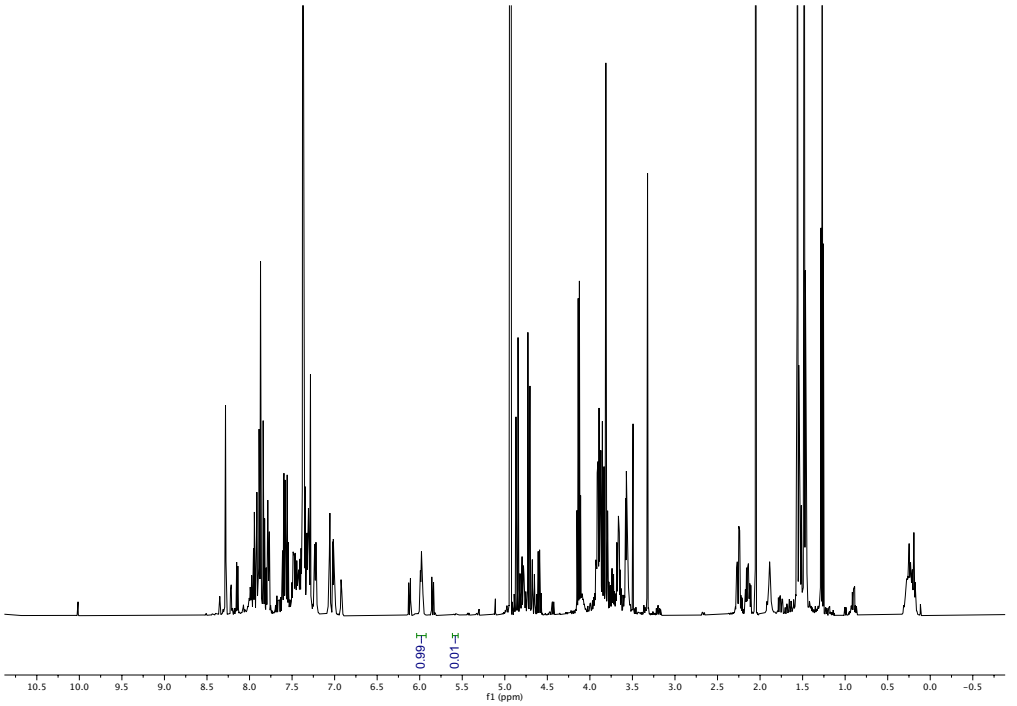

Crude ^{1}H-NMR (400 MHz, $CDCl_3$) en route to **3q**

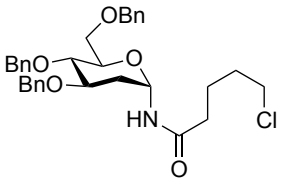

1-*N*-(4-chloropentoyl)-(2-deoxyl-3,4,6-*O*-benzyl-α-D-glucopyranosyl)-amine (3r). Following General Procedure A, 3,4,6-*O*-benzyl-D-glucal (0.2 mmol, 83 mg) and 3-(4-chlorobutyl)-1,4,2-dioxazol-5-one (0.4 mmol, 71 mg) were used, affording the title compound as a white solid (first run, 73 mg, 66%; second run, 68 mg, 62%). **^{1}H NMR** (500 MHz, CD_2Cl_2) δ 7.40 – 7.20 (m, 15H), 6.10 (d, J = 8.1 Hz, 1H), 5.68 (dt, J = 8.1, 4.0 Hz, 1H), 4.81 (d, J = 11.0 Hz, 1H), 4.66 (d, J = 11.7 Hz, 1H), 4.62 – 4.48 (m, 4H), 3.82 – 3.73 (m, 2H), 3.72 – 3.65 (m, 2H), 3.62 – 3.50 (m, 3H), 2.19 (t, J = 7.1 Hz, 2H), 2.16 – 2.09 (m, 1H), 1.99 – 1.87 (m, 1H), 1.84 – 1.68 (m, 4H) ppm. **^{13}C NMR** (126 MHz, CD_2Cl_2) δ 172.35, 139.06, 139.00, 128.92, 128.85, 128.48, 128.42, 128.20, 128.16, 128.11, 77.40,

77.04, 74.87, 73.92, 73.35, 71.89, 69.61, 45.39, 36.09, 33.88, 32.51, 23.15 ppm. **IR (neat):** 3376, 3032, 2928, 2904, 2873, 1686, 1510, 1465, 1454, 1365, 1206, 1186, 1126, 1089, 1062, 1029, 1003, 967, 754, 731, 694, 610, 581, 529 cm^{-1}. **HRMS (ESI)** *calcd.* for ($C_{32}H_{38}ClNNaO_5$) $[M+Na]^+$: 574.2331, *found* 574.2343. **M.P.**: 101 °C.

NMR spectroscopy of the crude reaction mixture prior to purification revealed the formation of **3r**-**4r** with a 94:6 α:β selectivity.

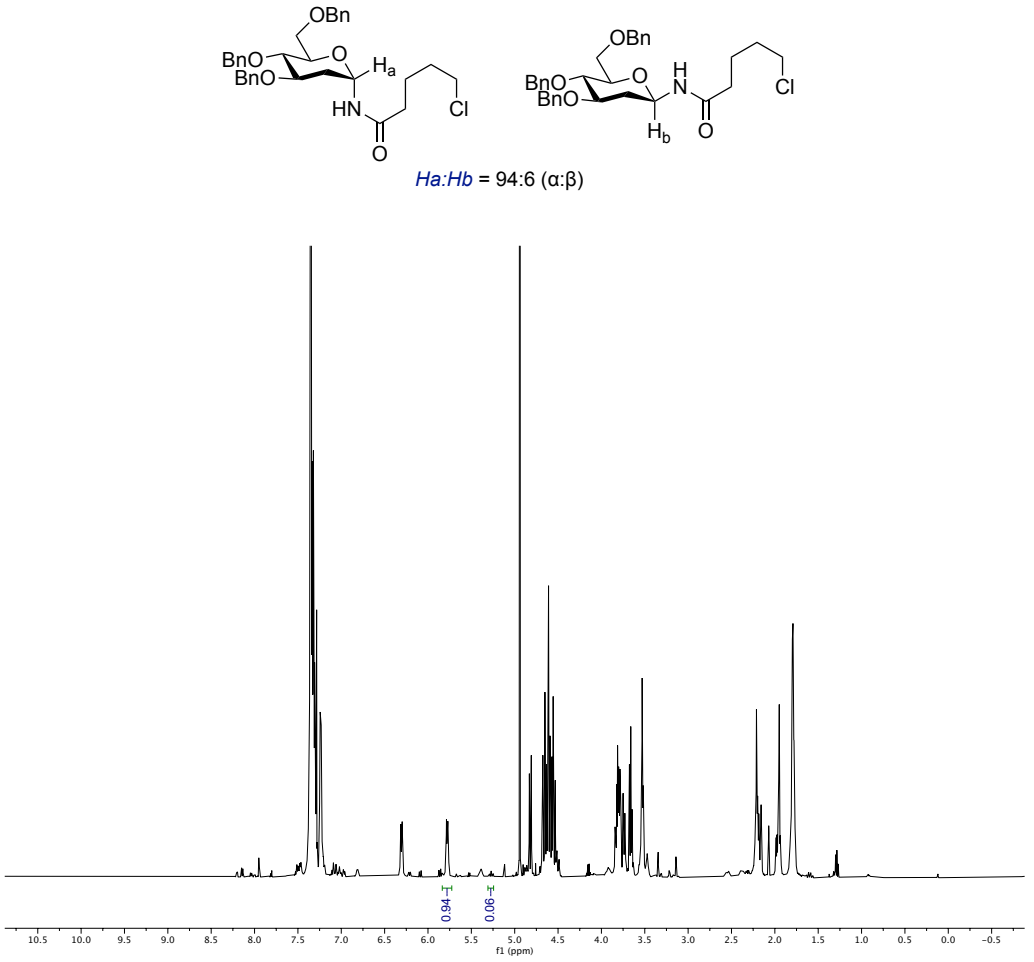

Crude ^{1}H-NMR (400 MHz, $CDCl_3$) en route to **3r**

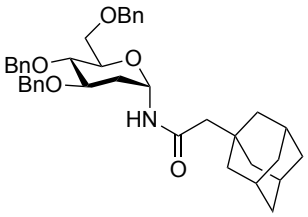

1-*N*-(2-(adamantan-1-yl)acetyl)-(2-deoxyl-3,4,6-*O*-benzyl-α-D-glucopyranosyl)-amine (3s). Following General Procedure A, 3,4,6-*O*-benzyl-D-glucal (0.2 mmol, 83 mg) and 3-((adamantan-1-yl)methyl)-1,4,2-dioxazol-5-one (0.4 mmol, 94 mg) were used, affording the title compound as a white solid (first run, 80 mg, 66%; second run, 91 mg, 75%). **^{1}H NMR** (500 MHz, CD_2Cl_2) δ 7.39 – 7.20 (m, 15H), 6.00 (d, *J* = 8.4 Hz, 1H), 5.78 – 5.63 (m, 1H), 4.83 (d, *J* = 10.9 Hz, 1H), 4.74 – 4.47 (m, 5H), 3.83 – 3.70 (m, 2H), 3.72 – 3.63 (m, 2H), 3.57 (t, *J* = 8.0 Hz, 1H), 2.18 – 2.05 (m, 1H), 1.99 – 1.90 (m, 4H), 1.76 – 1.54 (m, 14H) ppm. **^{13}C NMR** (126 MHz, CD_2Cl_2) δ 170.81, 139.08, 139.02, 128.92, 128.85, 128.55, 128.41, 128.21, 128.08, 77.72, 77.20, 75.02, 73.92, 73.88, 73.34, 71.91, 69.67, 52.16, 43.09, 37.26, 34.21, 33.35, 29.34 ppm. **IR (neat):** 3522, 3449, 3243, 3034, 2904, 2845, 1653, 1542, 1498, 1454, 1369, 1354, 1270, 1239, 1208, 1135, 1085, 1070, 1023, 1003, 990, 754, 730, 694, 629, 567 cm^{-1}. **HRMS (ESI)** *calcd*. for ($C_{39}H_{47}NNaO_5$) $[M+Na]^+$: 632.3346, *found* 632.3354. **M.P.**: 101 °C.

NMR spectroscopy of the crude reaction mixture prior to purification revealed the formation of **3s**-**4s** with a 95:5 α:β selectivity.

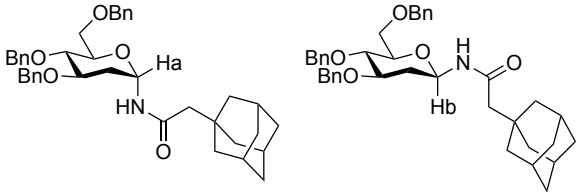

Ha:*Hb* = 95:5 (α:β)

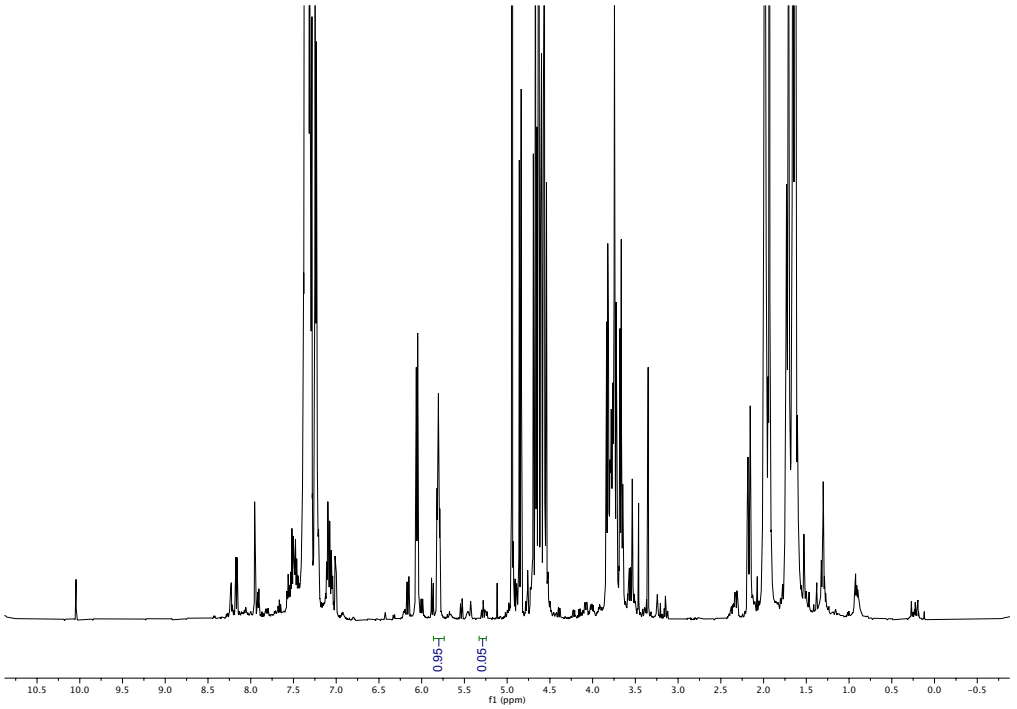

Crude ^{1}H-NMR (400 MHz, $CDCl_3$) en route to **3s**

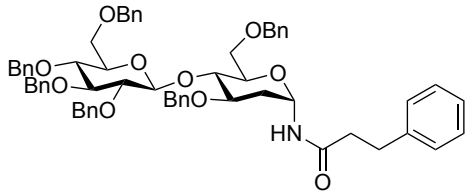

1-*N*-(phenpropoyl-(2-deoxyl-2',3,3',4',6,6'-*O*-benzyl-α-D-maltosyl)-amine (3t). Following General Procedure A, 2',3,3',4',6,6'-*O*-benzyl-D-cellobial (0.1 mmol, 1 equiv., 85 mg) and 3-phenethyl-1,4,2-dioxazol-5-one (0.2 mmol, 39 mg) were used, reactions were performed for 48 h, with additional DMMS (0.1 mmol, 12.5 μL) and TFE (0.1 mmol, 7.2 μL) added after 24 h, affording the title compound as a white solid (first run, 53 mg, 53%; second run, 47 mg, 47%). **^{1}H NMR** (500 MHz, CD_2Cl_2) δ 7.42 – 7.07 (m, 35H), 5.88 (d, *J* = 8.6 Hz, 1H), 5.62 (dt, *J* = 8.7, 5.5 Hz, 1H), 4.93 (d, *J* = 11.1 Hz, 1H), 4.89 (d, *J* = 11.0 Hz, 1H), 4.86 – 4.76 (m, 2H), 4.71 (d, *J* = 11.1 Hz, 1H), 4.68 (d, *J* = 12.1 Hz,

1H), 4.63 – 4.47 (m, 7H), 3.94 – 3.87 (m, 2H), 3.87 – 3.80 (m, 2H), 3.72 – 3.64 (m, 3H), 3.63 – 3.54 (m, 2H), 3.44 – 3.34 (m, 2H), 2.93 (t, J = 7.7 Hz, 2H), 2.56 – 2.39 (m, 2H), 1.95 – 1.86 (m, 2H) ppm. **^{13}C NMR** (126 MHz, CD_2Cl_2) δ 171.96, 141.52, 139.41, 139.32, 139.24, 139.04, 138.94, 129.01, 128.89, 128.83, 128.82, 128.78, 128.56, 128.40, 128.37, 128.35, 128.24, 128.15, 128.10, 128.08, 128.00, 126.72, 103.51, 85.16, 82.94, 78.31, 76.00, 75.36, 75.34, 75.32, 75.24, 75.18, 74.87, 73.86, 73.81, 72.14, 71.99, 69.51, 68.88, 38.72, 33.17, 31.77 ppm. **IR (neat):** 3304, 3062, 3030, 2901, 2866, 1651, 1526, 1496, 1452, 1395, 1351, 1307, 1271, 1197, 1070, 1027, 904, 728, 693, 459 cm^{-1}. **HRMS (ESI)** *calcd*. for ($C_{63}H_{67}NNaO_{10}$) $[M+Na]^+$: 1020.4657, *found* 1020.4660. **M.P.**: 146 °C.

NMR spectroscopy of the crude reaction mixture prior to purification revealed the formation of **3t**-**4t** with an exquisite α selectivity.

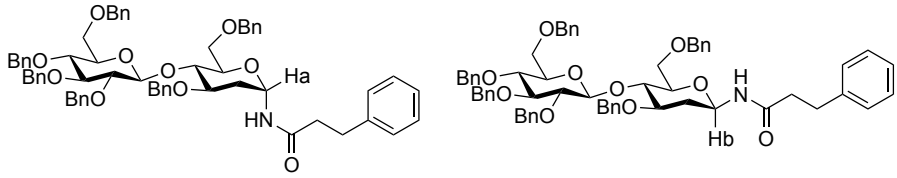

Ha:Hb > 99:1 (α:β)

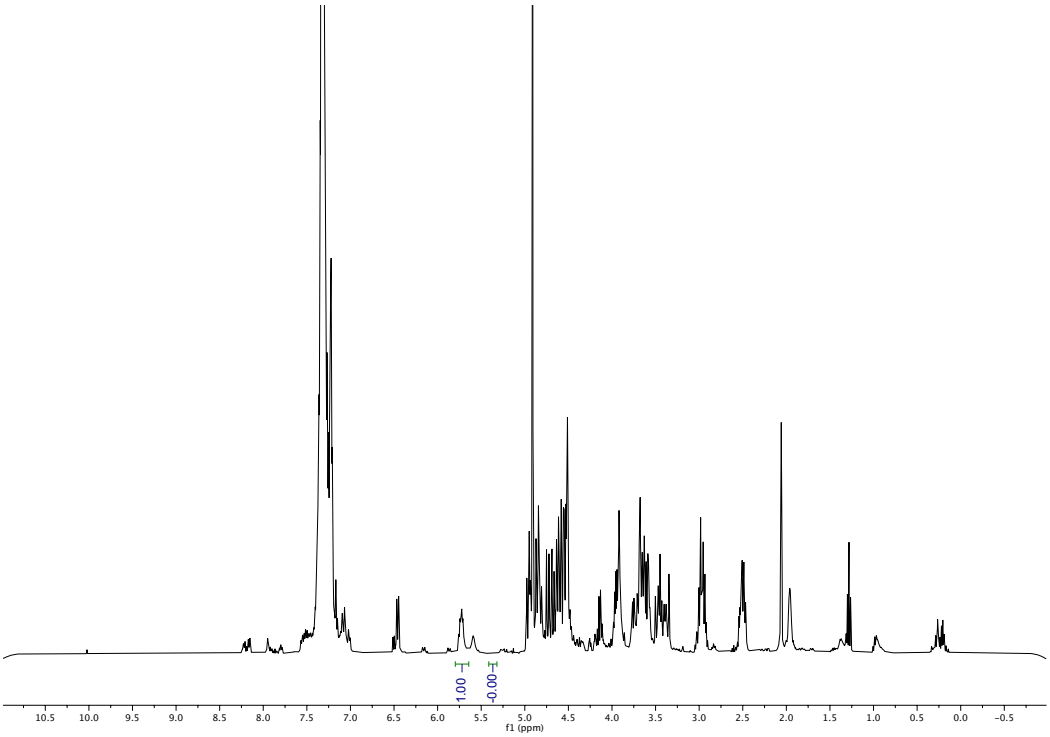

Crude ^{1}H-NMR (400 MHz, $CDCl_3$) en route to **3t**

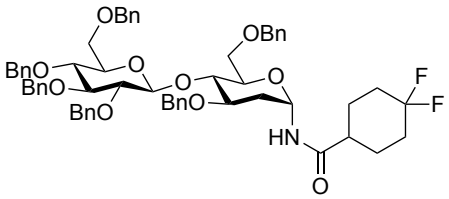

1-*N*-(4,4-difluorocyclohexane-1-carbonyl)-(2-deoxyl-2',3,3',4',6,6'-*O*-benzyl-α-D-maltosyl)-amine (3u). Following General Procedure A, 2',3,3',4',6,6'-*O*-benzyl-D-cellobial (0.1 mmol, 1 equiv., 85 mg) and 3-(4,4-difluorocyclohexyl)-1,4,2-dioxazol-5-one (0.2 mmol, 41 mg) were used, reactions were performed for 48 h, with additional DMMS (0.1 mmol, 12.5 μL) and TFE (0.1 mmol, 7.2 μL) added after 24 h, affording the title compound as a white solid (first run, 57 mg, 56%; second run, 46 mg, 45%). **^{1}H NMR** (400 MHz, CD_2Cl_2) δ 7.58 – 7.10 (m, 30H), 5.97 (d, *J* = 8.6 Hz, 1H), 5.69 – 5.60 (m, 1H), 4.97 (d, J = 11.0 Hz, 1H), 4.90 (d, *J* = 11.0 Hz, 1H), 4.86 – 4.77 (m, 2H), 4.73 (d, *J* = 11.0 Hz, 1H), 4.70 – 4.56 (m, 4H), 4.56 – 4.48 (m, 4H), 4.06 – 3.85 (m, 4H), 3.82 – 3.73 (m,

1H), 3.72 – 3.55 (m, 4H), 3.51 – 3.35 (m, 2H), 2.26 – 2.07 (m, 3H), 2.00 (t, *J* = 5.2 Hz, 2H), 1.93 – 1.84 (m, 2H), 1.83 – 1.68 (m, 4H) ppm. **^{13}C NMR** (101 MHz, CD_2Cl_2) δ 174.04, 139.42, 139.25, 139.16, 139.07, 139.04, 138.92, 128.88, 128.84, 128.80, 128.62, 128.43, 128.39, 128.30, 128.27, 128.18, 128.14, 128.08, 128.05, 123.44 (t, *J* = 241.3), 121.05, 103.62, 85.13, 82.92, 78.29, 76.02, 75.43, 75.36, 75.33, 75.27, 74.75, 73.90, 73.81, 72.06, 71.65, 69.55, 68.90, 43.10, 33.46, 33.22, 32.97, 32.82, 26.37, 26.32, 26.29, 26.23. **IR (neat):** 3291, 3063, 3031, 2901, 2869, 1647, 1535, 1496, 1452, 1358, 1271, 1196, 1071, 1027, 957, 728, 694 cm^{-1}. **HRMS (ESI)** *calcd*. for ($C_{61}H_{67}F_2NNaO_{10}$) $[M+Na]^+$: 1034.4625, *found* 1034.4628. **M.P.**: 167 °C.

NMR spectroscopy of the crude reaction mixture prior to purification revealed the formation of **3u** with an exquisite α selectivity.

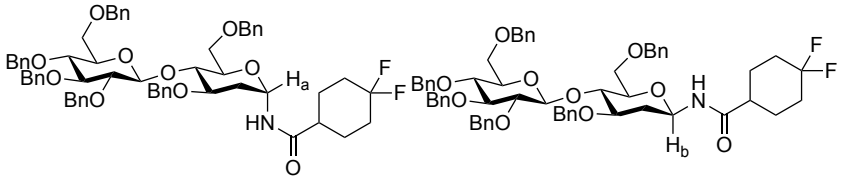

Ha:*Hb* > 99:1 (α:β)

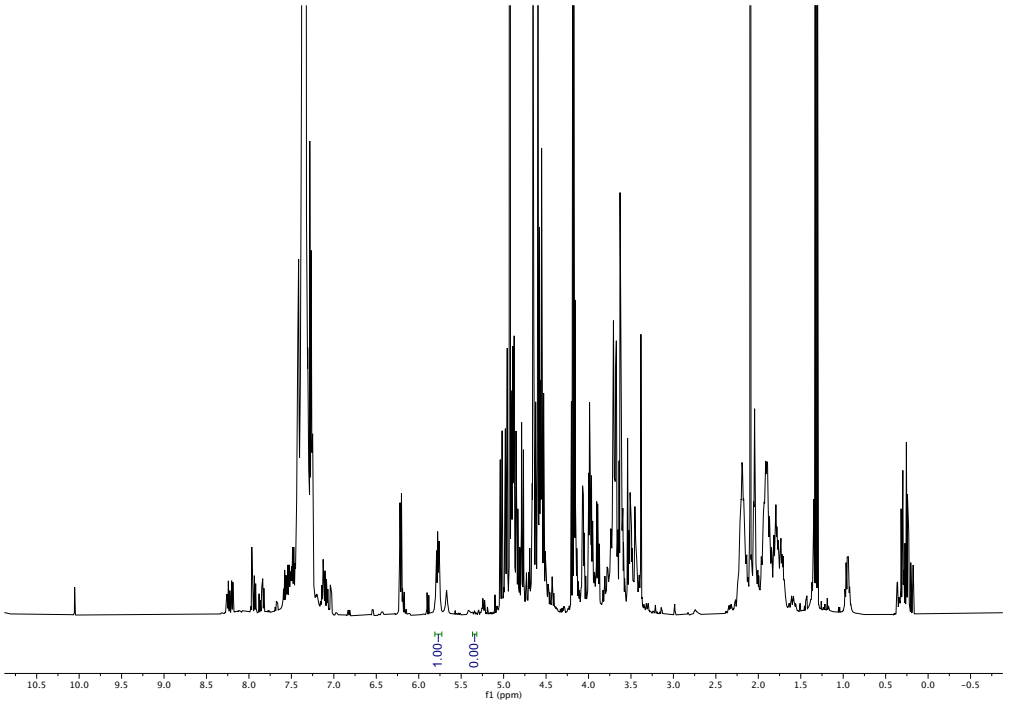

Crude ^{1}H-NMR (400 MHz, $CDCl_3$) en route to **3u**

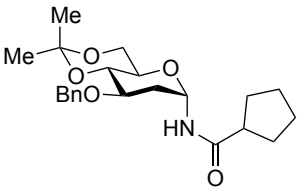

1-*N*-(cyclopentane-1-carbonyl)-(2-deoxyl-3-*O*-benzyl-4,6-di-*O*-isopropylidene-α-D-glucopyranosyl)-amine (3v). Following General Procedure A, 3-*O*-benzyl-4,6-di-*O*-isopropylidene-D-glucal (0.2 mmol, 55 mg) and 3-cyclopentyl-1,4,2-dioxazol-5-one (0.4 mmol, 62 mg) were used, affording the title compound as a colorless oil (first run, 49 mg, 63%; second run, 44 mg, 57%). **^{1}H NMR** (400 MHz, CD_2Cl_2) δ 7.41 – 7.24 (m, 5H), 6.18 (d, *J* = 7.9 Hz, 1H), 5.74 – 5.57 (m, 1H), 4.76 (d, *J* = 11.9 Hz, 1H), 4.66 (d, *J* = 11.9 Hz, 1H), 3.84 – 3.63 (m, 4H), 3.50 – 3.38 (m, 1H), 2.58 – 2.43 (m, 1H), 2.15 – 2.05 (m, 1H), 2.05 – 1.92 (m, 1H), 1.92 – 1.79 (m, 2H), 1.79 – 1.65 (m, 4H), 1.63 – 1.57 (m, 2H), 1.51 (s, 3H), 1.40 (s, 3H) ppm. **^{13}C NMR** (101 MHz, CD_2Cl_2) δ 176.21, 139.48, 128.83, 128.10,

128.06, 100.09, 76.99, 75.29, 73.58, 72.79, 65.48, 63.05, 46.19, 35.46, 30.97, 30.74, 29.66, 26.56, 26.53, 19.58 ppm. **IR (neat):** 3276, 2992, 2954, 2891, 2868, 1655, 1540, 1452, 1366, 1263, 1225, 1203, 1172, 1120, 1089, 1029, 985, 911, 856, 755, 734, 696 cm^{-1}. **HRMS (ESI)** *calcd*. for ($C_{22}H_{32}NO_5$) $[M+H]^+$: 390.2275, *found* 390.2266. **M.P.**: 135 °C.

NMR spectroscopy of the crude reaction mixture prior to purification revealed the formation of **3v**-**4v** with a 97:3 α:β selectivity.

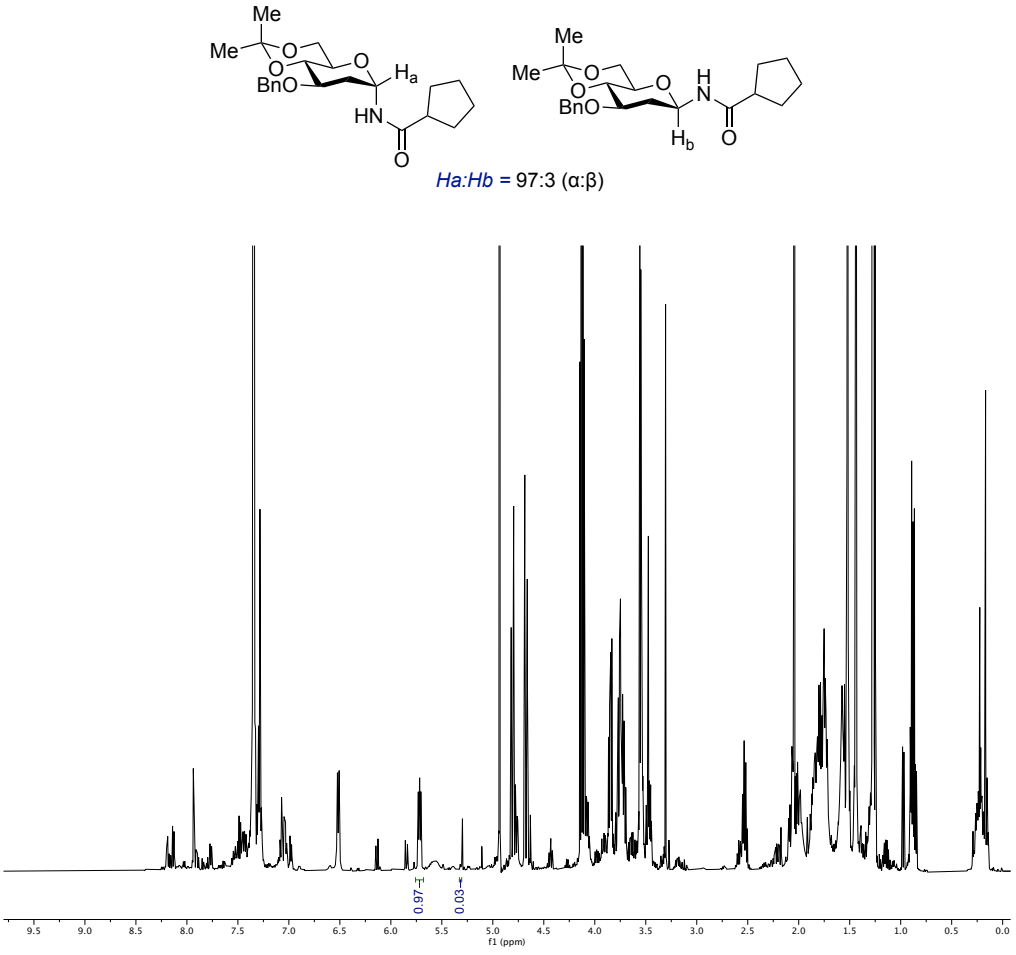

Crude ^{1}H-NMR (400 MHz, $CDCl_3$) en route to **3v**

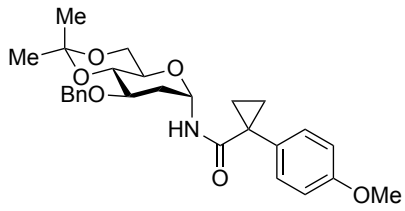

1-*N*-(1-(4-methoxyphenyl)cyclopropane-1-carbonyl)-(2-deoxyl-3-*O*-benzyl-4,6-di-*O*-isopropylidene-α-D-glucopyranosyl)-amine (3w). Following General Procedure A, 3-*O*-benzyl-4,6-di-*O*-isopropylidene-D-glucal (0.2 mmol, 55 mg) and 3-(1-(4-methoxyphenyl)cyclopropyl)-1,4,2-dioxazol-5-one (0.4 mmol, 93 mg) were used, affording the title compound as a colorless oil (first run, 50 mg, 53%; second run, 56 mg, 60%). **^{1}H NMR** (500 MHz, CD_2Cl_2) δ 7.40 – 7.16 (m, 7H), 7.00 – 6.89 (m, 2H), 6.07 (d, *J* = 8.1 Hz, 1H), 5.52 (dt, *J* = 8.0, 3.4 Hz, 1H), 4.61 (d, *J* = 11.9 Hz, 1H), 4.47 (d, *J* = 11.9 Hz, 1H), 3.83 (s, 3H), 3.80 – 3.73 (m, 1H), 3.73 – 3.58 (m, 2H), 3.19 – 3.07 (m, 2H), 1.89 – 1.82 (m, 2H), 1.54 – 1.47 (m, 2H), 1.46 (s, 3H), 1.36 (s, 3H), 1.04 (d, *J* = 3.3 Hz, 2H) ppm. **^{13}C NMR** (101 MHz, CD_2Cl_2) δ 174.38, 160.01, 139.26, 132.45, 131.56, 128.80, 128.07, 128.05, 115.09, 100.00, 76.71, 75.50, 73.39, 72.66, 65.52, 62.97, 55.88, 35.36, 30.07, 29.56, 19.52, 16.77, 16.40 ppm. **IR (neat):** 3428, 2993, 2954, 2924, 2885, 1679, 1610, 1512, 1494, 1465, 1374, 1293, 1246, 1204, 1174, 1118, 1089, 1030, 987, 945, 917, 855, 835, 735, 698, 553, 520 cm^{-1}. **HRMS (ESI)** *calcd*. for ($C_{27}H_{34}NO_6$) $[M+H]^+$: 468.2381, *found* 468.2366.

NMR spectroscopy of the crude reaction mixture prior to purification revealed the formation of **3w** with an exquisite α selectivity.

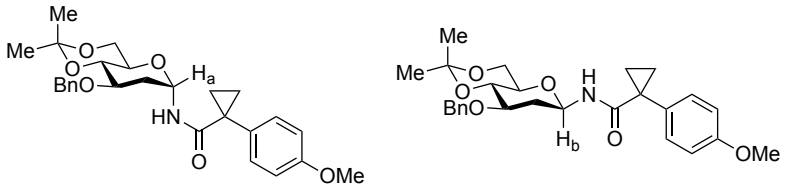

Ha:*Hb* > 99:1 (α:β)

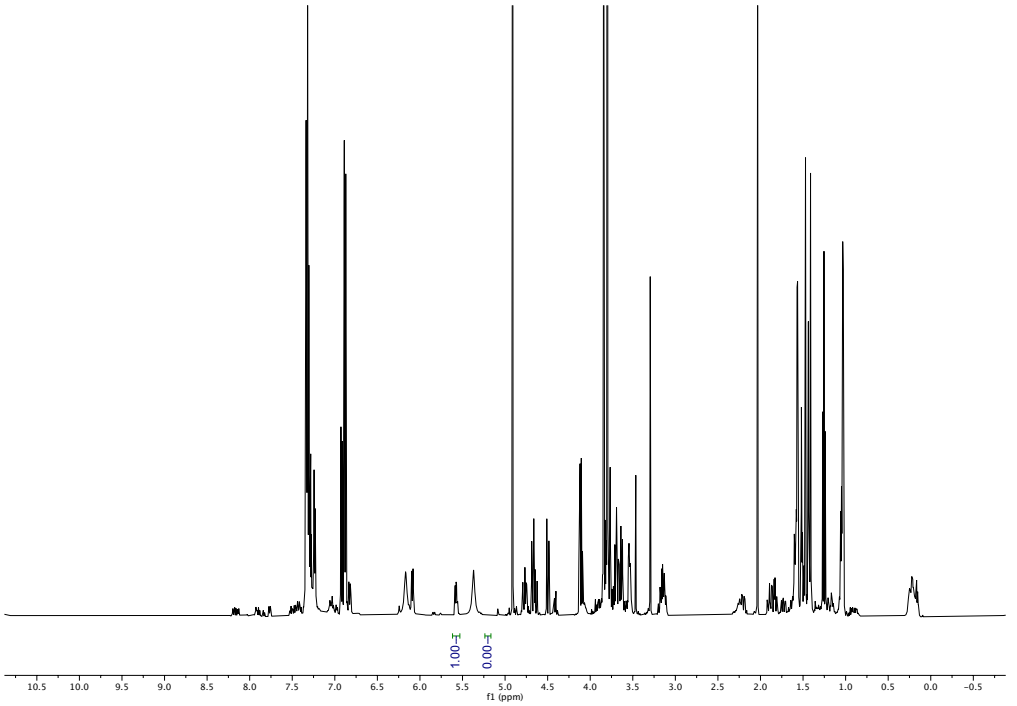

Crude ^{1}H-NMR (400 MHz, $CDCl_3$) en route to **3w**

3.9.4 Preparation of β-*N*-Glycosides

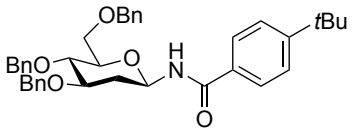

1-*N*-(4-*tert*-butylbenzoyl)-(2-deoxyl-3,4,6-tri-*O*-benzyl-β-D-glucopyranosyl)-amine (4k). Following General Procedure B, 3,4,6-tri-*O*-benzyl-D-glucal (0.2 mmol, 83 mg) and 3-(4-(*tert*-butyl)phenyl)-1,4,2-dioxazol-5-one (0.4 mmol, 88 mg) were used, affording the title compound as a white solid (first run, 84 mg, 71%; second run, 90 mg, 76%). **^{1}H NMR** (500 MHz, $CDCl_3$) δ 7.79 – 7.69 (m, 2H), 7.44 (d, *J* = 8.5 Hz, 2H), 7.38 – 7.23 (m, 13H), 7.21 – 7.12 (m, 2H), 6.78 (d, *J* = 9.1 Hz, 2H), 5.56 – 5.40 (m, 2H), 4.89 (d, *J* = 10.8 Hz, 1H), 4.68 (d, *J* = 11.6 Hz, 1H), 4.62 (d, *J* = 11.6 Hz, 1H), 4.59 – 4.49 (m, 2H), 4.43 (d, *J* = 12.1 Hz, 1H), 3.87 – 3.66 (m, 4H), 3.62 – 3.52 (m, 1H), 2.45 – 2.33 (m, 1H), 1.79 – 1.67 (m, 1H), 1.33 (s, 9H) ppm. **^{13}C NMR** (126 MHz, $CDCl_3$) δ 166.61, 155.64, 138.53, 138.41, 137.98, 130.91, 128.59, 128.51, 128.49, 128.27, 128.06, 127.88, 127.86, 127.82, 127.80, 127.18, 125.65, 79.97, 77.56, 76.84, 75.14, 73.69, 71.80, 68.65, 37.00, 35.11, 31.28 ppm. **IR (neat):** 3351, 3063, 3031, 2959, 2925, 2866, 1656, 1610, 1537, 1498, 1454, 1361, 1286, 1206, 1074, 1026, 990, 908, 852, 732, 696, 561 cm^{-1}. **HRMS (ESI)** *calcd.* for ($C_{38}H_{44}NO_5$) $[M+H]^+$: 594.3215, *found* 594.3214.

NMR spectroscopy of the crude reaction mixture prior to purification revealed the formation of **3k**-**4k** with a 7:93 α:β selectivity.

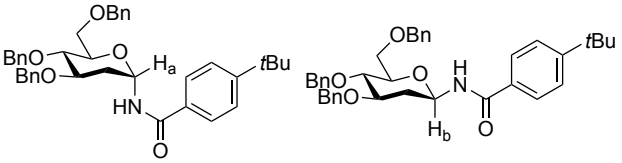

Ha:Hb: 7:93 (α:β)

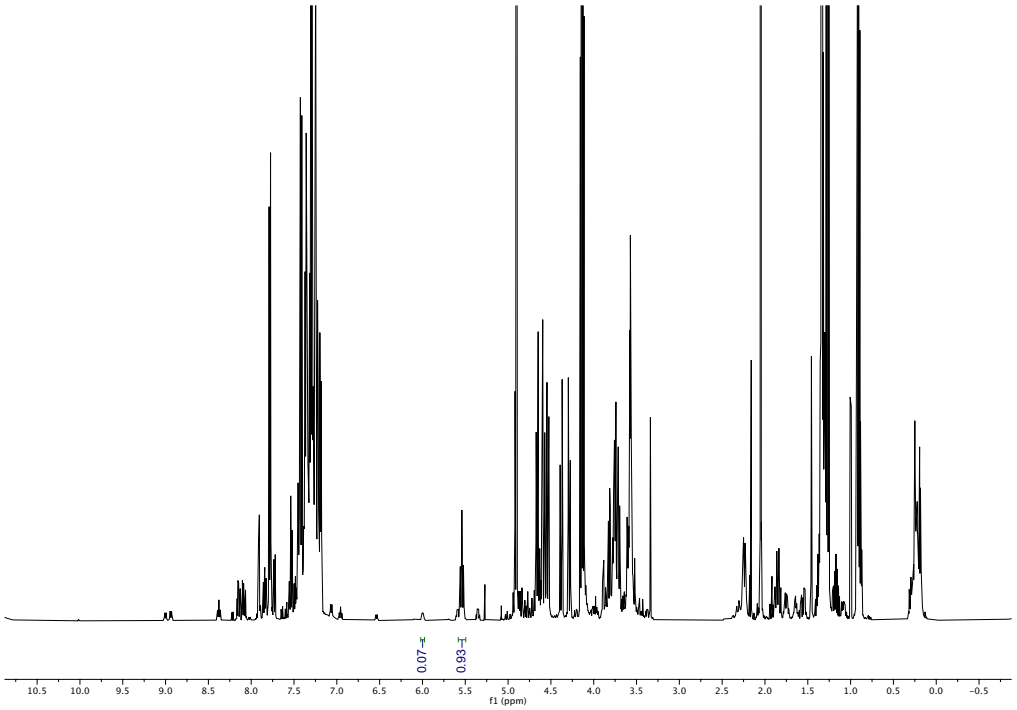

Crude ^{1}H-NMR (400 MHz, $CDCl_3$) en route to **4k**

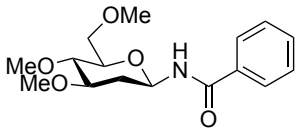

1-*N*-Benzoyl-(2-deoxyl-3,4,6-tri-*O*-methyl-β-D-glucopyranosyl)-amine (4b). Following General Procedure B, 3,4,6-tri-*O*-methyl-D-glucal (0.2 mmol, 38 mg) and **2a** (0.40 mmol, 65 mg) were used, the first step was performed for 72 h (additional DMMS (0.20 mmol, 25.0 μL) and TFE (0.1 mmol, 7.2 μL) were added after 48 h), affording the title compound as a colorless oil (first run, 39 mg, 63%; second run, 33 mg, 54%). **^{1}H NMR** (400 MHz, $CDCl_3$) δ 7.82 – 7.74 (m, 2H), 7.57 – 7.48 (m, 1H), 7.48 – 7.38 (m, 2H), 6.81 (m, 1H), 5.48 (m, 1H), 3.67 – 3.63 (m, 2H), 3.57 (s, 3H), 3.48 (s, 3H), 3.47 – 3.41 (m, 2H), 3.41 – 3.37 (m, 3H), 3.32 – 3.22 (m, 1H), 2.51 – 2.33 (m, 1H), 1.68 – 1.52 (m,

1H) ppm. **^{13}C NMR** (126 MHz, $CDCl_3$) δ 166.70, 133.76, 132.06, 128.69, 127.29, 81.42, 79.07, 76.92, 76.70, 71.00, 60.64, 59.23, 57.39, 36.37 ppm. **IR (neat):** 3336, 2991, 2952, 2923, 2894, 2869, 2855, 2808, 1655, 1602, 1528, 1489, 1440, 1387, 1320, 1295, 1192, 1176, 1135, 1119, 1089, 1056, 988, 968, 946, 896, 721, 691, 646, 629, 599 cm^{-1}. **HRMS (ESI)** *calcd*. for ($C_{16}H_{23}NNaO_5$) $[M+Na]^+$: 332.1468, *found* 332.1474. M.P.: 155 ºC.

NMR spectroscopy of the crude reaction mixture prior to purification revealed the formation of **3b**-**4b** with a 7:93 α:β selectivity.

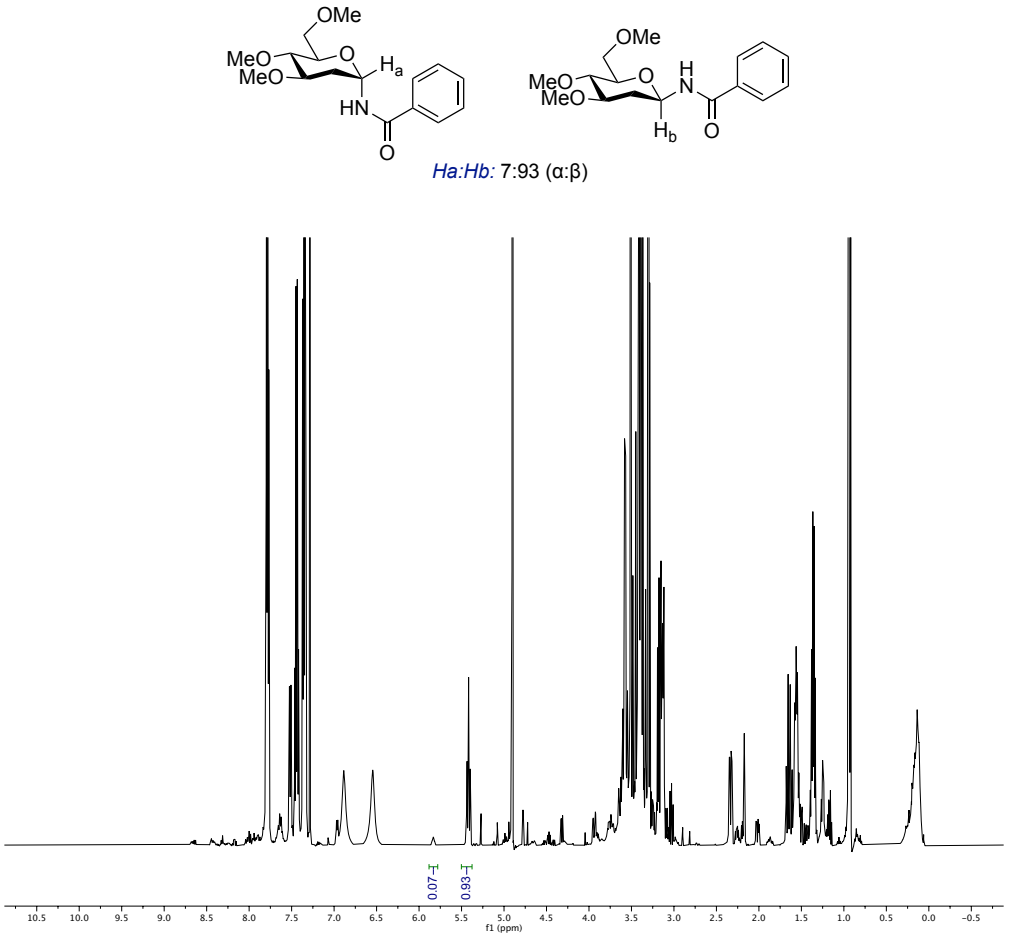

Crude ^{1}H-NMR (400 MHz, $CDCl_3$) en route to **4b**

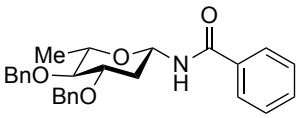

1-*N*-Benzoyl-(2,6-deoxyl-3,4-*O*-benzyl-β-L-glucopyranosyl)-amine (4f). Following General Procedure B, 3,4-di-*O*-benzyl-L-rhamnal (0.2 mmol, 62 mg) and **2a** (0.40 mmol, 65 mg) were used, affording the title compound as a white solid (first run, 47 mg, 54%; second run, 43 mg, 50%). **^{1}H NMR** (400 MHz, CD_2Cl_2) δ 7.84 – 7.71 (m, 2H), 7.61 – 7.51 (m, 1H), 7.49 – 7.43 (m, 2H), 7.40 – 7.25 (m, 10H), 6.66 (d, *J* = 9.0 Hz, 1H), 5.48 – 5.35 (m, 1H), 4.95 (d, *J* = 11.0 Hz, 1H), 4.77 – 4.58 (m, 3H), 3.84 – 3.70 (m, 1H), 3.59 – 3.45 (m, 1H), 3.13 (t, *J* = 8.9 Hz, 1H), 2.51 – 2.40 (m, 1H), 1.73 – 1.61 (m, 1H), 1.31 (d, *J* = 6.2 Hz, 3H) ppm. **^{13}C NMR** (101 MHz, CD_2Cl_2) δ 166.82, 139.35, 139.19, 134.47, 132.44, 129.15, 128.91, 128.81, 128.54, 128.32, 128.16, 128.14, 127.62, 84.10, 80.18, 76.67, 75.58, 73.89, 72.07, 37.50, 18.76 ppm. **IR (neat):** 3324, 3062, 3030, 2955, 2926, 2894, 2852, 1650, 1527, 492, 1452, 1361, 1304, 1290, 1090, 1026, 1000, 730, 693, 651cm^{-1}. **HRMS (ESI)** *calcd.* for ($C_{27}H_{29}NNaO_4$) $[M+Na]^+$: 454.1989, *found* 454.2002. M.P.: 165 ºC.

NMR spectroscopy of the crude reaction mixture prior to purification revealed the formation of **3f-4f** with a 7:93 α:β selectivity.

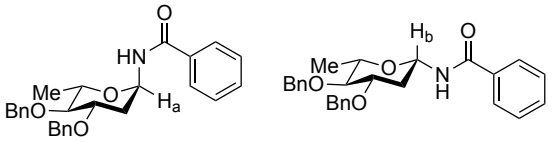

Ha:Hb: 7:93 (α:β)

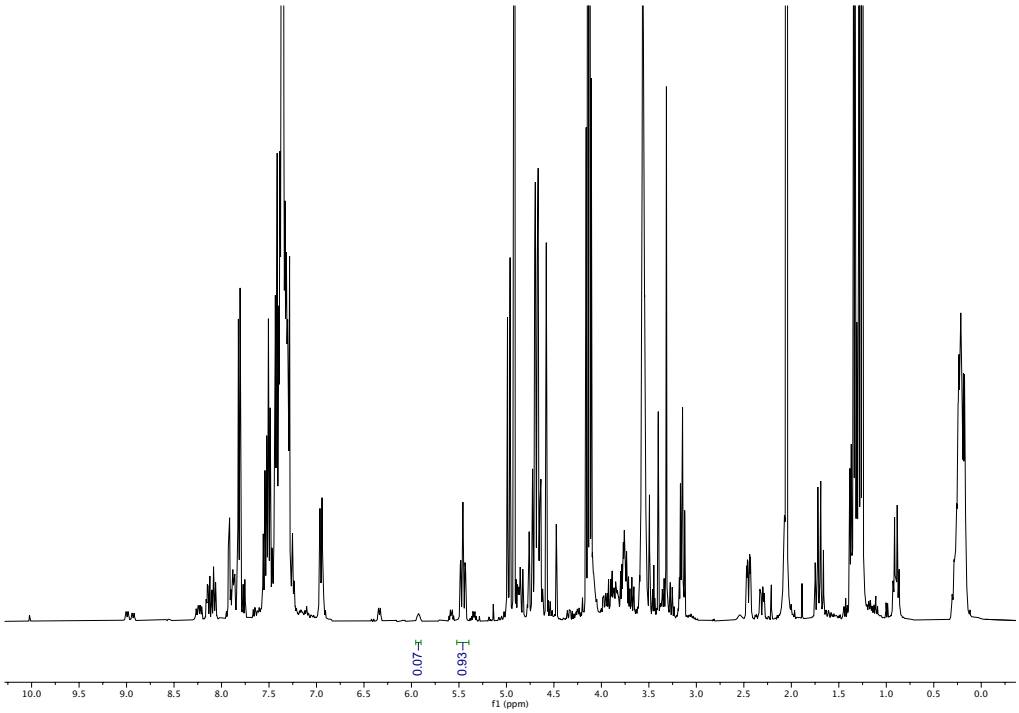

Crude ^{1}H-NMR (400 MHz, $CDCl_3$) en route to **4f**

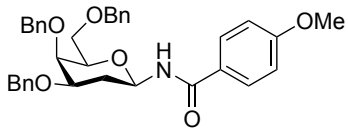

1-*N*-(4-methoxybenzoyl)-(2-deoxyl-3,4,6-*O*-benzyl-β-D-galactopyranosyl)-amine (4x). Following General Procedure B, 3,4,6-tri-*O*-benzyl-D-galactal (0.2 mmol, 83 mg) and 3-(4-methoxyphenyl)-1,4,2-dioxazol-5-one (0.4 mmol, 77 mg) were used, affording the title compound as a colorless oil (first run, 51 mg, 45%; second run, 64 mg, 56%). **^{1}H NMR** (500 MHz, CD_2Cl_2) δ 7.81 – 7.67 (m, 2H), 7.50 – 7.21 (m, 15H), 7.00 – 6.87 (m, 2H), 6.70 (d, *J* = 9.2 Hz, 1H), 5.41 (dt, *J* = 10.1, 3.0 Hz, 1H), 4.94 (d, *J* = 10.8 Hz, 1H), 4.66 (s, 2H), 4.57 (d, *J* = 10.8 Hz, 1H), 4.55 – 4.45 (m, 2H), 3.94 (d, *J* = 1.2 Hz, 1H), 3.83 (s, 3H), 3.80 – 3.69 (m, 2H), 3.68 – 3.55 (m, 2H), 2.22 – 2.00 (m, 2H) ppm. **^{13}C NMR** (126 MHz, CD_2Cl_2) δ 166.28, 163.14, 139.44, 139.04, 138.79, 129.52, 128.95, 128.91, 128.89, 128.81, 128.48, 128.23, 128.22, 128.15, 127.97, 126.56, 114.27, 78.30, 77.24,

75.94, 75.33, 73.94, 73.01, 71.04, 69.58, 55.97, 33.21 ppm. **IR (neat):** 3302, 3063, 3029, 2923, 2861, 1644, 1606, 1541, 1503, 1454, 1354, 1309, 1290, 1252, 1178, 1099, 1060, 1027, 846, 734, 695, 653, 612, 587 cm^{-1}. **HRMS (ESI)** *calcd.* for ($C_{35}H_{38}NO_6$) $[M+H]^+$: 568.2694, *found* 568.2707. **M.P.** :59 °C.

NMR spectroscopy of the crude reaction mixture prior to purification revealed the formation of **3x**-**4x** with a 9:91 α:β selectivity.

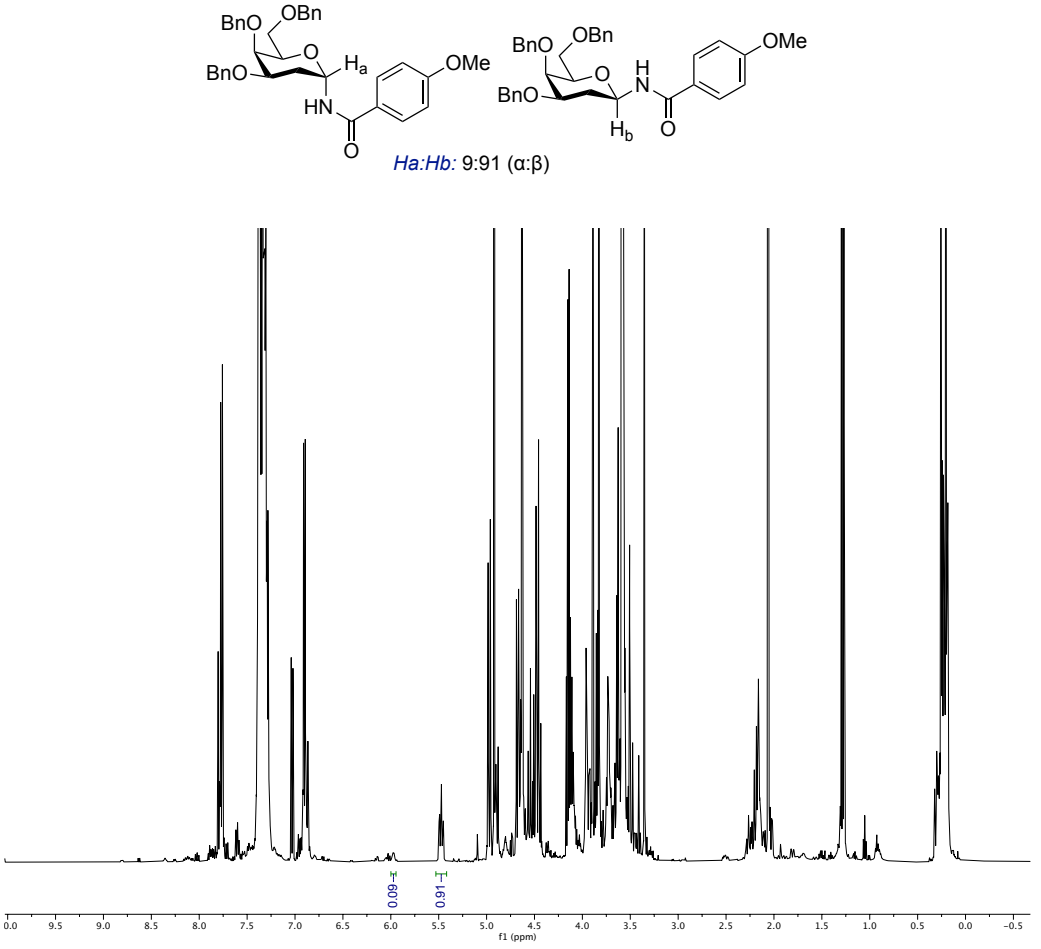

Crude ^{1}H-NMR (400 MHz, $CDCl_3$) en route to **4x**

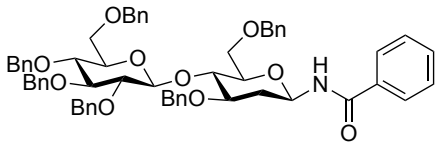

1-*N*-Benzoyl-(2-deoxyl-2',3,3',4',6,6'-*O*-benzyl-β-D-maltosyl)-amine (4j). Following General Procedure B, 2',3,3',4',6,6'-*O*-benzyl-D-cellobial (85 mg, 0.1 mmol, 1 equiv.) and **2a** (32 mg, 0.2 mmol, 2.0 equiv.) were used without TBAI, affording the title compound as a colorless oil (first run, 44 mg, 45%; second run; 38 mg, 39%). **^{1}H NMR** (500 MHz, $CDCl_3$) δ 7.80 – 7.72 (m, 2H), 7.60 – 7.48 (m, 1H), 7.42 (t, *J* = 7.6 Hz, 2H), 7.40 – 7.18 (m, 30H), 6.79 (d, *J* = 9.1 Hz, 1H), 5.50 (dt, *J* = 10.1, 2.3 Hz, 1H), 4.95 – 4.86 (m, 2H), 4.86 – 4.80 (m, 3H), 4.76 (d, *J* = 11.1 Hz, 1H), 4.70 (d, *J* = 12.3 Hz, 1H), 4.62 – 4.54 (m, 2H), 4.52 – 4.48 (m, 3H), 4.40 (d, *J* = 12.1 Hz, 1H), 4.06 (t, *J* = 8.7 Hz, 1H), 3.94 – 3.85 (m, 1H), 3.77 – 3.70 (m, 2H), 3.69 – 3.61 (m, 3H), 3.57 – 3.48 (m, 2H), 3.45 – 3.39 (m, 1H), 3.37 – 3.30 (m, 1H), 2.42 – 2.29 (m, 1H), 1.81 – 1.71 (m, 1H) ppm. **^{13}C NMR** (126 MHz, $CDCl_3$) δ 166.66, 139.10, 138.71, 138.53, 138.46, 138.42, 137.98, 133.78, 132.04, 128.70, 128.55, 128.51, 128.49, 128.47, 128.40, 128.39, 128.18, 127.98, 127.92, 127.85, 127.79, 127.77, 127.73, 127.53, 127.26, 102.71, 84.94, 82.79, 78.07, 77.03, 76.83, 76.60, 76.49, 75.75, 75.11, 75.09, 74.95, 73.51, 73.46, 72.53, 69.07, 68.28, 36.94 ppm. **IR (neat):** 3338, 3062, 3030, 2886, 1671, 1535, 1495, 1453, 1359, 1287, 1065, 1027, 909, 732, 695 cm^{-1}. **HRMS (ESI)** *calcd.* for ($C_{61}H_{63}NNaO_{10}$) $[M+Na]^+$: 992.4344, *found* 992.4323.

NMR spectroscopy of the crude reaction mixture prior to purification revealed the formation of **3j**-**4j** with a 10:90 α:β selectivity.

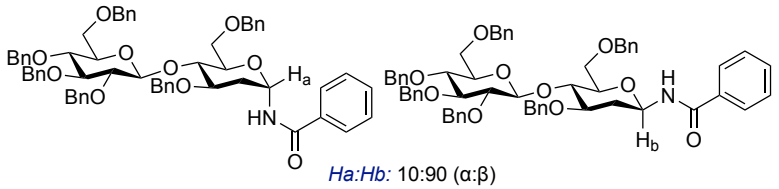

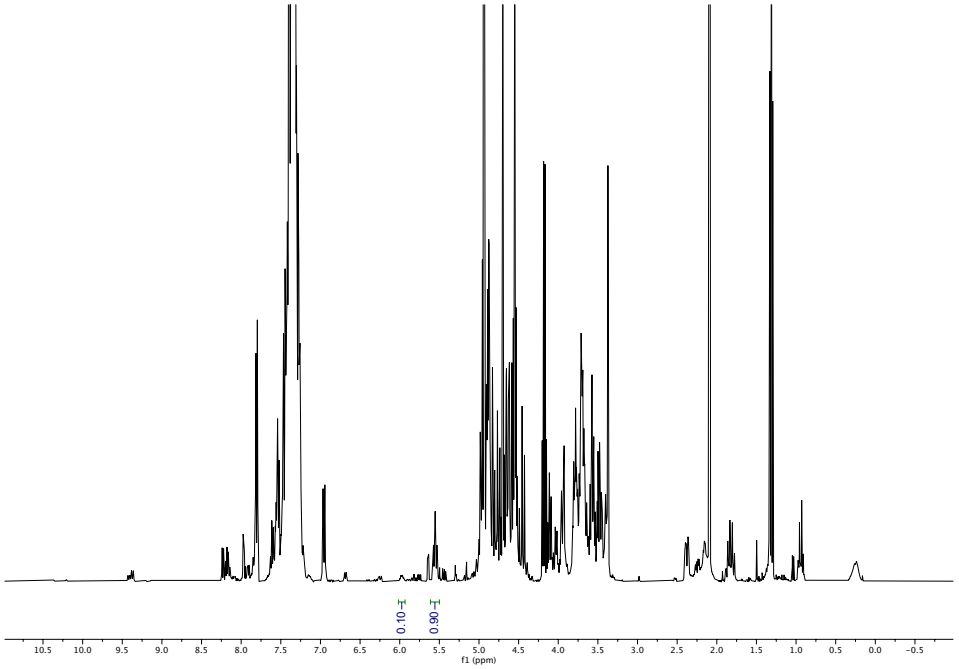

Crude ^{1}H-NMR (400 MHz, $CDCl_3$) en route to **4j**

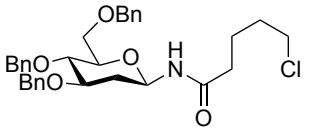

1-*N*-(4-chloropentoyl)-(2-deoxyl-3,4,6-*O*-benzyl-β-D-glucopyranosyl)-amine (4r). Following General Procedure B, 4,6-*O*-benzyl-D-glucal (0.2 mmol, 83 mg) and 3-(4-chlorobutyl)-1,4,2-dioxazol-5-one (0.4 mmol, 71 mg) were used, toluene (1 mL) was used for epimerization instead of MeCN, affording the title compound as a white solid (first run, 56 mg, 51%; second run, 51 mg, 46%). **^{1}H NMR** (400 MHz, $CDCl_3$) δ 7.39 – 7.22 (m, 13H), 7.21 – 7.12 (m, 2H), 6.20 (d, J = 9.3 Hz, 1H), 5.31 – 5.15 (m, 1H), 4.88 (d, J = 10.8 Hz, 1H), 4.72 – 4.56 (m, 3H), 4.50 (d, J = 10.8 Hz, 1H), 4.46 (d, J = 12.0 Hz, 1H), 3.80 – 3.65 (m, 3H), 3.62 (t, J = 9.1 Hz, 1H), 3.57 – 3.51 (m, 2H), 3.48 (dt, J = 9.5, 2.6 Hz, 1H), 2.30 – 2.11 (m, 3H), 1.87 – 1.72 (m, 4H), 1.61 – 1.49 (m, 1H) ppm. **^{13}C NMR** (101 MHz, $CDCl_3$) δ 171.92, 138.46, 138.34, 137.94, 128.60, 128.53, 128.49, 128.24, 128.04, 127.92, 127.89, 127.83, 79.89, 77.55, 76.63, 76.17, 75.12, 73.71, 71.88, 68.67,

44.69, 36.85, 35.62, 32.09, 22.57 ppm. **IR (neat):** 3303, 3064, 3029, 2924, 2867, 1650, 1539, 1495, 1452, 1361, 1302, 1267, 1228, 1208, 1105, 1089, 1074, 1037, 1026, 981, 949, 903, 735, 693, 643, 593, 563 cm^{-1}. **HRMS (ESI)** *calcd*. for ($C_{32}H_{38}ClNNaO_5$) $[M+Na]^+$: 574.2331, *found* 574.2339. **M.P.** :105 °C.

NMR spectroscopy of the crude reaction mixture prior to purification revealed the formation of **3r**-**4r** with a 6:94 α:β selectivity.

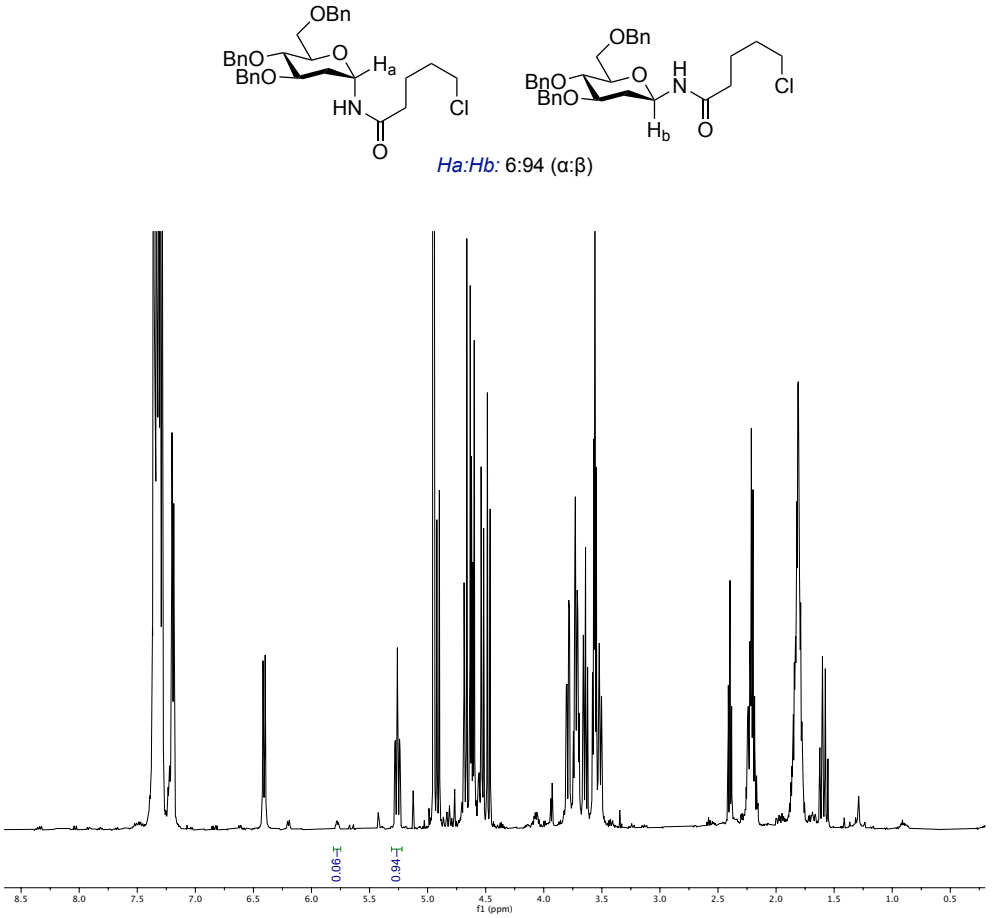

Crude ^{1}H-NMR (400 MHz, $CDCl_3$) en route to **4r**

3.9.5 Mechanistic Studies

Crossover experiments

Following General Procedure A, 3,4,6-tri-*O*-benzyl-D-glucal **1a** (0.2 mmol, 83 mg), 3-phenyl-1,4,2-dioxazol-5-one **2a** (0.3 mmol, 48 mg) and 4-methoxybenzamide (0.3 mmol, 45 mg) were used. The reaction resulted in **3a** (69 mg, 64%, 97:3 α:β), with not even traces of **3l** being detected in the crude mixtures. This experiment argues against a scenario consisting of nucleophilic addition of an amide to an in situ generated oxocarbenium ion.[28]

Isotope-labelling studies

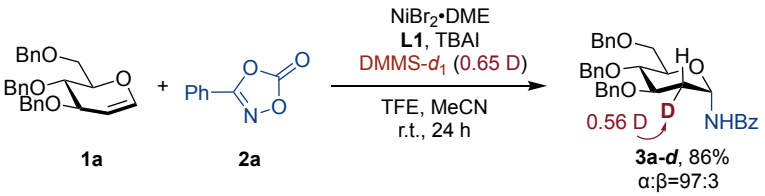

Following General Procedure A, 3,4,6-tri-*O*-benzyl-D-glucal **1a** (0.2 mmol, 83 mg) was reacted with 3-phenyl-1,4,2-dioxazol-5-one **2a** (0.4 mmol, 65 mg) and DMMS-d_1 (84.0 μL, 3.0 equiv., 0.65 D), affording **3a** (86%, 97:3 α:β). A significant deuterium incorporation was detected at C2. ^{1}H NMR (500 MHz, $CDCl_3$) δ 2.28 (dt, J = 13.5, 4.0 Hz, 0.44 H, Ha), 2.10 – 1.99 (m, 1H, Hb) ppm.

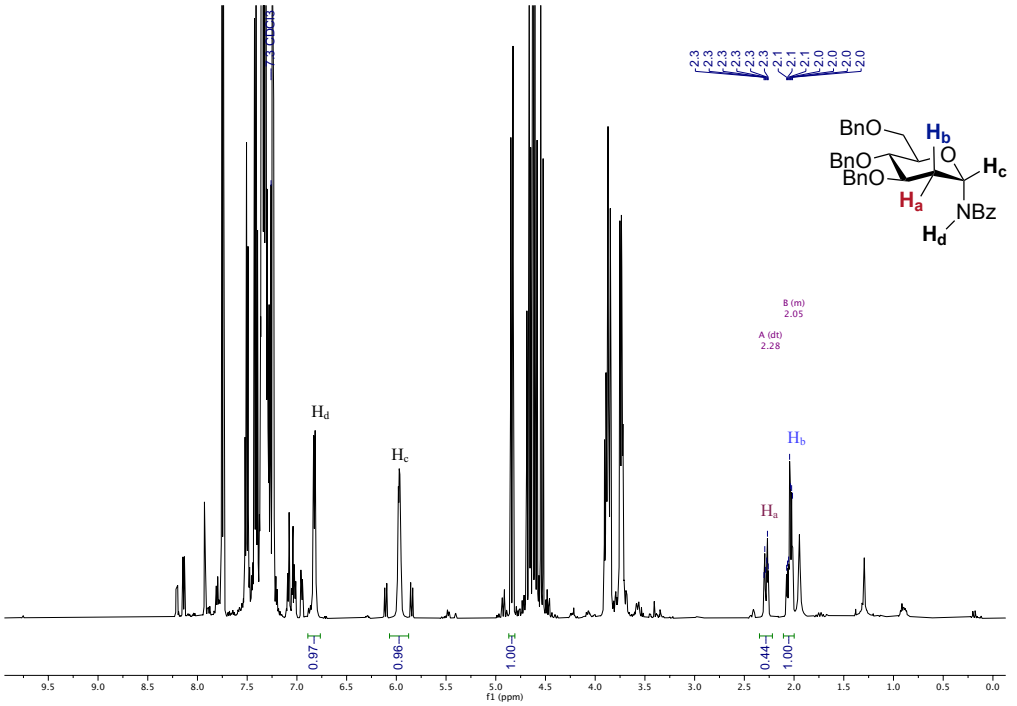
BnO
BnO
BnO
Hb
O
Hc
Ha
NBz
Hd
B (m)
2.05
A (dt)
2.28
Hd
Hc
Hb
Ha
0.97
0.96
1.00
0.44
1.00
f1 (ppm)

3.9.6 Crystallographic Data

X-ray diffraction of 3m

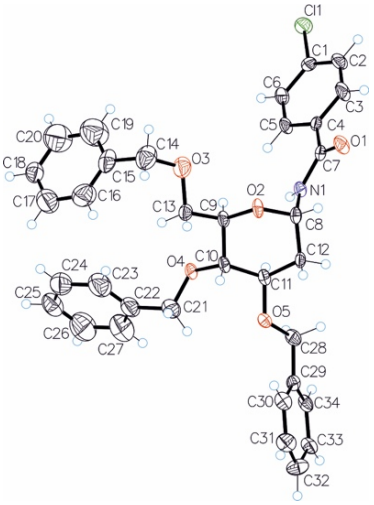

Figure 3.2 ORTEP diagram of **3m**, deposition number : 2386798

Table 3.7 Crystal data and structure refinement for **3m**.

Empirical formula	$C_{34}H_{34}ClNO_5$
Formula weight	572.07
Temperature/K	100.06
Crystal system	orthorhombic
Space group	$P2_12_12_1$
a/Å	5.0808(19)
b/Å	17.494(7)
c/Å	32.176(11)
α/°	90
β/°	90
γ/°	90
Volume/Å^3	2859.9(18)
Z	4
ρ_{calc}g/cm^3	1.329
μ/mm^{-1}	0.178

Table 3.7 Crystal data and structure refinement for **3m**.

F(000)	1208.0
Crystal size/mm^3	0.3 × 0.2 × 0.2
Radiation	MoKα (λ = 0.71073)
2Θ range for data collection/°	2.65 to 51.346
Index ranges	-6 ≤ h ≤ 5, -21 ≤ k ≤ 15, -39 ≤ l ≤ 38
Reflections collected	21354
Independent reflections	5399 [R_{int} = 0.0655, R_{sigma} = 0.0597]
Data/restraints/parameters	5399/193/469
Goodness-of-fit on F^2	1.030
Final R indexes [I>=2σ (I)]	R_1 = 0.0723, wR_2 = 0.1746
Final R indexes [all data]	R_1 = 0.0908, wR_2 = 0.1867
Largest diff. peak/hole / e Å^{-3}	0.72/-0.39
Flack parameter	0.08(5)

Table 3.8. Fractional Atomic Coordinates (×10^4) and Equivalent Isotropic Displacement Parameters (Å^2×10^3) for **3m**. U_{eq} is defined as 1/3 of the trace of the orthogonalised U_{IJ} tensor.

Atom	*x*	*y*	*z*	U(eq)
Cl1	11255(3)	11128.7(8)	4143.3(5)	35.1(4)
O1	2084(8)	8733(2)	4830.0(12)	32.4(10)
O2	6(7)	7453(2)	4043.4(11)	26.7(9)
O4	3469(9)	6289(2)	3284.1(11)	31.7(10)
O5	3959(8)	5408(2)	4052.9(11)	25.4(8)
N1	3890(10)	7904(3)	4371.9(13)	23.9(10)
C1	9184(12)	10371(3)	4270.7(17)	25.7(12)
C2	7690(14)	10409(4)	4625(2)	36.3(16)
C3	6006(16)	9813(4)	4718.2(19)	38.6(16)
C4	5778(11)	9189(3)	4459.6(16)	21.4(12)
C5	7310(11)	9160(3)	4106.3(17)	25.7(12)
C6	9028(13)	9746(3)	4008.0(18)	31.3(13)
C7	3758(12)	8599(3)	4570.7(16)	23.8(12)
C8	1734(11)	7370(3)	4393.5(16)	23.3(12)

Table 3.8. Fractional Atomic Coordinates ($\times 10^4$) and Equivalent Isotropic Displacement Parameters ($Å^2 \times 10^3$) for **3m**. U_{eq} is defined as 1/3 of the trace of the orthogonalised U_{IJ} tensor.

Atom	*x*	*y*	*z*	U(eq)
C9	1227(12)	7252(3)	3656.7(15)	23.6(12)
C10	2084(11)	6411(3)	3661.4(16)	23.3(12)
C11	3802(11)	6220(3)	4037.4(15)	23.2(11)
C12	2568(11)	6545(3)	4436.3(16)	22.3(12)
C28	6110(13)	5140(3)	4299.5(18)	29.5(13)
C29	6023(11)	4280(3)	4322.4(16)	23.0(12)
C32	6129(14)	2694(4)	4396(2)	39.2(16)
C30	3770(20)	3891(7)	4284(4)	30(3)
C31	3800(30)	3110(7)	4331(4)	38(3)
C33	8440(30)	3145(7)	4448(4)	31(3)
C34	8370(20)	3944(7)	4395(4)	29(3)
C30'	5180(20)	3809(7)	4003(4)	28(3)
C31'	5290(20)	2998(7)	4017(4)	30(3)
C33'	6900(20)	3075(7)	4700(5)	34(3)
C34'	6840(20)	3869(7)	4691(4)	26(3)
O3	-1340(20)	8161(8)	3275(5)	51(3)
C13	-710(30)	7325(7)	3313(5)	27(2)
C14	-3170(30)	8293(10)	2948(5)	60(4)
C15	-2056(19)	8227(6)	2515(2)	49(5)
C16	-2639(18)	7556(5)	2302(3)	65(4)
C17	-1690(19)	7446(5)	1901(3)	66(4)
C18	-158(18)	8006(6)	1713(2)	43(3)
C19	420(20)	8676(5)	1926(3)	90(6)
C20	-520(20)	8787(5)	2327(3)	90(5)
O3'	-570(50)	8296(17)	3271(10)	51(3)
C13'	-580(70)	7551(15)	3302(11)	27(2)
C14'	-2570(60)	8580(20)	2993(10)	60(4)
C15'	-2100(30)	8341(11)	2554(4)	60(12)
C16'	-3950(20)	8220(12)	2243(5)	78(8)
C17'	-3170(30)	8197(11)	1829(5)	70(8)
C18'	-540(30)	8294(10)	1726(4)	45(7)
C19'	1320(20)	8415(10)	2037(4)	39(5)

Table 3.8. Fractional Atomic Coordinates ($\times 10^4$) and Equivalent Isotropic Displacement Parameters ($Å^2 \times 10^3$) for **3m**. U_{eq} is defined as 1/3 of the trace of the orthogonalised U_{IJ} tensor.

Atom	*x*	*y*	*z*	U(eq)
C20'	540(30)	8438(10)	2450(4)	57(7)
C21	2950(30)	5561(7)	3103(3)	49(2)
C22	3768(18)	5584(5)	2657.0(17)	50(2)
C23	2123(14)	5954(5)	2376(2)	69(4)
C24	2758(15)	5967(5)	1956(2)	63(3)
C25	5037(16)	5611(5)	1816.7(18)	56(3)
C26	6682(15)	5241(5)	2097(3)	85(4)
C27	6047(17)	5228(5)	2517(2)	84(4)
C21'	4360(90)	5570(20)	3112(8)	49(2)
C22'	4350(50)	5671(12)	2644(5)	50(2)
C23'	4180(50)	6364(10)	2434(6)	48(8)
C24'	4230(50)	6377(10)	2002(6)	52(9)
C25'	4450(50)	5699(13)	1780(5)	56(3)
C26'	4630(60)	5006(10)	1990(7)	66(11)
C27'	4580(50)	4993(10)	2422(7)	55(10)

Table 3.9 Anisotropic Displacement Parameters ($Å^2 \times 10^3$) for **3m**. The Anisotropic displacement factor exponent takes the form: $-2\pi^2[h^2a^{*2}U_{11}+2hka^*b^*U_{12}+\ldots]$.

Atom	U_{11}	U_{22}	U_{33}	U_{23}	U_{13}	U_{12}
Cl1	42.0(8)	30.0(7)	33.3(8)	-0.8(7)	8.0(7)	-5.4(7)
O1	35(2)	37(2)	25(2)	-9.7(19)	12.6(18)	-6.1(19)
O2	24.4(18)	43(2)	12.9(18)	-4.8(17)	2.5(16)	5.0(18)
O4	48(3)	31(2)	15.5(18)	-4.7(17)	5.3(19)	10(2)
O5	30(2)	22.7(19)	23.6(19)	-3.8(16)	-4.8(18)	-4.2(17)
N1	28(2)	27(2)	16(2)	-2.9(19)	5(2)	3(2)
C1	30(3)	21(3)	25(3)	4(2)	3(3)	-2(2)
C2	55(4)	27(3)	26(3)	-8(3)	13(3)	-3(3)
C3	56(4)	39(4)	21(3)	-10(3)	18(3)	-12(3)
C4	28(3)	23(3)	13(2)	2(2)	1(2)	6(2)
C5	30(3)	29(3)	18(3)	-7(2)	7(2)	-1(2)
C6	40(3)	34(3)	20(3)	-4(2)	12(3)	2(3)
C7	32(3)	27(3)	13(2)	1(2)	0(3)	1(3)

Table 3.9 Anisotropic Displacement Parameters ($Å^2 \times 10^3$) for **3m**. The Anisotropic displacement factor exponent takes the form: $-2\pi^2[h^2a^{*2}U_{11}+2hka^*b^*U_{12}+\ldots]$.

Atom	U_{11}	U_{22}	U_{33}	U_{23}	U_{13}	U_{12}
C8	25(3)	32(3)	14(3)	-1(2)	3(2)	-1(2)
C9	26(3)	31(3)	14(3)	-4(2)	3(2)	5(3)
C10	26(3)	30(3)	14(3)	-5(2)	4(2)	-3(2)
C11	24(2)	28(3)	18(3)	-4(2)	1(2)	-3(3)
C12	29(3)	27(3)	11(3)	1(2)	0(2)	-2(2)
C28	27(3)	30(3)	31(3)	-6(2)	-5(3)	-5(3)
C29	22(3)	27(3)	20(3)	-1(2)	4(3)	-2(2)
C32	34(3)	30(3)	53(4)	9(3)	8(4)	1(3)
C30	20(5)	36(7)	33(7)	-6(5)	0(6)	2(6)
C31	34(7)	38(7)	43(8)	-1(6)	8(7)	-11(6)
C33	24(7)	33(7)	35(7)	-13(6)	-9(6)	13(5)
C34	22(6)	33(7)	30(7)	-11(5)	-12(5)	4(5)
C30'	33(6)	31(7)	19(6)	2(5)	-4(5)	1(5)
C31'	18(5)	28(7)	44(7)	-12(6)	11(5)	-1(5)
C33'	23(7)	26(7)	52(9)	10(6)	-9(7)	-3(5)
C34'	15(5)	38(7)	24(6)	-1(5)	-1(4)	1(5)
O3	60(5)	56(4)	37(3)	-4(3)	-6(4)	24(4)
C13	30(3)	31(5)	20(3)	1(4)	2(2)	4(4)
C14	59(5)	71(6)	49(4)	6(4)	1(4)	19(4)
C15	42(6)	71(7)	35(6)	5(5)	-2(4)	32(5)
C16	76(6)	57(6)	62(6)	8(5)	14(5)	-5(5)
C17	79(6)	64(6)	55(6)	-8(5)	6(5)	-7(5)
C18	43(5)	50(6)	36(5)	-2(4)	0(4)	12(5)
C19	93(8)	88(8)	89(7)	-2(6)	22(6)	-4(6)
C20	99(8)	84(7)	88(7)	-8(6)	21(6)	-6(6)
O3'	60(5)	56(4)	37(3)	-4(3)	-6(4)	24(4)
C13'	30(3)	31(5)	20(3)	1(4)	2(2)	4(4)
C14'	59(5)	71(6)	49(4)	6(4)	1(4)	19(4)
C15'	61(13)	67(13)	53(13)	2(6)	-1(7)	10(6)
C16'	74(10)	86(10)	74(10)	4(6)	1(7)	-1(7)
C17'	66(10)	79(10)	65(9)	-1(6)	3(6)	-2(6)
C18'	40(8)	55(9)	41(8)	-2(6)	2(6)	2(6)
C19'	31(7)	50(7)	37(7)	5(6)	-7(6)	11(6)

Table 3.9 Anisotropic Displacement Parameters ($Å^2 \times 10^3$) for **3m**. The Anisotropic displacement factor exponent takes the form: $-2\pi^2[h^2a^{*2}U_{11}+2hka^*b^*U_{12}+\ldots]$.

Atom	U_{11}	U_{22}	U_{33}	U_{23}	U_{13}	U_{12}
C20'	59(9)	61(9)	51(8)	5(6)	-17(6)	10(6)
C21	69(5)	40(4)	38(3)	-7(3)	9(4)	1(4)
C22	72(5)	42(4)	38(3)	-8(3)	12(3)	-8(4)
C23	89(6)	62(6)	57(5)	-9(5)	18(5)	-7(5)
C24	81(6)	55(5)	54(5)	0(4)	-1(5)	-17(5)
C25	61(5)	59(4)	48(4)	-13(3)	15(3)	-20(3)
C26	84(7)	93(7)	77(6)	-16(5)	17(5)	4(5)
C27	102(7)	84(6)	68(6)	-18(5)	3(6)	5(6)
C21'	69(5)	40(4)	38(3)	-7(3)	9(4)	1(4)
C22'	72(5)	42(4)	38(3)	-8(3)	12(3)	-8(4)
C23'	52(10)	47(10)	45(10)	1(6)	-2(6)	8(6)
C24'	51(10)	54(10)	50(10)	1(6)	2(6)	2(7)
C25'	61(5)	59(4)	48(4)	-13(3)	15(3)	-20(3)
C26'	68(12)	66(12)	63(12)	-8(7)	-2(7)	5(7)
C27'	58(11)	55(11)	51(11)	-2(6)	6(7)	5(7)

Table 3.10 Bond Lengths for **3m**.

Atom	Atom	Length/Å	Atom	Atom	Length/Å
Cl1	C1	1.742(6)	C30'	C31'	1.421(17)
O1	C7	1.214(7)	C33'	C34'	1.390(17)
O2	C8	1.435(7)	O3	C13	1.503(18)
O2	C9	1.434(6)	O3	C14	1.42(2)
O4	C10	1.420(6)	C14	C15	1.509(17)
O4	C21	1.424(12)	C15	C16	1.3900
O4	C21'	1.44(4)	C15	C20	1.3900
O5	C11	1.425(6)	C16	C17	1.3900
O5	C28	1.430(7)	C17	C18	1.3900
N1	C7	1.376(7)	C18	C19	1.3900
N1	C8	1.441(7)	C19	C20	1.3900

Table 3.10 Bond Lengths for **3m**.

Atom	Atom	Length/Å	Atom	Atom	Length/Å
C1	C2	1.372(8)	O3'	C13'	1.31(4)
C1	C6	1.384(8)	O3'	C14'	1.44(4)
C2	C3	1.382(9)	C14'	C15'	1.49(3)
C3	C4	1.377(8)	C15'	C16'	1.3900
C4	C5	1.379(8)	C15'	C20'	1.3900
C4	C7	1.498(8)	C16'	C17'	1.3900
C5	C6	1.383(9)	C17'	C18'	1.3900
C8	C12	1.512(8)	C18'	C19'	1.3900
C9	C10	1.535(8)	C19'	C20'	1.3900
C9	C13	1.485(18)	C21	C22	1.496(11)
C9	C13'	1.55(3)	C22	C23	1.3900
C10	C11	1.529(7)	C22	C27	1.3900
C11	C12	1.537(7)	C23	C24	1.3900
C28	C29	1.507(8)	C24	C25	1.3900
C29	C30	1.336(13)	C25	C26	1.3900
C29	C34	1.350(13)	C26	C27	1.3900
C29	C30'	1.386(13)	C21'	C22'	1.51(2)
C29	C34'	1.447(12)	C22'	C23'	1.3900
C32	C31	1.404(16)	C22'	C27'	1.3900
C32	C33	1.424(15)	C23'	C24'	1.3900
C32	C31'	1.396(15)	C24'	C25'	1.3900
C32	C33'	1.246(15)	C25'	C26'	1.3900
C30	C31	1.376(18)	C26'	C27'	1.3900
C33	C34	1.408(17)			

Table 3.11 Bond Angles for **3m**.

Atom	Atom	Atom	Angle/°	Atom	Atom	Atom	Angle/°
C9	O2	C8	113.1(4)	C29	C34	C33	118.3(10)
C10	O4	C21	113.1(6)	C29	C30'	C31'	123.8(10)
C10	O4	C21'	128.0(13)	C32	C31'	C30'	114.9(10)
C11	O5	C28	112.9(4)	C32	C33'	C34'	120.6(12)
C7	N1	C8	120.9(5)	C33'	C34'	C29	121.4(11)
C2	C1	Cl1	119.5(5)	C14	O3	C13	111.0(13)
C2	C1	C6	121.0(6)	C9	C13	O3	106.6(11)
C6	C1	Cl1	119.5(4)	O3	C14	C15	115.2(12)
C1	C2	C3	119.1(6)	C16	C15	C14	116.1(9)
C4	C3	C2	121.3(6)	C16	C15	C20	120.0
C3	C4	C5	118.7(6)	C20	C15	C14	123.9(9)
C3	C4	C7	117.3(5)	C15	C16	C17	120.0
C5	C4	C7	123.9(5)	C18	C17	C16	120.0
C4	C5	C6	121.2(5)	C19	C18	C17	120.0
C5	C6	C1	118.8(5)	C18	C19	C20	120.0
O1	C7	N1	121.6(5)	C19	C20	C15	120.0
O1	C7	C4	120.7(5)	C13'	O3'	C14'	113(3)
N1	C7	C4	117.7(5)	O3'	C13'	C9	113(3)
O2	C8	N1	111.2(4)	O3'	C14'	C15'	112(2)
O2	C8	C12	109.8(4)	C16'	C15'	C14'	127.9(16)
N1	C8	C12	114.2(5)	C16'	C15'	C20'	120.0
O2	C9	C10	110.4(4)	C20'	C15'	C14'	110.3(17)
O2	C9	C13	109.8(8)	C15'	C16'	C17'	120.0
O2	C9	C13'	107.4(13)	C18'	C17'	C16'	120.0
C10	C9	C13'	119.8(11)	C19'	C18'	C17'	120.0
C13	C9	C10	106.1(6)	C18'	C19'	C20'	120.0
O4	C10	C9	106.0(4)	C19'	C20'	C15'	120.0
O4	C10	C11	111.2(5)	O4	C21	C22	108.4(8)
C11	C10	C9	112.3(4)	C23	C22	C21	118.0(7)
O5	C11	C10	106.1(4)	C23	C22	C27	120.0
O5	C11	C12	111.2(4)	C27	C22	C21	121.9(7)
C10	C11	C12	110.3(4)	C24	C23	C22	120.0
C8	C12	C11	113.0(4)	C25	C24	C23	120.0
O5	C28	C29	109.4(5)	C24	C25	C26	120.0

Table 3.11 Bond Angles for **3m**.

Atom	Atom	Atom	Angle/°	Atom	Atom	Atom	Angle/°
C30	C29	C28	121.9(7)	C27	C26	C25	120.0
C30	C29	C34	123.4(8)	C26	C27	C22	120.0
C34	C29	C28	114.6(7)	O4	C21'	C22'	107(2)
C30'	C29	C28	124.5(7)	C23'	C22'	C21'	126(2)
C30'	C29	C34'	113.6(8)	C23'	C22'	C27'	120.0
C34'	C29	C28	121.9(7)	C27'	C22'	C21'	114(2)
C31	C32	C33	115.2(8)	C22'	C23'	C24'	120.0
C33'	C32	C31'	125.3(9)	C23'	C24'	C25'	120.0
C29	C30	C31	119.1(11)	C26'	C25'	C24'	120.0
C30	C31	C32	122.7(12)	C27'	C26'	C25'	120.0
C34	C33	C32	121.0(10)	C26'	C27'	C22'	120.0

Table 3.12 Torsion Angles for **3m**.

A	B	C	D	Angle/°	A	B	C	D	Angle/°
Cl1	C1	C2	C3	178.4(6)	C32	C33'	C34'	C29	-3.4(18)
Cl1	C1	C6	C5	-177.9(5)	C30	C29	C34	C33	-2.2(16)
O2	C8	C12	C11	54.6(6)	C31	C32	C33	C34	-5.7(16)
O2	C9	C10	O4	-174.8(4)	C33	C32	C31	C30	5.3(17)
O2	C9	C10	C11	-53.3(6)	C34	C29	C30	C31	1.8(16)
O2	C9	C13	O3	66.5(12)	C30'	C29	C34'	C33'	4.0(14)
O2	C9	C13'	O3'	70(3)	C31'	C32	C33'	C34'	3.7(18)
O4	C10	C11	O5	-74.0(5)	C33'	C32	C31'	C30'	-4.4(16)
O4	C10	C11	C12	165.5(4)	C34'	C29	C30'	C31'	-5.0(14)
O4	C21	C22	C23	-77.0(11)	O3	C14	C15	C16	102.8(13)
O4	C21	C22	C27	105.3(9)	O3	C14	C15	C20	-77.2(15)
O4	C21'	C22'	C23'	15(4)	C13	C9	C10	O4	66.2(8)
O4	C21'	C22'	C27'	-166(2)	C13	C9	C10	C11	-172.3(8)
O5	C11	C12	C8	-165.5(4)	C13	O3	C14	C15	-73.9(16)
O5	C28	C29	C30	-26.8(9)	C14	O3	C13	C9	179.3(11)
O5	C28	C29	C34	154.9(7)	C14	C15	C16	C17	-180.0(10)
O5	C28	C29	C30'	34.3(10)	C14	C15	C20	C19	180.0(10)
O5	C28	C29	C34'	-145.6(7)	C15	C16	C17	C18	0.0
N1	C8	C12	C11	-71.1(6)	C16	C15	C20	C19	0.0

Table 3.12 Torsion Angles for **3m**.

A	B	C	D	Angle/°	A	B	C	D	Angle/°
C1	C2	C3	C4	-0.8(11)	C16	C17	C18	C19	0.0
C2	C1	C6	C5	0.7(10)	C17	C18	C19	C20	0.0
C2	C3	C4	C5	1.3(10)	C18	C19	C20	C15	0.0
C2	C3	C4	C7	-175.6(6)	C20	C15	C16	C17	0.0
C3	C4	C5	C6	-0.7(9)	O3'	C14'	C15'	C16'	151(2)
C3	C4	C7	O1	13.2(9)	O3'	C14'	C15'	C20'	-44(3)
C3	C4	C7	N1	-166.2(6)	C13'	C9	C10	O4	59.6(15)
C4	C5	C6	C1	-0.3(9)	C13'	C9	C10	C11	-178.8(15)
C5	C4	C7	O1	-163.5(6)	C13'	O3'	C14'	C15'	-66(4)
C5	C4	C7	N1	17.1(8)	C14'	O3'	C13'	C9	-170(2)
C6	C1	C2	C3	-0.2(10)	C14'	C15'	C16'	C17'	163(2)
C7	N1	C8	O2	94.3(6)	C14'	C15'	C20'	C19'	-166.0(19)
C7	N1	C8	C12	-140.7(5)	C15'	C16'	C17'	C18'	0.0
C7	C4	C5	C6	176.0(6)	C16'	C15'	C20'	C19'	0.0
C8	O2	C9	C10	61.2(6)	C16'	C17'	C18'	C19'	0.0
C8	O2	C9	C13	178.0(6)	C17'	C18'	C19'	C20'	0.0
C8	O2	C9	C13'	-166.5(12)	C18'	C19'	C20'	C15'	0.0
C8	N1	C7	O1	13.9(8)	C20'	C15'	C16'	C17'	0.0
C8	N1	C7	C4	-166.8(5)	C21	O4	C10	C9	-141.6(7)
C9	O2	C8	N1	65.7(6)	C21	O4	C10	C11	96.2(8)
C9	O2	C8	C12	-61.8(6)	C21	C22	C23	C24	-177.8(8)
C9	C10	C11	O5	167.5(4)	C21	C22	C27	C26	177.7(9)
C9	C10	C11	C12	46.9(6)	C22	C23	C24	C25	0.0
C10	O4	C21	C22	162.2(7)	C23	C22	C27	C26	0.0
C10	O4	C21'	C22'	150.4(16)	C23	C24	C25	C26	0.0
C10	C9	C13	O3	-174.1(9)	C24	C25	C26	C27	0.0
C10	C9	C13'	O3'	-163(2)	C25	C26	C27	C22	0.0
C10	C11	C12	C8	-48.1(6)	C27	C22	C23	C24	0.0
C11	O5	C28	C29	176.3(4)	C21'	O4	C10	C9	-171(2)
C28	O5	C11	C10	161.5(4)	C21'	O4	C10	C11	67(2)
C28	O5	C11	C12	-78.5(6)	C21'	C22'	C23'	C24'	179(3)
C28	C29	C30	C31	-176.4(9)	C21'	C22'	C27'	C26'	-179(3)
C28	C29	C34	C33	176.1(9)	C22'	C23'	C24'	C25'	0.0
C28	C29	C30'	C31'	175.1(9)	C23'	C22'	C27'	C26'	0.0

Table 3.12 Torsion Angles for **3m**.

A	B	C	D	Angle/°	A	B	C	D	Angle/°
C28	C29	C34'	C33'	-176.1(9)	C23'	C24'	C25'	C26'	0.0
C29	C30	C31	C32	-3.5(19)	C24'	C25'	C26'	C27'	0.0
C29	C30'	C31'	C32	5.2(16)	C25'	C26'	C27'	C22'	0.0
C32	C33	C34	C29	4.3(18)	C27'	C22'	C23'	C24'	0.0

Table 3.13 Hydrogen Atom Coordinates ($Å \times 10^4$) and Isotropic Displacement Parameters ($Å^2 \times 10^3$) for **3m**.

Atom	*x*	*y*	*z*	U(eq)
H1	5310.27	7783.66	4229.75	29
H2	7811.89	10838.86	4804.55	44
H3	4984.95	9833.49	4965.3	46
H5	7183.72	8729.51	3927.3	31
H6	10082.64	9719.73	3764.55	38
H8	690.69	7501.53	4647.2	28
H9	2779.57	7589.53	3603.75	28
H9B	2883.1	7559.39	3640.41	28
H10	483.16	6078.12	3665.6	28
H11	5601.54	6440.45	3997.81	28
H12A	1012.99	6232.63	4511.08	27
H12B	3857.28	6502.18	4665.81	27
H28A	5993.91	5358.43	4582.72	35
H28B	7795.11	5306.21	4174.16	35
H32	6159.74	2151.57	4405.61	47
H32A	6110.47	2153.73	4424.4	47
H30	2173.67	4151.25	4224.68	36
H31	2180.31	2840.2	4318.08	46
H33	10052.77	2903.06	4518.11	37
H34	9937.58	4239.34	4411.13	34
H30'	4477.57	4042.17	3759.9	33

Table 3.13 Hydrogen Atom Coordinates (Å×10^4) and Isotropic Displacement Parameters (Å^2×10^3) for **3m**.

Atom	*x*	*y*	*z*	U(eq)
H31'	4834.35	2685.9	3786.87	36
H33'	7532.1	2819.23	4940.96	41
H34'	7341.48	4147.33	4931.37	31
H13A	-2317.48	7028.55	3375.92	32
H13B	54.51	7131.58	3049.84	32
H14A	-3920.31	8811.89	2981.58	72
H14B	-4637.38	7923.31	2975.79	72
H16	-3685.54	7173.08	2430.46	78
H17	-2087.92	6987.21	1755.9	79
H18	490.57	7930.26	1439.33	51
H19	1471.45	9059.18	1797.32	108
H20	-126.15	9245.07	2471.88	108
H13C	11.5	7328.05	3035.14	32
H13D	-2402.19	7374.87	3353.35	32
H14C	-2614.79	9142.21	3008.08	72
H14D	-4304.69	8382.8	3083.52	72
H16'	-5751.93	8153.61	2313.93	93
H17'	-4439.92	8114.1	1617.15	84
H18'	-3.91	8278.07	1443.15	55
H19'	3120.11	8481.58	1965.92	47
H20'	1808.15	8521.1	2662.71	69
H21A	1052.26	5440.7	3124.63	59
H21B	3949.72	5159.6	3252.39	59
H23	565.2	6197.93	2471.73	83
H24	1633.8	6220.2	1764.43	76
H25	5471.22	5619.9	1529.52	67
H26	8240.1	4997.33	2001.91	102

Table 3.13 Hydrogen Atom Coordinates (Å×10^4) and Isotropic Displacement Parameters (Å^2×10^3) for **3m**.

Atom	*x*	*y*	*z*	U(eq)
H27	7171.55	4975.05	2709.2	101
H21C	3163.02	5153.9	3194.39	59
H21D	6153.31	5453.56	3211.72	59
H23'	4021.39	6827.47	2585.68	58
H24'	4106.57	6850.72	1858.66	62
H25'	4487.21	5708.26	1485.24	67
H26'	4782.69	4542.55	1838.81	79
H27'	4697.51	4519.29	2565.83	66

Table 3.14 Atomic Occupancy for **3m**.

Atom	Occupancy	Atom	Occupancy	Atom	Occupancy
H9	0.500(8)	H9B	0.500(8)	H32	0.500(8)
H32A	0.500(8)	C30	0.500(8)	H30	0.500(8)
C31	0.500(8)	H31	0.500(8)	C33	0.500(8)
H33	0.500(8)	C34	0.500(8)	H34	0.500(8)
C30'	0.500(8)	H30'	0.500(8)	C31'	0.500(8)
H31'	0.500(8)	C33'	0.500(8)	H33'	0.500(8)
C34'	0.500(8)	H34'	0.500(8)	O3	0.652(10)
C13	0.652(10)	H13A	0.652(10)	H13B	0.652(10)
C14	0.652(10)	H14A	0.652(10)	H14B	0.652(10)
C15	0.652(10)	C16	0.652(10)	H16	0.652(10)
C17	0.652(10)	H17	0.652(10)	C18	0.652(10)
H18	0.652(10)	C19	0.652(10)	H19	0.652(10)
C20	0.652(10)	H20	0.652(10)	O3'	0.348(10)
C13'	0.348(10)	H13C	0.348(10)	H13D	0.348(10)

Atom	Occupancy	Atom	Occupancy	Atom	Occupancy
C14'	0.348(10)	H14C	0.348(10)	H14D	0.348(10)
C15'	0.348(10)	C16'	0.348(10)	H16'	0.348(10)
C17'	0.348(10)	H17'	0.348(10)	C18'	0.348(10)
H18'	0.348(10)	C19'	0.348(10)	H19'	0.348(10)
C20'	0.348(10)	H20'	0.348(10)	C21	0.759(10)
H21A	0.759(10)	H21B	0.759(10)	C22	0.759(10)
C23	0.759(10)	H23	0.759(10)	C24	0.759(10)
H24	0.759(10)	C25	0.759(10)	H25	0.759(10)
C26	0.759(10)	H26	0.759(10)	C27	0.759(10)
H27	0.759(10)	C21'	0.241(10)	H21C	0.241(10)
H21D	0.241(10)	C22'	0.241(10)	C23'	0.241(10)
H23'	0.241(10)	C24'	0.241(10)	H24'	0.241(10)
C25'	0.241(10)	H25'	0.241(10)	C26'	0.241(10)
H26'	0.241(10)	C27'	0.241(10)	H27'	0.241(10)

3.9.7 Representative set of NMR Spectra

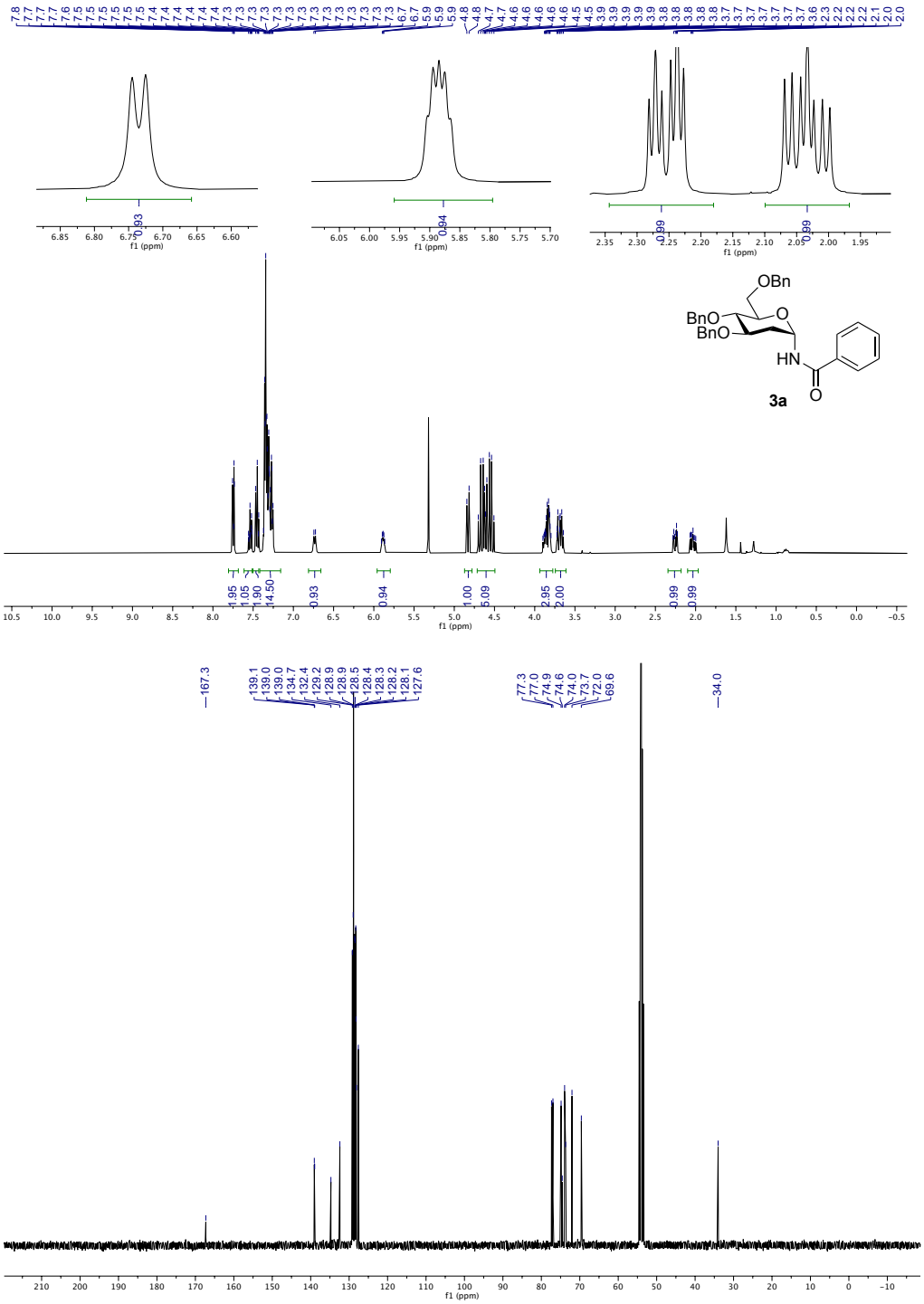
OBn
BnO
BnO
O
HN
O
3a
f1 (ppm)

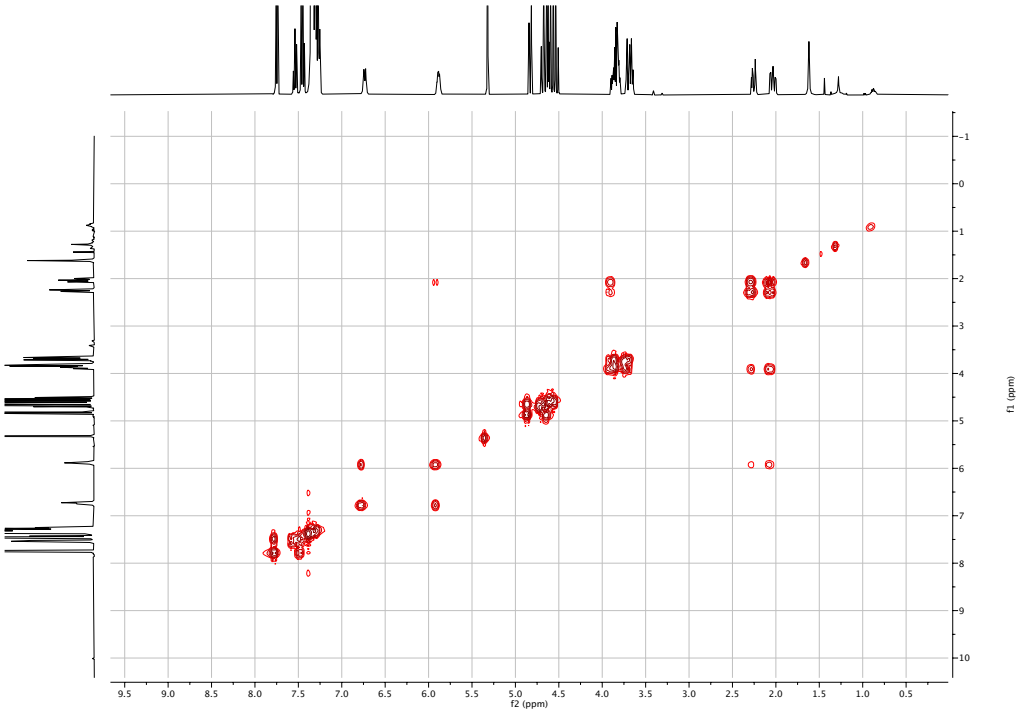
f2 (ppm)
f1 (ppm)

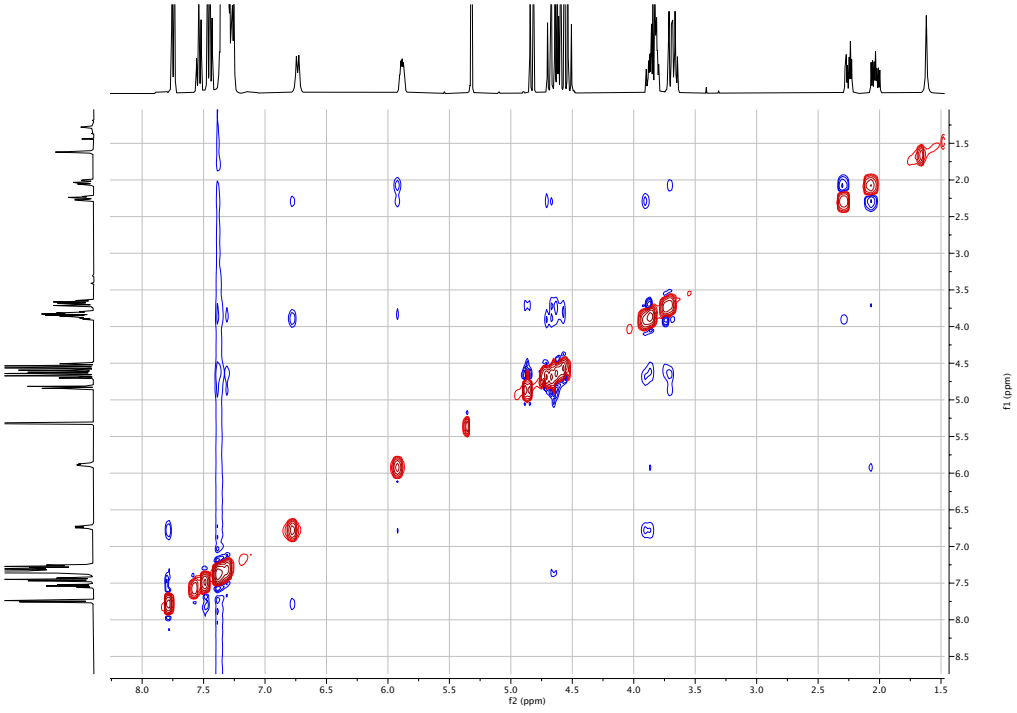
f2 (ppm)
f1 (ppm)

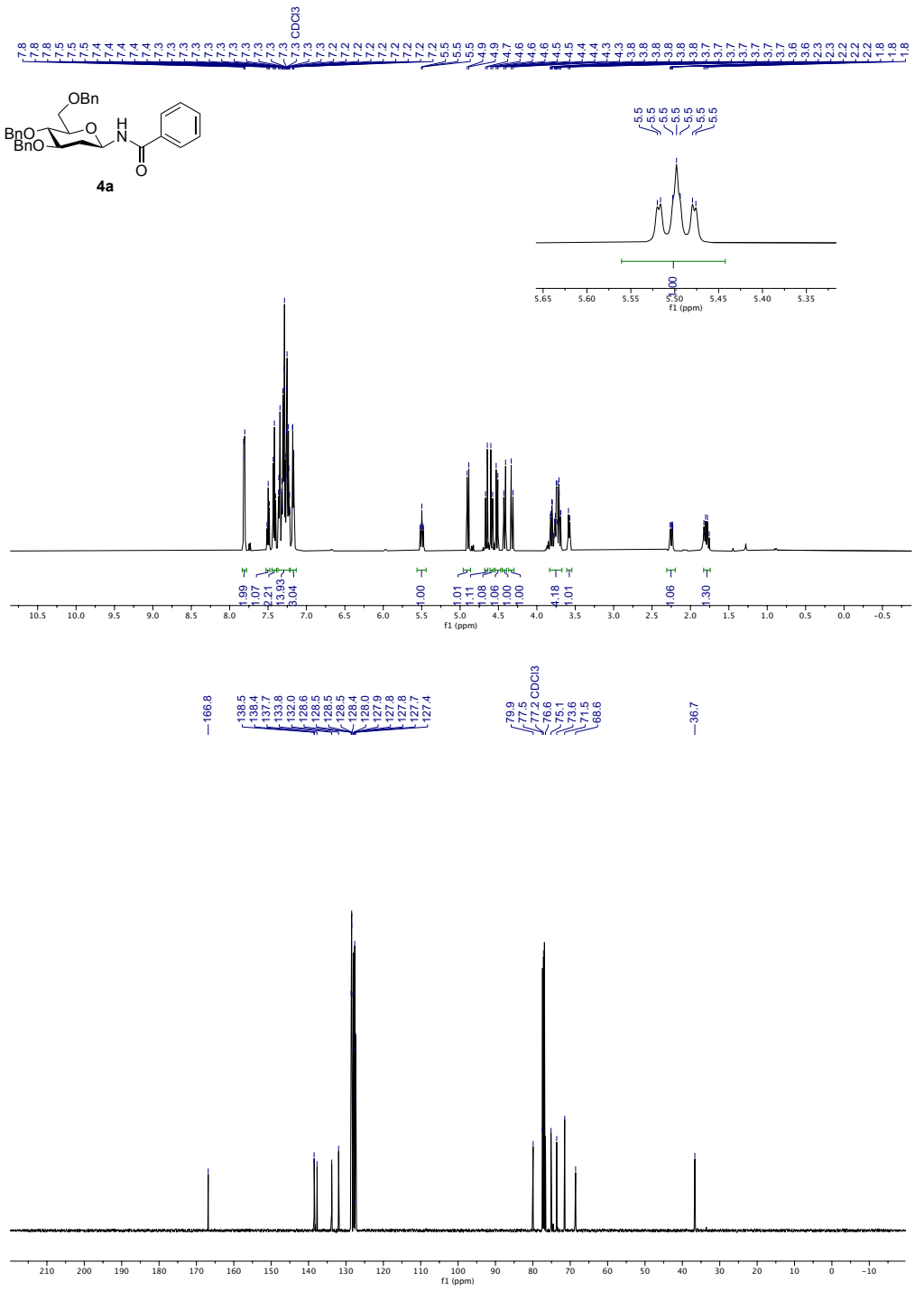
CDCl3
OBn
BnO
BnO
O
H
N
O
4a
f1 (ppm)
CDCl3

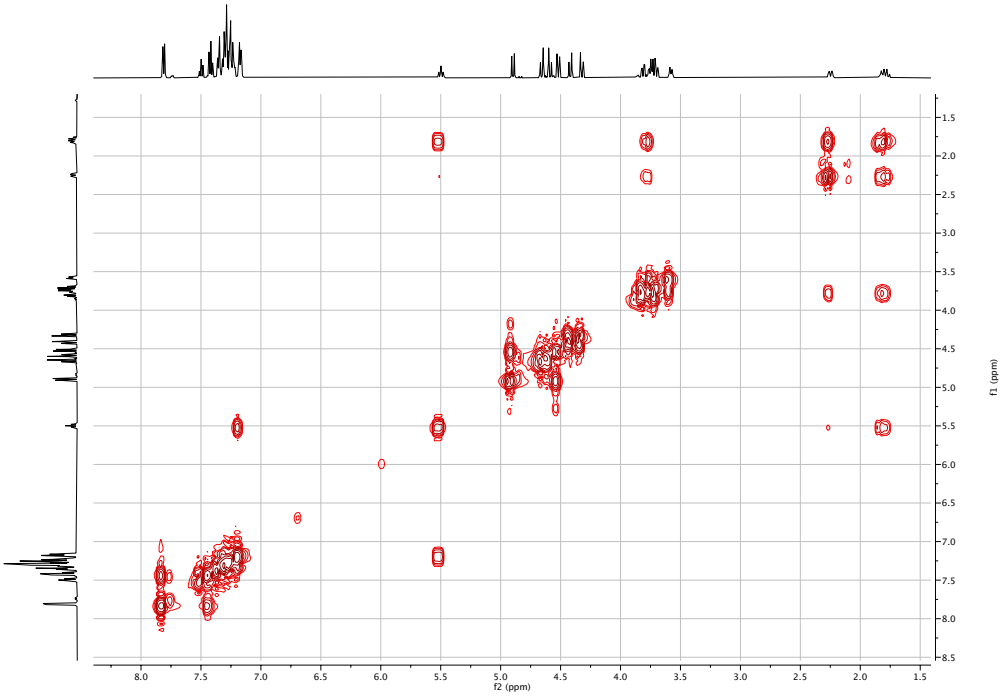
f2 (ppm)
f1 (ppm)

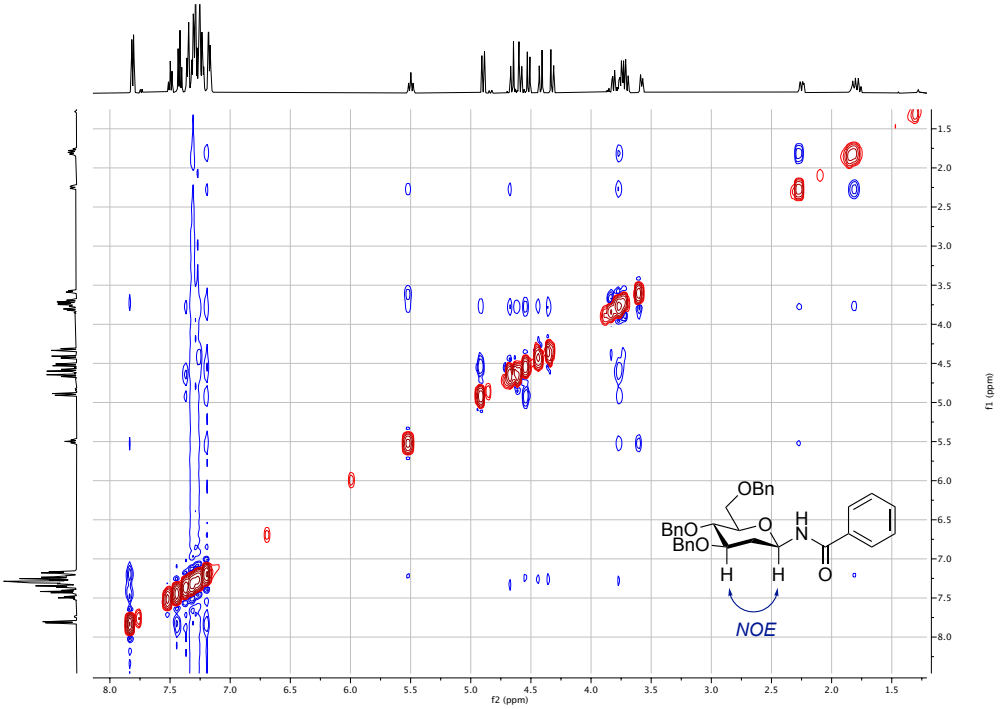
OBn
BnO
BnO
O
H
N
H
H
O
NOE
f2 (ppm)
f1 (ppm)

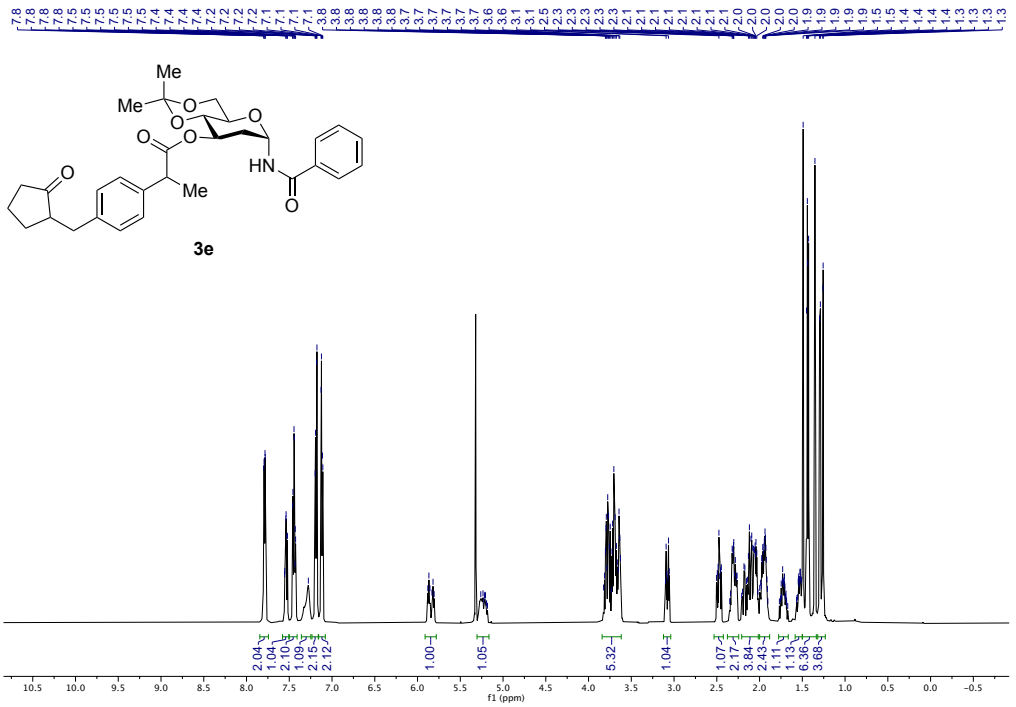
Me
Me
O
O
O
O
HN
O
O
Me
3e
f1 (ppm)

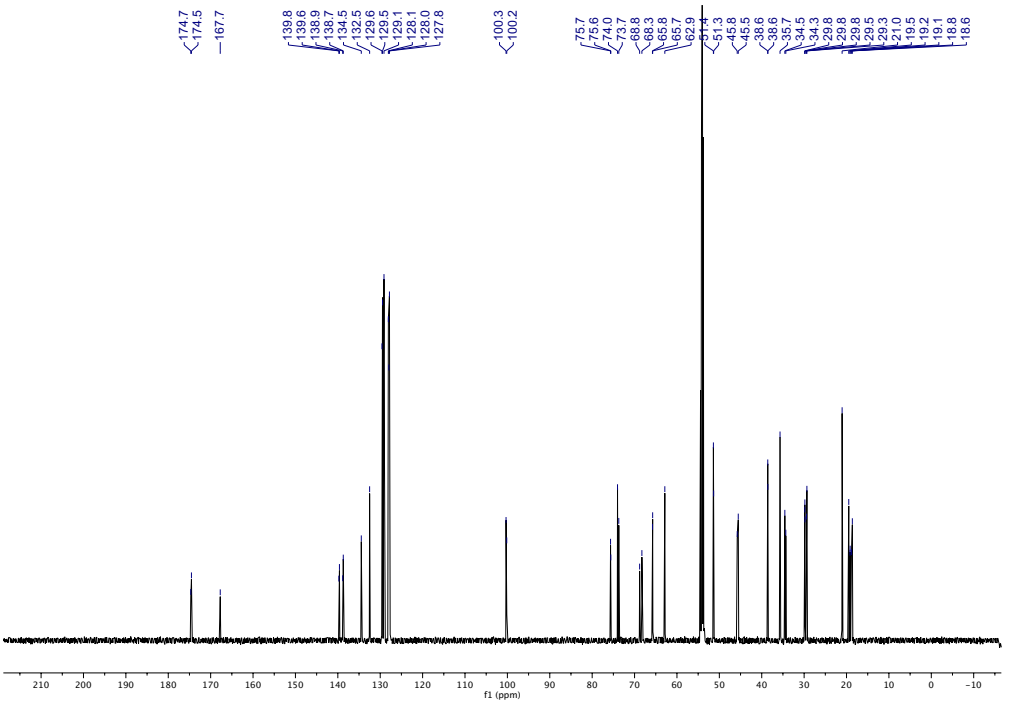
f1 (ppm)

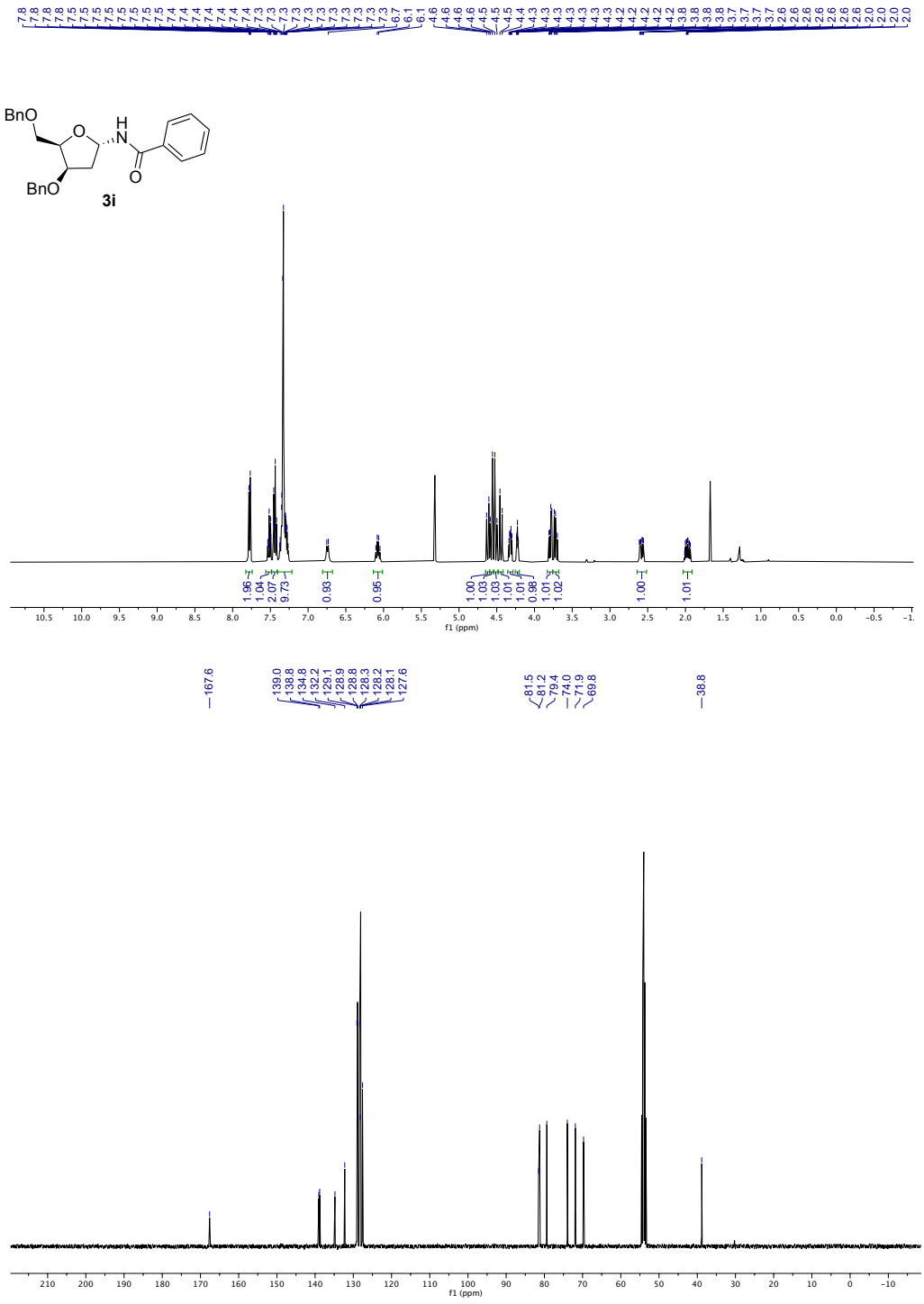
BnO
O
H
N
O
BnO
3i
f1 (ppm)
f1 (ppm)

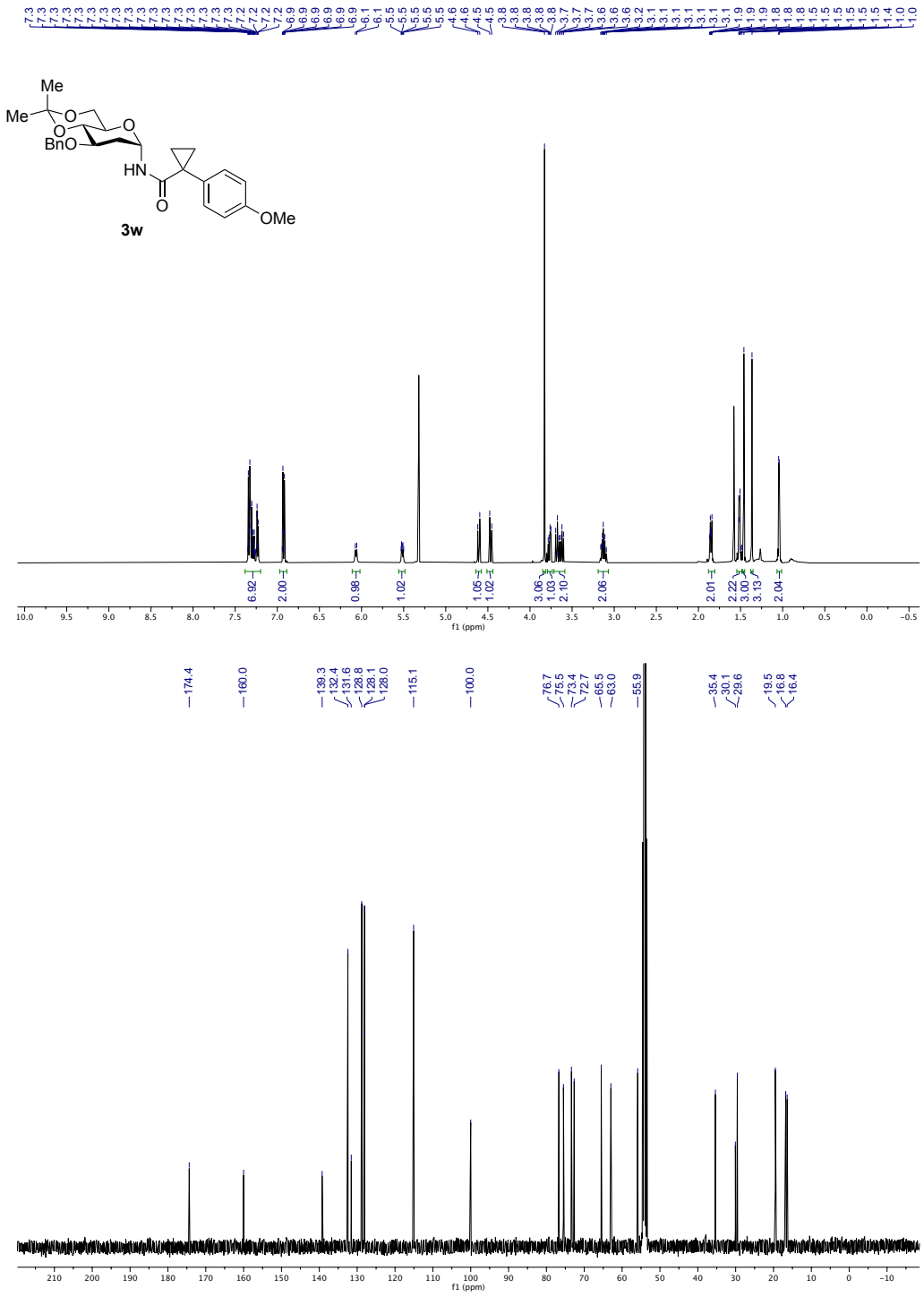
Me
Me
O
O
O
BnO
HN
O
OMe
3w
f1 (ppm)
f1 (ppm)

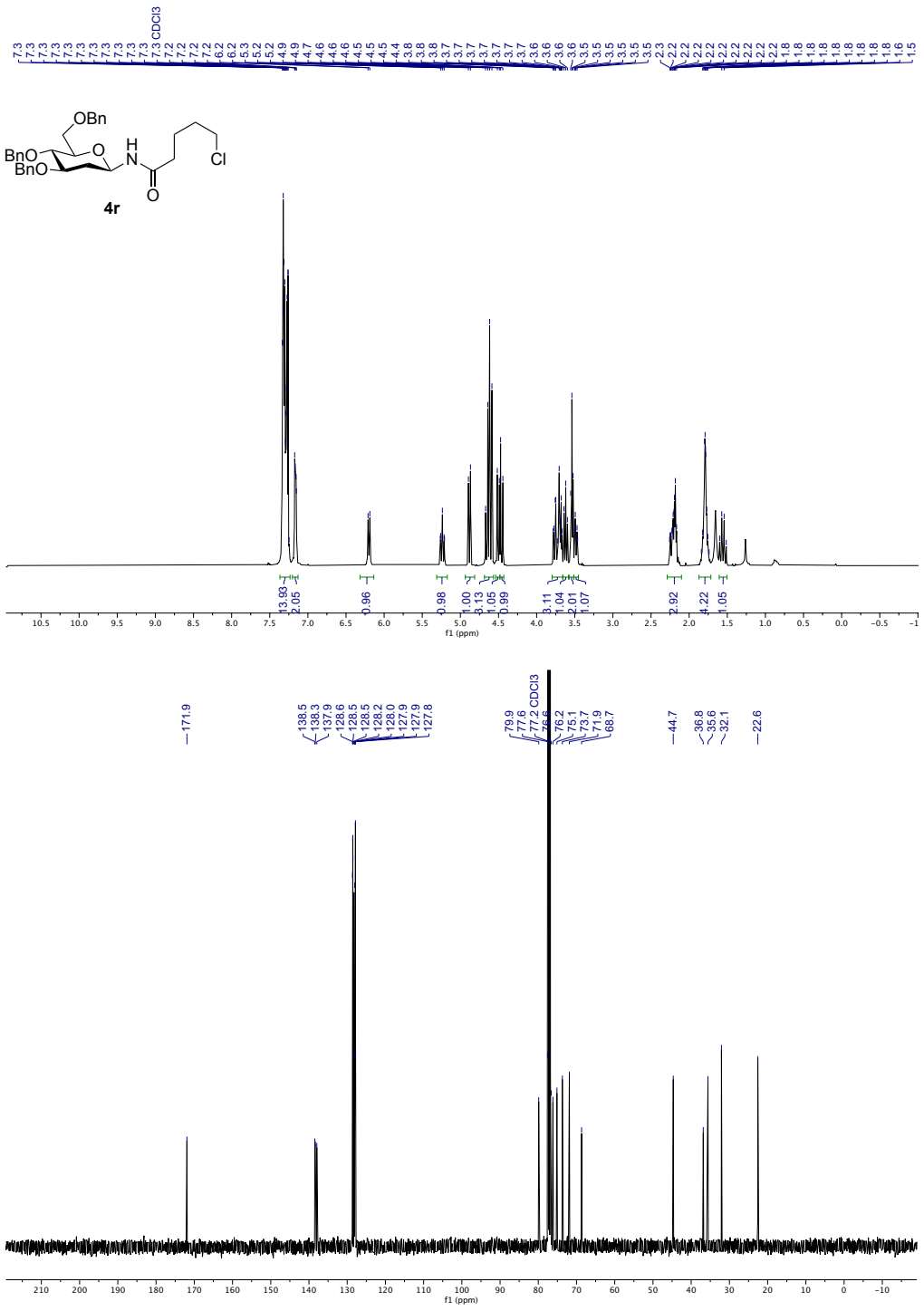
OBn
BnO
BnO
O
H
N
Cl
O
4r
CDCl3
f1 (ppm)

3.10 References

[1] M. Brito-Arias, N-Glycosides. In: Synthesis and Characterization of Glycosides. Springer, **2022**.

[2] A. Varki, D. C. Cummings, J. D Esko, H. H. Freeze, P. Stanley, C. R. Bertozzi, G. W. Hart, M. E. Etzler, In *Essentials of Glycobiology* 2nd ed.; Cold Spring Habor Laboratory Press: New York, **2009**.

[3] a) S. Ōmura, Y. Iwai, A. Hirano, A. Nakagawa, J. Awaya, H. Tsuchiya, Y. Takahashi, R. Asuma, *J. Antibiot.* **1977**, *30*, 275; b) S. Ōmura, Y. Asami, A. Crump, *J. Antibiot.* **2018**, *71*, 688; c) K. Pommerehne, J. Walisko, A. Ebersbach, R. Krull, *Appl. Microbiol. Biotechnol.* **2019**, *103*, 3267; d) H. Laube, *Clin. Drug Invest.* **2002**; *22*, 141.

[4] a) C. Reily, T. J. Stewart, M. B. Renfrow, J. Novak, *Nat. Rev. Nephrol.* **2019**, *15*, 346; b) S. Ōmura, Y. Iwai, A. Hirano, A. Nakagawa, J. Awaya, H. Tsuchiya, Y. Takahashi, R. Asuma, *J. Antibiot.* **1977**, *30*, 275; c) S. Ōmura, Y. Asami, A. Crump, *J. Antibiot.* **2018**, *71*, 688.

[5] H. Tanaka, Y. Iwata, D. Takahashi, M. Adachi, T. Takahashi, *J. Am. Chem. Soc.* **2005**, *127*, 1630.

[6] Y. Kobayashi, Y. Nakaysuji, S. Li, S. Tsuzuki, Y. Takemoto, *Angew. Chem. Int. Ed.* **2018**, *57*, 3646

[7] H. H. Kinfe, *Org. Biomol. Chem.* **2019**, *17*, 4153; S. J. Danishefsky, M. T. Bilodeau, *Angew. Chem. Int. Ed.* **1996**, *35*, 1380.

[8] Y. Nakatsuji, Y. Kobayashi, Y. Takemoto, *Angew. Chem. Int. Ed.* **2019**, *58*, 14115.

[9] J. Zheng, K. B. Urkalan, S. B. Herzon, *Angew. Chem. Int. Ed.* **2013**, *52*, 6068.

[10] S. Chakraborty, B, Mishra, P. K. Das, S. Pasari, A. Paul, S. Hotha, *Angew. Chem. Int. Ed.* **2023**, *62*, e202214167.

[11] Q. Sun, Q. Wang, W. Qin, K. Jiang, G. He, M. J. Koh, G. Chen, *Nat. Synth.* **2024**, *3*, 623.

[12] D. Liu, X. Zhang, S. Liu, X. Hu, *Nat. Commun.* **2024**, *15*, 3401.

[13] Z. Shen, G. Yin, Y. Li, *Chin. J. Chem.* **2024**, *42*, 2147.

[14] Selected reviews: a) S. Z. Tasker, E. A. Standley, T. F. Jamison, *Nature* **2014**, *509*, 299; b) K. E. Poremba, S. E. Dibrell, S. E. Reisman, *ACS Catal.* **2020**, *10*, 8237; c) C. Lee, H. Kang, S. Hong, *Chem. Sci.* **2024**, *15*, 442; d) L. Chen, S. E. Reisman, *Acc. Chem. Res.* **2024**, *57*, 751.

[15] Selected references: a) M. Ju, J. M. Schomaker, *Nat. Rev. Chem.* **2021**, *5*, 580; b) G. Dequirez, V. Pons, P. Dauban, *Angew. Chem. Int. Ed.* **2012**, *51*, 7384; *Angew. Chem.* **2012**, *124*, 7498; c) T. Shimbayashi, K. Sasakura, A. Eguchi, K. Okamoto, K. Ohe, *Chem. Eur. J.* **2019**, *25*, 3156; d) Y. Park, Y. Kim, S. Chang, *Chem. Rev.* **2017**, *117*, 9247.

[16] a) R. J. Ferrier, N. Prasad, *J. Chem. Soc. C.* **1969**, 570; b) F. Ding, R. William, X.-W. Liu, *J. Org. Chem.* **2013**, *78*, 1293–1299; c) Y. Dai, J. Zheng, Q. Zhang, *Org. Lett.* **2018**, *20*, 3923; d) J. Yang, Y. Dai, R. Bartlett, Q. Zhang, *Org. Lett.* **2021**, *23*, 4008.

[17] a) T. Kumazawa, K. Odna, H. Okuyama, S. Matsuba, S. Sato, J. Onodera, *Carbohydr. Res.* **2002**, *337*, 1007; b) A. G. Santana, L. Montalvillo-Jimenez, L. Diaz-Casado, F. Corzana, P. Merino, F. J. Canada, G. Jimenez-Oses, J. Jimenez-Barbero, A, M. Gomez, J. L. Asensio, *J. Am. Chem. Soc.* **2020**, *142*, 12501; c) S. S. Nigudkar. A. V. Demchenko, *Chem. Sci.* **2015**, *6*, 2687.

[18] a) A. de Meijere, F. Diederich, *Metal-Catalyzed Cross-Coupling Reactions*, VCH, Weinheim, **2004**; b) R. Jana, T. P. Pathak, M. S. Sigman, *Chem. Rev.* **2011**, *111*, 1417; c) N. Kambe, T. Iwasakia, J. Terao, *Chem. Soc. Rev.* **2011**, *40*, 4937.

[19] a) Y. Wang, H. M. Carder, A. E. Wendlandt, *Nature* **2020**, *578*, 403; b) H. M. Carder, Y. Wang, A. E. Wendlandt. *J. Am. Chem. Soc.* **2022**, *144*, 11870. c) G. Zhao, U. Mukherjee. L. Zhou, J. N. Mauro, Y. Wu, P. Liu, M. Ngai. *CCS Chem.* **2023**, *5*, 106.

[20] a) X. Lyu, J. Zhang, D. Kim, S. Seo, S. Chang, *J. Am. Chem. Soc.* **2021**, *143*, 5867; b) X. Lyu, C. Seo, H. Jung, T. Faber, D. Kim, S. Seo, S. Chang, *Nat. Catal.* **2023**, *6*, 784; c) H. Keum, H. Ryoo, D. Kim, S. Chang, *J. Am. Chem. Soc.* **2024**, *146*, 1001; d) L. Meng, J. Yang, M. Duan, Y. Wang, S. Zhu, *Angew. Chem. Int. Ed.* **2021**, *60*, 23584; e) Y. Dong, R. M. Clarke, G. J. Porter, T. A. Betley, *J. Am. Chem. Soc.* **2020**, *142*, 10996.

[21] a) N. A. Eberhardt, H. Guan, *Chem. Rev.* **2016**, *116*, 8373; b) Y. Wang, Y. He, S. Zhu, *Acc. Chem. Res.* **2022**, *55*, 3519; c) Z. Zhang, S. Bera, C. Fan, X. Hu, *J. Am. Chem. Soc.* **2022**, 144, 7015; d) Y. K. Mirza, P. S. Bera, S. B. Mohite, *Org. Chem. Front.* **2024**, *11*, 4290.

[22] a) F. Zhu, M. A. Walczak, *J. Am. Chem. Soc.* **2020**, *142*, 15127; b) I. V. Alabugin, L. Kuhn, N. V. Krivoshchapov, P. Mehaffy, M. G. Medvedev, *Chem. Soc. Rev.* **2021**, *50*, 10212; c) Y. Wei, B. Ben-zvi, T. Diao, *Angew. Chem. Int. Ed.* **2021**, *60*, 9433.

[23] T. Wang, X.-Q. Hao, J.-J. Huang, K. Wang, J.-F. Gong, M.-P. Song, *Organometallics* **2014**, *33*, 194.

[24] B. Liu, D. Liu, X. Rong, X. Lu, Y. Fu, Q. Liu, *Angew. Chem. Int. Ed.* **2023**, *62*, e202218544.

[25] K. H. Dotz, F. Otto, M. Niegar, *J. Organomet. Chem.* **2001**, *621*, 77.

[26] J. J. Patroni, R. V. Stick, D. M. G. Tilbrook, B. W. Skelton, A. H. White, *Aust. J. Chem.* **1989**, *42*, 2127.

[27] a) K. M. van Vliet, B. de Bruin, *ACS Catal*. **2020**, *10*, 4751. b) X. Lyu, J. Zhang, D. Kim, S. Seo, S. Chang, *J. Am. Chem. Soc*. **2021**, *143*, 5867; c) B. Du, Y. Ouyang, Q. Chen, W.-Y. Yu, *J. Am. Chem. Soc.* **2021**, *143*, 14962.

[28] Y. Nakatsuji, Y. Kobayashi, Y. Takemoto, *Angew. Chem. Int. Ed.* **2019**, *58*, 14115.

Chapter 4. Site-Selective Remote C(sp^3)–H Bromination of Aliphatic Amines as a Gateway for Forging Nitrogen-Containing sp^3 Architectures.

———In collaboration with Clarence Tan, Dr. Jesús Rodrigalvarez and Shuai Zhang

4.1 General Introduction

Given that an increased number of saturated sp^3–hybridized carbons have been showed to improve several molecular attributes that contribute to clinical success,[1] C(sp^3)-H functionalization has emerged at the forefront of modern synthetic methodology development for forging new sp^3 architectures. This is not only due to its improved atom economy when compared to conventional protocols for forging sp^3 architectures, but also for accessing new chemical space not apparent at first sight, thus streamlining the access of added-value chemicals from simple precursors, particularly when dealing with late-stage functionalization (LSF) of advanced ingredients.[2] Driven by the ubiquity of amines in a myriad of biologically-relevant molecules, it comes as no surprise that chemists have been challenged to design catalytic C(sp^3)–H functionalization of amines as a new manifold to access amine-containing drug candidates.

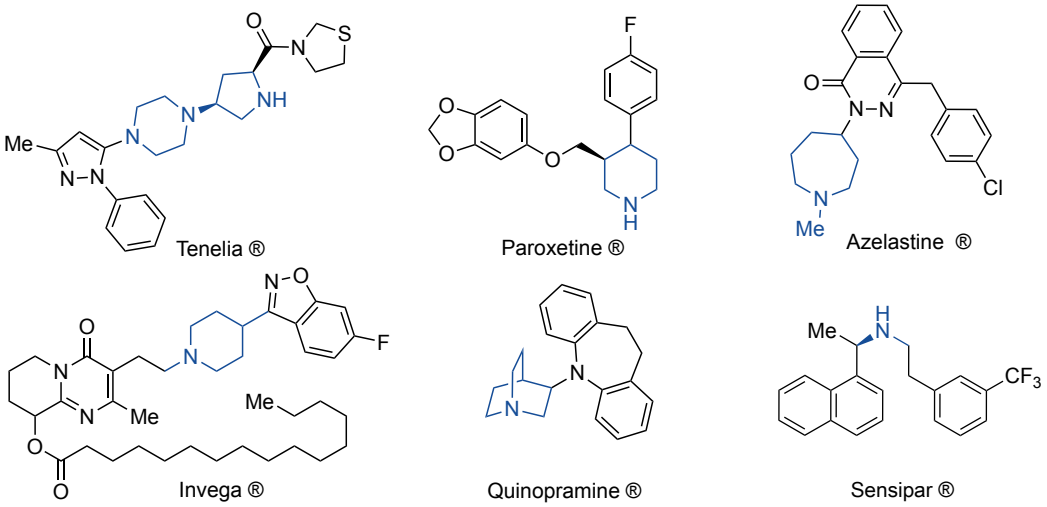

Scheme 4.1 Small molecular medicines containing amine groups.

In recent years, significant advances in α-C(sp^3)-H functionalization of amines have been reported in the context of hydrogen-atom transfer (HAT) processes at α to nitrogen atom[3] or via the intermediacy of iminium ions generated in the presence of appropriate oxidants (Scheme 4.2).[4] In addition, α-functionalization of amines can be enabled by

deprotonation with superbases followed by electrophilic substitution,[5] metal-catalyzed C(sp^3)–H functionalization events,[6] or carbene/nitrene-type insertion pathways.[7] In contrast, remote C(sp^3)-H functionalization of amines remains more challenging due to the lack of radical stabilization adjacent to the nitrogen atom and lower acidity of remote C(sp^3)–H bonds compared to α-C(sp^3)–H linkages. To overcome these drawbacks, several strategies have been developed to tackle the functionalization of remote C(sp^3)-H bonds of amines. For example, β-functionalization can be enabled via imine-enamine equilibrium. On the other hand, catalytic functionalization at γ-C(sp^3)–H sites can be achieved by metal-catalyzed strategies using native amine as directing groups, 1,5- or 1,6-HAT strategies aided by the intermediacy of amidyl radicals or at terminal C(sp^3)–H sites by means of Ir-catalyzed borylation events.

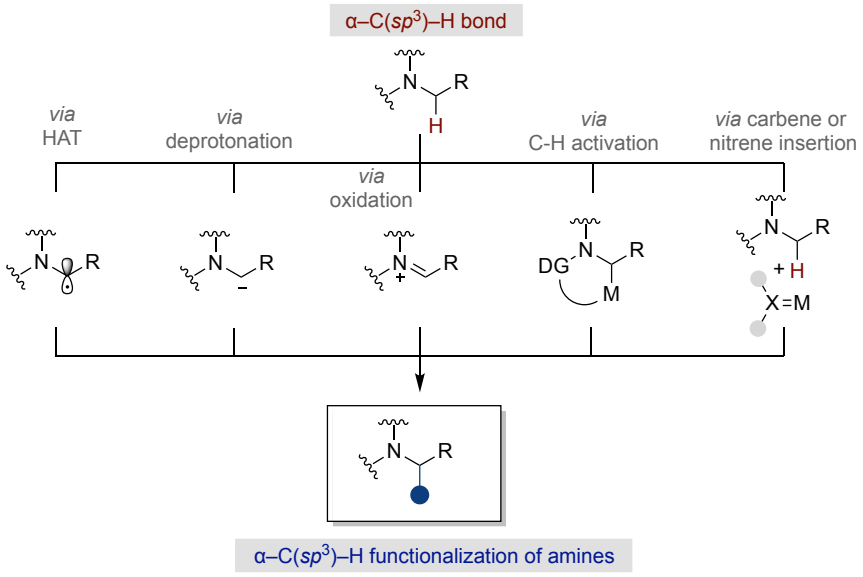

Scheme 4.2. Strategies for functionalization of α-C(sp^3)-H bonds of amines.

4.1.1 C(sp^3)–H Functionalization of Amine Derivatives via Deprotonation

Direct deprotonation of amines at the α-C(sp^3)–H bond in the presence of superbases followed by electrophilic substitution is a common strategy for enabling site-selective α-C(sp^3)-H functionalization of aliphatic amines.[8] For example, in 1995 Dieter developed an α-C(sp^3)-H arylation of amines enabled by deprotonation and palladium catalysis.[9] Exposure of Boc-protected amines to *s*-BuLi results in α-aminoalkyllithium species that undergo coupling with aryl iodides catalyzed by Pd[(*p*-MeOC$_6$H$_4$)$_3$P]$_4$ in one pot, leading to the corresponding α-arylated amines (Scheme 4.3).

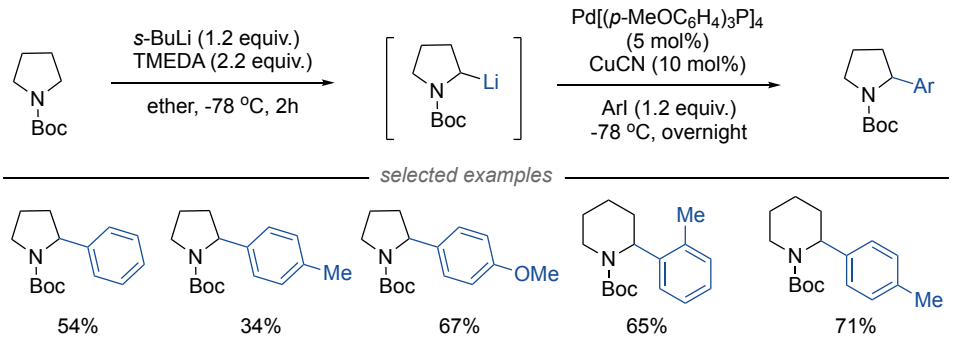

Scheme 4.3 α-C(sp^3)-H arylation of amines enabled by deprotonation.

Building on the elegant efforts of Baudoin and co-workers, this deprotonation strategy allowed to promote remote β-C–H functionalization through a sequential palladium-catalyzed Negishi coupling events (Scheme 4.4).[10] The use of flexible biarylphosphines as ligands facilitated the formation of the kinetically favored β-arylated products, an observation that is consistent with a sequence consisting of 1,2-palladium migration via β-hydride elimination and migratory insertion. Notably, more rigid biarylphosphines favored an α-arylation event. Unfortunately, the scope of amine derivatives was limited to six-membered piperidines, as no desired β-arylation products were observed for *N*-Boc-pyrrolidine, -azepane, or -azocane, respectively.

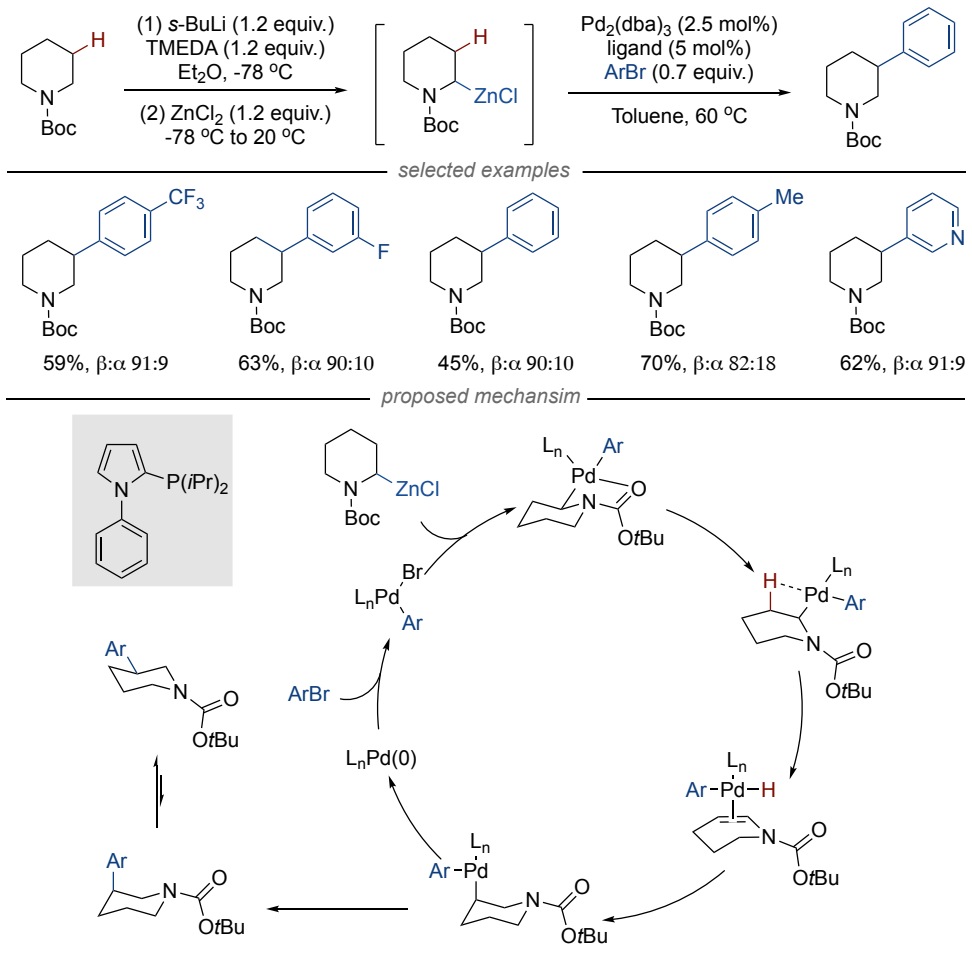

Scheme 4.4 β-C(sp^3)-H arylation of piperidine enabled by deprotonation.

In 2020, Seidel and co-workers described a facile multistep process that enables β-alkylation across various secondary alicyclic amines with different ring sizes, such as piperazine, azepane and others (Scheme 4.5).[11] In this process, alicyclic amine was first exposed to *n*-BuLi followed by treatment with a ketone oxidant, leading to an imine species via hydride transfer.[12] Subsequent deprotonation by LDA results in an endocyclic 1-azaallyl anion that then reacts with an electrophilic alkylating agent. Final reduction of newly formed imine ultimately affords the β-alkylated product.

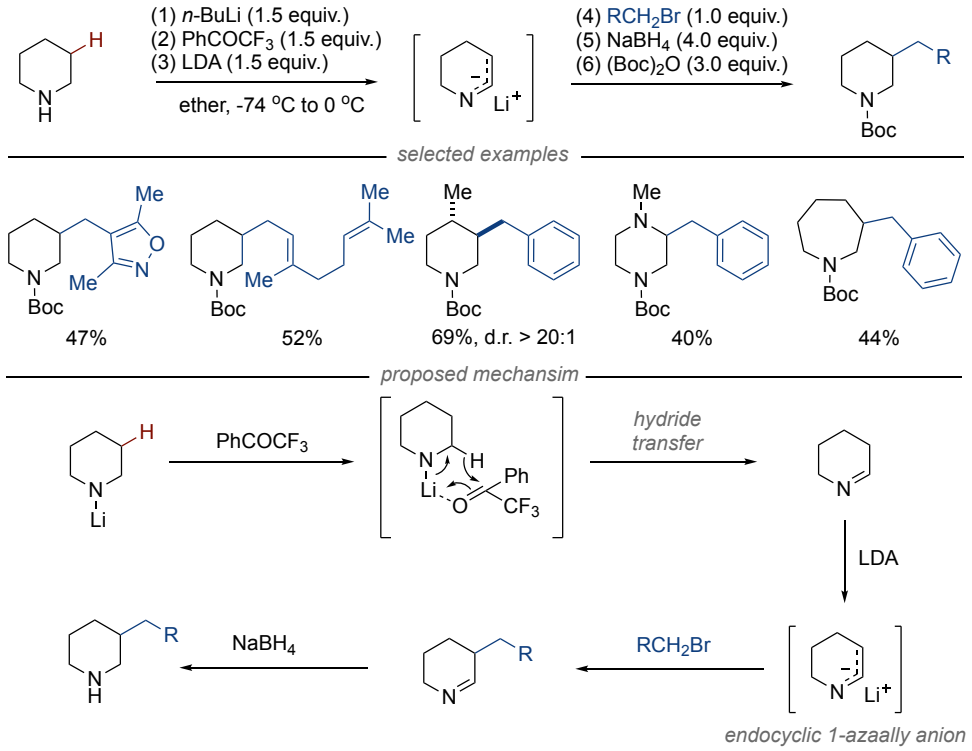

Scheme 4.5. β-C(sp^3)–H arylation of cyclic amines enabled by deprotonation.

4.1.2 Remote C(sp^3)–H Functionalization with Native Amine Directing Groups

The utilization of the nitrogen's native coordinating ability offers a strategic advantage for remote C(sp^3)–H functionalization (Scheme 4.6). In 2014, Gaunt reported a palladium-catalyzed β-C(sp^3)–H functionalization of secondary aliphatic amines via four-membered ring cyclopalladation.[13] This reaction is enabled by functionalization of the β-C(sp^3)-H bond, ultimately resulting in strained aziridines and β-lactams by utilizing $PhI(OAc)_2$ or carbon monoxide as oxidants, respectively. Notably, the presence of α-substituents were necessary to prevent parasitic β-hydride elimination. Subsequent mechanistic studies proposed amine coordination to the palladium center followed by intermolecular C(sp^3)–H functionalization to form a four-membered ring palladacycle intermediate. This intermediate is then oxidized by $PhI(OAc)_2$, generating a Pd(IV) species that facilitates acetic acid dissociation and reductive elimination to afford the aziridine.[14] Later on,

Gaunt, Yu, Shi and others expanded these conceptions to C(sp^3)-H acetoxylation,[15] alkenylation, arylation,[16] even in an enantioselective manner,[17] thus allowing to forge C(sp^3)–O, C(sp^3)–C(sp^3), C(sp^3)–C(sp^2) bonds at distal β- or γ-C–H sites in a series of primary, secondary, and tertiary aliphatic amines.

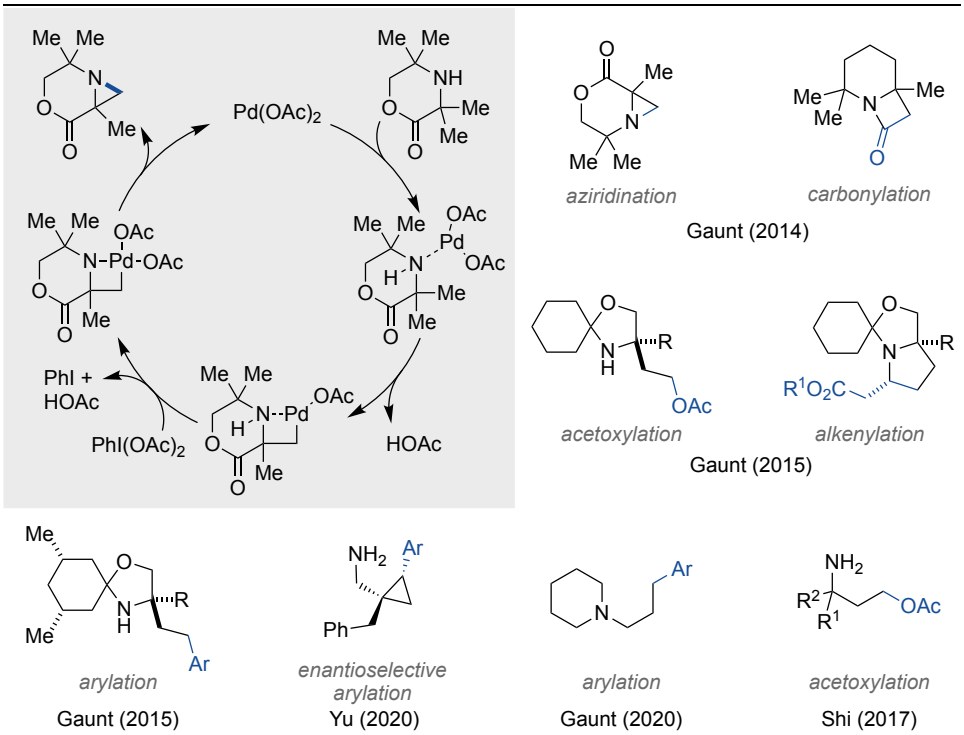

Scheme 4.6 Pd-catalyzed remote C(sp^3)-H functionalization directed by native amines.

4.1.3 Remote C–H Functionalization of Amines Driven by Steric Hindrance

In 2014, Hartwig and co-workers disclosed an iridium-catalyzed remote C(sp^3)–H borylation of amines (Scheme 4.7), with functionalization occurring predominantly at primary C(sp^3)–H bonds in tertiary amines.[18] Computational results confirmed Me_4phen-ligated iridium-trisboryl complex as the active catalyst, facilitating oxidative addition at terminal primary C(sp^3)–H bond followed by reductive elimination to deliver the desired

product. Further efforts from this group demonstrated that the utilization of 2-mphen as ligand led to functionalization at remote C(sp^3)–H bonds on steric grounds.[19]

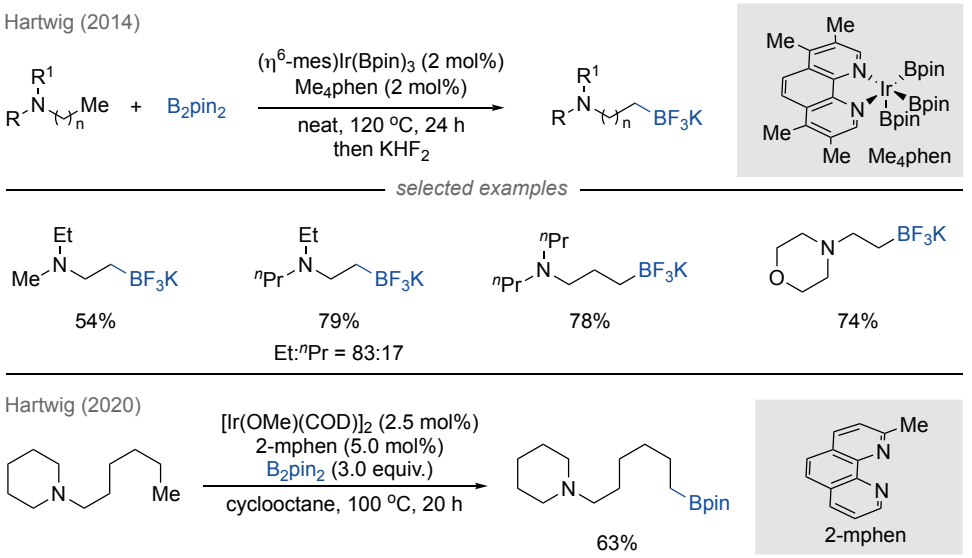

Scheme 4.7 Ir-catalyzed distal C(sp^3)–H Functionalization of amines.

4.1.4 Remote C(sp^3)–H Functionalization of Amines via HLF Reactions

Nitrogen-centered radicals represent highly effective intermediates capable of abstracting hydrogen atoms from unactivated C(sp^3)–H bonds due to their high BDE (N–H: 95-107 kcal/mol).[20] This property has been exploited for the remote functionalization of δ-C(sp^3)–H linkages in amine derivatives. From a mechanistic standpoint, nitrogen-centered radicals formed by homolysis of nitrogen-heteroatom bonds or via oxidation of N-H bonds are prone to selectively abstract δ-hydrogen atom through a favorable six-membered cyclic transition state (Scheme 4.8). The resulting open-shell carbon-centered radicals can then react with an appropriate radical acceptor to yield the corresponding δ-functionalized products.

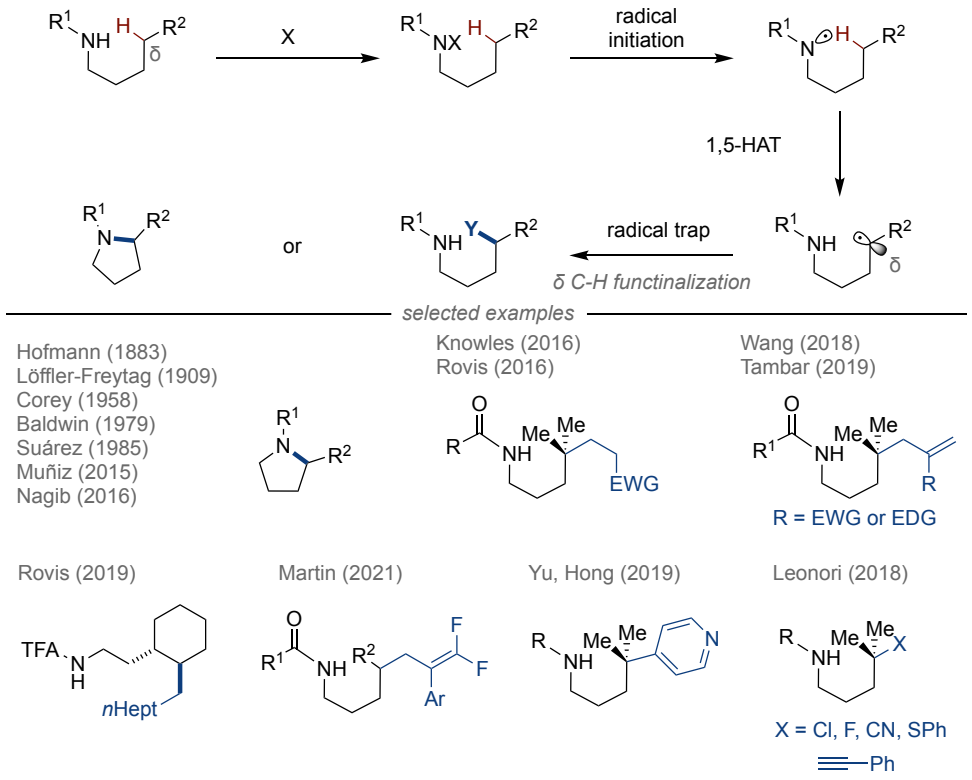

Scheme 4.8 δ-C(sp^3)-H Functionalization of amines via HLF process.

In 1883, Hofmann demonstrated that pyrrolidines are within reach from the corresponding halogenated tertiary amines, a process coined as Hofmann-Löffler-Freytag (HLF) reaction.[21] This strategy was later on applied by Corey in the context of synthesis of natural products.[22] Subsequent advances by Suárez and Muñiz, among others, revealed that *N*-halogen species could be generated in situ using oxidants, thus avoiding the need for prefunctionalization.[23] More recently, Knowles,[24] Rovis,[25] Martin,[26] among many others,[27] took advantage of oxidative proton-coupled electron transfer (PCET) to form nitrogen-centered radicals, thus facilitating the intervention of 1,5-HAT processes.[28] The resulting alkyl radical is then interfaced with either a radical acceptor or with a Ni intermediate, thus setting the basis for a subsequent C–C bond formation. Additionally, Leonori and Nagib expanded the scope of the HLF process to include halogenation,

thiolation, cyanation, and alkynylation of δ-C–H bonds in the presence of appropriate radical acceptors.[29]

4.1.5 Remote C–H Functionalization of Amines Enabled by Protonation

Although site-selective functionalization of proximal C(sp^3)-H bonds in amines or derivatives thereof can be readily accomplished due to hydridic properties of the C–H linkage, low BDEs, or/and stabilization effect from heteroatoms for these bonds, the functionalization at remote C–H bonds is significantly more challenging. In 2014, Radom and Chan revealed the BDEs of C–H bonds in butanol are significantly affected by protonation and deprotonation.[30] Compared to the neutral alcohol, protonation increases the BDEs of proximal C–H bonds, while deprotonation decreased them (Scheme 4.9).

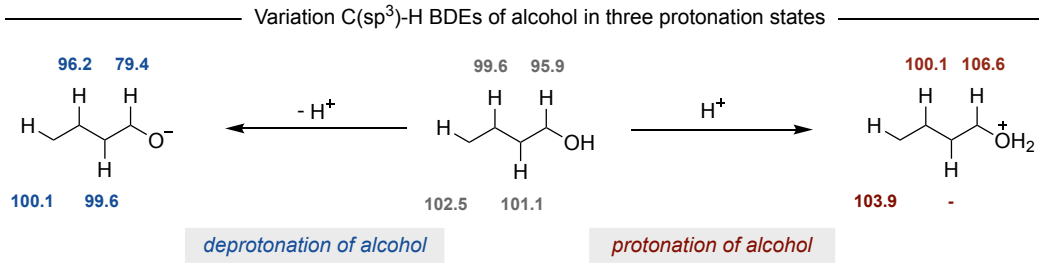

Scheme 4.9 Deactivation of proximal C(sp^3)-H bonds by protonation

In 1993, Asensio and co-workers demonstrated that the presence of HBF_4 facilitates the site-selective oxidation of distal secondary or tertiary C(sp^3)–H bonds in amines (Scheme 4.10).[31] Later on, Sanford,[32] White,[33] and Sigman[34] integrated transition catalysis into this deactivation strategy, facilitating the site-selective oxidation towards terminal primary or distal tertiary C(sp^3)–H linkages. Recent significant advances from Schultz and MacMillan combined this acid-mediated deactivation with photoredox catalysis, allowing to promote oxidation,[35] trifluoromethylation,[36] and sulfinylation[37] of remote C(sp^3)–H sites in aliphatic amines.

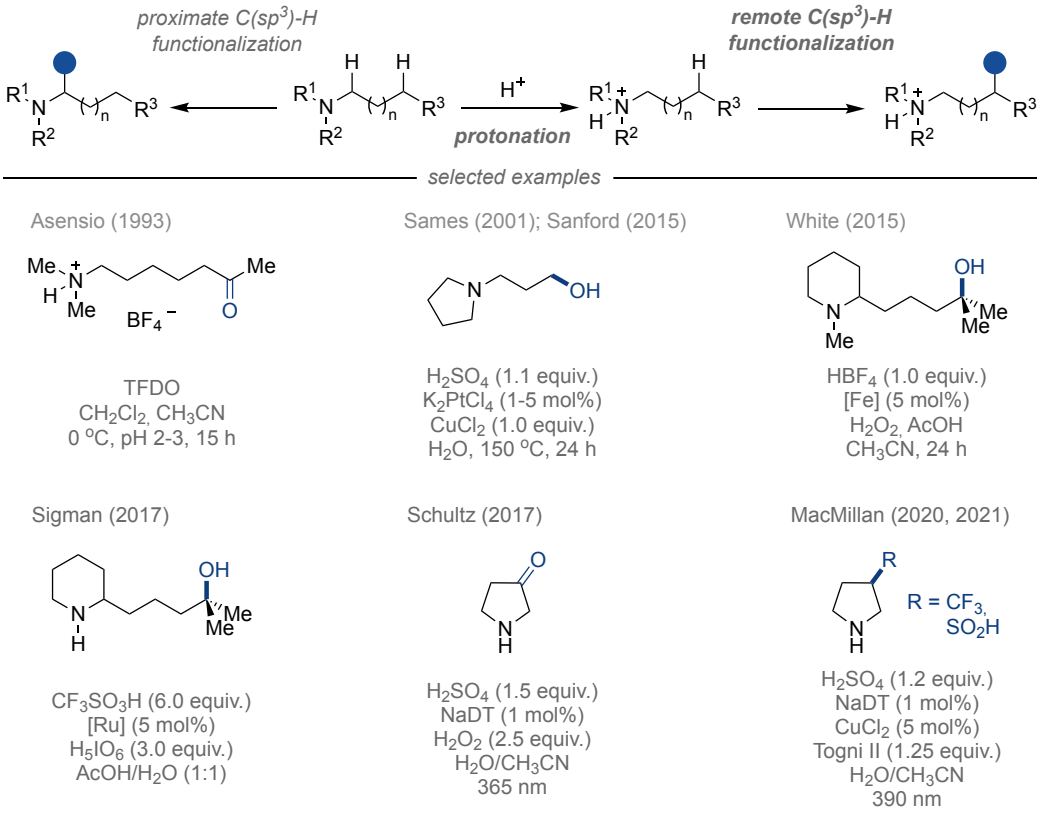

Scheme 4.10 Remote C(sp^3)-H functionalization of amines by protonation strategy.

4.2 General Aim of the Project

At the outset of our investigations, significant progress had been made on the remote C(sp^3)-H functionalization of amines. However, the development of a modular and general blueprint that incorporates with equal ease carbon-carbon or carbon-heteroatom bonds at distal C(sp^3)–H sites of unprotected aliphatic amines still represents a worthwhile endeavor for chemical invention. In this chapter, we propose that the site-selective installation of a versatile halogenated linchpin at remote C(sp^3)–H sites in unprotected amines could provide a new pathway for downstream applications, thus streamlining the access to advanced sp^3 architectures with an aliphatic amine core (Scheme 4.11).

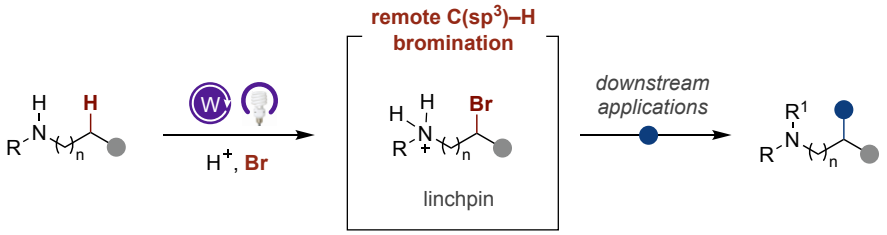

Scheme 4.11 Site-selective remote functionalization of aliphatic amines.

4.3 DFT Calculations

We began our investigations by evaluating the remote C(sp^3)–H functionalization of *n*-propyl amine (**1a**). As anticipated, density functional theory (DFT) calculations revealed that C–H bonds adjacent to the nitrogen atom are electronically perturbed upon protonation (Scheme 4.12). Interestingly, H_b in protonated congener **1a'** exhibited a lower BDEs, indicating that C–H_b cleavage would be expected to be more facile compared to H_a and H_c upon protonolysis of the amine function.

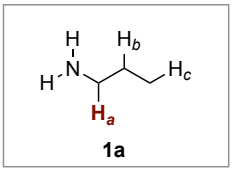

1a

acidic conditions

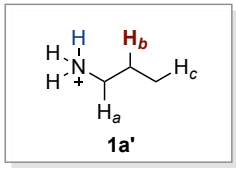

1a'

	H_a	H_b	H_c
NPA	0.167	0.189	0.197
BDE	91.9	97.4	101.3

	H_a	H_b	H_c
NPA	0.220	0.208	0.207
BDE	102.9	97.8	102.3

Scheme 4.12 DFT calculations: Natural Population Analysis (NPA) and bond dissociation energies (BDE, kcal·mol-1) of C–H bonds for **1a** and **1a'** (B3LYP/6-311+ +G(d.p)).

4.4 Optimization of the Reaction Conditions

Taking into considerations the previous DFT calculations, we started our work by examining the C(sp^3)–H bromination of **1a** in acidic media using 1,3-dibromo-5,5-dimethylhydantoin (DBDMH) as the bromine source, and tetra-*n*-butylammonium decatungstate (TBADT) (1 mol%) as the photocatalyst under 390nm light in acetonitrile (Table 4.1). Initial attempts with CH_3CO_2H did not yield the desired bromination product (entry 1) whereas the utilization of strong Brønsted acids such as TFA, HCl, H_2SO_4, and TfOH resulted in formation of the β-brominated product **2a'**, albeit in low yields (entries 2-5). Notably, the utilization of $HClO_4$ afforded **2a'** in 80% yield with 89% selectivity (entry 6), thus highlighting the significant influence of the escorting counterion on both reactivity and site-selectivity. Notably, no traces of **2a'** or **2a''** were observed when

promoting C(sp^3)–H functionalization with bulky Brookhart's acid (H[BArF]$_4$) or Lewis acid $BF_3 \cdot Et_2O$ (entries 7-8).

Table 4.1. Screening of acids with DBDMH as bromine source

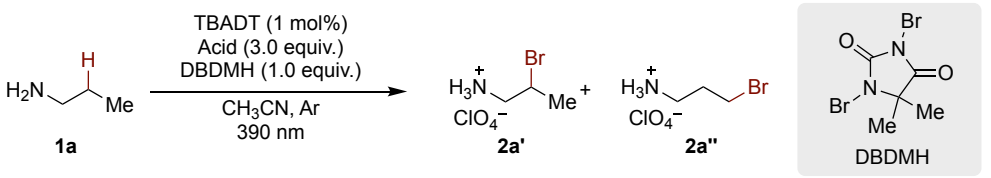

Entries	Acids	**2a'**(%)[a]	(**2a'**/(**2a'**+**2a''**))[b]
1	CH_3CO_2H	0	-
2	TFA	26	90%
3	HCl	21	88%
4	H_2SO_4	11	65%
5	TfOH	11	58%
6	$HClO_4$	80	89%
7	H[BArF]$_4$	0	-
8	BF_3•Et_2O	0	-

[a] ^{1}H-NMR yield using CH_2Br_2 as internal standard. [b] Regioselectivity en route to **2a'**.

Unfortunately, all our attempts to modify the decatungstate catalyst did not improve results (Table 4.2, entries 1-2). The utilization of benzophenone and anthraquinone as photocatalysts instead of TBADT led to significantly lower yields (entries 3-4), an observation that is probably ascribed to photocatalyst poisoning under the strong acidic conditions. Interestingly, bromination at primary the C(sp^3)–H site was primarily observed when *N*-chlorosuccinimide (NCS) was employed as HAT reagent (entry 6), underscoring the importance of judiciously selecting the HAT reagent for achieving high regioselectivity.[38] The utilization of Br_2 or *N*-bromosuccinimide (NBS) resulted in notably lower yields and selectivity for **2a'** (entries 7 and 8). Additionally, the inclusion of water as a co-solvent was detrimental to both yield and selectivity (entry 9). As initially

anticipated, control experiments confirmed that both the photocatalyst and acid were essential for the bromination's success, with the best results obtained when combining TBADT and $HClO_4$ (entry 10).

Table 4.2. Deviation standard conditions.

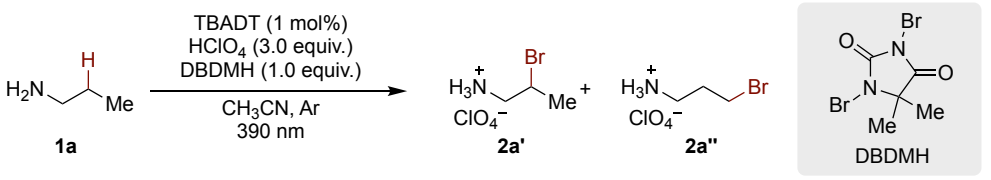

Entries	Deviation	**2a'**(%)[a]	(**2a'**/(**2a'**+**2a''**))[b]
1	*n*-Bu_3BnNDT instead of TBADT	72	89%
2	Ph_4PDT instead of TBADT	76	89%
3	Benzophenone instead of TBADT[c]	10	50%
4	Anthraquinone instead of TBADT[c]	7	70%
5	using (Mes-Acr-Ph)BF_4[d]	0	-
6	using NCS, CCl_3Br[e]	4	31%
7	Br_2 instead of DBDMH	11	61%
8	NBS instead of DBDMH	54	83%
9	CH_3CN:H_2O (10:1) as solvent	21	64%
10	No TBADT / acid	trace	-

[a] ^{1}H-NMR yield using CH_2Br_2 as internal standard. [b] Regioselectivity en route to **2a'**. [c] 5 mol% photocatalyst were used. [d] **1a** (0.40 mmol), (Mes-Acr-Ph)BF_4 (5 mol%), K_3PO_4 (0.30 mmol), DBDMH (0.20 mmol) in HFIP (1 mL) under 450 nm for 20 h. [e] **1a** (0.40 mmol), NCS (0.20 mmol), $HClO_4$ (0.60 mmol), CCl_3Br (1.0 mmol) in CH_3CN:H_2O 10:1 (1 mL) under 450 nm for 20 h.

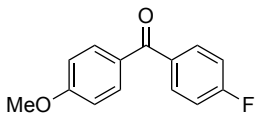

Benzophenone

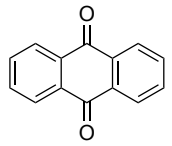

Anthraquinone

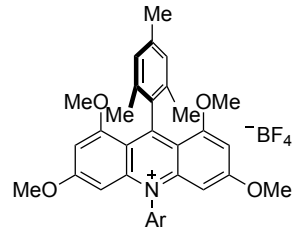

(Mes-Acr-Ph)BF_4

4.5 Substrate Scope

4.5.1 Scope of Acyclic Aliphatic Amines

With optimized conditions in hand, we turned our attention to study the generality of the remote C(sp^3)–H bromination across a wide range of aliphatic amines. As illustrated in Scheme 4.13, a variety of acyclic alkyl amines were successfully employed as substrates. Sequential addition of TsCl or CbzCl in a one-pot procedure enabled the isolation of the brominated products, thus laying the foundation for further functionalization events. As demonstrated by **2a**-**2c**, the C(sp^3)–H bromination occurred at distal unactivated methylene sites in both primary and secondary aliphatic amines. The utilization of *n*-pentyl amine containing multiple, yet similar C(sp^3)-H bonds, is particularly illustrative, as it gives access to **2d** with 70% selectivity at distal γ-methylene site. These results indirectly suggest that the electronic influence of protonation on hydrogen-atom transfer progressively weakens at long range. Importantly, unprotected amino acids, such as D-norvaline, γ-aminobutyric acid (GABA), and L-leucine were readily subjected to this protocol, affording **2e**, **2f**, and **2j**, respectively, thus offering access to unnatural amino acids and peptides in a straightforward manner. Notably, the presence of electron-withdrawing groups, such as carboxylic acids or a *gem*-difluoronated motifs led to a significant impact on site-selectivity, resulting in **2f** and **2g** with excellent β-selectivities. Moreover, C(sp^3)–H bromination could be accomplished at tertiary or benzylic sites (**2i**-**2l**) with equal ease, including the selective bromination of the commercial drug Baclofen®, thus holding promise to the implementation of this technique in the context of a late-stage functionalization of advanced ingredients.

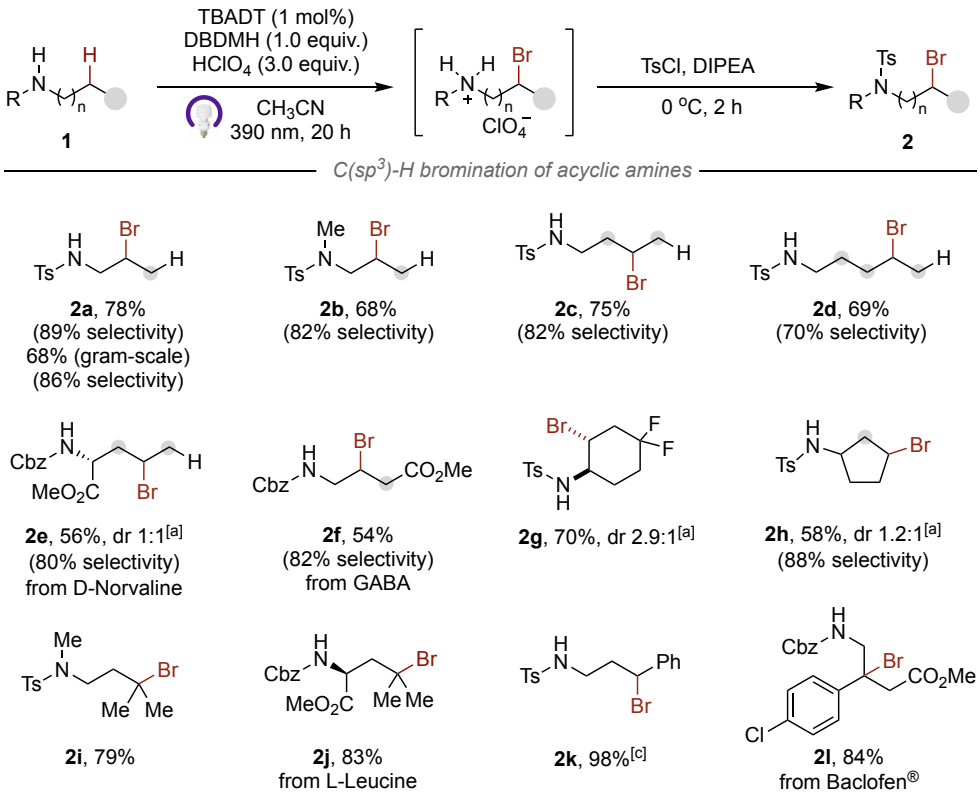

Scheme 4.13 C(sp^3)–H bromination of acyclic aliphatic amines. Reaction conditions: **1** (0.40 mmol), $HClO_4$ (0.60 mmol), TBADT (1 mol%), DBDMH (0.20 mmol) in CH_3CN (2 mL) under 390 nm for 20 h, then TsCl (0.60 mmol), DIPEA (1.50 mmol) at 0 º C for 2 h. See experimental section for further details. The selectivity corresponds to the ratio of product to the other regioisomers. [a] dr values refer to the main product. [c] without TBADT.

4.5.2 Scope of Alicyclic Amines

Driven by the prevalence of pyrrolidine, piperidine, and azepine scaffolds in the top-selling small-molecule pharmaceuticals and natural alkaloids,[39] we next sought to assess the suitability of a site-selective bromination of these heterocycles (Scheme 4.14). As illustrated by **2m**, exclusive β-bromination was obtained for pyrrolidine, whereas 57% γ-site-selectivity was observed in piperidine due to the similar electronic properties of the γ- and β-C–H bonds, as revealed by DFT calculations. Notably, introducing a methyl

group at the 3 or 4 position of piperidine core led to the bromination at tertiary C(sp^3)-H sites, affording **2o** and **2p** with high selectivity, respectively. The presence of an electron-withdrawing nitrile group in piperidine altered the site-selectivity, resulting in β-brominated **2q**, which is consistent with **2f** and **2g**. As anticipated, the presence of ethereal motives in amines led to preferential oxidation adjacent to the oxygen atom, affording the lactone **2r** and hemiacetal **2s**.[40] An excellent 88% γ-selective C(sp^3)–H bromination was observed for azepine core (**2t**), whereas the benzofused analogue (2-benzazepine) provided **2u** with exclusive benzylic selectivity. Moreover, the 7-azabicyclo[2.2.1] core proved to be compatible, leading to **2v** with exquisite endo selectivity.

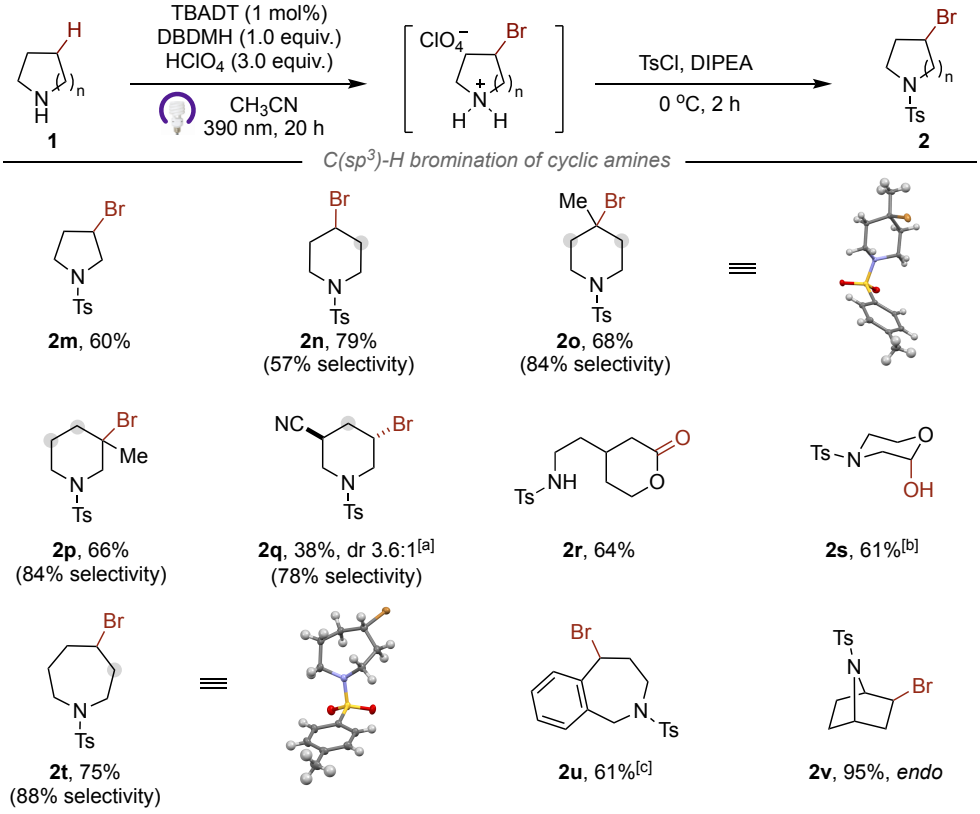

Scheme 4.14. C(sp^3)–H bromination of saturated nitrogen-containing heterocycles. Reaction conditions: **1** (0.40 mmol), $HClO_4$ (0.60 mmol), TBADT (1 mol%), DBDMH (0.20 mmol) in CH_3CN (2 mL) under 390 nm for 20 h, then TsCl (0.60 mmol), DIPEA (1.50 mmol) at 0 ° C for 2

h. See the experimental section for further details. The selectivity corresponds to the ratio of product to the other regioisomers. [a] dr values refer to the main product. [b] Further oxidation to the lactone was observed in 10% yield. [c] without TBADT.

4.6 One-pot Cyclization via C(sp^3)–H Bromination

Given the alkyl bromides can serve as synthons for further functionalization, we anticipated that the alkyl bromides generated by remote C(sp^3)–H functionalization of amines might constitute an ideal platform to access advanced heterocycles, prevalent motifs in medicinal chemistry, bioactive molecules, and natural products. Compared to the classic Hofmann–Löffler-Freytag reaction, which generates pyrrolidine or piperidine scaffolds via 1,5- or 1,6-HAT followed by *N*-nucleophilic substitution,[41] our protocol provides a more customizable, yet flexible strategy to assemble heterocycles with different size, which can be determined by the distance between nitrogen atom and the bromination site. As demonstrated in Scheme 4.15, small-ring systems such as aziridine (**3a**, **3b**, **3c**) and azetidine skeletons (**3d**), which possess significant ring strain, can be obtained from a series of simple amines through site-selective bromination/intramolecular nucleophilic substitution sequence in one pot. Additionally, this methodology enables the formation of γ-lactone (**3e)** via cyclization of amino acid, and 2-oxazolidones (**3f-3g)** through 1,3-dipolar cycloaddition with CO_2. Thus, this approach offers a complementary reactivity to existing processes for their synthesis, enabling the preparation of heterocycles from unprotected amines without the need for prefunctionalization.[42]

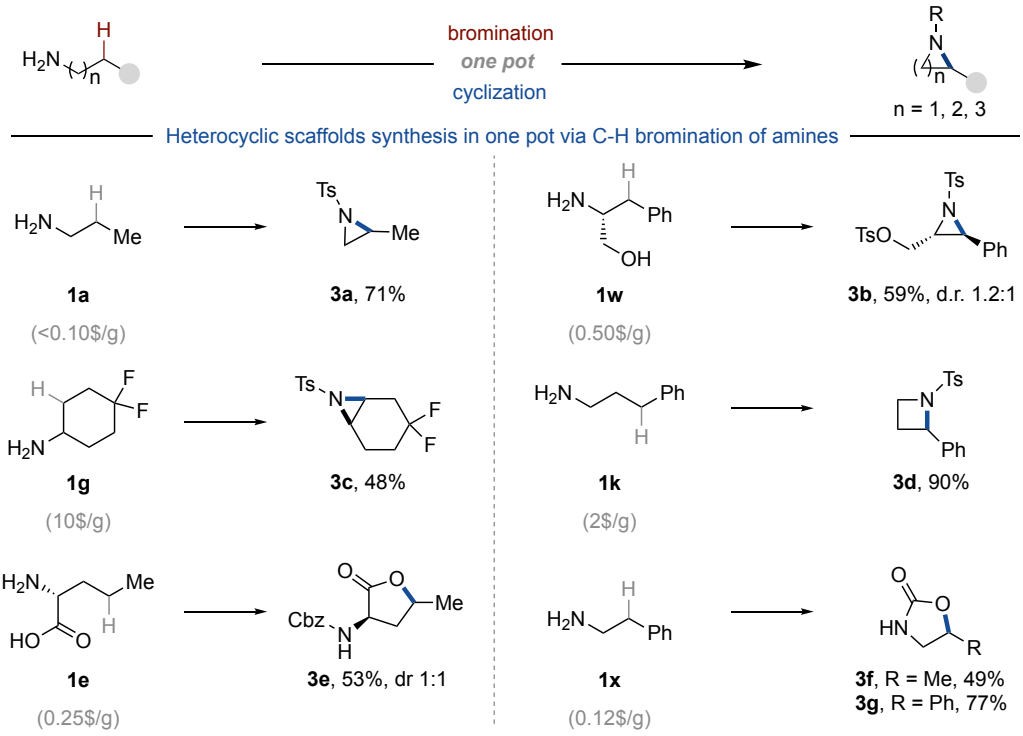

Scheme 4.15 Accessing advanced aliphatic amines by levering the potential of remote C(sp^3)–H functionalization, as for **Scheme 4.12** followed by exposure with base, see experimental section for further details.

4.7 Derivatization of Halogenated Amines

Considering the broad utility of alkyl halides in cross-coupling reactions to forge carbon-carbon and carbon-heteroatom bonds,[43] we hypothesized that our C(sp^3)–H bromination protocol could serve as a gateway to diverse functionalization of these sp^3-hybridized sites, enabling access to advanced amines. As demonstrated in Scheme 4.16, β-arylated pyrrolidine **4a** was readily obtained via silyl radical activation of β-C-Br bond.[44] Additionally, a nickel-catalyzed reductive cross-coupling of **2m** with 1-iodopropane successfully forged a C(sp^3)–C(sp^3) bond at remote site of pyrrolidine.[45] The reaction of **2m** with styrene en route to **4b** via Pd-catalyzed Heck-type process.[46] Nucleophilic substitution of **2m** with benzoate, amide, and azide provided access to

carbon−heteroatom (C−O/N) bonds (**4d-4f**) at this unconventional sp^3-hybridized site. Notably, the successful preparation of *N*-Ts-azelastine **4t** and *N*-Ts-fluoxetine **4y** from simple building blocks stand not only as a testament to the synthetic applicability for accessing advanced synthetic intermediates, but also offer improved flexibility in retrosynthetic design.

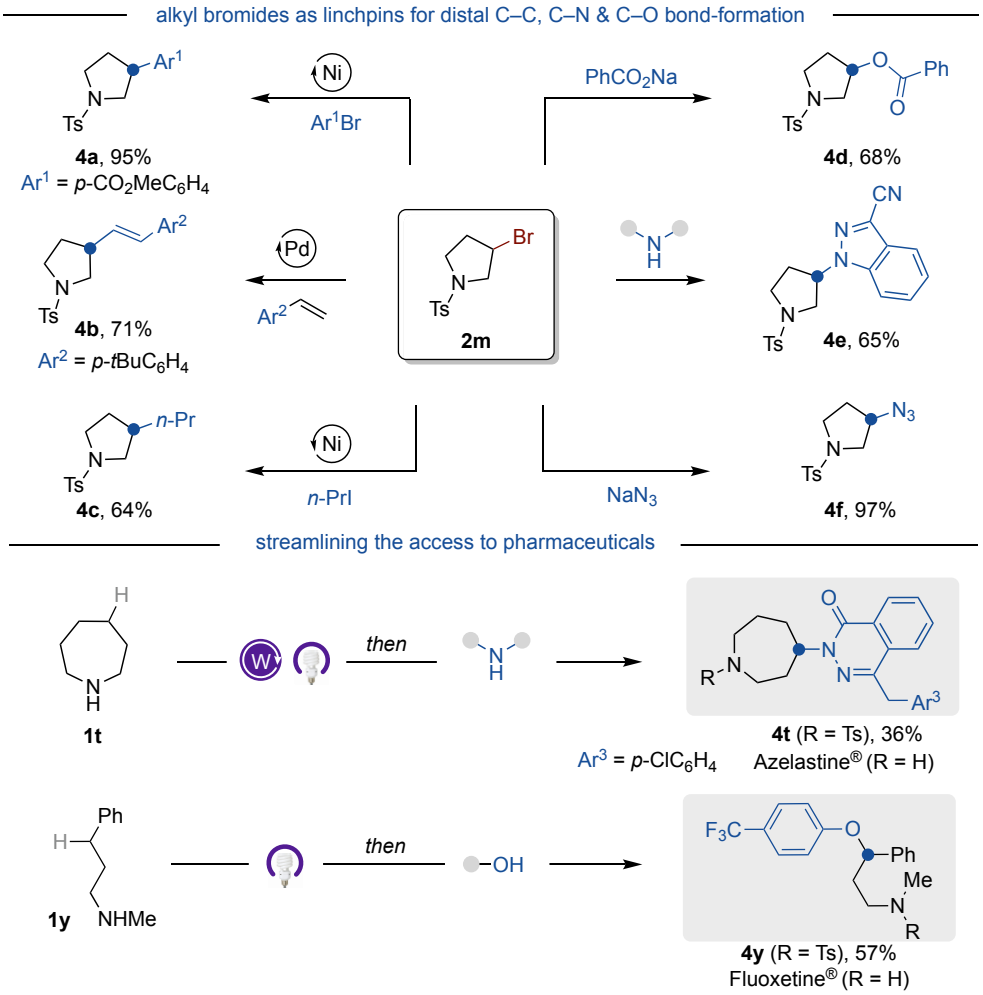

Scheme 4.16 Accessing advanced aliphatic amines by levering the potential of remote C(sp^3)–H functionalization *Top:* 1. Ir[dF(CF$_3$)ppy]$_2$(dtbbpy)PF$_6$ (1 mol%), Ni(dtbbpy)Br$_2$ (2 mol%), methyl 4-bromo benzoate (0.2 mmol), **2m** (0.3 mmol), TTMS (0.2 mmol), Na$_2$CO$_3$ (0.4 mmol), DME (2

mL), blue LED, 14 h. 2. $Pd(PPh_3)_4$ (5 mol%), dppf (7 mol%), **2m** (0.2 mmol),1-(tert-butyl)-4-vinylbenzene (0.4 mmol), LiI (0.4 mmol), Cy_2NMe (0.3 mmol,), $PhCF_3$ (1.0 mL), 110 °C, 36 h. 3. $Ni(COD)_2$ (10 mol%), (*S*)-*i*Pr-Pybox (8 mol%), **2m** (0.2 mmol), 1-iodopropane (0.6 mmol), Zn (0.6 mmol), DMA (1.5 mL), 25 ºC, 12 h. 4. **2m** (0.2 mmol), $PhCO_2Na$ (0.60 mmol) and KI (0.22 mmol), DMF (1 mL), 70 ºC, 16 h. 5. **2m** (0.2 mmol), 1*H*-Indazole-3-carbonitrile (0.60 mmol), K_2CO_3 (0.22 mmol), KI (0.22 mmol), DMF (1 mL), 70 ºC, 16 h. 6. **2m** (0.2 mmol), NaN_3 (1.0 mmol), DMF (1 mL), 80 ºC, 18 h. *Bottom:* as for **Scheme 4-13** followed by exposure with base, see experiment section for details.

4.8 Preliminary Mechanistic Studies

4.8.1 Radical Scavenger Experiments

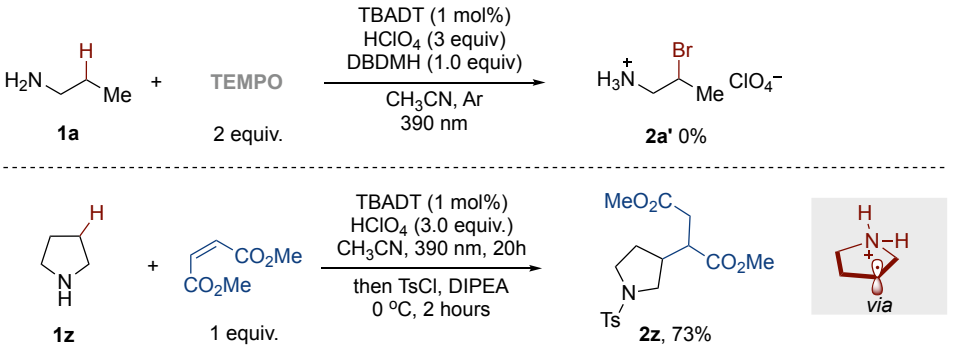

Scheme 4.17 Radical scavenger experiments

To gain insight into the possible reaction pathway of our C(sp^3)–H bromination protocol, a set of preliminary mechanistic experiments were conducted. As shown in Scheme 4.17, the addition of the radical scavenger–TEMPO completely inhibited the formation of **2a'**. Moreover, radical trapping experiments with dimethyl maleate resulted in the isolation of the radical addition product **2z** in 73% yield. These observations suggested the involvement of open-shell species in the bromination reaction.

4.8.2 Intermolecular Kinetic Isotope Effect

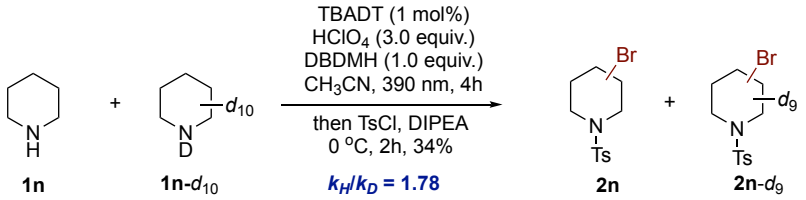

Scheme 4.18 Intermolecular kinetic isotope effect.

An intermolecular kinetic isotope effect (k_H/k_D=1.78) was observed by comparing the bromiantion of piperidine **1n** and **1n**-d_{10}, suggesting that C(sp^3)–H cleavage might not be involved in the rate-determining step of the reaction (Scheme 4.18).

4.8.3 Quantum Yields

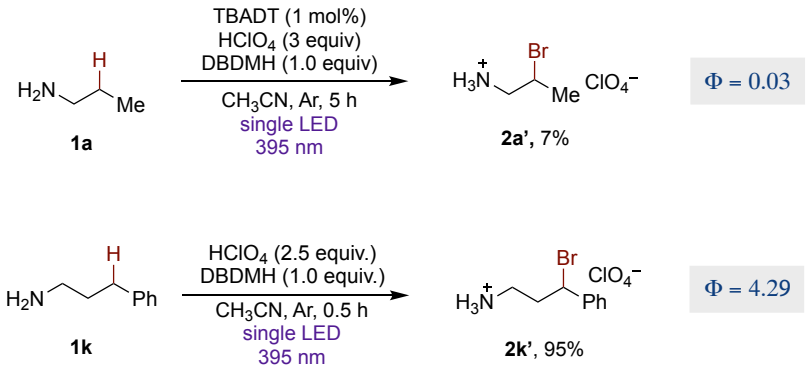

Scheme 4.19. Measurement of quantum yields for the reaction of **1a** and **1k**.

A quantum yield of 0.03 for the catalytic bromination of **1a** was observed (Scheme 4.19), suggesting that the reaction may not proceed through a canonical radical-chain propagation mechanism. In contrast, a quantum yield of 4.29 for the bromination of **1k** revealed that this process likely follows a radical-chain propagation mechanism, as each photon initiates multiple bromination events. This stark difference between the two reactions highlights distinct mechanistic pathways for bromination of unactivated C(sp^3)–H and benzylic C(sp^3)–H bonds.

4.8.4 Bromine Transfer Reactions

As shown in Scheme 4.18, 1-BrTMH (**b2**) and 3-BrTMH (**b3**) were prepared and tested with **1m'** respectively to identify which bromine is transferred from DBDMH (**b1**). The significantly higher yields observed with **b2** indicate that the N–Br bond at the 1-position is more active. However, this observation does not exclude the potential catalytic activity of the N–Br linkage at the 3-position.

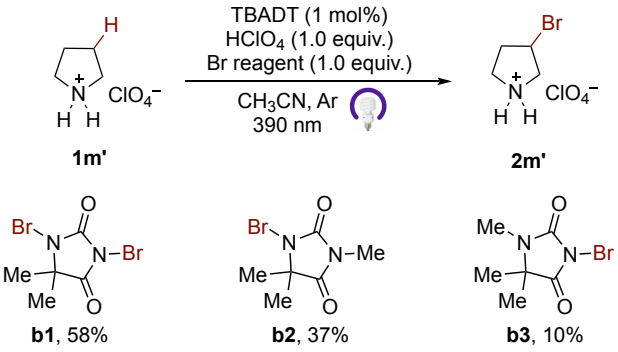

Scheme 4.18 Experiments with bromohydantoin reagents

4.8.5 Proposed Mechanism

With all this information in hand, we believe that our transformation follows the mechanistic rationale depicted in Figure 4.1.[47] Photoexcitation of the decatungstate anion $[W_{10}O_{32}]^{4-}$ (**I**) is followed by rapid intersystem crossing to generate the excited decatungstate triplet state $*[W_{10}O_{32}]^{4-}$ (**II**). This electrophilic species facilitates a hydrogen atom transfer at the remote C(sp^3)–H bond of ammonium salt **1a'**, resulting in the formation of a carbon centered radical **1a''** and reduced decatungstate $[W_{10}O_{32}]^{5-}$ **III** ($E[W_{10}O_{32}]^{4-}/[W_{10}O_{32}]^{5-} = -0.97$ V vs SCE).[48] This reduced decatungstate **III** undergoes disproportionation to regenerate the ground state decatungstate (**I**) and the doubly reduced decatungstate $[W_{10}O_{32}]^{6-}$ (**IV**). In parallel, a bromine atom transfer event between the carbon centered radical **1a''** and BDBMH yields the brominated **2a'** and an amidyl radical (**b4**). The formed amidyl subsequently oxidizes $[W_{10}O_{32}]^{6-}$ back to $[W_{10}O_{32}]^{5-}$, closing the reaction cycle ($E([W_{10}O_{32}]^{5-}/[W_{10}O_{32}]^{6-}) = -1.48$ V vs SCE).[49]

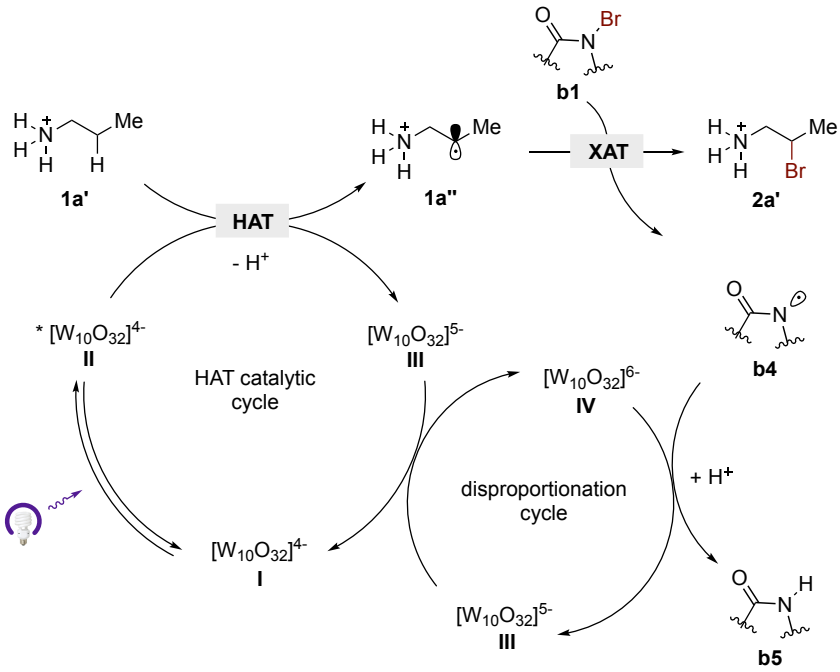

Figure 4.1 Proposed Mechanism.

4.9 Conclusion

This chapter summarizes our efforts towards the development of a predictable remote C(sp^3)–H bromination protocol for aliphatic primary and secondary amines. The reaction is achieved by an effective modulation of the electronic properties of proximal C(sp^3)–H bonds upon protonolysis of the amine function. This approach is distinguished by its broad applicability across a wide range of acyclic and heterocyclic amine scaffolds. Subsequent diversification of the carbon-halide bond offers a complementary platform for constructing heterocyclic motifs and forging C(sp^3)–C(sp^2), C(sp^3)–C(sp^3), and C(sp^3)–N/O architectures in common aliphatic amines, resulting in a site-selective protocol for incorporating functional groups at remote sp^3-hybridized sites.

4.10 Experimental Section

4.9.1 General Information

Analytical methods

^{1}H and ^{13}C NMR were recorded on Bruker 300 MHz, Bruker 400 MHz and Bruker 500 MHz at 20 °C. All ^{1}H NMR spectra are reported in parts per million (ppm) downfield of TMS and were calibrated using the residual solvent peak of $CHCl_3$ (7.26 ppm), unless otherwise indicated. All ^{13}C NMR spectra are reported in ppm relative to TMS, were calibrated using the signal of residual $CHCl_3$ (77.16 ppm). Coupling constants, J are reported in Hertz. Gas chromatographic analyses were performed on Hewlett-Packard 6890 gas chromatography instrument with FID detector. Melting points were measured using open glass capillaries in a Büchi B540 apparatus. Infrared spectra (FT-IR) measurements were carried out on a Bruker Optics FT-IR Alpha spectrometer equipped with a DTGS detector, KBr beamsplitter at 4 cm-1 resolution using a one bounce ATR accessory with diamond windows. High-resolution mass spectra were recorded on a Waters LCT Premier spectrometer or in a MicroTOF Focus, Bruker Daltonics spectrometer. UV/Vis absorption spectra were recorded using a Agilent Technologies Cary 300 UV/Vis spectrophotometer and UV-1800PC spectrophotometer in quartz cuvettes with a path length of 1.0 cm. Flash chromatography was performed with EM Science silica gel 60 (230-400 mesh). Thin layer chromatography was used to monitor reaction progress and analyzed fractions from column chromatography. To this purpose TLC Silica gel 60 F254 aluminium sheets from Merck were used and visualization was achieved using UV irradiation and/or staining with Potassium Permanganate or Phosphomolybdic acid solution. The yields reported refer to isolated yields and represent an average of at least two independent runs. The procedures described in this section are representative. Thus, the yields may differ slightly from those given in the tables of the manuscript.

Reagents

Commercially available materials were used as received without further purification. DBDMH (98% purity) was purchased from Fluorochem. $HClO_4$ (70% w/w solution) was purchased from Aldrich. Anhydrous MeCN (99.5% purity) was purchased from PanReac AppliChem. Anhydrous pivalonitrile (*t*-BuCN, 98% purity) was purchased from Aldrich.

Synthesis of catalysis

Synthesis of tetra-*n*-butylammonium decatungstate (TBADT). The title compound was prepared via modification of a literature procedure.[50] To a 2 L beaker wrapped in aluminum foil for insulation and equipped with a stir bar was added tetrabutylammonium bromide (4.80 g, 14.9 mmol, 0.49 equiv.) and deionized water (1600 mL). In a separate 4 L beaker wrapped in aluminum foil for insulation and equipped with a stir bar was added $Na_2WO_4 \cdot 2H_2O$ (10 g, 30.3 mmol, 1.00 equiv.) and deionized water (1600 mL). Both solutions were rapidly stirred and heated to 90 °C. When both solutions reached 90 °C, concentrated HCl was added to each solution until pH stabilized at 2. At this point, the acidified solutions were combined in the 4 L beaker, and the resultant suspension was stirred at 90 °C for an additional 30 minutes. The reaction mixture was cooled to room temperature, then filtered and the solids were washed with water and EtOAc, then left to dry under vacuum overnight, afford TBADT as white powder (5.33 g, 1.6 mmol, 53%). The quality of synthesized TBADT was measured by UV spectroscopy.[51]

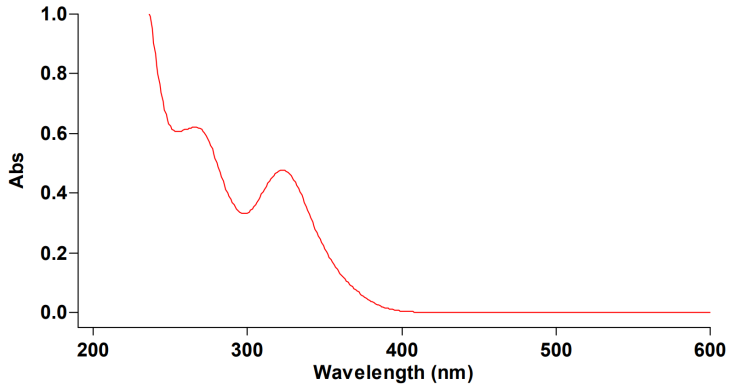

Figure 4-2. UV absorption spectrum of synthesized TBADT.

Synthesis of *n*-Bu_3BnNDT. To a 2 L beaker wrapped in aluminum foil for insulation and equipped with a stir bar was added benzyltributylammonium bromide (5.31 g, 14.9 mmol, 0.49 equiv.) and deionized water (1600 mL). In a separate 4 L beaker wrapped in aluminum foil for insulation and equipped with a stir bar was added Na_2WO_4•2H2O (10 g, 30.3 mmol, 1.00 equiv.) and deionized water (1600 mL). Both solutions were rapidly stirred and heated to 90 °C. When both solutions reached 90 °C, concentrated HCl was added to each solution until pH stabilized at 2. At this point, the acidified solutions were combined in the 4 L beaker, and the resultant suspension was stirred at 90 °C for an additional 30 minutes. The reaction mixture was cooled to room temperature, then filtered and the solids were washed with water and EtOAc, then left to dry under vacuum overnight, afford *n*-Bu_3BnNDT as white powder (4.78 g, 1.4 mmol, 47%). The quality of synthesized *n*-Bu_3BnNDT was measured by UV spectroscopy.

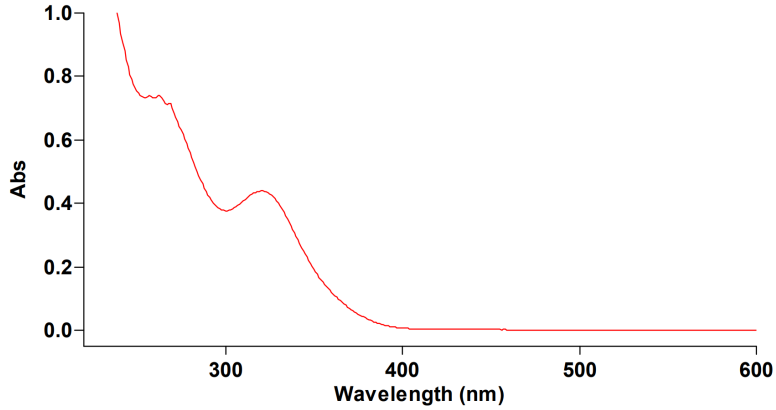

Figure 4-3 UV absorption spectrum of synthesized *n*-Bu_3BnNDT.

Synthesis of Ph_4PDT. To a 2 L beaker wrapped in aluminum foil for insulation and equipped with a stir bar was added tetraphenylphosphonium bromide (6.25 g, 14.9 mmol, 0.49 equiv.) and deionized water (1600 mL). In a separate 4 L beaker wrapped in aluminum foil for insulation and equipped with a stir bar was added Na_2WO_4•2H_2O (10 g, 30.3 mmol, 1.00 equiv.) and deionized water (1600 mL). Both solutions were rapidly stirred and heated to 90 °C. When both solutions reached 90 °C, concentrated HCl was

added to each solution until pH stabilized at 2. At this point, the acidified solutions were combined in the 4 L beaker, and the resultant suspension was stirred at 90 °C for an additional 30 minutes. The reaction mixture was cooled to room temperature, then filtered and the solids were washed with water and EtOAc, then left to dry under vacuum overnight, afford Ph_4PDT as white powder (4.25 g, 1.1 mmol, 37%). The quality of synthesized Ph_4PDT was measured by UV spectroscopy.

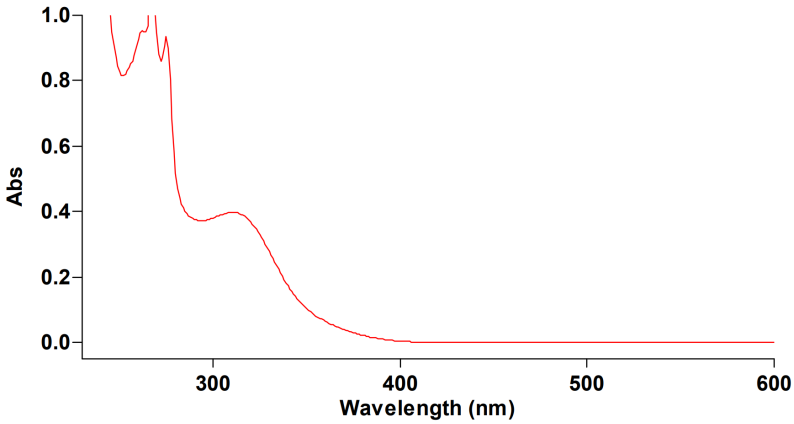

Figure 4-4 UV absorption spectrum of synthesized Ph_4PDT.

Standard reaction setup

8 vials photoreactor (UFO reactor). Eight vials were used in the photoreactor setup (UFO reactor).[52] Simultaneous irradiation of eight reactions took place using the photoreactor, with a 40W Kessil PR160L-390 nm LED lamp serving as the light source. A fan was placed beneath the reactor, thus ensuring that the reaction temperature remained below 30 °C. The entire setup was positioned behind UV-light shielding amber acrylic throughout the course of the reaction.

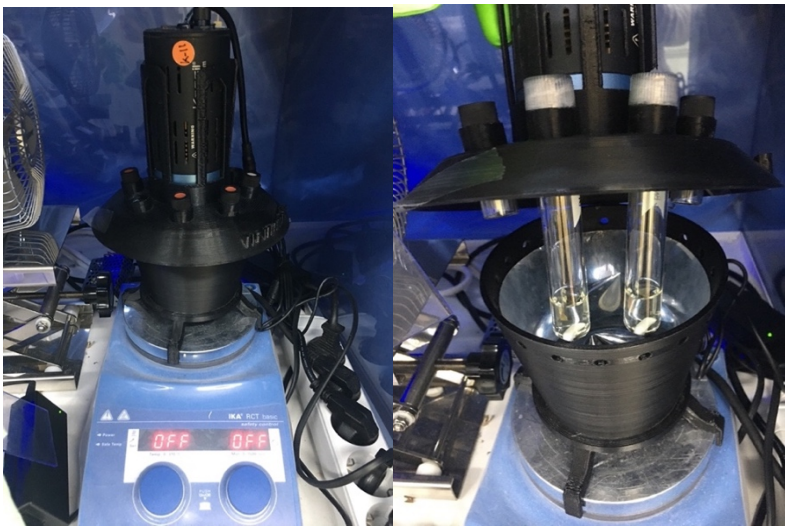

Optimization of the Reaction conditions.

Procedure for optimization of C(sp^3)–H Bromination of *n*-propylamine (1a) with TBADT as photocatalyst and DBDMH as bromine source.) An oven-dried 10 mL screw-cap reaction tube containing a stir bar was charged with TBADT (1 mol%, 6.6 mg) and the DBDMH (0.2 mmol, 1 equiv., 57 mg). The reaction tube was capped with a Teflon-lined rubber septum and connected to a vacuum line where it was evacuated and backfilled with Ar three times. In a separate 4 mL Teflon-capped glass vial, *n*-propylamine **1a** (0.4 mmol, 2 equiv., 24 mg) and CH_3CN (2 mL) were subsequently added by syringe followed by sequential addition of the corresponding acid (0.6 mmol, 3.0 equiv.). This solution was then transferred to the reaction tube by syringe after sparging with Ar for 5 minutes. The reaction tube was sealed with parafilm and irradiated by a 390 nm Kessil Lamp in a UFO Reactor under stirring at 600 rpm for 20 h. The reaction was then stopped and cooled to r.t.. The yield was determined via ^{1}H-NMR spectroscopy using CH_2Br_2 (0.2 mmol, 35mg, 13.5 μL) as internal standard.

C(sp^3)–H Bromination of *n*-propylamine (1a) with NCS as HAT reagent and CCl_3Br as bromine source.[53]

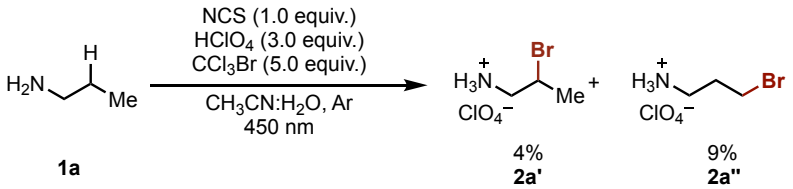

To an oven-dried 10 mL vial containing a stir bar was charged with *N*-chlorosuccinimide (NCS, 0.2 mmol, 1.0 equiv. 27 mg). The reaction tube was capped with a Teflon-lined rubber septum and connected to a vacuum line where it was evacuated and backfilled with Ar three times. In a separate 4 mL Teflon-capped glass vial was added amine **1a** (0.4 mmol, 2 equiv., 24 mg) and solvent (CH_3CN:H_2O (10:1), 2.2 mL), followed by sequential addition of $HClO_4$ (0.6 mmol, 3.0 equiv., 51μL). This solution was then transferred to the reaction tube by syringe after sparging with Ar for 5 minutes followed by addition of CCl_3Br (1.0 mmol, 5 equiv., 198 mg). The reaction tube was sealed with parafilm and irradiated by a 450 nm Kessil Lamp in a UFO Reactor under stirring at 600 rpm for 16 h. The reaction was stopped and cooled to r.t. The yield of **2a'** and **2a''** was determined via ^{1}H-NMR using CH_2Br_2 (0.2 mmol, 35mg, 13.5 μL) as internal standard. NMR spectroscopy of the crude revealed a 31% β-regioselectivity (**2a'**/(**2a'**+**2a''**) for **2a'**.

C(sp^3)–H Bromination of *n*-propylamine (1a) with *t*Bu$_2$-Mes-Acr$^+$ (PC1) as photocatalyst.

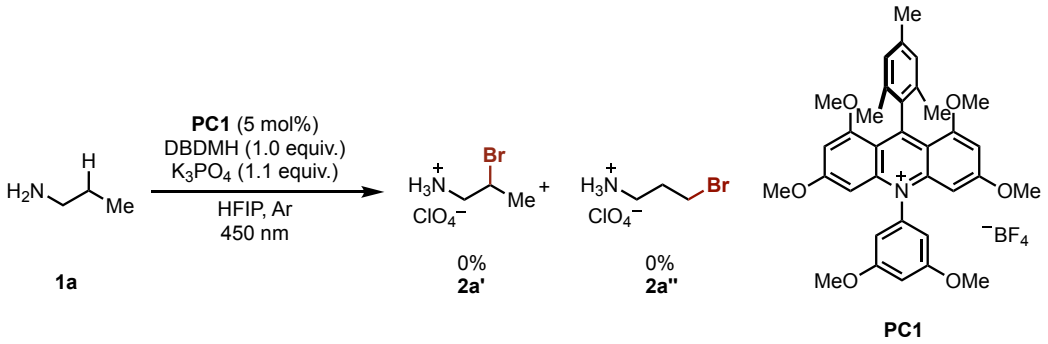

An oven-dried 10 mL screw-cap reaction tube containing a stir bar was charged with *t*Bu$_2$-Mes-Acr$^+$ (**PC1**, 5 mol%, 6.4 mg) K_3PO_4 (0.22 mmol, 1.1 equiv., 47 mg) and

DBDMH (0.2 mmol, 1 equiv, 57 mg). The reaction tube was capped with a Teflon-lined rubber septum and connected to a vacuum line where it was evacuated and backfilled with Ar three times. To this tube was added HFIP (2 mL) and amine **1a** (0.4 mmol, 2 equiv., 24 mg). The reaction mixture was sparged with Ar for 5 minutes, sealed with parafilm and irradiated by a 450 nm Kessil Lamp in a UFO Reactor under stirring at 600 rpm for 16 h. The reaction was stopped and cooled to r.t. The yield of **2a'** and **2a''** was determined via ^{1}H-NMR using CH_2Br_2 (0.2 mmol, 35mg, 13.5 μL) as internal standard.

Procedure for optimization of C(sp^3)–H Bromination of 3-phenylpropylamine (1k) with DBDMH as bromine source. An oven-dried 10 mL screw-cap reaction tube containing a stir bar was charged with DBDMH (0.2 mmol, 1.0 equiv., 57 mg). The reaction tube was capped with a Teflon-lined rubber septum and connected to a vacuum line where it was evacuated and backfilled with Ar three times. In a separate 4ml Teflon-capped glass vial, 3-phenylpropylamine (0.3 mmol, 1.5 equiv., 41 mg) and CH_3CN (2 mL) were added, followed by addition of $HClO_4$ (0.5 mmol, 2.5 equiv., 43 μL). This solution was transferred to the reaction tube by syringe after sparging with Ar for 5 minutes. The reaction tube was sealed with parafilm and irradiated by a 390 nm Kessil Lamp in a UFO Reactor under stirring at 600 rpm for 4 h (maintaining a temperature below 30°C). The reaction was then stopped and cooled to r.t.. The yield was determined via ^{1}H-NMR spectroscopy using CH_2Br_2 (0.2 mmol, 35mg, 13.5 μL) as internal standard.

4.9.2 C(sp^3)-H bromination of Aliphatic and Cyclic Amines

General procedure for C(sp^3)-H functionalization

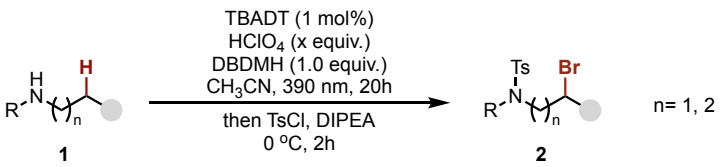

General Procedure A. An oven-dried 10 mL screw-cap reaction tube containing a stir bar was charged with TBADT (1 mol%, 6.6 mg) and DBDMH (0.2 mmol, 1.0 equiv., 57

mg). The reaction tube was capped with a Teflon-lined rubber septum and connected to a vacuum line where it was evacuated and backfilled with Ar three times. In a separate 4ml Teflon-capped glass vial, the corresponding amine (0.4-0.6 mmol, 2-3 equiv.) and CH_3CN (2 mL) were added by syringe, followed by the sequential addition of $HClO_4$ (0.6-0.8 mmol, 3.0-4.0 equiv., 51-68 μL). This solution was then transferred to the reaction tube by syringe after sparging with Ar for 5 minutes. The reaction tube was sealed with parafilm and irradiated by a 390 nm Kessil Lamp in a UFO Reactor under stirring at 600 rpm for 20 h. Then, the reaction mixture was cooled to 0 °C. TsCl (0.6-0.8 mmol, 3.0-4.0 equiv., 114-152 mg) and DIPEA (1.5-2.0 mmol, 7.5-10.0 equiv., 260-348 μL) were added sequentially to the reaction tube, and the mixture was stirred at 0 °C for 2 h. Subsequently, the reaction mixture was concentrated under vacuum, passed through a thin pad of silica with Hexane:EtOAc, and then concentrated under vacuum. The targeted compounds were purified by column chromatography on silica gel.

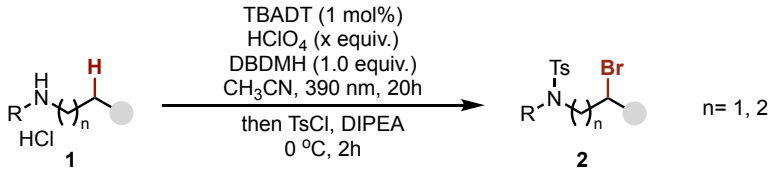

General Procedure B *(this procedure was utilized with hydrochloride salts as starting precursors)*. An oven-dried 10 mL screw-cap reaction tube containing a stir bar was charged with TBADT (1 mol%, 6.6 mg) and DBDMH (0.2 mmol, 1.0 equiv., 57 mg). The reaction tube was capped with a Teflon-lined rubber septum and connected to a vacuum line where it was evacuated and backfilled with Ar three times. In a separate 4ml Teflon-capped glass vial, amine HCl salt (0.4-0.6 mmol, 2.0-3.0 equiv.) and CH_3CN (2 mL) were added, followed by addition of $HClO_4$ (0.6-0.8 mmol, 3.0-4.0 equiv., 51-68 μL). This solution was concentrated under vacuum to remove HCl. After addition of 2 ml of CH_3CN and sparging with Ar for 5 minutes, this mixture was transferred to the reaction tube by syringe. The reaction tube was sealed with parafilm and irradiated by a 390 nm Kessil Lamp in a UFO Reactor under stirring at 600 rpm for 20 h (maintaining a temperature between 50 °C-60 °C). After reaction completion, the reaction mixture was cooled to 0 °C.

TsCl (0.6-0.8 mmol, 3.0-4.0 equiv., 114-152 mg) and DIPEA (1.5-2.0 mmol, 7.5-10.0 equiv., 260-348 μL) were added to the reaction tube and the mixture was stirred at 0 °C for another 2 hours. Subsequently, the reaction mixture was concentrated, passed through a thin pad of silica with Hexane:EtOAc, and concentrated under vacuum. The targeted compounds were purified by column chromatography on silica gel.

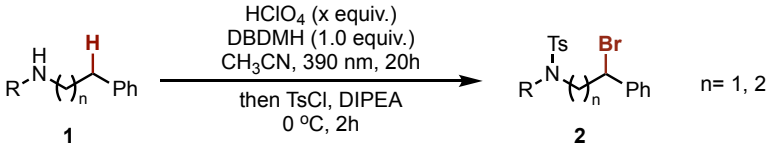

General Procedure C (*this procedure was utilized with aliphatic amines possessing arenes on the side-chain)*. An oven-dried 10 mL screw-cap reaction tube containing a stir bar was charged with DBDMH (0.2 mmol, 1.0 equiv., 57 mg). The reaction tube was capped with a Teflon-lined rubber septum and connected to a vacuum line where it was evacuated and backfilled with Ar three times. In a separate 4ml Teflon-capped glass vial, the amine (0.2-0.4 mmol, 1-2 equiv.) and CH_3CN (2 mL) were added, followed by addition of $HClO_4$ (0.4-0.6 mmol, 2.0-3.0 equiv., 26-51 μL). This solution was transferred to the reaction tube by syringe after sparging with Ar for 5 minutes. The reaction tube was sealed with parafilm and irradiated by a 390 nm Kessil Lamp in a UFO Reactor under stirring at 600 rpm for 4 h (maintaining a temperature below 30°C). After cooling the reaction to 0 °C, TsCl (0.4-0.6 mmol, 2.0-3.0 equiv., 76-114 mg) and DIPEA (1.5-2.0 mmol, 7.5-10.0 equiv., 260-348 μL) were added to the reaction tube, and the mixture was stirred at 0 °C for another 2 hours. Subsequently, the reaction mixture was concentrated, passed through a thin pad of silica with Hexane:EtOAc, and concentrated under vacuum. The targeted compounds were purified by column chromatography on silica gel.

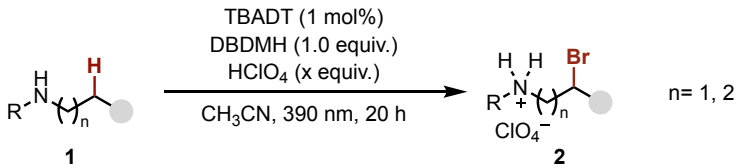

General Procedure D. (*this procedure was for determining NMR yield and site-selectivity without isolation).* An oven-dried 10 mL screw-cap reaction tube containing a stir bar was charged with TBADT (1 mol%, 6.6 mg) and DBDMH (0.2 mmol, 1.0 equiv., 57 mg). The reaction tube was capped with a Teflon-lined rubber septum and connected to a vacuum line where it was evacuated and backfilled with Ar three times. In a separate 4ml Teflon-capped glass vial, the corresponding amine (0.4-0.6 mmol, 2-3 equiv.) and CH_3CN (2 mL) were added by syringe, followed by the sequential addition of $HClO_4$ (0.6-0.8 mmol, 3.0-4.0 equiv., 51-68 μL). This solution was then transferred to the reaction tube by syringe after sparging with Ar for 5 minutes. The reaction tube was sealed with parafilm and irradiated by a 390 nm Kessil Lamp in a UFO Reactor under stirring at 600 rpm for 20 h. Then, the reaction was cooled to r.t. and the yield and selectivity were determined via ^{1}H-NMR spectroscopy using CH_2Br_2 (0.2 mmol, 35mg, 13.5 μL) as internal standard.

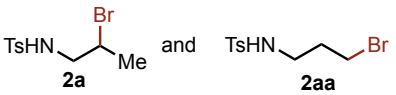

***N*-(2-bromopropyl)-4-methylbenzenesulfonamide (2a) and *N*-(3-bromopropyl)-4-methylbenzenesulfonamide (2aa).** Following General Procedure A, *n*-propylamine (0.4 mmol, 24 mg) and $HClO_4$ (0.6 mmol, 51μL) were used, affording **2a** (45 mg, 78%, white powder) and **2aa** (6 mg, 10%, colorless oil) with 89% β-regioselectivity (**2a**/(**2a**+**2aa**)).

2a: **^{1}H NMR** (400 MHz, $CDCl_3$) δ 7.75 (d, *J* = 8.3 Hz, 2H), 7.32 (d *J* = 7.9, 2H), 5.03 – 4.93 (m, 1H), 4.17 – 4.04 (m, 1H), 3.31 (m, 1H), 3.13 (m, 1H), 2.43 (s, 3H), 1.65 (d, *J* = 6.7, 3H) ppm. **^{13}C NMR** (101 MHz, $CDCl_3$) δ 143.9, 137.0, 129.7, 127.1, 51.2, 48.9, 23.3, 21.7 ppm. **IR (neat):** 3273, 1423, 1315, 1149, 1086, 809, 657, 548, 526 cm^{-1}. **HRMS (ESI)** *calcd*. for ($C_{10}H_{14}BrNNaO_2S$) $[M+Na]^+$: 313.9821, *found* 313.9810. **M.P.**: 76 °C.

2aa: **^{1}H NMR** (400 MHz, $CDCl_3$) δ 7.75 (d, *J* = 8.3 Hz, 2H), 7.32 (d, *J* = 8.0 Hz, 2H), 4.60 (t, *J* = 6.4 Hz, 1H), 3.42 (t, *J* = 6.3 Hz, 2H), 3.12 (q, *J* = 6.5 Hz, 2H), 2.44 (s, 3H), 2.03 (m, 2H) ppm. **^{13}C NMR** (101 MHz, $CDCl_3$) δ 143.8, 136.9, 130.0, 127.3, 41.6, 32.5, 30.3, 21.7 ppm. **IR (neat):** 3295, 1415, 1319, 1304, 1153, 1091, 1058, 946, 817, 666, 578, 545 cm^{-1}. **HRMS (ESI)** *calcd*. for ($C_{10}H_{14}BrNNaO_2S$) $[M+Na]^+$: 313.9821, *found* 313.9809.

Gram-scale synthesis of 2a

An oven-dried 100 mL round bottom flask containing a stir bar was charged with TBADT (1 mol%, 19.8 mg) and DBDMH (6.0 mmol, 1.0 equiv., 1.7 g). The reaction tube was capped with a septum and connected to a vacuum line where it was evacuated and backfilled with Ar three times. In a separate 100 mL round bottom flask, *n*-propylamine (12.0 mmol, 720 mg) and CH_3CN (30 mL) were added by syringe, followed by the sequential addition of $HClO_4$ (18.0 mmol, 3.0 equiv., 1.5 mL). This solution was concentrated under vacuum to remove water, another 60 mL of CH_3CN was add to this mixture which was then transferred to first 100 mL round bottom flask by syringe after

sparging with Ar for 10 minutes. The round bottom flask was sealed with parafilm and irradiated by two 390 nm Kessil Lamps under stirring at 610 rpm for 36 h. Then, the reaction mixture was cooled to 0 °C. TsCl (18.0 mmol, 3.0 equiv., 3.4 g) and DIPEA (45.0 mmol, 7.5 equiv., 7.8 mL) were added sequentially to the reaction tube, and the mixture was stirred at 0 °C for 2 h. Subsequently, the reaction mixture was concentrated under vacuum, diluted with EtOAc (70 mL) and 0.5 M HCl (90 mL), extracted by EtOAc three times, dried with anhydrous Na_2SO_4, then concentrated under vacuum to give a crude product, which was purified by column chromatography, affording **2a** (1.2 g, 68%, white powder) and **2aa** (173 mg, 10%, colorless oil) with 86% alpha-regioselectivity (**2a**/(**2a**+**2aa**)).

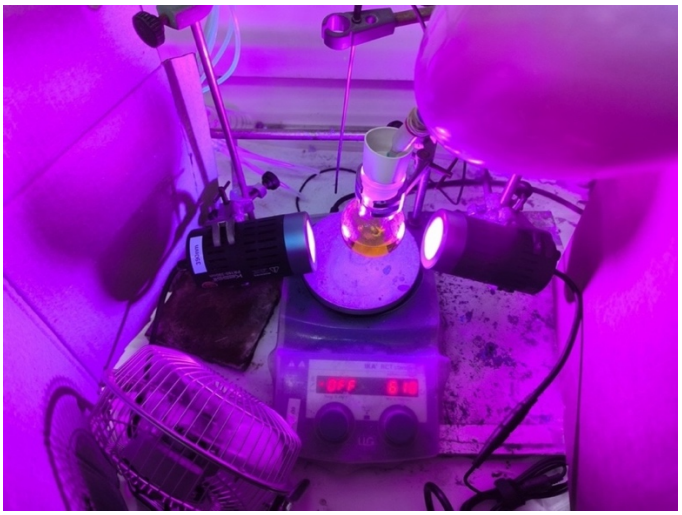

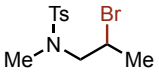

***N*-(2-bromopropyl)-*N*,4-dimethylbenzenesulfonamide (2b).** Following General Procedure A, *N*-methyl propylamine (0.4 mmol, 29 mg) and $HClO_4$ (0.6 mmol, 51μL) were used, affording the title compound as a white powder (42 mg, 68%). **^{1}H NMR** (400 MHz, $CDCl_3$) δ 7.68 (d, *J* = 8.3 Hz, 2H), 7.33 (d, *J* = 7.9 Hz, 2H), 4.23 (m, 1H), 3.36 (dd, *J* = 14.1, 8.0 Hz, 1H), 3.20 (dd, *J* = 14.1, 6.2 Hz, 1H), 2.81 (s, 3H), 2.44 (s, 3H), 1.76 (d, *J* = 6.7 Hz, 3H) ppm. **^{13}C NMR** (101 MHz, $CDCl_3$) δ 143.8, 134.6, 130.0, 127.6, 58.5,

46.4, 36.9, 23.4, 21.7 ppm. **IR (neat):** 2976, 1453, 1332, 1306, 1159, 1088, 965, 890, 814, 748, 655, 570, 548 cm^{-1}. **HRMS (ESI)** *calcd*. for ($C_{11}H_{16}BrNNaO_2S$) $[M+Na]^+$: 327.9977, *found* 327.9984. **M.P.**: 71 °C.

Following general procedure D (using *N*-methyl propylamine (0.4 mmol, 29 mg) and $HClO_4$ (0.6 mmol, 51μL)), NMR spectroscopy of the crude mixture revealed a 82% γ-regioselectivity (**2ba**/(**2ba**+**2ba'**) using benzoic acid (0.2 mmol, 24 mg) as internal standard.

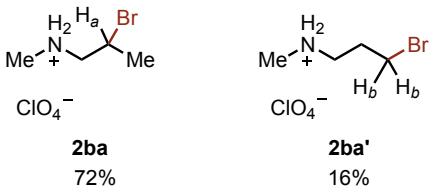

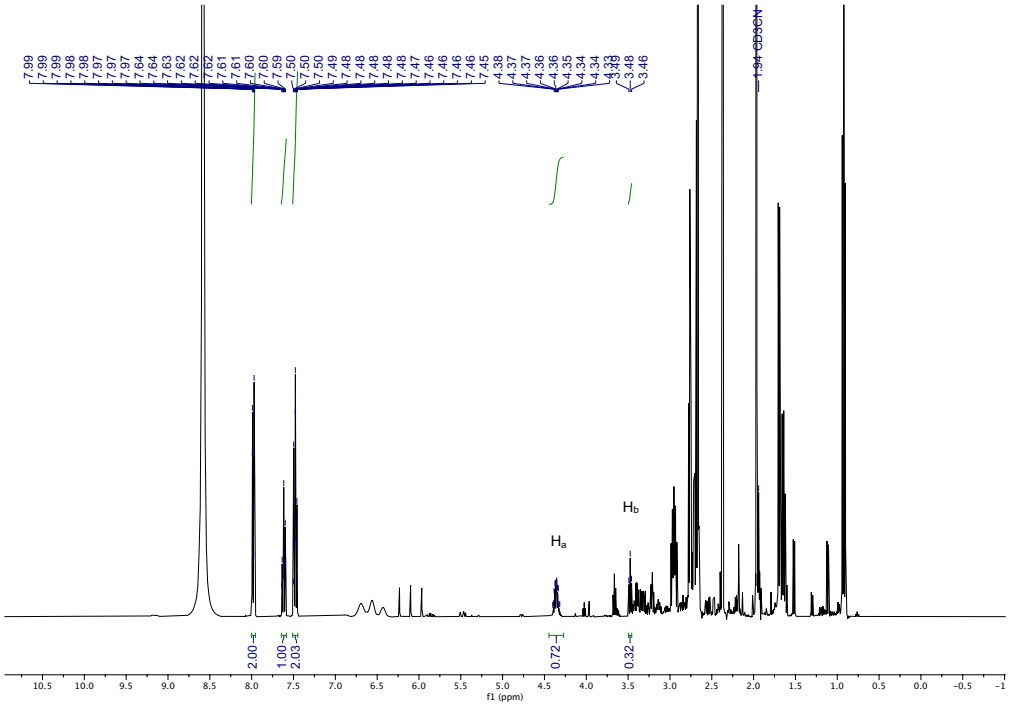

Crude ^{1}H-NMR (400 MHz, CD_3CN) en route to **2ba**:**2ba'**.

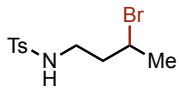

***N*-(3-bromobutyl)-4-methylbenzenesulfonamide (2c).** Following General Procedure A, *n*-butylamine (0.4 mmol, 29 mg) and $HClO_4$ (0.6 mmol, 51μL) were used, affording the title compound as a colorless oil (41 mg, 75%). **^{1}H NMR** (400 MHz, $CDCl_3$) δ 7.75 (d, *J* = 8.3 Hz, 2H), 7.32 (d, *J* = 8.5 Hz, 1H), 4.76 (t, *J* = 6.4 Hz, 1H), 4.14 (m, 1H), 3.20 – 3.03 (m, 2H), 2.43 (s, 3H), 2.00 (m, 1H), 1.89 (m, 1H), 1.68 (d, *J* = 6.6 Hz, 3H). **^{13}C NMR** (101 MHz, $CDCl_3$) (101 MHz, $CDCl_3$) δ 143.8, 136.9, 129.9, 127.2, 48.0, 41.9, 40.7, 26.6, 21.7. **IR (neat):** 3292, 1414, 1323, 1301, 1150, 1082, 813, 760, 664, 543 cm^{-1}. **HRMS (ESI)** *calcd.* for ($C_{11}H_{15}BrNO_2S$) $[M-H]^+$: 304.0012, *found* 304.0019.

Following general procedure D (using *n*-butylamine (0.4 mmol, 29 mg) and $HClO_4$ (0.6 mmol, 51μL), NMR spectroscopy of the crude mixture revealed a 82% γ-regioselectivity (**2ca**/(**2ca**+**2ca'**+**2ca''**)) using CH_2Br_2 (0.2 mmol, 35mg, 13.5 μL) as internal standard.

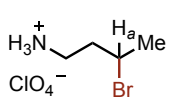

2ca
75%

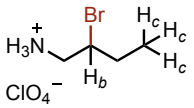

2ca'
11%

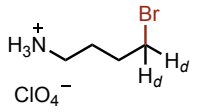

2ca''
5%

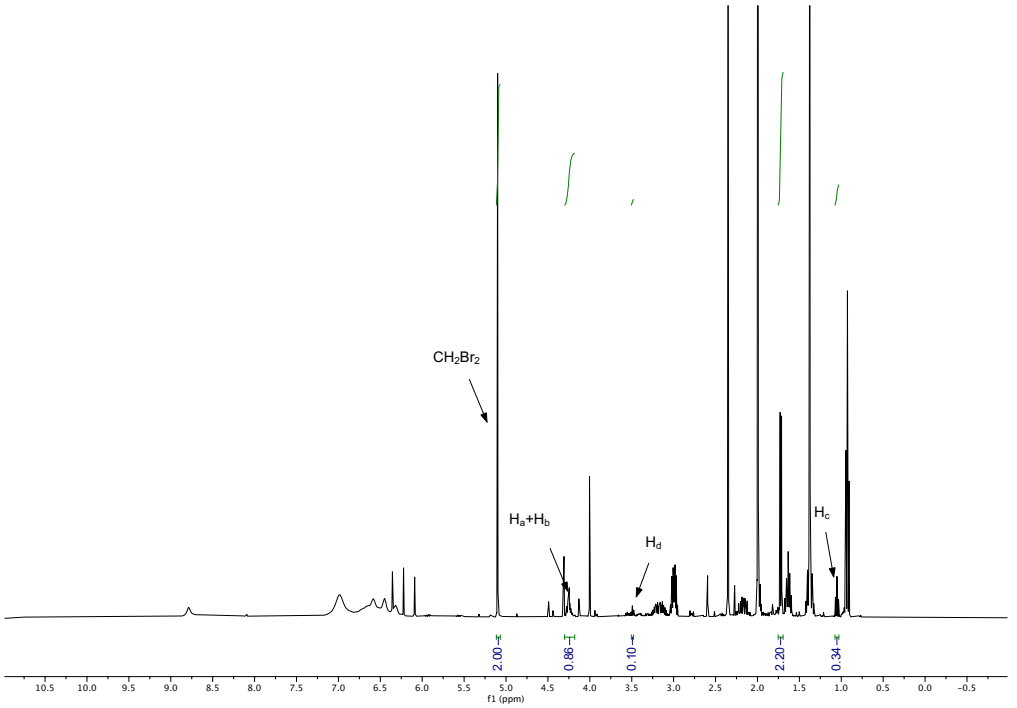

Crude ^{1}H-NMR (400 MHz, CD_3CN) en route to **2ca**:**2ca'**:**2ca''**

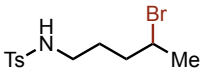

***N*-(4-bromopentyl)-4-methylbenzenesulfonamide (2d).** Following General Procedure A, amylamine (0.4 mmol, 35 mg) and $HClO_4$ (0.6 mmol, 51 μL) were used, affording the title compound as a colorless oil (44 mg, 69%). **^{1}H NMR** (400 MHz, $CDCl_3$) δ 7.75 (d, *J* = 8.3 Hz, 2H), 7.30 (d, *J* = 7.9 Hz, 1H), 4.89 (t, *J* = 6.3 Hz, 1H), 4.36 – 3.82 (m, 1H), 2.94 (q, *J* = 6.6 Hz, 2H), 2.42 (s, 3H), 1.75 (m, 2H), 1.73 – 1.38 (m, 5H). **^{13}C NMR** (101 MHz, $CDCl_3$) δ 143.6, 136.9, 129.9, 127.2, 50.8, 42.6, 37.8, 27.9, 26.5, 21.6. **IR (neat):** 3280, 1321, 1154, 1092, 910, 813, 730, 660, 548 cm^{-1}. **HRMS (ESI)** *calcd*. for ($C_{12}H_{17}BrNO_2S$) $[M\text{-}H]^+$: 318.0169, *found* 318.0164.

NMR spectroscopy of the crude mixture prior to purification revealed the formation of four different regioisomers **2d-2d'''** and 70% δ-regioselectivity (**2d**/(**2d**+**2d'**+**2d''**+**2d'''**) by utilizing CH_2Br_2 (0.1 mmol, 7 μL) as internal standard.

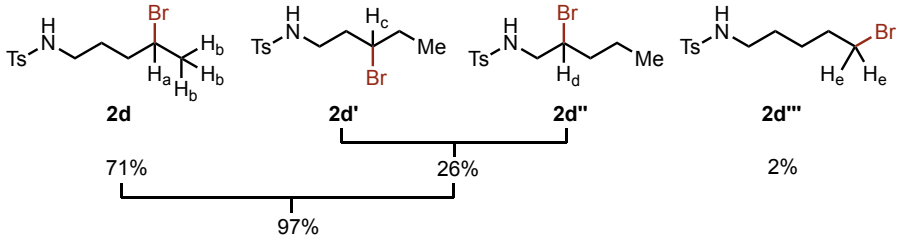

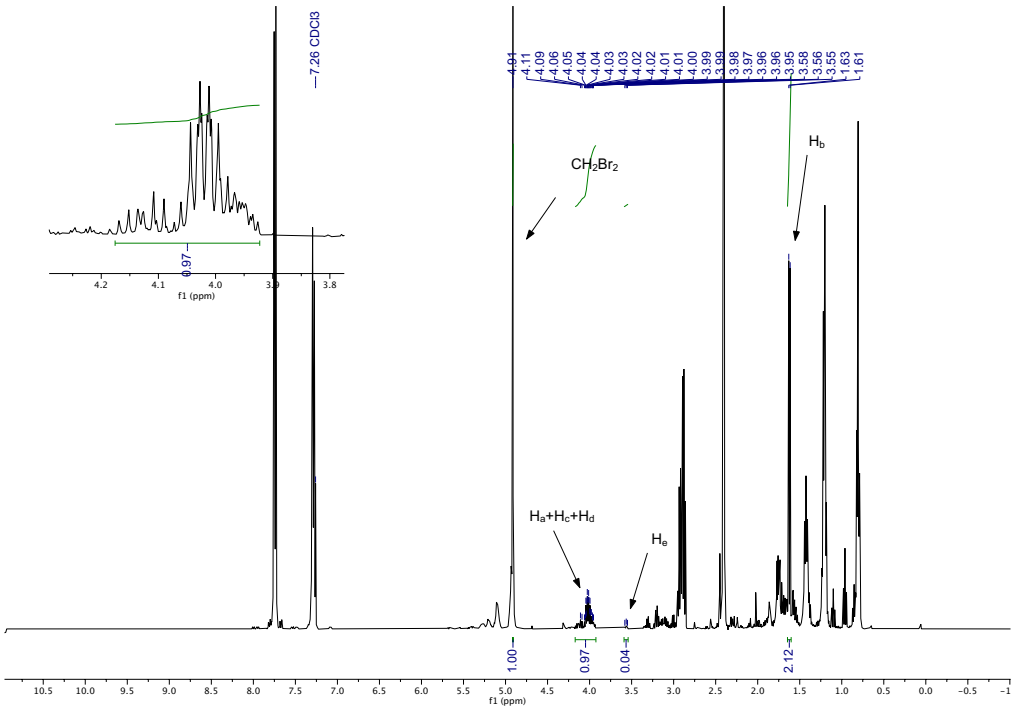

Crude ^{1}H-NMR (400 MHz, $CDCl_3$) en route to **2d**

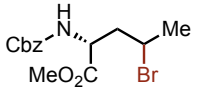

methyl (2*R*)-2-(((benzyloxy)carbonyl)amino)-4-bromopentanoate (2e). An oven-dried 10 mL screw-cap reaction tube containing a stir bar was charged with TBADT (1.0 mol%, 6.6 mg) and DBDMH (0.2 mmol, 1 equiv., 57 mg). The reaction tube was capped with a teflon-lined rubber septum and connected to a vacuum line where it was evacuated and backfilled with Ar three times. To a 4ml Teflon-capped glass vial was added *D*-Norvaline (0.6 mmol, 3 equiv., 70 mg) and CH_3CN (2 mL) before sequential addition of $HClO_4$ (0.8 mmol, 4 equiv., 68 μL). The reaction mixture was transferred to the reaction tube by syringe after sparging with Ar for 5 minutes. The reaction tube was then sealed with parafilm and irradiated by a 390 nm Kessil Lamp in a UFO Reactor (maintaining a temperature between 50 °C-60 °C) under stirring at 600 rpm for 20 h. After completion of the bromination, the reaction mixture concentrated under vacuum to remove CH_3CN completely, then cooled to 0 °C, MeOH (2 mL) and $SOCl_2$ (1.2 mmol, 6 equiv., 87 μL) were added to the reaction tube and the mixture was stirred at 0 °C to r.t. overnight. After the methylation reaction was complete, the reaction mixture concentrated under vacuum completely, then cooled to 0 °C, CH_3CN (2 mL), CbzCl (0.8 mmol, 4 equiv., 113 μL) and DIPEA (2.0 mmol, 10.0 equiv., 348 μL) were added to the reaction tube and the mixture was stirred at 0 °C for 2 hours. After the reaction was complete, the mixture was concentrated under vacuum, passed through a thin pad of silica with Hexane:EtOAc, then concentrated under vacuum to give a crude product, which was purified by column chromatography, which was purified by column chromatography, affording the brominated compound **2e** as colorless oil (38 mg, 56%; dr = 1:1). **^{1}H NMR** (500 MHz, CD_3CN) δ 7.67 – 7.22 (m, 5H), 5.98 (d, *J* = 7.3 Hz, 1H), 5.09 (s, 2H), 4.50 – 4.32 (m, 1H), 4.32 – 4.14 (m, 1H), 3.68 (s, 3H), 2.29 – 2.20 (m, 1H), 2.11 – 2.00 (m, 1H), 1.72 (d, *J* = 6.7 Hz, 3H). **^{13}C NMR** (126 MHz, CD_3CN) δ 173.3, 157.3, 138.0, 129.4, 128.9, 128.7, 67.2, 54.3, 53.0, 49.0, 42.9, 26.8. **IR (neat):** 3332, 2954, 1699, 1525, 1454, 1435, 1265, 1213, 1177, 1041, 1028, 738, 696 cm^{-1}. **HRMS (ESI)** *calcd*. for ($C_{14}H_{19}BrNO_4$) $[M+H]^+$: 344.0492, *found* 344.0505.

Following general procedure D (using *D*-Norvaline (0.6 mmol, 3 equiv., 70 mg) and $HClO_4$ (0.8 mmol, 4 equiv., 68 μL), NMR spectroscopy of the crude mixture revealed a

80% γ-regioselectivity (**2ea**/(**2ea**+**2ea'**+**2ea''**)) by using CH_2Br_2 (0.2 mmol, 13.5 μL) as internal standard.

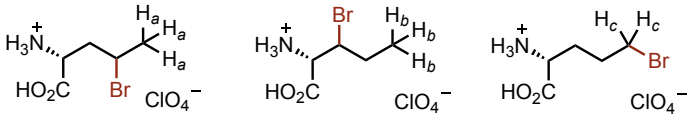

2ea 71%　　**2ea'** 10%　　**2ea''** 8%

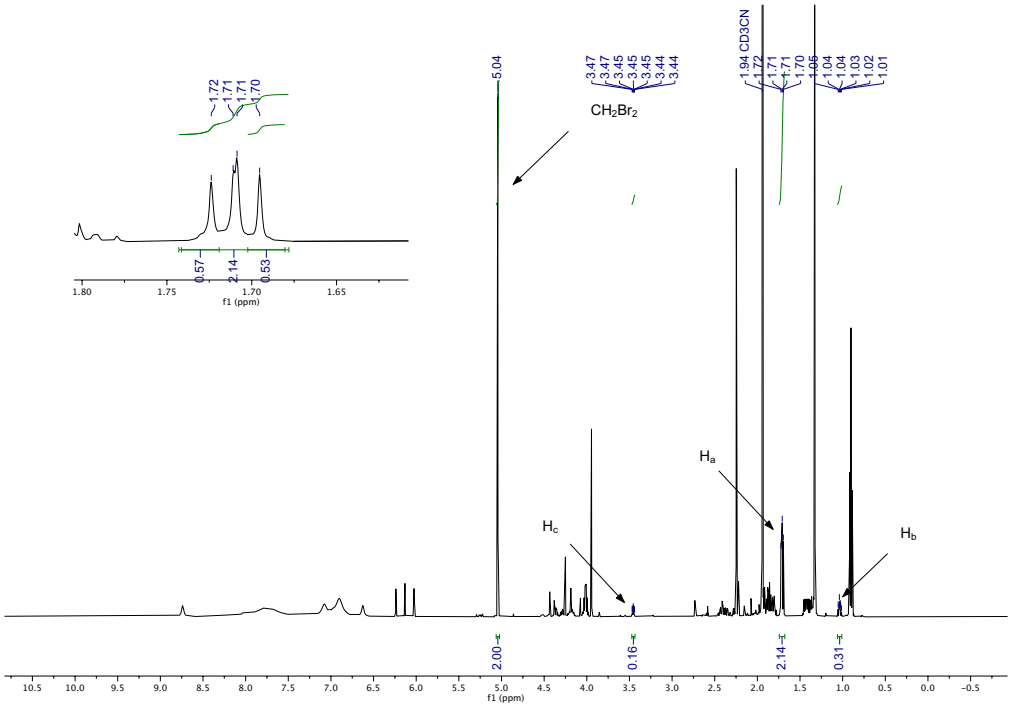

Crude ^{1}H-NMR (400 MHz, CD_3CN) en route to **2ea**

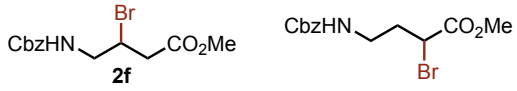

2f　　**2f'**

Methyl 4-(((benzyloxy)carbonyl)amino)-3-bromobutanoate (2f) and methyl 4-(((benzyloxy)carbonyl)amino)-2-bromobutanoate (2f'). An oven-dried 10 mL screw-

cap reaction tube containing a stir bar was charged with TBADT (1.0 mol%, 6.6 mg) and DBDMH (0.2 mmol, 1 equiv., 57 mg). The reaction tube was capped with a teflon-lined rubber septum and connected to a vacuum line where it was evacuated and backfilled with Ar three times. To a 4ml Teflon-capped glass vial was added 4-aminobutyric acid (GBAB) (0.4 mmol, 2 equiv. 41 mg) and CH_3CN (2 mL) before sequential addition of $HClO_4$ (0.6 mmol, 3 equiv., 51 μL). The reaction mixture was transferred to the reaction tube by syringe after sparging with Ar for 5 minutes. The reaction tube was then sealed with parafilm and irradiated by a 390 nm Kessil Lamp in a UFO Reactor (the temperature remained below 30 °C) under stirring at 600 rpm for 20 h. After completion of the bromination, the reaction mixture concentrated under vacuum to remove CH_3CN completely, then cooled to 0 °C, MeOH (2 mL) and $SOCl_2$ (1.2 mmol, 6 equiv., 87 μL) were added to the reaction tube and the mixture was stirred at 0 °C to r.t. overnight. After the methylation reaction was complete, the reaction mixture concentrated under vacuum completely, then cooled to 0 °C, CH_3CN (2 mL), CbzCl (0.6 mmol, 3 equiv., 85 μL) and DIPEA (1.7mmol, 8.5 equiv., 300 μL) were added to the reaction tube and the mixture was stirred at 0 °C to r.t. for 2 hours. After the reaction was complete, the mixture was concentrated under vacuum, passed through a thin pad of silica with Hexane:EtOAc, then concentrated under vacuum to give a crude product, which was purified by column chromatography, which was purified by column chromatography, affording the brominated compound **2f** and **2f'** (2:1 ratio) as colorless oil (35 mg, 54%).

^{1}H NMR (500 MHz, $CDCl_3$, **2f** and **2f'** (rr 2:1)) for δ 7.39 – 7.28 (m, 5H), 5.24 (s, 0.67H), 5.11 (s, 2.33H), 4.95 (s, 0.26H), 4.47 – 4.38 (m, 0.70H), 4.33-4.30 (m, 0.30), 3.76 (s, 0.91H), 3.72 (s, 2.09H), 3.69 – 3.53 (m, 2H), 3.40 (m, 0.32H), 3.32 (m, 0.36H), 2.96 (m, 0.74H), 2.87 (m, 0.85H), 2.35 (m, 0.28H), 2.23 – 2.11 (m, 0.31H). **^{13}C NMR** (126 MHz, $CDCl_3$, **2f** and **2f'** (rr 2:1)) δ 170.3, 170.1, 156.4, 136.4, 136.3, 128.7, 128.7, 128.4, 128.4, 128.3, 67.3, 67.0, 53.2, 52.3, 48.2, 47.3, 43.1, 41.0, 38.9, 34.9. **IR (neat):** 3339, 2953, 1721, 1529, 1438, 1247, 1154, 1012, 698 cm^{-1}. **HRMS (ESI)** *calcd*. for ($C_{13}H_{16}BrNNaO_4$) $[M+Na]^+$: 352.0155, *found* 352.0164.

Following general procedure D (using 4-aminobutyric acid (GBAB) (0.4 mmol, 2 equiv. 41 mg) and $HClO_4$ (0.6 mmol, 3 equiv., 51 μL), NMR spectroscopy of the crude mixture revealed a 82% β-regioselectivity (**2fa**/(**2fa**+**2fa'**) by using CH_2Br_2 (0.2 mmol, 13.5 μL) as internal standard.

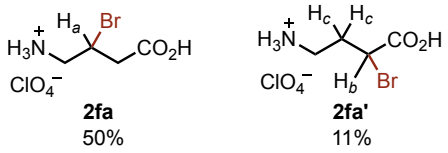

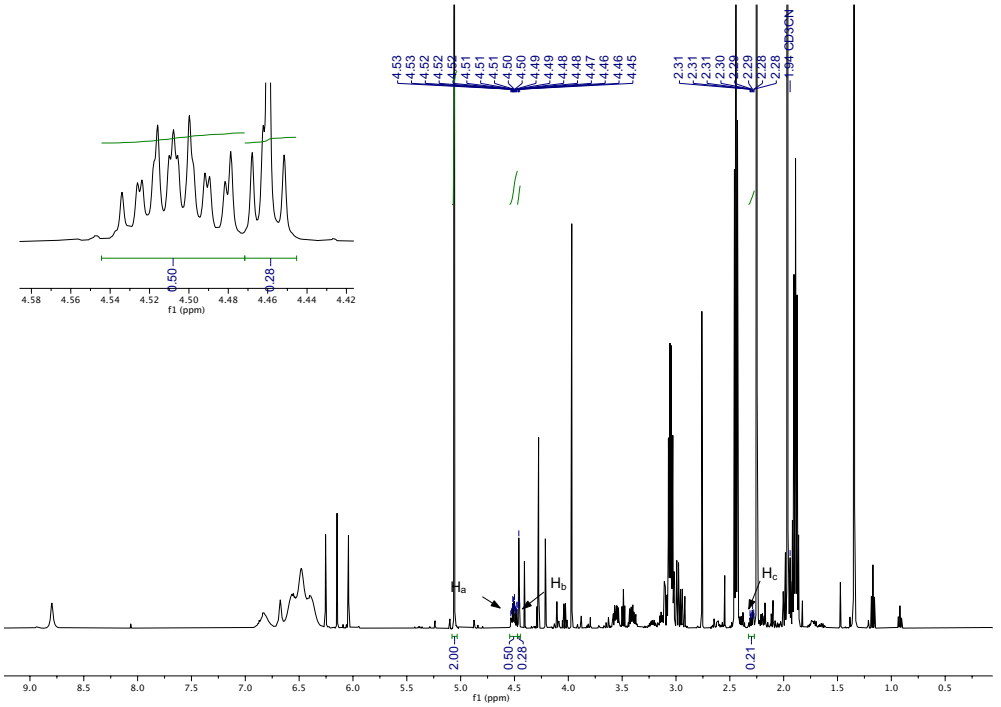

Crude ^{1}H-NMR (400 MHz, CD_3CN) en route to **2fa**

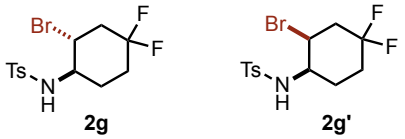

(±)-*N*-((1*R*,2*R*)-2-bromo-4,4-difluorocyclohexyl)-4-methylbenzenesulfonamide (2g) and **(±)-*N*-((1*R*,2*S*)-2-bromo-4,4-difluorocyclohexyl)-4-methylbenzenesulfonamide (2g').** Following General Procedure B, 4,4-difluorocyclohexylamine hydrochloride (0.6 mmol, 103 mg), $HClO_4$ (0.8 mmol, 68 μL), Tosylation was carried out at 0 °C for 1.5 hours, affording **2g** (38 mg, 52%, colorless oil) and **2g'** (13 mg, 18%, colorless oil) in a 2.9:1 ratio.

2g: **^{1}H NMR** (500 MHz, CD_3Cl_3) δ 7.78 (d, *J* = 8.3 Hz, 2H), 7.32 (d, J = 7.9 Hz, 2H), 4.94 (d, *J* = 5.5 Hz, 1H), 3.91 – 3.80 (m, 1H), 3.19 (m, 1H), 2.79 – 2.67 (m, 1H), 2.44 (s, 3H), 2.37 (m, 1H), 2.30 – 2.20 (m, 1H), 2.18 – 2.07 (m, 1H), 1.89 – 1.73 (m, 1H), 1.70 – 1.54 (m, 2H). **^{13}C NMR** (126 MHz, CD_3Cl_3) δ 144.1, 136.8, 129.9, 127.6, 120.8 (dd, *J* = 247.3, 240.4 Hz), 57.9, 47.70 (d, *J* = 11.5 Hz), 43.6 (t, *J* = 26.0 Hz), 31.9 (dd, *J* = 25.2, 23.5 Hz), 28.7 (d, *J* = 9.3 Hz), 21.7. **IR (neat):** 3304, 2924, 1597, 1449, 1369, 1310,1291, 1158, 1139, 1107, 1088, 994, 972, 949, 905, 847, 809, 664, 570, 552 cm^{-1}. **HRMS (ESI)** *calcd*. for ($C_{13}H_{16}BrF_2NNaO_2S$) $[M+Na]^+$: 389.9945, *found* 389.9930.

2g': **^{1}H NMR** (500 MHz, CD_3Cl_3) δ 7.77 (d, *J* = 8.3 Hz, 2H), 7.34 (d, *J* = 7.7 Hz, 2H), 4.88 (d, *J* = 5.0 Hz, 1H), 4.19 (dt, *J* = 8.7, 4.1 Hz, 1H), 3.34 (m, 1H), 2.44 (m, 5H), 2.29 (m, 1H), 2.21 – 2.07 (m, 1H), 1.90 (m, 1H), 1.67 (m, 1H). **^{13}C NMR** (126 MHz, CD_3Cl_3) δ 144.3, 136.3, 130.1, 127.5, 123.2-118.4 (m), 53.2, 48.8, 40.0 (t, *J* = 25.9 Hz), 29.5 (t, *J* = 23.1 Hz), 25.8-25.6 (m), 21.7. **IR (neat):** 3270, 2924, 1433, 1309, 1125, 1093, 1080, 964, 913, 809, 665, 586, 555, 543 cm^{-1}. **HRMS (ESI)** *calcd*. for ($C_{13}H_{16}BrF_2NNaO_2S$) $[M+Na]^+$: 389.9945, *found* 389.9927.

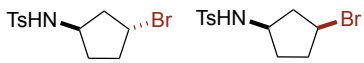

2h **2h'**

***N*-3-bromocyclopentyl)-4-methylbenzenesulfonamide 2h and 2h'.** Following General Procedure A, cyclopentylamine (0.4 mmol, 34 mg) and $HClO_4$ (0.6 mmol, 51 μL) were used, affording **2h** (20 mg, 32%, colorless oil) and **2h'** (16 mg, 26%, colorless oil), in a 1.2:1 ratio.

2h: **^{1}H NMR** (400 MHz, $CDCl_3$) δ 7.76 (d, *J* = 8.3 Hz, 2H), 7.31 (d, *J* = 8.6 Hz, 2H), 4.90 (d, *J* = 9.5 Hz, 1H), 4.33 (m, 1H), 3.93 – 3.81 (m, 1H), 2.43 (s, 3H), 2.36 (m, 1H), 2.18 – 2.01 (m, 2H), 2.01 – 1.87 (m, 2H), 1.85 – 1.73 (m, 1H). **^{13}C NMR** (101 MHz, $CDCl_3$) δ 143.6, 138.0, 129.9, 127.2, 53.5, 50.6, 44.8, 36.7, 32.6, 21.7. **IR (neat):** 3253, 2923, 1426, 1331, 1306, 1150, 1091, 903, 813, 669, 543 cm^{-1}. **HRMS (ESI)** *calcd*. for ($C_{12}H_{16}BrNNaO_2S$) $[M+Na]^+$: 339.9977, *found* 339.9984.

2h': ^{1}H NMR (400 MHz, $CDCl_3$) δ 7.77 (d, *J* = 8.3 Hz, 2H), 7.32 (d, *J* = 7.9 Hz, 2H), 4.87 (d, *J* = 7.2 Hz, 1H), 4.39 (m, 1H), 3.95 (m, 1H), 2.44 (s, 3H), 2.35 – 2.23 (m, 2H), 2.23 – 2.11 (m, 1H), 2.07 – 1.93 (m, 2H), 1.45 (m, 1H).**^{13}C NMR** (101 MHz, $CDCl_3$) δ 143.8, 137.4, 130.0, 127.3, 53.4, 49.5, 45.3, 36.1, 31.8, 21.7. **IR (neat):** 3267, 2976, 1440, 1319, 1304, 1153, 1091, 905, 813, 729, 663, 597, 547 cm^{-1}. **HRMS (ESI)** *calcd*. for ($C_{12}H_{16}BrNNaO_2S$) $[M+Na]^+$: 339.9977, *found* 339.9984.

NMR spectroscopy of the crude mixture prior to purification revealed the formation of 4 compounds **2h-2h''',** with 88% γ-regioselectivity ((**2h**+**2h'**)/(**2h**+**2h'**+**2h''**+**2h'''**)) by utilizing CH_2Br_2 (0.1 mmol, 7 μL) as internal standard.

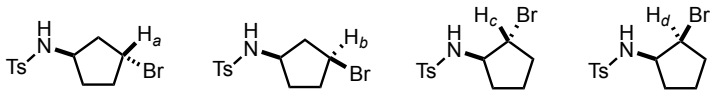

2h 34%　　**2h'** 27%　　**2h''** 4%　　**2h'''** 4%

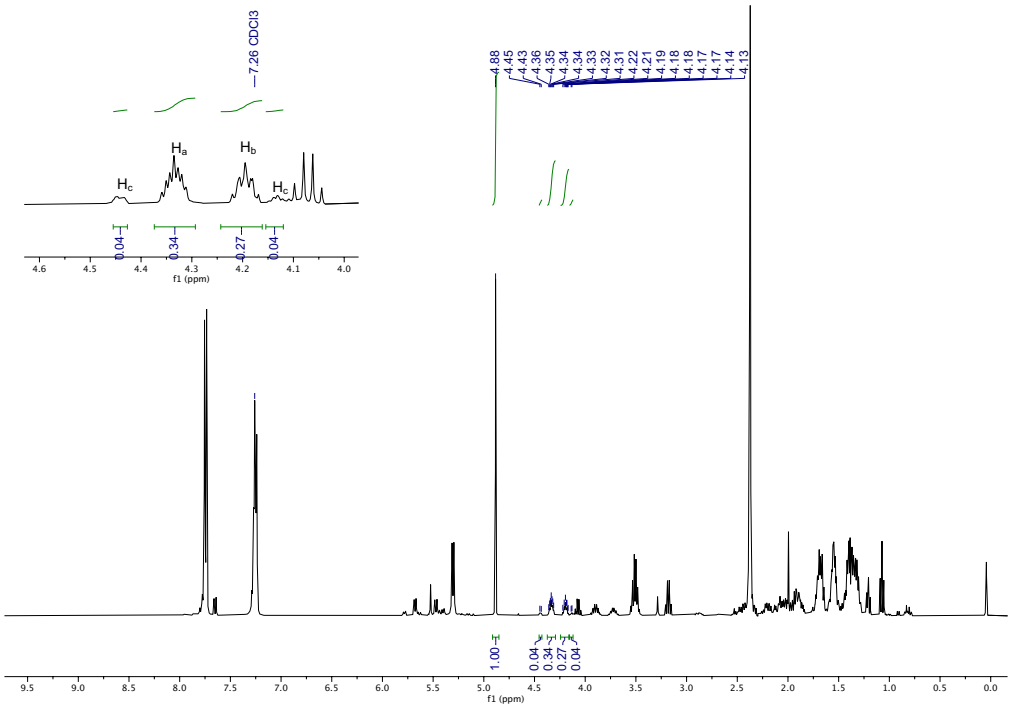

Crude ^{1}H-NMR (400 MHz, $CDCl_3$) en route to **2h**

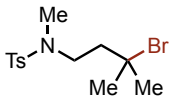

***N*-(3-bromo-3-methylbutyl)-*N*,4-dimethylbenzenesulfonamide (2i).** Following General Procedure A, *N*-methylisoamylamine (0.4 mmol, 49 mg) and $HClO_4$ (0.6 mmol, 51 µL) were used, affording the title compound as a colorless oil (53 mg, 79%). **^{1}H NMR** (300 MHz, $CDCl_3$) δ 7.68 (d, J = 8.2 Hz, 2H), 7.33 (d, J = 7.9 Hz, 2H), 3.39 – 3.15 (m, 2H), 2.76 (s, 3H), 2.43 (s, 3H), 2.24 – 1.96 (m, 2H), 1.77 (s, 6H). **^{13}C NMR** (75 MHz, $CDCl_3$) δ 143.6, 134.7, 129.9, 127.5, 64.9, 48.4, 44.9, 35.3, 34.5, 21.7. **IR (neat):** 2989, 2917, 1459, 1335, 1191, 1158, 1129, 1088, 938, 812, 735, 652, 568, 547, 513 cm^{-1}. **HRMS (ESI)** *calcd*. for ($C_{13}H_{20}BrNNaO_2S$) $[M+Na]^+$: 356.0290, *found* 356.0275.

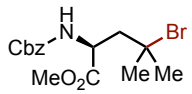

Methyl (*S*)-2-(((benzyloxy)carbonyl)amino)-4-bromo-4-methylpentanoate (2j). Following General Procedure B, *L*-Leucine methyl ester hydrochloride (0.4 mmol, 72 mg) and $HClO_4$ (0.6 mmol, 51 μL) were used, affording the title compound as a colorless oil (60 mg, 83%). **^{1}H NMR** (400 MHz, CD_3CN) δ 7.45 – 7.24 (m, 5H), 6.12 (d, *J* = 7.8 Hz, 1H), 5.09 (d, *J* = 2.2 Hz, 2H), 4.54 – 4.44 (m, 1H), 3.68 (s, 3H), 2.54 – 2.45 (m, 1H), 2.17 – 2.06 (m, 1H), 1.80 (s, 3H), 1.77 (s, 3H). **^{13}C NMR** (101 MHz, CD_3CN) δ 173.5, 156.9, 138.1, 129.4, 128.9, 128.6, 67.2, 53.9, 53.0, 48.5, 35.5, 34.0. **IR (neat):** 3336, 2954, 1701, 1524, 1437, 1302, 1214, 1117, 1114, 1047, 739, 697 cm^{-1}. **HRMS (ESI)** *calcd.* for ($C_{15}H_{21}BrNO_4$) $[M+H]^+$: 358.0648, *found* 358.0660.

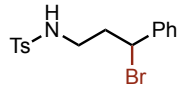

***N*-(3-bromo-3-phenylpropyl)-4-methylbenzenesulfonamide (2k).** Following General Procedure C, 3-phenylpropylamine (0.24 mmol, 32 mg) and $HClO_4$ (0.6 mmol, 51 μL) were used, affording the title compound as a colorless oil (72 mg, 98%). **^{1}H NMR** (500 MHz, $CDCl_3$) δ 7.81 – 7.72 (m, 2H), 7.32 – 7.24 (m, 7H), 5.09 (t, *J* = 6.3 Hz, 1H), 5.01 (dd, *J* = 9.3, 5.6 Hz, 1H), 3.10 (dt, *J* = 7.1, 6.1 Hz, 2H), 2.42 (s, 3H), 2.41 – 2.35 (m, 1H), 2.27 (m, 1H). **^{13}C NMR** (101 MHz, $CDCl_3$) δ 143.7, 141.3, 136.8, 129.9, 128.9, 128.7, 127.3, 127.2, 52.0, 41.8, 39.6, 21.6. **IR (neat):** 3262. 1997, 1436, 1323, 1153, 1091, 1068, 810, 697, 548 cm^{-1}. **HRMS (ESI)** *calcd.* for ($C_{16}H_{19}BrNO_2S$) $[M+H]^+$: 368.0314, *found* 368.0323.

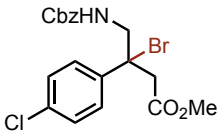

Methyl 4-(((benzyloxy)carbonyl)amino)-3-bromo-3-(4-chlorophenyl)butanoate (2l). An oven-dried 10 mL screw-cap reaction tube containing a stir bar was charged with TBADT (1.0 mol%, 6.6 mg) and DBDMH (0.2 mmol, 1 equiv., 57 mg). The reaction tube was capped with a teflon-lined rubber septum and connected to a vacuum line where it was evacuated and backfilled with Ar three times. To a 4ml Teflon-capped glass vial was added Baclofen (0.4 mmol, 2 equiv., 85 mg) and CH_3CN (2 mL) before sequential addition of $HClO_4$ (0.6 mmol, 3 equiv., 51 μL). The reaction mixture was transferred to the reaction tube by syringe after sparging with Ar for 5 minutes. The reaction tube was then sealed with parafilm and irradiated by a 390 nm Kessil Lamp in a UFO Reactor (ensuring the temperature remained below 30 °C) under stirring at 600 rpm for 20 h. After completion of the bromination, the reaction mixture was concentrated under vacuum to remove CH_3CN completely, then cooled to 0 °C, MeOH (2 mL) and $SOCl_2$ (1.2 mmol, 6 equiv., 87 μL) were added to the reaction tube and the mixture was stirred at 0 °C to r.t. overnight. After the methylation reaction was complete, the reaction mixture concentrated under vacuum completely. CH_3CN (2 mL) was added to the reaction tube, then cooled to 0 °C, CbzCl (0.6 mmol, 3 equiv., 85 μL) and DIPEA (1.7 mmol, 8.5 equiv., 300 μL) were added to the reaction tube and the mixture was stirred at 0 °C to r.t. for 2 hours. After the reaction was complete, the mixture was concentrated under vacuum, passed through a thin pad of silica with Hexane:EtOAc, then concentrated under vacuum to give a crude product, which was purified by column chromatography, affording the title compound as a colorless oil (73 mg, 84%). **^{1}H NMR** (500 MHz, CD_3CN) δ 7.57 (d, J = 8.8 Hz, 2H), 7.47 – 7.20 (m, 7H), 5.92 (s, 1H), 5.02 (s, 2H), 4.04 (m, 2H), 3.56 (s, 3H), 3.52 – 3.40 (m, 2H). **^{13}C NMR** (126 MHz, CD_3CN) δ 170.1, 157.4, 141.1, 138.1, 134.4, 130.1, 129.4, 129.0, 128.8, 128.6, 68.2, 67.1, 52.7, 52.3, 45.6. **IR (neat):** 3342, 2951, 1719, 1513, 1494, 1435, 1217, 1171, 1096, 1011, 827, 728, 696 cm^{-1}. **HRMS (ESI)** *calcd*. for ($C_{19}H_{19}BrClNNaO_4$) $[M+Na]^+$: 462.0078, *found* 462.0094.

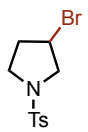

3-bromo-1-tosylpyrrolidine (2m). Following a modified General Procedure A, pyrrolidinium perchlorate (0.4 mmol, 68 mg) and $HClO_4$ (0.2 mmol, 17 μL) was used, affording the title compound as a white solid (34 mg, 60%). **^{1}H NMR** (400 MHz, $CDCl_3$) δ 7.73 (d, *J* = 8.3 Hz, 2H), 7.33 (d, *J* = 7.8 Hz, 2H), 4.33 (m, 1H), 3.86 (dd, *J* = 12.1, 5.2 Hz, 1H), 3.58 (m, 1H), 3.52 (m, 1H), 3.46 (m, 1H), 2.43 (s, 3H), 2.36 – 2.23 (m, 1H), 2.14 (m, 1H). **^{13}C NMR** (101 MHz, $CDCl_3$) δ 143.9, 133.9, 129.9, 127.7, 57.3, 46.3, 45.6, 36.5, 21.7. **IR (neat):** 1328, 1156, 1091, 1010, 818, 660, 589, 546 cm^{-1}. **HRMS (ESI)** *calcd*. for ($C_{11}H_{14}BrNNaO_2S$) $[M+Na]^+$: 325.9821, *found* 325.9827. **M.P.** :95 °C.

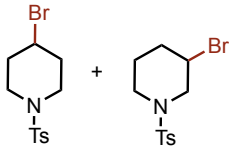

2n **2n'**

4-bromo-1-tosylpiperidine (2n) and 3-bromo-1-tosylpiperidine (2n'). Following General Procedure A, piperidine (0.6 mmol, 51 mg) and $HClO_4$ (0.8 mmol, 68 μL) was used, affording **2n** and **2n'** as colorless oil (50 mg, 79%). The ratio of **2n**: **2n'** is 1.3:1. **^{1}H NMR** (500 MHz, $CDCl_3$) δ 7.64 (d, *J* = 8.3 Hz, 3H), 7.33 (d, *J* = 8.3 Hz, 3H), 4.24 (m, 1H), 4.06 (m, 0.5H), 3.94 (m, 0.5H), 3.59 (m, 0.5H), 3.19 (m, 2H), 3.09 (m, 2H), 2.63 (m, 0.5H), 2.44 (m, 5H), 2.28 – 2.13 (m, 2.6H), 2.05 (m, 2H), 1.83 (m, 0.5H), 1.77 – 1.56 (m, 1.5H). **^{13}C NMR** (101 MHz, $CDCl_3$) δ 144.0, 143.9, 133.6, 133.4, 129.9, 129.9, 127.7, 127.7, 53.6, 48.0, 45.8, 45.3, 43.9, 35.0, 34.8, 25.5, 21.7. **IR (neat):** 2956, 2923, 1597, 1445, 1339, 1279, 1161, 1091, 928, 712, 549 cm^{-1}. **HRMS (ESI)** *calcd*. for ($C_{12}H_{16}BrNNaO_2S$) $[M+Na]^+$: 339.9977, *found* 339.9975.

NMR spectroscopy of the crude mixture prior to purification revealed a 57% γ-regioselectivity (**2n**/(**2n**+**2n'**) by using CH_2Br_2 (0.1 mmol, 7 μL) as internal standard.

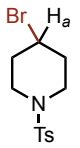

2n
46%

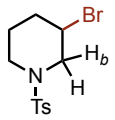

2n'
35%

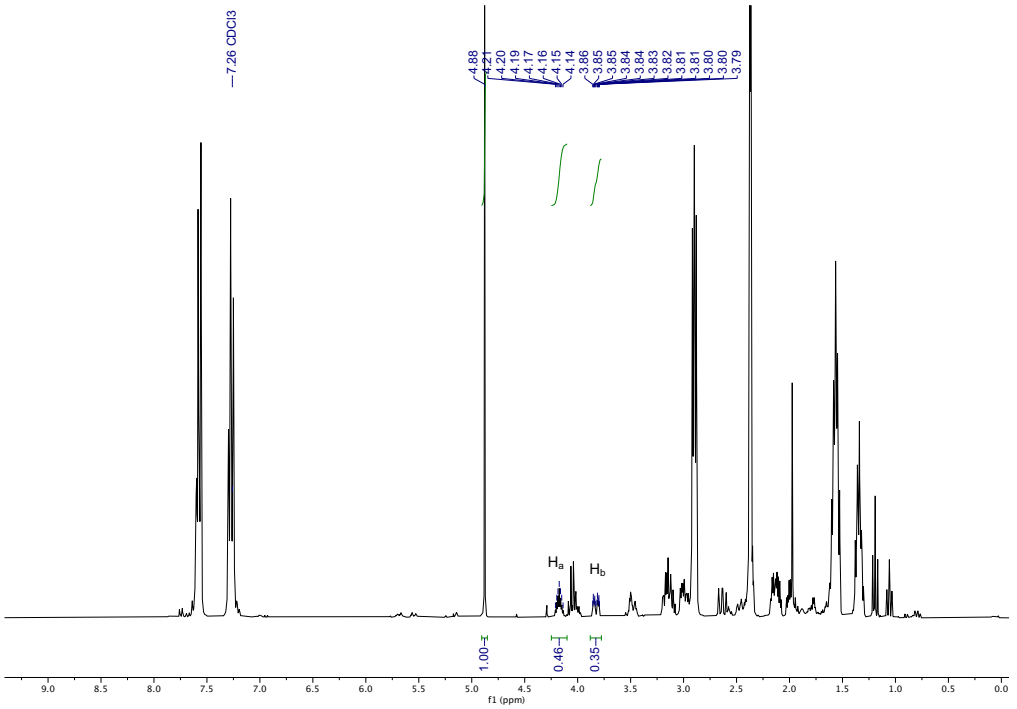

Crude ^{1}H-NMR (400 MHz, $CDCl_3$) en route to **2n**

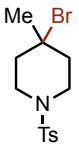

4-bromo-4-methyl-1-tosylpiperidine (2o). Following General Procedure A, 4-methylpiperidine (0.4 mmol, 40 mg) and $HClO_4$ (0.6 mmol, 51 μL) was used, affording the title compound as a colorless oil (45 mg, 68%). **^{1}H NMR** (300 MHz, $CDCl_3$) δ 7.65 (d, *J* = 8.3 Hz, 2H), 7.33 (d, *J* = 7.9 Hz, 2H), 3.75 – 3.63 (m, 2H), 2.80 – 2.64 (m, 2H),

2.43 (s, 3H), 2.12 – 1.96 (m, 2H), 1.91 – 1.69 (m, 5H). **^{13}C NMR** (126 MHz, $CDCl_3$) δ 143.8, 133.6, 129.9, 127.7, 66.1, 43.6, 41.3, 34.9, 21.7. **IR (neat):** 2945, 2923, 1598, 1338, 1283, 1151, 1089, 936, 901, 805, 750, 656, 589, 548 cm^{-1}. **HRMS (ESI)** *calcd.* for ($C_{13}H_{18}BrNNaO_2S$) $[M+Na]^+$: 354.0134, *found* 354.0132. **M.P.**: 84 °C.

NMR spectroscopy of the crude mixture prior to purification revealed the formation of **2o-2o'** with 84% γ-regioselectivity (**2o**/(**2o**+**2o'**)) by utilizing CH_2Br_2 (0.1 mmol, 7 μL) as internal standard.

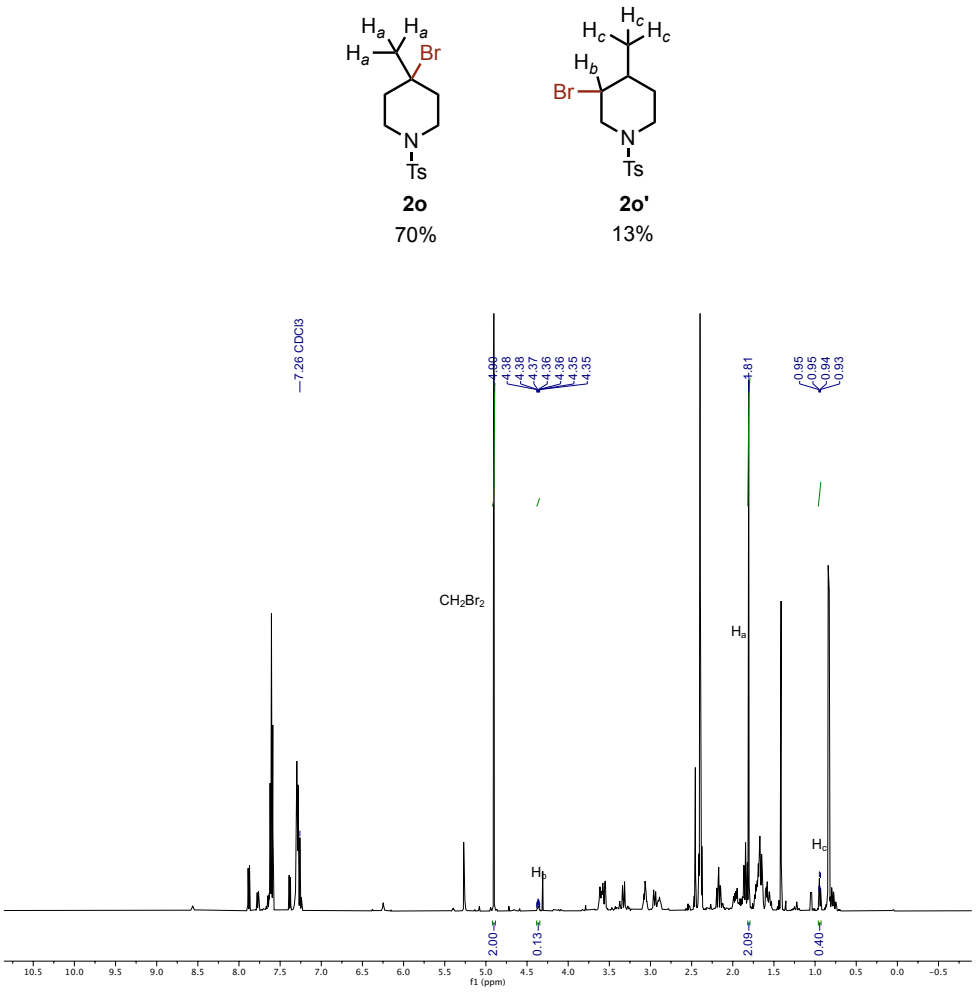

Crude ^{1}H-NMR (400 MHz, $CDCl_3$) en route to **2o**

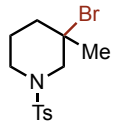

3-bromo-3-methyl-1-tosylpiperidine (2p). Following General Procedure A, 3-methylpiperidine (0.4 mmol, 40 mg) and $HClO_4$ (0.6 mmol, 51μL) was used, affording the title compound as a colorless oil (44 mg, 66%). **^{1}H NMR** (500 MHz, $CDCl_3$) δ 7.65 (d, *J* = 8.3 Hz, 2H), 7.32 (d, *J* = 7.9 Hz, 2H), 3.31 (m, 1H), 3.10 – 2.93 (m, 3H), 2.43 (s, 3H), 2.07 – 1.93 (m, 1H), 1.93 – 1.86 (m, 1H), 1.85 (s, 3H), 1.79 – 1.65 (m, 2H). **^{13}C NMR** (126 MHz, $CDCl_3$) δ 143.8, 133.8, 129.9, 127.7, 61.6, 58.9, 46.0, 40.9, 30.2, 23.2, 21.7. **IR (neat):** 2945, 2924, 1338, 1164, 1151, 1089, 937, 901, 806, 751, 656, 589, 549 cm^{-1}. **HRMS (ESI)** *calcd*. for ($C_{13}H_{18}BrNNaO_2S$) $[M+Na]^+$: 354.0134, *found* 354.0125.

NMR spectroscopy of the crude mixture prior to purification revealed the formation of **2p-2p''** with 84% β-regioselectivity (**2p**/(**2p**+**2p'**+**2p''**)) by utilizing CH_2Br_2 (0.1 mmol, 7 μL) as internal standard.

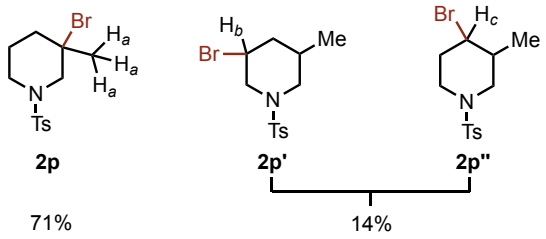

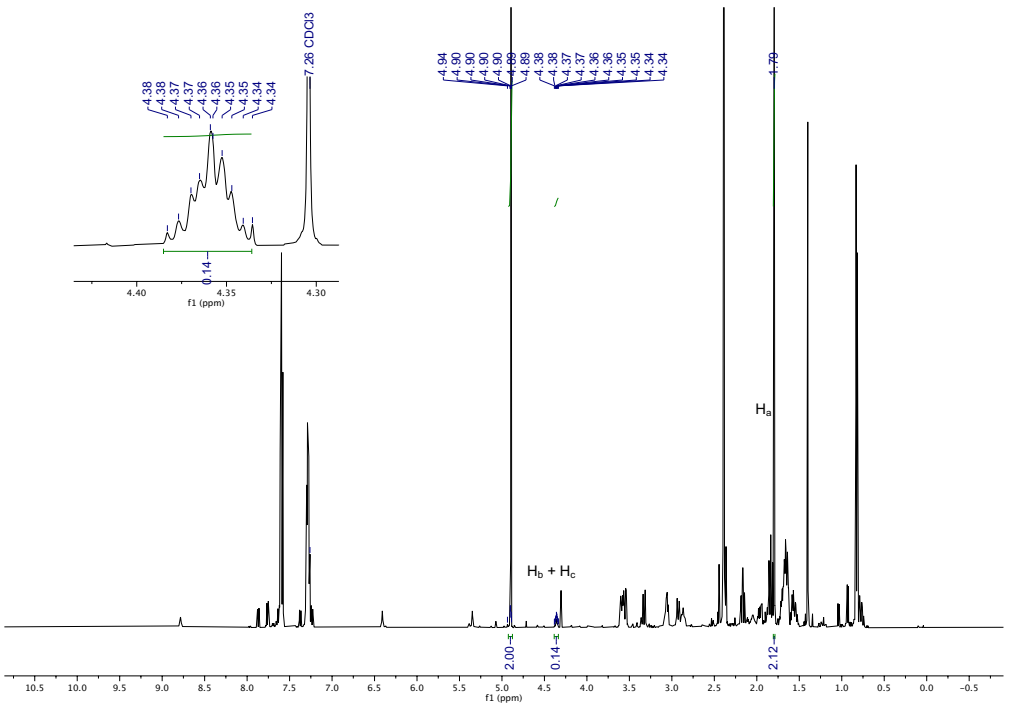

Crude ^{1}H-NMR (400 MHz, $CDCl_3$) en route to **2p**

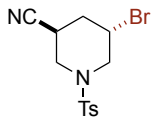

(±)-(3*S*,5*S*)-5-bromo-1-tosylpiperidine-3-carbonitrile (2q). Following General Procedure A, piperidine-3-carbonitrile (0.6 mmol, 66 mg) and $HClO_4$ (0.8 mmol, 68µL) were used, affording the title compound as a white solid (26 mg, 38%; dr = 3.6:1). **^{1}H NMR** (500 MHz, $CDCl_3$) δ 7.67 (d, *J* = 8.3 Hz, 2H), 7.36 (d, *J* = 7.9 Hz, 2H), 4.35 (m, 1H), 3.48 (m, 1H), 3.31 (m, 2H), 3.28 – 3.18 (m, 2H), 2.45 (s, 3H), 2.30 (m, 1H), 2.14 (m, 1H). **^{13}C NMR** (126 MHz, $CDCl_3$) δ 144.7, 133.4, 130.2, 127.8, 118.6, 52.5, 47.1, 41.5, 36.4, 26.5, 21.7. **IR (neat):** 2922, 2244, 1597, 1342, 1327, 1158, 1086, 911, 811, 723, 661, 549 cm^{-1}. **HRMS (ESI)** *calcd.* for ($C_{13}H_{15}BrN2NaO_2S$) $[M+Na]^+$: 364.9930, *found* 364.9927. **M.P.** :157 °C.

Following general procedure D (using piperidine-3-carbonitrile (0.6 mmol, 66 mg) and $HClO_4$ (0.8 mmol, 68μL), NMR spectroscopy of the crude mixture revealed a 78% β-regioselectivity en route to **2qa/2qa'** ((**2qa**+**2qa'**)/(**2qa**+**2qa'**+**2qa''**)), by using CH_2Br_2 (0.2 mmol, 35mg, 13.5 μL) as internal standard.

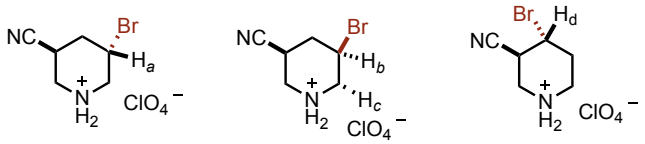

2qa 40% **2qa'** 11% **2qa''** 14%

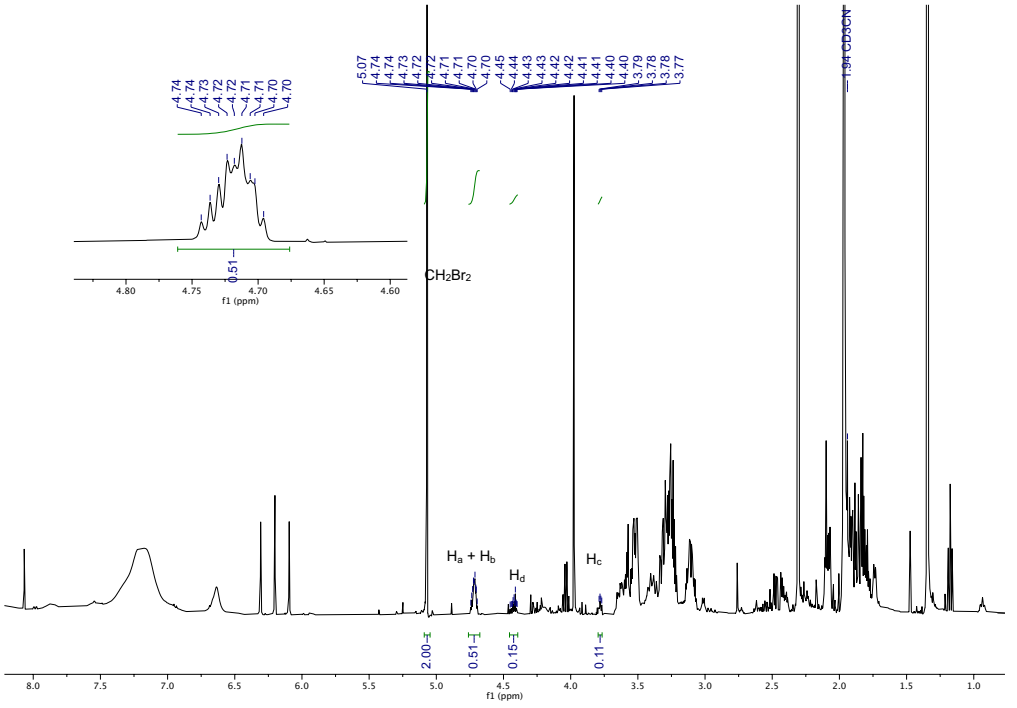

Crude ^{1}H-NMR (400 MHz, $CDCl_3$) en route to **2qa**

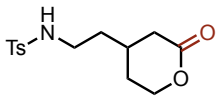

4-methyl-*N*-(2-(2-oxotetrahydro-2*H*-pyran-4-yl)ethyl)benzenesulfonamide (2r). Following General Procedure A, 2-(tetrahydro-2H-pyran-4-yl)ethan-1-amine (0.4 mmol, 52 mg), $HClO_4$ (0.6 mmol, 51 μL) and water (11 μL, 0.6 mmol) were used, affording the title compound as a colorless oil (38 mg, 64%). **^{1}H NMR** (500 MHz, $CDCl_3$) δ 7.78 – 7.74 (m, 2H), 7.35 (m, 2H), 4.74 (brt, J = 6.3 Hz, 1H), 4.40 (m, 1H), 4.24 (m, 1H), 3.00 (m, 2H), 2.71 – 2.60 (m, 1H), 2.46 (s, 3H), 2.21 – 2.06 (m, 2H), 2.03 – 1.89 (m, 1H), 1.61 – 1.45 (m, 3H). **^{13}C NMR** (126 MHz, $CDCl_3$) δ 170.8, 143.9, 136.8, 130.0, 127.2, 68.5, 40.4, 36.2, 36.0, 28.8, 28.6, 25.2, 21.7. **IR (neat):** 2982, 2928, 1754, 1487, 1450, 1332, 1223, 1158, 1101, 890, 862 cm^{-1}. **HRMS (ESI)** *calcd.* for ($C_{14}H_{19}NNaO_4S$) $[M+Na]^+$: 320.0927, *found* 320.0938.

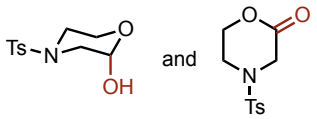

2s **2s'**

4-tosylmorpholin-2-ol (2s) and 4-tosylmorpholin-2-one (2s'). Following a modified General Procedure A, morpholine (0.6 mmol, 35 μL), water (10 μL) and $HClO_4$ (0.6 mmol, 51 μL) were used, affording **2s** (31 mg, 61%, colorless oil) and **2s'** (5 mg, 10%, colorless oil) in a 6:1 ratio.

2s: **^{1}H NMR** (500 MHz, $CDCl_3$) δ 7.64 (d, J = 8.3 Hz, 2H), 7.35 (d, J = 7.9 Hz, 2H), 4.98 (s, 1H), 4.04 (m, 1H), 3.69 (m, 1H), 3.31 – 3.26 (m, 1H), 3.22 (m, 1H), 3.09 (m, 1H), 2.88 (m, 1H), 2.72 (m, 1H), 2.45 (s, 3H). **^{13}C NMR** (126 MHz, $CDCl_3$) δ 144.3, 132.2, 130.0, 128.0, 91.2, 61.6, 50.4, 45.2, 21.7. **IR (neat):** 3312, 2942, 1482, 1380, 1239, 1197, 1112, 1022, 887 cm^{-1}. **HRMS (ESI)** *calcd.* for ($C_{11}H_{15}NNaO_4S$) $[M+Na]^+$: 280.0614, *found* 280.0617.

2s': **^{1}H NMR** (500 MHz, $CDCl_3$) δ 7.68 (d, *J* = 8.3 Hz, 2H), 7.39 (d, *J* = 7.9 Hz, 2H), 4.49 – 4.39 (m, 2H), 3.90 (s, 2H), 3.37 – 3.32 (m, 2H), 2.46 (s, 3H). **^{13}C NMR** (126 MHz, $CDCl_3$) δ 164.3, 145.2, 131.7, 130.4, 128.0, 67.8, 47.3, 42.6, 21.8. **IR (neat):** 2957, 2920, 1752, 1446, 1332, 1248, 1150, 1095, 890 cm^{-1}. **HRMS (ESI)** *calcd*. for ($C_{11}H_{13}NNaO_4S$) $[M+Na]^+$: 278.0457, *found* 278.0455.

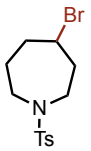

4-bromo-1-tosylazepane (2t). Following General Procedure A, azepane (0.4 mmol, 40 mg) and $HClO_4$ (0.6 mmol, 51 μL) were used, affording the title compound as a colorless oil (50 mg, 75%). **^{1}H NMR** (500 MHz, $CDCl_3$) δ 7.65 (d, *J* = 8.4 Hz, 2H), 7.29 (d, *J* = 7.9 Hz, 2H), 4.42 (m, 1H), 3.49 – 3.43 (m, 1H), 3.39 (m, 1H), 3.23 (m, 1H), 3.14 (m, 1H), 2.41 (s, 3H), 2.33 (m, 1H), 2.20 (m, 2H), 2.11 (m, 1H), 2.03 – 1.92 (m, 1H), 1.73 (m, 1H). **^{13}C NMR** (126 MHz, $CDCl_3$) δ 143.4, 136.2, 129.8, 127.0, 53.6, 47.3, 44.4, 40.6, 36.1, 24.9, 21.6. **IR (neat):** 2940, 2893, 1598, 1331, 1284, 1235, 1155, 1144, 1089, 1031, 996, 918, 809, 712, 649, 570, 545 cm^{-1}. **HRMS (ESI)** *calcd*. for ($C_{13}H_{18}BrNNaO_2S$) $[M+Na]^+$: 354.0134, *found* 354.0131.

NMR spectroscopy of the crude mixture prior to purification revealed the formation of **2t-2t'** and 88% γ-regioselectivity (**2t**/(**2t**+**2t'**)) by utilizing CH_2Br_2 (0.2 mmol, 13.5 μL) as internal standard.

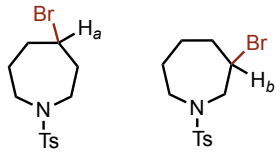

2t 78% **2t'** 11%

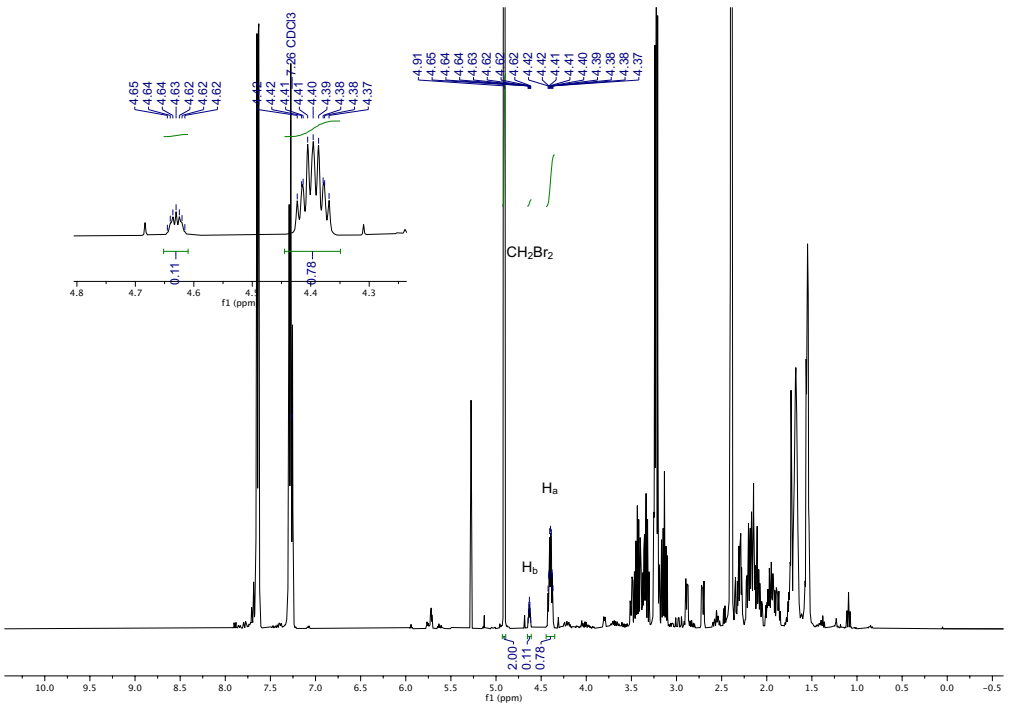

Crude ^{1}H-NMR (400 MHz, $CDCl_3$) en route to **2t**

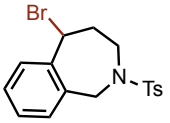

5-bromo-2-tosyl-2,3,4,5-tetrahydro-1*H*-benzo[c]azepine (2u). Following a modified General Procedure B, 2,3,4,5-tetrahydro-1*H*-benzo[c]azepine hydrochloride (0.4 mmol, 73 mg) and $HClO_4$ (0.6 mmol, 51 μL) were used in the absence of TBADT, affording the title compound as a colorless oil (46 mg, 61%). **^{1}H NMR** (500 MHz, $CDCl_3$) δ 7.59 – 7.54 (m, 2H), 7.32 (dd, *J* = 7.4, 1.5 Hz, 1H), 7.27 (m, 1H), 7.24 – 7.16 (m, 4H), 5.40 (t, *J* = 3.9 Hz, 1H), 4.73 (dd, *J* = 15.4, 1.8 Hz, 1H), 4.52 (d, *J* = 15.3 Hz, 1H), 4.04 (m, 1H), 3.71 (m, 1H), 2.38 (s, 3H), 2.15 (m, 2H). **^{13}C NMR** (126 MHz, $CDCl_3$) δ 143.3, 140.1, 138.5, 136.9, 130.7, 129.7, 129.3, 129.2, 128.1, 127.2, 56.8, 52.7, 47.3, 36.2, 21.6. **IR**

(neat): 2919, 1451, 1334, 1154, 1089, 1061, 942, 910, 875, 760, 731, 701, 651, 558, 546 cm^{-1}. **HRMS (ESI)** *calcd*. for ($C_{17}H_{19}BrNO_2S$) $[M+H]^+$: 380.0314, *found* 380.0316.

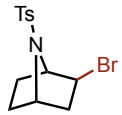

2-bromo-7-tosyl-7-azabicyclo[2.2.1]heptane (2v). Following General Procedure B, 7-azabicyclo[2.2.1]heptane hydrochloride (0.4 mmol, 53 mg) and $HClO_4$ (0.6 mmol, 51 μL) were used, affording the title compound as a colorless oil (62 mg, 95%). **^{1}H NMR** (400 MHz, $CDCl_3$) δ 7.88 (d, *J* = 8.3 Hz, 2H), 7.29 (d, *J* = 8.0 Hz, 2H), 4.29 – 4.24 (m, 1H), 4.23 (dd, *J* = 5.4, 1.0 Hz, 1H), 3.92 (dd, *J* = 7.5, 3.1 Hz, 1H), 2.42 (s, 3H), 2.26 (m, 1H), 2.15 (m, 1H), 2.11 – 2.02 (m, 1H), 1.97 (m, 1H), 1.47 (m, 1H), 1.37 (m, 1H). **^{13}C NMR** (101 MHz, $CDCl_3$) δ 143.8, 137.5, 129.6, 127.8, 67.2, 59.4, 48.3, 44.5, 29.0, 28.1, 21.7. **IR (neat):** 2957, 2922, 1594, 1330, 1153, 1086, 1055, 1013, 819, 794, 675, 651, 598, 578, 533 cm^{-1}. **HRMS (ESI)** *calcd*. for ($C_{13}H_{17}BrNO_2S$) $[M+H]^+$: 330.0158, *found* 330.0157. **M.P.**:113 °C.

4.9.3 One-pot cyclization via C(sp^3)–H bromination

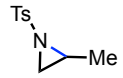

2-methyl-1-tosylaziridine (3a). An oven-dried 10 mL screw-cap reaction tube containing a stir bar was charged with TBADT (1 mol%, 6.6 mg) and DBDMH (0.2 mmol, 1 equiv., 57 mg). The reaction tube was capped with a Teflon-lined rubber septum and connected to a vacuum line where it was evacuated and backfilled with Ar three times. To a 4mL Teflon-capped glass vial was added *n*-propylamine (0.4 mmol, 2 equiv., 24 mg) and CH_3CN (2 mL) before sequential addition of $HClO_4$ (0.6 mmol, 3 equiv., 51 μL). The reaction mixture was transferred to the reaction tube by syringe after sparging with Ar for 5 minutes. The reaction tube was then sealed with parafilm and irradiated by a 390 nm Kessil Lamp in a UFO Reactor (maintaining a temperature between 50 °C-60 °C) under stirring at 600 rpm for 20 h. After completion of the bromination, the reaction was cooled to 0 °C. TsCl (0.6 mmol, 3 equiv., 114 mg) and NaOH (2.5 mmol, 12.5 equiv. 60 mg) were added to the reaction tube and the mixture was stirred at 0 °C to r.t. overnight. After the reaction was complete, the reaction mixture was concentrated under vacuum, diluted with EtOAc and brine, extracted with EtOAc three times, dried with anhydrous Na_2SO_4, and then concentrated under vacuum to give a crude product, which was purified by column chromatography, affording the title compound as a white solid (30 mg, 71%). **^{1}H NMR** (500 MHz, CD_3Cl_3) δ 7.82 (d, J = 8.3 Hz, 2H), 7.33 (d, J = 7.9 Hz, 2H), 2.82 (m, 1H), 2.61 (d, J = 7.0 Hz, 1H), 2.44 (s, 3H), 2.02 (d, J = 4.6 Hz, 1H), 1.25 (d, J = 5.6 Hz, 3H). **^{13}C NMR** (126 MHz, CD_3Cl_3) δ 144.5, 135.5, 129.8, 127.9, 36.0, 34.9, 21.8, 16.9. **IR (neat):** 2971, 2929, 1316, 1288, 1150, 1096, 1032, 984, 845, 814, 712, 688, 658, 565, 548 cm^{-1}. **HRMS (ESI)** *calcd.* for ($C_{10}H_{13}NNaO_2S$) $[M+Na]^+$: 234.0559, *found* 234.0565. **M.P.**: 63 °C.

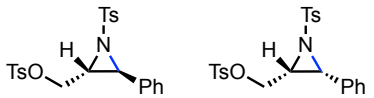

3b **3b'**

((2*S*,3*S*)-3-phenyl-1-tosylaziridin-2-yl)methyl 4-methylbenzenesulfonate (3b) and **((2*S*,3*R*)-3-phenyl-1-tosylaziridin-2-yl)methyl 4-methylbenzenesulfonate (3b').** An oven-dried 10 mL screw-cap reaction tube containing a stir bar was charged with TBADT (1 mol%, 6.6 mg) and DBDMH (0.2 mmol, 1 equiv., 57 mg). The reaction tube was capped with a Teflon-lined rubber septum and connected to a vacuum line where it was evacuated and backfilled with Ar three times. To a 4mL Teflon-capped glass vial was added *D*-phenylalaninol (Solriamfetol precursor, 0.4 mmol, 60 mg) and CH_3CN (2 mL) before sequential addition of $HClO_4$ (0.6 mmol, 3 equiv., 51 μL). The reaction mixture was transferred to the reaction tube by syringe after sparging with Ar for 5 minutes. The reaction tube was then sealed with parafilm and irradiated by a 390 nm Kessil Lamp in a UFO Reactor (maintaining a temperature below 30 °C) under stirring at 600 rpm for 20 h. After completion of the bromination, the reaction was cooled to 0 °C. TsCl (1.2 mmol, 6 equiv., 228 mg) and DIPEA (3.0 mmol, 15 equiv., 523 μL) were added to the reaction tube and the mixture was stirred at 0 °C to r.t. for 4 hours. After the reaction was complete, the reaction mixture was concentrated under vacuum, passed through a thin pad of silica with Hexane:EtOAc, then concentrated under vacuum to give a crude product, which was purified by column chromatography, affording **3b** (28 mg, 31%, colorless oil) and **3b'** (25 mg, 28%, colorless oil) in a 1.2:1 ratio.

3b: **^{1}H NMR** (400 MHz, $CDCl_3$) δ 7.85 (d, *J* = 8.3 Hz, 2H), 7.51 (d, *J* = 8.3 Hz, 2H), 7.38 – 7.33 (m, 2H), 7.29 – 7.20 (m, 5H), 7.15 – 7.11 (m, 2H), 4.05 (d, *J* = 7.0 Hz, 1H), 3.78 (dd, *J* = 11.0, 6.6 Hz, 1H), 3.69 (dd, *J* = 11.0, 6.2 Hz, 1H), 3.30 (q, *J* = 6.6 Hz, 1H), 2.46 (s, 3H), 2.43 (s, 3H). **^{13}C NMR** (101 MHz, $CDCl_3$) δ 145.3, 145.1, 134.3, 132.3, 131.2, 130.0, 130.0, 128.7, 128.5, 128.3, 128.0, 127.5, 65.9, 44.5, 42.5, 21.9, 21.8. **IR (neat):** 2920, 1736, 1597, 1455, 1360, 1342, 1176, 1161, 1019, 967, 807, 788, 759, 718, 698, 668, 576, 659, 505 cm^{-1}. **HRMS (ESI)** *calcd*. for ($C_{23}H_{23}NNaO_5S_2$) $[M+Na]^+$: 480.0910, *found* 480.0910.

3b': ^{1}H NMR (400 MHz, $CDCl_3$) δ 7.79 (m, 4H), 7.37 – 7.31 (m, 2H), 7.31 – 7.20 (m, 5H), 7.18 – 7.10 (m, 2H), 4.70 (dd, *J* = 11.4, 5.5 Hz, 1H), 4.61 (dd, *J* = 11.4, 7.4 Hz, 1H),

3.89 (d, J = 4.0 Hz, 1H), 3.14 (m, 1H), 2.45 (s, 3H), 2.41 (s, 3H). **^{13}C NMR** (101 MHz, $CDCl_3$) δ 145.4, 144.8, 136.4, 133.7, 132.7, 130.2, 129.8, 128.8, 128.7, 128.2, 127.7, 126.9, 66.8, 48.0, 47.4, 21.8, 21.8. **IR (neat):** 2923, 1736, 1597, 1362, 1323, 1175, 1158, 1088, 967, 911, 812, 757, 686, 661, 551 cm^{-1}. **HRMS (ESI)** *calcd*. for ($C_{23}H_{23}NNaO_5S_2$) $[M+Na]^+$: 480.0910, *found* 480.0908.

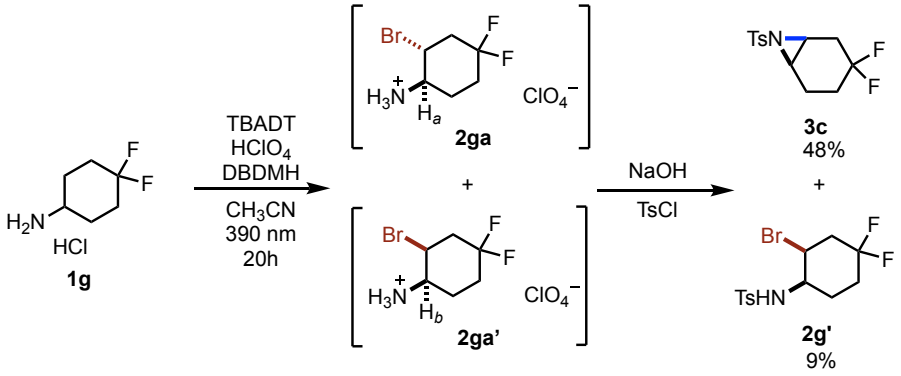

(±)-(1*S*,6*R*)-3,3-difluoro-7-tosyl-7-azabicyclo[4.1.0]heptane (3c) An oven-dried 10 mL screw-cap reaction tube containing a stir bar was charged with TBADT (1 mol%, 6.6 mg) and DBDMH (0.2 mmol, 1.0 equiv., 57 mg). The reaction tube was capped with a Teflon-lined rubber septum and connected to a vacuum line where it was evacuated and backfilled with Ar three times. In a separate 4ml Teflon-capped glass vial, 4,4-difluorocyclohexylamine hydrochloride (0.6 mmol, 3.0 equiv., 103 mg) and CH_3CN (2 mL) were added, followed by addition of $HClO_4$ (0.8 mmol, 4.0 equiv., 68 μL). This solution was concentrated under vacuum to remove HCl. After addition of 2 ml of CH_3CN and sparging with Ar for 5 minutes, this mixture was transferred to the reaction tube by syringe. The reaction tube was sealed with parafilm and irradiated by a 390 nm Kessil Lamp in a UFO Reactor under stirring at 600 rpm for 20 h (maintaining a temperature between 50 °C-60 °C). After reaction completion, the reaction mixture was cooled to 0 °C. TsCl (0.8 mmol, 4.0 equiv., 152 mg) and NaOH (2.5 mmol, 12.5 equiv., 60 mg) were added to the reaction tube and the mixture was stirred at 0 °C to r.t. overnight. Subsequently, the reaction mixture was concentrated, passed through a thin pad of silica with Hexane:EtOAc, and concentrated under vacuum to give a crude product, which was

purified by column chromatography, affording **3c** (28 mg, 48%, colorless oil) and **2g'** (7 mg, 9%, colorless oil) in a 4.8:1 ratio.

3c: **^{1}H NMR** (500 MHz, CD_3Cl_3) δ 7.83 (d, *J* = 8.3 Hz, 2H), 7.38 (d, *J* = 7.9 Hz, 2H), 3.13 – 3.07 (m, 1H), 3.04 (m, 1H), 2.48 (s, 3H), 2.46 – 2.35 (m, 1H), 2.20 – 2.02 (m, 3H), 1.90 – 1.76 (m, 2H). **^{13}C NMR** (126 MHz, CD_3Cl_3) δ 144.8, 135.3, 130.0, 127.9, 121.1 (dd, *J* = 243.2, 239.3 Hz), 38.9 (d, *J* = 1.7 Hz), 37.2 (d, *J* = 11.7 Hz), 32.4 (t, *J* = 27.9 Hz), 27.0 (dd, *J* = 25.3, 23.4 Hz), 21.8, 20.7 (dd, *J* = 9.6, 2.2 Hz). **IR (neat):** 2932, 1597, 1372, 1319, 1303, 1155, 1111, 1090, 1000, 922, 879, 825, 814, 718, 667, 580, 546 cm^{-1}. **HRMS (ESI)** *calcd.* for ($C_{13}H_{15}F_2NNaO_2S$) $[M+Na]^+$: 310.0684, *found* 310.0681.

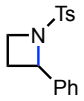

2-phenyl-1-tosylazetidine (3d). An oven-dried 10 mL screw-cap reaction tube containing a stir bar was charged DBDMH (0.2 mmol, 1 equiv., 57 mg). The reaction tube was capped with a teflon-lined rubber septum and connected to a vacuum line where it was evacuated and backfilled with Ar three times. To a 4 mL Teflon-capped glass vial was added 3-phenylpropylamine (0.4 mmol, 2 equiv., 54 mg) and CH_3CN (2 mL) before sequential addition of $HClO_4$ (0.6 mmol, 3 equiv., 51 μL). The reaction mixture was transferred to the reaction tube by syringe, then sparged with Ar for 5 minutes. The reaction tube was then sealed with parafilm and irradiated by a 390 nm Kessil Lamp in a UFO Reactor (maintaining a temperature below 30 °C) under stirring at 600 rpm for 4 h. After completion of the bromination, the reaction mixture was cooled to 0 °C. TsCl (0.6 mmol, 3 equiv., 114 mg), NaI (0.15 mmol, 0.75 equiv., 23 mg) and NaOH (2.5 mmol, 12.5 equiv., 60 mg) were added to the reaction tube and the mixture was stirred at 0 °C to r.t. overnight. After the reaction was complete, the reaction mixture was concentrated under vacuum, diluted with EtOAc and brine, extracted by EtOAc three times, dried by anhydrous Na_2SO_4, then concentrated under vacuum to give a crude product, which was purified by column chromatography, affording the title compound as a white solid (52 mg, 90%). **^{1}H**

NMR (500 MHz, $CDCl_3$) δ 7.68 (d, *J* = 8.3 Hz, 2H), 7.44 – 7.39 (m, 2H), 7.36 – 7.30 (m, 4H), 7.30 – 7.25 (m, 1H), 4.88 (t, *J* = 8.4 Hz, 1H), 3.83 – 3.69 (m, 2H), 2.44 (s, 3H), 2.38 – 2.27 (m, 1H), 2.26 – 2.16 (m, 1H). **^{13}C NMR** (126 MHz, $CDCl_3$) δ 144.1, 140.7, 132.3, 129.8, 128.6, 128.6, 128.1, 126.4, 65.8, 47.4, 25.9, 21.7. **IR (neat):** 2981, 2878, 1495, 1455, 1338, 1157, 1087, 1087, 1014, 964, 817, 751, 696, 665, 596, 544, 499 cm^{-1}. **HRMS (ESI)** *calcd*. for ($C_{16}H_{17}NNaO_2S$) $[M+Na]^+$: 310.0872, *found* 310.0885. **M.P.** :110 °C.

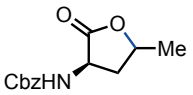

benzyl ((3*R*)-5-methyl-2-oxotetrahydrofuran-3-yl)carbamate (3e) An oven-dried 10 mL screw-cap reaction tube containing a stir bar was charged with TBADT (1 mol%, 6.6 mg) and DBDMH (0.2 mmol, 1 equiv., 57 mg). The reaction tube was capped with a Teflon-lined rubber septum and connected to a vacuum line where it was evacuated and backfilled with Ar three times. To a 4mL Teflon-capped glass vial was added *D*-Norvaline (0.4 mmol, 47 mg) and CH_3CN (2 mL) before sequential addition of $HClO_4$ (0.6 mmol, 3 equiv., 51 μL). The reaction mixture was transferred to the reaction tube by syringe after sparging with Ar for 5 minutes. The reaction tube was then sealed with parafilm and irradiated by a 390 nm Kessil Lamp in a UFO Reactor (maintaining a temperature between 50 °C-60 °C) under stirring at 600 rpm for 20 h. After completion of the bromination, the reaction was cooled to 0 °C. CbzCl (0.6 mmol, 3 equiv., 85 μL) and DIPEA (3.0 mmol, 15 equiv., 523 μL) were added to the reaction tube and the mixture was stirred at 0 °C to r.t. overnight. After the reaction was complete, the reaction mixture was concentrated under vacuum, passed through a thin pad of silica with Hexane:EtOAc, then concentrated under vacuum to give a crude product, which was purified by column chromatography, affording the title compound as a colorless oil (26 mg, 53%, dr 1:1). **^{1}H NMR** (500 MHz, $CDCl_3$) δ 7.42 – 7.29 (m, 5H), 5.41 (brs, 1H), 5.12 (s, 2H), 4.79 (d, *J* = 10.1 Hz, 0.4H), 4.66 – 4.41 (m, 1.54H), 2.85 (dt, *J* = 12.4, 6.1 Hz, 0.51H), 2.43 (t, *J* = 11.3 Hz, 0.4H), 2.33 (m, 0.5H), 1.78 (m, 0.58H), 1.45 (d, *J* = 6.1 Hz, 1.51H), 1.40 (d, *J* = 6.6 Hz, 1.46H). **^{13}C NMR** (126 MHz, $CDCl_3$) δ 174.9, 174.7, 156.2, 136.0, 128.7, 128.4, 128.3, 128.3,

74.9, 74.7, 67.5, 67.4, 52.3, 49.7, 38.5, 35.8, 21.3, 20.7. **IR (neat):** 3349, 2937, 1795, 1685, 1537, 1255, 1189, 970, 740, 699, 575 cm^{-1}. **HRMS (ESI)** *calcd*. for ($C_{13}H_{15}NNaO_4$) $[M+Na]^+$: 272.0893, *found* 272.0895.

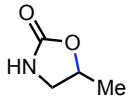

5-methyloxazolidin-2-one (3f). An oven-dried 10 mL screw-cap reaction tube containing a stir bar was charged with TBADT (1 mol%, 6.6 mg) and DBDMH (0.2 mmol, 1 equiv., 57 mg). The reaction tube was capped with a teflon-lined rubber septum and connected to a vacuum line where it was evacuated and backfilled with Ar three times. To a 4 mL Teflon-capped glass vial was added *n*-butylamine (0.4 mmol, 29 mg) and CH_3CN (2 mL) before sequential addition of $HClO_4$ (0.6 mmol, 3 equiv., 51 μL). The reaction mixture was transferred to the reaction tube by syringe after sparging with Ar for 5 minutes. The reaction tube was then sealed with parafilm and irradiated by a 390nm Kessil Lamp in a UFO Reactor (maintaining a temperature between 50 °C - 60 °C) under stirring at 600rpm for 20h. After completion of the bromination, the reaction mixture was cooled to r.t.. 2 mL of a saturated $NaHCO_3$ aqueous solution was added to the reaction tube and the mixture was stirred at 80 °C for 6 hours. After the reaction was complete, the reaction mixture was diluted with EtOAc, extracted by EtOAc three times, dried with anhydrous Na_2SO_4, then concentrated under vacuum to give a crude product, which was purified by column chromatography, affording the title compound as a colorless oil (10 mg, 49%). **^{1}H NMR** (500 MHz, $CDCl_3$) δ 5.53 (s, 1H), 4.78 (m, 1H), 3.70 (dt, J = 8.3, 0.7 Hz, 1H), 3.20 (dt, J = 8.0, 7.1, 0.9 Hz, 1H), 1.45 (d, J = 6.3 Hz, 3H). **^{13}C NMR** (126 MHz, $CDCl_3$) δ 160.0, 73.7, 47.5, 20.7. **IR (neat):** 3284, 2983, 1719, 1385, 1242, 1066, 970, 722 cm^{-1}. **HRMS (ESI)** *calcd*. for ($C_4H_7NNaO_2$) $[M+Na]^+$: 124.0369, *found* 124.0370.

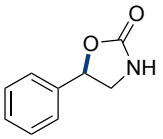

5-phenyloxazolidin-2-one (3g). An oven-dried 10 mL screw-cap reaction tube containing a stir bar was charged and DBDMH (0.2 mmol, 1 equiv., 57 mg). The reaction tube was capped with a teflon-lined rubber septum and connected to a vacuum line where it was evacuated and backfilled with Ar three times. To a 4 mL Teflon-capped glass vial was added 2-phenylethylamine (0.4 mmol, 2 equiv., 48 mg) and CH_3CN (2 mL) before sequential addition of $HClO_4$ (0.6 mmol, 3 equiv., 51 μL). The reaction mixture was transferred to the reaction tube by syringe after sparging with Ar for 5 minutes. The reaction tube was then sealed with parafilm and irradiated by a 390nm Kessil Lamp in a UFO Reactor (maintaining a temperature below 30 °C) under stirring at 600 rpm for 4 h. After completion of the bromination, the reaction mixture was cooled to r.t.. 2 mL of a saturated $NaHCO_3$ aqueous solution was added to the reaction tube and the mixture was stirred at 80 °C for 6 hours. After the reaction was complete, the reaction mixture was diluted with EtOAc, extracted by EtOAc three times, dried with anhydrous Na_2SO_4, then concentrated under vacuum to give a crude product, which was purified by column chromatography, affording the title compound as a white solid (23 mg, 77%). **^{1}H NMR** (300 MHz, $CDCl_3$) δ 7.52 – 7.30 (m, 5H), 6.07 (s, 1H), 5.62 (dd, J = 8.7, 7.7 Hz, 1H), 3.98 (td, J = 8.7, 0.8 Hz, 1H), 3.55 (dt, J = 8.6, 0.9 Hz, 1H). **^{13}C NMR** (126 MHz, $CDCl_3$) δ 160.0, 138.5, 129.1, 129.1, 125.8, 78.1, 48.5. **IR (neat):** 3264, 1715, 1496, 1366, 1237, 1077, 968, 928, 760, 694, 607 cm^{-1}. **HRMS (ESI)** *calcd*. for ($C_9H_9NNaO_2$) $[M+Na]^+$: 186.0525, *found* 186.0526. **M.P.** : 85 °C.

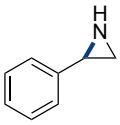

2-phenylaziridine (3h). An oven-dried 10 mL screw-cap reaction tube containing a stir bar was charged and DBDMH (0.2 mmol, 1 equiv., 57 mg). The reaction tube was capped with a teflon-lined rubber septum and connected to a vacuum line where it was evacuated and backfilled with Ar three times. To a 4 mL Teflon-capped glass vial was added 2-phenylethylamine (0.3 mmol, 1.5 equiv., 36 mg) and CH_3CN (2 mL) before sequential addition of $HClO_4$ (0.5 mmol, 2.5 equiv., 43 μL). The reaction mixture was transferred to

the reaction tube by syringe after sparging with Ar for 5 minutes. The reaction tube was then sealed with parafilm and irradiated by a 390nm Kessil Lamp in a UFO Reactor (maintaining a temperature below 30 °C) under stirring at 600 rpm for 4 h. After completion of the bromination, the reaction mixture was cooled to r.t.. NaOH (1.2 mmol, 6 equiv., 48 mg) was added to the reaction tube and the mixture was stirred at r.t. overnight. After the reaction was complete, the reaction mixture was diluted with H_2O and Et_2O, extracted by Et_2O three times, dried with anhydrous Na_2SO_4, then concentrated under vacuum to give a crude product, which was purified by column chromatography, affording the title compound as a colorless oil (20 mg, 85%). **^{1}H NMR** (500 MHz, $CDCl_3$) δ 7.34 – 7.29 (m, 2H), 7.26 – 7.21 (m, 3H), 3.01 (dd, J = 6.0, 3.4 Hz, 1H), 2.20 (d, J = 6.0 Hz, 1H), 1.80 (brs, 1H), 1.06 – 0.79 (brs, 1H). **^{13}C NMR** (126 MHz, $CDCl_3$) δ 140.5, 128.5, 127.1, 125.8, 32.2, 29.4.[5]

4.9.4 Derivatization of Halogenated Amines

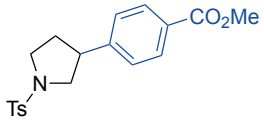

methyl 4-(1-tosylpyrrolidin-3-yl)benzoate (4a). To a 10 mL screw-cap reaction tube equipped with a stir bar was added photocatalyst Ir[dF(CF_3)ppy]$_2$(dtbbpy)PF_6 (1 mol%, 2.2 mg), methyl 4-bromo benzoate (0.2 mmol, 1 equiv., 43 mg.), 3-bromo-1-tosylpyrrolidine **2m** (0.3 mmol, 1.5 equiv., 91 mg,), Ni(4,4'-di-*tert*-butyl-2,2'-bipyridine)Br_2 (2 mol%, 2.0 mg,), tris(trimethylsilyl)silane (0.2 mmol, 1.0 equiv, 62 µL), and anhydrous sodium carbonate (0.4 mmol, 2 equiv., 42 mg). The tube was sealed and placed under nitrogen before 2 mL of DME was added. The reaction was stirred and irradiated with a 34 W blue LED lamp for 14 hours. The reaction was quenched by exposure to air and concentrated in vacuo. Purification by column chromatography yielded the title compound as a white solid (68 mg, 95%). **^{1}H NMR** (400 MHz, $CDCl_3$) δ 7.91 (d, *J* = 8.6 Hz, 2H), 7.73 (d, *J* = 8.3 Hz, 2H), 7.33 (d, *J* = 7.9 Hz, 2H), 7.15 (d, *J* = 8.1 Hz, 2H), 3.88 (s, 3H), 3.75 – 3.66 (m, 1H), 3.51 (m, 1H), 3.40 – 3.15 (m, 3H), 2.43 (s, 3H), 2.29 – 2.16 (m, 1H), 1.93 – 1.79 (m, 1H). **^{13}C NMR** (101 MHz, $CDCl_3$) δ 166.8, 146.2, 143.7, 133.8, 130.0, 129.8, 129.0, 127.6, 127.1, 53.9, 52.2, 47.8, 43.8, 32.8, 21.6. **IR (neat):** 2950, 2881, 1711, 1610, 1433, 1334, 1283, 1152, 1106, 1036, 1016, 809, 773, 704, 659, 590, 546 cm^{-1}. **HRMS (ESI)** *calcd*. for ($C_{19}H_{22}NO_4S$) $[M+H]^+$: 360.1264, *found* 360.1274. **M.P.**: 93 °C.

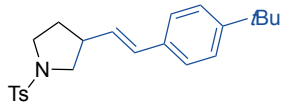

(*E*)-3-(4-(tert-butyl)styryl)-1-tosylpyrrolidine (4b). In a glove box, a 10 mL screw-cap reaction tube containing a magnetic stir bar was charged sequentially with $Pd(PPh_3)_4$ (5 mol%, 11.6 mg), dppf (7 mol%, 7.8 mg) and dry $PhCF_3$ (1.0 mL). After stirring at room

temperature for 30 minutes, 3-bromo-1-tosylpyrrolidine **2m** (0.2 mmol, 1 equiv., 61 mg), 1-(*tert*-butyl)-4-vinylbenzene (0.4 mmol, 2.0 equiv., 56 µL), LiI (0.4 mmol, 2.0 equiv., 54 mg) and Cy_2NMe (0.3 mmol, 1.5 equiv., 58 mg) were added sequentially via syringe. The reaction tube was capped and heated with vigorous stirring at 110 °C for 36 h. Then, the mixture was cooled to room temperature, diluted with diethyl ether and filtered through a short pad of silica gel to remove insoluble salts with three rounds of diethyl ether washings. The filtrate was concentrated under reduced pressure and the residue was subjected to silica gel flash chromatography, affording the title compound as a white solid (54 mg, 71%). **^{1}H NMR** (500 MHz, $CDCl_3$) δ 7.74 (d, *J* = 8.3 Hz, 2H), 7.36 – 7.29 (m, 4H), 7.18 (d, *J* = 8.3 Hz, 2H), 6.32 (d, *J* = 15.8 Hz, 1H), 5.85 (dd, *J* = 15.8, 7.8 Hz, 1H), 3.53 (dd, *J* = 10.0, 7.3 Hz, 1H), 3.40 (m, 1H), 3.31 (m, 1H), 3.03 (dd, *J* = 10.0, 7.9 Hz, 1H), 2.88 – 2.78 (m, 1H), 2.44 (s, 3H), 2.03 (m, 1H), 1.69 – 1.62 (m, 1H), 1.30 (s, 9H). **^{13}C NMR** (126 MHz, $CDCl_3$) δ 150.8, 143.6, 134.0, 134.0, 130.8, 129.8, 128.4, 127.7, 125.9, 125.6, 53.1, 47.6, 42.1, 34.7, 32.2, 31.4, 21.7. **IR (neat):** 2948, 2879, 1342, 1330, 1156, 1095, 1030, 965, 814, 655, 593, 546 cm^{-1}. **HRMS (ESI)** *calcd.* for ($C_{23}H_{30}NO_2S$) $[M+H]^+$: 384.1992, *found* 384.2003. **M.P.**: 87 °C.

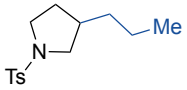

3-propyl-1-tosylpyrrolidine (4c). To a 10 mL screw-cap reaction tube equipped with a magnetic stir bar was loaded 3-bromo-1-tosylpyrrolidine **2m** (0.2 mmol, 1 equiv., 61 mg), followed by addition of (*S*)-^{i}Pr-Pybox (0.016 mmol, 8 mol%, 4.8 mg) and zinc powder (0.6 mmol, 3 equiv., 39 mg). The tube was moved into a dry glove box, at which point $Ni(COD)_2$ (10 mol%, 5.5 mg) was added. The tube was capped with a Teflon-lined rubber septum, and it was moved out of the glove box. 1-iodopropane (0.6 mmol, 3 equiv., 59 µL) and DMA (1.5 mL) were then added via syringe. After the reaction mixture was allowed to stir for 12 h under N_2 atmosphere at 25 ºC, the mixture was quenched by exposure to air, diluted with EtOAc and washed by water. The residue was concentrated under vacuum and purified by column chromatography, yielding the title compound as a

colorless oil (34 mg, 64%). **^{1}H NMR** (500 MHz, $CDCl_3$) δ 7.70 (d, *J* = 8.3 Hz, 2H), 7.31 (d, *J* = 7.9 Hz, 2H), 3.42 (dd, *J* = 9.7, 7.3 Hz, 1H), 3.32 (m, 1H), 3.17 (m, 1H), 2.75 (dd, *J* = 9.7, 8.1 Hz, 1H), 2.42 (s, 3H), 1.99 (m, 1H), 1.94 – 1.86 (m, 1H), 1.34 (m, 1H), 1.27 – 1.13 (m, 4H), 0.83 (t, *J* = 6.9 Hz, 3H). **^{13}C NMR** (101 MHz, $CDCl_3$) δ 143.4, 134.1, 129.7, 127.6, 53.4, 47.7, 38.7, 35.4, 31.6, 21.6, 21.3, 14.2. **IR (neat):** 2957, 2927, 1342, 1159, 1094, 816, 661, 589, 547 cm^{-1}. **HRMS (ESI)** *calcd.* for ($C_{14}H_{22}NO_2S$) $[M+H]^+$: 268.1366, *found* 268.1374.

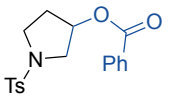

1-tosylpyrrolidin-3-yl benzoate (4d). To a 10 mL screw-cap reaction tube equipped with a magnetic stir bar was loaded sodium benzoate (0.60 mmol, 3.0 equiv., 86 mg) and potassium iodide (0.22 mmol, 1.1 equiv., 37 mg). The tube was sealed and placed under nitrogen before 1.0 mL of DMF was added. After stirring at room temperature for 30 minutes, a solution of 3-bromo-1-tosylpyrrolidine **2m** (0.2 mmol, 1.0 equiv., 61 mg) in 1 mL DMF was added via syringe. The reaction mixture was allowed to stir for 16 h at 70 ºC. Then, the mixture was diluted with EtOAc, washed with water and dried with anhydrous Na_2SO_4. The mixture was concentrated under vacuum and purified by column chromatography, affording the title compound as a white solid (47 mg, 68%). **^{1}H NMR** (500 MHz, $CDCl_3$) δ 7.71 (d, *J* = 8.3 Hz, 2H), 7.70 – 7.66 (m, 2H), 7.54 (m, 1H), 7.40 – 7.33 (m, 2H), 7.22 (d, *J* = 7.8 Hz, 2H), 5.36 (m, 1H), 3.63 (dd, *J* = 12.4, 4.6 Hz, 1H), 3.60 – 3.51 (m, 2H), 3.37 (m, 1H), 2.29 (s, 3H), 2.19 – 2.09 (m, 2H). **^{13}C NMR** (126 MHz, $CDCl_3$) δ 165.7, 143.7, 133.5, 133.4, 129.8, 129.6, 129.5, 128.4, 127.7, 73.9, 53.8, 46.5, 31.8, 21.6. **IR (neat):** 1719, 1328, 1287, 1267, 1158, 1117, 1095, 1023, 1013, 710, 658, 596, 551 cm^{-1}. **HRMS (ESI)** *calcd.* for ($C_{18}H_{19}NNaO_4S$) $[M+Na]^+$: 368.0927, *found* 368.0926. **M.P.**: 145 °C.

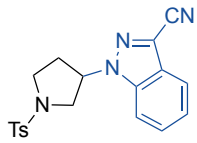

1-(1-tosylpyrrolidin-3-yl)-1*H*-indazole-3-carbonitrile (4e). To a 10 mL screw-cap reaction tube equipped with a magnetic stir bar was loaded *1*H-Indazole-3-carbonitrile (0.60 mmol, 3.0 equiv., 86 mg), potassium carbonate (0.22 mmol, 1.1 equiv., 30 mg), and potassium iodide (0.22 mmol, 1.1 equiv., 37 mg). The tube was sealed and placed under nitrogen before 1.0 mL of DMF was added. After stirring at room temperature for 30 minutes, a solution of 3-bromo-1-tosylpyrrolidine **2m** (0.2 mmol, 1.0 equiv., 61 mg) in 1 mL DMF was added via syringe. The reaction mixture was allowed to stir for 16 h at 70 ºC. Then, the mixture was diluted with EtOAc, washed with water and dried with anhydrous Na_2SO_4. The mixture was concentrated and purified by column chromatography, affording the title compound as a white solid (48 mg, 65%). **^{1}H NMR** (500 MHz, $CDCl_3$) δ 7.77 (dt, *J* = 8.2, 1.0 Hz, 1H), 7.58 (d, *J* = 8.3 Hz, 2H), 7.54 – 7.45 (m, 2H), 7.36 (m, 1H), 7.22 (d, J = 7.9 Hz, 2H), 5.22 – 5.13 (m, 1H), 3.94 (dd, *J* = 11.3, 6.4 Hz, 1H), 3.73 – 3.62 (m, 2H), 3.58 (m, 1H), 2.56 (m, 1H), 2.52 – 2.42 (m, 4H). **^{13}C NMR** (126 MHz, $CDCl_3$) δ 144.2, 139.0, 133.1, 129.9, 128.2, 127.5, 125.7, 124.1, 119.9, 118.0, 113.3, 109.9, 58.2, 53.0, 47.0, 31.0, 21.8. **IR (neat):** 2966, 2920, 2234, 1469, 1331, 1299, 1154, 1094, 1026, 1007, 769, 749, 664, 597, 582, 547 cm^{-1}. **HRMS (ESI)** *calcd.* for ($C_{19}H_{19}N_4O_2S$) $[M+H]^+$: 367.1223, *found* 367.1229. **M.P.**: 148 °C.

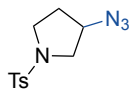

3-azido-1-tosylpyrrolidine (4f). To a 10 mL screw-cap reaction tube equipped with a magnetic stir bar was loaded 3-bromo-1-tosylpyrrolidine **2m** (0.2 mmol, 1 equiv., 61 mg), NaN_3 (1.0 mmol, 5 equiv., 65 mg) and DMF (1 mL). The tube was capped with a rubber septum, and the reaction mixture was allowed to stir for 18 h at 80 ºC. Then, the mixture was diluted with EtOAc, washed with water and dried with anhydrous Na_2SO_4. The

mixture was concentrated under vacuum and purified by column chromatography, affording the title compound as a white solid (51 mg, 97%). **^{1}H NMR** (500 MHz, $CDCl_3$) δ 7.71 (d, *J* = 8.3 Hz, 2H), 7.33 (d, *J* = 7.9 Hz, 2H), 4.06 (m, 1H), 3.47 (dd, *J* = 11.2, 5.5 Hz, 1H), 3.41 (m, 1H), 3.29 – 3.18 (m, 2H), 2.43 (s, 3H), 2.04 – 1.96 (m, 1H), 1.87 (m, 1H). **^{13}C NMR** (126 MHz, $CDCl_3$) δ 143.9, 133.6, 129.9, 127.6, 60.0, 52.8, 46.1, 31.3, 21.6. **IR (neat):** 2979, 2135, 2097, 1341, 1310, 1275, 1153, 1086, 1004, 814, 706, 658, 587, 546 cm^{-1}. **HRMS (ESI)** *calcd*. for ($C_{11}H_{14}N_4NaO_2S$) $[M+Na]^+$: 289.0730, *found* 289.0728. **M.P.**: 66 °C.

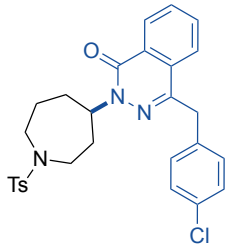

4-(4-chlorobenzyl)-2-(1-tosylazepan-4-yl)phthalazin-1(2*H*)-one (4t). To a 10 mL screw-cap reaction tube equipped with a magnetic stir bar was loaded 4-(4-chlorobenzyl)phthalazin-1(2*H*)-one (0.20 mmol, 2.0 equiv., 54 mg), potassium carbonate (0.11 mmol, 1.1 equiv., 15 mg), and potassium iodide (0.11 mmol, 1.1 equiv., 18 mg). The tube was sealed and placed under nitrogen before 1.0 mL of DMF was added. After stirring at room temperature for 30 minutes, a solution of 4-bromo-1-tosylazepane **2t** (0.1 mmol, 1.0 equiv., 33 mg) in 0.5 mL DMF was added via syringe. The reaction mixture was allowed to stir for 48 h at 70 ºC. Then, the mixture was diluted with EtOAc, washed with water and dried with anhydrous Na_2SO_4. The mixture was concentrated under vacuum and purified by column chromatography, affording the title compound as a white solid (25 mg, 48%). **^{1}H NMR** (500 MHz, $CDCl_3$) δ 8.48 – 8.42 (m, 1H), 7.75 – 7.66 (m, 5H), 7.36 – 7.31 (m, 2H), 7.29 – 7.24 (m, 2H), 7.23 – 7.15 (m, 2H), 5.24 – 5.13 (m, 1H), 4.26 (s, 2H), 3.74 – 3.67 (m, 1H), 3.52 – 3.33 (m, 2H), 3.19 – 3.12 (m, 1H), 2.43 (s, 3H), 2.33 – 2.25 (m, 1H), 2.20 – 2.11 (m, 1H), 2.08 – 1.96 (m, 2H), 1.83 – 1.62 (m, 2H). **^{13}C NMR** (126 MHz, $CDCl_3$) δ 158.6, 144.8, 143.3, 136.5, 136.3, 133.1, 132.7, 131.4, 129.9,

129.9, 129.0, 128.7, 128.3, 127.6, 127.2, 124.8, 56.8, 48.1, 44.7, 38.5, 34.6, 31.8, 25.1, 21.6. **IR (neat):** 2922, 2856, 1646, 1585, 1490, 1328, 1154, 1090, 1015, 797, 712, 690, 547 cm^{-1}. **HRMS (ESI)** *calcd.* for ($C_{28}H_{28}ClN_3NaO_3S$) $[M+Na]^+$: 544.1432, *found* 544.1417.

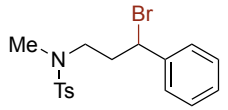

***N*-(3-bromo-3-phenylpropyl)-*N*,4-dimethylbenzenesulfonamide (2y).** Following General Procedure C, *N*-methyl-3-phenylpropan-1-amine (0.3 mmol, 45 mg) and $HClO_4$ (0.6 mmol, 51 μL) was used, affording the title compound as a colorless oil (51 mg, 67%). **^{1}H NMR** (400 MHz, $CDCl_3$) δ 7.65 (d, *J* = 8.2 Hz, 2H), 7.43 – 7.27 (m, 7H), 5.06 (dd, *J* = 9.0, 5.5 Hz, 1H), 3.25 – 3.04 (m, 2H), 2.75 (s, 3H), 2.57 – 2.26 (m, 5H). **^{13}C NMR** (101 MHz, $CDCl_3$) δ 143.7, 141.6, 134.3, 129.9, 128.9, 128.7, 127.6, 127.4, 52.0, 49.1, 38.5, 35.9, 21.6. **IR (neat):** 2923, 1454, 1337, 1156, 1088, 814, 736, 696, 648, 548 cm^{-1}. **HRMS (ESI)** *calcd.* for ($C_{17}H_{21}BrNO_2S$) $[M+H]^+$: 382.0471, *found* 382.0474.

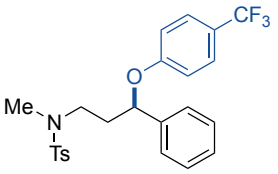

***N*-tosylfluoxetine (4y).** To a 10 mL screw-cap reaction tube equipped with a magnetic stir bar was loaded 4-Trifluoromethylphenol (0.24 mmol, 1.2 equiv., 39 mg) and potassium carbonate (0.24 mmol, 1.2 equiv, 33 mg). The tube was sealed and placed under nitrogen before 1.0 mL of acetone was added. After stirring at room temperature for 1 hour, a solution of **2y** (0.2 mmol, 1.0 equiv., 76 mg) in acetone (1.0 mL) was added via syringe. The reaction mixture was allowed to stir for 48 hours at room temperature. Then the mixture was concentrated and purified by column chromatography, affording the title compound as a white solid (78.7 mg, 85%). **^{1}H NMR** (300 MHz, $CDCl_3$) δ 7.64 (d, *J* = 8.3 Hz, 2H), 7.46 – 7.40 (m, 2H), 7.37 – 7.23 (m, 7H), 6.90 (d, *J* = 8.3 Hz, 2H), 5.30 (dd,

J = 8.6, 4.2 Hz, 1H), 3.28 (m, 1H), 3.10 (m, 1H), 2.74 (s, 3H), 2.42 (s, 3H), 2.28 – 2.00 (m, 2H). **^{13}C NMR** (126 MHz, $CDCl_3$) δ 160.4, 143.5, 140.5, 134.2, 129.8, 128.9, 128.1, 127.5, 126.9 (q, *J* = 3.7 Hz), 125.9, 123.1, 122.9 (q, *J* = 32.6 Hz), 116.0, 77.4, 47.1, 37.2, 35.5, 21.5. **IR (neat):** 2927, 1614, 1517, 1323, 1247, 1157, 1108, 1066, 835, 815, 716, 700, 647, 548 cm^{-1}. **HRMS (ESI)** *calcd.* for ($C_{24}H_{24}F_3NNaO_3S$) $[M+Na]^+$: 486.1321, *found* 486.1328.

4.9.5 Mechanistic Studies

Radical scavenger experiments

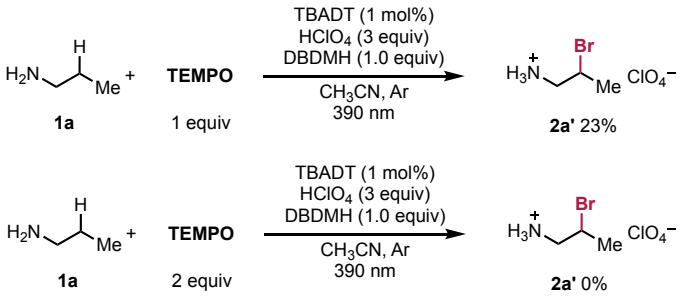

An oven-dried 10 mL screw-cap reaction tube containing a stir bar was charged with TBADT (1 mol%, 6.6 mg), TEMPO (0.2-0.4 mmol, 1 or 2 equiv., 31-62 mg) and DBDMH (0.2 mmol, 1 equiv, 57 mg). The reaction tube was capped with a Teflon-lined rubber septum and connected to a vacuum line where it was evacuated and backfilled with Ar three times. To a 4ml Teflon-capped glass vial was added *n*-propyl-amine **1a** (0.4 mmol, 2 equiv, 24 mg) and CH_3CN (2 mL) before sequential addition of $HClO_4$ (0.6 mmol, 3 equiv, 51 μL). The reaction mixture was transferred to the reaction tube by syringe, then sparged with Ar for 5 minutes. The reaction tube was then sealed with parafilm and irradiated by a 390 nm Kessil Lamp in a UFO Reactor under stirring at 600 rpm for 20 h. The reaction mixture was then quenched with air. The yield was determined via ^{1}H-NMR using CH_2Br_2 (0.2 mmol, 14 μL) as internal standard.

Intercepting radical intermediates with methyl acrylate

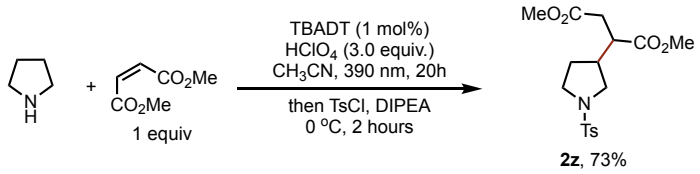

An oven-dried 10 mL screw-cap reaction tube containing a stir bar was charged with catalyst TBADT (1 mol%, 6.6 mg). The reaction tube was capped with a teflon-lined rubber septum and connected to a vacuum line where it was evacuated and backfilled with Ar three times. To a 4 mL Teflon-capped glass vial was added pyrrolidine **1m** (0.4 mmol, 2 equiv., 28 mg) and CH_3CN (2 mL) before sequential addition of $HClO_4$ (0.6 mmol, 3 equiv., 51 μL). The reaction mixture was transferred to the reaction tube by syringe, then sparged with Ar for 5 minutes and dimethyl maleate (0.2 mmol, 1 equiv., 29 mg) was added. The reaction tube was then sealed with parafilm and irradiated by a 390 nm Kessil Lamp in a UFO Reactor under stirring at 600 rpm for 20 h. After the reaction was complete, the reaction mixture was concentrated under vacuum, passed through a thin pad of silica with Hexane and EtOAc, then concentrated under vacuum to give a crude product, which was purified by column chromatography delivering **2z** (53 mg, 73%) as a colorless oil.

Dimethyl 2-(1-((4-methylphenyl)sulfonamido)propan-2-yl)succinate (2z). Colorless oil. **^{1}H NMR** (400 MHz, $CDCl_3$) δ 7.69 (d, *J* = 8.3 Hz, 2H), 7.33 (d, *J* = 8.6 Hz, 2H), 3.72 – 3.60 (m, 6H), 3.46 – 3.32 (m, 2H), 3.21 – 3.07 (m, 1H), 3.02 – 2.83 (m, 1H), 2.74 – 2.61 (m, 2H), 2.46 – 2.41 (m, 3H), 2.24 (m, 1H), 2.00 – 1.81 (m, 1H), 1.62 – 1.39 (m, 2H). **^{13}C NMR** (126 MHz, $CDCl_3$) δ 173.8, 173.7, 171.9, 171.8, 143.8, 143.7, 133.6, 133.6, 129.9, 129.9, 127.7, 127.7, 52.3, 52.2, 52.1, 52.1, 51.5, 51.3, 47.6, 47.5, 44.2, 43.9, 40.4, 40.2, 35.0, 34.7, 29.6, 29.4, 21.7. **HRMS (ESI)** *calcd*. for ($C_{17}H_{23}NNaO_6S$) $[M+Na]^+$: 392.1138, *found* 392.1152.

Intermolecular Kinetic Isotope Effect

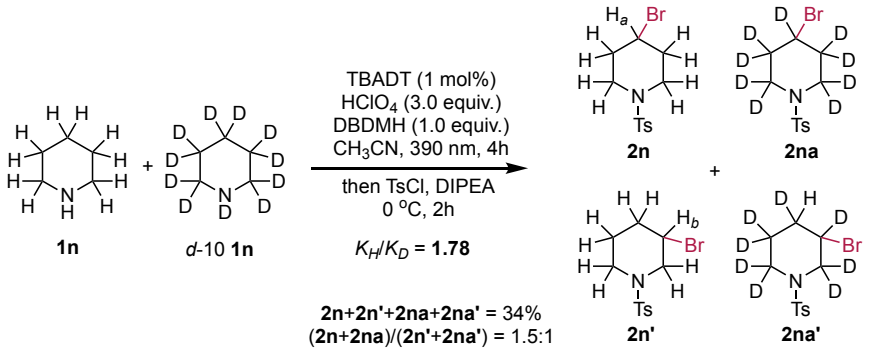

Following a modified General Procedure A, piperidine (0.2 mmol, 1 equiv) and piperidine-d_{10} (0.2 mmol, 1 equiv) were treated with $HClO_4$ (0.6 mmol, 3 equiv) and irradiated with a 390 nm Kessil lamp for 4 hours. The reaction mixture was purified by column chromatography, yielding a 1.5:1 mixture of *N*-tosyl 4-bromopiperidine and *N*-tosyl 3-bromopiperidine (22.0 mg, 34% yield).

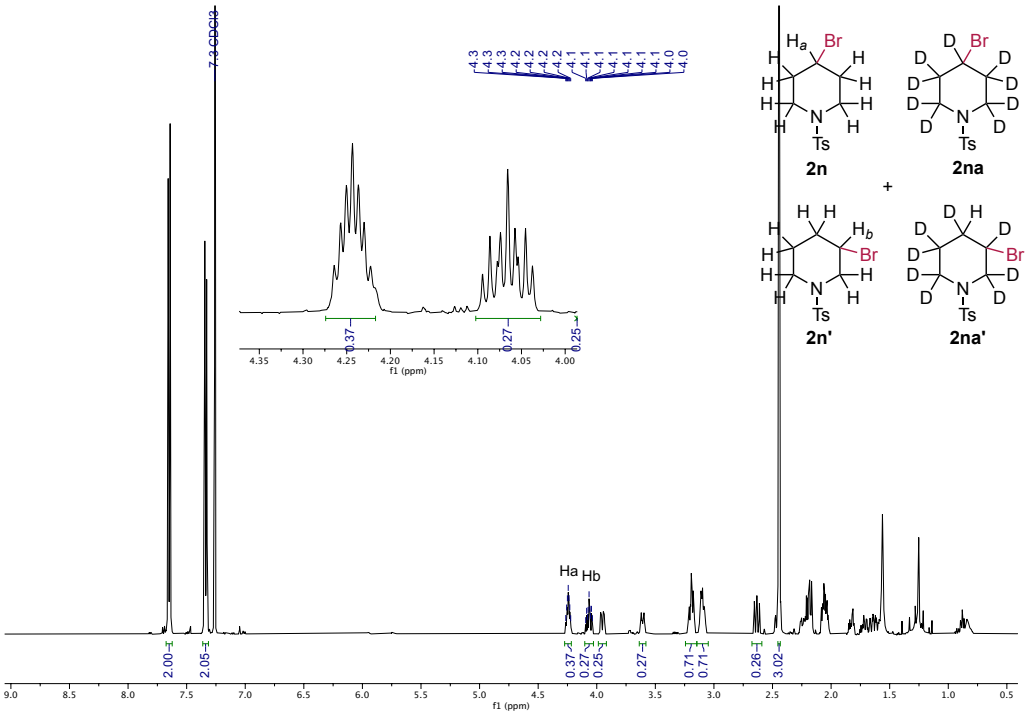

^{1}H NMR (500 MHz, $CDCl_3$) of brominated **1n** and **1n**-d_{10}**,** δ 4.24 (m, 0.37H, Ha), 4.07 (m, 0.27H, Hb).

KIE = (Ha+Hb)/(1-(Ha+Hb)) = 0.64H/0.36D = **1.78**

Quantum Yield

The quantum yield was measured for the C(sp^3)–H bromination of **1a** and **1k**. The reactions were performed in a quartz cuvette (path length (l) = 1.0 cm) positioned 1 cm away from a single blue LED (λmax = 395 nm).

Determination of the Photon Flux:

The photon flux of the blue LED set-up was determined using standard ferrioxalate actinometry.[54] A 0.012 M ferrioxalate solution (solution a) was prepared by dissolving 59 mg of potassium ferrioxalate trihydrate in 10 mL of 0.05 M aq. H_2SO_4. A buffered 5.5 mM phenanthroline solution (solution b) was prepared by dissolving 10 mg of 1,10-phenanthroline and 2.25 g of $NaOAc \cdot 3H_2O$ in 10 mL of 0.5 M aq. H_2SO_4. Both solutions were stored in amber vessels in the dark. Whilst working under red light, 2 mL of solution a) was transferred into a cuvette. This operation was repeated three times to get 3 identical solutions: one of them was kept in the dark (Blank), while the other cuvettes (Test 1 and Test 2) were placed 1 cm from a single 395nm LED and irradiated for 60 seconds. After irradiation, 25 μL of each of the three solutions were withdrawn and diluted with 2.5 mL of solution b) each. The mixtures were left to stand for approximately 15 min. Then, a single-beam spectrophotometer was used to read the difference of absorbance (ΔA) at λ = 510 nm between Test 1 and 2 and the Blank. ε is the molar absorptivity of the $Fe(phen)_3^{2+}$ complex at λ = 510 nm (11100 L mol^{-1} cm^{-1}).

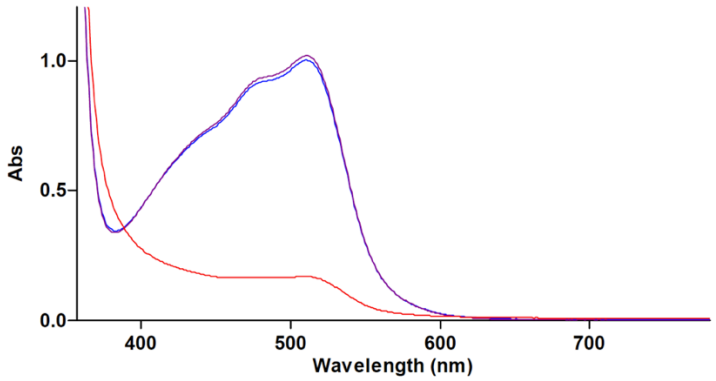

Figure 4-5 UV absorption spectrum of Test 1 (blue) and Test 2 (purple) and the Blank (red).

for Test 1: $\Delta A = 0.83303$

for Test 2: $\Delta A = 0.85051$

The number of moles of Fe^{2+} formed was calculated using:

$$\text{mol } Fe^{2+} = \frac{\Delta A \times 2.0 \times 10^{-3}\ \text{L} \times \dfrac{2.75 \times 10^{-3}\ \text{L}}{0.25 \times 10^{-3}\ \text{L}}}{\varepsilon \times l}$$

for Test 1: mol $Fe^{2+} = 1.65 \times 10^{-6}$

for Test 2: mol $Fe^{2+} = 1.69 \times 10^{-6}$

The photon flux was calculated using:

$$\text{photon flux } (\text{E} \bullet s^{-1}) = \frac{\text{mol } Fe^{2+}}{\Phi \times t \times f}$$

Where Φ is the quantum yield for the ferrioxalate actinometer (1.13 at $\lambda = 395$ nm),[55] t is the irradiation time (60 s), and f is the fraction of light absorbed at $\lambda = 395$ nm, where f

$= 1 - 10^{-A(395\ nm)}$. The absorbance of the above ferrioxalate solution at 395 nm was measured to be 3.098, therefore $f = 0.9992$.

Determination of the Quantum Yields:

*Quantum Yield for the formation of **2a'** :*

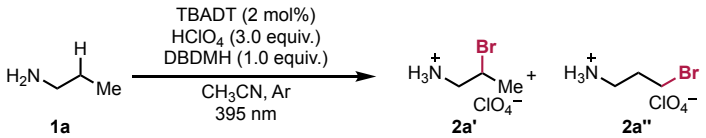

A 4.5 mL quartz cuvette (path length: l = 1.0 cm) containing a stir bar was charged with TBADT (2 mol%, 13 mg) and DBDMH (0.2 mmol, 1 equiv., 57 mg). The cuvette was capped with a Teflon-lined rubber septum and connected to a vacuum line where it was evacuated and backfilled with Ar three times. To a 4 mL Teflon-capped glass vial, *n*-propylamine **1a** (0.4 mmol, 2 equiv., 24 mg) and CH_3CN (2 mL) were added, followed by the sequential addition of $HClO_4$ (0.6 mmol, 3.0 equiv., 51 µL). This solution was then transferred to the cuvette by syringe after sparging with Ar for 5 minutes. The cuvette was sealed with parafilm and positioned 1 cm away from a single 395 nm LED, stirred and irradiated for 5 h. The reaction mixture was then quenched with air. The yield was determined via ^{1}H-NMR assay using CH_2Br_2 (0.2 mmol, 13.5 µL) as an internal standard. We calculated the quantum yield after 5 h of reaction, when 1.4×10^{-5} moles (7% yield) of product **2a'** were formed. QY (Φ) was calculated from the ratio between the moles of product produced after 5 h and the moles of photon reaching the reaction vial in 5 h.

Entry	ΔA	mol Fe^{2+}	E • s^{-1}	E in 5 h	mol $_{prod}$	Φ
1	0.83303	1.65×10^{-6}	2.44×10^{-8}	4.39×10^{-4}	1.40×10^{-5}	0.03
2	0.85051	1.69×10^{-6}	2.49×10^{-8}	4.48×10^{-4}	1.40×10^{-5}	0.03

Quantum yield was determined to be 0.03 (as average of two experiments), indicating that the process does not follow a canonical radical-chain propagation.

*Quantum Yield for the formation of **2k'*** :

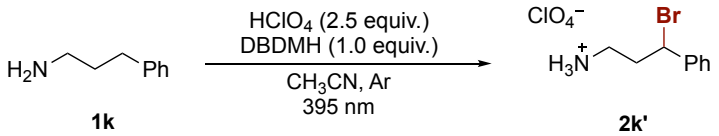

A 4.5 mL quartz cuvette (path length: l = 1.0 cm) containing a stir bar was charged with DBDMH (0.2 mmol, 1 equiv., 57 mg). The cuvette was capped with a Teflon-lined rubber septum and connected to a vacuum line where it was evacuated and backfilled with Ar three times. To a 4 mL Teflon-capped glass vial, 3-phenylpropylamine **1k** (0.25 mmol, 34 mg) and CH_3CN (2 mL) were added, followed by the sequential addition of $HClO_4$ (0.5 mmol, 43 µL). This solution was then transferred to the cuvette by syringe after sparging with Ar for 5 minutes. The cuvette was sealed with parafilm and positioned 1 cm away from a single 395 nm LED, stirred and irradiated for 0.5 h. The reaction mixture was then quenched with air. The yield was determined via ^{1}H-NMR assay using CH_2Br_2 (0.2 mmol, 13.5 µL) as an internal standard. We calculated the quantum yield after 0.5 h of reaction, when 1.90×10^{-4} moles (95% yield) of product **2k'** were formed. QY (Φ) was calculated from the ratio between the moles of product produced after 0.5 h and the moles of photon reaching the reaction vial in 0.5 h.

Entry	ΔA	mol Fe^{2+}	E • s^{-1}	E in 0.5 h	mol $_{prod}$	Φ
1	0.83303	1.65×10^{-6}	2.44×10^{-8}	4.39×10^{-5}	1.90×10^{-4}	4.33
2	0.85051	1.69×10^{-6}	2.49×10^{-8}	4.48×10^{-5}	1.90×10^{-4}	4.24

Quantum yield was determined to be 4.29 (as average of two experiments), indicating that the process might follow a radical-chain propagation.

4.9.6 DFT Calculations

To better understand the rule of selectivity in this distal bromination event, BDE and NPA analysis of amines and ammonia salts were collected. The following results do not only predict the more electron-rich hydrogen with lower BDE amenable for hydrogen atom transfer (HAT) but also explain the site-selectivity in the presence of additional electron-rich C(sp^3)–H linkages.

All calculations were performed using the Gaussian 09 program. All geometries were optimized at the B3LYP/6-31G(d,p) level of theory, accounting for solvation effects using the self-consistent reaction field polarizable continuum model (IEF-PCM) in acetonitrile, T=295.15K. Natural population analysis (NPA) was performed on the energy minimized structure at the B3LYP/6-311++G(d,p) level of theory to obtain natural partial atomic charges for all hydrogen atoms (lower values indicate the site is more electron rich).[56]

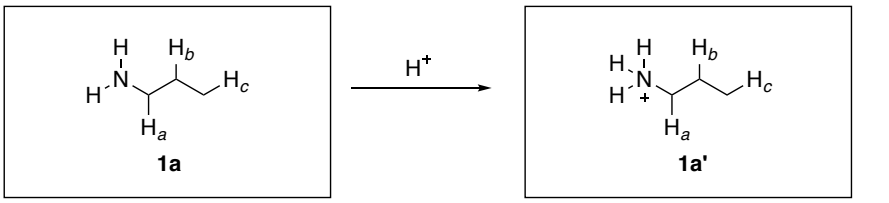

NPA	BDE	NPA	BDE
H_a = 0.167	H_a = 91.9 kcal	H_a = 0.220	H_a = 102.9 kcal
H_b = 0.189	H_b = 97.4 kcal	H_b = 0.208	H_b = 97.8 kcal
H_c = 0.197	H_c = 101.3 kcal	H_c = 0.207	H_c = 102.3 kcal

Table 4.4 The NPA and BDE analysis of **1a** and **1a'**.

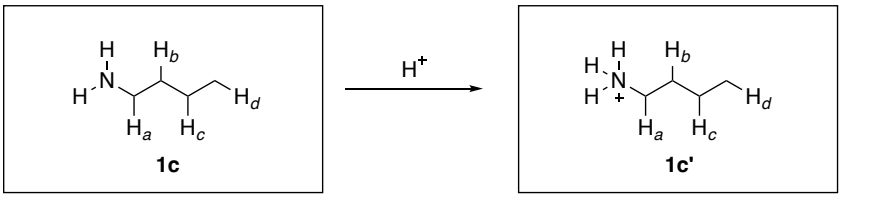

NPA	BDE	NPA	BDE
H_a = 0.168	H_a = 91.7 kcal	H_a = 0.220	H_a = 102.9 kcal
H_b = 0.188	H_b = 98.1 kcal	H_b = 0.208	H_b = 98.2 kcal
H_c = 0.187	H_c = 97.6 kcal	H_c = 0.197	H_c = 98.3 kcal
H_d = 0.195	H_d = 101.4 kcal	H_d = 0.200	H_d = 101.8 kcal

Table 4.5 The NPA and BDE analysis of **1c** and **1c'**.

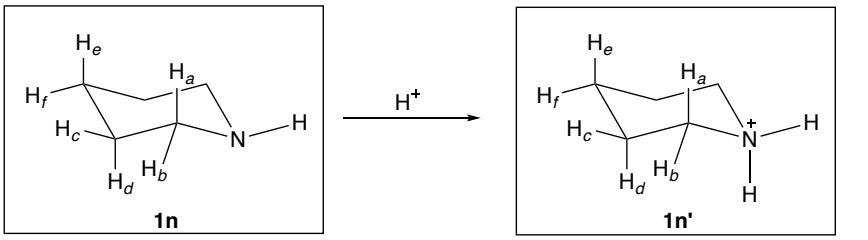

NPA	BDE	NPA	BDE
H_a = 0.156	$H_{a/b}$ = 91.9 kcal	H_a = 0.218	$H_{a/b}$ = 102.6 kcal
H_b = 0.193		H_b = 0.229	
H_c = 0.201	$H_{c/d}$ = 99.4 kcal	H_c = 0.232	$H_{c/d}$ = 99.0 kcal
H_d = 0.191		H_d = 0.210	
H_e = 0.188	$H_{e/f}$ = 98.3 kcal	H_e = 0.204	$H_{e/f}$ = 99.2 kcal
H_f = 0.200		H_f = 0.219	

Table 4.6 The NPA and BDE analysis of **1n** and **1n'**.

(For DFT Calculations details, see the SI of *Angew. Chem. Int. Ed.* **2024**, *63*, e202406485.)

4.9.7 Crystallographic Data

X-ray diffraction of 2o

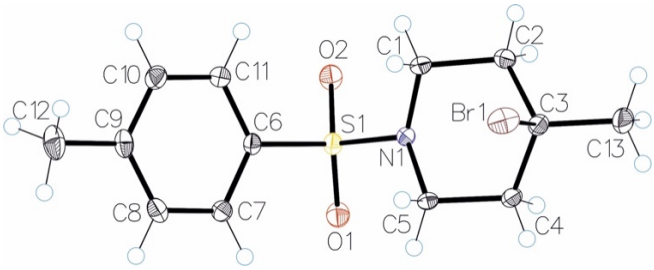

Figure 4.6 ORTEP diagram of **2o**, CCDC: 2325216

Table 4.7 Crystal data and structure refinement for **2o**.

Empirical formula	$C_{13}H_{18}BrNO_2S$
Formula weight	332.25
Temperature/K	100
Crystal system	monoclinic
Space group	$P2_1/n$
a/Å	13.9183(4)
b/Å	5.98420(10)
c/Å	17.7637(4)
α/°	90
β/°	105.466(3)
γ/°	90
Volume/Å^3	1425.96(6)
Z	4
ρ_{calc}g/cm^3	1.548
μ/mm^{-1}	3.023
F(000)	680.0
Crystal size/mm^3	0.5 × 0.5 × 0.5
Radiation	MoKα (λ = 0.71073)
2Θ range for data collection/°	4.328 to 64.72

Table 4.7 Crystal data and structure refinement for **2o**.

Index ranges	$-20 \le h \le 15$, $-7 \le k \le 9$, $-26 \le l \le 26$
Reflections collected	22453
Independent reflections	4686 [R_{int} = 0.0247, R_{sigma} = 0.0242]
Data/restraints/parameters	4686/0/165
Goodness-of-fit on F^2	1.044
Final R indexes [I>=2σ (I)]	R_1 = 0.0279, wR_2 = 0.0645
Final R indexes [all data]	R_1 = 0.0354, wR_2 = 0.0667
Largest diff. peak/hole / e $Å^{-3}$	0.80/-0.41

Table 4.8 Fractional Atomic Coordinates ($\times 10^4$) and Equivalent Isotropic Displacement Parameters ($Å^2 \times 10^3$) for **2o**. U_{eq} is defined as 1/3 of the trace of the orthogonalised U_{IJ} tensor.

Atom	*x*	*y*	*z*	U(eq)
Br1	3665.4(2)	9416.8(3)	5077.9(2)	23.83(5)
S1	4765.3(2)	6171.2(6)	2573.7(2)	13.46(7)
O1	4378.2(7)	7436.8(18)	1873.0(6)	18.8(2)
O2	4788.2(8)	3768.7(17)	2543.7(6)	19.0(2)
N1	4078.7(8)	6794.8(19)	3159.2(7)	13.0(2)
C5	3815.4(10)	9157(2)	3227.6(8)	13.7(2)
C4	2816.4(10)	9217(2)	3425.1(8)	15.0(3)
C6	5996.8(9)	7083(2)	2998.7(8)	13.4(2)
C3	2799.8(10)	7854(2)	4145.3(8)	15.5(3)
C7	6297.6(10)	9182(2)	2812.7(8)	15.4(3)
C2	3230.7(11)	5528(2)	4111.2(9)	16.1(3)
C11	6653.6(11)	5679(2)	3514.1(9)	17.5(3)
C9	7949.8(10)	8477(3)	3658.0(8)	18.2(3)
C8	7277.7(11)	9858(2)	3141.2(9)	17.5(3)
C1	4221.7(10)	5547(2)	3892.4(8)	15.7(3)
C10	7625.9(11)	6389(3)	3836.4(9)	20.0(3)
C13	1759.3(11)	7756(3)	4268.7(10)	25.5(3)
C12	9012.6(12)	9205(3)	4014.2(10)	27.8(4)

Table 4.9 Anisotropic Displacement Parameters ($Å^2×10^3$) for **2o**. The Anisotropic displacement factor exponent takes the form: $-2π^2[h^2a^{*2}U_{11}+2hka*b*U_{12}+…]$.

Atom	U_{11}	U_{22}	U_{33}	U_{23}	U_{13}	U_{12}
Br1	33.13(9)	22.56(8)	14.57(8)	-3.53(6)	4.19(6)	3.79(6)
S1	11.97(14)	13.38(15)	15.46(15)	-2.25(12)	4.42(11)	-0.67(11)
O1	16.9(5)	24.3(5)	14.6(5)	0.5(4)	3.1(4)	0.1(4)
O2	19.2(5)	13.4(5)	26.1(5)	-6.2(4)	9.1(4)	-1.5(4)
N1	13.0(5)	11.3(5)	15.9(5)	0.9(4)	6.0(4)	1.5(4)
C5	15.0(6)	9.4(6)	17.1(6)	1.3(5)	4.8(5)	1.8(4)
C4	14.9(6)	14.9(6)	15.6(6)	2.7(5)	4.6(5)	3.9(5)
C6	11.2(6)	14.6(6)	15.2(6)	-1.2(5)	4.9(5)	0.0(5)
C3	14.8(6)	17.8(6)	14.4(6)	1.8(5)	4.5(5)	3.1(5)
C7	15.9(6)	14.2(6)	17.1(6)	0.2(5)	6.1(5)	1.4(5)
C2	17.6(6)	13.7(6)	18.2(6)	2.6(5)	6.8(5)	0.8(5)
C11	16.2(6)	16.8(6)	20.3(7)	4.1(5)	6.2(5)	1.4(5)
C9	13.8(6)	26.3(7)	16.0(6)	-4.3(6)	6.3(5)	-2.4(5)
C8	17.8(6)	16.7(6)	20.3(7)	-2.3(5)	9.3(5)	-3.9(5)
C1	16.3(6)	12.4(6)	19.0(6)	3.4(5)	5.6(5)	3.1(5)
C10	14.7(6)	26.5(7)	18.0(7)	5.0(6)	3.1(5)	3.1(6)
C13	20.2(7)	33.6(9)	26.5(8)	9.6(7)	12.5(6)	8.2(6)
C12	15.8(7)	42.8(10)	24.5(8)	-3.9(7)	4.9(6)	-7.6(7)

Table 4.10 Bond Lengths for **2o**.

Atom	Atom	Length/Å	Atom	Atom	Length/Å
Br1	C3	2.0016(14)	C6	C11	1.391(2)
S1	O1	1.4336(11)	C3	C2	1.5234(19)
S1	O2	1.4394(11)	C3	C13	1.5226(19)
S1	N1	1.6323(11)	C7	C8	1.393(2)
S1	C6	1.7651(13)	C2	C1	1.5296(19)
N1	C5	1.4734(17)	C11	C10	1.388(2)
N1	C1	1.4681(18)	C9	C8	1.394(2)
C5	C4	1.5225(19)	C9	C10	1.393(2)
C4	C3	1.5228(19)	C9	C12	1.510(2)

Table 4.10 Bond Lengths for **2o**.

Atom	Atom	Length/Å	Atom	Atom	Length/Å
C6	C7	1.3915(19)			

Table 4.11 Bond Angles for **2o**.

Atom	Atom	Atom	Angle/°	Atom	Atom	Atom	Angle/°
O1	S1	O2	120.16(7)	C4	C3	C2	111.22(11)
O1	S1	N1	106.51(6)	C2	C3	Br1	107.67(9)
O1	S1	C6	107.77(6)	C13	C3	Br1	106.53(10)
O2	S1	N1	105.93(6)	C13	C3	C4	111.70(12)
O2	S1	C6	107.22(6)	C13	C3	C2	111.72(12)
N1	S1	C6	108.88(6)	C6	C7	C8	119.04(13)
C5	N1	S1	118.20(9)	C3	C2	C1	113.23(11)
C1	N1	S1	119.01(9)	C10	C11	C6	118.94(13)
C1	N1	C5	113.13(11)	C8	C9	C12	121.04(14)
N1	C5	C4	107.72(11)	C10	C9	C8	118.71(13)
C5	C4	C3	113.59(11)	C10	C9	C12	120.25(14)
C7	C6	S1	119.79(11)	C7	C8	C9	120.95(13)
C11	C6	S1	119.19(11)	N1	C1	C2	108.12(11)
C11	C6	C7	121.02(13)	C11	C10	C9	121.33(14)
C4	C3	Br1	107.72(9)				

Table 4.12 Torsion Angles for **2o**.

A	B	C	D	Angle/°	A	B	C	D	Angle/°
Br1	C3	C2	C1	-70.14(13)	C5	C4	C3	Br1	69.55(13)
S1	N1	C5	C4	151.01(9)	C5	C4	C3	C2	-48.22(16)
S1	N1	C1	C2	-151.46(10)	C5	C4	C3	C13	-173.80(13)
S1	C6	C7	C8	-178.72(11)	C4	C3	C2	C1	47.65(16)
S1	C6	C11	C10	178.93(11)	C6	S1	N1	C5	72.53(11)
O1	S1	N1	C5	-43.43(11)	C6	S1	N1	C1	-71.28(11)
O1	S1	N1	C1	172.76(10)	C6	C7	C8	C9	-0.9(2)
O1	S1	C6	C7	21.76(13)	C6	C11	C10	C9	0.5(2)
O1	S1	C6	C11	-158.00(11)	C3	C2	C1	N1	-53.95(15)
O2	S1	N1	C5	-172.44(10)	C7	C6	C11	C10	-0.8(2)
O2	S1	N1	C1	43.75(12)	C11	C6	C7	C8	1.0(2)

Table 4.12 Torsion Angles for **2o**.

A	B	C	D	Angle/°	A	B	C	D	Angle/°
O2	S1	C6	C7	152.43(11)	C8	C9	C10	C11	-0.4(2)
O2	S1	C6	C11	-27.32(13)	C1	N1	C5	C4	-63.15(14)
N1	S1	C6	C7	-93.38(12)	C10	C9	C8	C7	0.6(2)
N1	S1	C6	C11	86.86(12)	C13	C3	C2	C1	173.22(12)
N1	C5	C4	C3	54.51(15)	C12	C9	C8	C7	179.95(14)
C5	N1	C1	C2	63.00(14)	C12	C9	C10	C11	-179.74(14)

Table 4.13 Hydrogen Atom Coordinates ($Å \times 10^4$) and Isotropic Displacement Parameters ($Å^2 \times 10^3$) for **2o**.

Atom	*x*	*y*	*z*	U(eq)
H5A	3766.02	9948.35	2729.34	16
H5B	4333.29	9899.37	3644.23	16
H4A	2294.08	8643.16	2973.08	18
H4B	2650.57	10789.22	3511.18	18
H7	5841	10141.19	2466.74	18
H2A	2743.18	4620.98	3723.31	19
H2B	3330.98	4800.82	4627.06	19
H11	6440.28	4255.62	3643.43	21
H8	7491.14	11279.61	3011.03	21
H1A	4743.82	6269.31	4311.2	19
H1B	4434.99	3998.22	3825.14	19
H10	8079.57	5432.74	4185.78	24
H13A	1788.07	6991.71	4762.26	38
H13B	1314.33	6934.71	3836.67	38
H13C	1505.82	9276.94	4286.71	38
H12A	9461.38	8319.15	3791.02	42
H12B	9184.07	8977.68	4580.75	42
H12C	9082.34	10791.29	3901.89	42

X-ray diffraction of 2t

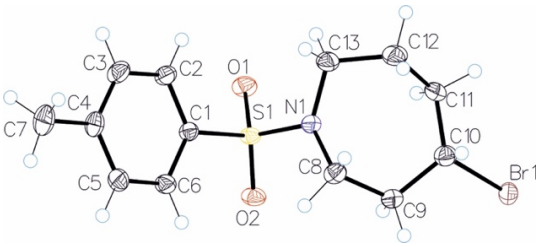

Figure 4.7 ORTEP diagram of **2t**, CCDC: 2325217

Table 4.14 Crystal data and structure refinement for **2t**.

Empirical formula	$C_{13}H_{18}BrNO_2S$
Formula weight	332.25
Temperature/K	100.00
Crystal system	monoclinic
Space group	$P2_1/n$
a/Å	14.4416(2)
b/Å	5.20660(10)
c/Å	18.4755(3)
α/°	90
β/°	90.8660(10)
γ/°	90
Volume/Å^3	1389.04(4)
Z	4
ρ_{calc}g/cm^3	1.589
μ/mm^{-1}	3.104
F(000)	680.0
Crystal size/mm^3	0.2 × 0.2 × 0.2
Radiation	MoKα (λ = 0.71073)
2Θ range for data collection/°	5.642 to 68.9
Index ranges	$-21 \le h \le 22$, $-8 \le k \le 8$, $-28 \le l \le 27$
Reflections collected	40216
Independent reflections	5702 [R_{int} = 0.0385, R_{sigma} = 0.0213]
Data/restraints/parameters	5702/0/164

Goodness-of-fit on F^2	1.061
Final R indexes [I>=2σ (I)]	R_1 = 0.0374, wR_2 = 0.1029
Final R indexes [all data]	R_1 = 0.0436, wR_2 = 0.1059
Largest diff. peak/hole / e $Å^{-3}$	1.96/-0.67

Table 4.15 Fractional Atomic Coordinates ($\times 10^4$) and Equivalent Isotropic Displacement Parameters ($Å^2 \times 10^3$) for **2t**. U_{eq} is defined as 1/3 of the trace of the orthogonalised U_{IJ} tensor.

Atom	*x*	*y*	*z*	U(eq)
Br1	6788.9(2)	-313.5(4)	2869.2(2)	25.87(6)
C2	1689.3(12)	4422(4)	4230.9(10)	23.3(3)
O2	3510.2(10)	-919(3)	4506.7(7)	24.7(3)
C3	1190.3(13)	6148(4)	4648.4(11)	27.2(3)
C4	1378.5(12)	6447(4)	5386.9(10)	24.2(3)
C5	2080.2(14)	4970(4)	5704.4(10)	24.9(3)
C6	2586.9(12)	3228(4)	5295.9(9)	22.6(3)
C7	840.9(15)	8344(5)	5832.6(13)	34.1(4)
C8	4665.8(12)	3302(4)	4083.7(10)	23.5(3)
O1	2454.3(10)	-84(3)	3457.2(8)	25.3(3)
N1	3852.6(10)	2552(3)	3648.4(8)	20.7(3)
C1	2387.5(11)	2970(3)	4560.2(9)	18.3(3)
S1	3051.2(3)	864.3(8)	4028.5(2)	18.14(8)
C9	5508.6(12)	1749(4)	3854.2(9)	23.3(3)
C10	5841.0(13)	2316(4)	3094.7(10)	24.8(3)
C11	5131.6(13)	2351(4)	2476.2(9)	24.4(3)
C12	4455.2(15)	4617(4)	2542.8(12)	29.5(4)
C13	3612.4(14)	4091(4)	3000.6(10)	25.7(3)

Table 4.16 Anisotropic Displacement Parameters ($Å^2 \times 10^3$) for **2t**. The Anisotropic displacement factor exponent takes the form: $-2\pi^2[h^2a^{*2}U_{11}+2hka^*b^*U_{12}+\ldots]$.

Atom	U_{11}	U_{22}	U_{33}	U_{23}	U_{13}	U_{12}
Br1	21.69(9)	29.03(10)	27.06(10)	5.47(6)	5.47(6)	3.58(6)
C2	21.1(7)	26.5(8)	22.1(7)	-1.8(6)	-3.0(6)	4.8(6)
O2	32.6(7)	21.1(6)	20.4(5)	1.6(4)	-2.6(5)	9.0(5)
C3	22.5(7)	27.9(9)	31.1(9)	-2.1(7)	-1.3(6)	7.8(7)

Table 4.16 Anisotropic Displacement Parameters ($Å^2×10^3$) for **2t**. The Anisotropic displacement factor exponent takes the form: $-2π^2[h^2a^{*2}U_{11}+2hka*b*U_{12}+…]$.

Atom	U_{11}	U_{22}	U_{33}	U_{23}	U_{13}	U_{12}
C4	21.4(7)	22.4(7)	28.9(8)	-5.6(6)	5.0(6)	1.1(6)
C5	25.5(8)	29.1(8)	20.3(7)	-5.3(6)	1.7(6)	1.7(6)
C6	24.4(7)	25.8(8)	17.6(6)	-2.0(6)	-1.1(5)	5.0(6)
C7	28.9(9)	32.5(10)	41.3(11)	-12.0(9)	8.8(8)	4.1(8)
C8	22.8(7)	24.9(8)	22.6(7)	-6.1(6)	-3.3(6)	2.1(6)
O1	27.8(6)	26.8(6)	21.0(6)	-7.0(5)	-6.4(5)	0.4(5)
N1	19.5(6)	25.2(7)	17.4(6)	0.2(5)	-1.1(4)	2.8(5)
C1	18.6(6)	18.3(6)	18.1(6)	-1.7(5)	-0.2(5)	2.0(5)
S1	21.33(17)	17.90(16)	15.09(15)	-2.12(12)	-3.12(12)	3.56(13)
C9	22.0(7)	26.9(8)	20.9(7)	1.2(6)	-3.0(5)	1.7(6)
C10	24.3(7)	24.7(8)	25.4(8)	3.1(6)	-1.3(6)	1.1(6)
C11	26.9(7)	28.0(8)	18.2(7)	5.4(6)	0.5(6)	3.0(6)
C12	29.7(9)	27.6(9)	31.3(9)	11.6(7)	-2.2(7)	1.4(7)
C13	28.9(8)	25.8(8)	22.5(7)	4.7(6)	0.3(6)	7.6(7)

Table 4.17 Bond Lengths for **2t**

Atom	Atom	Length/Å	Atom	Atom	Length/Å
Br1	C10	1.9847(19)	C8	C9	1.527(3)
C2	C3	1.392(3)	O1	S1	1.4399(14)
C2	C1	1.393(2)	N1	S1	1.6215(16)
O2	S1	1.4368(13)	N1	C13	1.477(2)
C3	C4	1.396(3)	C1	S1	1.7646(16)
C4	C5	1.394(3)	C9	C10	1.519(3)
C4	C7	1.509(3)	C10	C11	1.523(3)
C5	C6	1.394(2)	C11	C12	1.538(3)
C6	C1	1.392(2)	C12	C13	1.518(3)
C8	N1	1.466(2)			

Table 4-18. Bond Angles for **2t**.

Atom	Atom	Atom	Angle/°	Atom	Atom	Atom	Angle/°
C3	C2	C1	119.06(17)	O2	S1	O1	119.65(9)

Table 4-18. Bond Angles for **2t**.

Atom	Atom	Atom	Angle/°	Atom	Atom	Atom	Angle/°
C2	C3	C4	121.24(17)	O2	S1	N1	106.90(8)
C3	C4	C7	120.82(18)	O2	S1	C1	107.97(8)
C5	C4	C3	118.64(16)	O1	S1	N1	106.96(8)
C5	C4	C7	120.54(18)	O1	S1	C1	107.28(8)
C6	C5	C4	120.99(17)	N1	S1	C1	107.56(8)
C1	C6	C5	119.27(16)	C10	C9	C8	114.72(15)
N1	C8	C9	109.98(14)	C9	C10	Br1	106.77(12)
C8	N1	S1	118.55(12)	C9	C10	C11	118.50(15)
C8	N1	C13	118.42(16)	C11	C10	Br1	107.99(13)
C13	N1	S1	118.98(12)	C10	C11	C12	111.70(17)
C2	C1	S1	119.33(13)	C13	C12	C11	114.95(16)
C6	C1	C2	120.79(15)	N1	C13	C12	111.65(15)
C6	C1	S1	119.84(13)				

Table 4.19 Torsion Angles for **2t**.

A	B	C	D	Angle/°	A	B	C	D	Angle/°
Br1	C10	C11	C12	-170.97(13)	C8	N1	S1	O1	-167.28(13)
C2	C3	C4	C5	-0.2(3)	C8	N1	S1	C1	77.75(14)
C2	C3	C4	C7	179.30(19)	C8	N1	C13	C12	46.7(2)
C2	C1	S1	O2	-162.86(15)	C8	C9	C10	Br1	-170.71(13)
C2	C1	S1	O1	-32.66(17)	C8	C9	C10	C11	-48.7(2)
C2	C1	S1	N1	82.10(16)	N1	C8	C9	C10	66.8(2)
C3	C2	C1	C6	0.1(3)	C1	C2	C3	C4	0.1(3)
C3	C2	C1	S1	-177.71(15)	S1	N1	C13	C12	-156.24(15)
C3	C4	C5	C6	0.1(3)	C9	C8	N1	S1	107.42(15)
C4	C5	C6	C1	0.1(3)	C9	C8	N1	C13	-95.42(19)
C5	C6	C1	C2	-0.2(3)	C9	C10	C11	C12	67.6(2)
C5	C6	C1	S1	177.61(15)	C10	C11	C12	C13	-87.3(2)
C6	C1	S1	O2	19.34(17)	C11	C12	C13	N1	39.7(2)
C6	C1	S1	O1	149.55(15)	C13	N1	S1	O2	164.97(14)
C6	C1	S1	N1	-95.69(15)	C13	N1	S1	O1	35.69(16)
C7	C4	C5	C6	-179.39(19)	C13	N1	S1	C1	-79.28(15)
C8	N1	S1	O2	-38.00(15)					

Table 4.20 Hydrogen Atom Coordinates (Å×10^4) and Isotropic Displacement Parameters (Å^2×10^3) for **2t**.

Atom	*x*	*y*	*z*	U(eq)
H2	1555.46	4237.37	3728.61	28
H3	712.76	7141.04	4426.51	33
H5	2214.96	5152.87	6206.65	30
H6	3063.09	2228.82	5517.4	27
H7A	971.87	10092.06	5666.08	51
H7B	1024.96	8178.14	6343.2	51
H7C	176.69	7994.92	5778.14	51
H8A	4544.93	2995.33	4602.61	28
H8B	4789.37	5157.17	4017.57	28
H9A	6023.13	2090.3	4201.1	28
H9B	5355.51	-100.37	3886.47	28
H10	6155.35	4027.06	3105.59	30
H11A	4778.62	720.9	2476.17	29
H11B	5457.63	2476.1	2009.98	29
H12A	4794.52	6098.1	2753.51	35
H12B	4241.8	5118.15	2051.04	35
H13A	3337.76	5743.3	3153.51	31
H13B	3142.78	3160.57	2705.93	31

4.9.8 Representative set of NMR Spectra

For all the spectra, see the SI of *Angew. Chem. Int. Ed.* **2024**, *63*, e202406485.

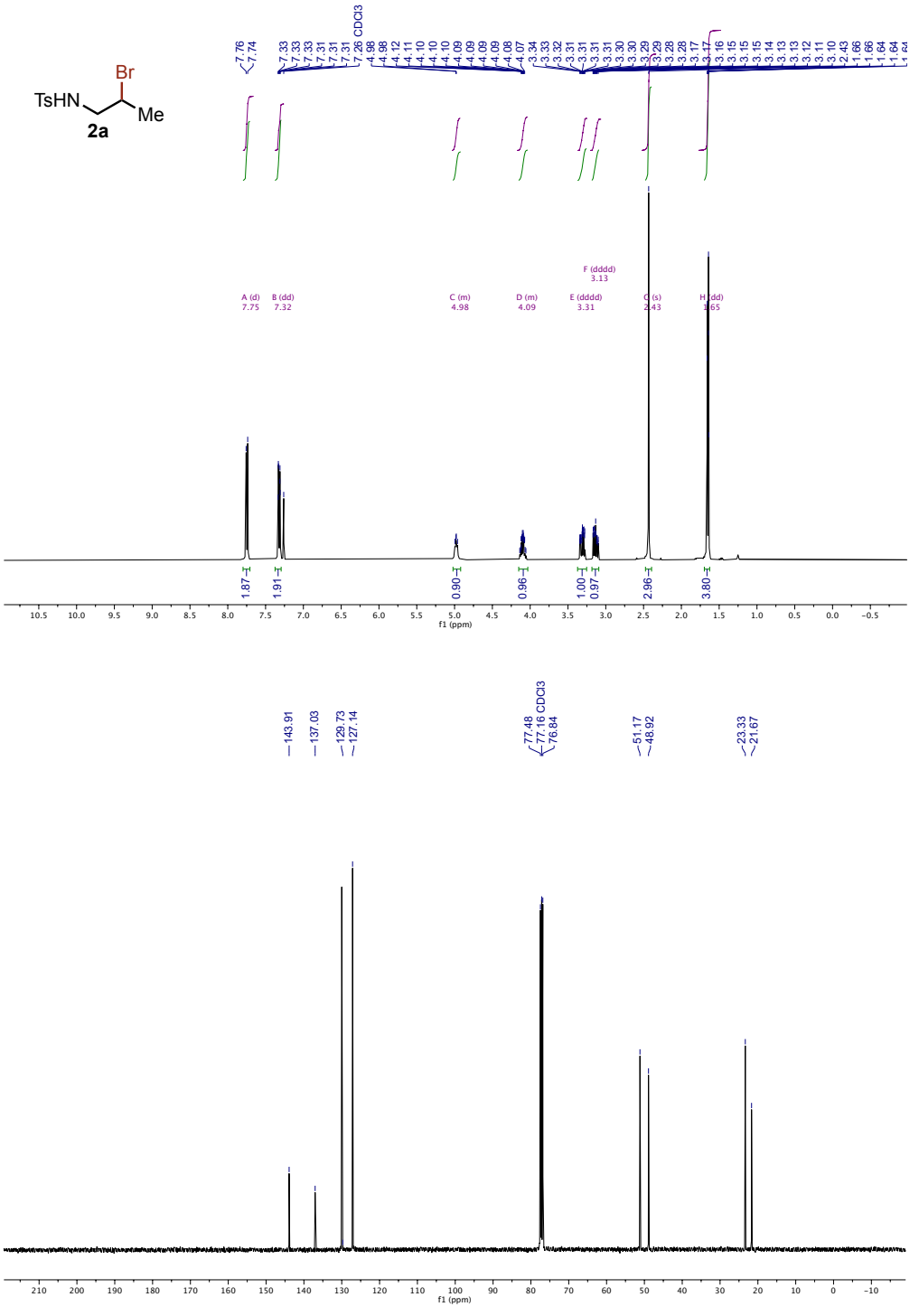
Br
TsHN
Me
2a
CDCl3
A (d) 7.75
B (dd) 7.32
C (m) 4.98
D (m) 4.09
E (dddd) 3.31
F (dddd) 3.13
G (s) 2.43
H (dd) 1.65
1.87
1.91
0.90
0.96
1.00
0.97
2.96
3.80
f1 (ppm)
143.91
137.03
129.73
127.14
77.48
77.16 CDCl3
76.84
51.17
48.92
23.33
21.67
f1 (ppm)

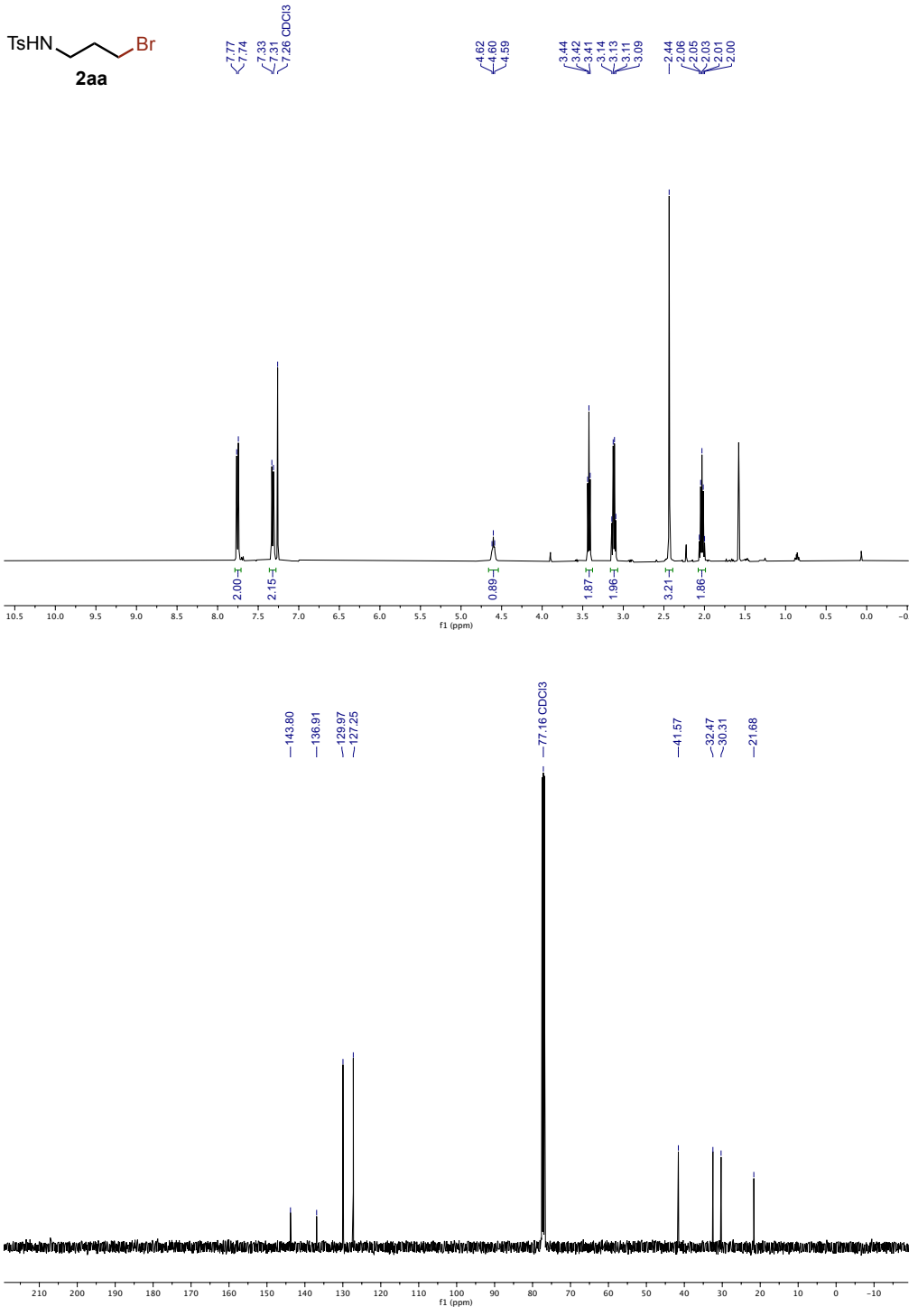
TsHN
Br
2aa
7.77
7.74
7.33
7.31
7.26 CDCl3
4.62
4.60
4.59
3.44
3.42
3.41
3.14
3.13
3.11
3.09
2.44
2.06
2.05
2.03
2.01
2.00
2.00
2.15
0.89
1.87
1.96
3.21
1.86
f1 (ppm)
143.80
136.91
129.97
127.25
77.16 CDCl3
41.57
32.47
30.31
21.68
f1 (ppm)


7.76
7.73
7.31
7.29
7.26 CDCl3
4.90
4.89
4.87
4.07
4.06
4.06
4.05
4.04
4.04
4.04
4.03
4.02
4.02
4.02
4.01
4.01
4.00
3.99
2.97
2.95
2.94
2.92
2.42
1.78
1.78
1.78
1.77
1.77
1.77
1.76
1.76
1.76
1.75
1.75
1.74
1.74
1.73
1.73
1.72
1.72
1.71
1.71
1.70
1.70
1.69
1.69
1.69
1.68
1.68
1.67
1.67
1.67
1.66
1.66
1.65
1.63
1.63
1.61
1.61
1.60
1.59
1.58
1.57
1.56
1.56
1.54

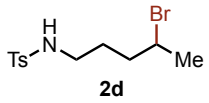
H
N
Ts
Br
Me

2d

2.16
2.29
0.99
1.02
2.06
3.48
2.35
5.16
f1 (ppm)

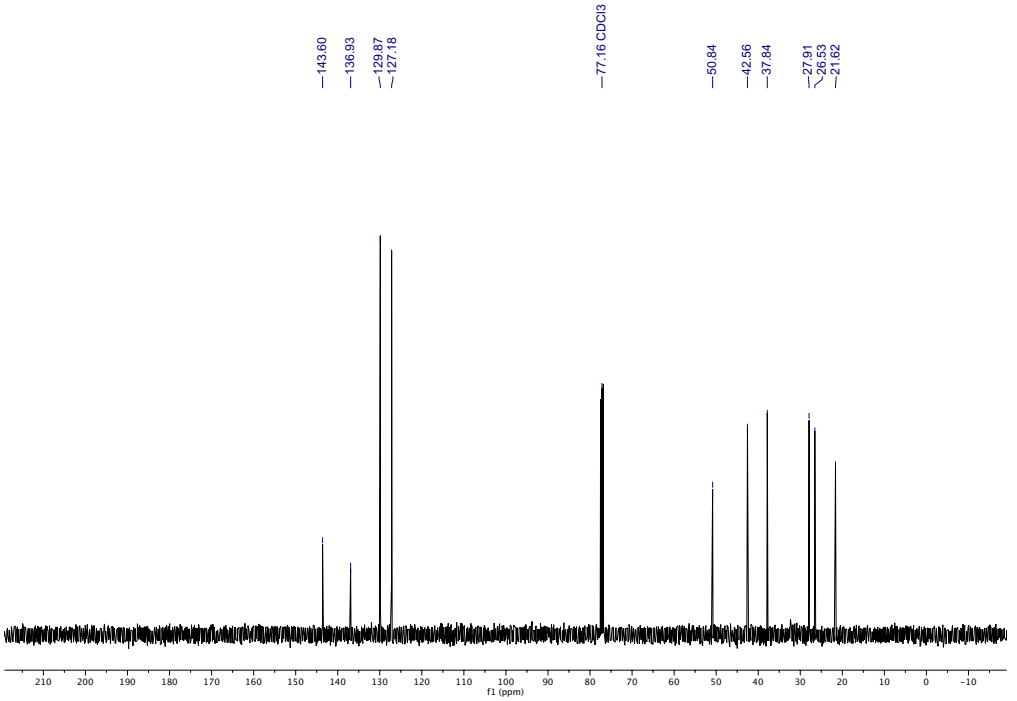
143.60
136.93
129.87
127.18
77.16 CDCl3
50.84
42.56
37.84
27.91
26.53
21.62
f1 (ppm)

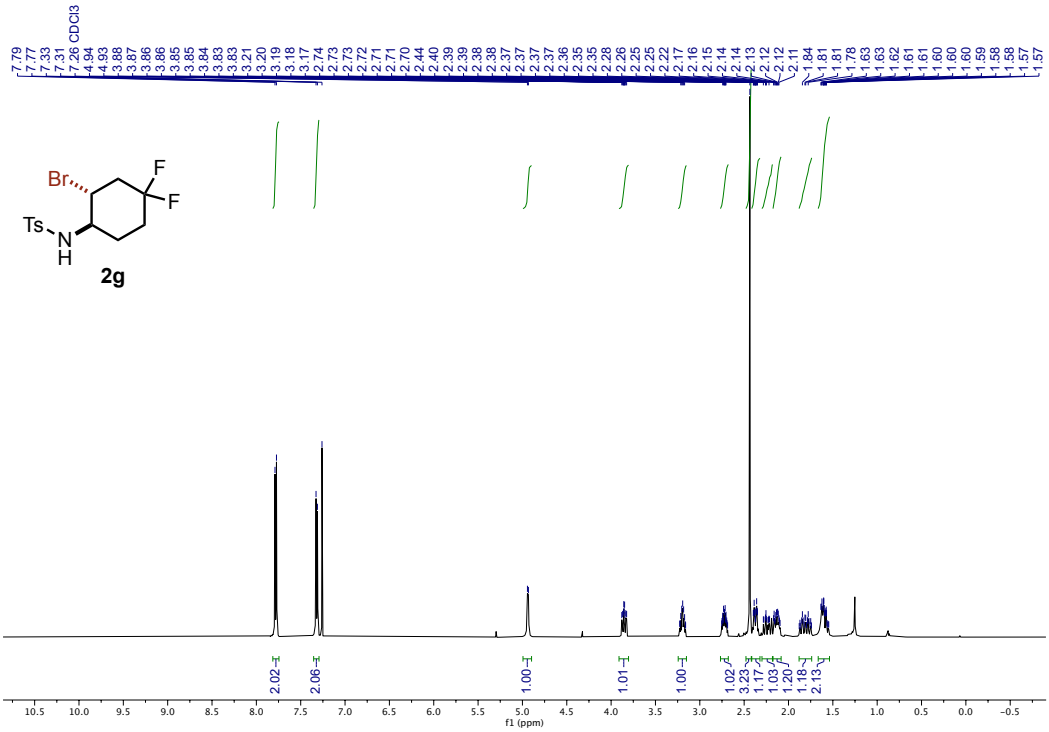
Br
F
F
Ts
N
H
2g
f1 (ppm)

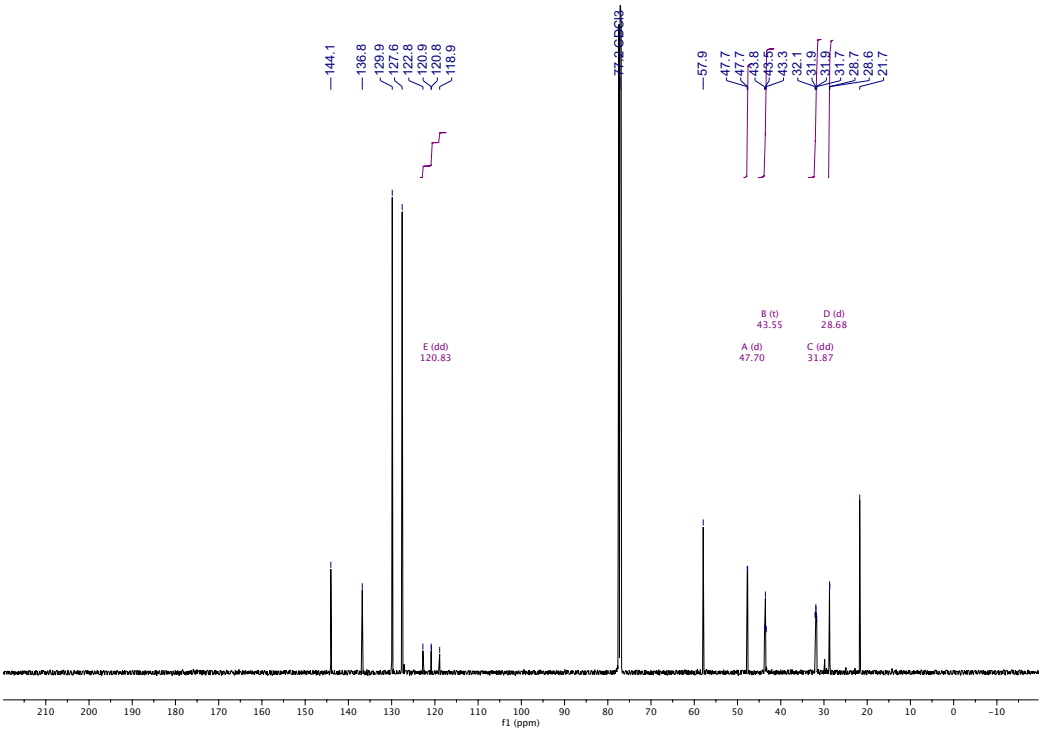
E (dd)
120.83
B (t)
43.55
D (d)
28.68
A (d)
47.70
C (dd)
31.87
f1 (ppm)

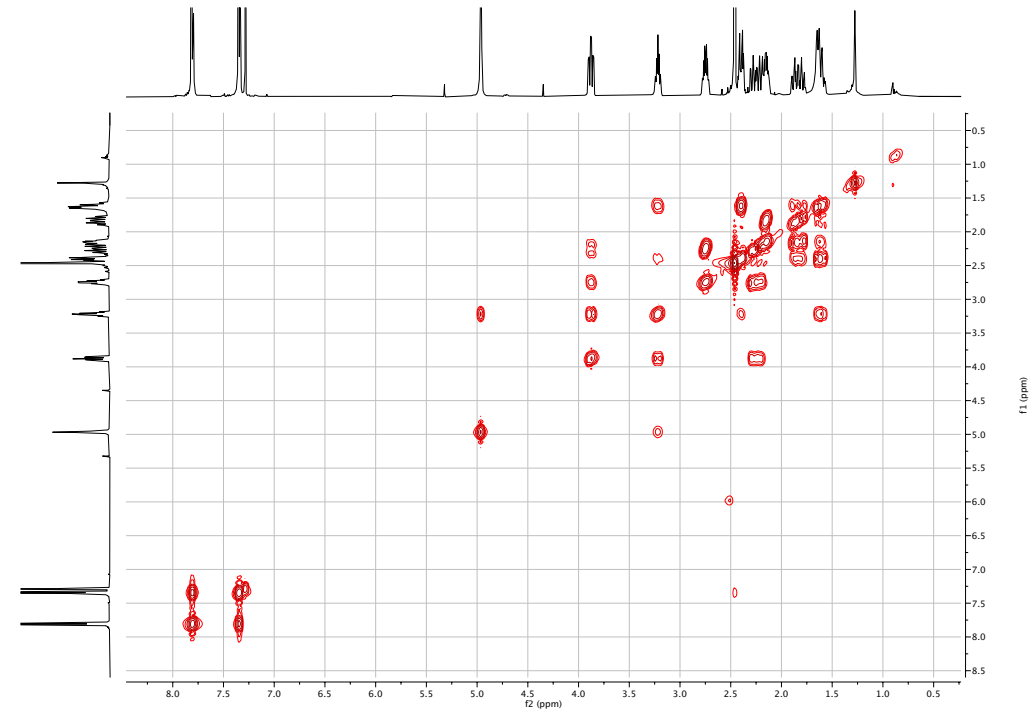
f2 (ppm)
f1 (ppm)

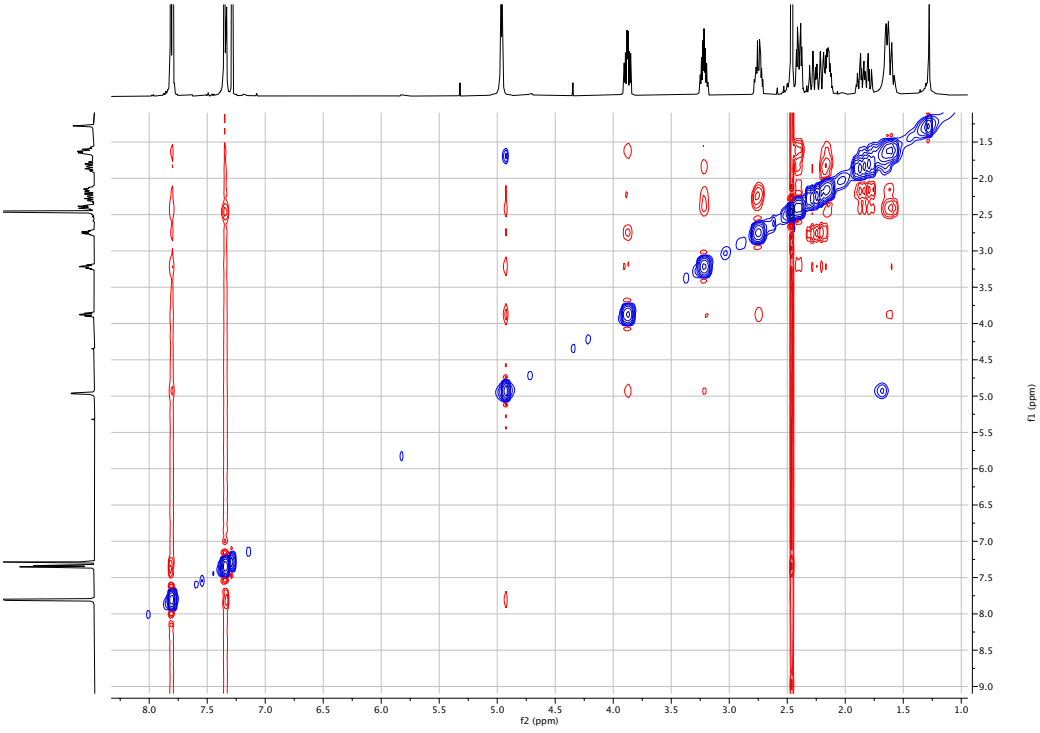
f2 (ppm)
f1 (ppm)

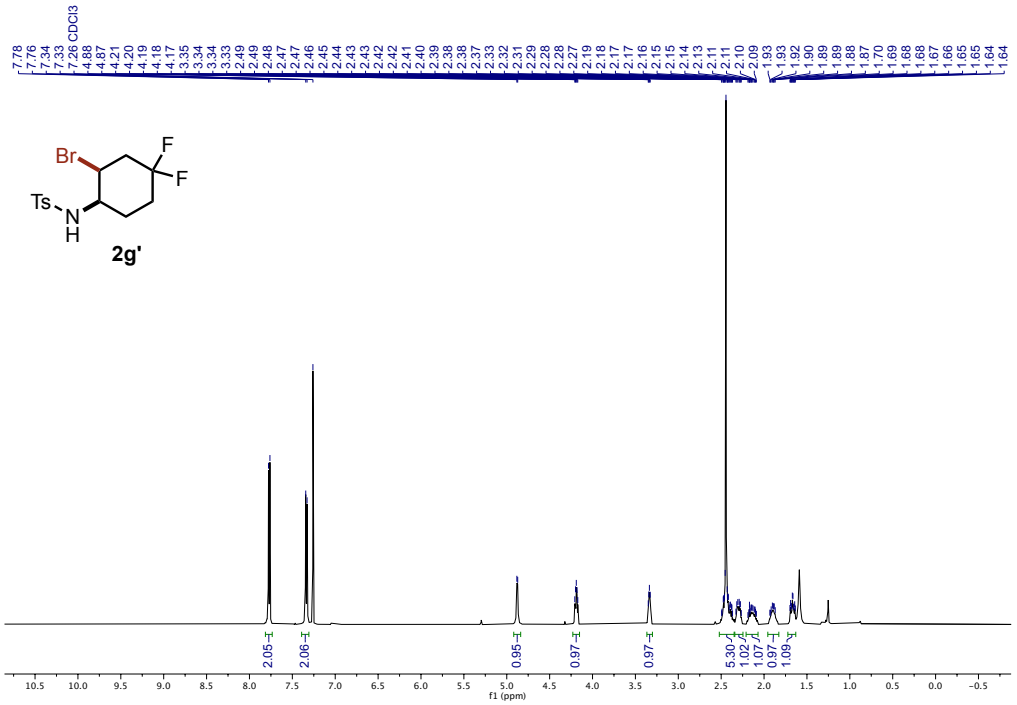
Br
F
F
Ts
N
H
2g'
f1 (ppm)

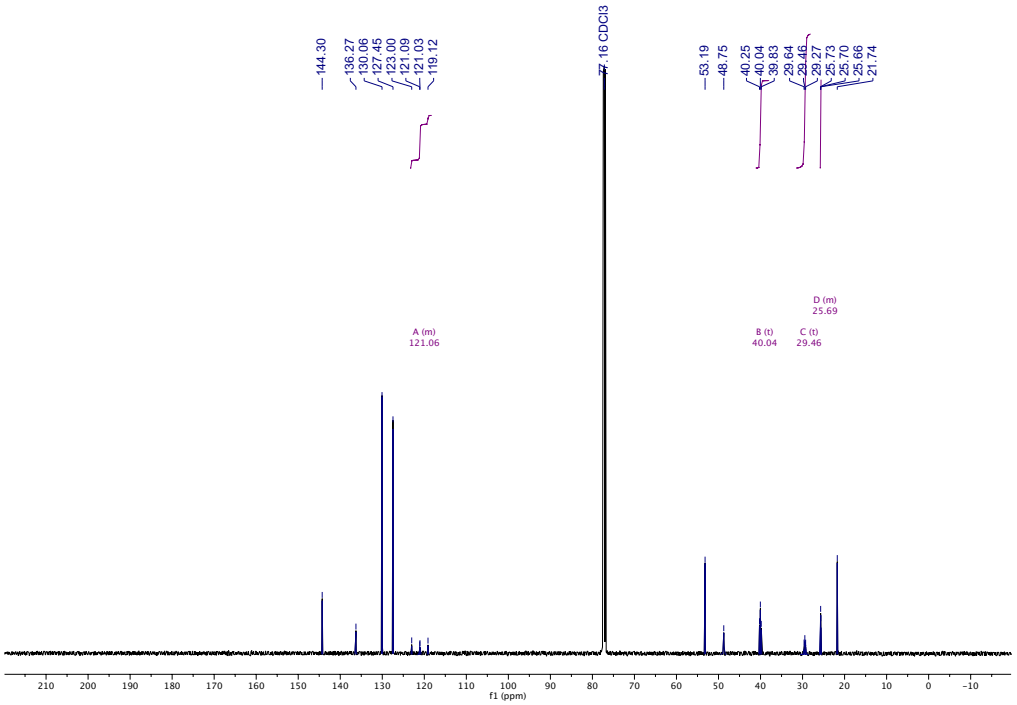
77.16 CDCl3
A (m)
121.06
B (t)
40.04
C (t)
29.46
D (m)
25.69
f1 (ppm)

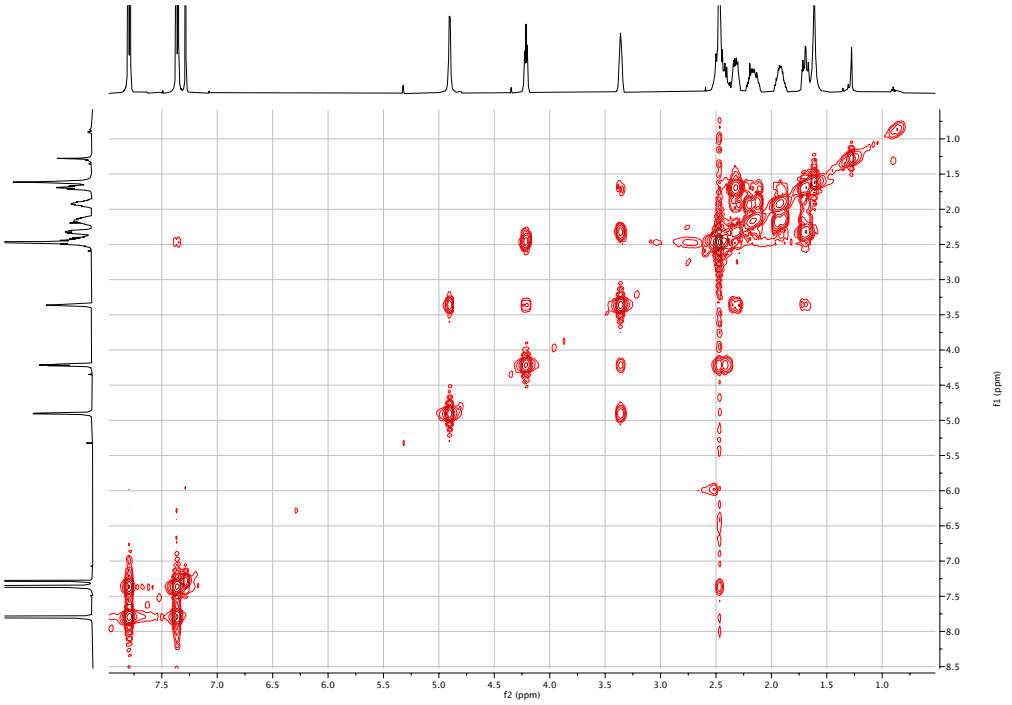
f2 (ppm)
f1 (ppm)

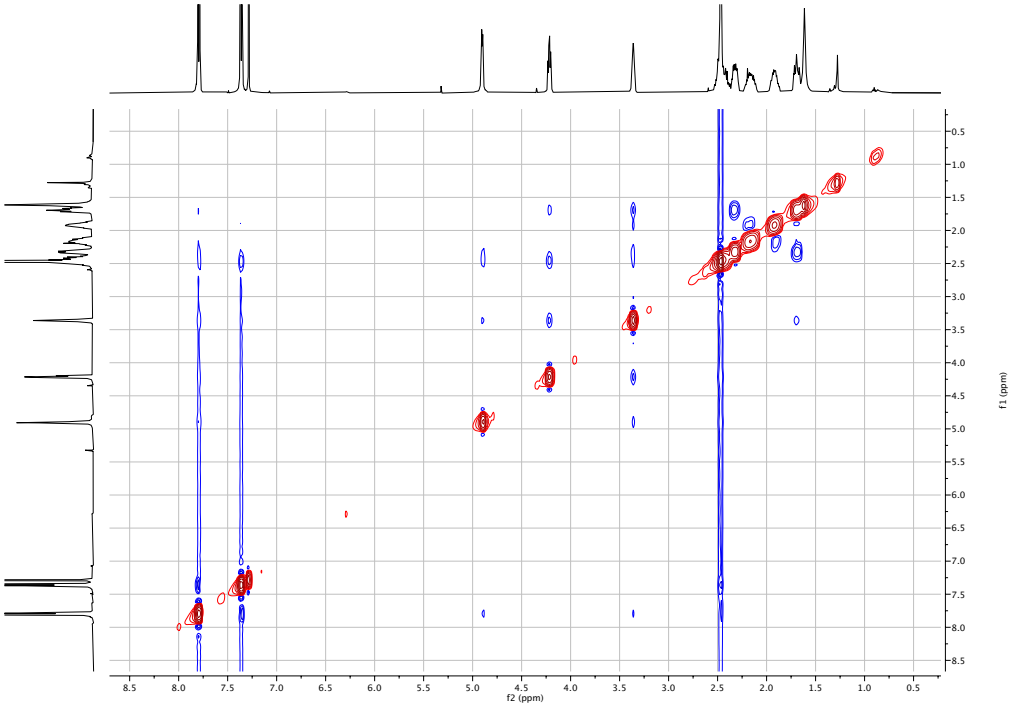
f2 (ppm)
f1 (ppm)

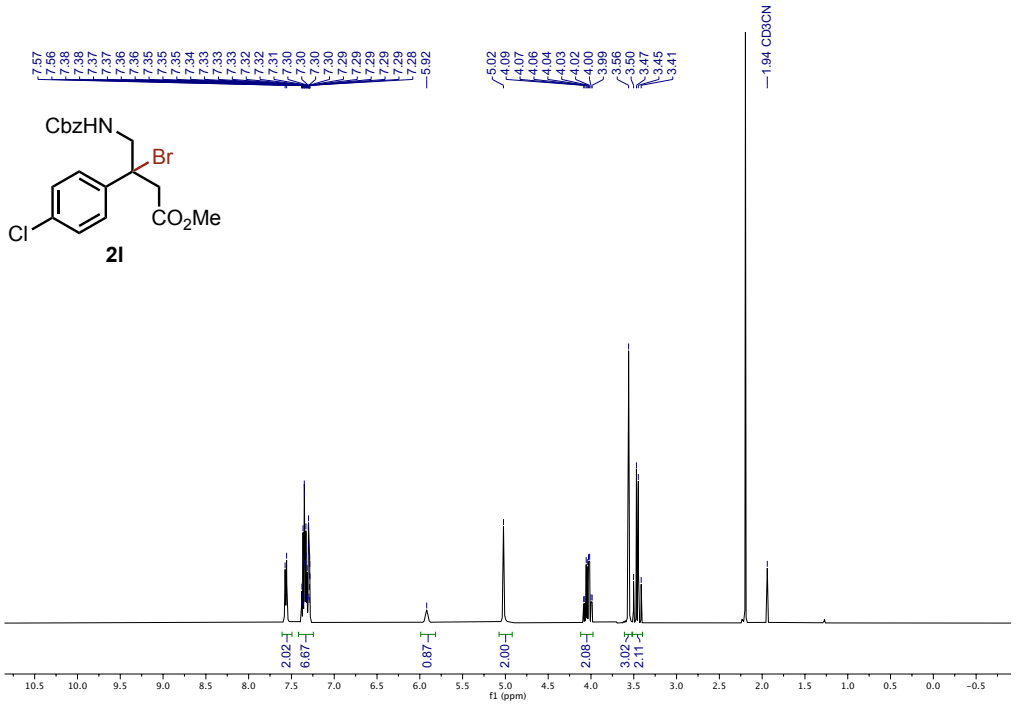
7.57
7.56
7.38
7.38
7.37
7.37
7.36
7.36
7.35
7.35
7.35
7.34
7.33
7.33
7.33
7.32
7.32
7.31
7.30
7.30
7.30
7.29
7.29
7.29
7.29
7.28
5.92
5.02
4.09
4.07
4.06
4.04
4.03
4.02
4.00
3.99
3.56
3.50
3.47
3.45
3.41
1.94 CD3CN
CbzHN
Br
Cl
CO2Me
2l
2.02
6.67
0.87
2.00
2.08
3.02
2.11
f1 (ppm)

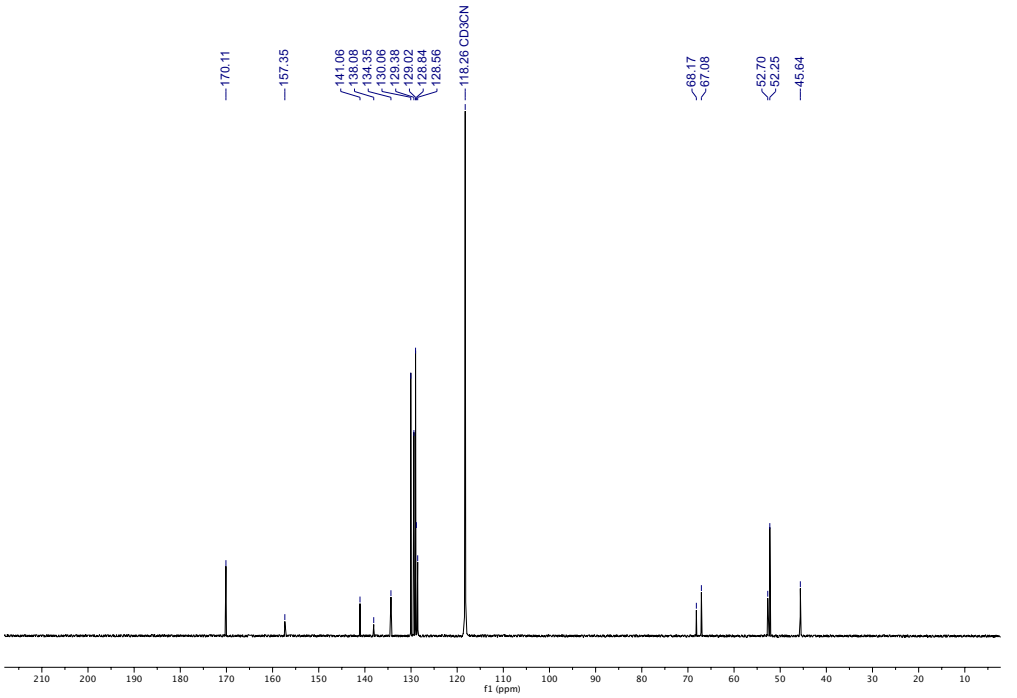
170.11
157.35
141.06
138.08
134.35
130.06
129.38
129.02
128.84
128.56
118.26 CD3CN
68.17
67.08
52.70
52.25
45.64
f1 (ppm)

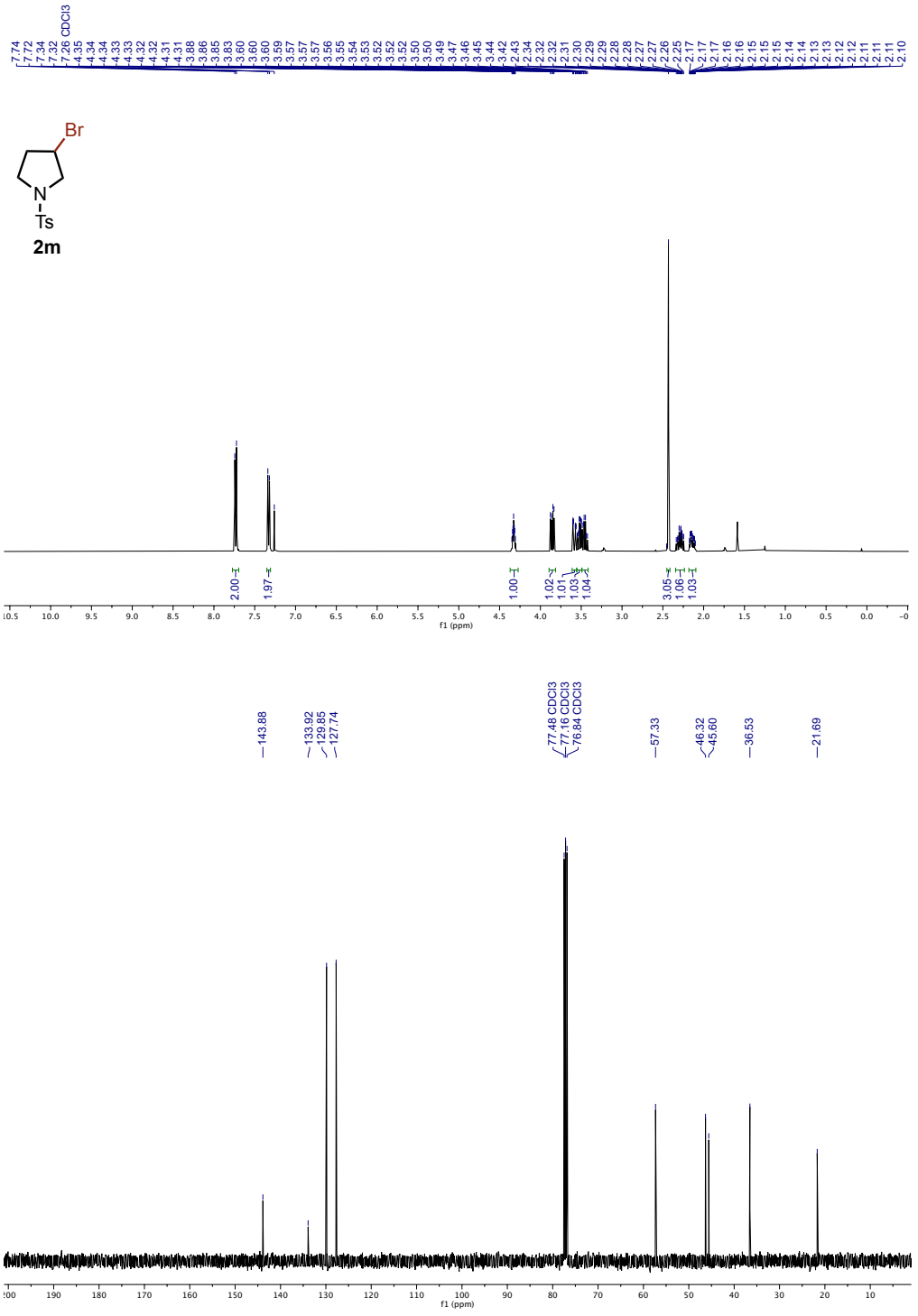
CDCl3
Br
N
Ts
2m
f1 (ppm)
143.88
133.92
129.85
127.74
77.48 CDCl3
77.16 CDCl3
76.84 CDCl3
57.33
46.32
45.60
36.53
21.69

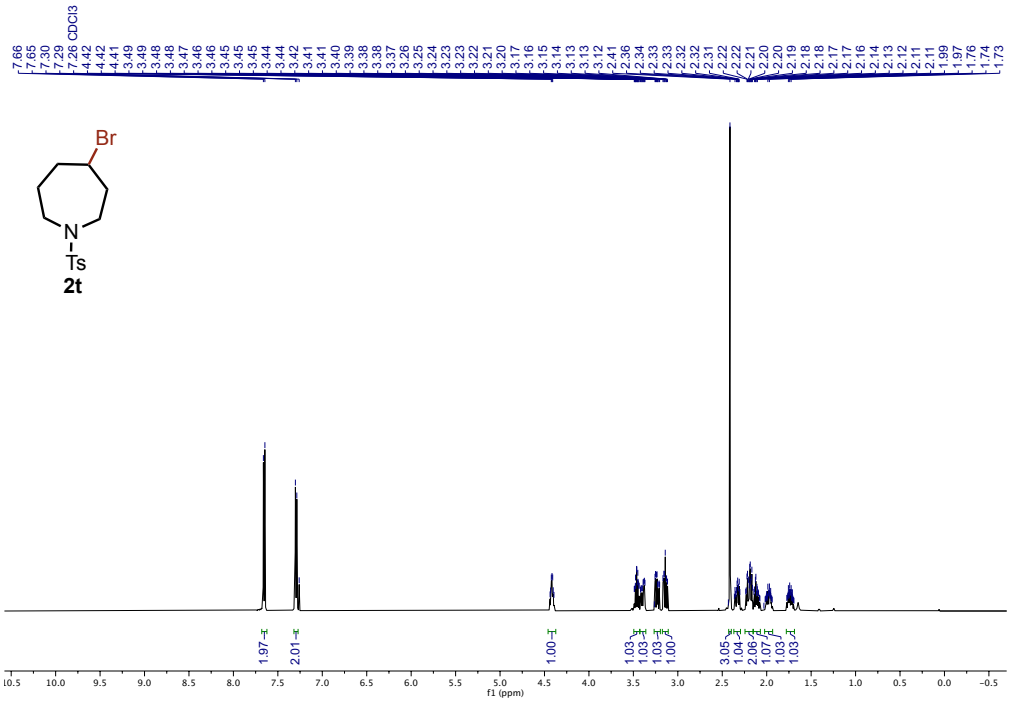
7.66
7.65
7.30
7.29
7.26 CDCl3
Br
N
Ts
2t
1.97
2.01
1.00
1.03
1.03
1.03
1.00
3.05
1.04
2.06
2.07
1.03
1.03
f1 (ppm)

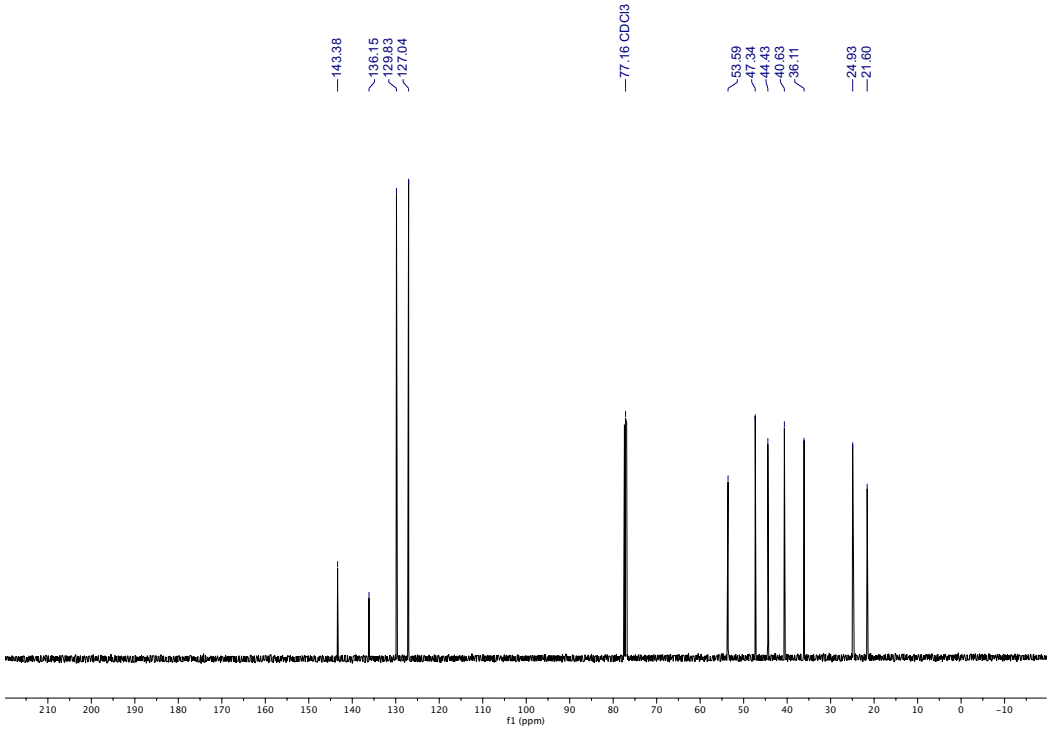
143.38
136.15
129.83
127.04
77.16 CDCl3
53.59
47.34
44.43
40.63
36.11
24.93
21.60
f1 (ppm)

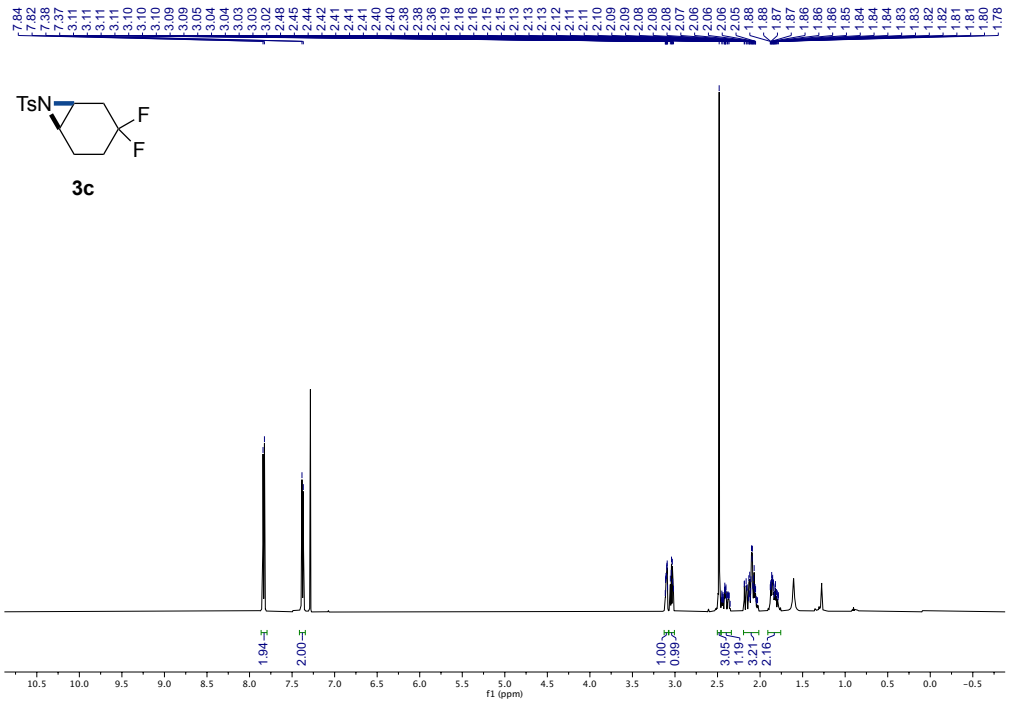
TsN
F
F
3c
f1 (ppm)

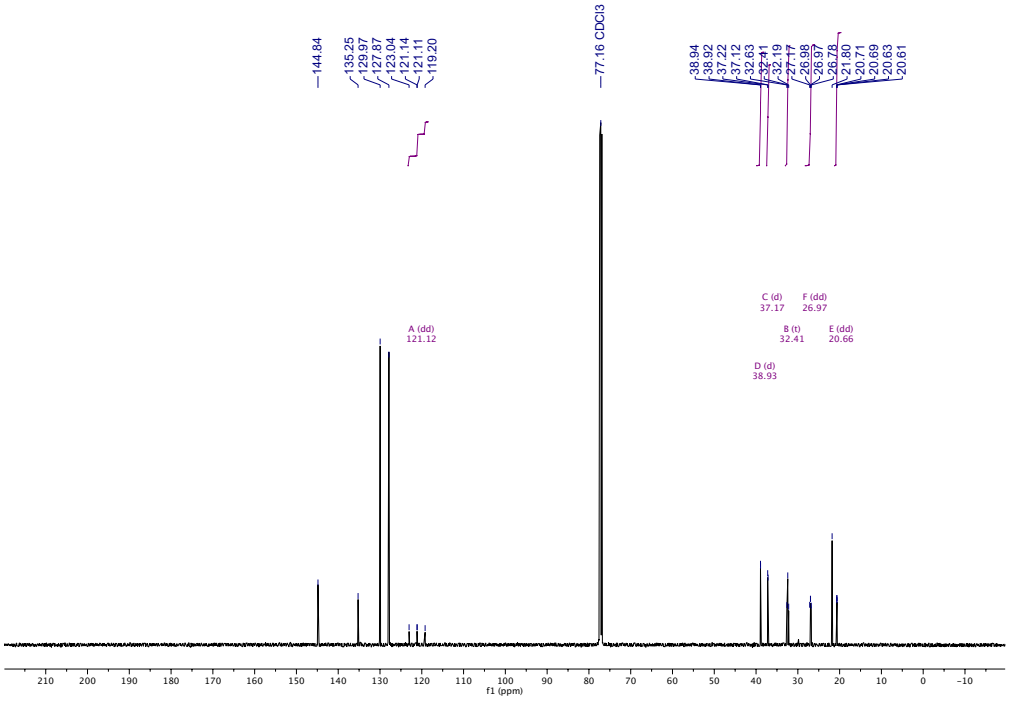
144.84
135.25
129.97
127.87
123.04
121.14
121.11
119.20
77.16 CDCl3
38.94
38.92
37.22
37.12
32.63
32.41
32.19
27.17
26.98
26.97
26.78
21.80
20.71
20.69
20.63
20.61
A (dd)
121.12
C (d)
37.17
F (dd)
26.97
B (t)
32.41
E (dd)
20.66
D (d)
38.93
f1 (ppm)

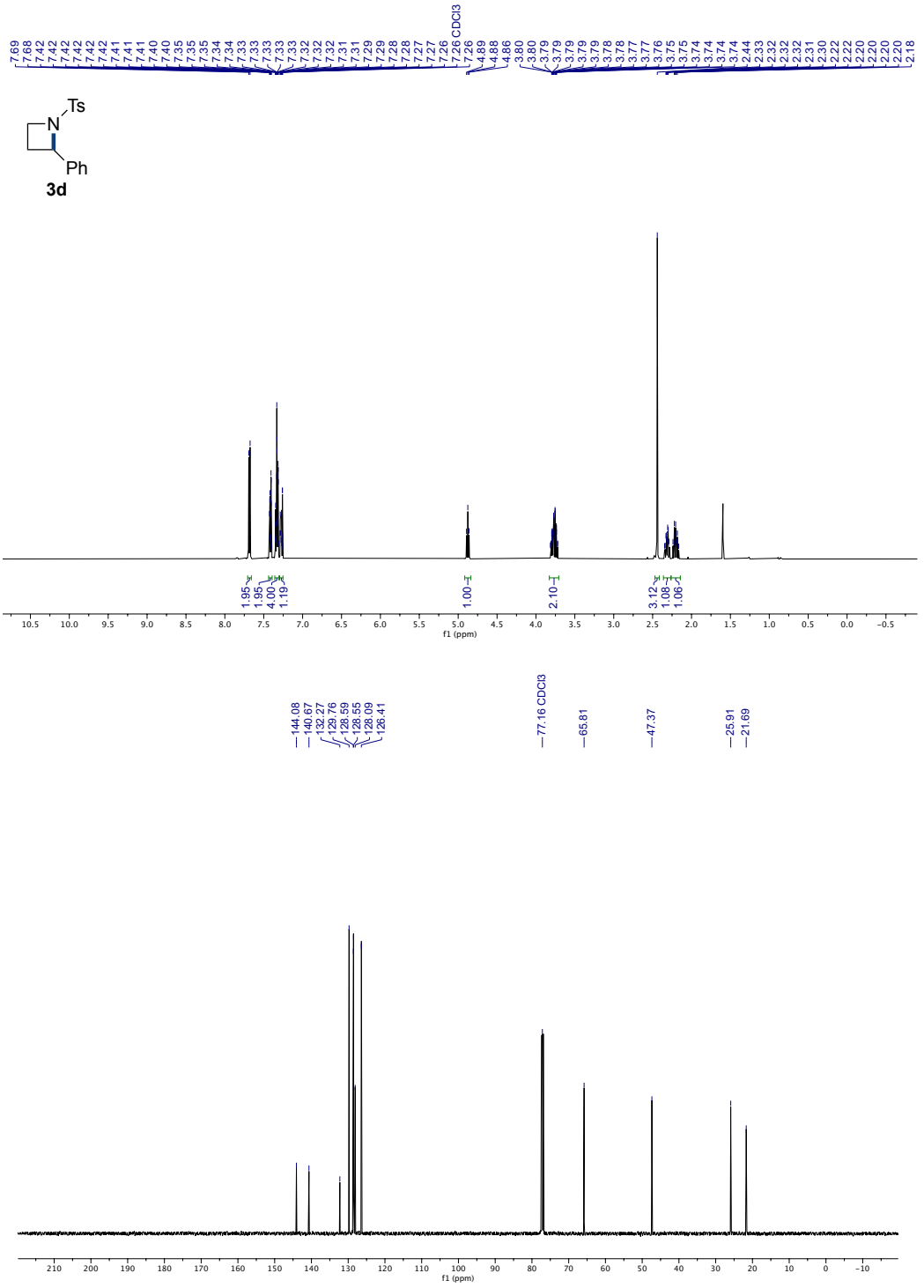
7.69 7.68 7.42 7.42 7.42 7.42 7.42 7.42 7.41 7.41 7.40 7.40 7.40 7.35 7.35 7.35 7.34 7.34 7.33 7.33 7.33 7.33 7.33 7.32 7.32 7.32 7.31 7.31 7.29 7.29 7.28 7.28 7.28 7.27 7.27 7.26 7.26 CDCl3 7.26 4.89 4.88 4.86 3.80 3.80 3.79 3.79 3.79 3.79 3.79 3.78 3.78 3.77 3.77 3.76 3.75 3.75 3.74 3.74 3.74 3.74 2.44 2.33 2.32 2.32 2.31 2.30 2.22 2.22 2.20 2.20 2.20 2.20 2.18
Ts
N
Ph
3d
1.95 1.95 4.00 1.19 1.00 2.10 3.12 1.08 1.06
f1 (ppm)
144.08 140.67 132.27 129.76 128.59 128.55 128.09 126.41 77.16 CDCl3 65.81 47.37 25.91 21.69
f1 (ppm)

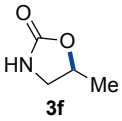
O
O
HN
Me

3f

7.26 CDCl3
5.53
4.81
4.80
4.80
4.79
4.79
4.78
4.78
4.78
4.77
4.77
4.77
4.77
4.76
4.76
4.75
4.74
3.72
3.72
3.70
3.70
3.68
3.68
3.21
3.21
3.20
3.20
3.20
3.18
3.18
1.46
1.45
1.07
1.00
1.05
1.05
3.23
f1 (ppm)

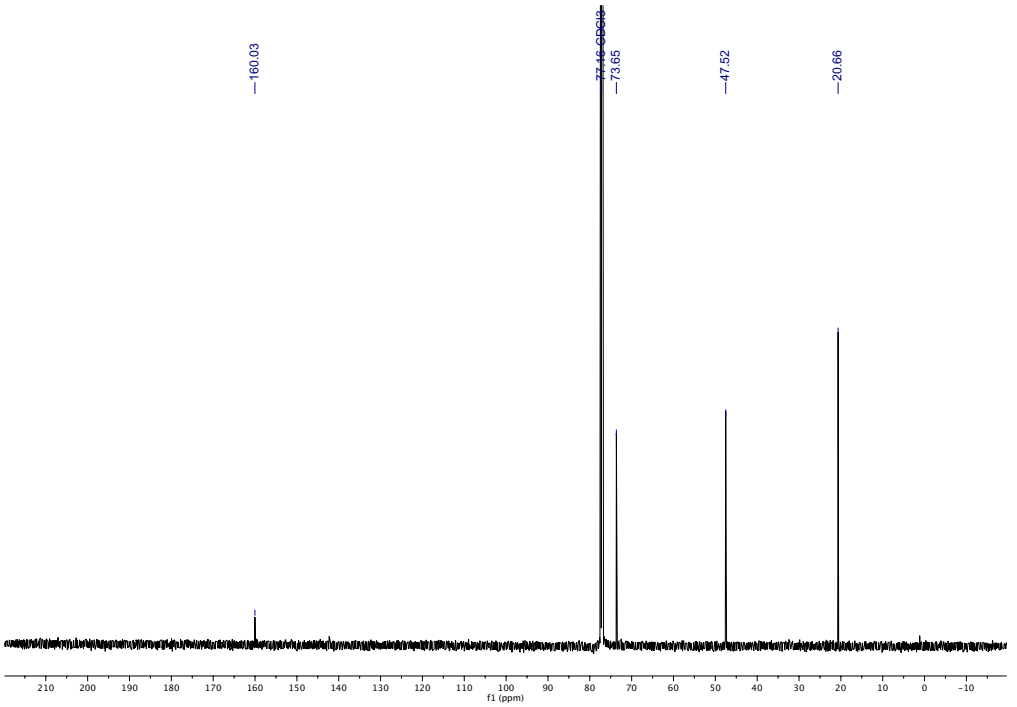
160.03
77.16 CDCl3
73.65
47.52
20.66
f1 (ppm)

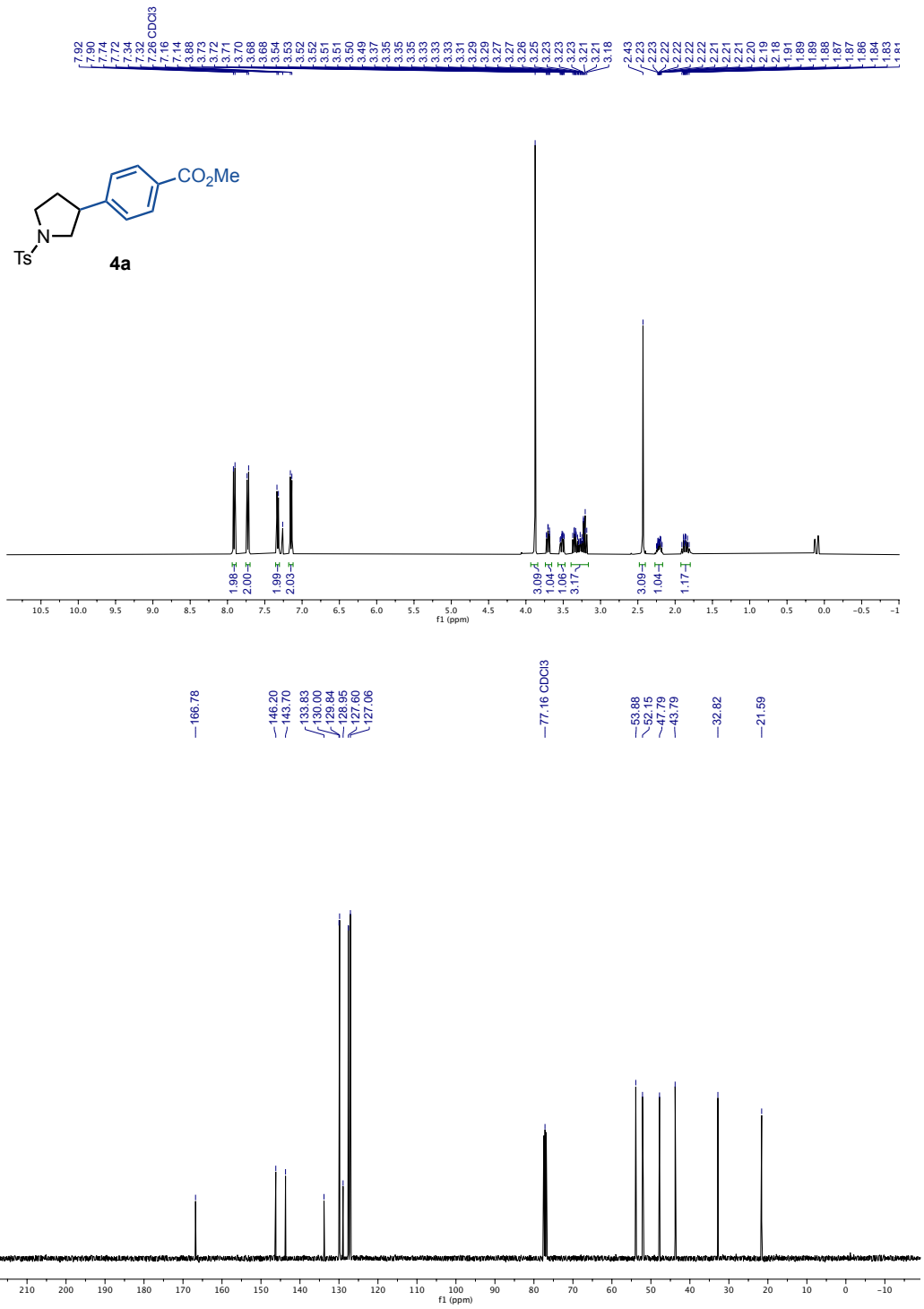
CO2Me
Ts
N
4a
f1 (ppm)

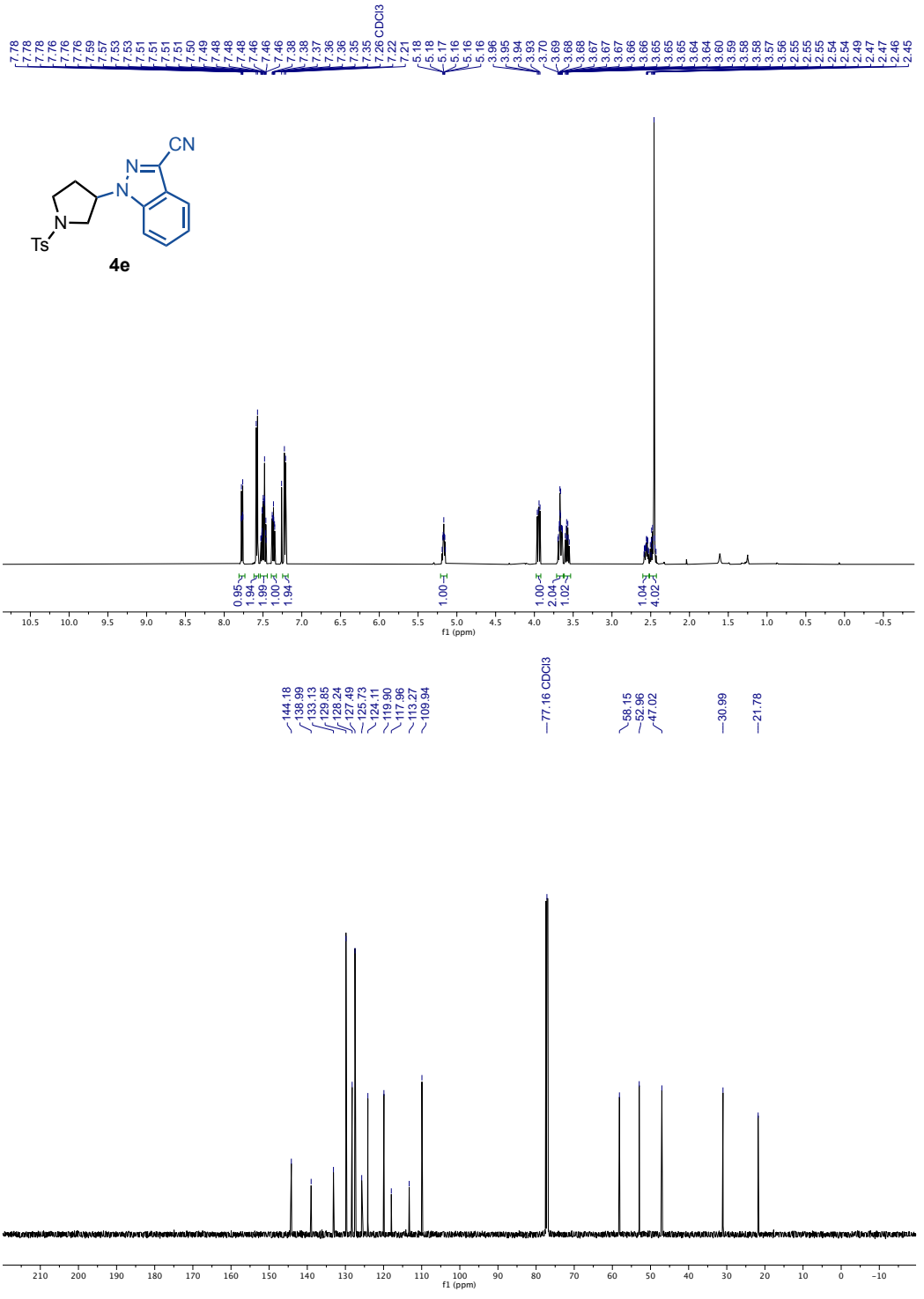
7.78 7.78 7.78 7.76 7.76 7.76 7.59 7.57 7.53 7.53 7.51 7.51 7.51 7.50 7.49 7.48 7.48 7.48 7.46 7.46 7.46 7.38 7.38 7.37 7.36 7.36 7.35 7.35 7.26 CDCl3 7.21 5.18 5.17 5.16 5.16 5.16 3.96 3.95 3.94 3.93 3.70 3.69 3.68 3.68 3.67 3.67 3.67 3.66 3.66 3.65 3.65 3.65 3.64 3.64 3.60 3.59 3.58 3.58 3.57 3.56 2.55 2.55 2.55 2.54 2.54 2.49 2.47 2.47 2.46 2.45
CN
N
N
N
Ts
4e
0.95 1.94 1.99 1.00 1.94 1.00 1.00 2.04 1.02 1.04 4.02
f1 (ppm)
144.18 138.99 133.13 129.85 128.24 127.49 125.73 124.11 119.90 117.96 113.27 109.94 77.16 CDCl3 58.15 52.96 47.02 30.99 21.78
f1 (ppm)

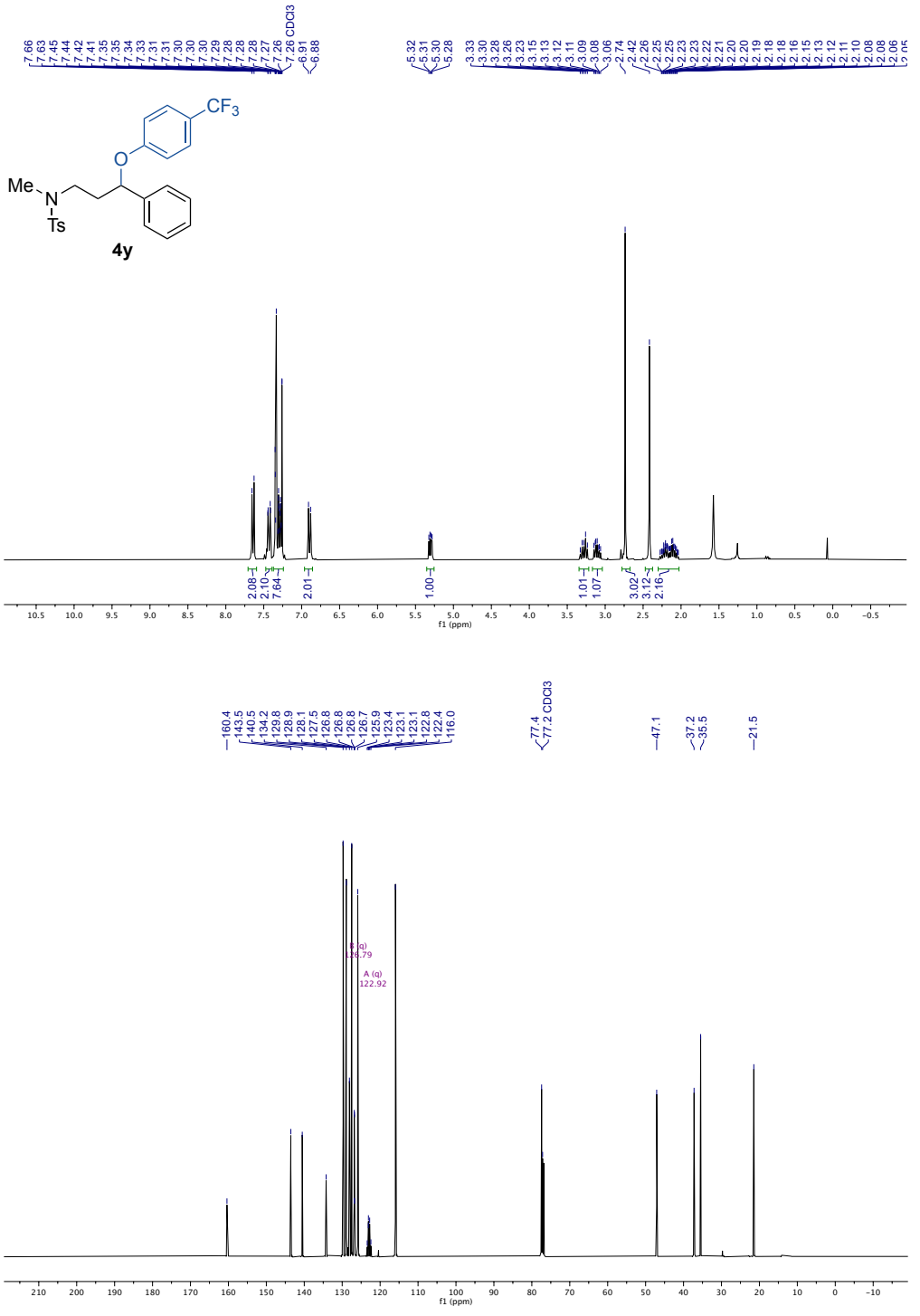
CF3
O
Me
N
Ts
4y
f1 (ppm)
f1 (ppm)

4.11 References

[1] a) F. Lovering, J. Bikker, C. Humblet, *J. Med. Chem.* **2009**, *52*, 6752; b) W. Wei, S. Cherukupalli, L. Jing, X. Liu, P. Zhan, *Drug. Discov. Today* **2020**, *25*, 1839.

[2] T. Rogge, N. Kaplaneris, N. Chatani, J. Kim, S. Chang, B. Punji, L. L. Schafer, D. G. Musaev, J. Wencel-Delord, C. A. Roberts, R. Sarpong, Z. E. Wilson, M. A. Brimble, M. J. Johansson, L. Ackermann, *Nat. Rev. Methods Primers* **2021**, *1*, 43.

[3] a) K. Nakajima, Y. Miyake, Y. Nishibayashi, *Acc. Chem. Res.* **2016**, *49*, 1946; b) A. McNally, C. K. Prier, D. W. C. MacMillan, *Science* **2011**, *334*, 1114.

[4] Z. Li, C.-J. Li, *J. Am. Chem. Soc.* **2004**, *126*, 11810.

[5] C. J. Cordier, R. J. Lundgren, G. C. Fu, *J. Am. Chem. Soc.* **2013**, *135*, 10946.

[6] a) S. J. Pastine, D. V. Gribkov, D. Sames, *J. Am. Chem. Soc.* **2006**, *128*, 14220; b) P. Jain, P. Verma, G. Xia, J.-Q. Yu, *Nature Chem.* **2017**, *9*, 140.

[7] H. M. L. Davies, T. Hansen, D. W. Hopper, S. A. Panaro, *J. Am. Chem. Soc.* **1999**, *121*, 6509.

[8] K. R. Campos, *Chem. Soc. Rev.* **2007**, *36*, 1069.

[9] R. K. Dieter, S. Li, *Tetrahedron Lett.* **1995**, *36*, 3613.

[10] A. Millet, P. Larini, E. Clot, O. Baudoin, *Chem. Sci.* **2013**, *4*, 2241.

[11] W. Chen, A. Pual, A. K. Abboud, D. Seidel, *Nat. Chem.* **2020**, *12*, 545.

[12] M. C. Haibach, D. Seidel, *Angew. Chem., Int. Ed.* **2014**, 53, 5010.

[13] A. McNakky, B. Haffemayer, B. S. L. Collins, M. J. Gaunt, *Nature* **2014**, *510*, 129.

[14] A. P. Smalley, M. J. Gaunt, *J. Am. Chem. Soc.* **2015**, *137*, 10632.

[15] a) J. Calleja, D. Pla, T. W. Gorman, V. Domingo, B. Haffemayer, M. J. Gaunt, *Nat. Chem.* **2015**, *7*, 1009; b) K. Chen, D. Wang, Z.-W. Li, Z. Liu, F. Pan, Y.-F. Zhang, Z.-J. Shi, *Org. Chem. Front.* **2017**, *4*, 2097.

[16] J. Rodrigalvarez, M. Nappi, H. Azuma, N. J. Flodén, M. E. Burns, M. J. Gaunt, *Nat. Chem.* **2020**, *12*, 76.

[17] Z. Zhuang, J.-Q. Yu, *J. Am. Chem. Soc.* **2020**, *142*, 12015.

[18] Q. Li, C. W. Liskey, J. F. Hartwig, *J. Am. Chem. Soc.* **2014**, *136*, 8755.

[19] R. Oeschger, B. Su, L. Yu, C. Ehinger, E. Romero, S. He, J. Hartwig, *Science* **2020**, *368*, 736.

[20] S. Chiba, H. Chen, *Org. Biomol. Chem.* **2014**, *12*, 4051.

[21] a) A. W. Hofmann, *Chem. Ber.* **1883**, *16*, 558; b) K. Löffler, C. Freytag, *Chem. Ber.* **1909**, 42, 3427.

[22] a) E. J. Corey, W. R. Hertler, *J. Am. Chem. Soc.* **1958**, *80*, 2903; b) S. W. Baldwin, R. J. Doll, *Tetrahedron Lett.* **1979**, *20*, 3275.

[23] a) P. D. Armas, R. Carrau, J. I. Concepción, C. G. Francisco, R. Hernández, E. Suárez, *Tetrahedron Lett.* **1985**, *26*, 2493; b) C. Martínez, K. Muñiz, *Angew. Chem. Int. Ed.* **2015**, *54*, 8287.

[24] G. J. Choi, Q. Zhu, D. C. Miller, C. J. Gu, R. R. Knowles, *Nature* **2016**, *539*, 268.

[25] a) J. C. K. Chu, T. Rovis, *Nature* **2016**, *539*, 272; b) S. M. Thullen, S. M. Treacy, T. Rovis, J. *Am. Chem. Soc.* **2019**, *141*, 14062.

[26] W. J. Yue, C. S. Day, R. Martin, *J. Am. Chem. Soc.* **2021**, *143*, 6395.

[27] a) R. T. Simons, M. Nandakumar, K. Kwon, S. K. Ayer, N. M. Venneti, J. L. Roizen, *J. Am. Chem. Soc.* **2023**, *145*, 3882; b) X. Wu, C. Zhu, *CCS Chemistry*. **2020**, *2*, 813.

[28] D. R. Weinberg, C. J. Gagliardi, J. F. Hull, C. F. Murphy, C. A. Kent, B. C. Westlake, A. Paul, D. H. Ess, D. Granville McCafferty, T. J. Meyer, *Chem. Rev.* **2012**, *112*, 4016.

[29] a) S. P. Morcillo, E. M. Dauncey, J. H. Kim, J. J. Douglas, N. S. Sheikh, D. Leonori, *Angew. Chem. Int. Ed.* **2018**, *57*, 12945; b) Z. Zhang, X. Zhang, D. A. Nagib, *Chem.* **2019**, *5*, 3127.

[30] M. Morris, B. Chan, L. Radom, *J. Phys. Chem. A* **2014**, *118*, 2810.

[31] G. Asensio, M. E. González-Núñez, C. B. Bernardini, R. Mello, W. Adam, *J. Am. Chem. Soc.* **1993**, *115,* 7250.

[32] a) B. D. Dangel, J. A. Johnson, D. Sames, *J. Am. Chem. Soc.* **2001**, *123*, 8149; b) M. Lee, M. S. Sanford, *J. Am. Chem. Soc.* **2015**, *137*, 12796.

[33] J. M. Howell, K. Feng, J. R. Clark, L. J. Trzepkowski, M. C. White, *J. Am. Chem. Soc.* **2015**, *137*, 14590.

[34] J. B. C. Mack, J. D. Gipson, J. Du Bois, M. S. Sigman, *J. Am. Chem. Soc.* **2017**, *139*, 9503.

[35] D. M. Schultz, F. Lévesque, D. A. DiRocco, M. Reibarkh, Y. Ji, L. A. Joyce, J. F Dropinski, H. Sheng, B. D. Sherry, I. W. Davies. *Angew. Chem. Int. Ed.* **2017**, *56*, 15274.

[36] P. J. Sarver, V. Bacauanu, D. M. Schultz, D. A. DiRocco, Y.-H. Lam, E. C. Sherer, D. W. C. MacMillan, *Nat. Chem.* **2020**, *12*, 459.

[37] P. J. Sarver, N. B. Bissonnette, D. W. C. MacMillan, *J. Am. Chem. Soc.* **2021**, *143*, 9737.

[38] a) B. J. Shields, A. G. Doyle, *J. Am. Chem. Soc.* **2016**, *138*, 12719; b) H.-P. Deng, Q. Zhou, J. Wu, *Angew. Chem. Int. Ed.* **2018**, *57*, 12661; *Angew. Chem*. **2018**, *130*, 12843; c) M. I. Gonzalez, D. Gygi, Y. Qin, Q. Zhu, E. J. Johnson, Y. Chen, D. G. Nocera, *J. Am. Chem. Soc.* **2022**, *144*, 1464; d) O. L. Garry, M. Heilmann, J. Chen, Y. Liang, X. Zhang, X. Ma, C. S. Yeung, D. J. Bennett, D. W. C. MacMillan, *J. Am. Chem. Soc.* **2023**, *145*, 3092; e) M. Wang, Y. Huang, P. Hu, *Science* **2024**, *383*, 537.

[39] E. Vitaku, D. T. Smith, J. T. Njardarson, *J. Med. Chem.* **2014**, *57*, 10257.

[40] a) A. K. Fazlur-Rahman, J. C. Chai, K. M. Nicholas, *J. Chem. Soc., Chem. Commun.* **1992**, 1334; b) A. Sen, M. Lin, L. C. Kao, A. C. Hutson, *J. Am. Chem. Soc.***1992**,*114*, 6385; c) M. T. Reezt, K. Tollner, *Tetrahedron Lett.* **1995**, *36*, 9461; d) M. Sasidharan, A. Bhaumik, *J. Mol. Catal. A Chem.* **2011**, *338*, 105; e) A. Gonzalez-de-Castro, C. M. Robertson, J. Xiao, *J. Am. Chem. Soc.* **2014**, *136*, 8350.

[41] M. E. Wolff, *Chem. Rev.* **1963**, *63*, 55.

[42] a) R. Sarpong, J. L. Jeffrey, *Chem. Sci.* **2013**, *4*, 4092; b) H. J. Dequina, C. L. Jones, J. M. Schomaker, *Chem* **2023**, *9*, 1658.

[43] a) A. C. Frisch, M. Beller. *Angew. Chem. Int. Ed.* **2005**, *44*, 674; b) B. D. Sherry, A. Fürstner, *Acc. Chem. Res.* **2008**, *41*, 1500; c) J. Terao, N. Kambe, *Acc. Chem. Res.* **2008**, *41*, 1545; d) A. Rudolph, M. Lautens, *Angew. Chem. Int. Ed.* **2009**, *48*, 2656; e) D. A. Everson, R. Shrestha, D. J. Weix, *J. Am. Chem. Soc.* **2010**, *132*, 920; f) R. Jana, T. P. Pathak, M. S. Sigman, *Chem. Rev.* **2011**, *111*, 1417; g) N. Kambe, T. Iwasakia, J. Terao, *Chem. Soc. Rev.* **2011**, *40*, 4937; h) J. Gu, X. Wang, W. Xue, H. Gong, *Org. Chem. Front.*

2015, 2, 1411; i) C. P. Johnston, R. T. Smith, S. Allmendinger, D. W. C. MacMillan. *Nature* **2016**, *536*, 322; j) J. Liu, Y. Ye, J. L. Sessler, H. Gong, *Acc. Chem. Res.* **2020**, 53, 1833; k) F. Juliá, T. Constantin, D. Leonori, *Chem. Rev.* **2022**, *122*, 2292.

[44] P. Zhang, C. C. Le, D. W. C. MacMillan, *J. Am. Chem. Soc.* **2016**, *138*, 8084.

[45] X. Yu, T. Yang, S. Wang, H. Xu, H. Gong, *Org. Lett.* **2011**, *13*, 2138.

[46] Y. Zou, J. Zhou, *Chem. Commun.* **2014**, *50*, 3725.

[47] V. D. Waele, O. Poizat, M. Fagnoni, A. Bagno, D. Ravelli, *ACS Catal.* **2016**, *6*, 7174.

[48] R. F. Renneke, M. Pasquali, C. L. Hill, *J. Am. Chem. Soc.* **1990**, *112*, 6585.

[49] P. J. Sarver, N. B. Bissonnette, D. W. C. MacMillan, *J. Am. Chem. Soc.* **2021**, *143*, 9737.

[50] . B. Perry, T. F. Brewer, P. J. Sarver, D. M. Schultz, D. A. DiRocco, D. W. C. MacMillan, *Nature* **2018**, *560*, 70.

[51] T. Yamase, N. Takabayashi, M. Kaji, *J. Chem. Soc., Dalton Trans.* **1984**, 793.

[52] A. Pulcinella, S. Bonciolini, F. Lukas, A. Sorato, T. Noël, *Angew. Chem. Int. Ed.* **2023**, *62*, e202215374.

[53] O. L. Garry, M. Heilmann, J. Chen, Y. Liang, X. Zhang, X. Ma, C. S. Yeung, D. J. Bennett, D. W. C. MacMillan, *J. Am. Chem. Soc.* **2023**, *145*, 3092.

[54] Atchard, C. G. H. A new sensitive chemical actinometer II. Potassium ferrioxalate as a standard chemical actinometer. vol. 8 https://royalsocietypublishing.org/.

[55] J. Liu, W. Zhang, X. Tao, Q. Wang, X. Wang, Y. Pan, J. Ma, L. Yan, Y. Wang, *Org. Lett.* **2023**, *25*, 3083.

[56] P. E. Gormisky, M. C. White, *J. Am. Chem. Soc.* **2013**, *135*, 3083.

UNIVERSITAT ROVIRA I VIRGILI
Synthesis of Advanced Aliphatic Amines via Catalytic C(sp3)–N Bond-Formation or C(sp3)–H Functionalization
JINHONG CHEN

Chapter 5. General Conclusions

UNIVERSITAT ROVIRA I VIRGILI
Synthesis of Advanced Aliphatic Amines via Catalytic C(sp3)–N Bond-Formation or C(sp3)–H Functionalization
JINHONG CHEN

This thesis describes the efficient manifolds for accessing advanced aliphatic amines via catalytic C(sp^3)–N bond-formation or C(sp^3)–H functionalization, highlighting their potential application in medicinal development. The main achievements of the initial program are highlighted herein:

Chapter 2:

- A nickel-catalyzed intermolecular, site-selective C(sp^3)–H amidation via nitrene transfer has been developed. The method is characterized by its ease of execution, mild conditions, and broad substrate scope.

- The protocol is distinguished by a predictable reactivity pattern using dioxazolones as nitrene precursors, allowing to forge C(sp^3)–N linkages at sp^3 sites adjacent to nitrogen or oxygen atoms in either cyclic or acyclic frameworks.

- Preliminary mechanistic experiments revealed the involvement of open-shell carbon-centered radicals generated via hydrogen atom transfer by the nickel-nitrenoid intermediate. In addition, a prepared bathocuproine-ligated Ni(I) complex was found to be component as reaction intermediate.

Chapter 3:

- A switchable, stereodivergent nickel-catalyzed *N*-glycosylation of readily accessible glycals has been developed.

- The method involves the incorporation of a hydrogen atom across an olefin prior to C(sp^3)–N bond formation, thus offering a new way to access α-*N*-glycosides. The corresponding β-*N*-glycosides can be easily accessed by epimerization of the former α-*N*-glycosides in acidic media.

- Isotope-labelling studies suggest a mechanism consisting of a nickel-hydride migratory insertion into the glycal from α-face, an observation that is likely dictated by a kinetic metalloanomeric effect.

Chapter 4:

- A photocatalyzed, site-selective remote bromination of C(sp^3)–H bonds in primary or secondary aliphatic amines has been developed.

- The approach was achieved by modulating the electronics properties of the proximal C–H bonds via protonation of the amine function, allowing to promote functionalization at remote sp^3 C–H bonds.

- The resulting halogenated building blocks serve as synthetic linchpins, as these intermediates can be engaged in a series of C(sp^3)–C, C(sp^3)–N or C(sp^3)–O bond-forming reactions, thus offering a new platform to incorporate different moieties at remote positions of simple aliphatic amine backbones.

UNIVERSITAT ROVIRA I VIRGILI
Synthesis of Advanced Aliphatic Amines via Catalytic C(sp3)–N Bond-Formation or C(sp3)–H Functionalization
JINHONG CHEN

UNIVERSITAT ROVIRA I VIRGILI
Synthesis of Advanced Aliphatic Amines via Catalytic C(sp3)–N Bond-Formation or C(sp3)–H Functionalization
JINHONG CHEN

UNIVERSITAT ROVIRA I VIRGILI
Synthesis of Advanced Aliphatic Amines via Catalytic C(sp3)–N Bond-Formation or C(sp3)–H Functionalization
JINHONG CHEN

UNIVERSITAT ROVIRA I VIRGILI
Synthesis of Advanced Aliphatic Amines via Catalytic C(sp3)–N Bond-Formation or C(sp3)–H Functionalization
JINHONG CHEN

UNIVERSITAT
ROVIRA i VIRGILI